

POLSKIE TOWARZYSTWO MIKROBIOLOGÓW
POLISH SOCIETY OF MICROBIOLOGISTS

Polish Journal of Microbiology

2019

CONTENTS

MINIREVIEW

Antibiotic resistance among uropathogenic <i>Escherichia coli</i> KOT B.	403
Colistin resistance in Enterobacterales strains – a current view STEFANIUK E.M., TYSKI S.	417

ORIGINAL PAPERS

Molecular identification of <i>Vibrio alginolyticus</i> causing vibriosis in shrimp and its herbal remedy HANNAN MD. A., RAHMAN MD. M., MONDAL MD. N., DEB S.C., CHOWDHURY G., ISLAM MD. T.	429
<i>Salmonella</i> -infected aortic aneurysm: investigating pathogenesis using <i>Salmonella</i> serotypes CHU C., WONG M.Y., CHIU C.-H., TSENG Y.-H., CHEN C.-L., HUANG Y.-K.	439
Molecular epidemiology of hepatitis B virus in Turkish Cypriot SUMER U., SAYAN M.	449
Cytokine levels in the <i>in vitro</i> response of T cells to planktonic and biofilm <i>Corynebacterium amycolatum</i> OLENDER A., BOGUT A., MAGRYŚ A., TABARKIEWICZ J.	457
The diversity of the endobiotic bacterial communities in the four jellyfish species LIU Q., CHEN X., LI X., HONG J., JIANG G., LIANG H., LIU W., XU Z., ZHANG J., WANG W., XIAO L.	465
Inhibition of drug resistance of <i>Staphylococcus aureus</i> by efflux pump inhibitor and autolysis inducer to strengthen the antibacterial activity of β -lactam drugs LUAN W., LIU X., WANG X., AN Y., WANG Y., WANG C., SHEN K., XU H., LI S., LIU M., YU L.	477
Diversity, virulence factors, and antifungal susceptibility patterns of pathogenic and opportunistic yeast species in rock pigeon (<i>Columba livia</i>) fecal droppings in Western Saudi Arabia ABULREESH H.H., ORGANJI S.R., ELBANNA K., OSMAN G.E.H., ALMALKI M.H.K., ABDEL-MALEK A.Y., GHYATHUDDIN A.A.K., AHMAD I.	493
The composition of fungal communities in the rumen of gayals (<i>Bos frontalis</i>), yaks (<i>Bos grunniens</i>), and Yunnan and Tibetan yellow cattle (<i>Bos taurus</i>) WANG H., LI P., LIU X., ZHANG C., LU Q., XI D., YANG R., WANG S., BAI W., YANG Z., ZHOU R., CHENG X., LENG J.	505
New look on antifungal activity of silver nanoparticles (AgNPs) ŻAROWSKA B., KOŹLECKI T., PIEGZA M., JAROS-KOŹLECKA K., ROBAK M.	515
Illumina MiSeq analysis and comparison of freshwater microalgal communities on Ulleungdo and Dokdo Islands YUN X.-S., KIM Y.-S., YOON H.-S.	527
Epidemiology, drug resistance, and virulence of <i>Staphylococcus aureus</i> isolated from ocular infections in Polish patients KŁOS M., POMORSKA-WESOŁOWSKA M., ROMANISZYN D., CHMIELARCZYK A., WÓJKOWSKA-MACH J.	541
Structural changes of <i>Bacillus subtilis</i> biomass on biosorption of Iron (II) from aqueous solutions: isotherm and kinetic studies KANAMARLAPUDI S.L.R.K., MUDDADA S.	549

SHORT COMMUNICATIONS

Differentially marked IncP-1 β R751 plasmids for cloning via recombineering and conjugation BAINS A., WILSON J.W.	559
---	-----

INSTRUCTIONS FOR AUTHORS

Instructions for authors: https://www.exeley.com/journal/polish_journal_of_microbiology



**Ministry of Science
and Higher Education**

Republic of Poland

Purchase of DOI numbers for articles and implementation
of a modern publication platform
for the Polish Journal of Microbiology are funded with the financial support
of the Ministry of Science and Higher Education
under agreement No. 659/P-DUN/2018 for science dissemination activities.

Antibiotic Resistance Among Uropathogenic *Escherichia coli*

BARBARA KOT[✉]

Department of Microbiology, Faculty of Natural Sciences, Siedlce University of Natural Sciences and Humanities,
Siedlce, Poland

Submitted 30 June 2019, revised 9 September 2019, accepted 24 September 2019

Abstract

Urinary tract infections (UTIs) belong to the most common community-acquired and nosocomial infections. A main etiological factor of UTIs is uropathogenic *Escherichia coli* (UPEC). This review describes the current state of knowledge on the resistance of UPEC to antibiotics recommended for the treatment of UTIs based on the available literature data. Nitrofurantoin and fosfomycin are recommended as first-line therapy in the treatment of uncomplicated cystitis, and the resistance to these antimicrobial agents remains low between UPEC. Recently, in many countries, the increasing resistance is observed to trimethoprim-sulfamethoxazole, which is widely used as the first-line antimicrobial in the treatment of uncomplicated UTIs. In European countries, the resistance of UPEC to this antimicrobial agent ranges from 14.6% to 60%. The widespread use of fluoroquinolones (FQs), especially ciprofloxacin, in the outpatients is the cause of a continuous increase in resistance to these drugs. The resistance of UPEC to FQs is significantly higher in developing countries (55.5–85.5%) than in developed countries (5.1–32.0%). Amoxicillin-clavulanic acid is recommended as first line-therapy for pyelonephritis or complicated UTI. Resistance rates of UPEC to amoxicillin-clavulanic acid are regionally variable. In European countries the level of resistance to this antimicrobial ranges from 5.3% (Germany) to 37.6% (France). Increasing rates of UPEC resistance to antimicrobials indicate that careful monitoring of their use for UTI treatment is necessary.

Key words: uropathogenic *Escherichia coli*, antibiotic resistance, antibiotic therapy, urinary tract infections, treatment of UTIs

Introduction

Urinary tract infections (UTIs) are among the most common bacterial infections in humans (Bischoff et al. 2018). It is estimated that 40% of women and 12% of men experience a minimum one symptomatic UTI episode during their lifetimes, and 27 to 48% of the affected women suffer from recurrent UTIs (Braumbaugh et al. 2013; Micali et al. 2014). UTIs comprise about 40% of all hospital-acquired infections and 50% of bacterial infections that contribute to increased morbidity causing prolonged hospitalization (Asadi Karam et al. 2019). UTIs are also an economic problem. In the United States, about 11 million people per year have been treated due to UTIs, generating the cost of about \$6 billion (Mann et al. 2017). Healthcare-associated infections (HAI) are a serious threat for patients in terms of morbidity and mortality, with the healthcare-associated urinary tract infections (HAUTI) being among the most frequent HAI. In Europe, HAUTI

account for 19.0% of all HAI (ECDCP 2013). Community- or healthcare-acquired UTIs are clinically divided into complicated or uncomplicated, and among many other factors, this classification determines what antimicrobial agents can be applied for treatment (Zacchè and Giarenis 2016). Complicated UTIs require prolonged therapy and occur in patients with renal failure, anatomical urinary tract abnormalities such as urinary obstruction and retention or in patients that use medical devices such as a catheter. Complicated UTIs are also associated with immunosuppression and previous antibiotic exposure. This category of UTIs increases the risk of chronic and/or recurrent infections. Uncomplicated UTIs are found in patients who have no anatomical urinary tract abnormalities and do not use the urinary tract instrumentation. In uncomplicated UTIs, host immune response may successfully fight infection without antibiotic therapy (Mann et al. 2017). The symptomatic UTIs are classified as urosepsis, pyelonephritis (infection of the upper UTI) or

* Corresponding author: B. Kot, Department of Microbiology, Faculty of Natural Sciences, Siedlce University of Natural Sciences and Humanities, Siedlce, Poland; e-mail: barbara.kot@uph.edu.pl

© 2019 Barbara Kot

This work is licensed under the Creative Commons Attribution-NonCommercial-NoDerivatives 4.0 License (<https://creativecommons.org/licenses/by-nc-nd/4.0/>).

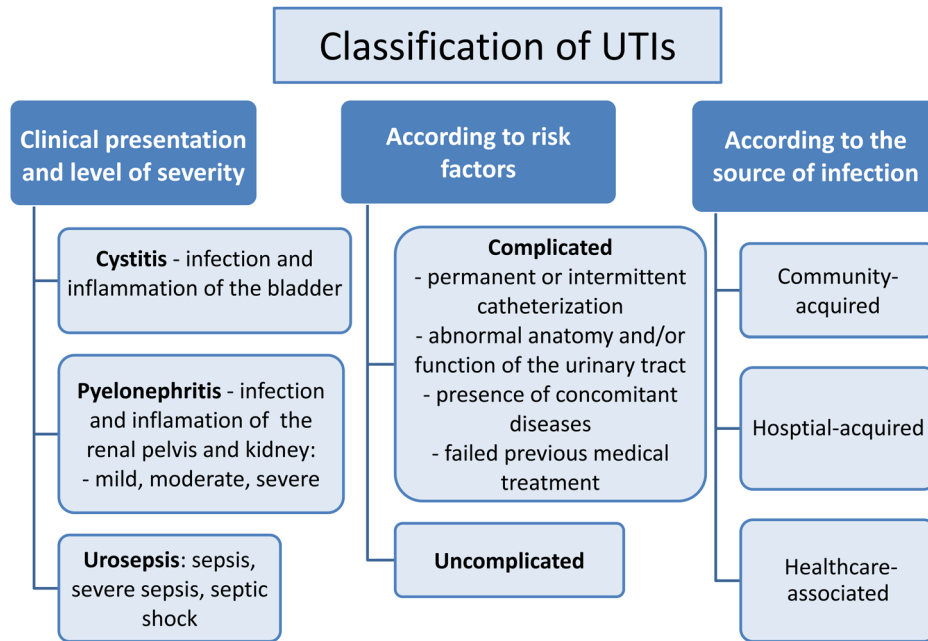


Fig. 1. Classification of urinary tract infections (Bartoletti et al. 2016).

cystitis (infection of the lower UTI) (Terlizzi et al. 2017) (Fig. 1). The presence of numerous UPEC cells in the urine ($\geq 10^5$ CFU/ml) without the clinical symptoms is called asymptomatic bacteriuria (ABU) and in healthy non-pregnant women is not treated in 20–80% of cases (Schneeberger et al. 2014).

The increase of antibiotic resistance and appearance of multi-drug resistant (MDR) pathogens in the course of UTI is related to high rates of inadequate antibiotic empirical therapies prescribed without the antibiotic susceptibility testing and finally result in an ineffective UTI treatment (Adamus-Białek 2018). Wagenlehner et al. (2016) showed that among 27 542 patients from 856 urology units in 70 countries, 56% of the hospitalized patients were treated with antimicrobials. Among them, 46% received prophylactic antibiotic treatment, 26% of them had the antimicrobials prescribed for the microbiologically proven UTI, 21% – for suspected UTI, and 7% for other infections. The above study also has revealed that broad-spectrum antibiotics were applied such as fluoroquinolones (35%), cephalosporins (27%), and penicillins (16%). The results obtained by Cek et al. (2014) showed the correlation between the increased use of broad-spectrum antibiotics and increased antimicrobial resistance and multi-resistance of bacteria. These authors also observed that prophylactic antibiotic treatment of urological patients occurred most frequently in Asia, Africa, and Latin America (86%, 85%, and 84%, respectively), followed by Europe (67%). The increasing number of MDR isolates from UTIs of outpatients makes treatment more difficult. Risk factors of MDR isolated from UTIs include prior use of antimicrobials, hospitalization, genitourinary disturbances,

age, and recurrent UTIs (Walker et al. 2016). Tenney et al. (2018) have recently analyzed the published data (25 studies including 31 284 patients with the confirmed UTI) to determine the risk factors for MDR isolated from UTIs and revealed that previous antibiotic treatment applied from 2 to 365 days earlier was the most commonly identified risk factor. The analysis by Tenney et al. (2018) showed also that urinary catheterization, previous hospitalization, and residence in a nursing home were strong risk factors of MDR isolated from UTI. Present work aimed to review the available literature published in 2016–2019 to investigate the prevalence of UPEC resistant to antibiotics recommended for the treatment of UTIs. The resistance to antibiotics of UPEC isolated in different regions of the world (European countries, North America, Asia, and some countries of Africa) was compared. The increase of resistance to fluoroquinolones, which was significantly higher in developing countries than in developed countries, has been revealed. Also, the resistance mechanisms identified in these pathogens were discussed.

***Escherichia coli* as a main etiological agent of UTIs**

The bacteria belonging to the *Enterobacteriaceae* such as *Klebsiella pneumoniae* (about 7%), *Proteus mirabilis* (about 5%), *Citrobacter*, *Enterobacter*, and other bacteria such as *Pseudomonas aeruginosa*, *Acinetobacter baumannii*, *Staphylococcus aureus*, *Staphylococcus saprophiticus*, *Enterococcus faecalis*, *Streptococcus bovis*, and the fungus *Candida albicans* can cause UTIs (Hof

2017; Mann et al. 2017). However, among the bacterial species involved in UTIs, uropathogenic *Escherichia coli* strains (UPEC) are the most common. UPEC account for about 80% of uncomplicated UTIs, 95% of community-acquired infections, and 50% of hospital-acquired infections (Tabasi et al. 2016). UPEC also remains the most frequent pathogen in complicated UTIs (Bartoletti et al. 2016).

UPEC is a heterogeneous group of extraintestinal pathogenic *E. coli* (ExPEC) that seem to originate from the gut. Many studies suggest that farm animals may be reservoirs of *E. coli* strains carrying virulence genes responsible for UTI in humans. Comparison of the antimicrobial resistance profiles and genetic virulence determinants in the *E. coli* strains isolated from UTI patients, farm animals or meat (particularly chicken) showed high similarity (Jakobsen et al. 2010; Mellata et al. 2018). Food-borne urinary tract infections (FUTI) include UTIs acquired from bacteria-contaminated food (Nordstrom et al. 2013). ExPEC can survive in the alimentary tract but do not cause diseases of the digestive system. However, ExPEC strains present in other sites such as central nervous system, blood or the urinary tract may cause serious illness. Four main UPEC phylogroups (A, B1, B2, and D) were identified based on the genomic Pathogenicity Islands (PAI) occurrence and strains belonging to B2 and D groups are isolated most frequently from UTI (Kot et al. 2016; Asadi Karam et al. 2019). The intestinal *E. coli* enters the urinary tract system and colonizes the periurethral and vaginal areas and the urethra. After that, bacteria reach the bladder and attach to the surface epithelium using fimbrial and non-fimbrial adhesins (Mann et al. 2017). Adhering bacteria may be internalized into the uroepithelial facet cells, and then they can enter the cytoplasm, replicate and form intracellular bacterial communities (IBCs) being a source of quiescent intracellular reservoirs (QIRs) (Asadi Karam et al. 2019). The host immune system may remove some of the IBCs by exfoliation of bladder surface facet cells and excreting them with the urine but the remaining bacteria can grow as a biofilm resistant to immune mechanisms and antibacterial agents (McLellan and Hunstad 2016). Some of these bacteria escape from the biofilm, convert to motile form and disseminate into the bladder lumen or even ascend into the kidneys, causing pyelonephritis (Flores-Mireles et al. 2015). UPEC may also spread from the urinary tract to the bloodstream causing bacteremia. For 15% to 23% of episodes of UTI positive blood cultures could be obtained (Velasco et al. 2003; Bahagon et al. 2007; van Nieuwkoop et al. 2010). The results presented by Abernethy et al. (2017) suggest that treatment failure in UTIs, as well as an inappropriate use and management of urinary catheters in the hospital and community, are important risk factors for the development of *E. coli* bacteremia.

Treatment of UTIs

Based on the general European susceptibility patterns and according to the European Association of Urology guidelines, the following antimicrobial agents are recommended for treatment of uncomplicated cystitis in premenopausal women and uncomplicated pyelonephritis in all European countries: nitrofurantoin, fosfomicin trometamol and trimethoprim-sulfamethoxazole (TMP-SMZ) (Bartoletti et al. 2016). Nitrofurantoin and fosfomicin trometamol are recommended as first-line therapy for uncomplicated cystitis (Bonkat et al. 2017; Asadi Karam et al. 2019). TMP-SMZ is not indicated as the empirical treatment due to the high prevalence of bacterial resistance and can be considered only for the patients with a low prevalence of resistant *E. coli* (<20%) (Bartoletti et al. 2016; Bonkat et al. 2017). Fluoroquinolones (ciprofloxacin and levofloxacin) play an important role in the treatment of more severe infections and septicemia, and thus, ciprofloxacin should be considered as an alternative, not as a first-line antibiotic, in the treatment of uncomplicated cystitis (Bartoletti et al. 2016). Ciprofloxacin could be used as second-line empiric therapy in cases of mild and moderate pyelonephritis or complicated UTI treatment, and as third-line empiric treatment for uncomplicated cystitis. Amoxicillin-clavulanic acid is recommended as first line-therapy for mild and moderate pyelonephritis or complicated UTI, as well as alternative empiric therapy for uncomplicated cystitis. For complicated UTI (high fever, sepsis, vomiting) or severe pyelonephritis, amoxicillin with gentamicin or a second-generation cephalosporin with an aminoglycoside are recommended as first-line empiric therapy, and third-generation cephalosporin applied intravenously as alternative empiric therapy (Bonkat et al. 2017; Cheung et al. 2017). The choice of antimicrobials for the treatment of UTI is also based on local resistance profiles of the pathogen.

Antimicrobial resistance of UPEC

UTIs are associated with significant use of antibiotics that cause implications for bacterial ecology and spread of resistance to antibiotics, especially when it stems from the empirical antimicrobial treatment of recurrent UTIs. Antimicrobial resistance in UPEC and the spreading of MDR UPEC in recent decades is a clinical problem, particularly in women with recurrent UTIs. The increasing frequency of MDR UPEC, especially in developing countries, results in excessive use of broad-spectrum antibiotics such as fluoroquinolones, cephalosporins, and aminoglycosides that raise the cost of treatment and hospitalization (Bartoletti et al. 2016;

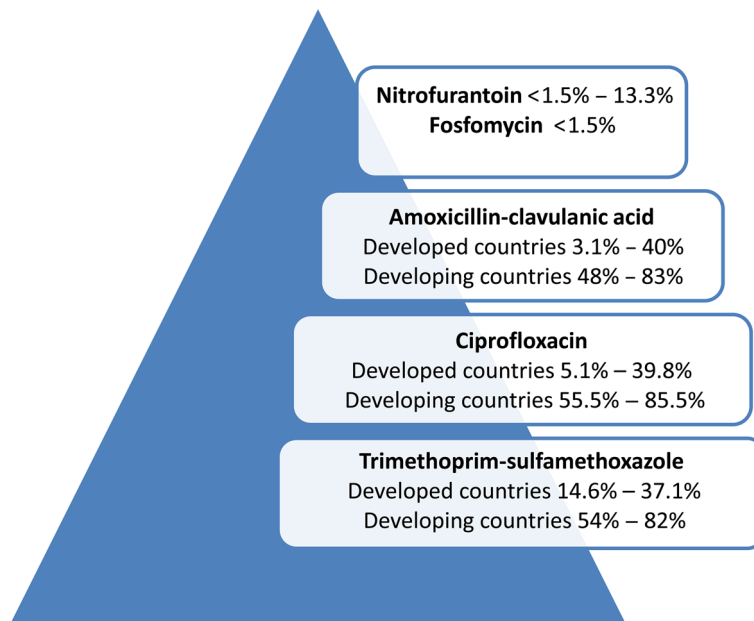


Fig. 2. The resistance of UPEC to antimicrobials using in the treatment of UTIs.

Amoxicillin-clavulanic acid; the developed countries (USA, 3.1–40%; Germany, 5.3%; Poland, 13.9%; England, 30%; France, 37.6%), developing countries (Nepal, 48%; Pakistan, 71%; Jordan, 83%). **Ciprofloxacin**; developed countries (USA, 5.1–12.1%; Belgium, 12.9%; Germany, 10.5–17.3%; Switzerland, 17.4%; England, 20.4%; France, 24.8%; Spain, 39.8%), developing countries (Jordan, 55.5%; Mongolia, 58.1%; Pakistan, 60.8%; Nepal, 64.6%; Ethiopia, 85.5%). **Trimethoprim-sulfamethoxazole**; developed countries (Belgium, 14.6%; USA, 17.4%; Germany, 18.45%; Poland, 21.4%; Switzerland, 24.5%; Spain, 30.9%; France, 37.1%), developing countries (Iran, 54%; Mexico, 66%; Ethiopia, 68.5%; Mongolia, 70.9%; Jordan, 73.1%; Pakistan, 82%).

Sanchez et al. 2016). Antimicrobial resistance between UPEC is increasing in many countries and shows the time- and area-related variability (Fig. 2).

Resistance to nitrofurantoin

According to the European Association of Urology guidelines (Bonkat et al. 2017), nitrofurantoin is recommended for the treatment of uncomplicated cystitis as first-line empiric therapy. At present, the resistance of UPEC to nitrofurantoin is very low, favoring its use as a first-line antibacterial agent. A retrospective analysis performed by Sanchez et al. (2016) showed that in the United States nitrofurantoin retains a high level of antibiotic activity against urinary *E. coli*. A comparison of the reports from the period of 2003 to 2012 revealed that resistance of *E. coli* isolates from adults to nitrofurantoin only slightly increased (from 0.7% to 0.9%). The rates of UPEC resistance in Germany, Belgium, and Spain in 2013–2014 were below 1.5% (Kresken et al. 2016). A slightly higher percentage of UPEC resistant to nitrofurantoin was observed among isolates from elderly hospitalized patients in Argentina (2.3%) (Delpech et al. 2018). While in Brazil the rate of UPEC isolates resistant to nitrofurantoin was 6.6% (Cunha et al. 2016). In European countries (Romania, Poland, France) the percentage of nitrofurantoin

resistant UPEC isolated from outpatients and hospitalized patients ranged from 3% to 3.8% (Ciontea et al. 2018; Kot et al. 2016; Lavigne et al. 2016). The study concerning *E. coli* resistance rates at urology clinics in the Netherlands revealed that nitrofurantoin was active against 95% of strains (van der Donk et al. 2012). Among UPEC from inpatients and outpatients in Bosnia and Herzegovina, 8.23% isolates were resistant to nitrofurantoin (Abduzaimovic et al. 2016). Lack of susceptibility to nitrofurantoin among *E. coli* isolates from the urine of patients hospitalized in different hospitals in England was low (4.6–6.9%) (Abernethy et al. 2017). *E. coli* strains isolated from the hospitalized patients with UTIs in Mongolia (Munkhdelger et al. 2017), Pakistan (Ali et al. 2016), and Iran (Raeispour and Ranjbar 2018) showed that 5.4%, 6%, and 10% of strains were resistant to this antimicrobial agent, respectively. The study conducted by Prasada et al. (2019) in India showed that the resistance of UPEC isolated from hospitalized patients to nitrofurantoin was 13.3% and did not significantly change over 5 years (2013–2017). A similar rate of UPEC resistance to nitrofurantoin (12.7%) in Mexico was reported by Ramírez-Castillo et al. (2018). These results show that nitrofurantoin remains the drug of choice for the treatment of uncomplicated cystitis, although it should not be used for the treatment of pyelonephritis since its concentration in the renal parenchyma is too low. Additional

characteristics, as high efficiency, cost-effectiveness, and weak adverse environmental impact suggest that nitrofurantoin should be the first-choice treatment in uncomplicated UTI in women.

Resistance to fosfomycin

Fosfomycin is an “old” antibiotic used for the treatment of drug-resistant bacterial infections. Fosfomycin shows activity against several *Enterobacteriaceae* species, including those expressing extended-spectrum β -lactamases (ESBL) and metallo- β -lactamases (MBL). Fosfomycin is currently approved for use in some European countries as a single 3 g dose for treating uncomplicated UTIs caused by *E. coli* in women (Dijkmans et al. 2017). The results of Hirsch et al. (2015) showed that all *E. coli* strains investigated were susceptible to fosfomycin. The comparative study on UPEC susceptibility to fosfomycin conducted in Germany, Belgium, and Spain, showed that only <1.5% of isolates were resistant to this antibiotic (Kresken et al. 2016). In UTI caused by non-resistant uropathogens, clinical cure rates ranged from 87% to 93%, while microbiological cure rates ranged from 80% to 83%. The treatments of UTIs caused by MDR uropathogens with fosfomycin demonstrated an overall microbiological cure rate of 59% (Neuner et al. 2012). Antibacterial efficacy of fosfomycin is weaker compared to other first-line agents used in the treatment of uncomplicated UTIs, and thus this drug should be avoided if there is a suspicion of early pyelonephritis.

Resistance to trimethoprim-sulfamethoxazole

TMP-SMZ is another important and widely used first-line antimicrobial in the treatment of uncomplicated cystitis. The comparative study performed in the USA by Yamaji et al. (2018) showed that frequencies of TMP-SMZ resistance in UPEC isolates obtained from outpatients with UTI symptoms in 1999–2000 and in 2016–2017 did not significantly change (resistance slightly increased from 16.9% to 17.1%). However, increasing resistance to this drug has recently been observed in many countries. A majority of studies show resistance at or above the accepted level of 20%, and thus TMP-SMZ should not be used in empiric treatment (Bartoletti et al. 2016). High resistance rate to TMP-SMZ (24.5%) among *E. coli* isolated from urine in 2012–2015 was reported in Switzerland by Erb et al. (2018). The considerable geographic and age-related differences in resistance of UPEC to TMP-SMZ were observed, and the highest resistance was noted in certain regions of Europe in young women. Studies of

TMP-SMZ activity against UPEC revealed resistance in European countries (Belgium, Germany, Poland, Switzerland, France, Spain, Bosnia and Herzegovina, and Romania) between 14.6% and 60% (Abduzaimovic et al. 2016; Kot et al. 2016; Kresken et al. 2016; Lavigne et al. 2016; Ciontea et al. 2018; Erb et al. 2018; Hitzentbichler et al. 2018). The TMP-SXT resistance rate in India in 2013 was 52%, and in 2017 it increased up to 59.6% (Prasada et al. 2019). A similar rate of resistance of UPEC isolates against TMP-SXT (50.6%) was observed in Brazil (Cunha et al. 2016). The activity of TMP-SMZ against UPEC in other regions of the world was significantly lower as the frequencies of TMP-SMZ resistant UPEC isolates ranged from 72.7% in Mexico to 82% in Pakistan (Ali et al. 2016; Ramírez-Castillo et al. 2018). High resistance to TMP-SMZ was also observed in Iran (54%), Ethiopia (68.5%), Mongolia (70.9%), and Jordan (73.1%) (Raeispour and Ranjbar 2016; Munkhdelger et al. 2017; Regasa Dadi et al. 2018; Shakhathreh et al. 2018). These results indicate that in many countries TMP-SMZ should not be used in empiric UTI therapy due to the high frequency of UPEC resistant to this antimicrobial.

Resistance to fluoroquinolones

Fluoroquinolones (FQs) are recommended for empirical oral antimicrobial therapy in uncomplicated pyelonephritis (Bonkat et al. 2017) and they are frequently used for the treatment of UTIs (Drekonja et al. 2013; Yamasaki et al. 2015; Walker et al. 2016). The increasing emergence of *E. coli* resistant to FQs was reported worldwide, and it has emerged probably due to the excessive use of these antibiotics. The resistance of UPEC to FQs was reported from different countries and the level of resistance is significant. The results of Prasada et al. (2019) revealed a high rate of fluoroquinolone resistance in UPEC in India (>60%). The results of the meta-analysis on resistance to ciprofloxacin in the community- and hospital-acquired UTIs showed that UPEC resistance to ciprofloxacin was higher in the hospital when compared to the community setting (Fasugba et al. 2015). In Europe, resistance to FQs was reported in 22% of strains, and the prevalence of fluoroquinolone-resistant UPEC strains was about 31% among hospitalized patients in the United States (Asadi Karam et al. 2019). In many parts of the world, >20% of *E. coli* isolated from patients with community-acquired uncomplicated UTI and >50% of *E. coli* isolated from complicated UTI showed resistance to FQs (Talan et al. 2016). In Poland, resistance to FQs was observed in about 30% of UPEC (Michno et al. 2018). MDR UPEC demonstrated much higher rates of resistance to FQs, ranging from 49% to 72% (Walker et al. 2016). Among

FQs, ciprofloxacin is the most commonly prescribed for UTIs because it is available in oral and intravenous preparations. In the group of UPEC strains isolated in 2013–2014 from outpatients in Brasilia, 18.8% were resistant to ciprofloxacin, and resistance to ciprofloxacin was associated with multidrug resistance (Moreira da Silva et al. 2017). In the United States in the period from 2013 to 2014, 12.1% of *E. coli* isolates from patients with acute uncomplicated and complicated pyelonephritis were resistant to this antibiotic (Talan et al. 2016). A similar percentage of UPEC resistant to ciprofloxacin was noted in other research conducted in the United States in 2016–2017 for isolates from the urine samples from outpatients with symptoms of UTI (Yamaji et al. 2018). While a higher rate of resistance to ciprofloxacin was detected in UPEC from elderly hospitalized patients in Argentina (42.8%) (Delpech et al. 2018), and in UPEC isolates from the community and hospital-acquired infections in Mexico (47.3%) (Ramírez-Castillo et al. 2018). Blaettler et al. (2009) found that in Switzerland, over 10 years (1997–2007), resistance to ciprofloxacin increased significantly from 1.8% to 15.9%, which coincided with an increase in ciprofloxacin use in this country. In 2000 in Switzerland FQs were prescribed for treatment of uncomplicated UTIs in 64% of cases. In the recent study conducted in Switzerland in 2012–2015, an increase of resistance to ciprofloxacin from 15.9% (Blaettler et al. 2009) to 17.4% (Erb et al. 2018) was reported. Although total antibiotic usage in Switzerland is lower than in other European countries, the fluoroquinolone consumption in this country for treatments of urological outpatients comprises 20.1% of all antibiotics (Helsana 2014) and it is rather high when compared to an average of 7.3% in other European countries (Filippini et al. 2004), which may explain the increasing fluoroquinolone resistance in UPEC isolates. In 2013–2014 in Belgium, Germany, and Spain the percentage of ciprofloxacin-resistant UPEC strains was 12.9, 17.3, and 39.8%, respectively (Kresken et al. 2016). The research conducted in England showed that among *E. coli* isolates from the urine samples from patients, who later developed bacteremia, 20.4% and 15.5% of isolates were resistant to ciprofloxacin in the year and four weeks before the bacteremia onsets. (Abernethy et al. 2017). Resistance to ciprofloxacin was significantly higher in developing countries (Ethiopia – 85.5%, Nepal – 64.6%, Pakistan – 60.8%, Mongolia – 58.1%, Jordan – 55.5%) (Ali et al. 2016, Khatri et al. 2017; Munkhdelger et al. 2017; Regasa Dadi et al. 2018; Shakhathreh et al. 2018) than in developed countries (USA – 5.1%, Germany – 10.5%, Switzerland – 17.4%, France – 24.8%) (Lavigne et al. 2016; Erb et al. 2018; Hitzenbichler et al. 2018; Yamaji et al. 2018). The study conducted in Switzerland showed also that patient age over 65 years was associated with higher

E. coli resistance to ciprofloxacin (Erb et al. 2018). According to many authors, the widespread use of fluoroquinolones in the outpatients is the cause of the continuous increase in resistance to this drug. Therefore, ciprofloxacin should be avoided in first-line treatment of UTIs and be used only in more severe infections or as an alternative when the recommended agents cannot be used. Restrictions of ciprofloxacin usage should be enhanced especially in developing countries, where no regulations concerning the use of this antibiotic currently apply (Asadi Karam et al. 2019).

Resistance to amoxicillin-clavulanic acid

Amoxicillin-clavulanic acid was recommended as first-line therapy for mild and moderate pyelonephritis or complicated UTI or as an alternative empiric therapy for uncomplicated cystitis (Cheung et al. 2017). Resistance rates for amoxicillin-clavulanic acid vary regionally. In the United States in 2012, the prevalence of UPEC isolates resistant to this antibiotic in the age groups: below 17, 18–64, and over 65 years were 3.1%, 3.9%, and 5.5%, respectively (Sanchez et al. 2016). Morrill et al. (2017) studied *E. coli* urinary isolates collected in the period from 2009 to 2013 from inpatients and outpatients in the Veterans Affairs Care System in the United States and showed that rates of resistance to amoxicillin or ampicillin/beta-lactamase inhibitors were approximately 40%. Ramírez-Castillo et al. (2018) have recently found that 23.6% of UPEC isolates were resistant to amoxicillin-clavulanic acid in Mexico. The resistance rate to amoxicillin-clavulanic acid among *E. coli* isolates from the urine samples taken from patients of tertiary care hospital in Germany in 2015–2017 was 5.3% (Hitzenbichler et al. 2018). Between 2015 and 2017 in Romania, (Ciontea et al. 2018), and in Bosnia and Herzegovina in 2016, 29.0% and 19.6% of UPEC isolates collected from outpatients were resistant to amoxicillin-clavulanic acid (Abduzaimovic et al. 2016). In Poland in women with uncomplicated UTIs 3.3% of UPEC were resistant to amoxicillin-clavulanic acid in 2003–2006 (Naber et al. 2008). In 2007–2008 the percentage of amoxicillin-clavulanic acid-resistant UPEC isolated from hospital-acquired UTIs in Poland was 13.9% (Kot et al. 2016). In the group of UPEC isolates obtained in 2009–2010 in the urology units in France, 37.6% were resistant to this antimicrobial (Lavigne et al. 2016) Among UPEC isolated in Argentina from patients over 70 years old with UTIs, without urinary catheters and antimicrobial therapy, 28.6% were resistant to this antibacterial agent (Delpech et al. 2018). In England, 30% of *E. coli* isolates from the urine samples from hospitalized patients showed resistance to amoxicillin-clavulanic acid (Abernethy et al. 2017).

High level of resistance to this antimicrobial was reported for UPEC isolates from children hospitalized in 2015–2016 in Nepal (48%) (Parajuli et al. 2017), and in Pakistan in the group of UPEC isolated from outpatients (71%) (Ali et al. 2016). While very high resistance to amoxicillin-clavulanic acid (83%) was showed for UPEC isolates from hospitalized patients in Jordan (Shakhathreh et al. 2018). These results demonstrate that the levels of UPEC resistance to amoxicillin-clavulanic acid varied between geographical regions or patient populations. For this reason, the empiric regimens for uncomplicated and complicated UTIs should be guided by the local susceptibility of *E. coli*. However, definitive regimens should be developed according to the susceptibility results of UPEC, when available.

Resistance to other antibiotics

Some UPEC isolates can be resistant to ampicillin and first-generation oral cephalosporins (Moya-Dionisio et al. 2016). The resistance to cefuroxime (second-generation cephalosporin) in Belgium, Germany, and Spain was 5.5%, 12.8%, and 16.6%, respectively (Kresken et al. 2016). *E. coli* isolates from the urine samples from hospitalized patients in England were found to be resistant (13.8–21.3%) to third-generation cephalosporins (cefotaxime/ceftazidime) (Abernethy et al. 2017). The percentage of UPEC susceptible to third generation cephalosporins in Romania was 87% (Ciontea et al. 2018). While, the other research conducted in this country demonstrated that the resistance rate was 47.52% for ampicillin, and 41.16% for tetracycline (Cristea et al. 2019). The resistance of *E. coli* isolates from the urinary tract isolated in the urology department in France to amoxicillin, ticarcillin, nalidixic acid was high and reached 61.4%, 59%, and 31.9%, respectively (Lavigne et al. 2016). In Iran, the resistance to ampicillin, ceftazidime and nalidixic acid was higher than 50%, while amikacin and gentamicin showed high activity against UPEC (89.1% and 82.4% of sensitive isolates, respectively) (Faghri et al. 2016). The resistance against gentamicin and amikacin of UPEC isolated from outpatients in Pakistan was 29%, and 4%, respectively (Ali et al. 2016). In Mexico, the resistance rates to antibiotics belonging to aminoglycosides were 28.2%, 19.1%, 10%, and 5.5% for gentamycin, tobramycin, amikacin, and netilmicin, respectively (Ramírez-Castillo et al. 2018). The carbapenems, piperacillin-tazobactam, and amikacin were highly active (>95% susceptibility) against *E. coli* isolates from UTIs collected from 2010 to 2014 in Canada and the United States (Lob et al. 2016). Carbapenems (ertapenem, imipenem, meropenem, doripenem) are recommended for the treatment of acute uncomplicated pyelonephritis, complicated UTI, and

urosepsis (Bonkat et al. 2017). Shahbazi et al. (2018) showed that all UPEC isolates from patients with UTI in Teheran were negative for carbapenemases. Another study on UPEC isolates from Iran confirmed a lack of resistance to meropenem in isolates from outpatients and inpatients (Faghri et al. 2016). Ali et al. (2016) described a high activity of meropenem in Pakistan since only 1.3% of UPEC were resistant to this antibiotic. However, a recent study from Saudi Arabia about the presence of carbapenem-resistant uropathogenic *E. coli* clones in community-acquired UTIs reported the occurrence of carbapenemases NDM-1 and 5 (the New Delhi metallo-lactamase), and carbapenemases of the OXA-181 type in these strains (Abd El Ghany et al. 2018). The emergence of carbapenem-resistant uropathogenic *E. coli* isolates makes treatment of these infections increasingly challenging.

Mechanisms of UPEC resistance to antibiotics

Resistance to β -lactams is related to the production of different types of β -lactamase enzymes. Among the genes often located on plasmids are those coding multiple types of β -lactamases (*bla* genes) (Adamus-Białek et al. 2018). β -lactamases hydrolyze the amide bond of the four-membered β -lactam ring of β -lactam antibiotics (penicillin, cephalosporin, monobactams, and carbapenems) (Noyal et al. 2009). ESBL are enzymes that confer resistance to β -lactam antibiotics (all penicillins, cephalosporins, and monobactams), except for carbapenems, cephamycins, and β -lactamase inhibitors (Baudry et al. 2009). ESBL are the predominant source of *Enterocacteriaceae* resistance to 3rd- and 4th-generation cephalosporins and they developed as a result of mutations in the genes coding for ancestral enzymes blaTEM-1, blaTEM-2, and blaSHV-1 (Dashti et al. 2006). Three classes of β -lactamases including TEM and SHV, and since 2000 a new group of ESBL, CTX-M (cefotaximases), were observed among ESBL produced by UPEC (Ojdana et al. 2014; Shahbazi et al. 2018). Genetic analyses of UPEC from hospitalized patients in different hospital wards in Lodz (Poland) revealed that TEM-1 was present in almost all investigated strains (Adamus-Białek et al. 2018). Among UPEC isolated from 2013 to 2015 from patients hospitalized in a Department of Internal Medicine and Nephrology in southern Poland, 8% of the strains produced ESBL (Michno et al. 2018). In France, 7.6% of UPEC produce ESBL with the predominance of CTX-M (Lavigne et al. 2016). The CTX-M enzymes are active against cefotaxime and ceftriaxone and less active against ceftazidime (Bhat et al. 2012). UPEC producing ESBL are particularly often detected in developing countries (Iran – 37.1%, Nepal – 38.9%, Pakistan

– 40%, and Jordan – about 50%) (Ali et al. 2016; Parajuli et al. 2017; Shakhathreh et al. 2018). Prasada et al. (2019) revealed that in India the percentage of ESBL-producing UPEC increased from 45.2 to 59.6% over 5 years (2013–2017). The frequency of ESBL-producing *E. coli* isolates is different in various parts of the world and sometimes even in various hospitals within the country. In addition to resistance to β -lactam antibiotics, ESBL-producing *E. coli* isolates are also resistant to other antimicrobial agents, such as aminoglycosides, tetracycline, and trimethoprim/sulfamethoxazole (Rezai et al. 2015). Shahbazi et al. (2018) has found that higher number of ESBL-producing UPEC isolates were resistant to aminoglycosides and quinolones when compared to the UPEC strains that not produce ESBL. Carbapenems (imipenem and meropenem) represent the best option for the treatment of UTIs caused by ESBL-producing strains (Idil et al. 2016). Cephalosporins, penicillins, and monobactams should be used with β -lactamase inhibitors (Bartoletti et al. 2016).

Quinolones and fluoroquinolones are extensively used worldwide in the treatment of UTIs and their common use led to increased resistance in UPEC. The mechanism of fluoroquinolone action is based on binding to and impeding the activity of topoisomerase II (DNA gyrase) and topoisomerase IV (parC and parE) (Komp Lindgren et al. 2003). DNA gyrase is encoded by the *gyrA* and *gyrB* genes (Pourahmad Jaktaji and Mohiti 2010). The resistance of *E. coli* to quinolones frequently results from a mutation in the *gyrA* and *gyrB* genes that catalyze DNA supercoiling. The point mutations in *gyrA* protein N-terminal sequence (amino acids 67 (Ala-67) to 106 (Gln-106)) strongly correlate with phenotypic resistance to quinolones and fluoroquinolones, and this sequence is named a quinolone resistance-determining region (QRDR) (Friedman et al. 2001). Investigation of mutations in codons 83 and 106 of the *gyrA* gene in UPEC isolates in Iran presented the significant relationship between mutations in the *gyrA* gene and quinolone and fluoroquinolone resistance pattern of UPEC isolates (Shenagari et al. 2018). Other genes responsible for the resistance to quinolones and fluoroquinolones are the *qnr* genes (*qnrA*, *qnrB*, and *qnrC*), being the most important PMQR (plasmid-mediated quinolone resistance) genes that induce antibiotic resistance by inhibition of binding of quinolones to DNA gyrase and topoisomerases (Shahbazi et al. 2018).

Other mechanisms of *E. coli* resistance to quinolones and fluoroquinolones are related to the presence of efflux pumps and decreased uptake of the antibiotics due to changes in the outer membrane porin proteins (Asadi Karam et al. 2019). Abdelhamid and Abozahra (2017) showed that the increased expression of the efflux pump-coding genes *acrA* and *mdfA* was related to the growing resistance to levofloxacin, which confirms

that efflux pump systems contribute to fluoroquinolone resistance in urinary *E. coli* isolates.

The mechanism of fosfomycin action is unique because it irreversibly inhibits an early stage of bacterial cell wall biosynthesis, leading to bacterial cell lysis and death (Dijkmans et al. 2017). The active transport proteins used to transport both glucose-6-P and glycerol-3-P are also used by fosfomycin to reach bacterial cytoplasm (Popovic et al. 2010). Fosfomycin in the cytoplasm is an analog of phosphoenolpyruvate (PEP) and binds UDP-GlcNAc enolpyruvyl transferase, inactivating this enzyme, which is essential for peptidoglycan biosynthesis. The resistance to fosfomycin is due to three mechanisms that have already been described. One of them is based on decreased uptake of fosfomycin by the bacterial cells due to mutations in the genes that encode the glycerol-3-phosphate transporter or the glucose-6-phosphate transporter (Kadner and Winkler 1973; Tsuruoka and Yamada 1975). The second mechanism is based on point mutations in the binding site of UDP-GlcNAc enolpyruvyl transferase (Kim et al. 1996). The third mechanism of resistance is related to the inactivation of fosfomycin by enzymatic cleavage of the oxirane ring of the antibiotic or by phosphorylation of the phosphonate group. The opening of the oxirane ring may be catalyzed by glutathione transferase (FosA), L-cysteine thiol transferase (FosB) or fosfomycin-specific epoxide hydrolase (FosX) (Rigsby et al. 2005).

Nitrofurantoin is recommended for the treatment of uncomplicated cystitis and, currently, the resistance of UPEC to nitrofurantoin is very low. Resistance to nitrofurantoin did not evolve as fast as to other drugs because of this antimicrobial acts at multiple targets in the bacterial cell (Veeraraghavan and Shakti 2015). Sandegren et al. (2008) identified mutations conferring resistance to nitrofurantoin and found that the mutation frequency is approximately 10^{-7} /cell in *E. coli*. The mutations in the *nsfA* and *nfsB* genes that encode oxygen-insensitive nitroreductases were responsible for nitrofurantoin resistance. It was also found that the growth of bacterial cells in the presence of nitrofurantoin at therapeutic concentrations was greatly reduced in nitrofurantoin-resistant mutants. It may indicate that resistant mutants in the presence of nitrofurantoin were probably unable to establish an infection (Sandegren et al. 2008).

The resistance of UPEC lineages

The multilocus sequence-typing (MLST) technique is widely used to study ExPEC lineages. Sequence types (STs) 10, 69, 73, 95, 127, and 131 defined by MLST were isolated as pandemic clones of ExPEC from human infections, including UTIs and bloodstream infections (Tartof et al. 2005; Adams-Sapper et al. 2013;

Riley 2014). Globally, these genotypes account for more than 50% of ExPEC infections (Gibreel et al. 2012; Adams-Sapper et al. 2013; Kallonen et al. 2017). The isolates belonging to the lineage ST131 are multidrug-resistant (Banerjee and Johnson 2014; Petty et al. 2014). Adams-Sapper et al. (2013) who investigated *E. coli* isolates from bloodstream infections in the United States, found that ST131 was the most common genotype, including 92% of multidrug-resistant isolates. UPEC isolates from patients in the Northwest region of England that belonged to lineage ST131 exhibited higher levels of antibiotic resistance when compared to ST127 isolates that were the most widely susceptible to antibiotics (Gibreel et al. 2012). The UPEC of ST131 line from a tertiary care hospital in Saudi Arabia was also significantly associated with high levels of antibiotic resistance and 60% of ST131 carried CTX-M-14 and CTX-M-15 (Alghoribi et al. 2015). ST73 was the lineage most frequently identified by Kallonen et al. (2017) among isolates associated with bacteremia in England, and isolates belonging to this lineage were susceptible to most antibiotics. The authors suggested that drug resistance was not a primary determinant for the prevalence of *E. coli* lineages responsible for invasive diseases, and the frequency of *E. coli* lineages is associated with the presence of new lineages outside the hospital. Yamaji et al. (2018) compared the clonal distribution of UPEC in the same community during two periods. The UPEC strains belonging to ST 95, 127, 73, 69, 131, and 10 were responsible for 56% of UTI cases in 1999–2000. In the period 2016–2017, the same STs caused 64% of UTI cases. The study of Yamaji et al. (2018) showed that 46.4% of the isolates resistant to ampicillin in 2016–2017 belonged to four genotypes (ST 95, 127, 73, and 131), while in 1999–2000 they comprised only 21.8%. The increase of resistance to ampicillin was observed only in these genotypes. Yamaji et al. (2018) reported that ST69 included the highest percentage of TMP-SMZ-resistant isolates during two study periods. In 2016–2017, 58% of ciprofloxacin-resistant isolates represented the ST131 lineage. ST69, 127, and 131 comprised 70% of isolates with CTX-M. Among *E. coli* extraintestinal isolates from Iran, the highest rates of the multidrug-resistance phenotype were detected in ST131 (85.7%), and ST69 (41.7%) lineages (Hojabri et al. 2019). Similarly to the results by Yamaji et al. (2018), the resistance to TMP-SMZ was detected mainly in the ST69 lineage. The widespread occurrence of new multidrug-resistant *E. coli* clonal group ST1193 has recently been demonstrated in the United States (Tchesnokova et al. 2019). This clonal group of strains was isolated from younger adults. ST1193 isolates were resistant to fluoroquinolones and often co-resistant to TMP-SXT and tetracycline, but currently, remain susceptible to most β -lactam antibiotics.

Conclusion

The antibiotic therapy is important in the UTI treatment but in recent years it is becoming more challenging due to increasing resistance of UTIs to routinely applied antibiotics. High resistance of UPEC to FQs used as third-line empiric treatment for therapy of uncomplicated cystitis in pyelonephritis or second-line empiric treatment in complicated UTI requires a rational policy of prescription of these drugs. The awareness of the resistance rates of *E. coli* in a given area and the established guidelines for appropriate first-line antibiotic treatment should be critical in the empirical treatment of UTIs, especially for the controlled use of fluoroquinolones.

ORCID

Barbara Kot 0000-0002-6191-8275

Acknowledgments

This work was supported by the Siedlce University of Natural Science and Humanities (Scientific Research Project No. 316/12/S).

Conflict of interest

The author does not report any financial or personal connections with other persons or organizations, which might negatively affect the contents of this publication and/or claim authorship rights to this publication.

Literature

- Abd El Ghany M, Sharaf H, Al-agamy MH, Shibl A, Hill-Cawthorne GA, Hong PY. Genomic characterization of NDM-1 and 5, and OXA-181 carbapenemases in uropathogenic *Escherichia coli* isolates from Riyadh, Saudi Arabia. *PLoS One*. 2018 Aug 15; 13(8):e0201613. <https://doi.org/10.1371/journal.pone.0201613>
- Abdelhamid SM, Abozahra RR. Expression of the fluoroquinolones efflux pump genes *acrA* and *mdfA* in urinary *Escherichia coli* isolates. *Pol J Microbiol*. 66(1):25–30.
- Abduzaimovic A, Aljicevic M, Rebic V, Vranic S, Abduzaimovic K, Sestic S. Antibiotic resistance in urinary isolates of *Escherichia coli*. *Mater Sociomed*. 2016;28(6):416–419. <https://doi.org/10.5455/msm.2016.28.416-419>
- Abernethy J, Guy R, Sheridan EA, Hopkins S, Kiernan M, Wilcox MH, Johnson AP, Hope R. *E. coli* bacteraemia sentinel surveillance group. *Epidemiology of Escherichia coli* bacteraemia in England: results of an enhanced sentinel surveillance programme. *J Hosp Infect*. 2017;95(4):365–375. <https://doi.org/10.1016/j.jhin.2016.12.008>
- Adams-Sapper S, Diep BA, Perdreau-Remington F, Riley LW. Clonal composition and community clustering of drug-susceptible and -resistant *Escherichia coli* isolates from bloodstream infections. *Antimicrob Agents Chemother*. 2013 Jan;57(1):490–497. <https://doi.org/10.1128/AAC.01025-12>
- Adamus-Białek W, Baraniak A, Wawszczak M, Głuszek S, Gad B, Wróbel K, Bator P, Majchrzak M, Parniewski P. The genetic background of antibiotic resistance among clinical uropathogenic *Escherichia coli* strains. *Mol Biol Rep*. 2018 Oct;45(5):1055–1065. <https://doi.org/10.1007/s11033-018-4254-0>
- Alghoribi MF, Gibreel TM, Farnham G, Al Johani SM, Balkhy HH, Upton M. Antibiotic-resistant ST38, ST131 and ST405 strains are

- the leading uropathogenic *Escherichia coli* clones in Riyadh, Saudi Arabia. *J Antimicrob Chemother*. 2015 Oct;70(10):2757–2762. <https://doi.org/10.1093/jac/dkv188>
- Ali I, Rifaque Z, Ahmed S, Malik S, Dasti JI. Prevalence of multi-drug resistant uropathogenic *Escherichia coli* in Potohar region of Pakistan. *Asian Pac J Trop Biomed*. 2016 Jan;6(1):60–66. <https://doi.org/10.1016/j.apjtb.2015.09.022>
- Asadi Karam MR, Habibi M, Bouzari S. Urinary tract infection: Pathogenicity, antibiotic resistance and development of effective vaccines against Uropathogenic *Escherichia coli*. *Mol Immunol*. 2019 Apr;108:56–67. <https://doi.org/10.1016/j.molimm.2019.02.007>
- Bahagon Y, Raveh D, Schlesinger Y, Rudensky B, Yinnon AM. Prevalence and predictive features of bacteremic urinary tract infection in emergency department patients. *Eur J Clin Microbiol Infect Dis*. 2007 May 4;26(5):349–352. <https://doi.org/10.1007/s10096-007-0287-3>
- Banerjee R, Johnson JR. A new clone sweeps clean: the enigmatic emergence of *Escherichia coli* sequence type 131. *Antimicrob Agents Chemother*. 2014 Sep;58(9):4997–5004. <https://doi.org/10.1128/AAC.02824-14>
- Bartoletti R, Cai T, Wagenlehner FM, Naber K, Bjerklund Johansen TE. Treatment of urinary tract infections and antibiotic stewardship. *Eur Urol Suppl*. 2016 Jul;15(4):81–87. <https://doi.org/10.1016/j.eursup.2016.04.003>
- Baudry PJ, Nichol K, DeCorby M, Lagacé-Wiens P, Olivier E, Boyd D, Mulvey MR, Hoban DJ, Zhanel GG. Mechanisms of resistance and mobility among multidrug-resistant CTX-M-producing *Escherichia coli* from Canadian intensive care units: the 1st report of QepA in North America. *Diagn Microbiol Infect Dis*. 2009 Mar;63(3):319–326. <https://doi.org/10.1016/j.diagmicrobio.2008.12.001>
- Bhat MA, Sageerabano S, Kowsalya R, Sarkar G. The occurrence of CTX-M3 type extended spectrum beta lactamases among *Escherichia coli* causing urinary tract infections in a tertiary care hospital in puducherry. *J Clin Diagn Res*. 2012;6(7):1203–1206.
- Bischoff S, Walter T, Gerigk M, Ebert M, Vogelmann R. Empiric antibiotic therapy in urinary tract infection in patients with risk factors for antibiotic resistance in a German emergency department. *BMC Infect Dis*. 2018 Dec;18(1):56. <https://doi.org/10.1186/s12879-018-2960-9>
- Blaettler L, Mertz D, Frei R, Elzi L, Widmer AF, Battegay M, Flückiger U. Secular trend and risk factors for antimicrobial resistance in *Escherichia coli* isolates in Switzerland 1997–2007. *Infection*. 2009 Dec;37(6):534–539. <https://doi.org/10.1007/s15010-009-8457-0>
- Bonkat G, Pickard R, Bartoletti R, Bruyère F, Geerlings SE, Wagenlehner F, Wullt B. Guidelines on urological infections [Internet]. Arnhem (The Netherlands): European Association of Urology; 2017 [cited 2019 May 31]. Available from <https://uroweb.org/wp-content/uploads/Urological-Infections-2017-pocket.pdf>
- Brumbaugh AR, Smith SN, Mobley HLT. Immunization with the yersiniabactin receptor, FyuA, protects against pyelonephritis in a murine model of urinary tract infection. *Infect Immun*. 2013 Sep; 81(9):3309–3316. <https://doi.org/10.1128/IAI.00470-13>
- Cek M, Tandoğdu Z, Wagenlehner F, Tenke P, Naber K, Bjerklund-Johansen TE. Healthcare-associated urinary tract infections in hospitalized urological patients – a global perspective: results from the GPIU studies 2003–2010. *World J Urol*. 2014 Dec;32(6): 1587–1594. <https://doi.org/10.1007/s00345-013-1218-9>
- Cheung A, Karmali G, Noble S, Song H. Antimicrobial stewardship initiative in treatment of urinary tract infections at a rehabilitation and complex continuing care hospital. *Can J Hosp Pharm*. 2017 Apr 28;70(2):144–149. <https://doi.org/10.4212/cjhp.v70i2.1648>
- Ciontea AS, Cristea D, Andrei MM, Popa A, Usein CR. *In vitro* antimicrobial resistance of urinary *Escherichia coli* isolates from outpatients collected in a laboratory during two years, 2015–2017. *Roum Arch Microbiol Immunol*. 2018;77(1):28–32.
- Cristea VC, Gheorghe I, Barbu IC, Popa LI, Ispas B, Grigore GA, Bucatariu I, Popa GL, Angelescu M-C, Velican A, et al. Snapshot of phylogenetic groups, virulence, and resistance markers in *Escherichia coli* uropathogenic strains isolated from outpatients with urinary tract infections in Bucharest, Romania. *BioMed Res Int*. 2019; Article ID 5712371, 8 pages. <https://doi.org/10.1155/2019/5712371>
- Cunha MA, Assunção GLM, Medeiros IM, Freitas MR. Antibiotic resistance patterns of urinary tract infections in a northeastern Brazilian capital. *Rev Inst Med Trop São Paulo*. 2016;58(0):2. <https://doi.org/10.1590/S1678-9946201658002>
- Dashti AA, West P, Paton R, Amyes SG. Characterization of extended-spectrum -lactamase (ESBL)-producing Kuwait and UK strains identified by the Vitek system, and subsequent comparison of the Vitek system with other commercial ESBL-testing systems using these strains. *J Med Microbiol*. 2006 Apr 01;55(4):417–421. <https://doi.org/10.1099/jmm.0.46177-0>
- Delpech G, Allende NG, Lissarrague S, Sparo M. Antimicrobial resistance of uropathogenic *Escherichia coli* from elderly patients at a general hospital, Argentina. *Open Infect Dis J*. 2018 Jul 19;10(1): 79–87. <https://doi.org/10.2174/1874279301810010079>
- Dijkmans AC, Zacarias NVO, Burggraaf J, Mouton JW, Wilms E, van Nieuwkoop C, Touw DJ, Stevens J, Kamerling IMC. Fosfomicin: pharmacological, clinical and future perspectives. *Antibiotics (Basel)*. 2017 Oct 31;6(4):24. <https://doi.org/10.3390/antibiotics6040024>
- Drekonja DM, Rector TS, Cutting A, Johnson JR. Urinary tract infection in male veterans: treatment patterns and outcomes. *JAMA Intern Med*. 2013 Jan 14;173(1):62–68. <https://doi.org/10.1001/2013.jamainternmed.829>
- Erb S, Frei R, Tschudin Sutter S, Egli A, Dangel M, Bonkat G, Widmer AF. Basic patient characteristics predict antimicrobial resistance in *E. coli* from urinary tract specimens: a retrospective cohort analysis of 5246 urine samples. *Swiss Med Wkly*. 2018 Nov 15;148:w14660. <https://doi.org/10.4414/sm.w.2018.14660>
- ECDCP. Point prevalence survey of healthcare associated infections and antimicrobial use in European Acute Care Hospitals, 2011–2012. Stockholm (Sweden): European Center for Disease Control and Prevention; 2013.
- Faghri J, Dehbanipour R, Rastaghi S, Sedighi M, Maleki N. High prevalence of multidrug-resistance uropathogenic *Escherichia coli* strains, Isfahan, Iran. *J Nat Sci Biol Med*. 2016;7(1):22–26. <https://doi.org/10.4103/0976-9668.175020>
- Fasugba O, Gardner A, Mitchell BG, Mnatzaganian G. Ciprofloxacin resistance in community- and hospital-acquired *Escherichia coli* urinary tract infections: a systematic review and meta-analysis of observational studies. *BMC Infect Dis*. 2015 Dec;15(1):545. <https://doi.org/10.1186/s12879-015-1282-4>
- Filippini M, Masiero G, Moschetti K. Socioeconomic determinants of regional differences in outpatient antibiotic consumption: evidence from Switzerland. *Health Policy*. 2006 Aug;78(1):77–92. <https://doi.org/10.1016/j.healthpol.2005.09.009>
- Flores-Mireles AL, Walker JN, Caparon M, Hultgren SJ. Urinary tract infections: epidemiology, mechanisms of infection and treatment options. *Nat Rev Microbiol*. 2015 May;13(5):269–284. <https://doi.org/10.1038/nrmicro3432>
- Friedman SM, Lu T, Drlica K. Mutation in the DNA gyrase A Gene of *Escherichia coli* that expands the quinolone resistance-determining region. *Antimicrob Agents Chemother*. 2001 Aug 01; 45(8):2378–2380. <https://doi.org/10.1128/AAC.45.8.2378-2380.2001>
- Gibreel TM, Dodgson AR, Cheesbrough J, Fox AJ, Bolton FJ, Upton M. Population structure, virulence potential and antibiotic

- susceptibility of uropathogenic *Escherichia coli* from Northwest England. *J Antimicrob Chemother.* 2012 Feb 01;67(2):346–356. <https://doi.org/10.1093/jac/dkr451>
- Habibi A, Khameneie MK.** Antibiotic resistance properties of uropathogenic *Escherichia coli* isolated from pregnant women with history of recurrent urinary tract infections. *Trop J Pharm Res.* 2016 Sep 05;15(8):1745–1750. <https://doi.org/10.4314/tjpr.v15i8.21>
- Helsana.** Helsana-arzneimittelreport. Zürich (Switzerland): Helsana-Gruppe; 2014.
- Hirsch EB, Raux BR, Zucchi PC, Kim Y, McCoy C, Kirby JE, Wright SB, Eliopoulos GM.** Activity of fosfomycin and comparison of several susceptibility testing methods against contemporary urine isolates. *Int J Antimicrob Agents.* 2015 Dec;46(6):642–647. <https://doi.org/10.1016/j.ijantimicag.2015.08.012>
- Hitzenbichler F, Simon M, Holzmann T, Iberer M, Zimmermann M, Salzberger B, Hanses F.** Antibiotic resistance in *E. coli* isolates from patients with urinary tract infections presenting to the emergency department. *Infection.* 2018 Jun;46(3):325–331. <https://doi.org/10.1007/s15010-018-1117-5>
- Hof H.** [Candiduria! What now? Therapy of urinary tract infections with Candida]. *Urologe.* 2017 Feb;56(2):172–179. <https://doi.org/10.1007/s00120-016-0219-x>
- Hojabri Z, Mirmohammadhani M, Darabi N, Arab M, Pajand O.** Characterization of antibiotic-susceptibility patterns and virulence genes of five major sequence types of *Escherichia coli* isolates cultured from extraintestinal specimens: a 1-year surveillance study from Iran. *Infect Drug Resist.* 2019 Apr;12:893–903. <https://doi.org/10.2147/IDR.S199759>
- Idil N, Candan ED, Rad AY, Aksoz N.** High trimethoprim-sulfamethoxazole resistance in ciprofloxacin-resistant *Escherichia coli* strains isolated from urinary tract infection. *Minerva Biotechnol.* 2016;28(3):159–163.
- Jakobsen L, Spangholm DJ, Pedersen K, Jensen LB, Emborg HD, Agerød Y, Aarestrup FM, Hammerum AM, Frimodt-Møller N.** Broiler chickens, broiler chicken meat, pigs and pork as sources of ExPEC related virulence genes and resistance in *Escherichia coli* isolates from community-dwelling humans and UTI patients. *Int J Food Microbiol.* 2010 Aug 15;142(1-2):264–272. <https://doi.org/10.1016/j.ijfoodmicro.2010.06.025>
- Kadner RJ, Winkler HH.** Isolation and characterization of mutations affecting the transport of hexose phosphates in *Escherichia coli*. *J Bacteriol.* 1973 Feb;113(2):895–900.
- Kallonen T, Brodrick HJ, Harris SR, Corander J, Brown NM, Martin V, Peacock SJ, Parkhill J.** Systematic longitudinal survey of invasive *Escherichia coli* in England demonstrates a stable population structure only transiently disturbed by the emergence of ST131. *Genome Res.* 2017 Aug;27(8):1437–1449. <https://doi.org/10.1101/gr.216606.116>
- Khatri S, Pant ND, Neupane S, Bhandari S, Banjara MR.** Biofilm production in relation to extended spectrum beta-lactamase production and antibiotic resistance among uropathogenic *Escherichia coli*. *Janaki Medical College J Med Sci.* 2017 Aug 09;5(1):61–63. <https://doi.org/10.3126/jmcjms.v5i1.17989>
- Kim DH, Lees WJ, Kempell KE, Lane WS, Duncan K, Walsh CT.** Characterization of a Cys115 to Asp substitution in the *Escherichia coli* cell wall biosynthetic enzyme UDP-GlcNAc enolpyruvyl transferase (MurA) that confers resistance to inactivation by the antibiotic fosfomycin. *Biochemistry.* 1996 Jan;35(15):4923–4928. <https://doi.org/10.1021/bi952937w>
- Komp Lindgren P, Karlsson A, Hughes D.** Mutation rate and evolution of fluoroquinolone resistance in *Escherichia coli* isolates from patients with urinary tract infections. *Antimicrob Agents Chemother.* 2003 Oct 01;47(10):3222–3232. <https://doi.org/10.1128/AAC.47.10.3222-3232.2003>
- Kot B, Wicha J, Gruzewska A, Piechota M, Wolska K, Obregńska M.** Virulence factors, biofilm-forming ability, and antimicrobial resistance of urinary *Escherichia coli* strains isolated from hospitalized patients. *Turk J Med Sci.* 2016;46(6):1908–1914. <https://doi.org/10.3906/sag-1508-105>
- Kresken M, Körber-Irrgang B, Biedenbach DJ, Batista N, Besard V, Cantón R, García-Castillo M, Kalka-Moll W, Pascual A, Schwarz R, et al.** Comparative *in vitro* activity of oral antimicrobial agents against *Enterobacteriaceae* from patients with community-acquired urinary tract infections in three European countries. *Clin Microbiol Infect.* 2016 Jan;22(1):63.e1–63.e5. <https://doi.org/10.1016/j.cmi.2015.08.019>
- Lavigne JP, Thibault M, Costa P, Combescure C, Sotto A, Cariou G, Ronco E, Lanotte P, Bruyère F, Coloby P, et al.** Resistance and virulence potential of uropathogenic *Escherichia coli* strains isolated from patients hospitalized in urology departments: a French prospective multicentre study. *J Med Microbiol.* 2016 Jun 01;65(6):530–537. <https://doi.org/10.1099/jmm.0.000247>
- Lob SH, Nicolle LE, Hoban DJ, Kazmierczak KM, Badal RE, Sahn DF.** Susceptibility patterns and ESBL rates of *Escherichia coli* from urinary tract infections in Canada and the United States, SMART 2010–2014. *Diagn Microbiol Infect Dis.* 2016 Aug;85(4):459–465. <https://doi.org/10.1016/j.diagmicrobio.2016.04.022>
- Mann R, Mediati DG, Duggin IG, Harry EJ, Bottomley AL.** Metabolic adaptations of uropathogenic *E. coli* in the urinary tract. *Front Cell Infect Microbiol.* 2017 Jun 08;7:241. <https://doi.org/10.3389/fcimb.2017.00241>
- McLellan LK, Hunstad DA.** Urinary tract infection: pathogenesis and outlook. *Trends Mol Med.* 2016 Nov;22(11):946–957. <https://doi.org/10.1016/j.molmed.2016.09.003>
- Mellata M, Johnson JR, Curtiss R 3rd.** *Escherichia coli* isolates from commercial chicken meat and eggs cause sepsis, meningitis and urinary tract infection in rodent models of human infections. *Zoonoses Public Health.* 2018 Feb;65(1):103–113. <https://doi.org/10.1111/zph.12376>
- Micali S, Isgro G, Bianchi G, Miceli N, Calapai G, Navarra M.** Cranberry and recurrent cystitis: more than marketing? *Crit Rev Food Sci Nutr.* 2014 Jan;54(8):1063–1075. <https://doi.org/10.1080/10408398.2011.625574>
- Michno M, Sydor A, Wałaszek M, Sulowicz W.** Microbiology and drug resistance of pathogens in patients hospitalized at the Nephrology Department in the South of Poland. *Pol J Microbiol.* 2018;67(4):517–524. <https://doi.org/10.21307/pjm-2018-061>
- Moreira da Silva RCR, de Oliveira Martins Júnior P, Gonçalves LF, de Paulo Martins V, de Melo ABE, Pitondo-Silva A, de Campos TA.** Ciprofloxacin resistance in uropathogenic *Escherichia coli* isolates causing community-acquired urinary infections in Brasília, Brazil. *J Glob Antimicrob Resist.* 2017 Jun;9:61–67. <https://doi.org/10.1016/j.jgar.2017.01.009>
- Morrill HJ, Morton JB, Caffrey AR, Jiang L, Dosa D, Mermel LA, LaPlante KL.** Antimicrobial Resistance of *Escherichia coli* Urinary Isolates in the Veterans Affairs Health Care System. *Antimicrob Agents Chemother.* 2017 May;61(5):e02236-16. <https://doi.org/10.1128/AAC.02236-16>
- Moya-Dionisio V, Díaz-Zabala M, Ibáñez-Fernández A, Suárez-Leiva P, Martínez-Suárez V, Ordóñez-Álvarez FA, Santos-Rodríguez F.** [Uropathogen pattern and antimicrobial susceptibility in positive urinary cultures isolates from paediatric patients]. *Rev Esp Quimioter.* 2016 Jun;29(3):146–150.
- Munkhdelger Y, Gunregjav N, Dorjpurev A, Juniichiro N, Sarantuya J.** Detection of virulence genes, phylogenetic group and antibiotic resistance of uropathogenic *Escherichia coli* in Mongolia. *J Infect Dev Ctries.* 2017 Jan 30;11(01):51–57. <https://doi.org/10.3855/jidc.7903>

- Naber KG, Schito G, Botto H, Palou J, Mazzei T. Surveillance study in Europe and Brazil on clinical aspects and Antimicrobial Resistance Epidemiology in Females with Cystitis (ARESC): implications for empiric therapy. *Eur Urol*. 2008 Nov;54(5):1164–1178. <https://doi.org/10.1016/j.eururo.2008.05.010>
- Neuner EA, Sekeres J, Hall GS, van Duin D. Experience with fosfomycin for treatment of urinary tract infections due to multidrug-resistant organisms. *Antimicrob Agents Chemother*. 2012 Nov;56(11):5744–5748. <https://doi.org/10.1128/AAC.00402-12>
- Nordstrom L, Liu CM, Price LB. Foodborne urinary tract infections: a new paradigm for antimicrobial-resistant foodborne illness. *Front Microbiol*. 2013;4:29. <https://doi.org/10.3389/fmicb.2013.00029>
- Noyal MJC, Menezes GA, Harish BN, Sujatha S, Parija SC. Simple screening tests for detection of carbapenemases in clinical isolates of nonfermentative Gram-negative bacteria. *Indian J Med Res*. 2009 Jun;129(6):707–712.
- Ojdana D, Sacha P, Wiczorek P, Czaban S, Michalska A, Jaworowska J, Jurczak A, Poniatowski B, Tryniszewska E. The occurrence of *bla*CTX-M, *bla*SHV, and *bla*TEM genes in extended-spectrum β -lactamase-positive strains of *Klebsiella pneumoniae*, *Escherichia coli*, and *Proteus mirabilis* in Poland. *Int J Antibiot*. 2014; Art. ID 935842: 7 pages. <http://doi.org/10.1155/2014/935842>
- Paniagua-Contreras GL, Monroy-Pérez E, Rodríguez-Moctezuma JR, Domínguez-Trejo P, Vaca-Paniagua F, Vaca S. Virulence factors, antibiotic resistance phenotypes and O-serogroups of *Escherichia coli* strains isolated from community-acquired urinary tract infection patients in Mexico. *J Microbiol Immunol Infect*. 2017 Aug;50(4):478–485. <https://doi.org/10.1016/j.jmii.2015.08.005>
- Parajuli NP, Maharjan P, Parajuli H, Joshi G, Paudel D, Sayami S, Khanal PR. High rates of multidrug resistance among uropathogenic *Escherichia coli* in children and analyses of ESBL producers from Nepal. *Antimicrob Resist Infect Control*. 2017 Dec;6(1):9. <https://doi.org/10.1186/s13756-016-0168-6>
- Petty NK, Ben Zakour NL, Stanton-Cook M, Skippington E, Totsika M, Forde BM, Phan MD, Gomes Moriel D, Peters KM, Davies M, et al. Global dissemination of a multidrug resistant *Escherichia coli* clone. *Proc Natl Acad Sci USA*. 2014 Apr 15; 111(15):5694–5699. <https://doi.org/10.1073/pnas.1322678111>
- Popovic M, Steinort D, Pillai S, Joukhadar C. Fosfomycin: an old, new friend? *Eur J Clin Microbiol Infect Dis*. 2010 Feb;29(2):127–142. <https://doi.org/10.1007/s10096-009-0833-2>
- Pourahmad Jaktaji R, Mohiti E. Study of Mutations in the DNA gyrase *gyrA* Gene of *Escherichia coli*. *Iran J Pharm Res*. 2010 Winter; 9(1):43–48.
- Prasada S, Bhat A, Bhat S, Shenoy Mulki S, Tulasidas S. Changing antibiotic susceptibility pattern in uropathogenic *Escherichia coli* over a period of 5 years in a tertiary care center. *Infect Drug Resist*. 2019 May;12:1439–1443. <https://doi.org/10.2147/IDR.S201849>
- Raeispour M, Ranjbar R. Antibiotic resistance, virulence factors and genotyping of Uropathogenic *Escherichia coli* strains. *Antimicrob Resist Infect Control*. 2018 Dec;7(1):118. <https://doi.org/10.1186/s13756-018-0411-4>
- Ramírez-Castillo FY, Moreno-Flores AC, Avelar-González FJ, Márquez-Díaz F, Harel J, Guerrero-Barrera AL. An evaluation of multidrug-resistant *Escherichia coli* isolates in urinary tract infections from Aguascalientes, Mexico: cross-sectional study. *Ann Clin Microbiol Antimicrob*. 2018 Dec;17(1):34. <https://doi.org/10.1186/s12941-018-0286-5>
- Regasa Dadi B, Abebe T, Zhang L, Mihret A, Abebe W, Amogne W. Drug resistance and plasmid profile of uropathogenic *Escherichia coli* among urinary tract infection patients in Addis Abeba. *J Infect Dev Ctries*. 2018 Aug 31;12(08):608–615. <https://doi.org/10.3855/jidc.9916>
- Rezai MS, Salehifar E, Rafiei A, Langaee T, Rafati M, Shafahi K, Eslami G. Characterization of multidrug resistant extended-spectrum beta-lactamase-producing *Escherichia coli* among uropathogens of pediatrics in North of Iran. *BioMed Res Int*. 2015;2015:1–7. <https://doi.org/10.1155/2015/309478>
- Rigsby RE, Fillgrove KL, Beihoffer LA, Armstrong RN. Fosfomycin resistance proteins: a nexus of glutathione transferases and epoxide hydrolases in a metalloenzyme superfamily. *Methods Enzymol*. 2005;401:367–379. [https://doi.org/10.1016/S0076-6879\(05\)01023-2](https://doi.org/10.1016/S0076-6879(05)01023-2)
- Riley LW. Pandemic lineages of extraintestinal pathogenic *Escherichia coli*. *Clin Microbiol Infect*. 2014 May;20(5):380–390. <https://doi.org/10.1111/1469-0691.12646>
- Sanchez GV, Babiker A, Master RN, Luu T, Mathur A, Bordon J. Antibiotic resistance among urinary isolates from female outpatients in the United States in 2003 and 2012. *Antimicrob Agents Chemother*. 2016 May;60(5):2680–2683. <https://doi.org/10.1128/AAC.02897-15>
- Sandegren L, Lindqvist A, Kahlmeter G, Andersson DI. Nitrofurantoin resistance mechanism and fitness cost in *Escherichia coli*. *J Antimicrob Chemother*. 2008 Jun 10;62(3):495–503. <https://doi.org/10.1093/jac/dkn222>
- Sarowska J, Futoma-Koloch B, Jama-Kmieciak A, Frej-Madrzak M, Ksiazczyk M, Bugla-Ploskonska G, Choroszy-Krol I. Virulence factors, prevalence and potential transmission of extraintestinal pathogenic *Escherichia coli* isolated from different sources: recent reports. *Gut Pathog*. 2019 Dec;11(1):10. <https://doi.org/10.1186/s13099-019-0290-0>
- Schneeberger C, Kazemier BM, Geerlings SE. Asymptomatic bacteriuria and urinary tract infections in special patient groups: women with diabetes mellitus and pregnant women. *Curr Opin Infect Dis*. 2014 Feb;27(1):108–114. <https://doi.org/10.1097/QCO.0000000000000028>
- Shahbazi S, Asadi Karam MR, Habibi M, Talebi A, Bouzari S. Distribution of extended-spectrum β -lactam, quinolone and carbapenem resistance genes, and genetic diversity among uropathogenic *Escherichia coli* isolates in Tehran, Iran. *J Glob Antimicrob Resist*. 2018 Sep;14:118–125. <https://doi.org/10.1016/j.jgar.2018.03.006>
- Shakhatreh MAK, Swedan SF, Al-Odat MA, Khabour OF. Uropathogenic *Escherichia coli* (UPEC) in Jordan: prevalence of urovirulence genes and antibiotic resistance. *JKSUS*. 2018. <https://doi.org/10.1016/j.jksus.2018.03.009>
- Shenagari M, Bakhtiari M, Mojtahedi A, Atrkar Roushan Z. High frequency of mutations in *gyrA* gene associated with quinolones resistance in uropathogenic *Escherichiacoli* isolates from the north of Iran. *Iran J Basic Med Sci*. 2018 Dec;21(12):1226–1231.
- Smelov V, Naber K, Bjerklund Johansen TE. Improved classification of urinary tract infection: future considerations. *Eur Urol Suppl*. 2016 Jul;15(4):71–80. <https://doi.org/10.1016/j.eursup.2016.04.002>
- Tabasi M, Karam MR, Habibi M, Mostafavi E, Bouzari S. Genotypic characterization of virulence factors in *Escherichia coli* isolated from patients with acute cystitis, pyelonephritis and asymptomatic bacteriuria. *J Clin Diagn Res*. 2016;10(12):DC01–DC07. <https://doi.org/10.7860/JCDR/2016/21379.9009>
- Talan DA, Takhar SS, Krishnadasan A, Abrahamian FM, Mower WR, Moran GJ; EMERGENCY ID Net Study Group. Fluoroquinolone-resistant and extended-spectrum β -lactamase-producing *Escherichia coli* infections in patients with pyelonephritis, United States. *Emerg Infect Dis*. 2016 Sep;22(9). <https://doi.org/10.3201/eid2209.160148>
- Tartof SY, Solberg OD, Manges AR, Riley LW. Analysis of a uropathogenic *Escherichia coli* clonal group by multilocus sequence typing. *J Clin Microbiol*. 2005 Dec 01;43(12):5860–5864. <https://doi.org/10.1128/JCM.43.12.5860-5864.2005>

- Tchesnokova VL, Rechkina E, Larson L, Ferrier K, Weaver JL, Schroeder DW, She R, Butler-Wu SM, Agüero-Rosenfeld ME, Zerr D, et al. Rapid and extensive expansion in the United States of a new multidrug-resistant *Escherichia coli* clonal group, sequence type 1193. *Clin Infect Dis*. 2019 Jan 07;68(2):334–337. <https://doi.org/10.1093/cid/ciy525>
- Tenney J, Hudson N, Alnifaidy H, Li JTC, Fung KH. Risk factors for acquiring multidrug-resistant organisms in urinary tract infections: A systematic literature review. *Saudi Pharm J*. 2018 Jul;26(5):678–684. <https://doi.org/10.1016/j.jsps.2018.02.023>
- Terlizzi ME, Gribaudo G, Maffei ME. Uropathogenic *Escherichia coli* (UPEC) infections: virulence factors, bladder responses, antibiotic, and non-antibiotic antimicrobial strategies. *Front Microbiol*. 2017 Aug 15;8:1566. <https://doi.org/10.3389/fmicb.2017.01566>
- Tsuruoka T, Yamada Y. Characterization of spontaneous fosfomycin (phosphonomycin)-resistant cells of *Escherichia coli* B *in vitro*. *J Antibiot (Tokyo)*. 1975;28(11):906–911. <https://doi.org/10.7164/antibiotics.28.906>
- van der Donk CFM, van de Bovenkamp JHB, De Brauwier EIGB, De Mol P, Feldhoff KH, Kalka-Moll WM, Nys S, Thoelen I, Trienekens TAM, Stobberingh EE. Antimicrobial resistance and spread of multi drug resistant *Escherichia coli* isolates collected from nine urology services in the Euregion Meuse-Rhine. *PLoS One*. 2012 Oct 17;7(10):e47707. <https://doi.org/10.1371/journal.pone.0047707>
- van Nieuwkoop C, Bonten TN, Wout JW, Becker MJ, Groeneveld GH, Jansen CL, van der Vorm ER, IJzerman EP, Rothbarth PH, TerMeer-Veringa EM, et al. Risk factors for bacteremia with uropathogen not cultured from urine in adults with febrile urinary tract infection. *Clin Infect Dis*. 2010 Jun;50(11):e69–e72. <https://doi.org/10.1086/652657>
- Veeraraghavan B, Shakti L. Advantage and limitations of nitrofurantoin in multi-drug resistant Indian scenario. *Indian J Med Microbiol*. 2015;33(4):477–481. <https://doi.org/10.4103/0255-0857.167350>
- Velasco M, Martínez JA, Moreno-Martínez A, Horcajada JB, Ruiz J, Barranco M, Almela M, Vila J, Mensa J. Blood cultures for women with uncomplicated acute pyelonephritis: are they necessary? *Clin Infect Dis*. 2003 Oct 15;37(8):1127–1130. <https://doi.org/10.1086/378291>
- Wagenlehner F, Tandogdu Z, Bartoletti R, Cai T, Cek M, Kulchavenya E, Köves B, Naber K, Perepanova T, Tenke P, et al. The global prevalence of infections in urology study: a long-term, worldwide surveillance study on urological infections. *Pathogens*. 2016 Jan 19;5(1):10. <https://doi.org/10.3390/pathogens5010010>
- Walker E, Lyman A, Gupta K, Mahoney MV, Snyder GM, Hirsch EB. Clinical management of an increasing threat: outpatient urinary tract infections due to multidrug-resistant uropathogens. *Clin Infect Dis*. 2016 Oct 01;63(7):960–965. <https://doi.org/10.1093/cid/ciw396>
- Yamaji R, Rubin J, Thys E, Friedman CR, Riley LW. Persistent pandemic lineages of uropathogenic *Escherichia coli* in a college community from 1999 to 2017. *J Clin Microbiol*. 2018 Feb 07;56(4):e01834-17. <https://doi.org/10.1128/JCM.01834-17>
- Yamasaki E, Yamada C, Jin X, Nair GB, Kurazono H, Yamamoto S. Expression of *marA* is remarkably increased from the early stage of development of fluoroquinolone-resistance in uropathogenic *Escherichia coli*. *J Infect Chemother*. 2015 Feb;21(2):105–109. <https://doi.org/10.1016/j.jiac.2014.10.007>
- Zacchè MM, Giarenis I. Therapies in early development for the treatment of urinary tract inflammation. *Expert Opin Investig Drugs*. 2016 May 03;25(5):531–540. <https://doi.org/10.1517/13543784.2016.1161024>

Colistin Resistance in Enterobacterales Strains – A Current View

ELŻBIETA M. STEFANIUK^{1*} and STEFAN TYSKI^{1,2}

¹Department of Antibiotics and Microbiology, National Medicines Institute, Warsaw, Poland

²Department of Pharmaceutical and Microbiology, Medical University of Warsaw, Warsaw, Poland

Submitted 18 June 2019, revised 5 November 2019, accepted 5 November 2019

Abstract

Colistin is a member of cationic polypeptide antibiotics known as polymyxins. It is widely used in animal husbandry, plant cultivation, animal and human medicine and is increasingly used as one of the last available treatment options for patients with severe infections with carbapenem-resistant Gram-negative bacilli. Due to the increased use of colistin in treating infections caused by multidrug-resistant (MDR) bacteria, the resistance to this antibiotic ought to be monitored. Bacterial resistance to colistin may be encoded on transposable genetic elements (e.g. plasmids with the *mcr* genes). Thus far, nine variants of the *mcr* gene, *mcr-1* – *mcr-9*, have been identified. Chromosomal resistance to colistin is associated with the modification of lipopolysaccharide (LPS). Various methods, from classical microbiology to molecular biology methods, are used to detect the colistin-resistant bacterial strains and to identify resistance mechanisms. The broth dilution method is recommended for susceptibility testing of bacteria to colistin.

Key words: Enterobacterales, polymyxins and their use, colistin-resistance and detection methods, treatment options

Pharmacology and application

Colistin is a cationic polypeptide antibiotic, a member of the polymyxin family of molecules. It was isolated for the first time in 1949 as a product of *Paenibacillus polymyxa* (formerly *Bacillus polymyxa*), which is an industrially significant facultative anaerobic, non-pathogenic, and endospore-forming bacillus. The polymyxin molecule consists of a peptide and a fatty acid residue. Based on the amino acid sequence of the peptide, five polymyxin (A – E) variants can be distinguished but only two variants are used in medicine, B and E (colistin). The antibacterial effect of colistin is concentration-dependent (Li 2005; Das et al. 2017). Colistin is only active against Gram-negative bacteria (GNB), such as the aerobic Enterobacterales ord. nov. (except *Proteus* spp., *Providencia* spp., *Serratia* spp., *Edwardsiella* spp., *Morganella* spp., and *Hafnia* spp.), non-fermenting rods of *Pseudomonas*, *Acinetobacter* and *Burkholderia*, and anaerobic bacteria, e.g. *Fusobacterium* and *Bacteroides* (except *Bacteroides fragilis*) (Li et al. 2005). Its antibacterial mechanism is based on the electrostatic interaction between colistin amino groups and lipid A subunits of lipopolysaccharide (LPS). Colis-

tin displaces Mg²⁺ and Ca²⁺ ions from LPS, leading to disturbances in the outer membrane structure of the cell. This leads to increased permeability of the cell membrane and, consequently, to cell death (Schindler and Osborn 1979).

As polymyxins are poorly absorbed from the digestive tract, orally administered polymyxins are only active on bacteria in the gastrointestinal system. Polymyxins do not diffuse well into tissues and do not penetrate the cerebrospinal fluid or the pleural and peritoneal cavity. Colistin has numerous side effects, including nephrotoxicity and neurotoxicity; therefore, it cannot be used in patients with renal failure (Kostowski and Herman 2010). The levels of nephrotoxicity and neurotoxicity were the reason for its discontinued use in human medicine after 1970 (Tullu and Dhariwal 2013).

In medicine, two physical forms of colistin are available, colistin sulphate (CS) for oral and topical use, and colistin methanesulphonate (CMS) for parenteral use (Kwa et al. 2005; Li et al. 2005). Nephrotoxicity and neurotoxicity are dose-dependent (Ordoeji Javan et al. 2015). Risk factors for nephrotoxicity include colistin plasma levels > 2.5–3 g/l, concomitant administration of other nephrotoxic drugs (such as anti-inflammatory

* Corresponding author: Elżbieta M. Stefaniuk, Department of Antibiotics and Microbiology, National Medicines Institute, Warsaw, Poland; e-mail: e.stefaniuk@nil.gov.pl

© 2019 Elżbieta M. Stefaniuk and Stefan Tyski

This work is licensed under the Creative Commons Attribution-NonCommercial-NoDerivatives 4.0 License (<https://creativecommons.org/licenses/by-nc-nd/4.0/>).

drugs, vancomycin and aminoglycosides), the advanced age of patient, and severity of the disease (rates of nephrotoxicity 14–53%) (Kwon et al. 2010; Pogue et al. 2011). Neurotoxicity is reversible and manifests itself, among others, in the form of peripheral and facial paresthesia, dizziness/vertigo, weakness, visual disturbances, and ataxia (4–6% of patients) (Koch-Weser et al. 1970; Spapen et al. 2011). Colistin methanesulphonate has no antimicrobial activity and acts as a colistin pro-drug that does not bind to plasma proteins. After parenteral administration, approximately 20% of CMS is hydrolyzed to colistin. This is an important feature in reducing toxicity, especially nephrotoxicity (Falagas et al. 2005). When given intravenously, a large portion of CMS is eliminated mainly through the kidneys by glomerular filtration and tubular secretion, which allows the use of CMS in urinary tract infections (Kostowski and Herman 2010). The intravenous (IV) form of the drug may also be administered by inhalation (Li et al. 2005). Inhaled colistin is used for treating pneumonia and ventilator-associated pneumonia (VAP) caused by multidrug-resistant (MDR) Gram-negative microorganisms, while it is also used prophylactically in patients with cystic fibrosis. Colistin also causes the release of histamine and serotonin by monocytes, which can lead to acute respiratory failure; therefore, care is needed when administering this drug in the form of an aerosol (Dzierżanowska 2018).

In the last 20 years, the emergence of MDR Gram-negative bacilli has led to polymyxins B and E being used once again, as a “salvage” therapy in the patients with CRE (carbapenems-resistant *Enterobacteriaceae*) infections for which we do not have the better treatment options (Li et al. 2006; Nation and Li 2009; Lim et al. 2010). Orally and topically administered colistin sulphate and parenteral colistin methanesulphonate sodium are designed for the treatment of life-threatening human infections caused by Gram-negative rods. Colistin has been approved by the American Thoracic Society and Infectious Diseases Society of America, who have provided guidelines for the treatment of VAP caused by MDR Gram-negative rods (American Thoracic Society and Infectious Diseases Society of America 2005). The parenteral form of colistin has also been evaluated for the treatment of other serious infections caused by MDR *P. aeruginosa*, *A. baumannii*, and *Enterobacteriaceae*, such as sepsis, abdominal infections, bone and joint infections, urinary tract infections, and meningitis (Falagas et al. 2005; Walkty et al. 2009; Batirel et al. 2014). Recent studies have demonstrated acceptable effectiveness and considerably less toxicity than had been reported on polymyxins in older studies (Ordoeji Javan et al. 2015). However, randomized controlled trials are urgently needed to further clarify the issues surrounding the efficacy and safety of polymyxins.

Colistin resistance mechanisms

Bacteria acquire resistance to colistin as a result of mutations and adaptation mechanisms. Different molecular mechanisms are associated with colistin resistance in Gram-negative bacteria; there are, among others, changes in the two-component systems: *pmrA/pmrB* (*Escherichia coli*, *Klebsiella pneumoniae*, *Salmonella* spp., *Acinetobacter baumannii*, and *Pseudomonas aeruginosa*), *phoP/phoQ* (*K. pneumoniae*, *Salmonella* spp.), *parR/parS* (*P. aeruginosa*), *colR/colS* (*P. aeruginosa*), and *cprR/cprS* (*Campylobacter jejuni*) (Olaitan et al. 2014b). Mechanisms of resistance differ among Gram-negative bacterial species. The most important chromosomal mechanism of colistin resistance in *K. pneumoniae* is an alteration of the *mgrB* gene, which encodes a negative regulator of *phoP/phoQ* system (Jayol et al. 2015). Colistin resistance is mainly achieved by modification of LPS, which is the main target of colistin in the bacterial cell. Mutations that lead to the addition of cationic groups to lipid A weaken the binding of polymyxins (Olaitan et al. 2014b; Baron et al. 2016). In the case of *A. baumannii*, similar changes in the *lpxA*, *lpxC* and *lpxD* genes as described above, cause inhibition of lipid A biosynthesis and thus loss of the polymyxin target in the bacteria (Moffatt et al. 2010). There is the hypothesis that colistin resistance of clinical isolates results from a combination of porin mutations and overexpression of efflux pump systems (Olaitan et al. 2014b).

Bacterial colistin resistance may be coded on transposable genetic elements (mostly plasmids with the *mcr* genes). Thus far, nine variants of the *mcr* genes, *mcr-1* – *mcr-9*, have been identified in various Enterobacteriales and *Moraxella* species. The first plasmid-mediated colistin resistance was detected in an *E. coli* strain collected from food animals in China in 2015 (Liu et al. 2016). Since then, the plasmid-mediated colistin resistance in Enterobacteriales has been reported worldwide, including human infections, also from Poland (Izdebski et al. 2016). The *mcr-1* gene modifies LPS by encoding phosphoethanolamine transferase (pEtN transferase), which mediates the addition of pEtN to lipid A (Baron et al. 2016). Generally, *E. coli* strains with the *mcr-1* gene are characterized by the low-level colistin resistance with a minimum inhibitory concentration (MIC) in the range of 2–8 mg/l. Zhang et al. (2019) have shown that the expression of the *mcr-1* gene in *E. coli* led to a higher mutation rate in the chromosomal polymyxin resistance cascade genes and produced higher MIC values (≥ 64 mg/l).

The *mcr-2* gene was first identified by Xavier and colleagues in *E. coli* strains isolated from calves and pigs in Belgium; MCR-1 and MCR-2 proteins showed 80.65% identity (Xavier et al. 2016). In 2017, a third mobile

colistin resistance gene, *mcr-3*, was described in *E. coli* by Yin et al. (2017). The amino acid sequence of the *mcr-3* gene product, MCR-3, showed 32.5 and 31.7% amino acid identity to MCR-1 and MCR-2, respectively (Yin et al. 2017). Also, Carrattoli et al. (2017) in 2017 detected a new plasmid-mediated colistin gene, *mcr-4*, in *Salmonella* on a small, not self-conjugative plasmid. For the first time, Borowiak et al. (2017) described a novel transposon-associated phosphoethanolamine transferase gene, *mcr-5*, which conferred colistin resistance in d-tartrate-fermenting *Salmonella enterica* subsp. *enterica* serovar Paratyphi B. In 2018, further variants, the *mcr-6* – *mcr-8* genes, were described (AbuOun et al. 2017; 2018; Wang et al. 2018; Yang et al. 2018).

Recently, Carroll et al. (2019) have described the *mcr-9* gene, a novel *mcr* homologue detected in MDR colistin-susceptible *Salmonella enterica* serovar Typhimurium strain isolated from a patient in the Washington State in 2010. This strain was phenotypically sensitive to colistin with a MIC value of 2 mg/l, according to the European Committee on Antimicrobial Susceptibility Testing (EUCAST) recommendations. The *mcr-9* gene was cloned into colistin-sensitive *E. coli* and the expression-conferred *E. coli* NEB5 α strain with resistance to 1, 2 and 2.5 mg/l colistin. Pairwise comparison of the predicted protein structures of all nine *mcr* homologues (*mcr-1* to *mcr-9*) revealed that the *mcr-3*, *mcr-4*, *mcr-7*, and *mcr-9* genes share a high degree of similarity at the structural level (Carroll et al. 2019).

Colistin uses in human medicine

Colistin is used for treating infections with carbapenem-resistant *Enterobacteriaceae* (CRE) that belong to multi-resistant isolates and have already been reported worldwide (Grundmann et al. 2010). The seriousness of the problem is underlined by high (>30%) mortality of hospitalized patients infected with carbapenem-resistant strains (Capone et al. 2013; Ghafur et al. 2014; Guducuoglu et al. 2018; Zhang et al. 2018). Such infections are difficult to treat and with limited therapeutic options (Parisi et al. 2015; Baraniak et al. 2016). Tumbarello et al. (2012) analyzed the course of *K. pneumoniae* KPC-positive infection in the patients; combination therapy with tigecycline, colistin, and meropenem was associated with a lower risk of mortality (12.5%). The authors also indicate that incorrect empirical therapy is a significant factor in the mortality rate of the patients infected with carbapenem-resistant *K. pneumoniae* (Tumbarello et al. 2012; Tumbarello et al. 2015).

Moreover, the development of outbreaks by colistin-resistant Gram-negative bacilli producing carbapenemases is a great problem (Antoniadou et al. 2007;

Marchaim et al. 2011; Monaco et al. 2014; Olaitan et al. 2014a; Parisi et al. 2015; Jayol et al. 2016; Gundogdu et al. 2018). In 2013, the colistin resistance rate has risen to an average of over 30% of CRE isolates, including Italy, Spain, and Greece, and constituted accordingly 43, 31, and 20.8%, respectively (ECDC 2014; Monaco et al. 2014; Pena et al. 2014; Meletis et al. 2015). The increased mortality is also related to infections with colistin-resistant strains (Capone et al. 2013). Colistin resistance makes the choice of antimicrobial agents difficult, and the use of therapeutic options for colistin-resistant MDR isolates depends on the sensitivity phenotype of the isolates, the infection type and site, antimicrobial PK/PD properties, and potential side effects (Petrosillo et al. 2019).

Due to the increasing role of colistin in the treatment of human infections with MDR bacteria, the resistance to this antibiotic should be carefully monitored. The use of colistin in human medicine is assumed to be a cause for the occurrence of colistin resistance in Enterobacterales, particularly in *K. pneumoniae* (Sandri et al. 2013; Vicari et al. 2013).

Ceftazidime/avibactam, as a combination of β -lactam and β -lactamases inhibitor, plays an important role in the treatment of MDR *K. pneumoniae* infections, including colistin-resistant isolates producing KPC (Jayol et al. 2018a). It is registered for the treatment of abdominal infections, urinary tract infections and nosocomial pneumonia (Zhanel et al. 2013). Avibactam inhibits class A, C, and D β -lactamases, including KPC and OXA-48 carbapenemases (Shields et al. 2015; Pogue et al. 2019), but does not inhibit metallo- β -lactamases (Ambler class B) due to the absence of the active-site serine residue in these enzymes (Davido et al. 2017). The combination of ceftazidime/avibactam with aztreonam showed activity against *K. pneumoniae* strains, regardless of the type of carbapenemase produced (Davido et al. 2017; Jayol et al. 2018a). Ceftazidime/avibactam therapy is less nephrotoxic compared to aminoglycosides or colistin (Zhanel et al. 2013). However, it has been reported that *K. pneumoniae* acquired resistance to ceftazidime with avibactam during treatment (Shields et al. 2017; Gaibani et al. 2018).

The combination of meropenem with vaborbactam is the new antimicrobial agent active against KPC-positive *K. pneumoniae* (Pfaller et al. 2018; Pogue et al. 2019), and it is registered for the treatment of respiratory pneumonia and bacteraemia (U.S. National Library from Medicine 2019). Vaborbactam does not inhibit class D or class B carbapenemases and due to the risk of developing resistance, meropenem/vaborbactam should be reserved for the treatment of infections caused by MDR strains, including colistin-resistant *K. pneumoniae* KPC-positive (Lomovskaya et al. 2017).

Methods for susceptibility testing

It is highly important to develop phenotypic tests capable of detecting the colistin resistance in Gram-negative rods. Until recently, there was no consensus as to the methodology for colistin susceptibility testing. The disc diffusion method and gradient tests proved to be unreliable due to the poor diffusion of colistin in agar (Galani et al. 2008; Behera et al. 2010; Dafopoulos et al. 2015; Chew et al. 2017; Vasoo 2017; Giske and Kahlmeter 2018). Therefore, disk diffusion and gradient diffusion are not valid techniques for the determination of susceptibility to polymyxins.

In 2016, both EUCAST and the Clinical and Laboratory Standards Institute (CLSI) recommended the International Standard Organization (ISO) 20776 standard broth dilution method for testing of the MIC values of colistin (CLSI 2016; EUCAST 2016). However, the reference broth microdilution method is difficult to apply in routine microbiological diagnostics. The EUCAST does not recommend the use of automated systems to determine the phenotype of bacterial sensitivity such as Vitek 2, (bioMérieux, France), BD Phoenix (Becton Dickinson, USA), as well as Walk-Away (Beckman Coulter, USA) for the analysis of the sensitivity of Gram-negative bacilli to colistin. This is because these systems have fairly limited accuracy in determining colistin MIC, particularly in the range of 2–4 mg/l when compared to the reference method (Nordmann et al. 2016b; Bosacka et al. 2018; Matuschek et al. 2018b; Lellouche et al. 2019).

The literature data indicate the usefulness of several commercially available systems that are based on the broth microdilution method, such as the MIC-Strip Colistin (Merlin, Germany), Microlatest MIC Colistin (Erba Lachema, Czech Republic), Sensitest Colistin (Liofilchem, Italy), and MIC COL (Diagnostics, Slovakia) for the evaluation of the sensitivity of Enterobacterales and non-fermenting rods to colistin (Nordmann et al. 2016b; Matuschek et al. 2018a; Bosacka et al. 2018; Lellouche et al. 2019). Members of colistin-resistant bacilli are usually correctly categorized as resistant using the above-mentioned methods (Chew et al. 2017; Poirel et al. 2017). An increasing number of recent reports point to the heterogeneity of strains detected *via* microdilution in broth (Chew et al. 2017).

Methods for the detection of colistin resistance

The innovatory technique for the identification of colistin resistance is the Rapid Polymyxin NP (Nordmann/Poirel) test. It was developed by the Nordmann's group for the colistin susceptibility testing in Enterobacterales (Nordmann et al. 2016b). Currently, the

researchers are underway to use this test for the detection of colistin resistance in non-fermenting bacilli. The Rapid Polymyxin NP test detects fermentation of glucose associated with bacterial growth in the presence of a defined concentration of polymyxin E or B; the presence of acid metabolites is evidenced by the change in the pH and the indicator (red phenol) color from orange to yellow. The sensitivity and specificity of the test are highly comparable to the reference broth microdilution method (99.3 and 95.4%, respectively). This test is easy to perform and provides a result in less than 2 hours (Nordmann et al. 2016b).

Chromogenic media are commonly used for screening; they allow the growth of sought bacteria as properly colored colonies. The first agar medium for detecting colistin-resistant Gram-negative rods from bacterial cultures and rectal swab samples was the SuperPolymyxin screening medium (Nordmann et al. 2016a); the commercial version of this medium is SuperPolymyxin medium (ELITechGroup, Puteaux, France) for detecting colistin-resistant Enterobacterales strains, including these with the low MIC values (mg/l) that harbor the *mcr-1* gene (Jayol et al. 2018). It is composed of eosin methylene blue (EMB) agar and includes colistin, daptomycin, and amphotericin B (3.5, 10, and 5 µg/ml, respectively). The other medium, CHROMagar COLAPSE medium for the detection of colistin-resistant strains was compared to the SuperPolymyxin medium (Abdul Momin et al. 2017); this medium differentiates colistin-resistant Enterobacterales strains from non-fermenting rods. Bardet et al. (2017) described the LBJMR medium, a new polyvalent culture medium for the isolation and selection of colistin-resistant bacteria and vancomycin-resistant bacteria. This medium was developed by the addition of colistin sulphate salt (4 µg/ml), vancomycin (50 µg/ml), and a substrate for fermentation (7.5 g/l of glucose) to a Purple Agar Base (31 g/l). In early 2018, a new chromogenic medium, CHROMID Colistin R agar (COLR; bioMérieux, France) came into the market and allowed the screening of colistin-resistant *Enterobacteriaceae* in clinical samples, such as stools and rectal swabs. The COLR is a manual qualitative diagnostic test, which allows colistin-resistant isolates to be distinguished from those that are susceptible. Colistin-resistant strains forming colored colonies on chromogenic media and their color depends on the species. By contrast, colistin-susceptible isolates do not grow on the COLR plate (García-Fernández et al. 2019).

The chromogenic method is based on the dilution in agar, although EUCAST does not recommend this procedure for the determination of bacterial susceptibility to colistin, as the threshold of the detectability increases with the growth of the bacterial inoculum (Matuschek et al. 2018b). However, Turlej-Rogacka et al. (2018) reported that when compared to broth

dilution methods, the method of the dilution in agar yields more accurate results in the evaluation of the colistin MIC values (Turlej-Rogacka et al. 2018). Behera and colleagues (2010) confirmed the high correlation of results between the reference method and the agar dilution method (Behera et al. 2010; Dafopouolu et al. 2015). The greatest challenge in colistin handling is its binding to plastic (Humphries 2015; Matuschek et al. 2018b). According to the above-mentioned authors, the agar dilution method significantly reduces the phenomenon of colistin-plastic binding, and the MICs results obtained with this method are characterized by a high accuracy (Behera et al. 2010; Humphries 2015; Matuschek et al. 2018).

The COLR medium uses the borderline colistin concentrations that allow qualification of the strains studied as susceptible or resistant. This chromogenic medium is a qualitative method of Enterobacterales detection and does not allow the determination of the colistin MIC values against the bacterial strains analyzed. As such, it should only be regarded as a screening test. On the other hand, in treating the infections caused by colistin-resistant bacteria, the clinical interpretation is significant. This entails the categorization of colistin resistance rather than the determination of the specific MIC value since maximum dosages of the medication are prescribed independently of precise susceptibility levels. However, the MIC values are important in monitoring the increase in the resistance to colistin observed in the intestinal bacteria.

Other new-generation methods have been developed recently to detect colistin-resistant strains: the loop-mediated isothermal amplification (LAMP) for nucleic acid detection (Zou et al. 2017), and a microarray CT103XL (Bernasconi et al. 2017). Zou et al. (2017) showed that the LAMP test is ten times more sensitive than the conventional PCR and confirmed its usefulness for the detection of the *mcr-1* gene in Enterobacterales strains from stool samples. Similarly, Bernasconi et al. (2017) demonstrated the usefulness of the new CT103XL microarray for the rapid characterization of multidrug-resistant Gram-negative bacteria through simultaneously identifying the *mcr-1*, *mcr-2*, and clinically important *bla* genes.

Colistin in veterinary medicine and agriculture

Colistin sulphate has also been widely and heavily used for decades in veterinary medicine for the treatment of intestinal infections in pigs, poultry, and cattle, which were caused by Enterobacterales strains, mainly *E. coli* and *Salmonella* spp. (Liu et al. 2016). In these situations, colistin is chiefly used in an oral form, and its usage varies widely among different countries. In Spain,

it is used during gestation and lactation, the post-weaning period, and for metaphylactic intestinal disease control (Casal et al. 2007). During the post-weaning period, it is used in 50% and 35% of pig farms in France and Austria, respectively (Kempf et al. 2013; Trauffler et al. 2014). In Sweden, colistin was the most frequently used antibiotic in 18% of weaned piglet herds (Sjölund et al. 2015). A German study on antimicrobial use in pigs has revealed that polypeptides accounted for 4.2% of the total use per kg but regarding treatment units, they were among the three most frequently used antimicrobial classes (van Rennings et al. 2015). A Netherland study has shown that colistin, as one of the most used antimicrobials next to tetracyclines, trimethoprim/sulfonamides, macrolides, and lincosamides was available on the prescription and deliveries for pigs, veal calves, and broilers in the country (Bos et al. 2013).

In Asian countries, the use of antibiotics, particularly colistin, in animal husbandry also takes place on a large scale. China is one of the world's largest users of colistin in agriculture; over 11 thousand tons of colistin is being used (QYResearch Medical Research Centre 2015). Considering this upward trend, the consumption of colistin in Chinese agriculture is estimated to reach more than 16 thousand tons in 2021 (QYResearch Medical Research Centre 2015). China remains the largest user of colistin in agriculture worldwide. In the Red River Delta region of Vietnam, colistin was also used as a feed additive for growth promotion in pig production (Kim et al. 2013). This was a cause of concern because colistin is an unapproved antibiotic for growth promotion in Vietnam (MARD 2006; 2009). These facts illustrate the sheer scale of antibiotic consumption in animal and poultry husbandry.

Alarming data on the use of antibiotics in veterinary medicine, in particular colistin, has led to efforts to limit their use. The different monitoring systems for the use of antibiotics in animals and the surveillance of resistance to antibiotics were established in European countries (BTK 2015; Borck Høg et al. 2017; SDa Autoriteit Diergenesmiddelen 2018; SWEDRES/SVARM 2018; MARAN 2019). In 2015, Nunan and Young (2015) reported that antibiotics, particularly colistin, should not be routinely used as prophylactics in animal farms in the United Kingdom (UK). The authors added that colistin accounted for only 0.2% of all antibiotics that were used in breeding in the UK and was only used by veterinarians to treat sick animals (EMA/CVMP 2010; Nunan and Young 2015; Catry et al. 2015).

In a national report on antibiotics consumption in the Australian pig industry, Jordan et al. (2009) found that colistin was not used during the study period in the production of pigs.

Until recently, there were no recommendations on the need of conducting the screening tests to find

the carriage of colistin-resistant bacteria, but under a 'One Health' perspective, it is necessary to monitor the colistin resistance among Gram-negative bacteria in veterinary and human medicine. Currently, at least in the veterinarian sector in Germany, screening for colistin resistance is recommended and carried out routinely, and efforts are being made to implement colistin screening also for human isolates. It, therefore, seems justified to develop a chromogenic agar medium for detecting colistin-resistant rods directly from clinical material other than stools and rectal swabs, e.g. samples from the lower respiratory tract or urine samples.

Colistin-resistant strains in plant food and the environment

There are progressively more and more reports on the culture of the colistin-resistant Enterobacterales strains from vegetables and fruits samples (Liu et al. 2014; Jones-Dias et al. 2016; Luo et al. 2017). A study by Zhon et al. (2017) showed that water, where live bacteria may have come from the excrements, can be the source of plant contamination with Gram-negative bacilli (Zhon et al. 2017). Jung et al. (2014) analyzed the relationship between the plant food production chain and the incidence of foodborne disease outbreaks, and the consumption of contaminated raw vegetables has been linked with these outbreaks (Jung et al. 2014). Liu et al. (2014) studied the samples of vegetables (carrots, pak choi, green peppers, and leaf lettuce) from supermarkets or farmers' markets in nine provinces of China; about 4% of the vegetable samples (3.6%) carried one or more the *mcr*-positive isolates (*E. coli* and *Enterobacter cloacae*); the dissemination of the *mcr-1* gene was mediated by plasmids. All isolates were MDR; however, they were susceptible to meropenem and tigecycline (Liu et al. 2014). Jones-Dias et al. (2016) showed the presence of the *mcr-1* gene in lettuce samples in Portugal (Jones-Dias et al. 2016).

Zurfuh et al. (2016) reported the presence of the plasmid-borne *mcr-1* colistin resistance gene in the extended-spectrum β -lactamase (ESBL) producing *E. coli* strains from rivers and lakes in Switzerland, and the ready-to-eat imported vegetables from Asian countries (Zurfuh et al. 2016). The *E. coli* strains with the *mcr-1* genes belonged to different multilocus sequence types (MLSTs), which harbored different the *bla*_{ESBL} genes. This suggests that the *mcr-1* gene can be spread on different plasmids. Luo et al. (2017) described the identification of the *mcr-1* gene in *E. coli* and *Raoultella ornithinolytica* ESBL-producing isolates collected from fresh vegetable samples in Guangzhou, China. *Raoultella ornithinolytica* belongs to a genus closely related to *Klebsiella* and is an environmental microorganism

associated with community-acquired infections, but the number of *R. ornithinolytica* infections might have been underestimated due to its misidentification as a *Klebsiella* spp. (Luo et al. 2017). Li et al. (2017) showed that the *mcr-1* gene in isolates from Guangzhou was located on IncHI2/ST3, IncI2, and IncX4 plasmids in both isolates from animals and humans. The studies cited here differ in the number and variety of the vegetables examined; however, as vegetables are often consumed raw, the presence of bacteria carrying the *mcr-1* gene may pose a threat to public health.

Summary

The resistance of Gram-negative rods to colistin, including Enterobacterales, is a serious public health problem. The colistin use in animal husbandry and agriculture has an impact on the spread of colistin resistance (Catry et al. 2015). The *mcr* genes were found in bacteria isolated from various food sources as animal meat and vegetables as well as the environment (including rivers and lakes water), infected patients, and asymptomatic human carriers. The detection of the antimicrobial resistance genes is critical for the prevention of the spread of bacterial resistance. There are several phenotypic and genotypic methods to detect colistin-resistant strains, determine the colistin MIC values and identify colistin resistance mechanisms. The easy transmission of resistance genes among microorganisms poses a challenge to the therapy of MDR bacterial infections, especially caused by carbapenem-resistant Enterobacterales. Therefore, resistance to colistin in the members of the Enterobacterales should be perceived as an important global health problem, requiring multi-sectoral, further research as well as a proper monitoring and surveillance systems.

ORCID

Elżbieta M. Stefaniuk [0000-0002-8169-6964](https://orcid.org/0000-0002-8169-6964)

Stefan Tyski [0000-0003-3352-038X](https://orcid.org/0000-0003-3352-038X)

Conflict of interest

The authors do not report any financial or personal connections with other persons or organizations, which might negatively affect the contents of this publication and/or claim authorship rights to this publication.

Literature

Abdul Momin MHF, Bean DC, Hendriksen RS, Haenni M, Phee LM, Wareham DW. CHROMagar COL-APSE: a selective bacterial culture medium for the isolation and differentiation of colistin-resistant Gram-negative pathogens. J Med Microbiol. 2017 Nov 01;66(11):1554–1561. <https://doi.org/10.1099/jmm.0.000602>

- AbuOun M, Stubberfield EJ, Duggett NA, Kirchner M, Dormer L, Nunez-Garcia J, Randall LP, Lemma F, Crook DW, Teale C, et al. *mcr-1* and *mcr-2* (*mcr-6.1*) variant genes identified in *Moraxella* species isolated from pigs in Great Britain from 2014 to 2015. J Antimicrob Chemother. 2017 Oct 01;72(10):2745–2749. <https://doi.org/10.1093/jac/dkx286>
- AbuOun M, Stubberfield EJ, Duggett NA, Kirchner M, Dormer L, Nunez-Garcia J, Randall LP, Lemma F, Crook DW, Teale C, et al. *mcr-1* and *mcr-2* (*mcr-6.1*) variant genes identified in *Moraxella* species isolated from pigs in Great Britain from 2014 to 2015. J Antimicrob Chemother. 2018 Oct 01;73(10):2904. <https://doi.org/10.1093/jac/dky272>
- American Thoracic Society; Infectious Diseases Society of America. Guidelines for the management of adults with hospital-acquired, ventilator-associated, and healthcare-associated pneumonia. Am J Respir Crit Care Med. 2005 Feb 15;171(4):388–416. <https://doi.org/10.1164/rccm.200405-644ST>
- Antoniadou A, Kontopidou F, Poulakou G, Koratzanis E, Galani I, Papadomichelakis E, Kopterides P, Souli M, Armaganidis A, Giamarellou H. Colistin-resistant isolates of *Klebsiella pneumoniae* emerging in intensive care unit patients: first report of a multiclonal cluster. J Antimicrob Chemother. 2007 Apr 01;59(4):786–790. <https://doi.org/10.1093/jac/dkl562>
- Baraniak A, Izdebski R, Fiett J, Gawryszewska I, Bojarska K, Herda M, Literacka E, Żabicka D, Tomczak H, Pewińska N, et al. NDM-producing Enterobacteriaceae in Poland, 2012–14: inter-regional outbreak of *Klebsiella pneumoniae* ST11 and sporadic cases. J Antimicrob Chemother. 2016 Jan;71(1):85–91. <https://doi.org/10.1093/jac/dkv282>
- Bardet L, Le Page S, Leangapichart T, Rolain JM. LBJMR medium: a new polyvalent culture medium for isolating and selecting vancomycin and colistin-resistant bacteria. BMC Microbiol. 2017 Dec; 17(1):220. <https://doi.org/10.1186/s12866-017-1128-x>
- Baron S, Hadjadj L, Rolain JM, Olaitan AO. Molecular mechanisms of polymyxin resistance: knowns and unknowns. Int J Antimicrob Agents. 2016 Dec;48(6):583–591. <https://doi.org/10.1016/j.ijantimicag.2016.06.023>
- Batirel A, Balkan II, Karabay O, Agalar C, Akalin S, Alici O, Alp E, Altay FA, Altin N, Arslan F, et al. Comparison of colistin-carbapenem, colistin-sulbactam, and colistin plus other antibacterial agents for the treatment of extremely drug-resistant *Acinetobacter baumannii* bloodstream infections. Eur J Clin Microbiol Infect Dis. 2014 Aug;33(8):1311–1322. <https://doi.org/10.1007/s10096-014-2070-6>
- Behera B, Mathur P, Das A, Kapil A, Gupta B, Bhoi S, Farooque K, Sharma V, Misra MC. Evaluation of susceptibility testing methods for polymyxin. Int J Infect Dis. 2010 Jul;14(7):e596–e601. <https://doi.org/10.1016/j.ijid.2009.09.001>
- Bernasconi OJ, Principe L, Tinguely R, Karczarek A, Perreten V, Luzzaro F, Endimiani A. Evaluation of a new commercial microarray platform for the simultaneous detection of β -lactamase and *mcr-1* and *mcr-2* genes in Enterobacteriaceae. J Clin Microbiol. 2017 Oct;55(10):3138–3141. <https://doi.org/10.1128/JCM.01056-17>
- Borck Høg B, Korsgaard HB, Wolff Sönksen U, Bager H, Bortolonia V, Ellis-Iversen J, Hendriksen RS, Jensen LB, Korsgaard HB, Vorobieva V. DANMAP 2016 – Use of antimicrobial agents and occurrence of antimicrobial resistance in bacteria from food animals, food and humans in Denmark. Statens Serum Institut, National Veterinary Institute, Technical University of Denmark National Food Institute, Technical University of Denmark. 2017. https://orbit.dtu.dk/ws/files/161713656/Rapport_DANMAP_2017.pdf
- Borowiak M, Fischer J, Hammerl JA, Hendriksen RS, Szabo I, Malorny B. Identification of a novel transposon-associated phosphoethanolamine transferase gene, *mcr-5*, conferring colistin resistance in d-tartrate fermenting *Salmonella enterica* subsp. *enterica* serovar Paratyphi B. J Antimicrob Chemother. 2017 Dec 01;72(12):3317–3324. <https://doi.org/10.1093/jac/dkx327>
- Bos ME, Taverne FJ, van Geijlswijk IM, Mouton JW, Mevius DJ, Heederik DJ; Netherlands Veterinary Medicines Authority SDA. Consumption of antimicrobials in pigs, veal calves, and broilers in the Netherlands: quantitative results of nationwide collection of data in 2011. PLoS One. 2013 Oct 21;21;8(10):e77525. <https://doi.org/10.1371/journal.pone.0077525>
- Bosacka K, Kozińska A, Stefaniuk E, Rybicka J, Mikołajczyk A, Młodzińska E, Hryniewicz W. Colistin antimicrobial susceptibility testing of Gram-negative bacteria – evaluation of tests available in Poland. ECCMID 2018 Abstract publication E0116, 21–24 April 2018; Available from https://www.escmid.org/escmid_publications/escmid_elibrary/?q=Bosacka+K&id=2173&L=0&x=28&y=20
- BTK. Guidelines for the prudent use of veterinary antimicrobial drugs – with notes for guidance. Federal Veterinary Surgeons' Association (BTK = Bundestierärztekammer). Addendum to the German Veterinary Gazette 2015;(3/2015). Available from <https://www.bundestieraerztekammer.de/tieraerzte/leitlinien/>
- Capone A, Giannella M, Fortini D, Giordano A, Meledandri M, Ballardini M, Venditti M, Bordi E, Capozzi D, Balice MP, et al. High rate of colistin resistance among patients with carbapenem-resistant *Klebsiella pneumoniae* infection accounts for an excess of mortality. Clin Microbiol Infect. 2013 Jan;19(1):E23–E30. <https://doi.org/10.1111/1469-0691.12070>
- Carattoli A, Villa L, Feudi C, Curcio L, Orsini S, Luppi A, Pezzotti G, Magistrali CF. Novel plasmid-mediated colistin resistance gene *mcr-4* gene in *Salmonella* and *Escherichia coli*, Italy 2013, Spain and Belgium, 2015 to 2016. Euro Surveill. 2017 Aug 3;22(31). <https://doi.org/10.2807/1560-7917.ES.2017.22.31.30589>
- Carroll LM, Gaballa A, Guldemann C, Sullivan G, Henderson LO, Wiedmann M. Identification of novel mobilized colistin resistance gene *mcr-9* in a multidrug-resistant, colistin-susceptible *Salmonella enterica* serotype Typhimurium isolate. MBio. 2019;10(3):e00853-19. <https://doi.org/10.1128/mBio.00853-19>
- Casal J, Mateu E, Mejia W, Martin M. Factors associated with routine mass antimicrobial usage in fattening pig units in a high pig-density area. Vet Res. 2007 May;38(3):481–492. <https://doi.org/10.1051/vetres:2007010>
- Catry B, Cavaleri M, Baptiste K, Grave K, Grein K, Holm A, Jukes H, Liebana E, Navas AL, Mackay D, et al. Use of colistin-containing products within the European Union and European Economic Area (EU/EEA): development of resistance in animals and possible impact on human and animal health. Int J Antimicrob Agents. 2015 Sep;46(3):297–306. <https://doi.org/10.1016/j.ijantimicag.2015.06.005>
- Chew KL, La MV, Lin RTP, Teo JWP. Colistin and polymyxin B susceptibility testing for carbapenem-resistant and *mcr* -positive Enterobacteriaceae: comparison of sensititre, MicroScan, Vitek 2, and Etest with broth microdilution. J Clin Microbiol. 2017 Sep; 55(9):2609–2616. <https://doi.org/10.1128/JCM.00268-17>
- CLSI. Performance standards for antimicrobial susceptibility testing. 26th ed. CLSI supplement M100S. Wayne (PA): Clinical and Laboratory Standards Institute; 2016.
- Dafopoulou K, Zarkotou O, Dimitroulia E, Hadjichristodoulou C, Gennimata V, Pournaras S, Tsakris A. Comparative evaluation of colistin susceptibility testing methods among carbapenem-non-susceptible *Klebsiella pneumoniae* and *Acinetobacter baumannii* clinical isolates. Antimicrob Agents Chemother. 2015 Aug;59(8):4625–4630. <https://doi.org/10.1128/AAC.00868-15>
- Das P, Sengupta K, Goel G, Bhattacharya S. Colistin: Pharmacology, drug resistance and clinical applications. J Acad Clin Microbiol. 2017;19(2):77–85. https://doi.org/10.4103/jacm.jacm_31_17
- Davidó B, Fellous L, Lawrence C, Maxime V, Rottman M, Dinh A. Ceftazidime-avibactam and aztreonam, an interesting

- strategy to overcome β -lactam resistance conferred by metallo- β -lactamases in *Enterobacteriaceae* and *Pseudomonas aeruginosa*. *Antimicrob Agents Chemother*. 2017 Sep;61(9):e01008-17. <https://doi.org/10.1128/AAC.01008-17>
- Dzierżanowska D.** Antybiotyko-terapia praktyczna (in Polish). Bielsko-Biala (Poland): α -medica Press; 2018. p. 206–209.
- ECDC. Antimicrobial Resistance Surveillance in Europe, 2013; Annual Report of the European Antimicrobial Resistance Surveillance Network (EARS-Net). Stockholm (Sweden): European Centre for Disease Prevention and Control; 2014 [cited 2019 Jun 11]. Available from <https://ecdc.europa.eu/en/publications-data/surveillance-antimicrobial-resistance-europe-2013>
- EMA/CVMP. Opinion following an Article 35 referral for veterinary medicinal formulations containing colistin at 2 000 000 IU per ml and intended for administration in drinking water to food producing species. Amsterdam (The Netherlands): European Medicines Agency, Committee for Medical Products for Veterinary Use; 2010 [cited 2019 Jun 11]. Available from http://www.ema.europa.eu/docs/en_GB/document_library/Referrals_document/Colistin_25/WC500093733.pdf.
- EUCAST. Breakpoint tables for interpretation of MICs and zone diameters. Version 6.0, 2016.; Basel (Switzerland): The European Committee on Antimicrobial Susceptibility Testing; 2016 [cited 2019 Jun 11]. Available from <http://www.eucast.org>
- Falagas ME, Kasiakou SK, Saravolatz LD.** Colistin: the revival of polymyxins for the management of multidrug-resistant gram-negative bacterial infections. *Clin Infect Dis*. 2005 May 01;40(9):1333–1341. <https://doi.org/10.1086/429323>
- Gaibani P, Campoli C, Lewis RE, Volpe SL, Scaltriti E, Giannella M, Pongolini S, Berlingeri A, Cristini F, Bartoletti M, et al.** *In vivo* evolution of resistant subpopulations of KPC-producing *Klebsiella pneumoniae* during ceftazidime/avibactam treatment. *J Antimicrob Chemother*. 2018 Jun 01;73(6):1525–1529. <https://doi.org/10.1093/jac/dky082>
- Galani I, Kontopidou F, Souli M, Rekatsina PD, Koratzanis E, Deliolanis J, Giamarellou H.** Colistin susceptibility testing by Etest and disk diffusion methods. *Int J Antimicrob Agents*. 2008 May; 31(5):434–439. <https://doi.org/10.1016/j.ijantimicag.2008.01.011>
- Gao B, Li X, Yang F, Chen W, Zhao Y, Bai G, Zhang Z.** Molecular epidemiology and risk factors of ventilator-associated pneumonia infection caused by carbapenem-resistant *Enterobacteriaceae*. *Front Pharmacol*. 2019 Mar 22;10:262. <https://doi.org/10.3389/fphar.2019.00262>
- García-Fernández S, García-Castillo M, Ruiz-Garbajosa P, Morosini MI, Bala Y, Zambardi G, Cantón R.** Performance of CHROMID® Colistin R agar, a new chromogenic medium for screening of colistin-resistant Enterobacterales. *Diagn Microbiol Infect Dis*. 2019 Jan;93(1):1–4. <https://doi.org/10.1016/j.diagmicrobio.2018.07.008>
- Ghafur A, Vidyalakshimi PR, Murali A, Priyadarshini K, Thirunarayan MA.** Emergence of Pan-drug resistance amongst gram negative bacteria! The First case series from India. *J Microbiol Infect Dis*. 2014 Sep 01;4(3):86–91. <https://doi.org/10.5799/ahinjs.02.2014.03.0145>
- Giske CG, Kahlmeter G.** Colistin antimicrobial susceptibility testing – can the slow and challenging be replaced by the rapid and convenient? *Clin Microbiol Infect*. 2018 Feb;24(2):93–94. <https://doi.org/10.1016/j.cmi.2017.10.007>
- Grundmann H, Livermore DM, Giske CG, Canton R, Rossolini GM, Campos J, Vatopoulos A, Gniadkowski M, Toth A, Pfeifer Y, Jarlier V, Carmeli Y; CNSE Working Group.** Carbapenem-non-susceptible *Enterobacteriaceae* in Europe: conclusions from a meeting of national experts. *Euro Surveill*. 2010 Nov 18; 15(46):19711.
- Guducuoglu H, Gursoy NC, Yakupogullari Y, Parlak M, Karasin G, Sunnetcioglu M, Otlu B.** Hospital outbreak of a colistin-resistant, NDM-1- and OXA-48-producing *Klebsiella pneumoniae*: high mortality from pandrug resistance. *Microb Drug Resist*. 2018 Sep;24(7):966–972. <https://doi.org/10.1089/mdr.2017.0173>
- Gundogdu A, Ulu-Kilic A, Kilic H, Ozhan E, Altun D, Cakir O, Alp E.** Could frequent carbapenem use be a risk factor for colistin resistance? *Microb Drug Resist*. 2018 Jul;24(6):774–781. <https://doi.org/10.1089/mdr.2016.0321>
- Humphries RM.** Susceptibility testing of the polymyxins: where are we now? *Pharmacotherapy*. 2015 Jan;35(1):22–27. <https://doi.org/10.1002/phar.1505>
- Izdebski R, Baraniak A, Bojarska K, Urbanowicz P, Fiett J, Pomorska-Wesołowska M, Hryniewicz W, Gniadkowski M, Żabicka D.** Mobile MCR-1-associated resistance to colistin in Poland: Table 1. *J Antimicrob Chemother*. 2016 Aug;71(8):2331–2333. <https://doi.org/10.1093/jac/dkw261>
- Jayol A, Nordmann P, Brink A, Poirel L.** Heteroresistance to colistin in *Klebsiella pneumoniae* associated with alterations in the PhoPQ regulatory system. *Antimicrob Agents Chemother*. 2015 May;59(5):2780–2784. <https://doi.org/10.1128/AAC.05055-14>
- Jayol A, Nordmann P, Poirel L, Dubois V.** Ceftazidime/avibactam alone or in combination with aztreonam against colistin-resistant and carbapenemase-producing *Klebsiella pneumoniae*. *J Antimicrob Chemother*. 2018 Feb 01;73(2):542–544. <https://doi.org/10.1093/jac/dkx393>
- Jayol A, Poirel L, André C, Dubois V, Nordmann P.** Detection of colistin-resistant Gram-negative rods by using the SuperPolymyxin medium. *Diagn Microbiol Infect Dis*. 2018 Oct;92(2):95–101. <https://doi.org/10.1016/j.diagmicrobio.2018.05.008>
- Jayol A, Poirel L, Dortet L, Nordmann P.** National survey of colistin resistance among carbapenemase-producing *Enterobacteriaceae* and outbreak caused by colistin-resistant OXA-48-producing *Klebsiella pneumoniae*, France, 2014. *Euro Surveill*. 2016; 21(37):30339. <https://doi.org/10.2807/1560-7917.ES.2016.21.37.30339>
- Jones-Dias D, Manageiro V, Ferreira E, Barreiro P, Vieira L, Moura IB, Caniça M.** Architecture of class 1, 2, and 3 integrons from Gram negative bacteria recovered among fruits and vegetables. *Front Microbiol*. 2016;7:1400. <https://doi.org/10.3389/fmicb.2016.01400>
- Jordan D, Chin JJ-C, Fahy VA, Barton MD, Smith MG, Trott DJ.** Antimicrobial use in the Australian pig industry: results of a national survey. *Aust Vet J*. 2009 Jun;87(6):222–229. <https://doi.org/10.1111/j.1751-0813.2009.00430.x>
- Jung Y, Jang H, Matthews KR.** Effect of the food production chain from farm practices to vegetable processing on outbreak incidence. *Microb Biotechnol*. 2014 Nov;7(6):517–527. <https://doi.org/10.1111/1751-7915.12178>
- Kempf I, Fleury MA, Drider D, Bruneau M, Sanders P, Chauvin C, Madec JY, Jouy E.** What do we know about resistance to colistin in *Enterobacteriaceae* in avian and pig production in Europe? *Int J Antimicrob Agents*. 2013 Nov;42(5):379–383. <https://doi.org/10.1016/j.ijantimicag.2013.06.012>
- Kim DP, Saegerman C, Douny C, Dinh TV, Xuan BH, Vu BD, Hong NP, Scippo M-L.** First survey on the use of antibiotics in pig and poultry production in the Red River Delta region of Vietnam. *Food Public Health*. 2013;3(5):247–256. <https://doi.org/10.5923/j.fph.20130305.03>
- Koch-Weser J, Sidel VW, Federman EB, Kanarek P, Finer DC, Eaton AE.** Adverse effects of sodium colistimethate. Manifestations and specific reaction rates during 317 courses of therapy. *Ann Intern Med*. 1970 Jun 01;72(6):857–868. <https://doi.org/10.7326/0003-4819-72-6-857>

- Kostowski W, Herman ZS. Farmakologia (in Polish). Warsaw (Poland): PZWL Press; 2010. p. 341–342.
- Kwa ALH, Loh C, Low JGH, Kurup A, Tam VH. Nebulized colistin in the treatment of pneumonia due to multidrug-resistant *Acinetobacter baumannii* and *Pseudomonas aeruginosa*. Clin Infect Dis. 2005 Sep 01;41(5):754–757. <https://doi.org/10.1086/432583>
- Kwon JA, Lee JE, Huh W, Peck KR, Kim YG, Kim DJ, Oh HY. Predictors of acute kidney injury associated with intravenous colistin treatment. Int J Antimicrob Agents. 2010 May;35(5):473–477. <https://doi.org/10.1016/j.ijantimicag.2009.12.002>
- Lellouche J, Schwartz D, Elmalech N, Ben Dalak MA, Temkin E, Paul M, Geffen Y, Yahav D, Eliakim-Raz N, Durante-Mangoni E, et al.; AIDA study group. Combining VITEK² with colistin agar dilution screening assist timely reporting of colistin susceptibility. Clin Microbiol Infect. 2019 Jun;25(6):711–716. <https://doi.org/10.1016/j.cmi.2018.09.014>
- Li J, Nation RL, Milne RW, Turnidge JD, Coulthard K. Evaluation of colistin as an agent against multi-resistant Gram-negative bacteria. Int J Antimicrob Agents. 2005 Jan;25(1):11–25. <https://doi.org/10.1016/j.ijantimicag.2004.10.001>
- Li J, Nation RL, Turnidge JD, Milne RW, Coulthard K, Rayner CR, Paterson DL. Colistin: the re-emerging antibiotic for multidrug-resistant Gram-negative bacterial infections. Lancet Infect Dis. 2006 Sep;6(9):589–601. [https://doi.org/10.1016/S1473-3099\(06\)70580-1](https://doi.org/10.1016/S1473-3099(06)70580-1)
- Li J. Difficulty in assaying colistin methanesulphonate. Clin Microbiol Infect. 2005 Sep;11(9):773–774. <https://doi.org/10.1111/j.1469-0691.2005.01218.x>
- Li R, Xie M, Zhang J, Yang Z, Liu L, Liu X, Zheng Z, Chan EWC, Chen S. Genetic characterization of *mcr-1*-bearing plasmids to depict molecular mechanisms underlying dissemination of the colistin resistance determinant. J Antimicrob Chemother. 2017 Feb;72(2):393–401. <https://doi.org/10.1093/jac/dkw411>
- Lim LM, Ly N, Anderson D, Yang JC, Macander L, Jarkowski A 3rd, Forrest A, Bulitta JB, Tsuji BT. Resurgence of colistin: a review of resistance, toxicity, pharmacodynamics, and dosing. Pharmacotherapy. 2010 Dec;30(12):1279–1291. <https://doi.org/10.1592/phco.30.12.1279>
- Liu B-T, Li X, Zhang Q, Shan H, Zou M, Song F-J. Colistin-resistant *mcr*-positive *Enterobacteriaceae* in fresh vegetables, an increasing infectious threat in China. Int J Antimicrob Agents. 2019;54(1):89–94. <https://doi.org/10.1016/j.ijantimicag.2019.04.013>
- Liu YY, Wang Y, Walsh TR, Yi LX, Zhang R, Spencer J, Doi Y, Tian G, Dong B, Huang X, et al. Emergence of plasmid-mediated colistin resistance mechanism MCR-1 in animals and human beings in China: a microbiological and molecular biological study. Lancet Infect Dis. 2016 Feb;16(2):161–168. [https://doi.org/10.1016/S1473-3099\(15\)00424-7](https://doi.org/10.1016/S1473-3099(15)00424-7)
- Lomovskaya O, Sun D, Rubio-Aparicio D, Nelson K, Tsvikovski R, Griffith DC, Dudley MN. Vaborbactam: spectrum of beta-lactamase inhibition and impact of resistance mechanisms on activity in *Enterobacteriaceae*. Antimicrob Agents Chemother. 2017 Nov;61(11):e01443-17. <https://doi.org/10.1128/AAC.01443-17>
- Luo J, Yao X, Lv L, Doi Y, Huang X, Huang S, Liu JH. Emergence of *mcr-1* in *Raoultella ornithinolytica* and *Escherichia coli* isolates from retail vegetables in China. Antimicrob Agents Chemother. 2017 Oct;61(10):e01139-17. <https://doi.org/10.1128/AAC.01139-17>
- MARAN. NethMap 2019: Consumption of antimicrobial agents and antimicrobial resistance among medically important bacteria in the Netherlands/MARAN 2019: Monitoring of Antimicrobial Resistance and Antibiotic Usage in Animals in the Netherlands in 2018. Wageningen (The Netherlands): Wageningen University & Research; 2019 [cited 2019 Jun 11]. Available from https://www.wur.nl/upload_mm/a/7/9/89640bbc-53a2-40f0-ba4a-a9a34a7bf416_Nethmap%20Maran%202019.pdf
- Marchaim D, Chopra T, Pogue JM, Perez F, Hujer AM, Rudin S, Endimiani A, Navon-Venezia S, Hothi J, Slim J, et al. Outbreak of colistin-resistant, carbapenem-resistant *Klebsiella pneumoniae* in metropolitan Detroit, Michigan. Antimicrob Agents Chemother. 2011 Feb;55(2):593–599. <https://doi.org/10.1128/AAC.01020-10>
- MARD (Ministry of Agriculture and Rural Development). 2009. Livestock development strategy to 2020, Amended and Reprinted in the first time. Publishing House for Science and Technology.
- MARD. (Ministry of Agriculture and Rural Development). Standard TCN. 2006;861:2006. [Animal feeding stuffs – Maximum levels of antibiotics and drugs in complete feed.].
- Matuschek E, Ahman J, Webster C, Kahlmeter G. Antimicrobial susceptibility testing of colistin – evaluation of seven commercial MIC products against standard broth microdilution for *Escherichia coli*, *Klebsiella pneumoniae*, *Pseudomonas aeruginosa*, and *Acinetobacter* spp. Clin Microbiol Infect. 2018a Aug;24(8):865–870. <https://doi.org/10.1016/j.cmi.2017.11.020>
- Matuschek E, Davies L, Ahman J, Kahlmeter G, Wootton M. Can agar dilution be used for colistin MIC determination? Session: Colistin antimicrobial susceptibility testing – which methods are available? ECCMID 2018, 24 April 2018, Abstract publication O0954. 2018b [cited 2019 Jun 11]. Available from https://www.escmid.org/escmid_publications/escmid_elibrary/?q=Matuschek+E&id=2173&L=0&x=21&y=24
- Meletis G, Oustas E, Botziori C, Kakasi E, Koteli A. Containment of carbapenem resistance rates of *Klebsiella pneumoniae* and *Acinetobacter baumannii* in a Greek hospital with a concomitant increase in colistin, gentamicin and tigecycline resistance. New Microbiol. 2015 Jul;38(3):417–421.
- Moffatt JH, Harper M, Harrison B, Hale JD, Vinogradov E, Seemann T, Henry R, Crane B, St Michael E, Cox AD, et al. Colistin resistance in *Acinetobacter baumannii* is mediated by complete loss of lipopolysaccharide production. Antimicrob Agents Chemother. 2010;54(12):4971–4977. <https://doi.org/10.1128/AAC.00834-10>
- Monaco M, Giani T, Raffone M, Arena F, Garcia-Fernandez A, Pollini S; Network EuSCAPE-Italy, Grundmann H, Pantosti A, Rossolini GM. Colistin resistance superimposed to endemic carbapenem-resistant *Klebsiella pneumoniae*: a rapidly evolving problem in Italy, November 2013 to April 2014. Euro Surveill. 2014;19(42):20939. <https://doi.org/10.2807/1560-7917.es2014.19.42.20939>
- Nation RL, Li J. Colistin in the 21st century. Curr Opin Infect Dis. 2009 Dec;22(6):535–543. <https://doi.org/10.1097/QCO.0b013e328332e672>
- Nordmann P, Jayol A, Poirel L. A universal culture medium for screening polymyxin-resistant Gram-negative isolates. J Clin Microbiol. 2016 May;54(5):1395–1399. <https://doi.org/10.1128/JCM.00446-16>
- Nordmann P, Jayol A, Poirel L. Rapid detection of polymyxin resistance in *Enterobacteriaceae*. Emerg Infect Dis. 2016 Jun;22(6):1038–1043. <https://doi.org/10.3201/eid2206.151840>
- Nunan C, Young R. Use of antibiotics in animals and people. Vet Rec. 2015 Nov 07;177(18):468.2–470. <https://doi.org/10.1136/vr.h5934>
- Olaitan AO, Diene SM, Kempf M, Berrazeg M, Bakour S, Gupta SK, Thongmalayong B, Akkhavong K, Somphavong S, Paboriboune P, et al. Worldwide emergence of colistin resistance in *Klebsiella pneumoniae* from healthy humans and patients in Lao PDR, Thailand, Israel, Nigeria and France owing to inactivation of the PhoP/PhoQ regulator mgrB: an epidemiological and molecular study. Int J Antimicrob Agents. 2014 Dec;44(6):500–507. <https://doi.org/10.1016/j.ijantimicag.2014.07.020>
- Olaitan AO, Morand S, Rolain JM. Mechanisms of polymyxin resistance: acquired and intrinsic resistance in bacteria. Front Microbiol. 2014 Nov 26;5:643. <https://doi.org/10.3389/fmicb.2014.00643>

- Ordooei Javan A, Shokouhi S, Sahraei Z. A review on colistin nephrotoxicity. *Eur J Clin Pharmacol*. 2015 Jul;71(7):801–810. <https://doi.org/10.1007/s00228-015-1865-4>
- Parisi SG, Bartolini A, Santacatterina E, Castellani E, Ghirardo R, Berto A, Franchin E, Menegotto N, De Canale E, Tommasini T, et al. Prevalence of *Klebsiella pneumoniae* strains producing carbapenemases and increase of resistance to colistin in an Italian teaching hospital from January 2012 To December 2014. *BMC Infect Dis*. 2015 Dec;15(1):244. <https://doi.org/10.1186/s12879-015-0996-7>
- Pena I, Picazo JJ, Rodríguez-Avial C, Rodríguez-Avial I. Carbapenemase-producing *Enterobacteriaceae* in a tertiary hospital in Madrid, Spain: high percentage of colistin resistance among VIM-1-producing *Klebsiella pneumoniae* ST11 isolates. *Int J Antimicrob Agents*. 2014 May;43(5):460–464. <https://doi.org/10.1016/j.ijantimicag.2014.01.021>
- Petrosillo N, Taglietti F, Granata G. Treatment Options for Colistin Resistant *Klebsiella pneumoniae*: Present and Future. *J Clin Med*. 2019;28;8(7):E934. <https://doi.org/10.3390/jcm8070934>
- Pfaller MA, Huband MD, Mendes RE, Flamm RK, Castanheira M. *In vitro* activity of meropenem/vaborbactam and characterisation of carbapenem resistance mechanisms among carbapenem-resistant *Enterobacteriaceae* from the 2015 meropenem/vaborbactam surveillance programme. *Int J Antimicrob Agents*. 2018 Aug;52(2):144–150. <https://doi.org/10.1016/j.ijantimicag.2018.02.021>
- Pogue JM, Bonomo RA, Kaye KS. Ceftazidime/avibactam, meropenem/vaborbactam, or both? Clinical and formulary considerations. *Clin Infect Dis*. 2019 Jan 18;68(3):519–524. <https://doi.org/10.1093/cid/ciy576>
- Pogue JM, Lee J, Marchaim D, Yee V, Zhao JJ, Chopra T, Lephart P, Kaye KS. Incidence of and risk factors for colistin-associated nephrotoxicity in a large academic health system. *Clin Infect Dis*. 2011 Nov 01;53(9):879–884. <https://doi.org/10.1093/cid/cir611>
- Poirel L, Jayol A, Nordmann P. Polymyxins: antibacterial activity, susceptibility testing, and resistance mechanisms encoded by plasmids or chromosomes. *Clin Microbiol Rev*. 2017 Apr;30(2):557–596. <https://doi.org/10.1128/CMR.00064-16>
- QYResearch Medical Research Centre. The global polymyxin industry report 2015. Ottawa (Canada): QYResearch Medical Research Centre; 2015 [cited 2019 Jun 11]. Available from <http://www.qyresearch.com>
- Sandri AM, Landersdorfer CB, Jacob J, Boniatti MM, Dal-rosa MG, Falci DR, Behle TF, Bordinhão RC, Wang J, Forrest A, et al. Population pharmacokinetics of intravenous polymyxin B in critically ill patients: implications for selection of dosage regimens. *Clin Infect Dis*. 2013 Aug 15;57(4):524–531. <https://doi.org/10.1093/cid/cit334>
- Schindler M, Osborn MJ. Interaction of divalent cations and polymyxin B with lipopolysaccharide. *Biochemistry*. 1979 Oct 02;18(20):4425–4430. <https://doi.org/10.1021/bi00587a024>
- SdA Autoriteit Diergezondheidszaken. Usage of antibiotics in agricultural livestock in the Netherlands in 2017. Trends and benchmarking of livestock farms and veterinarians. Utrecht (The Netherlands): SdA Autoriteit Diergezondheidszaken; 2018 [cited 2019 Jun 11]. Available from <https://www.autoriteitdiergezondheidszaken.nl/en/publications>
- Shields RK, Chen L, Cheng S, Chavda KD, Press EG, Snyder A, Pandey R, Doi Y, Kreiswirth BN, Nguyen MH, et al. Emergence of ceftazidime-avibactam resistance due to plasmid-borne *bla*_{KPC-3} mutations during treatment of carbapenem-resistant *Klebsiella pneumoniae* infections. *Antimicrob Agents Chemother*. 2017 Mar; 61(3):e02097-16. <https://doi.org/10.1128/AAC.02097-16>
- Shields RK, Clancy CJ, Hao B, Chen L, Press EG, Iovine NM, Kreiswirth BN, Nguyen MH. Effects of *Klebsiella pneumoniae* carbapenemase subtypes, extended-spectrum β -lactamases, and porin mutations on the *in vitro* activity of ceftazidime-avibactam against carbapenem-resistant *K. pneumoniae*. *Antimicrob Agents Chemother*. 2015 Sep;59(9):5793–5797. <https://doi.org/10.1128/AAC.00548-15>
- Sjölund M, Backhans A, Greko C, Emanuelson U, Lindberg A. Antimicrobial usage in 60 Swedish farrow-to-finish pig herds. *Prev Vet Med*. 2015 Oct;121(3-4):257–264. <https://doi.org/10.1016/j.prevetmed.2015.07.005>
- Spapen H, Jacobs R, Van Gorp V, Troubleyn J, Honoré PM. Renal and neurological side effects of colistin in critically ill patients. *Ann Intensive Care*. 2011 Dec;1(1):14. <https://doi.org/10.1186/2110-5820-1-14>
- SWEDRES/SVARM. Consumption of antibiotics and occurrence of antibiotic resistance in Sweden. Solna/Uppsala (Sweden): Public Health Agency of Sweden and National Veterinary Institute; 2018 [cited 2019 Jun 11]. Available from <https://www.folkhalsomyndigheten.se/contentassets/d8f6b3d187a94682a1d50a48f0a4fb3d/swedres-svarm-2018.pdf>
- Trautfler M, Griesbacher A, Fuchs K, Köfer J. Antimicrobial drug use in Austrian pig farms: plausibility check of electronic on-farm records and estimation of consumption. *Vet Rec*. 2014 Oct 25;175(16):402. <https://doi.org/10.1136/vr.102520>
- Tullu MS, Dhariwal AK. Colistin: re-emergence of the ‘forgotten’ antimicrobial agent. *J Postgrad Med*. 2013;59(3):208–215. <https://doi.org/10.4103/0022-3859.118040>
- Tumbarello M, Trecarichi EM, De Rosa FG, Giannella M, Giacobbe DR, Bassetti M, Losito AR, Bartoletti M, Del Bono V, Corcione S, et al.; ISGRI-SITA (Italian Study Group on Resistant Infections of the Società Italiana Terapia Antinfettiva). Infections caused by KPC-producing *Klebsiella pneumoniae*: differences in therapy and mortality in a multicentre study. *J Antimicrob Chemother*. 2015 Jul 01;70(7):2133–2143. <https://doi.org/10.1093/jac/dkv086>
- Tumbarello M, Viale P, Viscoli C, Trecarichi EM, Tumietto F, Marchese A, Spanu T, Ambretti S, Ginocchio F, Cristini F, et al. Predictors of mortality in bloodstream infections caused by *Klebsiella pneumoniae* carbapenemase-producing *K. pneumoniae*: importance of combination therapy. *Clin Infect Dis*. 2012 Oct 01;55(7):943–950. <https://doi.org/10.1093/cid/cis588>
- Turlej-Rogacka A, Xavier BB, Janssens L, Lammens C, Zarkotou O, Pournaras S, Goossens H, Malhotra-Kumar S. Evaluation of colistin stability in agar and comparison of four methods for MIC testing of colistin. *Eur J Clin Microbiol Infect Dis*. 2018 Feb;37(2):345–353. <https://doi.org/10.1007/s10096-017-3140-3>
- U.S. National Library of Medicine. A study of meropenem-vaborbactam versus piperacillin/tazobactam in participants with hospital-acquired and ventilator-associated bacterial pneumonia (TANGOIII). <https://clinicaltrials.gov/ct2/show/NCT03006679>
- van Rennings L, von Münchhausen C, Otilie H, Hartmann M, Merle R, Honscha W, Käsbohrer A, Kreienbrock L. Cross-sectional study on antibiotic usage in pigs in Germany. *PLoS ONE*. 2015; 0(3): e0119114. <https://doi.org/10.1371/journal.pone.0119114>
- Vasoo S. Susceptibility testing for the polymyxins: two steps back, three steps forward? *J Clin Microbiol*. 2017;55(9):2573–2582. <https://doi.org/10.1128/JCM.00888-17>
- Vicari G, Bauer SR, Neuner EA, Lam SW. Association between colistin dose and microbiologic outcomes in patients with multi-drug-resistant Gram-negative bacteremia. *Clin Infect Dis*. 2013;56: 398–404. <https://doi.org/10.1093/cid/cis909>
- Walkty A, DeCorby M, Nichol K, Karlowsky JA, Hoban DJ, Zhanel GG. *In vitro* activity of colistin (polymyxin E) against 3,480 isolates of gram-negative bacilli obtained from patients in Canadian

- hospitals in the CANWARD study, 2007–2008. *Antimicrob Agents Chemother.* 2009 Nov 01;53(11):4924–4926. <https://doi.org/10.1128/AAC.00786-09>
- Wang X, Wang Y, Zhou Y, Li J, Yin W, Wang S, Zhang S, Shen J, Shen Z, Wang Y. Emergence of a novel mobile colistin resistance gene, *mcr-8*, in NDM-producing *Klebsiella pneumoniae*. *Emerg Microbes Infect.* 2018 Dec;7(1):1–9. <https://doi.org/10.1038/s41426-018-0124-z>
- Xavier BB, Lammens C, Ruhul R, Kumar-Singh S, Butaye P, Goossens H, Malhotra-Kumar S. Identification of a novel plasmid-mediated colistin-resistance gene, *mcr-2*, in *Escherichia coli*. *Euro Surveill.* 2016;21(27):30280. <https://doi.org/10.2807/1560-7917.ES.2016.21.27.30280>
- Yang Y-Q, Li Y-X, Lei C-W, Zhang A-Y, Wang H-N. 2018. Novel plasmid mediated colistin resistance gene *mcr-7.1* in *Klebsiella pneumoniae*. *J Antimicrob Chemother.* 73(7):1791–1795. <https://doi.org/10.1093/jac/dky111>
- Yin W, Li H, Shen Y, Liu Z, Wang S, Shen Z, Zhang R, Walsh RT, Shen J, Wang Y. 2017. Novel plasmid-mediated colistin resistance gene *mcr-3* in *Escherichia coli*. *MBio.* 8:e0054317. <https://doi.org/10.1128/mBio.00543-17>
- Zhanell GG, Lawson CD, Adam H, Schweizer F, Zelenitsky S, Lagacé-Wiens PR, Denisuk A, Rubinstein E, Gin AS, Hoban DJ, et al. Ceftazidime-avibactam: a novel cephalosporin/β-lactamase inhibitor combination. *Drugs.* 2013;73(2):159–77. <https://doi.org/10.1007/s40265-013-0013-7>
- Zhang H, Zhao D, Quan J, Hua X, Yu Y. *mcr-1* facilitated selection of high-level colistin-resistant mutants in *Escherichia coli*. *Clin Microbiol Infect.* 2019;25(4):517.e1–517.e4. <https://doi.org/10.1016/j.cmi.2018.12.014>
- Zhang Y, Wang Q, Yin Y, Chen H, Jin L, Gu B, Xie L, Yang C, Ma X, Li H, et al. Epidemiology of carbapenem-resistant *Enterobacteriaceae* infections: report from the China CRE Network. *Antimicrob Agents Chemother.* 2018;62(2): e01882-17. <https://doi.org/10.1128/AAC.01882-17>
- Zhon HW, Zhang T, Ma JH, Fang Y, Wang HY, Huang ZX, Wang Y, Wu C, Chen GX. Occurrence of plasmid- and chromosome-carried *mcr-1* in water-borne *Enterobacteriaceae* in China. *Antimicrob Agents Chemother.* 2017;61(8):e00017-17. <https://doi.org/10.1128/AAC.00017-17>
- Zou D, Huang S, Lei H, Yang Z, Su Y, He X, Zhao Q, Wang Y, Liu W, Huang L. Sensitive and rapid detection of the plasmid-encoded colistin-resistance gene *mcr-1* in *Enterobacteriaceae* isolates by loop-mediated isothermal amplification. *Front Microbiol.* 2017;8:2356. <https://doi.org/10.3389/fmicb.2017.02356>
- Zurfluh K, Poirel L, Nordmann P, Nuesch-Inderbinen M, Hachler H, Stefan R. Occurrence of the plasmid-borne *mcr-1* colistin resistance gene in extended-spectrum-beta-lactamase-producing *Enterobacteriaceae* in river water and imported vegetables was identified in Switzerland. *Antimicrob Agents Chemother.* 2016;60(4):2594–2595. <https://doi.org/10.1128/AAC.00066-16>

Molecular Identification of *Vibrio alginolyticus* Causing Vibriosis in Shrimp and Its Herbal Remedy

MD. ABDUL HANNAN¹, MD. MAHBUBUR RAHMAN^{2*}, MD. NURUNNABI MONDAL³,
SUZAN CHANDRA DEB², GAZLIMA CHOWDHURY⁴ and MD. TOFAZZAL ISLAM²

¹Department of Aquatic Animal Health Management, Sher-e-Bangla Agricultural University, Dhaka, Bangladesh

²Institute of Biotechnology and Genetic Engineering, Bangabandhu Sheikh Mujibur Rahman Agricultural University, Gazipur, Bangladesh

³Department of Fisheries Management, Bangabandhu Sheikh Mujibur Rahman Agricultural University, Gazipur, Bangladesh

⁴Department of Aquatic Environment and Resource Management, Sher-e-Bangla Agricultural University, Dhaka, Bangladesh

Submitted 19 April 2019, revised 5 August 2019, accepted 5 August 2019

Abstract

Penaeus monodon is highly susceptible to vibriosis disease. Aims of the study were to identify the pathogen causing vibriosis in *P. monodon* through molecular techniques and develop a biocontrol method of the disease by application of herbal extracts. Shrimp samples were collected aseptically from the infected farm and the bacteria were isolated from the infected region of those samples. Based on phenotypic identification, several isolates were identified as *Vibrio* sp. 16S rRNA gene sequences of the selected isolates exhibited 100% homology with *V. alginolyticus* strain ATCC 17749. An *in vivo* infection challenge test was performed by immersion method with *V. alginolyticus* where these isolates caused high mortality in juvenile shrimp with prominent symptoms of hepatopancreatic necrosis. Antibiogram profile of the isolates was determined against eleven commercial antibiotic discs whereas the isolates were found resistant to multiple antibiotics. A total of twenty-one herbal extracts were screened where *Emblia officinalis*, *Allium sativum*, and *Syzygium aromaticum* strongly inhibited the growth of *V. alginolyticus* in *in vitro* conditions. In *in vivo* conditions, the ethyl acetate extracts of *E. officinalis* and *A. sativum* successfully controlled the vibriosis disease in shrimp at a dose of 10 mg/g feed. This is the first report on molecular identification and biocontrol of *V. alginolyticus* in shrimp in Bangladesh.

Key words: *Penaeus monodon*, hepatopancreatic necrosis, *in vivo* challenge test, *Emblia officinalis*, *Allium sativum*

Introduction

Shrimp culture is one of the fastest-growing aquaculture industries in Bangladesh. A dramatic expansion of shrimp culture occurred in the 1980s significantly contributed to the economy of Bangladesh (Paul and Vogl 2011; Hossain et al. 2013). However, in the recent years, shrimp production in Bangladesh has severely been affected by the outbreak of various diseases such as black spot, softshell, external fouling, broken appendages, hepatopancreatic infection, and vibriosis (Chowdhury et al. 2015; Ali et al. 2018). Among these diseases, vibriosis is considered as one of the most important bacterial diseases in shrimp farms of Bangladesh. Vibriosis infects both penaeids and non-penaeid shrimps (Chowdhury

et al. 2015) and is responsible for high mortality in aquaculture worldwide (Lightner 1988; Sparagano 2002), and can devastate the entire shrimp farm (Wei and Wendy 2012). Several members of *Vibrio* genus such as *V. harveyi*, *V. anguillarum*, *V. splendidus*, *V. parahaemolyticus*, *V. fluvialis*, and *V. alginolyticus* are reported as the causative agents of vibriosis in shrimp (de la Pena et al. 1993; Karunasagar et al. 1994; Lee et al. 1996; Lightner 1996; Austin and Zhang 2006; Chatterjee and Halder 2012). No molecular level study has so far been conducted to precisely identify the causal agent of vibriosis in shrimp in Bangladesh and the required effective management for this worrisome disease.

A number of antibiotics and chemotherapeutic agents have been used in shrimp farms to prevent and

* Corresponding author: Md. M. Rahman, Fisheries Biotechnology Discipline, Institute of Biotechnology and Genetic Engineering, Bangabandhu Sheikh Mujibur Rahman Agricultural University, Gazipur, Bangladesh; e-mail: mahbub-biotech@bsmrau.edu.bd
© 2019 Md. Abdul Hannan et al.

This work is licensed under the Creative Commons Attribution-NonCommercial-NoDerivatives 4.0 License (<https://creativecommons.org/licenses/by-nc-nd/4.0/>).

control of microbial diseases including vibriosis (Mohney et al. 1992; Hossain et al. 2012; Karim et al. 2018). But indiscriminate and careless use of antibiotics leads to the development of antibiotic resistance in microorganisms (Karunasagar et al. 1994), which is now a major health concern worldwide (Karim et al. 2018). Therefore, an alternative approach is needed for effective and sustainable management of vibriosis in shrimp. Herbal extracts could be used as safe and alternative to synthetic antibiotics for the management of vibriosis in shrimp. Although *Vibrio* sp. is the important causal pathogen in shrimp farms, the investigation of the herbal remedy of vibriosis in shrimp is very limited in Bangladesh. Bangladesh is rich in diversified medicinal plants (Yusuf et al. 2009) and some of them have been found effective in the management of fish diseases. It has been demonstrated that methanol extracts of *A. sativum*, and methanol and acetone extracts of *S. aromaticum* significantly reduce the mortality of tilapia fish, artificially infected with *Enterococcus faecalis* as both preventive and therapeutic agents (Sindermann 1990). However, no study has so far been conducted in Bangladesh for the management of shrimp diseases caused by *Vibrio* sp. using herbal extracts. Therefore, the objectives of this study were to (i) identify the causal agent(s) of vibriosis in shrimp through physiological, biochemical and molecular techniques, (ii) assess the antibiotic susceptibility profile in the isolated shrimp pathogenic *Vibrio* sp., and (iii) control of vibriosis through the treatment with herbal extracts.

Experimental

Materials and Methods

Isolation and phenotypic identification of bacteria from the infected shrimp. Shrimp (*P. monodon*) suspected to be suffering from vibriosis were collected from different farms located in Satkhira district (near to Sundarbans mangrove forest at the south-west part of Bangladesh). The moribund shrimp were collected and individually kept in sterilized polythene bags and transported to the laboratory of the Faculty of Fish-

eries of Bangabandhu Sheikh Mujibur Rahman Agricultural University, Gazipur, Bangladesh maintaining proper icing and aseptic condition. The symptoms of the infected shrimp such as deformed and discolored (blackish or yellowish) hepatopancreas and reddening of the body (Table I) were recorded. The hepatopancreas of the shrimps were dissected and the samples were serially diluted. Hundred microliters of the diluted (10^{-5} to 10^{-7}) samples were spread on nutrient agar (NA; supplemented with 2% NaCl) and thiosulfate citrate bile salt (TCBS) agar plates to isolate the bacteria (Shaanmugasundaram et al. 2015). The agar plates were incubated at 28°C for 24–48 hours in an incubator (Liu et al. 2004). Several colonies were randomly selected from each plate and inoculated on NA media to obtain a pure culture. The isolates were routinely sub-cultured on NA plates and stock cultures were maintained in nutrient broth supplemented with 2% NaCl and 10% glycerol and stored in a freezer at –20°C. Individual colonies grown on NA or TCBS plates were observed and colony characteristics such as colony size, shape, color, type, etc. were recorded. To identify the isolates, Gram's staining, bacterial shape, motility, catalase, oxidase, oxidative-fermentative (O-F) test, acetoin production, indole production, arginine dihydrolase, lysine decarboxylase, hydrogen sulfide (H_2S) production, acid production from glucose, arabinose, mannitol, sorbitol and sucrose, sensitivity to Vibriostatic agent 0/129, growth at 4°C and 40°C were observed (Alsina and Blanch 1994; Rahman et al. 2010). Growth of the bacterial isolates in different salt concentrations was studied by supplementing the NA media with 2, 4, 6, and 8% of NaCl and incubated at 28°C. Growth in the absence of NaCl was studied by removing the NaCl from the NA.

Molecular identification of *Vibrio* isolates. Of a total of 20 isolates, genomic DNA of four representatives of *Vibrio* isolates (2A1a, 2A3, 2A11 and 2V21) was extracted using a commercial DNA extraction kit (GeneJET Genomic DNA purification Kit K0721, Thermo Scientific). The quantity of the extracted DNA was checked by electrophoresis on 0.8% agarose gel and compared with a lambda DNA marker (Promega). The DNA was stored at –20°C for further use. Polymerase chain reaction (PCR) for amplification of the targeted

Table I
External symptoms of vibriosis and the site of isolation of pathogen from infected shrimp collected from the shrimp farms.

Sample No.	Symptoms	Site of isolation
01–04	Deformed and yellowish colored hepatopancreas	Hepatopancreas
05–06	Blackish colored hepatopancreas	Hepatopancreas
07–11	Discolored hepatopancreas	Hepatopancreas
12–13	Yellowish colored hepatopancreas	Hepatopancreas
14–15	No visible symptom	Hepatopancreas

16S rRNA gene sequences of the isolates was performed with universal primer sets 27F (5'-AGAGTTTGATCCTGGCTCAG-3') and 1492R (5'-GGTTACCTTGT-TACGACTT-3') (Sigma Ltd.). Each PCR mixture contained 6 µl of 25 mM MgCl₂, 10 µl of 10×PCR buffer, 2.0 µl of 10 mM deoxyribonucleotide triphosphate, 5.0 µl of a 20 µM solution of each primers, 100–200 ng of DNA template, 0.5 µl of *Taq* DNA polymerase (Promega) at 5 U µl/l, and sterile double-distilled water in a total volume of 100 µl. The PCR amplification was performed in a PCR thermocycler (Eppendorf Ltd.). The optimal conditions for PCR were set as follows: an initial denaturation step at 94°C for 5 min; 35 cycles of a denaturation step at 94°C for 1 min, an annealing at 57°C for 40 second, and an extension at 72°C for 1 min and a final extension step at 72°C for 7 min. A small portion (usually 5 µl) of the PCR amplicons were mixed with 1–2 µl of 6× loading dye and loaded in a 1.5% agarose gel with 1 Kb ladder marker (Promega). Then, electrophoresis was performed in 0.5× Tris-Borate-EDTA (TBE) buffer for 40 min at 70 volts. Amplicons were visualized with UV light in a gel documentation system (Weltec KETA G, Weltec Corp.). The PCR product was purified using a commercial Gel/PCR Purification Kit (FavorPrep™, Favorgen® Biotech Corp.) following the manufacturer's protocol. The DNA sequencing was done in the Center for Advanced Research in Sciences (CARS) at the University of Dhaka in a DNA sequencer (ABI-3130, Applied BioSystems). The sequence data was extracted by using BIOAD software as FASTA format. The DNA sequences (FASTA format) of the isolates were then analyzed using web-based Basic Local Alignment Search Tool (BLAST) program of National Centre for Biotechnology Information (NCBI) and phylogenetic analysis was done using the Phylogeny.fr web-based software.

***In vivo* challenge test.** To evaluate the pathogenic potential of the isolates, four representatives of *Vibrio* sp. isolates (2A1a, 2A3, 2A11 and 2V21) were used for *in vivo* challenge test following the immersion method with three replications. We followed Completely Randomized Design (CRD) for the experiment. Juvenile shrimp (average length 3.5 ± 0.13 cm, weight 2.1 ± 0.4 g) were collected from a nursery pond of a private hatchery and acclimatized in an aquarium at room temperature and continued for seven days. Bacterial inoculums for infection challenge test were prepared by adding 30 ml of 24 hours TCBS broth culture into 2970 ml sterile saline solution (2% w/v NaCl). TCBS broth culture was used for specific and better growth of *Vibrio* bacterium. The density of the inoculums was 4.2 × 10⁶, 3.8 × 10⁶, 5.6 × 10⁶, and 5.4 × 10⁶ CFU/ml for the isolates 2A1a, 2A3, 2A11, and 2V21, respectively. Sixty juvenile shrimp (twenty juveniles in each aquarium) were immersed into individual bacterial suspension for 20 minutes at room temperature (about 25°C) and then transferred

to three separate aquaria containing 15 l saline water. A group of shrimp was maintained as a negative control, which was not inoculated with any bacterial suspension. The treated juveniles were regularly monitored at six hours interval for seven days, and the signs of infection and/or mortality was recorded. The mortality data were analyzed by ANOVA at <0.05> level of significance. Bacteria were re-isolated from the hepatopancreases of dead and infected shrimps on NA agar supplemented with 2% NaCl and identified based on their phenotypic characteristics (Rahman et al. 2017).

***In vitro* antibiogram assay.** Susceptibility profile of four representatives of *Vibrio* isolates (2A1a, 2A3, 2A11 and 2V21) was determined by disc diffusion method (Jorgensen and Ferraro 2009; Rahman and Hossain 2010) against of eleven commercial antibiotic discs. Antibiotic discs used in this study were erythromycin (15 µg/disc), penicillin (10 µg/disc), cefradine (25 µg/disc), levofloxacin (5 µg/disc), azithromycin (30 µg/disc), amoxicillin (30 µg/disc), cefuroxime (30 µg/disc), vancomycin (30 µg/disc), nitrofurantoin (30 µg/disc), ampicillin (25 µg/disc), and gentamycin (10 µg/disc) (manufactured by HiMedia Laboratories Pvt. Ltd.). Bacterial culture was spread on the Isosensei test agar plates (Traub et al. 1998; BSAC 2015; Rahman et al. 2017) and the antibiotic discs were placed on the culture plates and incubated at 37°C for 24 hours in an incubator. After incubation, the diameter of the inhibition zone (if any) was measured. The isolates were considered as sensitive or resistant according to CLSI-specified interpretive criteria (CLSI 2005).

***In vitro* inhibitory activity of herbal extracts.** Twenty-one medicinal herb extracts were used in this study to screen their inhibitory activity against the *Vibrio* isolates (Table II). The plants were selected based on their recognized medicinal properties described elsewhere (Muniruzzaman and Chowdhury 2004; Rahman and Hossain 2010; Rahman et al. 2017). For the preparation of herb extracts, 25 g of dried fresh herb materials were added into 100 ml sterile distilled water, *n*-hexane, ethyl acetate, acetone, and methanol. The samples were gently rotated in an orbital shaker at room temperature for 72 hours and then evaporated in a rotary evaporator at 50°C. The dried extracts were dissolved in respective solvents to adjust the concentration at 25 mg/ml. Sterilized filter paper discs were soaked with 30 µl (25 mg/ml solvent) of aqueous, *n*-hexane, ethyl acetate, acetone, and methanol extracts and their inhibitory activities were determined as described elsewhere (Rahman et al. 2017). All plates were incubated at 37°C for 24 hours and the diameter of the discs and the zone of inhibition were measured, and ratios between the diameters were calculated (Rahman et al. 2017). Data were collected from three replicated plates for each plant extract and calculated the mean value with standard deviation.

Table II
Medicinal herbs used for *in vitro* antibacterial assay against
V. alginolyticus isolates.

Sl. No.	English name	Scientific name	Plant parts used
1	Zinger	<i>Zingiber officinale</i>	Rhizome
2	Turmeric	<i>Curcuma longa</i>	Rhizome
3	Clove	<i>Syzygium aromaticum</i>	Bud
4	Garlic	<i>Allium sativum</i>	Bulb
5	Onion	<i>Allium cepa</i>	Bulb
6	Black cumin	<i>Nigella sativa</i>	Seed
7	Mehogoni	<i>Swietenia mahagoni</i>	Seed
8	Bottle gourd	<i>Lagania siceraria</i>	Seed, Fruit
9	Guava	<i>Psidium guajava</i>	Fruit
10	Olive	<i>Olea europaea</i>	Fruit
11	Chilli	<i>Capsicum pendulum</i>	Fruit
12	Rose periwinkle	<i>Catharanthus roseus</i>	Leaf and flower
13	Amla	<i>Emblica officinalis</i>	Leaf
14	Tamarind	<i>Tamarindus indica</i>	Leaf
15	Arjun	<i>Terminalia arjuna</i>	Leaf
16	Papaya	<i>Carica papaya</i>	Leaf
17	Carunda	<i>Carissa carandas</i>	Leaf
18	Bermuda grass	<i>Cynodon dactylon</i>	Leaf
19	Neem	<i>Azadirachta indica</i>	Leaf
20	Pomegranate	<i>Punica granatum</i>	Leaf
21	Carambola	<i>Averrhoa carambola</i>	Leaf

***In vivo* control of vibriosis infection by application of herbal extracts.** *In vivo* effects of ethyl acetate extract of *E. officinalis* leaf, ethyl acetate, and methanol extracts of *A. sativum* bulb, methanol, and acetone extracts of *S. aromaticum* bud, and acetone extract of *T. indica* leaf used as therapeutic agents against vibriosis infection in shrimp were evaluated in laboratory conditions. For this purpose, the stock solutions of 25 mg/ml ethyl acetate extracts of *E. officinalis*, ethyl acetate and methanol extract of *A. sativum*, methanol and acetone extract of *S. aromaticum* and acetone extract of *T. indica* were prepared. The herbal extracts were mixed with a commercial feed for juvenile shrimp at the dose of 5, 10, and 15 mg extract/g feed (0.2, 0.4, 0.6 ml from stock solution). Juvenile shrimp were exposed with 24 h culture suspension of a representative *V. alginolyticus* isolate (2A1a) as described earlier. The different groups of *V. alginolyticus* exposed shrimp, each of which had 3 replicates (n = 20), were transferred to different aquarium. A group of juvenile shrimp exposed to the bacterial suspension and fed with normal commercial feed (without any plant extract) was described as control group-2. Another group of shrimp not exposed to the bacterial suspension and fed with normal commercial feed (without any herb extract) was known as control

group-1. The rest groups of juvenile shrimp exposed to bacterial suspension were fed with commercial feed supplemented with ethyl acetate extracts of *E. officinalis*, ethyl acetate and methanol extract of *A. sativum*, methanol and acetone extract of *S. aromaticum* and acetone extract of *T. indica* at different doses (5, 10, and 15 mg extract/g feed). The juvenile shrimp were supplied feed at a rate of 10% of their body weight. Shrimp were fed twice in a day at 12 hours interval. Continuous aeration was maintained in the aquarium and approximately 50% of water was exchanged in two days interval. The experiment was continued for seven days.

Statistical analysis of data. Experiments for *in vivo* challenge test and *in vivo* control of the vibriosis infection by application of herbal extracts were carried out using a complete randomized design (CRD). Data were analyzed by one-way analysis of variance (ANOVA) and the mean values were separated by LSD posthoc statistic. The level of significance was $p < 0.05$. All the analyses were performed using Statistics 10. Mean value \pm standard error of 3 replications was used in Tables and Figures.

Results

Isolation, phenotypic, and molecular characterization of the pathogen causing vibriosis in shrimp. The infected shrimps were collected from the farms near Sundarbans mangrove forest. The high mortality of shrimps (approximately 65%) was observed in these farms. The infected shrimps exhibited reduced feeding and lethargic in swimming at the edges and surface of the water body. No symptoms of white spot syndrome virus disease (WSSV) were observed in the infected farms. The farms were also free from pollution. Water quality parameters of the infected farms were 7.8 ± 0.2 , 30 ± 1.6 , 8.6 ± 1.0 , 0.2 ± 0.08 , and 4.5 ± 0.5 for pH, temperature ($^{\circ}\text{C}$), salinity (ppt), ammonia (mg/l), and dissolved oxygen (mg/l), respectively. Twenty-five bacterial isolates were randomly selected (18 from TCBS and 7 from NA) as suspected *Vibrio* sp. based on their colony characteristics for preliminary phenotypic identification. Among these, a total of 20 isolates (16 from TCBS and 4 from NA) were Gram-negative, rod-shaped, fermentative, motile bacteria, susceptible to vibriostatic agent 0/129, and were positive in oxidase test, catalase test, indole production, and lysine decarboxylase test but negative in acetoin and hydrogen sulfide (H_2S) production test (Table III). Isolates were able to grow in the presence of 2, 4, 6, and 8% NaCl but did not grow in the absence of NaCl. They were unable to grow at 4°C but grew well at 40°C temperature. The isolates produced acid from glucose, sorbitol, mannitol, and sucrose but did not produce acid from arabinose. Based on the

Table III
Colony, morphological, and biochemical characteristics of *Vibrio* sp. isolates.

Test Type	Test	Characteristics
Colony characteristics	Color in NA media	Brownish
	Color in TCBS media	Yellowish
	Size	Large
	Shape	Round
	Elevation	Convex
Morphological characteristics	Shape	Comma
	Motility	+
	Growth in 0% NaCl	-
	Growth in 2,4 and 8% NaCl containing media	+
	Growth at 4°C	-
	Growth at 40°C	+
Biochemical characteristics	Gram's staining	-
	Oxidative-Fermentative	F
	Oxidase	+
	Catalase	+
	Acetoin production	-
	H ₂ S production	-
	Indole	+
	Sensitivity to a vibriostatic agent 0/129	+
	Arginine dihydrolase	-
	Lysine decarboxylase	+
Acid production from	Glucose	+
	Arabinose	-
	Manitol	+
	Sorbitol	+
	Sucrose	+

Note: + = Positive reaction; - = Negative reaction; F = Fermentative

colony's morphological and biochemical characteristics, twenty isolates were phenotypically identified as *Vibrio* sp. (Farmer et al. 2005; Jayasree et al. 2006; Nelapati et al. 2012). The phenotypic and biochemical characteristics of these twenty isolates were very similar to the characteristics described for *V. alginolyticus* (Lie et al. 2004).

Among twenty isolates, four (2A1a, 2A3, 2A11 and 2V21) were randomly selected for further molecular, pathological, antibiotic susceptibility and herbal disease control studies. The 16S rRNA gene sequence data of these four selected isolates exhibited 100% homology with *V. alginolyticus* strain ATCC 17749. The sequences of the isolates 2A1a, 2A3, 2A11, and 2V21 have been deposited to NCBI Gen Bank with accession numbers MG757701, MG757699, MG757700, and MG757703, respectively. In the phylogenetic tree, these four isolates shared a common ancestor and formed a cluster with *V. alginolyticus* (Fig. 1).

In vivo challenge of the isolated *V. alginolyticus*. To observe whether *V. alginolyticus* isolates were pathogenic to juvenile shrimp, we conducted an *in vivo*

challenge test under laboratory conditions. All of the four *V. alginolyticus* isolates tested (2A1a, 2A3, 2A11, and 2V21) produced disease symptoms in the juvenile shrimp and caused high mortality ranged from $81.67 \pm 2.29\%$ to $86.67 \pm 2.29\%$ (Fig. 2). In juvenile shrimp, mortality was observed from 24 to 96 hours after inoculation and the highest mortality was recorded within 72 hours. Hepatopancreatic discoloration, the main symptom of infection, was observed clearly in the challenged shrimp within 96–144 hours. The infected shrimp exhibited feeding redundancy and lethargic swimming at the surface of the aquarium.

Antibiogram profile of *V. alginolyticus* isolates. To find out whether the shrimp pathogenic *V. alginolyticus* isolates had any resistance against commercial antibiotics, we screened them against eleven antibiotics using disc diffusion assay. *V. alginolyticus* isolates exhibited resistance against various antibiotics such as erythromycin, penicillin, amoxicillin, vancomycin, ampicillin, and cefradine (Table IV). However, they were found sensitive to levofloxacin, cefuroxime, azithromycin,

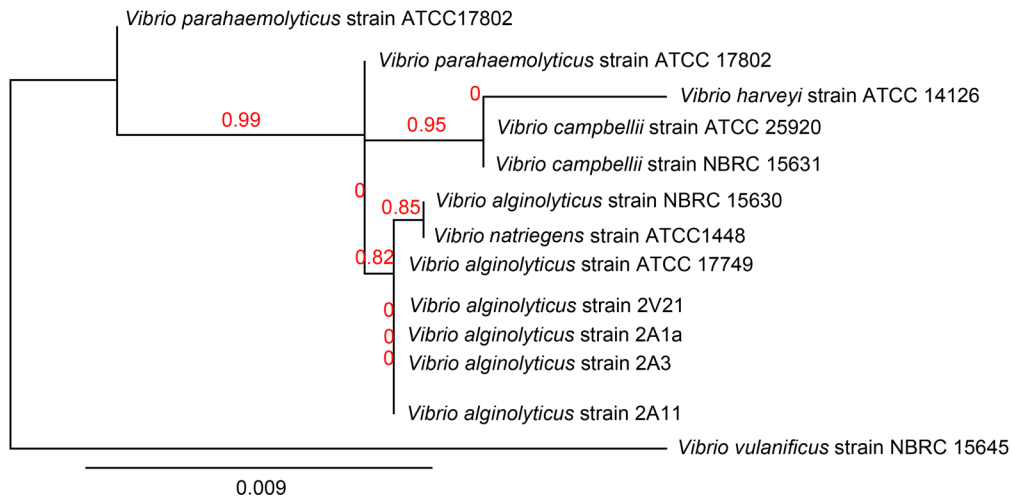


Fig. 1. Unrooted phylogenetic tree showing evolutionary relationship of *V. alginolyticus* isolates with other maximum identical related species on the basis of 16S rRNA gene sequences evolutionary distance.

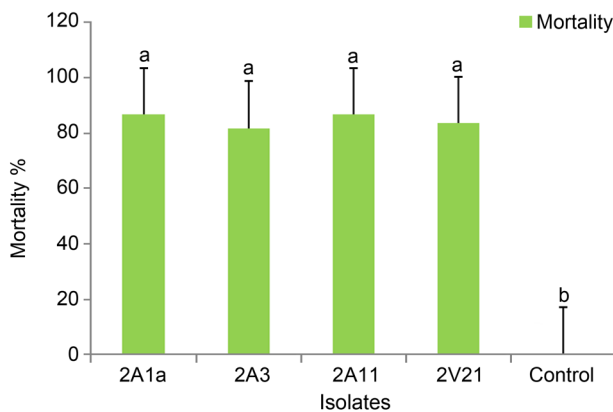


Fig. 2. Mortality of juvenile shrimp exposed to *V. alginolyticus* isolates in laboratory conditions. One way ANOVA was performed at ≤ 0.05 level of significance. Same letters indicate there is no significant variations in mortality of shrimp in different groups challenged with different isolates of *V. alginolyticus*.

nitrofurantoin, and gentamicin. The maximum and minimum inhibition zone was observed for levofloxacin and azithromycin, respectively.

In vitro inhibitory effects of herbal extracts. The shrimp pathogenic *V. alginolyticus* isolates were suscep-

tible to crude aqueous extracts of the leaf of *E. officinalis*, the bulb of *A. sativum*, the bud of *S. aromaticum*, and the leaf of *T. indica*. The *E. officinalis* extracts displayed the highest antibacterial activity (Table V). The bulb extract of *A. sativum* and bud extract of *S. aromaticum* also showed high inhibitory activity against *V. alginolyticus* whereas, lowest antibacterial activity against the *V. alginolyticus* isolates was observed for the leaf extract of *T. indica*. The ethyl acetate extract of the *E. officinalis* leaf strongly inhibited the growth of *V. alginolyticus* with maximum zone ratio 6.4 ± 0.19 but methanol, *n*-hexane, and acetone extracts of the leaf of *E. officinalis* caused no inhibition. The ethyl acetate extract of the bulb of *A. sativum* also highly inhibited *V. alginolyticus* (Fig. 3) followed by methanol extract. Acetone and methanol extracts of the bud of *S. aromaticum* also strongly inhibited the growth of *V. alginolyticus* isolates. The acetone, *n*-hexane, methanol, and ethyl acetate extracts of the leaf of *T. indica* inhibited the growth of *V. alginolyticus* but the zone ratios were not satisfactory.

An in vivo effect of herbal extracts as therapeutic agents against vibriosis in shrimps. Juvenile shrimps were fed with various herbal extracts mixed feed after

Table IV

In vitro antibiogram profiles of the *V. alginolyticus* isolates. Eleven commercial antibiotic discs were used.

Isolates	Inhibition zone ratio against different antibiotics										
	Er	Pe	Am	Va	Amp	Le	Cx	Az	Ni	Ce	Ge
2A1a	R	R	R	R	R	7.3 ± 0.2	4.6 ± 0.3	3.8 ± 0.3	6.8 ± 0.1	R	6 ± 0.2
2A3	R	R	R	R	R	7.3 ± 0.3	3.7 ± 0.2	3.3 ± 0.1	7 ± 0.1	R	5.7 ± 0.1
2A11	R	R	R	R	R	7.2 ± 0.1	4.8 ± 0.6	3.7 ± 0.6	6.5 ± 0.5	R	5.8 ± 0.1
2V21	R	R	R	R	R	7.0 ± 0.1	4.2 ± 0.2	3.3 ± 0.2	7.0 ± 0.2	R	5.7 ± 0.3

Note: Er = Erythromycin (15 µg/disc), Pe = Penicillin (10 µg/disc), Am = Amoxycillin (30 µg/disc), Va = Vancomycin (30 µg/disc), Amp = Ampicillin (25 µg/disc), Le = Levofloxacin (5 µg/disc), Cx = Cefuroxime (30 µg/disc), Az = Azithromycin (30 µg/disc), Ni = Nitrofurantoin (30 µg/disc), Ce = Cefradine (25 µg/disc), Ge = Gentamicin (10 µg/disc), R = Resistant.

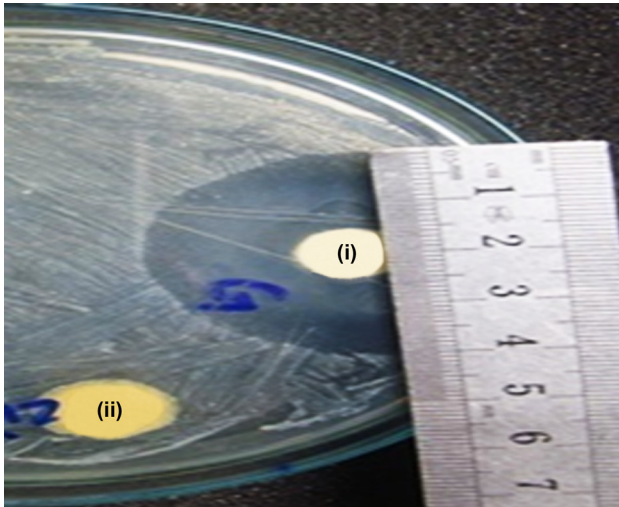


Fig. 3. An *in vitro* antibacterial activity of disc containing organic solvent extracts of herbs. (i) EtOAc extract of *A. sativum*, and (ii) control (no plant extract).

exposing them to the highly virulent isolate of *V. alginolyticus* (2A1a). Interestingly, $100 \pm 0.0\%$ of the challenged shrimp were survived when fed with ethyl acetate extract of *E. officinalis* and *A. sativum* at the rate of 10 mg/g of feed (Fig. 4). Survival of shrimp was also

high ($86.7 \pm 5.8\%$) when fed with methanol extract of *A. sativum* at the rate of 10 mg/g of feed. However, only $16.7 \pm 2.87\%$ shrimp survived when challenged with the pathogenic *Vibrio* isolate 2A1a in control group 2 (normal feed without any herbal treatment). The lower rate of survival ($35.0 \pm 7.07\%$) was also observed in the shrimp when fed with acetone extract of *T. indica* at a rate of 15 mg/g feed.

Discussion

Vibriosis is one of the most important bacterial diseases of shrimp caused by several species of *Vibrio*. This study isolated and identified (phenotypically) twenty isolates of *Vibrio* sp. from the infected shrimp with vibriosis symptoms collected from shrimp farms of Bangladesh. Among twenty, four virulent isolates were identified as *V. alginolyticus* by 16S rRNA gene sequencing (Fig. 1). These *V. alginolyticus* isolates exhibited a high level of virulence against juvenile shrimp ($81.67 \pm 2.29\%$ to $86.67 \pm 2.29\%$ mortality) in an *in vivo* challenged study. Liu et al. (2004) also obtained 80% mortality in shrimp in an *in vivo* challenge test

Table V
An *in vitro* inhibitory activity of herbal extracts on shrimp pathogenic *V. alginolyticus* isolates.

Plants	Type of extracts	Inhibition zone ratio of herbal extracts for <i>V. alginolyticus</i> isolates			
		2A1a	2A3	2A11	2V21
<i>E. officinalis</i>	Aqueous extract	5.33 ± 0.64	4.17 ± 0.38	4.67 ± 0.12	4.10 ± 0.44
	<i>n</i> -Hexane extract	-	-	-	-
	EtOAc extract	6.1 ± 0.19	5.6 ± 0.20	5.0 ± 0.23	6.1 ± 0.07
	MeOH extract	-	-	-	-
	Acetone extract	-	-	-	-
<i>A. sativum</i>	Aqueous extract	4.00 ± 0.46	4.10 ± 0.10	4.60 ± 0.53	3.80 ± 0.66
	<i>n</i> -Hexane extract	1.9 ± 0.06	1.8 ± 0.15	1.6 ± 0.05	1.8 ± 0.17
	EtOAc extract	4.1 ± 0.11	4.3 ± 0.03	3.3 ± 0.05	3.8 ± 0.25
	MeOH extract	2.5 ± 0.06	2.1 ± 0.25	2.4 ± 0.11	1.9 ± 0.15
	Acetone extract	1.5 ± 0.25	1.4 ± 0.15	1.4 ± 0.36	1.5 ± 0.06
<i>S. aromaticum</i>	Aqueous extract	3.93 ± 0.15	3.47 ± 0.55	3.93 ± 0.21	3.50 ± 0.53
	<i>n</i> -Hexane extract	3.5 ± 0.04	3.6 ± 0.24	3.6 ± 0.13	3.8 ± 0.14
	EtOAc extract	-	-	-	-
	MeOH extract	4.9 ± 0.21	4.6 ± 0.17	4.0 ± 0.06	4.4 ± 0.08
	Acetone extract	4.3 ± 0.12	4.4 ± 0.06	4.0 ± 0.15	4.1 ± 0.22
<i>T. indica</i>	Aqueous extract	1.17 ± 0.40	0.97 ± 0.21	1.20 ± 0.36	0.93 ± 0.15
	<i>n</i> -Hexane extract	1.9 ± 0.09	1.8 ± 0.06	1.5 ± 0.09	1.8 ± 0.21
	EtOAc extract	1.8 ± 0.14	1.9 ± 0.21	1.9 ± 0.06	1.5 ± 0.08
	MeOH extract	1.5 ± 0.22	1.5 ± 0.19	1.4 ± 0.08	1.4 ± 0.11
	Acetone extract	2.3 ± 0.12	1.8 ± 0.11	1.5 ± 0.13	1.8 ± 0.05

Note: Eight millimeter diameter filter paper discs were soaked with 30 microliter of aqueous, *n*-hexane, ethyl acetate (EtOAc), methanol (MeOH) and acetone extracts (25 mg/ml) of *E. officinalis*, *A. sativum*, *S. aromaticum*, and *T. indica* and then allowed to dry in a laminar airflow cabinet before placing them to the NBA petri dish inoculated with respective isolates of the pathogen. Each treatment was replicated for three times. Data presented here is the mean \pm SE.

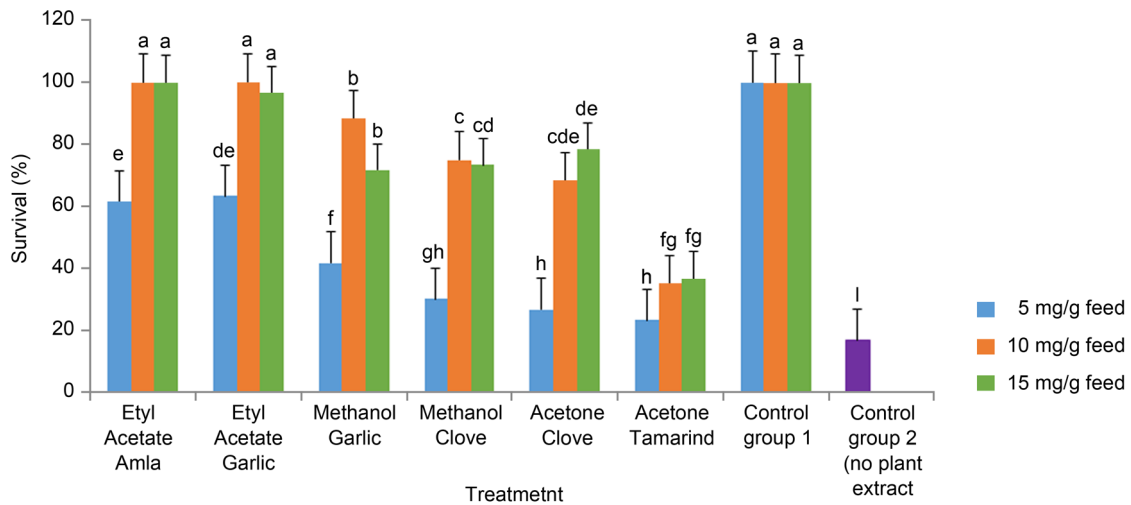


Fig. 4. Survival rate of shrimps fed with herbal extracts at day 7 after infection with a virulent strain of *V. alginolyticus* 2A1a. One way ANOVA was used for analysis of the data and mean value with standard deviation in the bar followed by the same letter (s) are not significantly different as assessed by LSD (Least Significance Difference) at $p \leq 0.05$. Control group-1 was not exposed to the pathogen; Control group-2 was infected with the pathogen but fed normal commercial feed.

with *V. alginolyticus* (CH003). In this study, the infected shrimp in *in vivo* challenge test exhibited almost identical symptoms as found in the naturally infected shrimp (Lightner 1993; Anderson et al. 1998).

One of the important findings of this study is that the shrimp pathogenic *V. alginolyticus* isolates showed resistance against various antibiotics but exhibited the high level of susceptibility to both aqueous and organic solvent extracts of herbs such as *E. officinalis*, *A. sativum*, *S. aromaticum*, and *T. indica* (Table V). Among these, ethyl acetate extract of *E. officinalis* strongly inhibited the growth of *V. alginolyticus* strains followed by ethyl acetate and methanol extract of *A. sativum*, and methanol extract of *S. aromaticum*. However, lower inhibition was obtained for both aqueous and organic extracts of *T. indica*. Medicinal plants are used to treat a variety of diseases for thousands of years of civilizations (Petrovska 2012). An *in vitro* antibacterial activity of numerous plants against both Gram-positive and Gram-negative marine bacteria has been reported elsewhere (Castro et al. 2008; Roomiani et al. 2013). Ethanol extract of turmeric (*Curcuma longa*) was reported to inhibit the shrimp pathogen *Vibrio* sp. (Lawhavinit et al. 2011). *In vitro* inhibitory activities of both aqueous and organic solvent extracts of *A. sativum*, *S. aromaticum*, and *T. indica* against fish pathogenic *Enterococcus faecalis* have also been reported (Rahman et al. 2017).

The most remarkable finding of this study is that ethyl acetate extracts of *E. officinalis* and *A. sativum* remarkably protected the juvenile shrimp (up to 100%) from vibriosis by a virulent isolate of *V. alginolyticus* (Fig. 4). High to moderate survival rates were also obtained in shrimp fed with methanol extracts of *A. sativum* and *S. aromaticum*, and acetone extract of

S. aromaticum. Inhibition of *V. alginolyticus* both in *in vitro* and *in vivo* conditions by organic solvent extracts of *E. officinalis*, *A. sativum*, and *S. aromaticum* suggests that these herbal extracts contain antibacterial secondary metabolite(s). Medicinal herbs are considered as one of the most important sources for medicine and drugs, as many secondary metabolites including antimicrobial substances are obtained from various herbs. Plants possess complex chemicals with varied biological activities, making plants suitable for the treatment of multifactorial diseases, and makes plants a suitable alternative to antibiotics with little risk for development of resistance (Gostner et al. 2012; Srivastava et al. 2014). *A. sativum* contains several bioactive compounds such as ajone, allicin and diallyl sulfides that possess potential antibacterial activity against different microorganisms (Naganawa et al. 1996; Ankri and Mirelman 1999; O'Gara et al. 2000). *S. aromaticum* contains eugenol that is reported to exhibit strong antibacterial activity against *Staphylococcus aureus* (Xu et al. 2016). Cinnamaldehyde and its derivatives obtained from cinnamon were reported to reduce the virulence in *Vibrio* sp. causing vibriosis (Brackman et al. 2008). *S. cumini* leaf powder also reported to increase immunity in juvenile shrimp (*Litopenaeus vannamei*) against *V. parahaemolyticus* infection (Prabu et al. 2018). Organic solvent extracts of *A. sativum* and *S. aromaticum* also reported to significantly increase the survival of *Oreochromis niloticus* from infection against *E. faecalis* (Rahman et al. 2017). Herbal extracts are also reported to stimulate immunity and develop disease resistance in shrimp (Raja Rajeswari et al. 2012; Yogeewaran et al. 2012). Dietary administration of *Gynura bicolor* extract was reported to enhance the innate immunity and antio-

xidant enzyme activities of shrimp against *V. alginolyticus* and WSSV infection (Wu et al. 2015). The purified garlic compounds allicin and ajoene demonstrated immune stimulant capacity against fish pathogenic protozoa *Spiroucleus vortens* and *Ichthyophthirius multifiliis*, and the bacteria *A. hydrophila* (Nya et al. 2010; Tanekhy and Fall 2016). Recently, Foysal et al. (2019) reported that dietary administration of garlic could modulate gut microbiota, increase recovery from streptococcus infection and upregulate the expression of immune genes in the intestinal tissue of tilapia. Since crude plant extracts contain multiple secondary metabolites, the chances of development of resistance in the pathogens against these extracts are likely lesser than those of pure antibiotics (Rahman et al. 2017). Valuable drugs could be developed from these herbal extracts to control vibriosis in shrimp and other fish diseases. The extracts of *E. officinalis* and *A. sativum* could be used as alternative therapeutic agents against vibriosis disease in shrimp.

ORCID

Md. Mahbubur Rahman 0000-0001-6203-3375

Acknowledgements

The authors acknowledge the Ministry of Science and Technology, Government of Bangladesh for providing special allocation under a research project titled “Molecular Detection and Bio-control of the Pathogen Causing Vibriosis and Black Spot Diseases in Prawn and Shrimp” to conduct the research work. Thanks to Mr. Nabangshu Shekhar Das of the University of Calgary, Canada for English language correction.

Conflict of interest

The authors do not report any financial or personal connections with other persons or organizations, which might negatively affect the contents of this publication and/or claim authorship rights to this publication.

Literature

- Ali H, Rahman MM, Rico A, Jaman A, Basak SK, Islam MM, Khan N, Keus HJ, Mohan CV. An assessment of health management practices and occupational health hazards in tiger shrimp (*Penaeus monodon*) and freshwater prawn (*Macrobrachium rosenbergii*) aquaculture in Bangladesh. *Vet Anim Sci*. 2018 Jun;5:10–19. <https://doi.org/10.1016/j.vas.2018.01.002>
- Alsina M, Blanch AR. A set of keys for biochemical identification of environmental *Vibrio* species. *J Appl Bacteriol*. 1994 Jan;76(1):79–85. <https://doi.org/10.1111/j.1365-2672.1994.tb04419.x>
- Anderson IG, Shamsudin MN, Shariff M. Bacterial septicemia in juvenile tiger shrimp, *Penaeus monodon*, cultured in Malaysian brackishwater ponds. *Asian Fish Sci*. 1988;2:93–108.
- Ankri S, Mirelman D. Antimicrobial properties of allicin from garlic. *Microbes Infect*. 1999 Feb;1(2):125–129. [https://doi.org/10.1016/S1286-4579\(99\)80003-3](https://doi.org/10.1016/S1286-4579(99)80003-3)
- Austin B, Zhang XH. *Virbio harveyi*: a significant pathogen of marine vertebrates and invertebrates. *Lett Appl Microbiol*. 2006;43:119–124. <https://doi.org/10.1111/j.1472-765X.2006.01989.x>
- Brackman G, Defoirdt T, Miyamoto C, Bossier P, Van Calenberg S, Nelis H, Coenye T. Cinnamaldehyde and cinnamaldehyde derivatives reduce virulence in *Vibrio* spp. by decreasing the DNA-binding activity of the quorum sensing response regulator LuxR. *BMC Microbiol*. 2008;8(1):149. <https://doi.org/10.1186/1471-2180-8-149>
- BSAC. BSAC Methods for Antimicrobial Susceptibility Testing. Version 14 January 2015. Birmingham (United Kingdom): The British Society for Antimicrobial Chemotherapy; 2015.
- Castro SBR, Leal CAG, Freire FR, Carvalho DA, Oliveira DF, Figueiredo HCP. Antibacterial activity of plant extracts from Brazil against fish pathogenic bacteria. *Braz J Microbiol*. 2008 Dec;39(4):756–760. <https://doi.org/10.1590/S1517-83822008000400030>
- Chatterjee S, Halder S. *Vibrio* related diseases in aquaculture and development of rapid and accurate identification methods. *J Marine Sci Res Dev*. 2012;1:002.
- Chowdhury G, Rahman MM, Mondal MN, Alam MS, Hannan MA, Rahman M, Deb SC. Studies on pathogens associated with black spot disease of prawn and shrimp in Bangladesh. Abstract: 23rd Bangladesh Science Conference. Dhaka, Bangladesh; 2015. p. 73.
- CLSI. Performance standards for antibiotic susceptibility testing: Fifteenth informational supplement. Wayne (USA): Clinical & Laboratory Standards Institute; 2005.
- de la Peña LD, Tamaki T, Momoyama K, Nakai T, Muroga K. Characteristics of the causative bacterium of vibriosis in the kuruma prawn, *Penaeus japonicus*. *Aquaculture*. 1993 Aug;115(1-2): 1–12. [https://doi.org/10.1016/0044-8486\(93\)90353-Z](https://doi.org/10.1016/0044-8486(93)90353-Z)
- Farmer JJ, Janda M, Brenner FW, Cameron DN, Birkhead KM. Genus I. *Vibrio Pacini* 1854, 411. *Bergey's Manual of Systematic Bacteriology*. 2005;2:494–546.
- Foysal MJ, Alam M, Momtaz F, Chaklader MR, Siddik MAB, Cole AJ, Fotedar R, Rahman MM. Dietary supplementation of garlic (*Allium sativum*) modulate gut microbiota and health status of tilapia (*Oreochromis niloticus*) against *Streptococcus iniae* infection. *Aquacult Res*. 2019;00:1–10. <https://doi.org/10.1111/are.14088>
- Gostner JM, Wrulich OA, Jenny M, Fuchs D, Ueberall F. An update on the strategies in multicomponent activity monitoring within the phytopharmaceutical field. *BMC Complement Altern Med*. 2012 Dec;12(1):528. <https://doi.org/10.1186/1472-6882-12-18>
- Hossain MS, Aktaruzzaman M, Fakhruddin ANM, Uddin MJ, Rahman SH, Chowdhury MAZ, Alam MK. Antimicrobial susceptibility of *Vibrio* species isolated from brackish water shrimp culture environment. *J Bangladesh Acad Sci*. 2012 Dec 14;36(2):213–220. <https://doi.org/10.3329/jbas.v36i2.12964>
- Hossain MS, Uddin MJ, Fakhruddin ANM. Impacts of shrimp farming on the coastal environment of Bangladesh and approach for management. *Rev Environ Sci Biotechnol*. 2013 Sep;12(3):313–332. <https://doi.org/10.1007/s11157-013-9311-5>
- Jayasree L, Janakiram P, Madhavi R. Characterization of *Vibrio* spp. associated with diseased shrimp from culture ponds of Andhra Pradesh (India). *J World Aquacult Soc*. 2006 Dec;37(4):523–532. <https://doi.org/10.1111/j.1749-7345.2006.00066.x>
- Jorgensen JH, Ferraro MJ. Antimicrobial susceptibility testing: a review of general principles and contemporary practices. *Clin Infect Dis*. 2009 Dec;49(11):1749–1755. <https://doi.org/10.1086/647952>
- Karim MR, Uddin MN, Rahman MK, Uddin MA. Microbiological study of coastal shrimp aquaculture production system of Bangladesh. *J Biol Life Sci*. 2018;9(1). <https://doi.org/10.5296/jbls.v9i1.12195>
- Karunasagar I, Pai R, Malathi GR, Karunasagar I. Mass mortality of *Penaeus monodon* larvae due to antibiotic-resistant *Vibrio* harveyi infection. *Aquaculture*. 1994 Dec;128(3–4):203–209. [https://doi.org/10.1016/0044-8486\(94\)90309-3](https://doi.org/10.1016/0044-8486(94)90309-3)
- Lawhavit OA, Sincharoenpokai P, Sunthornandh P, Kaset-sart J. Effects of ethanol turmeric (*Curcuma longa* Linn.) extract

- against shrimp pathogenic *Vibrio* sp. and on growth performance and immune status of white shrimp (*Litopenaeus vannamei*). *Nat Sci*. 2011;45:70–77.
- Lee KK, Yu SR, Chen FR, Yang TI, Liu PC. Virulence of *Vibrio alginolyticus* isolated from diseased tiger prawn, *Penaeus monodon*. *Curr Microbiol*. 1996 Apr 1;32(4):229–231. <https://doi.org/10.1007/s002849900041>
- Lightner DV. A hand book of pathology and diagnostic procedures for disease of penaeid shrimp. Baton Rouge (USA): World Aquacult Soc; 1996. p. 236.
- Lightner DV. Diseases of cultured penaeid shrimp and shrimps. In: Sindermann CJ, Lightner DV, editors. Disease diagnosis and control in North American marine aquaculture. Amsterdam (Netherlands): Elsevier; 1988. p. 8–127.
- Lightner DV. Diseases of cultured penaeid shrimp. In: McVey JP, editor. CRC Handbook of mariculture: crustacean aquaculture. Boca Raton (USA): CRC Press; 1993, p. 393–486.
- Liu CH, Cheng W, Hsu JP, Chen JC. *Vibrio alginolyticus* infection in the white shrimp *Litopenaeus vannamei* confirmed by polymerase chain reaction and 16S rDNA sequencing. *Dis Aquat Organ*. 2004;61(1–2):169–174. <https://doi.org/10.3354/dao061169>
- Mohney LL, Bell TA, Lightner DV. Shrimp antimicrobial testing *in vitro* susceptibility of thirteen Gram negative bacteria to twelve antibiotics. *J Aquat Anim Health*. 1992 Dec;4(4):257–261. [https://doi.org/10.1577/1548-8667\(1992\)004<0257:SATIIIV>2.3.CO;2](https://doi.org/10.1577/1548-8667(1992)004<0257:SATIIIV>2.3.CO;2)
- Muniruzzaman M, Chowdhury MBR. Sensitivity of fish pathogenic bacteria to various medicinal herbs. *Bangl. J Vet Med*. 2004; 2(1):75–82. <https://doi.org/10.3329/bjvm.v2i1.1941>
- Naganawa R, Iwata N, Ishikawa K, Fukuda H, Fujino T, Suzuki A. Inhibition of microbial growth by ajoene, a sulfur-containing compound derived from garlic. *Appl Environ Microbiol*. 1996 Nov; 62(11):4238–4242.
- Nelapati S, Nelapati K, Chinnam B. *Vibrio parahaemolyticus* – An emerging foodborne pathogen. *Vet World*. 2012;5(1):48–63. <https://doi.org/10.5455/vetworld.2012.48-63>
- Nya EJ, Dawood Z, Austin B. The garlic component, allicin, prevents disease caused by *Aeromonas hydrophila* in rainbow trout, *Oncorhynchus mykiss* (Walbaum). *J Fish Dis*. 2010 Apr;33(4):293–300. <https://doi.org/10.1111/j.1365-2761.2009.01121.x>
- O’Gara EA, Hill DJ, Maslin DJ. Activities of garlic oil, garlic powder, and their diallyl constituents against *Helicobacter pylori*. *Appl Environ Microbiol*. 2000 May 01;66(5):2269–2273. <https://doi.org/10.1128/AEM.66.5.2269-2273.2000>
- Paul BG, Vogl CR. Impacts of shrimp farming in Bangladesh: challenges and alternatives. *Ocean Coast Manage*. 2011 Mar;54(3): 201–211. <https://doi.org/10.1016/j.ocecoaman.2010.12.001>
- Petrovska B. Historical review of medicinal plants’ usage. *Pharmacogn Rev*. 2012;6(11):1–5. <https://doi.org/10.4103/0973-7847.95849>
- Prabu DL, Chandrasekar S, Ambashankar K, Dayal JS, Ebeneezar S, Ramachandran K, Kavitha M, Vijayagopal P. Effect of dietary *Syzygium cumini* leaf powder on growth and non-specific immunity of *Litopenaeus vannamei* (Boone 1931) and defense against virulent strain of *Vibrio parahaemolyticus*. *Aquaculture*. 2018 Mar;489:9–20. <https://doi.org/10.1016/j.aquaculture.2018.01.041>
- Rahman M, Rahman MM, Deb SC, Alam MS, Alam MJ, Islam MT. Molecular identification of multiple antibiotic resistant fish pathogenic *Enterococcus faecalis* and their control by medicinal herbs. *Sci Rep*. 2017 Dec;7(1):3747. <https://doi.org/10.1038/s41598-017-03673-1>
- Rahman MM, Hossain MN. Antibiotic and herbal sensitivity of some *Aeromonas* sp. isolates collected from diseased carp fishes. *Progress Agric*. 2010;21(1–2):117–129.
- Rahman S, Khan SN, Naser MN, Karim MM. Isolation of *Vibrio* sp. from penaeid shrimp hatcheries and coastal waters of Cox’s Bazar, Bangladesh. *Asian J Exp Biol Sci*. 2010;1(2):288–293.
- Raja Rajeswari P, Velmurugan S, Michael Babu M, Albin Dhas S, Kesavan K, Citarasu T. A study on the influence of selected Indian herbal active principles on enhancing the immune system in *Fenneropenaeus indicus* against *Vibrio harveyi* infection. *Aquacult Int*. 2012 Oct;20(5):1009–1020. <https://doi.org/10.1007/s10499-012-9525-5>
- Roomiani L, Soltani M, Akhondzadeh Basti A, Mahmoodi A, Taheri, Mirghaed A, Yadollahi F. Evaluation of the chemical composition and *in vitro* antimicrobial activity of *Rosmarinus officinalis*, *Zataria multiflora*, *Anethum graveolens* and *Eucalyptus globulus* against *Streptococcus iniae*; the cause of zoonotic disease in farmed fish. *Iran J Fish Sci*. 2013;12:702–716.
- Shanmugasundaram S, Mayavu P, Manikandarajan T, Suriya M, Eswar A, Anbarasu R. Isolation and identification of *Vibrio* sp. in the Hepatopancreas of cultured white pacific shrimp (*Litopenaeus vannamei*). *Int Lett Nat Sci*. 2015 Sep;46:52–59. <https://doi.org/10.18052/www.scipress.com/ILNS.46.52>
- Sindermann CJ. Principal Diseases of Marine Fish and Shellfish. New York (USA): Academic Press; 1990.
- Sparagano OAE, Robertson PAW, Purdom I, McINNES J, Li Y, Yu DH, Du ZJ, Xu HS, Austin B. PCR and molecular detection for differentiating *Vibrio* species. *Ann N Y Acad Sci*. 2002 Oct; 969(1):60–65. <https://doi.org/10.1111/j.1749-6632.2002.tb04351.x>
- Srivastava J, Chandra H, Nautiyal AR, Kalra SJS. Antimicrobial resistance (AMR) and plant-derived antimicrobials (PDA_{ns}) as an alternative drug line to control infections. *3 Biotech*. 2014 Oct;4(5):451–460. <https://doi.org/10.1007/s13205-013-0180-y>
- Tanekhy M, Fall J. Expression of innate immunity genes in kuruma shrimp *Marsupenaeus japonicus* after *in vivo* stimulation with garlic extract (allicin). *Vet Med (Praha)*. 2016 Jul 15;60(1):39–47. <https://doi.org/10.17221/7924-VETMED>
- Traub WH, Geipel U, Leonhard B. Antibiotic susceptibility testing (agar disk diffusion and agar dilution) of clinical isolates of *Enterococcus faecalis* and *E. faecium*: comparison of Mueller-Hinton, Iso-Sensitest, and Wilkins-Chalgren agar media. *Chemotherapy*. 1998;44(4):217–229. <https://doi.org/10.1159/000007118>
- Wei LS, Wendy W. Characterization of *Vibrio alginolyticus* isolated from white leg shrimp (*Litopenaeus vannamei*) with emphasis on its antibiogram and heavy metal resistance pattern. *Vet Arh*. 2012; 82(2):221–227.
- Wu CC, Chang YP, Wang JJ, Liu CH, Wong SL, Jiang CM, Hsieh SL. Dietary administration of *Gynura bicolor* (Roxb. Willd.) DC water extract enhances immune response and survival rate against *Vibrio alginolyticus* and white spot syndrome virus in white shrimp *Litopenaeus vannamei*. *Fish Shellfish Immunol*. 2015 Jan;42(1):25–33. <https://doi.org/10.1016/j.fsi.2014.10.016>
- Xu JG, Liu T, Hu QP, Cao XM. Chemical composition, antibacterial properties and mechanism of action of essential oil from clove bud against *Staphylococcus aureus*. *Molecules*. 2016 Sep 08;21(9):1194. <https://doi.org/10.3390/molecules21091194>
- Yogeewaran A, Velmurugan S, Punitha SMJ, Babu MM, Selvaraj T, Kumaran T, Citarasu T. Protection of *Penaeus monodon* against white spot syndrome virus by inactivated vaccine with herbal immunostimulants. *Fish Shellfish Immunol*. 2012 Jun; 32(6):1058–1067. <https://doi.org/10.1016/j.fsi.2012.02.029>
- Yusuf M, Begum J, Haque MN, Chowdhury JU. Medicinal plants of Bangladesh. Dhaka (Bangladesh): Bangladesh Council of Scientific and Industrial Research; 2009.

***Salmonella*-Infected Aortic Aneurysm: Investigating Pathogenesis Using *Salmonella* Serotypes**

CHISHIH CHU¹, MIN YI WONG², CHENG-HSUN CHIU^{3,4}, YUAN-HSI TSENG²,
CHYI-LIANG CHEN³ and YAO-KUANG HUANG^{2*} 

¹Department of Microbiology, Immunology, and Biopharmaceuticals, National Chiayi University, Chiayi, Taiwan

²Division of Thoracic and Cardiovascular Surgery, Chiayi Chang Gung Memorial Hospital, Chiayi,
and College of Medicine, Chang Gung University, Taoyuan, Taiwan

³Molecular Infectious Disease Research Center, Chang Gung Memorial Hospital, Taoyuan, Taiwan

⁴Division of Pediatric Infectious Diseases, Department of Pediatrics, Chang Gung Children's Hospital
and Chang Gung University, Taoyuan, Taiwan

Submitted 17 April 2019, revised 15 August 2019, accepted 19 August 2019

Abstract

Salmonella infection is most common in patients with infected aortic aneurysm, especially in Asia. When the aortic wall is heavily atherosclerotic, the intima is vulnerable to invasion by *Salmonella*, leading to the development of infected aortic aneurysm. By using THP-1 macrophage-derived foam cells to mimic atherosclerosis, we investigated the role of three *Salmonella enterica* serotypes – Typhimurium, Enteritidis, and Choleraesuis – in foam cell autophagy and inflammasome formation. Herein, we provide possible pathogenesis of *Salmonella*-associated infected aortic aneurysms. Three *S. enterica* serotypes with or without virulence plasmid were studied. Through Western blotting, we investigated cell autophagy induction and inflammasome formation in *Salmonella*-infected THP-1 macrophage-derived foam cells, detected CD36 expression after *Salmonella* infection through flow cytometry, and measured interleukin (IL)-1 β , IL-12, and interferon (IFN)- α levels through enzyme-linked immunosorbent assay. At 0.5 h after infection, plasmid-bearing *S. Enteritidis* OU7130 induced the highest foam cell autophagy – significantly higher than that induced by plasmid-less OU7067. However, plasmid-bearing *S. Choleraesuis* induced less foam cell autophagy than did its plasmid-less strain. In foam cells, plasmid-less *Salmonella* infection (particularly *S. Choleraesuis* OU7266 infection) led to higher CD36 expression than did plasmid-bearing strains infection. OU7130 and OU7266 infection induced the highest IL-1 β secretion. OU7067-infected foam cells secreted the highest IL-12p35 level. Plasmid-bearing *S. Typhimurium* OU5045 induced a higher IFN- α level than did other *Salmonella* serotypes. *Salmonella* serotypes are correlated with foam cell autophagy and IL-1 β secretion. *Salmonella* may affect the course of foam cells formation, or even aortic aneurysm, through autophagy.

Key words: *Salmonella* serotype, virulence plasmid, foam cell, autophagy, inflammasome

Introduction

A healthy aortic wall is highly resistant to infection. However, when its intima is diseased, such as in patients with atherosclerosis, the wall becomes susceptible to infection. *Salmonella*, the most common genus of the pathogen associated with infected aortic aneurysms, often infects preexisting atherosclerotic aortic aneurysms. Atherosclerosis is a chronic inflammatory, lipid-driven disease. The formation of macrophage foam cells in the arterial intima is a known hallmark of early-stage atherosclerosis lesions (Yu et al. 2013). Within the intimal layer, monocyte-derived macrophage subsequently

takes up oxidized low-density lipoprotein (oxLDL) via type B scavenger receptors CD36 and scavenger receptor-A (SR-A), leading to cholesterol-laden foam cell formation (Bekkering et al. 2014).

Autophagy is an evolutionarily conserved process involved in bulk degradation of long-lived proteins and organelles through which these cytoplasmic components are sequestered within double-membrane vesicles, namely autophagosome followed by lysosomal degradation (Nishida et al. 2008; Martinet and De Meyer 2009). In general, this catabolic process is mediated by numerous autophagy and autophagy-related proteins. Two conjugation systems, Atg12-conjugation, and LC3

* Corresponding author: Y.-K. Huang, Division of Thoracic and Cardiovascular Surgery, Chiayi Chang Gung Memorial Hospital, Chiayi and College of Medicine, Chang Gung University, Taoyuan, Taiwan; huang137@icloud.com

© 2019 Chishih Chu et al.

This work is licensed under the Creative Commons Attribution-NonCommercial-NoDerivatives 4.0 License (<https://creativecommons.org/licenses/by-nc-nd/4.0/>).

(microtubule-associated protein light chain 3)-lipidation are essential for the dynamic process of autophagosome formation (Vural and Kehrl 2014). The conjugate of a phosphatidylethanolamine group to the carboxyl terminus of LC3-I to generate LC3-II, localized to outer and inner autophagosomal membranes, is useful as an autophagosomal marker.

Inflammasomes are important intracellular multiprotein complexes consisting of a cytosolic sensor belonging to the AIM2 (absent in melanoma 2), or NLR (NOD-like receptors), an adaptor protein ASC (an apoptosis-associated speck-like protein containing a CARD), and an effector caspase, primarily caspase-1. Inflammasomes which regulate the processing and releasing of mature pro-inflammatory cytokines interleukin-1 β (IL-1 β) and IL-18, are activated by a variety of PAMPs and DAMPs (Martinon et al. 2002). Caspase-1, caspase-4, and caspase-5 in humans are the inflammatory caspases that are activated through the stimulation of either the NLRC4 or NLRP3 inflammasome (Martinon and Tschopp 2007). In response to bacterial infection, NLRP3 and NLRC4 inflammasomes can lead to autocatalytic cleavage of caspase-1, followed by secretion of IL-1 β and IL-18 resulting in pyroptosis (Bergsbaken et al. 2009). Autophagy and inflammasome are functionally interconnected; they both control cell homeostatic processes such as critically control inflammation and the clearance of pathogens (Seveau et al. 2018). Autophagy can directly regulate IL-1 β activation, release, and signaling that are activated by inflammasome (Sun et al. 2017; Wang et al. 2018).

Salmonella species are the most common pathogens of infected aortic aneurysm in Asia. *Salmonella*-associated infected aortic aneurysms have a more favorable therapeutic response to endovascular repair compared with those associated with other organisms (e.g., *Staphylococcus*, *Streptococcus*, and *Enterococcus*). We previously demonstrated that different serotypes of *Salmonella* may affect clinical outcomes (Huang et al. 2014a). The link to atherosclerosis and its more favorable response to endovascular aortic repair are implicated in the unique pathogenesis of *Salmonella*-associated infected aortic aneurysms (Forbes and Harding 2006;

Huang et al. 2014b). In this study, we investigate the role of different serotypes of *Salmonella enterica*, including Typhimurium, Enteritidis, and Choleraesuis in foam cells autophagy and inflammasome during infection, and we provide possible pathogenesis of *Salmonella*-associated infected aortic aneurysms.

Experimental

Materials and Methods

Bacterial strains and growth conditions. The bacterial strains used in this study are listed in Table I. The wild type strains of *S. enterica* serovar Typhimurium OU5045, *S. enterica* serovar Enteritidis OU7130, and *S. enterica* serovar Choleraesuis OU7085 carried 90-, 60-, and 50-kb virulence plasmids, respectively. We also used strains without a virulence plasmid: *S. Typhimurium* OU5046, *S. Enteritidis* OU7067, and *S. Choleraesuis* OU7266. All bacterial strains used in this study were routinely grown on xylose lysine deoxycholate agar plate, and every single black colony was later grown in Luria-Bertani (LB) broth at 37°C overnight.

Cell culture and differentiation. The monocyte-like THP-1 cell line that derived from the peripheral blood of a childhood case of acute monocytic leukemia was obtained from the Bioresource Collection and Research Center, Taiwan. The cells were grown in RPMI 1640 (Sigma Aldrich, St. Louis, MO, R6504) supplemented with 10% preheated fetal bovine serum (FBS; Sigma Aldrich, St. Louis, MO), 2 mM L-glutamine (Sigma Aldrich, St. Louis, MO, G7513), and 1% penicillin-streptomycin (Sigma Aldrich, St. Louis, MO, P0781). The cells were cultured at 37°C in 5% CO₂ and 70% humidity. The culture medium was changed every 3–4 days. The cell density was maintained between 2 × 10⁵ and 1 × 10⁶ cells/ml. Furthermore, 5 × 10⁶ THP-1 cells/10 ml were seeded in a 10-cm dish and differentiated using 10⁻⁵ M phorbol myristate acetate (PMA; Sigma Aldrich, St. Louis, MO, P8139) for 48 h at 37°C in 5% CO₂. For foam cell preparation, the differentiated THP-1 cells were treated with 50 μ g/ml oxLDL (Biomedical Techno-

Table I
Characteristics of *S. Typhimurium*, *S. Enteritidis*, and *S. Choleraesuis* strains.

Serovars	Strains	Characteristics of virulence plasmid
<i>S. Typhimurium</i>	OU5045	With a 90-kb pSTV as a wild type
	OU5046	Without pSTV from wild type
<i>S. Enteritidis</i>	OU7130	With a 60-kb pSEV as a wild type
	OU7067	Without pSEV from wild type
<i>S. Choleraesuis</i>	OU7085	With a 50-kb pSCV as a wild type
	OU7266	Without pSCV from wild type

logies Inc., BT-910) for 24 h, and oil red O staining was performed to confirm foam cell formation.

Detection of CD36 expression. To detect cell surface expression of CD36, flow cytometric analysis was performed using monoclonal FITC-conjugated anti-CD36 antibody (Abcam, ab82443). The THP-1-derived macrophages were incubated with the aforementioned antibody for 40 min in a dark room and washed three times with chilled phosphate-buffered saline (PBS) containing 0.02% NaN₃. The cells were analyzed using flow cytometry.

***Salmonella* infection.** Each single *Salmonella* colony was inoculated in 5 ml of LB broth at 37°C for 16 h, and the overnight culture was subcultured for 3 h. The THP-1-derived macrophages and foam cells were treated with antibiotic-free RPMI 1640 containing exponentially grown bacteria at a multiplicity of infection of 5:1 in a 24-well plate. After 0.5 and 2 h at 37°C, the cells were harvested through centrifugation at 4°C for 5 min. The culture supernatants were collected for further cytokine detection. The cells were then washed three times with PBS and harvested by scraping for further protein extraction.

Cytokines determination. Quantitative determination of IL-1 β (R&D Systems, DLB50), IL-12p40 (BlueGene Biotech, Shanghai, China, E01I0045), IL-12p35 (BlueGene Biotech, Shanghai, China, E01I0030), and interferon (IFN)- α (PBL Interferon Source, 41100) was performed through enzyme-linked immunosorbent assay (ELISA) in culture supernatants according to the manufacturer's protocol. The experiments were performed in triplicate and presented as mean \pm SD.

Protein extraction and Western blotting. The cells were treated with RIPA buffer (150 mM NaCl, 20 mM Tris-HCl, pH 7.5, 1% Triton X-100, 1% NP-40, 0.1% sodium dodecyl sulfate, and 0.5% deoxycholate) on ice for 15 min and sonicated three times for 2 s. After centrifugation at 4°C and 15 000 \times g for 15 min, the supernatant was collected and stored at -30°C until used for Western blotting. Protein concentrations of the resultant supernatants were determined using a Pierce BCA protein assay kit (Thermo Scientific). Protein samples (50 μ g) were electrophoretically separated through 12% SDS-PAGE and subsequently transferred onto polyvinylidene difluoride membranes. For immunoblotting, membranes were blocked with 5% skim milk in Tris-buffered saline containing 0.1% Tween 20 (TBST) for 1 h. The membranes were then incubated at 4°C overnight with primary antibody against LC3-I/II (Medical & Biological Laboratories Co., Ltd.) or actin (Abcam). After washing five times with TBST, a secondary antibody, horseradish peroxidase-conjugated goat anti-rabbit immunoglobulin G (Abcam), was applied for 1 h. After five TBST washes of 5 min each, the blots were incubated in commer-

cial ECL reagents (GE Healthcare Life Sciences) and exposed to photographic film.

Statistical analysis. Statistical analyses were performed using SPSS (version 18.0). To compare the differences between means (two samples), Student's *t*-test was used. Differences among multiple means were assessed through two-factor analysis of variance, as indicated by Tukey's honestly significant difference test.

Results

Plasmid-bearing *S. Enteritidis* induces more macrophage autophagy. To investigate macrophage autophagy and inflammasome induction during the infection of different serotypes of *Salmonella*, we detected LC3 and apoptosis-associated speck-like protein containing C-terminal caspase recruitment domain (CARD) (ASC) expression of THP-1-derived macrophages. Plasmid-bearing *S. Enteritidis* OU7130 induced significantly more macrophage autophagy than did the plasmid-less strain OU7067 (Fig. 1A and 1B). Furthermore, plasmid-bearing *S. Typhimurium* OU5045 showed a slightly higher ratio of macrophage autophagy than did plasmid-less OU5046. However, the trend of macrophage autophagy induced by plasmid-bearing *S. Choleraesuis* OU7085 and plasmid-less OU7266 contradicted that of the *S. Typhimurium* strains. ASC protein induction did not significantly differ among *Salmonella* serotypes. However, infection by all *Salmonella* serotypes, particularly plasmid-bearing *S. Typhimurium* OU5045 and *S. Enteritidis* OU7130, induced more of macrophage autophagy than of inflammasome. The virulence plasmids of *Salmonella* OU7130 are therefore likely involved in the induction of macrophage autophagy. *Salmonella*-induced macrophage autophagy may reduce inflammasome activity.

Formation of macrophage foam cells, promoted by oxLDL in the arterial intima, is a hallmark of atherosclerosis development (Bobryshev 2006; Yu et al. 2013). To further investigate the induction of autophagy and inflammasome in foam cells during infection with different serotypes of *Salmonella*, THP-1 macrophages were transformed into foam cells through oxLDL uptake. Among different *Salmonella* serotypes, plasmid-bearing *S. Enteritidis* OU7130 showed most foam cell autophagy, at a level significantly higher than that demonstrated by plasmid-less strain OU7067 at 0.5 h after infection (Fig. 1C and 1D). However, a contrary trend, in which virulence plasmid-bearing strains induced less foam cell autophagy than did plasmid-less strains was observed for *S. Choleraesuis* infection. ASC protein induction by different serotypes of *Salmonella* demonstrated no significant difference. Consistent with the high ratio of macrophage autophagy, the

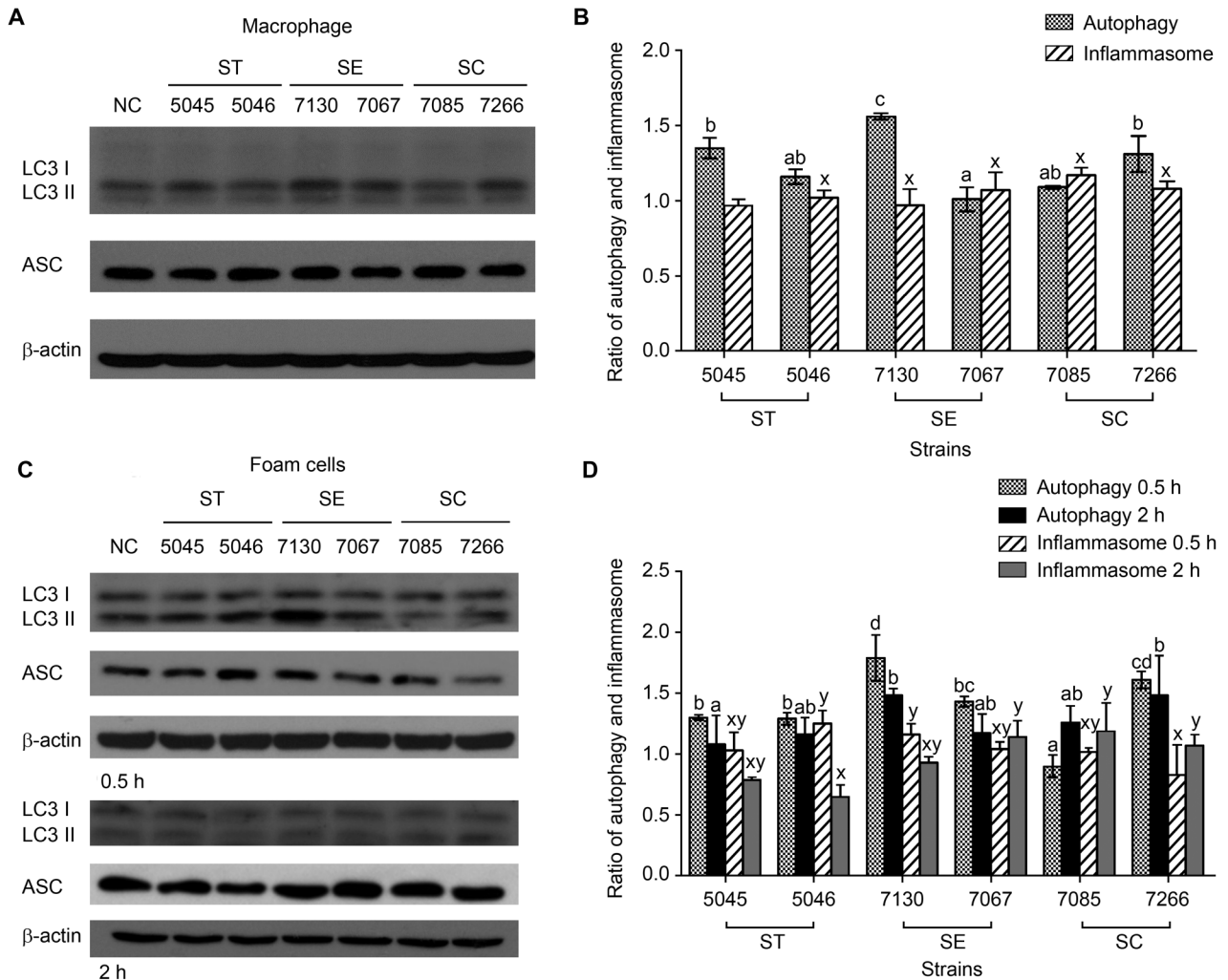


Fig. 1. Autophagy and inflammasome induced by *Salmonella* infection.

(A, C) Western blotting was performed with anti-LC3-I/II and anti-ASC antibodies. β -Actin Western blots were used as loading controls. LC3 was identified as a double band (i.e., LC3-I and LC3-II). (A) THP-1 macrophages and (C) THP-1 macrophage-derived foam cells were infected by different serotypes of *Salmonella* with or without virulence plasmid for 0.5 and 2 h. Uninfected macrophages and foam cells were the negative controls. (B, D) The LC3 I/II and ASC bands were quantified, and the ratios of autophagy and inflammasome were calculated from the ratios of infected to uninfected LC3-II/I cells and of infected to uninfected ASC, respectively. All values are represented as means \pm standard error ($n=3$). ^{a-c} indicate significant differences of autophagy formation between strains in the 0.5 and 2 h post-infection ($p<0.05$); ^{x,y,z} indicate significant differences of inflammasome formation between strains in the 0.5 and 2 h post-infection. ($p<0.05$). nc: uninfected cells.

virulence plasmid of *S. Enteritidis* OU7130 played a role in inducing both macrophage and foam cell autophagy. To assess the effect of *Salmonella* infection in foam cell autophagy and inflammasome at different infection stages, we detected LC3 and ASC expression at 0.5 and 2 h after infection. The ratio of foam cell autophagy significantly decreased from 0.5 to 2 h after infection, but the ratio of ASC expression did not change with infection time. Notably, the ratio of foam cell autophagy after plasmid-bearing *S. Choleraesuis* OU7085 infection increased from 0.5 to 2 h after infection, and ASC induction was higher than autophagy induction was at 0.5 h after infection. The mechanism used by plasmid-bearing *S. Choleraesuis* to induce autophagy is potentially different from that used by the other two *Salmonella* serotypes, *S. Enteritidis* and *S. Typhimurium*.

Plasmid-less *Salmonella* strains enhance foam cell surface CD36 expression. To understand infection by different serotypes *Salmonella* on foam cells within a preexisting atherosclerotic aortic aneurysm, we performed flow cytometric analysis and investigated CD36 expression in foam cells after *Salmonella* infection. CD36 functions as a high-affinity receptor responsible for oxLDL uptake by macrophages. The recognition and internalization of oxLDL particles by CD36, a specific macrophage scavenger receptor, is a critical step in foam cell formation (Rahaman et al. 2006). CD36 expression on foam cells infected by plasmid-less strains, particularly OU7266, was higher than that on those infected by plasmid-bearing strains (Table II and Fig. 2). The infection by plasmid-less *S. Choleraesuis* OU7266 induced foam cells to

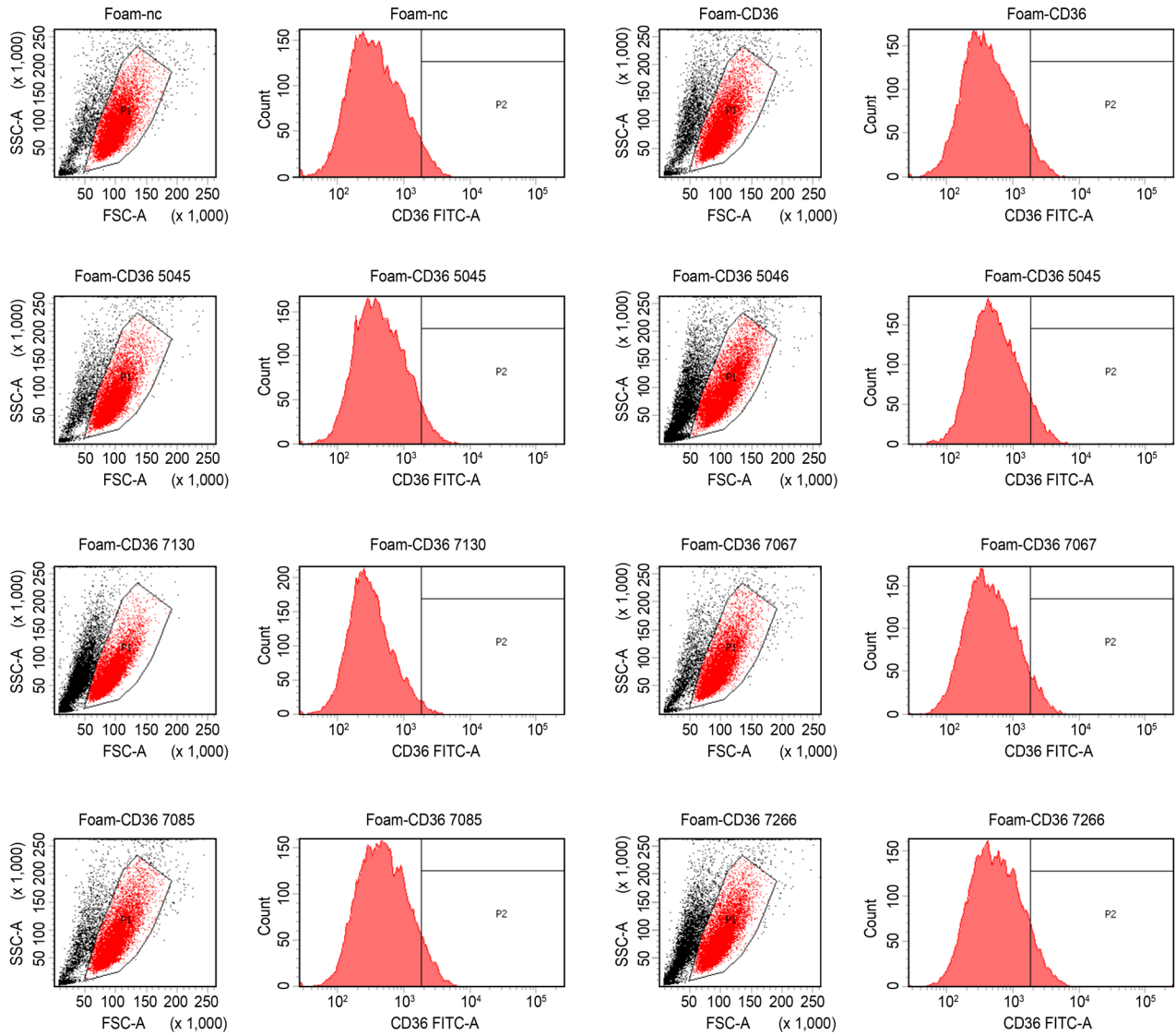


Fig. 2. CD36 expression in THP-1 macrophage-derived foam cells after different serotypes *Salmonella* infection. After treated with ox-LDL, THP-1 macrophage-derived foam cells were infected with plasmid-bearing and -less *S. Typhimurium*, *Enteritidis*, and *Choleraesuis*, respectively. CD36 expression was analyzed through flow cytometry.

express higher surface CD36 than did that by plasmid-bearing OU7085 to regulate foam cell autophagy. Notably, although plasmid-bearing *S. Enteritidis* OU7130

demonstrated the most foam cell autophagy, it exhibited the lowest CD36 expression, even lower than that in the uninfected cells.

Plasmid-bearing *S. Enteritidis* and plasmid-less *S. Choleraesuis* enhance IL-1 β secretion. Activation of the inflammasomes results in the processing and subsequent secretion of the pro-inflammatory cytokines IL-1 β and IL-18. To determine IL-1 β production after different serotypes of *Salmonella* infection, we performed ELISA to evaluate the IL-1 β secretion of infected THP-1 foam cells. Plasmid-bearing *S. Enteritidis* OU7130 and plasmid-less *S. Choleraesuis* OU7266 induced significantly higher IL-1 β secretion in foam cells than did plasmid-less *S. Enteritidis* OU7067 and plasmid-bearing *S. Choleraesuis* OU7085, respectively, at 0.5 and 2 hpi (Fig. 3). These results indicated that the virulence plasmid of *S. Enteritidis* is possibly

Table II

CD36 expression based on fluorescence density and gate (%) on foam cell interaction among different *Salmonella* serotypes.

Sample	%Parent	Mean
Foam NC	4.5	2 594
Foam NC-CD36 FITC	5.4	8 796
Foam 5045-CD36 FITC	5.2	7 204
Foam 5046-CD36 FITC	7.7	11 194
Foam 7130-CD36 FITC	1.8	4 807
Foam 7067-CD36 FITC	6.3	3 204
Foam 7085-CD36 FITC	7.2	5 341
Foam 7266-CD36 FITC	9.6	11 067

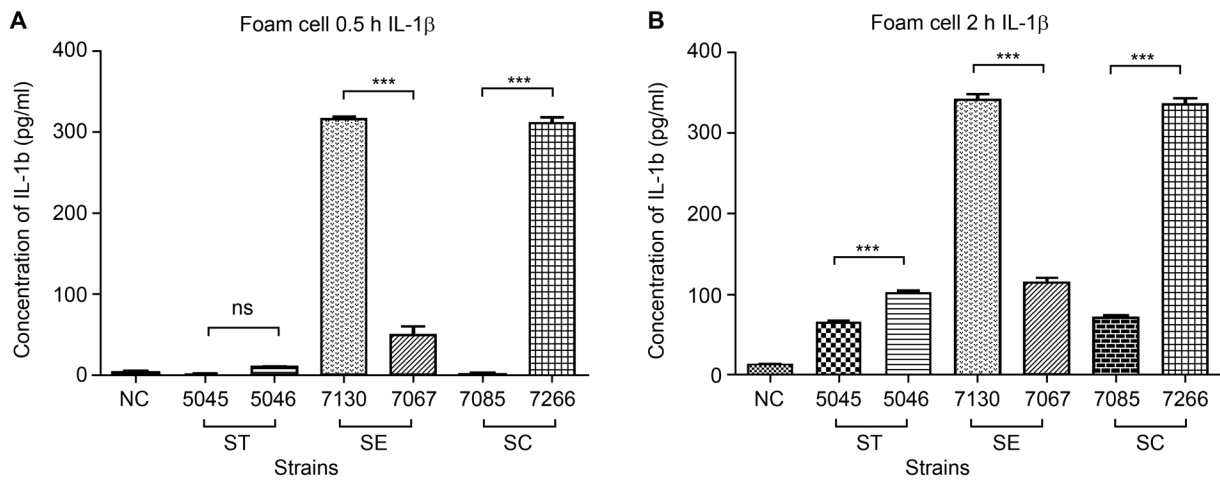


Fig. 3. IL-1 β production by THP-1 macrophage-derived foam cells after *Salmonella* infection.

ELISA was performed for IL-1 β produced after infection by different *Salmonella* serotypes. Foam cells were infected by plasmid-bearing *S. Typhimurium* OU5045, plasmid-less *S. Typhimurium* OU5046, plasmid-bearing *S. Enteritidis* OU7130, plasmid-less *S. Enteritidis* OU7067, and plasmid-bearing *S. Choleraesuis* OU7085 and plasmid-less *S. Choleraesuis* OU7266 for 0.5 and 2 h, and the supernatants were harvested and used for experiments. The experiments were performed in triplicate and presented as mean \pm SD. (***) $p < 0.005$, one-way ANOVA). NC: uninfected cells; ST: *S. Typhimurium*; SE: *S. Enteritidis*; SC: *S. Choleraesuis*.

involved in IL-1 β maturation during infection, whereas the virulence plasmid of *S. Choleraesuis* may play an opposite role.

***Salmonella*-infected foam cells secreted high IFN- α levels.** The cytokine IL-12 is a potent inducer of T helper 1 (Th1) cell differentiation and is required for resistance against bacterial infections. It is mostly produced by activated hematopoietic phagocytic cells (e.g., monocytes, macrophages, and neutrophils) and is composed of two chains, p40 and p35 (Trinchieri et al. 2003). To detect IL-12 secretion by foam cells after *Salmonella* infection, we performed ELISA. IL-12p40 secretion levels did not differ among different *Salmonella* serotypes (Fig. 4A). Nevertheless, the plasmid-less *S. Enteritidis* OU7067-infected foam cells secreted the highest IL-12p35 level among other infected cells and uninfected cells (Fig. 4B). *S. Enteritidis* infection may play a role in Th1-mediated immune response by increasing IL-12p35 secretion. In addition to IL-12, type I IFNs, considered primary cytokines produced directly in response to microbial products, are key regulators of both innate and adaptive immune responses. Stimulation with gram-negative bacteria, including *S. Typhimurium*, induces type I IFN production (Mancuso et al. 2007). The IFN- α level was significantly higher in *Salmonella*-infected foam cells than it was in uninfected foam cells (Fig. 4C). In foam cells, IFN- α was strongly expressed 0.5 h after infection; however, the IFN- α level decreased 2 h after infection. Plasmid-bearing *S. Typhimurium* OU5045-infected foam cells exhibited the highest IFN- α level 2 h after infection, suggesting that plasmid-bearing *S. Typhimurium* induces a higher level of immune response than other *Salmonella* serotypes do.

Discussion

Unlike other pathogens that cause infected aortic aneurysms (e.g., *Staphylococcus* and *Pseudomonas*), *Salmonella* resides in the phagosomes of the host macrophages and other antigen-presenting cells. Notably, compared with the endovascular repair of aortic aneurysms infected by other pathogens, the endovascular repair of *Salmonella*-infected aortic aneurysms by using graft-stents leads to fewer recurrent prosthetic infections (Huang et al. 2014b). *Salmonella* species may propagate by decreasing the innate immunity of the host and induce a systemic inflammatory response, possibly leading to degenerative aortic aneurysms. Foam cell formation from stimulated macrophages is a characteristic of atherosclerotic vascular degeneration. In this study, we investigated autophagy and inflammasome induction in foam cells after infection with different *Salmonella* serotypes to mimic the clinical scenario of *Salmonella*-associated infected aortic aneurysms.

Macrophage autophagy plays a protective role in atherosclerosis (Liao et al. 2012). Autophagy prevents macrophage apoptosis and defective efferocytosis, both of which promote plaque necrosis in advanced atherosclerosis. In this study, virulence plasmid-bearing *S. Enteritidis* OU7130 induced the most foam cell autophagy, whereas plasmid-bearing *S. Choleraesuis* OU7085 induced the least foam cell autophagy. Infection by plasmid-bearing *S. Choleraesuis* OU7085 induced less autophagy than did its plasmid-less strain, potentially promoting atherosclerosis formation. By contrast, infection by plasmid-bearing *S. Enteritidis* OU7130 induced more autophagy than did its plas-

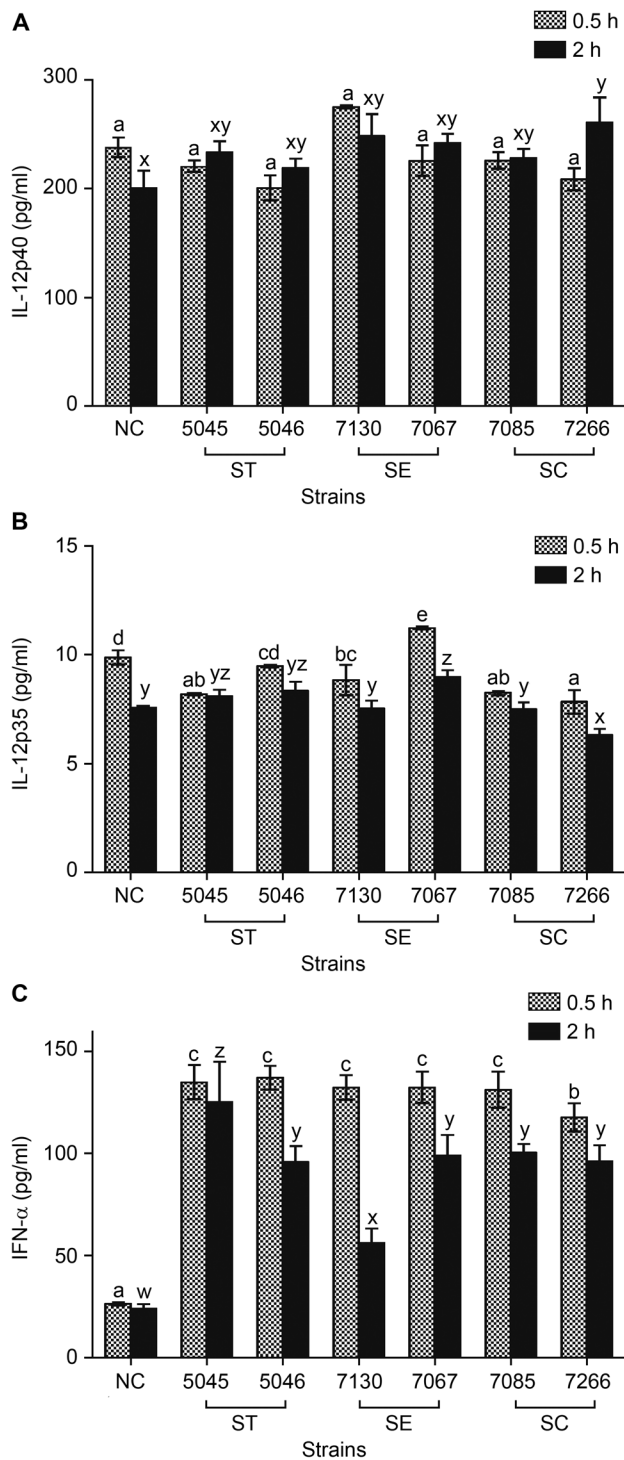


Fig. 4. Cytokines expression in response to *Salmonella* infection. ELISA for (A) interleukin (IL)-12p40, (B) IL-12p35, and (C) IFN- α produced after infection by different *Salmonella* serotypes. THP-1 macrophage-derived foam cells were infected by *Salmonella* with or without virulence plasmids for 0.5 and 2 h, and the supernatants were harvested and used for experiments. All values are presented as means \pm standard error ($n=3$). ^{a-z} indicate significant differences between strains 0.5 h after infection ($p < 0.05$); ^{w-z} indicate significant differences between strains 2 h after infection ($p < 0.05$). nc: uninfected cells.

mid-less strain, likely providing negligible promotion of atherosclerosis formation. Sower and Whelan (1962) demonstrated that *Salmonella* was a common cause of

infected aneurysms in patients with preexisting atherosclerosis. Wang et al. (1996) and Chan et al. (1995) have reported that the majority of infected aneurysms in Taiwan are caused by *S. Choleraesuis*. *S. Choleraesuis* may seed in atheroma and subsequently induce mycotic aortic aneurysm formation (Chiu et al. 2004). In addition, the virulence plasmid of *S. Choleraesuis* is possibly involved in inhibiting cell autophagy, causing the formation of atherosclerosis and infected aneurysm. A study also reported that most clinical isolates of *S. Choleraesuis* carry the virulence plasmid pSCV (Chu et al. 2001). Moreover, our clinical data from a previous study demonstrated that *S. Choleraesuis* affected surgical death and aneurysm-related death in a patient with infected aortic aneurysm (Huang et al. 2014a).

A crucial part of the innate immune response is the assembly of the inflammasome. Formation of the inflammasome in host cells in response to the detection of PAMPs facilitates the production of the proinflammatory cytokines IL-1 β and IL-18 (Man et al. 2014). ASC is a signal adaptor protein that is recruited to canonical inflammasomes, whereupon ASC polymerizes into a large, "speck"-like complex (Bierschenk et al. 2019). ASC specks are also formed during noncanonical inflammasome signaling. In this study, we investigated the induction of inflammasome by detecting ASC expression and IL-1 β secretion after *Salmonella* infection. We found that the ASC expression among different *Salmonella* serotypes infection was similar. Nevertheless, the secretion of IL-1 β was highly induced after plasmid-bearing *S. Enteritidis* OU7130 and plasmid-less *S. Choleraesuis* OU7266 infection, suggesting that the activation of inflammasome was induced by different *Salmonella* serotypes with or without virulence plasmid. The similar ASC expression after different *Salmonella* serotypes infection indicates that the role of ASC may be dispensable for different *Salmonella* serotypes with or without virulence plasmid infection. In all, the data indicate that the virulence plasmid of *S. Enteritidis* OU7130 plays a role in stimulating inflammasome formation while virulence plasmid of *S. Choleraesuis* OU7266 plays a suppression role.

The proinflammatory cytokine IL-12, produced by macrophages in response to microbial pathogens, comprises an α -chain p35 and β -chain p40. In the activated IL-12-producing antigen-presenting cells, p35 chain production is generally lower than p40 chain production, making p35 molecule formation a rate-limiting step in the bioactive IL-12 formation process (Snijders et al. 1996). The level of bioactive IL-12 production in monocytes in response to lipopolysaccharide and cytokines is determined by the level of p35 expression. In this study, we investigated IL-12 expression after infection by different *Salmonella* serotypes, and we found that infection by plasmid-less *S. Typhimurium*

and *S. Enteritidis* induced higher expression of IL-12p35 than did their plasmid-bearing strains. Even after 2 h of infection, plasmid-bearing *S. Enteritidis* induced lower IL-12p35 expression than did its plasmid-less strain. However, the expression of IL-12p35 after *S. Choleraesuis* infection demonstrated the opposite trend. These findings imply that *S. Typhimurium* and *S. Enteritidis* may induce higher inflammatory response after contact with foam cell or immune cells. By contrast, *S. Choleraesuis* suppresses inflammatory response and hides in foam cells; this makes eradication of atheromatous plaque difficult. After activation during atherosclerosis, macrophages produce IL-12, which drives inflammation and exacerbates atherosclerosis (Kleemann et al. 2008; Maiuri et al. 2013). Plasmid-bearing *S. Enteritidis* induces more cell autophagy as well as lower IL-12p35 expression than does the plasmid-less strain, suggesting that the virulence plasmid is involved in the induction of cell autophagy and reduction of inflammation to atherosclerosis development.

In conclusion, the virulence plasmid of *Salmonella* caused different effects after infection; plasmid-bearing *S. Enteritidis* induced more foam cell autophagy and IL-1 β secretion than did its plasmid-less strain, whereas plasmid-bearing *S. Choleraesuis* induced less foam cell autophagy and IL-1 β secretion than did its plasmid-less strain. *Salmonella* may affect the course of foam cells formation or even aortic aneurysm through autophagy.

ORCID

Yao-Kuang Huang [0000-0003-2699-2207](https://orcid.org/0000-0003-2699-2207)

Acknowledgments

We thank Wallace Academic Editing for editing this manuscript.

This study was supported by grants from the Ministry of Science and Technology of Taiwan (grant number: MOST 103-2314-B-182A-073-MY2) and Chang Gung Memorial Hospital, Chiayi, Taiwan (grant numbers: CMRPG6B0503, CMRPG6E0423, CMRPG6G0101, and CMRPG6H0121).

Conflict of interest

The authors do not report any financial or personal connections with other persons or organizations, which might negatively affect the contents of this publication and/or claim authorship rights to this publication.

Literature

- Bekkering S, Quintin J, Joosten LAB, van der Meer JWM, Netea MG, Riksen NP.** Oxidized low-density lipoprotein induces long-term proinflammatory cytokine production and foam cell formation via epigenetic reprogramming of monocytes. *Arterioscler Thromb Vasc Biol.* 2014 Aug;34(8):1731–1738. <https://doi.org/10.1161/ATVBAHA.114.303887>
- Bergsbaken T, Fink SL, Cookson BT.** Pyroptosis: host cell death and inflammation. *Nat Rev Microbiol.* 2009 Feb;7(2):99–109. <https://doi.org/10.1038/nrmicro2070>
- Bierschenk D, Monteleone M, Moghaddas F, Baker PJ, Masters SL, Boucher D, Schroder K.** The *Salmonella* pathogenicity island-2 subverts human NLRP3 and NLRC4 inflammasome responses. *J Leukoc Biol.* 2019 Feb;105(2):401–410. <https://doi.org/10.1002/JLB.MA0318-112RR>
- Bobryshev YV.** Monocyte recruitment and foam cell formation in atherosclerosis. *Micron.* 2006 Apr;37(3):208–222. <https://doi.org/10.1016/j.micron.2005.10.007>
- Chan P, Tsai CW, Huang JJ, Chuang YC, Hung JS.** Salmonellosis and mycotic aneurysm of the aorta. A report of 10 cases. *J Infect.* 1995 Mar;30(2):129–133. [https://doi.org/10.1016/S0163-4453\(95\)80007-7](https://doi.org/10.1016/S0163-4453(95)80007-7)
- Chiu S, Chiu C-H, Lin T-Y.** *Salmonella enterica* serotype Choleraesuis infection in a medical center in northern Taiwan. *J Microbiol Immunol Infect.* 2004 Apr;37(2):99–102.
- Chu C, Chiu CH, Wu WY, Chu CH, Liu TP, Ou JT.** Large drug resistance virulence plasmids of clinical isolates of *Salmonella enterica* serovar Choleraesuis. *Antimicrob Agents Chemother.* 2001 Aug 01;45(8):2299–2303. <https://doi.org/10.1128/AAC.45.8.2299-2303.2001>
- Forbes TL, Harding GEJ.** Endovascular repair of *Salmonella*-infected abdominal aortic aneurysms: A word of caution. *J Vasc Surg.* 2006 Jul;44(1):198–200. <https://doi.org/10.1016/j.jvs.2006.03.002>
- Huang YK, Chen CL, Lu MS, Tsai FC, Lin PL, Wu CH, Chiu CH.** Clinical, microbiologic, and outcome analysis of mycotic aortic aneurysm: the role of endovascular repair. *Surg Infect (Larchmt).* 2014a Jun;15(3):290–298. <https://doi.org/10.1089/sur.2013.011>
- Huang YK, Ko PJ, Chen CL, Tsai FC, Wu CH, Lin PJ, Chiu CH.** Therapeutic opinion on endovascular repair for mycotic aortic aneurysm. *Ann Vasc Surg.* 2014b Apr;28(3):579–589. <https://doi.org/10.1016/j.avsg.2013.07.009>
- Kleemann R, Zadelaar S, Kooistra T.** Cytokines and atherosclerosis: a comprehensive review of studies in mice. *Cardiovasc Res.* 2008 May 02;79(3):360–376. <https://doi.org/10.1093/cvr/cvn120>
- Liao X, Sluimer JC, Wang Y, Subramanian M, Brown K, Pattison JS, Robbins J, Martinez J, Tabas I.** Macrophage autophagy plays a protective role in advanced atherosclerosis. *Cell Metab.* 2012 Apr;15(4):545–553. <https://doi.org/10.1016/j.cmet.2012.01.022>
- Maiuri MC, Grassia G, Platt AM, Carnuccio R, Ialenti A, Maffia P.** Macrophage autophagy in atherosclerosis. *Mediators Inflamm.* 2013;2013:1–14. <https://doi.org/10.1155/2013/584715>
- Man SM, Hopkins LJ, Nugent E, Cox S, Glück IM, Tourlomis P, Wright JA, Cicuta P, Monie TP, Bryant CE.** Inflammasome activation causes dual recruitment of NLRC4 and NLRP3 to the same macromolecular complex. *Proc Natl Acad Sci USA.* 2014 May 20;111(20):7403–7408. <https://doi.org/10.1073/pnas.1402911111>
- Mancuso G, Midiri A, Biondo C, Beninati C, Zummo S, Galbo R, Tomasello F, Gambuzza M, Macrì G, Ruggeri A, et al.** Type I IFN signaling is crucial for host resistance against different species of pathogenic bacteria. *J Immunol.* 2007 Mar 01;178(5):3126–3133. <https://doi.org/10.4049/jimmunol.178.5.3126>
- Martinet W, De Meyer GRY.** Autophagy in atherosclerosis: a cell survival and death phenomenon with therapeutic potential. *Circ Res.* 2009 Feb 13;104(3):304–317. <https://doi.org/10.1161/CIRCRESAHA.108.188318>
- Martinon F, Burns K, Tschopp J.** The inflammasome: a molecular platform triggering activation of inflammatory caspases and processing of proIL- β . *Mol Cell.* 2002;10(2):417–426. [https://doi.org/10.1016/S1097-2765\(02\)00599-3](https://doi.org/10.1016/S1097-2765(02)00599-3)
- Martinon F, Tschopp J.** Inflammatory caspases and inflammasomes: master switches of inflammation. *Cell Death Differ.* 2007 Jan;14(1):10–22. <https://doi.org/10.1038/sj.cdd.4402038>
- Nishida K, Yamaguchi O, Otsu K.** Crosstalk between autophagy and apoptosis in heart disease. *Circ Res.* 2008 Aug 15;103(4):343–351. <https://doi.org/10.1161/CIRCRESAHA.108.175448>

- Rahaman SO, Lennon DJ, Febbraio M, Podrez EA, Hazen SL, Silverstein RL.** A CD36-dependent signaling cascade is necessary for macrophage foam cell formation. *Cell Metab.* 2006 Sep;4(3):211–221. <https://doi.org/10.1016/j.cmet.2006.06.007>
- Seveau S, Turner J, Gavrillin MA, Torrelles JB, Hall-Stoodley L, Yount JS, Amer AO.** Checks and balances between autophagy and inflammasomes during infection. *J Mol Biol.* 2018 Jan;430(2):174–192. <https://doi.org/10.1016/j.jmb.2017.11.006>
- Snijders A, Hilkens CM, van der Pouw Kraan TC, Engel M, Aarden LA, Kapsenberg ML.** Regulation of bioactive IL-12 production in lipopolysaccharide-stimulated human monocytes is determined by the expression of the p35 subunit. *J Immunol.* 1996 Feb 1;156(3):1207–1212.
- Sower ND, Whelan TJ Jr.** Suppurative arteritis due to *Salmonella*. *Surgery.* 1962 Dec;52(6):851–859.
- Sun Q, Fan J, Billiar TR, Scott MJ.** Inflammasome and autophagy regulation – a two-way street. *Mol Med.* 2017 Jan;23(1):188–195. <https://doi.org/10.2119/molmed.2017.00077>
- Trinchieri G, Pflanz S, Kastelein RA.** The IL-12 family of heterodimeric cytokines: new players in the regulation of T cell responses. *Immunity.* 2003 Nov;19(5):641–644. [https://doi.org/10.1016/S1074-7613\(03\)00296-6](https://doi.org/10.1016/S1074-7613(03)00296-6)
- Vural A, Kehrl JH.** Autophagy in macrophages: impacting inflammation and bacterial infection. *Scientifica (Cairo).* 2014;2014:1–13. <https://doi.org/10.1155/2014/825463>
- Wang JH, Liu YC, Yen MY, Wang JH, Chen YS, Wann SR, Cheng DL.** Mycotic aneurysm due to non-typhi *salmonella*: report of 16 cases. *Clin Infect Dis.* 1996 Oct 01;23(4):743–747. <https://doi.org/10.1093/clinids/23.4.743>
- Wang L, Yan J, Niu H, Huang R, Wu S.** Autophagy and ubiquitination in *Salmonella* infection and the related inflammatory responses. *Front Cell Infect Microbiol.* 2018 Mar 14;8:78. <https://doi.org/10.3389/fcimb.2018.00078>
- Yu XH, Fu YC, Zhang DW, Yin K, Tang CK.** Foam cells in atherosclerosis. *Clin Chim Acta.* 2013 Sep;424:245–252. <https://doi.org/10.1016/j.cca.2013.06.006>

Molecular Epidemiology of Hepatitis B Virus in Turkish Cypriot

UNAL SUMER^{1*} and MURAT SAYAN^{2,3}

¹Near East University, Faculty of Medicine, Department of Medical Microbiology,
Nicosia, Northern Cyprus

²Kocaeli University, Faculty of Medicine, Clinical Laboratory, PCR Unit, Kocaeli, Turkey

³Near East University, Research Centre of Experimental Health Sciences, Nicosia, Northern Cyprus

Submitted 25 June 2019, revised 21 August 2019, accepted 26 August 2019

Abstract

There is an increased demand for molecular and epidemiological information regarding Hepatitis B Virus (HBV) infection as the disease severity depends on these specifications. We have aimed to analyze nucleos(t)ide analogues (NA) resistance and typical HBsAg escape mutations with the dispersion of HBV genotype/subgenotype/HBsAg serotypes on overlapping *pol/S* gene regions in the Turkish population. Samples were collected in Northern Cyprus. Reverse transcriptase (*rt*) region between 80–250 amino acids were amplified. Typical HBsAg escape mutations were determined as HBIg escape (6.48%), vaccine escape (8.34%), HBsAg misdiagnosis (9.25%), and immune escape mutations (8.34%). NAs resistances were determined as primary (2.78%), partial (2.78%), and compensatory mutations (26.85%) in overlapping *pol/S* gene region. The study patients were predominantly infected with HBV genotype D/D1 (98%). However, the predominant HBsAg serotype was *ayw2* (99%). The most common NA resistance mutation was rtQ215H/P/S (16.67%), however, for *S* gene the misdiagnosis mutations were observed most frequently (9.25%). We can conclude that HBV D/D1 is the dominant strain and *ayw2* is the dominant serotype in the Turkish Cypriot. Cyprus is an island located in the Eastern Mediterranean region, and it is, therefore, a key location for human trafficking and immigration; as a result of this reputation, it is necessary to analyze HBV phylogenetically for local dynamics, and our results indicate that treatment naïve population is prone to these *pol/S* gene mutations. However, if HBV strains were also analyzed among Greek Cypriots too, this would enable a complete island survey. With this work, we believe that we have enlightened this subject for further research.

Key words: hepatitis B Virus, genotype, drug resistance, hepatitis B surface antigens

Introduction

Hepatitis B virus (HBV), which belongs to the family of *Hepadnaviridae* and is one of the smallest enveloped DNA viruses, is a global health concern as more than 2 billion of people are affected and around 260 million of people are chronically infected. In 2015, according to WHO, 275 million people live with HBV, and as estimated, 887 000 deceased as a result of the infection (WHO 2019). The virus is very old, as it has been infecting humans for at least 28 centuries. Humans are the only reservoir for this pathogen, which is 50–100 times more contagious than the Human Immunodeficiency Virus (Cheah et al. 2018). Both morbidity and mortality rates are high, as there is an increased lifetime risk of hepatocellular carcinoma, cirrhosis and liver disease (Bissinger et al. 2015; Cheah et al. 2018; Kostaki et al.

2018). Due to error-prone reverse transcriptase activity, a high nucleotide mismatch rate (10^5 change/base/replication) and a high replicative capacity ($> 10^{12}$ virion/day) are observed, and HBV is characterized by a significant degree of genetic heterogeneity (Kostaki et al. 2018). The HBV genome encloses four partially overlapping open reading frames, which are PreS1/S2/S, PreC/C, P, and X encoding seven different proteins. Most significantly, Reverse Transcriptase (*RT*) and HBsAg frames overlap at *RT* amino acid 8–236, with HBsAg frameshift downstream by one nucleotide. Therefore, it indicates that mutations in these specific areas might result in drug resistance (Zehender et al. 2014; Zamor et al. 2017).

The high degree of genomic heterogeneity categorizes HBV into 10 genotypes (A–J), and an intergroup difference of around 7.5% is observed. All genotypes, except E and G, are classified further into 25 different

* Corresponding author: U. Sumer, Near East University, Faculty of Medicine, Department of Medical Microbiology, Nicosia, Northern Cyprus. e-mail: usumer.lancetlab@gmail.com

© 2019 Unal Sumer and Murat Sayan

This work is licensed under the Creative Commons Attribution-NonCommercial-NoDerivatives 4.0 License (<https://creativecommons.org/licenses/by-nc-nd/4.0/>).

subgenotypes, with a difference of around 4% being observed (Kramvis et al. 2005; Kostaki et al. 2018). HBV-A and HBV-D are present around the globe, whereas HBV-A is mainly seen in Europe and Africa, and HBV-D in the Middle East and Europe. HBV-B and HBV-C are generally found in Oceania and Eastern Asia, HBV-E in both Central and Western Africa. HBV-F and HBV-H are found in Alaska and Latin America only. HBV-D is considered to be pandemic. HBV-D1 is dominant in Australia, Europe, Indonesia, North Africa, and Western Asia, whereas HBV-D2 is seen in Albania, Japan, Malaysia, North-Eastern Europe, Russia, and United Kingdom (Tallo et al. 2008; Bissinger et al. 2015; Kostaki et al. 2018). A recent study in Brazil showed that due to Italian colonization, the dominance of genotype D/D3 is observed (Paoli et al. 2018). A similar study was performed before in the same region, and once again, genotype D/D3 was found to be the most relevant genotype (Chacha et al. 2017).

The prevalence of HBV can be classified into three regions; low (<2%), middle (2–7%), and high (>8%) endemities. Turkey is categorized as middle endemicity with a prevalence rate of 0.8–5.7%, while the Turkish Republic of Northern Cyprus (TRNC) falls into a low category with a rate of 1.2% (Arikan et al. 2016; Ozguler and Sayan 2018). However, Cyprus is an island located in the Eastern Mediterranean, to the south of Turkey. Since 1974, there have been two communities living separately on the island: Turkish and Greek Cypriots. The exact population of North Cyprus is not known as the population number is dynamic, this is due to sex worker and immigrant trafficking that occurs along with constant international student and tourist travel. However, there is no data regarding HBV dynamics for South Cyprus. The South of the island is subject to more immigrations and human trafficking (Kaptanoglu et al. 2013; U.S. Department of State Publication 2018).

Cyprus had an estimated population of 1 193 635 in 2011. Around 352 000 were believed to live in North Cyprus, but the number has climbed up to half a million. Half of these are Cypriot-born children or Turkish settlers. Around 230 000 of those are classified as native-born TRNC citizens. The exact population remains unknown as North Cyprus has a dynamic society of students and tourists who regularly visit the island (Christou 2018; World Population Review 2018). Immunisation against HBV in the TRNC was rare in the late 80s, and the program was first introduced in the country in July 1998 (Kurugol et al. 2009). Between 2014 and 2018, 3149 HBsAg positive Turkish citizens were living in the TRNC, where 98.16% were of Turkish origin and 1.84% was Turkish Cypriots (KKTC Sağlık Bakanlığı 2019). Previous studies have concluded that the overall HBsAg positivity rate for the TRNC is 1.2% (Arikan et al. 2016).

There is a high demand for genotype information and investigation regarding HBV infected individuals. This importance rules to be informed regarding molecular and epidemiological specifications. As with the aim of this importance, we have aimed to analyze the dispersion of genotype/subgenotype/serotype together with *pol* gene mutations, which are related to NA therapy, and *S* gene mutations.

Experimental

Materials and Methods

Patients Samples. HBsAg reactive serum samples were collected and stored at -80°C in the Near East University Laboratory, Nicosia and Lancet Medical Diagnostic Laboratory, Famagusta between the dates of January 2015 and August 2018. This project obtained the Ethical Committee approval on 29 March 2018 from the Near East University Ethical Committee (Approval Number YDU/2018/56-539). As part of the Ethical approval, Helsinki Declaration principles were followed. Samples were taken from patients who presented to either of the health centers for residential permit screening, pre/post-operation screening, blood bank screening, and privately requested tests. The total number of samples in our study ($n = 170$) represented the total number of HBsAg reactive diagnoses made between the dates of January 2015 and August 2018. Unfortunately, information on the HBV infection status or phase of the patients is not available as they were not follow-up patients.

Serological Analysis. These samples were all screened for Anti-HCV, HBsAg, HIV Ag/Ab and Syphilis TP using Abbott Architect i1000SR/i2000SR automated analyzers. Out of the samples, only Turkish and Turkish Cypriot samples were selected ($n = 170$). Only HBsAg levels of the samples were measured primarily, and no other Hepatitis B serological markers were studied (such as AntiHBc).

Genotyping, subgenotyping, serotyping and mutation analysis. Out of 170 samples, only 108 were sequenced, as rest of the samples did not yield any HBV DNA load. The clinical demographics of the samples are given in Table I. For HBV genotypes/subgenotypes, nucleos(t)ide analogue (NA) drug resistance analysis, and *S* gene analysis the overlapping the *Pol/S* gene region (*rt* region, between amino acids 80–250) were chosen. For HBV *pol* gene amplification (742 base pairs), forward (F: 5'-TCGTGGTGGAC TTCTCTCA ATT-3') and backward (R: 5'-CGTTGACAGAC TTTC CAATCAAT-3') primers were designed and used. HBV *Pol* gene amplification and Sanger dideoxy sequencing protocols were all performed as described previously by Sayan et al. (2010).

Table I
Demographic characteristics of the patients.

Characteristics	Patient group	Study group
Patients, n	170	108
Gender, M/F, n (%)	106 (63) / 64 (37)	68 (63) / 40 (37)
Age, years (mean \pm SD)	49 \pm 31	41.5 \pm 23.5
Nationality Turkish	122 (71)	83 (77)
Turkish Cypriot	48 (29)	25 (23)
HBsAg value, S/Co* (mean \pm SD)	3882.5 \pm 3712.5	3882.5 \pm 3712.5

Abbreviations: M – male; F – female; *S/Co: Sample/Cut-off.
HBsAg value was obtained using Abbott Architect i1000SR/i2000SR systems (Abbott, USA).

Sequences obtained were subsequently analyzed using a special online tool, the Geno2pheno (Centre of Advanced European Studies and Research, Bonn, Germany) drug resistance platform. The following target region and amino acid positions were analyzed for the determination of antiviral drug-associated potential vaccine-escape mutations (ADAPVEM) regions 161, 164, 172, 173, 175, 176, 182, and 193–196; HBIg selected escape mutation regions 118, 120, 123, 124, 129, 133, 134, 144, and 145; vaccine escape mutation regions 120, 126, 133, 143–145, and 193; Hepatitis B misdiagnosis mutation regions 120, 131, 133, and 143; immune-selected mutation regions 100, 101, 105, 109, 110, 114, 117, 119, 120, 123, 127, 128, 130–134, 140, and 143–145. The target region and amino acid position for the determination of HBV *pol* gene mutation were as follows: overlapping surface gene segments 100, 101, 105, 109, 110, 114, 117–121, 123, 124, 126, 127, 128–135, 137, 139, 140–142, 144–149, 151–153, 155–157, 161, 172, 173, 175, 176, and 193–196. The following target region and amino acid position for the determination of HBV *pol* gene mutation were analyzed: *rt* gene segments 74, 80, 82, 84, 85, 139, 149, 156, 169, 173, 180, 181, 184, 194, 200, 202, 204, 214, 215, 233, 236, 237, 238, and 250 (Sayan et al. 2012; Asan et al. 2018).

HBV genotype/subgenotypes were also phylogenetically analyzed using the Neighbour-Joining method. Primarily, the sample sequences and reference sequences were all aligned. A phylogenetic tree was created using CLC Sequence Viewer 8.0 (CLC bio A/S, Qiagen, Denmark). A bootstrap value of 1000 was chosen.

Three HBsAg glycoproteins share an *a* determinant epitope, which is located at the position 127–147. There are two other determinants namely, *d/y* at the position 122, lysine/arginine residue and *w/r* at the position 160; lysine/arginine residue represents each determinant, respectively. At the position 127, residue further differentiates *w* into four subtypes. The *adr* subtype only is further divided into *q*⁻/*q*⁺. With these combinations, nine different subtypes of HBV have been

identified (Yokosuka and Arai 2006). The analysis of HBsAg serotypes was also performed using the CLC sequence viewer, as the geno2pheno tool is not able to detect this information. After aligning the sequences to reference sequences, the phylogenetic parameters of UPGMA/Jukes-Cantor were used and the bootstrap value of 1000 was used.

Results

Baseline data. Out of 170 samples included in the study, only 108 (63.5%) were sequenced. Demographic characteristics of the patients from whom these samples were collected are listed in Table I. Genotypes/subgenotypes/HBsAg serotype analysis of 108 samples were performed following aligning for phylogenetic analysis (Fig. 1 and 2).

RT mutations. NA resistance mutations were detected in 35/108 (32.4%) of the samples, and as a novel data 2/108 (1.85%) of these samples confer ADAPVEMs (Table II). The compensatory resistance *pol* gene mutations were the most frequent as 29/108 (26.85%) of the samples comprise this category, followed by primary resistance mutations in 3/108 (2.78%), and lastly, partial resistance mutations in 3/108 (2.78%) samples analyzed. The most prevalent *pol* gene mutation was rtQ215H/P/S and it falls in the compensatory mutation category.

The S gene mutations. A total of 17/108 (15.74%) the S gene mutations were detected, together with 3/108 (2.78%) combined escape mutations in the same region (Table III). The highest S gene escape mutations were detected for HBsAg misdiagnosis 10/108 (9.25%), both vaccine and immune escape mutations in 9/108 (8.34%), and the lowest number mutations were observed for HBIg escape with a frequency of 6.48% (7/108).

Genotyping, subgenotyping and serotyping. According to our results, HBV-D/D1 was observed to be the major genotype/subgenotype with a prevalence of 106/108 (98%), and *ayw2* was the major serotype that accomplishes 99% (96/108) in Turkish Cypriots (Table IV). Also, it is important to mention that only 1/108 (1%) Turkish Cypriot were infected with HBV-D/D2, and 1/108 (1%) Turkish citizen were infected with HBV-E. A significant finding is that HBV-D/D2 was the only *ayw3* serotype 1/108 (1%).

Discussion

In our former research the following HBV genotypes were found, namely: D/D1; 70.6%, D/D2; 5.9%, D/D3; 1.5%, A/A1; 7.4%, A/A2; 2.9%, and E; 11.8% (Sayiner and Abacioglu 2010; Arikan et al. 2016). However, in this study, D/D1 was found in 98% of the

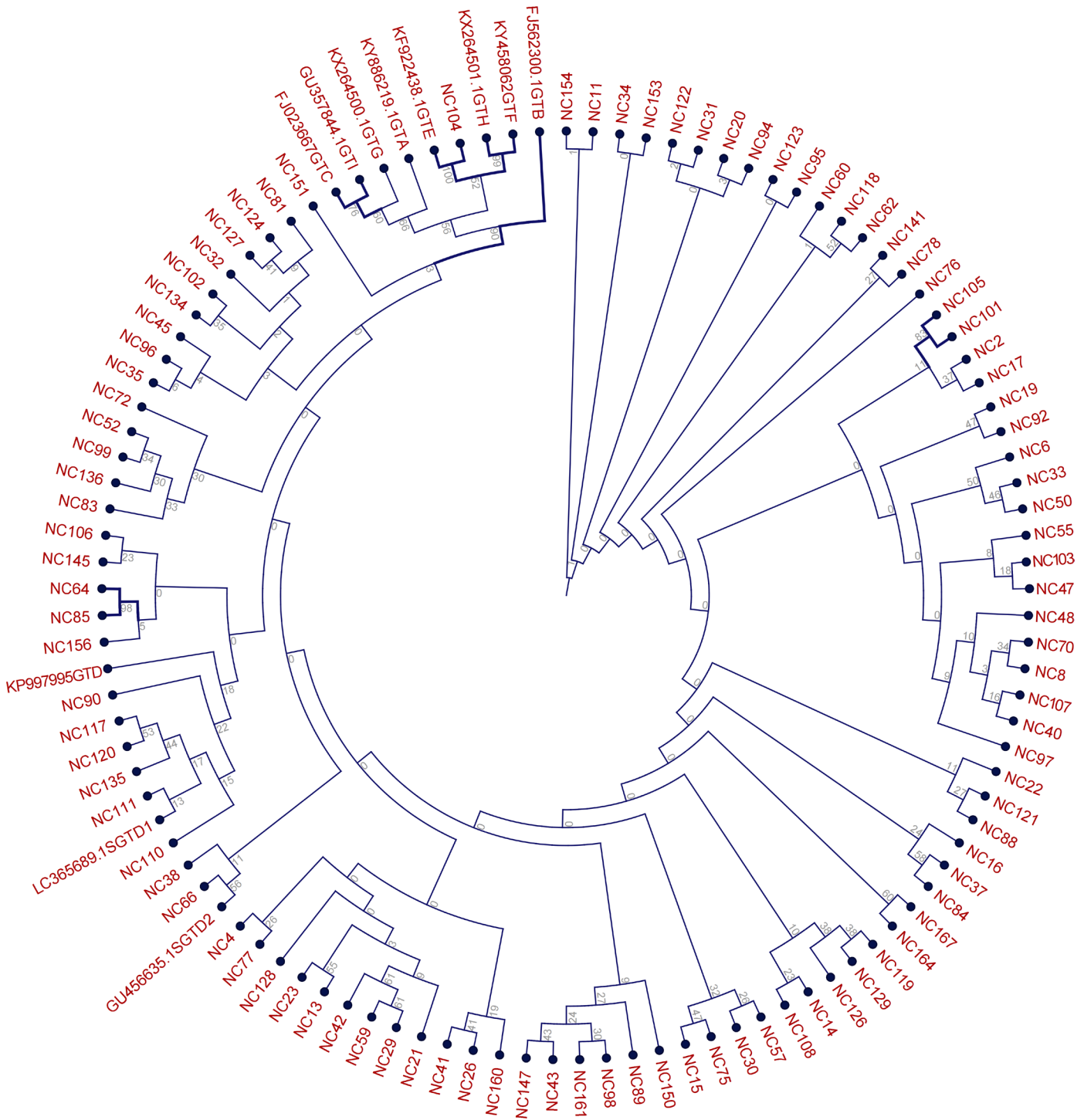


Fig. 1. Circular cladogram of HBV genotypes and subgenotypes. The phylogenetic tree was constructed using the CLC sequence viewer (CLC bio A/S, Qiagen, Denmark). The HBV reverse transcriptase region length was 495 base pairs in the alignment. The Neighbour-Joining and Jukes-Cantor methods were used. The Bootstrap value was chosen as 1000. HBV genotype A: KY886219.1, B: FJ562300.1, C: FJ023667 D: KP997995, D/D1: LC365689.1, D/D2:GU456635.1, E: KF922438.1, F: KY458062, G: KX264500.1, H: KX264501.1, I: GU357844.1 reference sequences were obtained from GenBank.

samples, and D/D2 and E only in 1% of the samples examined, respectively (Table IV). The most often detected genotype was D/D1 for both patient groups. This is the only similarity with our previous works and the main dissimilarity we observed in this study was that D/D2 was found in a Turkish Cypriot, and

a Turkish person was found to have genotype E, which has not been previously observed (Arikan et al. 2016).

Regarding other than Mediterranean region, high rates of genotype D have also been observed in the Middle East, South Asia, and North-East Europe (Sunbul et al. 2014; Zehender et al. 2014). Our results support

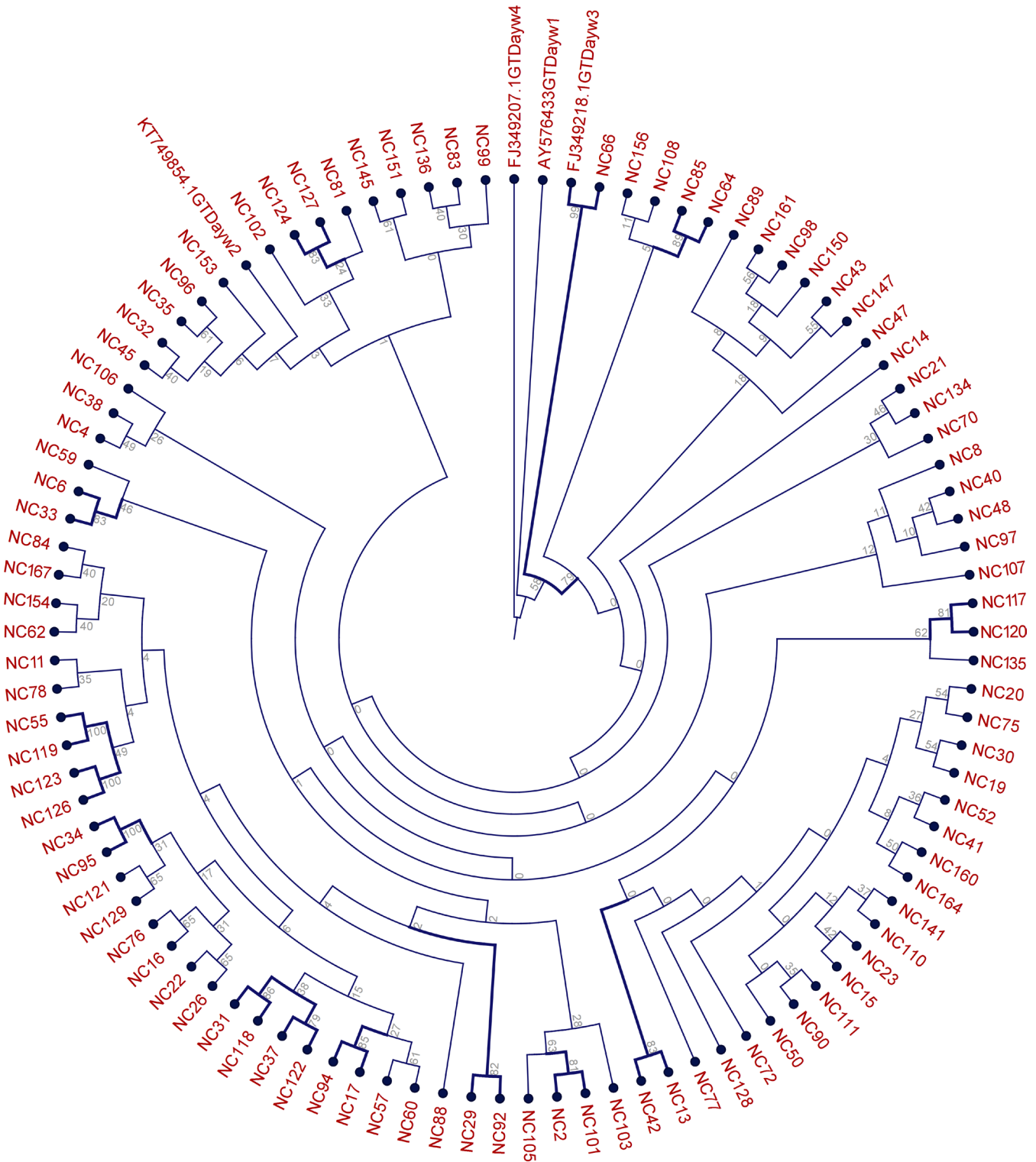


Fig. 2. Circular cladogram of HBsAg serotypes. The phylogenetic tree was constructed using the CLC sequence viewer (CLC bio A/S, Qiagen, Denmark). The HBV reverse transcriptase region length was 495 base pairs in the alignment. The UPGMA and Jukes-Cantor methods were used. The Bootstrap value was chosen as 1000. HBV D Serotype *ayw1*: AY576433, *ayw2*: KT749854.1, *ayw3*: FJ349218.1, *ayw4*: FJ349207.1 reference sequences were obtained from GenBank.

these findings as the majority of the students, sex workers, and labor workers mostly travel and immigrate to the TRNC from Europe, Turkey, and Africa. Therefore, we can state that genotype D was introduced into the society via migrations in the past several decades from

these regions, while other genotypes such as the serotype E could also be observed in the future (Zehender et al. 2014). In 2018, the article by Velkov et al. (2018) has been published that presents the global genotype distribution of HBV, assessing 125 countries and over

Table II
HBV *pol* gene mutation pattern and frequency in the study patients.

Mutation characteristic	Mutation pattern	Nucleos(t)ide analogue	Patient, n (%)
Primary resistance mutation	rtM204I	LAM, LDT, L-FMAU, FTC	2 (1.85)
	rtI233V	ADV	1 (0.92)
Total*	-	-	3 (2.78)
Partial resistance mutation	rtL80I	LAM, LDT	1 (0.92)
	rtL180M	LAM, LDT, L-FMAU, FTC	2 (1.85)
Total*	-	-	3 (2.78)
Compensatory mutation	rtL91I	LDT	7 (6.48)
	rtQ149K	ADV	7 (6.48)
	rtV214A	LAM, L-FMAU, FTC, TDF	2 (1.85)
	rtQ215H/P/S	LAM, L-FMAU, FTC, TDF	18 (16.67)
	rtN238D	ADV	6 (5.56)
Total*	-	-	29 (26.85)
ADAPVEM	rtM204I/sW196L	LAM, LDT	2 (1.85)
Total*	-	-	2 (1.85)

Abbreviations: LAM – lamivudine; LDT – telbivudine; L-FMAU – clevudine; FTC – emtricitabine; TDF – tenofovir; ADV – adefovir; ETV – entecavir; ADAPVEM – antiviral drug-associated potential vaccine escape mutant.

*Total: the number of total included *rt* gene mutations in 108 sequenced samples. The aa position 250 is where we expect a specific mutation to occur, two unknown mutations rtM250G/H detected were ETV related amino acid substitutions; these are not mutations which cause nucleoside resistance.

Table III
HBsAg escape mutations in the study patients.

HBsAg escape mutation category	Mutation pattern	Patient, n (%)	Combined pattern	Patient, n (%)
HBIG escape	sP120T, sQ129H, sM133I, sY134N, sD144E, sC147S	7 (6.48)	sM133I + sD144E	1 (0.92)
Vaccine escape	sP120S, sQ129H, sS143L, sD144E, sC147S, sS193L	9 (8.34)	sT126S + sS193L	1 (0.92)
HBsAg misdiagnosis	sP120T, sP120S, sR122K, sT131I, sM133I, sC147S	10 (9.25)	-	-
Immune escape	sQ101H, sG119R, sP120T, sT123N, sT131N, sY134F, sD144E	9 (8.34)	sG119R + sT123N	1 (0.92)
Total*	-	17 (15.74)	-	3 (2.78)

* The total number of patients which HBsAg mutation was detected.

Table IV
HBV genotypes, subgenotypes, and HBsAg serotypes of the samples.

HBV genotype	HBV subgenotype	Patients, n (%)	HBsAg serotype, n (%)*	Nationality
D	D1	106 (98)	ayw2, 96 (99)	TR, TRNC
	D2	1 (1)	ayw3, 1 (1)	TRNC
E	-	1 (1)	-	TR
Total	-	108 (100)	97 (100)	-

Abbreviations: TR – Turkey, TRNC – Turkish Republic of Northern Cyprus.

*Genotype E strain and short sequences (n = 11) were not included in serotype analysis.

900 publications. Their findings indicated that genotype D was dominant in Eastern Europe, the majority of Asia and North Africa. HBV genotype distribution shows a similar pattern among the countries in the same region but varies amongst different parts of the world.

Large population migrations can modify public health dynamics. High frequency of genotypes A-D was

observed in North America following migrations from Asia and Europe. A similar situation was observed in the Caribbean where genotypes A and D were found as a result of migrations from the African continent (Velkov et al. 2018; Al-Sadeq et al. 2019). We can see that migrations mainly from Turkey for working and living, and other parts of the Middle East for other purposes such

as studying have caused genotype D to be dominant and new genotypes such as E introduced to the TRNC.

In this study, a total of 3/108 (2.78%) primary, 3/108 (2.78%) partial and 29/108 (26.85%) compensatory mutations were observed in the *rt* gene (Table II). However, previously, primary/partial resistance mutations occurred with a frequency of 1% and compensatory mutations were of 37% (Arikan 2015). When analyzed in greater details, rtM204I, rtI233V, rtL80I, and rtL180M mutations were not detected before, and these mutations, particularly rtL80I and rtL180M, restore the activity of viral polymerase to near wild type levels, which helps to promote the replication of mutants (Lazarevic 2014). This indicates that treatment naïve population is prone to such mutations, and has a significant impact on the treatment procedures and costs. Also, primary/compensatory mutations alone may increase HBV DNA levels and cause failure in future treatment (Sayan 2010; Sayan et al. 2010; Sayan et al. 2011).

The *S* gene mutations; however, indicate different structure when compared to earlier work. In our study, the total number of the *S* gene mutations was 17/108 (15.74%), and combined *S* gene mutations were 3/108 (2.78%) (Table III). The previous work revealed the frequency of 29% and 9%, respectively (Arikan et al. 2016). HBV selected escape mutations in former work was 6%; however, in this study, different mutation pattern is observed with a similar percentage of 7/108 (6.48%); (Table III) (Arikan et al. 2016). sQ129H, sM133I, and sY134N mutations are associated with occult infection with D genotype; also they impair *S* protein secretion (Lazarevic 2014). HBV vaccine escape mutations in the prior work were observed with the frequency of 10% (Arikan et al. 2016). In this study, it was observed in 9/108 (8.34%) of the samples analyzed (Table III). Hepatitis B misdiagnosis mutation patterns in earlier work were only 4%, whereas in this study it was higher, and accounted for 9.25% (10/108) (Table III). Lastly, immune escape mutations in previous work were as often as in 24% of the samples. On the other hand, in this study, only 9/108 (8.34%) samples carried these mutations (Table III) (Arikan et al. 2016). Combined HBsAg mutations in this research were dissimilar to earlier study as 9% of the samples had such mutations, but in this study only 3/108 (2.78%) samples carried them (Arikan 2015). In summary, *S* gene mutations may lead to misdiagnoses (false-negative results) and cause insufficient protection using HBVg.

In the study by Al-Sadeq et al. (2019) performed in the Middle East and North Africa region, *S* gene mutations were detected in Egyptian, Saudi, Palestinian and Tunisian patients, in whom the genotypes B, D/D1, D/D3, and D/D7 were identified. We have detected only five common mutations and all the *S* gene mutations were observed only in D/D1 patients (Table III). This

indicates that different geographical regions may have different *S* gene mutation profiles, even though the genotypes of the patients are the same. The ADAPVEM analysis revealed 2/108 (1.85%) of the samples carried such mutations. These were rtM204I/sW196L mutations (Table II). In Turkey, the same mutation pattern was observed in 8.7% of the patients together with other ADAPVEMs. The ADAPVEM status has not yet been known for the TRNC, these results are initial data for monitoring of such mutations in the future. (Sayan et al. 2013; Asan et al. 2018; Ozguler and Sayan 2018).

In conclusion, HBV-D/D1 was the dominant strain, and *ayw2* is the serotype most often detected among Turkish Cypriots. Cyprus is an island located in the Eastern Mediterranean region, a strategic location for human trafficking and immigration, and as a result of this reputation, it is necessary to analyze HBV phylogenetically for international and local importance. However, data from Greek Cypriot is necessary, as it would enable a complete island survey to be performed. With this work, we believe that we have set the ground for further research of this topic.

One of the limitations of this study is a sample size, as larger samples will generate more significant results. The lack of prior work is another limitation as there is only one previous study, and additional work will uncover significant results in the future. Another limitation is that information is not available about the HBV infection status or phase of the patients as they were not follow-up patients.

Ethical approval

This project obtained Ethical Committee approval on 29 March 2018 from Near East University Ethical Committee. The Approval Number is YDU/2018/56-539, Project Number 539, and Committee Number 2018/56. Also, as part of Ethical approval, Declaration of Helsinki was respected.

Acknowledgments

We would like to thank the Near East University Laboratory and Lancet Medical Diagnostic Laboratory for the selection of the samples and assistance. Our thanks go to the Kocaeli University PCR unit for their valuable help on sequencing. We also thank Mr. Simon Thompson, Near East University, and Assoc. Prof. Dr. Bahire Ozad, Eastern Mediterranean University for their help on editing.

Conflict of interest

This is a Ph.D. thesis project.

The authors do not report any financial or personal connections with other persons or organizations, which might negatively affect the contents of this publication and/or claim authorship rights to this publication.

Literature

Al-Sadeq DW, Taleb SA, Zaied RE, Fahad SM, Smatti MK, Rizeq BR, Al Thani AA, Yassine HM, Nasrallah GK. Hepatitis B virus molecular epidemiology, host-virus interaction, coinfection,

- and laboratory diagnosis in the MENA Region: an update. *Pathogens*. 2019 May 11;8(2):63. <https://doi.org/10.3390/pathogens8020063>
- Arikan A, Şanlıdağ T, Süer K, Sayan M, Akçali S, Güler E.** [Molecular epidemiology of hepatitis B virus in Northern Cyprus] (in Turkish). *Mikrobiyol Bul.* 2016 Jan 7;50(1):86–93. <https://doi.org/10.5578/mb.10292>
- Arikan A.** Nucleoside analogue resistance and genotype/subgenotype dispersion of treatment naïve hepatitis B patients in Northern Cyprus [PhD thesis]. Institute of Health and Medical Sciences, Near East University, Nicosia; 2015.
- Asan A, Sayan M, Akhan S, Tekin Koruk S, Aygen B, Sirmatel F, Eraksoy H, Tuna N, Köse S, Kaya A, et al.** Molecular characterization of drug resistance in hepatitis B viruses isolated from patients with chronic infection in Turkey. *Hepat Mon.* 2018 Jan 24;18(1):e12472. <https://doi.org/10.5812/hepatmon.12472>
- Bissinger AL, Fehrle C, Werner CR, Lauer UM, Malek NP, Berg CP.** Epidemiology and genotyping of patients with chronic Hepatitis B: genotype shifting observed in patients from Central Europe. *Pol J Microbiol.* 2015;64(1):15–21.
- Chacha SGF, Gomes-Gouvêa MS, Malta FM, Ferreira SDC, Villanova MG, Souza FF, Teixeira AC, Passos ADDC, Pinho JRR, Martinelli ALC.** Distribution on HBV sungenotypes in Ribeirao Preto, Southeastern Brazil: a region with history of intense Italian immigration. *Braz J Infect Dis.* 2017;21(4):424–432. <https://doi.org/10.1016/j.bjid.2017.01.011>
- Cheah BC, Davies J, Singh GR, Wood N, Jackson K, Littlejohn M, Davison B, McIntyre P, Locarnini S, Davis JS, et al.** Sub-optimal protection against past hepatitis B virus infection where subtype mismatch exists between vaccine and circulating viral genotype in northern Australia. *Vaccine.* 2018 Jun;36(24):3533–3540. <https://doi.org/10.1016/j.vaccine.2018.01.062>
- Christou J.** Foreign students propel sharp population increase in north. *Cyprus Mail* [Internet]. 2018 Apr 3 [cited 2018 Dec 28]. Available from <https://cyprus-mail.com/2018/04/03/foreign-students-propel-sharp-population-increase-north/>
- Kaptanoğlu AF, Süer K, Diktaş H, Hınçal E.** Knowledge, attitudes and behaviour towards sexually transmitted diseases in Turkish Cypriot adolescents. *Cent Eur J Public Health.* 2013 Mar 1;21(1):54–58. <https://doi.org/10.21101/cejph.a3808>
- KKTC Sağlık Bakanlığı.** 2019 [cited 2019 Feb 2]. Available from <http://saglik.gov.ct.tr/>
- Kostaki EG, Karamitros T, Stefanou G, Mamais I, Angelis K, Hatzakis A, Kramvis A, Paraskevis D.** Unravelling the history of hepatitis B virus genotypes A and D infection using a full-genome phylogenetic and phylogeographic approach. *eLife.* 2018 Aug 07;7:e36709. <https://doi.org/10.7554/eLife.36709>
- Kramvis A, Kew M, François G.** Hepatitis B virus genotypes. *Vaccine.* 2005 Mar;23(19):2409–2423. <https://doi.org/10.1016/j.vaccine.2004.10.045>
- Kurugöl Z, Koturoğlu G, Akşit S, Ozacar T, Kayimbaşoğlu S, Ozbalkıç S, Erçal G, Güllüelli E, Bakkaloğlu F, Doğan E, et al.; Northern Cyprus Study Team.** Seroprevalence of hepatitis B infection in the Turkish population in Northern Cyprus. *Turk J Pediatr.* 2009 Mar-Apr;51(2):120–126.
- Lazarevic I.** Clinical implications of hepatitis B virus mutations: recent advances. *World J Gastroenterol.* 2014;20(24):7653–7664. <https://doi.org/10.3748/wjg.v20.i24.7653>
- Özgüler M, Sayan M.** Could resistant and escape variants of hepatitis B virus be a problem in the future? *Future Virol.* 2018 Mar;13(3):171–179. <https://doi.org/10.2217/fvl-2017-0144>
- Paoli J, Wortmann AC, Klein MG, Pereira VRZB, Cirolini AM, Godoy BA, Fagundes NJR, Wolf JM, Lunge VR, Simon D.** HBV epidemiology and genetic diversity in an area of high prevalence of hepatitis B in southern Brazil. *Braz J Infect Dis.* 2018 Jul;22(4):294–304. <https://doi.org/10.1016/j.bjid.2018.06.006>
- Sayan M, Akhan SC, Senturk O.** Frequency and mutation patterns of resistance in patients with chronic hepatitis B infection treated with nucleos(t)ide analogs in add-on and switch strategies. *Hepat Mon.* 2011 Oct 01;11(10):835–842. <https://doi.org/10.5812/kowsar.1735143X.1004>
- Sayan M, Buğdaci MS.** [HBV vaccine escape mutations in a chronic hepatitis B patient treated with nucleos(t)ide analogues] (in Turkish). *Mikrobiyol Bul.* 2013 Jul 29;47(3):544–549. <https://doi.org/10.5578/mb.5442>
- Sayan M, Cavdar C, Dogan C.** Naturally occurring polymerase and surface gene variants of hepatitis B virus in Turkish hemodialysis patients with chronic hepatitis B. *Jpn J Infect Dis.* 2012;65(6):495–501. <https://doi.org/10.7883/yoken.65.495>
- Sayan M, Şanlıdağ T, Akçali S, Arikan A.** [Hepatitis B virus genotype E infection in Turkey: the detection of the first case] (in Turkish). *Mikrobiyol Bul.* 2014 Oct 28;48(4):683–688. <https://doi.org/10.5578/mb.4769>
- Sayan M, Şentürk Ö, Akhan SÇ, Hülügü S, Çekmen MB.** Monitoring of hepatitis B virus surface antigen escape mutations and concomitantly nucleos(t)ide analog resistance mutations in Turkish patients with chronic hepatitis B. *Int J Infect Dis.* 2010 Sep; 14 Suppl 3:136–e141. <https://doi.org/10.1016/j.ijid.2009.11.039>
- Sayan M.** Molecular diagnosis of entecavir resistance. *Hepat Mon.* 2010;10(1):42–47.
- Sayiner A, Abacioglu H.** Epidemiology of hepatitis B in Turkey. In: Van Damme P, Vorsters A, Van Herck K, Hendrickx G, editors. *Viral Hepatitis.* Antwerp (Belgium): Viral hepatitis prevention board; 2010;18(2). p. 5–7.
- Sunbul M.** Hepatitis B virus genotypes: global distribution and clinical importance. *World J Gastroenterol.* 2014;20(18):5427–5434. <https://doi.org/10.3748/wjg.v20.i18.5427>
- Tallo T, Tefanova V, Priimägi L, Schmidt J, Katargina O, Michailov M, Mukomolov S, Magnius L, Norder H.** D2: major subgenotype of hepatitis B virus in Russia and the Baltic region. *J Gen Virol.* 2008 Aug 01;89(8):1829–1839. <https://doi.org/10.1099/vir.0.83660-0>
- U.S. Department of State Publication.** Trafficking in persons report. United States Department of State, Office of the Under Secretary for Civilian Security, Democracy, and Human Rights (USA): A/GIS/GPS; 2018. p. 159–162.
- Velkov S, Ott J, Protzer U, Michler T.** The global hepatitis B virus genotype distribution approximated from available genotyping data. *Genes (Basel).* 2018 Oct 15;9(10):495. <https://doi.org/10.3390/genes9100495>
- WHO.** Hepatitis B [Internet]. Geneva (Switzerland): World Health Organization; 2019 [cited 2019 Jul 23]. Available from <https://www.who.int/news-room/fact-sheets/detail/hepatitis-b>
- World Population Review.** Cyprus Population. Walnut (USA): World Population Review; 2018 [cited 2018 Dec 28]. Available from <http://worldpopulationreview.com/countries/cyprus-population/>
- Yokosuka O, Arai M.** Molecular biology of hepatitis B virus: effect of nucleotide substitutions on the clinical features of chronic hepatitis B. *Med Mol Morphol.* 2006 Sep 26;39(3):113–120. <https://doi.org/10.1007/s00795-006-0328-5>
- Zamor PJ, deLemos AS, Russo MW.** Viral hepatitis and hepatocellular carcinoma: etiology and management. *J Gastrointest Oncol.* 2017 Apr;8(2):229–242. <https://doi.org/10.21037/jgo.2017.03.14>
- Zehender G, Ebranati E, Gabanelli E, Sorrentino C, Lo Presti A, Tanzi E, Ciccozzi M, Galli M.** Enigmatic origin of hepatitis B virus: an ancient travelling companion or a recent encounter? *World J Gastroenterol.* 2014;20(24):7622–7634. <https://doi.org/10.3748/wjg.v20.i24.7622>

Cytokine Levels in the *In Vitro* Response of T Cells to Planktonic and Biofilm *Corynebacterium amycolatum*

ALINA OLENDER^{1*}, AGNIESZKA BOGUT¹, AGNIESZKA MAGRYŚ¹
and JACEK TABARKIEWICZ²

¹ Chair and Department of Medical Microbiology, Medical University of Lublin, Lublin, Poland

² Department of Human Immunology, Faculty of Medicine, University of Rzeszów, Rzeszów, Poland

Submitted 28 May 2019, revised 2 September 2019, accepted 16 September 2019

Abstract

Unravelling of the interplay between the immune system and non-diphtheria corynebacteria would contribute to understanding their increasing role as medically important microorganisms. We aimed at the analysis of pro- (TNF, IL-1 β , IL-6, IL-8, and IL-12p70) and anti-inflammatory (IL-10) cytokines produced by Jurkat T cells in response to planktonic and biofilm *Corynebacterium amycolatum*. Two reference strains: *C. amycolatum* ATCC 700207 (R-CA), *Staphylococcus aureus* ATCC 25923 (R-SA), and ten clinical strains of *C. amycolatum* (C-CA) were used in the study. Jurkat T cells were stimulated *in vitro* by the planktonic-conditioned medium (PCM) and biofilm-conditioned medium (BCM) derived from the relevant cultures of the strains tested. The cytokine concentrations were determined in the cell culture supernatants using the flow cytometry. The levels of the cytokines analyzed were lower after stimulation with the BCM when compared to the PCM derived from the cultures of C-CA; statistical significance ($p < 0.05$) was observed for IL-1 β , IL-12 p70, and IL-10. Similarly, planktonic R-CA and R-SA stimulated a higher cytokine production than their biofilm counterparts. The highest levels of pro-inflammatory IL-8, IL-1 β , and IL-12p70 were observed after stimulation with planktonic R-SA whereas the strongest stimulation of anti-inflammatory IL-10 was noted for the BCM derived from the mixed culture of both reference species. Our results are indicative of weaker immunostimulatory properties of the biofilm *C. amycolatum* compared to its planktonic form. It may play a role in the persistence of biofilm-related infections. The extent of the cytokine response can be dependent on the inherent virulence of the infecting microorganism.

Key words: *Corynebacterium amycolatum*, biofilm, planktonic cells, cytokines, Jurkat T cells

Introduction

Within recent years there has been a considerable increase in the number of literature data reporting non-diphtherial corynebacteria (also known as diphtheroids) as the causative agents of opportunistic and nosocomial infections in humans (De Miguel-Martinez et al. 1996; Yoon et al. 2011; Bernard 2012b; Nhan et al. 2012; Qin et al. 2017; Santos et al. 2017; Kang et al. 2018). These bacteria are members of the microbiota of the skin and mucous membranes (Qin et al. 2017; Santos et al. 2017; Kang et al. 2018). The potential association between coryneforms and clinical infections can be attributed to immunosuppression, severe underlying medical disorders or invasive procedures (Nhan et al. 2012; Cacopardo et al. 2013; Kimura et al. 2017; Qin et al. 2017). In order to shed more light on the role

of diphtheroids as medically relevant microorganisms, their inherent low virulence should be confronted to the increasingly reported multidrug resistance (Yoon et al. 2011; Bernard 2012b; Kimura et al. 2017; Qin et al. 2017), and the ability to adhere to biotic and abiotic surfaces and/or to form biofilms (Kwaszewska et al. 2006; Souza et al. 2015a; Souza et al. 2015b; Qin et al. 2017; Kang et al. 2018).

The biofilm-producing bacteria are protected both against antibiotics (Fux et al. 2005; Lebeaux et al. 2014), and the host innate and adaptive immune responses (Souza et al. 2015b). Biofilm infections are associated with simultaneous activation of both arms of the host immune response. Neither of them, however, can eliminate the biofilm pathogen, but instead, in synergy, causes collateral surrounding tissue damage due to the release of phagocytic enzymes, oxidative radicals

* Corresponding author: A. Olender, Chair, and Department of Medical Microbiology, Medical University of Lublin, Lublin, Poland; e-mail: alina.olender@umlub.pl

© 2019 Alina Olender et al.

This work is licensed under the Creative Commons Attribution-NonCommercial-NoDerivatives 4.0 License (<https://creativecommons.org/licenses/by-nc-nd/4.0/>).

and/or due to formation of immune complexes (antigen-antibody) (Costerton et al. 1999; Jensen et al. 2010). Moreover, during a biofilm-related infection, planktonic bacteria released from the biofilm can spread into the bloodstream or in the vicinity the source of the infection. These strategies favor microbial persistence and chronicization of the infectious process which significantly complicates the therapy of biofilm-associated infections (Costerton et al. 1999; Lebeaux et al. 2014).

Although studies focused on the investigation and comparison of immune mechanisms stimulated in response to planktonic and biofilm types of bacterial growth have already been undertaken for medically important bacteria such as *Staphylococcus aureus* (Leid et al. 2002; Secor et al. 2011; Brady et al. 2018), *Enterococcus faecalis* (Mathew et al. 2010; Daw et al. 2012; Jarzembowski et al. 2018) or *Pseudomonas aeruginosa* (Jensen et al. 2010), little is known about mechanisms involved in the stimulation of immune responses by opportunistic *Corynebacterium* spp. Another issue worth a thorough investigation is an interplay between the immune system and polymicrobial biofilms what have been increasingly reported in chronic infections such as diabetic foot ulcers or surgical site infections (Dowd et al. 2008; Wolcott et al. 2009).

Hence, the aim of the study was the investigation of the impact of *Corynebacterium amycolatum* soluble products of the planktonic-conditioned medium (PCM) and biofilm-conditioned medium (BCM) on human Jurkat T cells. The production of cytokines demonstrating pro-inflammatory (TNF, IL-1 β , IL-6, IL-8, IL-12p70) and anti-inflammatory properties (IL-10) was analyzed. The research was conducted with the use of clinical strains of *C. amycolatum*. Additionally, two reference strains represented by *C. amycolatum* ATCC 700207 and *S. aureus* ATCC 25923 were used to analyze the potential immunostimulatory effect of their mono- and mixed cultures.

Experimental

Materials and Methods

Bacterial strains. Two reference strains: *C. amycolatum* ATCC 700207, *S. aureus* ATCC 25923, and ten clinical strains of *C. amycolatum* isolated from patients with bacteremia were used in the study. The preliminary characterization of the isolated clinical strains to the species level was based on the analysis of their biochemical profile (APICoryne; bioMérieux, France). The phenotypic identification was followed by the analysis of the sequences of the specific fragment of the 16S rRNA gene (Genomed, Poland) (Drancourt et al. 2000; Bernard et al. 2002a; Fernández-Natal et al. 2008).

Cell culture. Human T lymphocytes cell line (Jurkat, Clone E6-1 ATCC[®]TIB-152) was used in the study. Cells were cultured in RPMI 1640 culture medium (Sigma Aldrich, USA) containing 10% heat-inactivated fetal calf serum (FCS) (Merck, USA), supplemented with 1% solution of antibiotics and antimycotic (Antibiotic, Solution Stabilized, Sigma Aldrich, USA). All cultures were kept in a humidified 5% CO₂ incubator at 37°C.

Planktonic and biofilm *C. amycolatum* culture and preparation of the planktonic-conditioned media (PCM) and the biofilm-conditioned media (BCM). The strains were initially assessed for the biofilm production using the assay with crystal violet that was carried out as previously described (Alves et al. 2016) with some modifications. The assay was performed in the 96-well microtiter plates (NUNC, Thermo Fisher Scientific Inc, Denmark). Overnight cultures of bacterial isolates (ca. McFarland 4 turbidity) were diluted 1:100 in RPMI 1640 medium containing 10% FCS. Aliquots (200 μ l) of each diluted bacterial culture were inoculated into five consecutive wells of the microtiter plate. The RPMI 1640 broth (200 μ l) was used as a negative control. Biofilms were grown statically for 24, 48, 72, and 96 h at 37°C in aerobic conditions. Following incubation, the wells were carefully washed twice with 0.9% NaCl, and dried for 1 h at 50°C. Biofilms in the wells were stained with 0.1% crystal violet (CV; 200 μ l) for 15 min to determine total biofilm biomass. After staining, the wells were washed by flushing the plate three times with 200 ml of distilled water to remove the unbound CV and air-dried. The biofilm-bound dye was extracted with 200 μ l of 70% (v/v) ethanol. The optical density (OD) was determined at 570 nm using the microplate reader. Based on the mean OD values for each strain at the time points mentioned above, the optimal biofilm incubation period was determined for the harvesting of BCM for the stimulation of the Jurkat T cells.

After confirmation of the ability to produce biofilm of a given strain, its planktonic and biofilm culture was performed in order to obtain PCMs and BCMs used subsequently to stimulate the Jurkat T cell lines. This was done for each of ten *C. amycolatum* strains.

Planktonic and biofilm cultures of the reference strains: *C. amycolatum* ATCC 700207, and *S. aureus* ATCC 25923 were also performed in monoculture and the mixed cultures. The “mixed cultures” were achieved in the proportion of 1:1 of two bacterial species when their suspensions of the 0.5 McFarland density (1.5×10^8 CFU/ml) were mixed and grown together. It provided the same number of bacterial cells (of both species) in the final volume at the beginning of the mixed culture growth.

Planktonic cultures of the strains tested were grown in glass tubes (with the inoculum of McFarland 0.5 turbidity, approximately corresponding to 1.5×10^8 CFU/ml)

in RPMI 1640 medium supplemented with 10% FCS, and gently agitated for 48 hours at 37°C. Biofilms were grown from the bacterial inoculum (McFarland 0.5 turbidity) of each strain in RPMI 1640 medium supplemented with 10% FCS in 24-well plates (volume 1000 µl, Nunc, USA) for 48 hours at 37°C. Both types of bacterial cultures resulted in the different number of bacterial cells following the incubation. For *C. amycolatum*, the planktonic and biofilm cultures resulted in the cell density of approximately 9.0×10^8 CFU/ml (McFarland 3.0 turbidity) and 1.2×10^9 CFU/ml (McFarland 4.0 turbidity), respectively. For *S. aureus*, the planktonic and biofilm cultures resulted in the cell density of approximately 6×10^8 CFU/ml (McFarland 2.0 turbidity) and 9×10^8 CFU/ml (McFarland 3.0 turbidity), respectively. For the mixture of *S. aureus* and *C. amycolatum*, the planktonic (PCMmix) and biofilm (BCMmix) cultures resulted in the cell density of approximately 6×10^8 CFU/ml (McFarland 2.0 turbidity) and 9×10^8 CFU/ml (McFarland 3.0 turbidity), respectively. For each of ten clinical *C. amycolatum* strains, and the reference *C. amycolatum* ATCC 700207 and *S. aureus* ATCC 25923 strains, the supernatants were preserved after 48-hour culture of the planktonic and biofilm bacteria. The supernatants were filtered with the use of the MILIPORE filters (the pore size: 0.22 µm) (Merck, USA). The supernatants were prepared directly before their inoculation into to the human cell culture (1:10 dilution, a final volume of the cells culture medium – 1000 µl).

The whole protein content was measured in the supernatants of all bacterial strains investigated before inoculation of the medium for growth of Jurkat T cells. For this purpose, the absorbance was measured in the BioPhotometer (Eppendorf BioPhotometer, Germany) at a wavelength of 280 nm. The absorbance values ranged from 0.018 to 0.720 (planktonic cultures) and from 0.022 to 0.776 (biofilm cultures). The protein content expressed by the optical density (OD) was higher in the biofilm culture of each investigated isolate when compared to its planktonic culture. These supernatants were subsequently used to stimulate cytokine production in Jurkat T cells.

In vitro stimulation of Jurkat T cells with PCM, BCM, PCMmix, BCMmix. For the experiments, Jurkat T cells (at the density of 1×10^5 cells/well) were seeded independently three times in the wells of 24-well culture plates (Nunc, USA) and incubated with the bacterial conditioned media (PCM, BCM, PCMmix or BCMmix) for 24 h at 37°C and 5% CO₂ at a ratio of 1:10 (total volume – 1000 µl). After incubation, the supernatants of the cell culture were collected and analyzed for cytokine concentrations.

Detection of cytokines by flow cytometry. The level of cytokines in the supernatants of Jurkat T cell

culture after their exposure to the PCM, BCM, PCMmix, and BCMmix was determined using the BD Cytometric Bead Array (CBA) Human Inflammatory Cytokines Kit (Becton Dickinson, USA), according to the manufacturer's protocol. The method was based on the cytokine binding to the specific antibody (conjugated to phycoerythrin). The resulting complex emitted a fluorescent signal in the proportion to the concentration of the cytokine that was recorded with the flow cytometer. The fluorescence intensity allowed distinguishing between different cytokines (TNF, IL-1β, IL-6, IL-8, IL-12p70, and IL-10) and the mean fluorescence intensity represented the concentration of cytokines. The results were acquired and analyzed on a FACSCalibur (BD Bioscience, USA) flow cytometer using the Cellquest software (BD Bioscience, USA).

Statistical analysis. Statistical analysis was conducted with the use of Statistica 9.0PL software (Statsoft, Poland). Distribution of variables was checked with the Kolmogorov-Smirnow test with Lilliefors correction and with W Shapiro-Wilk test. Due to the non-Gaussian distribution of variables we used non-parametric tests for further analyses. The assessment of differences between groups was done with the Kruskal-Wallis ANOVA test and paired posthoc test.

Differences were considered statistically significant with $p < 0.05$. Results are shown as median value (Me), mean value (\bar{x}), minimal (min) and maximal values (max).

All experiments were performed in triplicate in three independent experiments.

Results

The range of OD values for *C. amycolatum* strains tested for the ability to produce biofilm were as follows: at 24 h – from 0.089 to 0.101 (mean: 0.097), at 48 h – from 0.113 to 0.385 (mean: 0.201), at 72 h from 0.101 to 0.437 (mean: 0.142), at 96 h from 0.088 to 0.199 (mean: 0.139). Since the highest mean OD was recorded at the 48 h-time point, this period of incubation was used in further research.

Stimulation of the Jurkat T cells line with ten clinical strains of *C. amycolatum* revealed significant differences in the effects exerted by to the PCM and BCM derived from the planktonic and biofilm cultures, respectively.

The level of two cytokines, namely IL-1β and IL-12p70, produced by Jurkat T cells was significantly ($p=0.0027$ and $p=0.0222$, respectively) lower after stimulation with the BCM when compared to the PCM (Fig. 1A, Fig. 1B). The level of the remaining pro-inflammatory cytokines, TNF, IL-6, and IL-8, was also lower but the differences did not achieve statistical significance (. 1C-E).

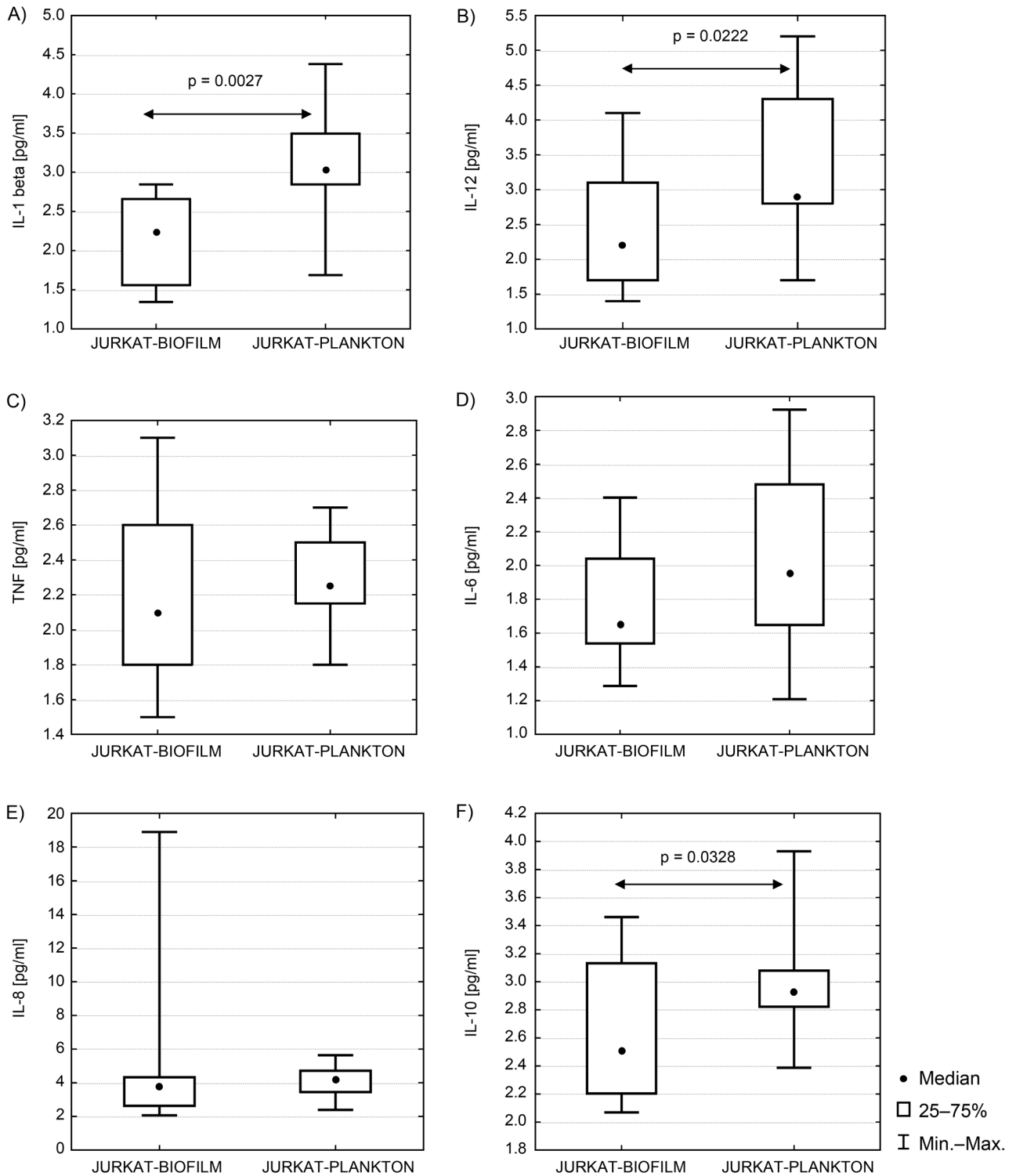


Fig. 1. Concentrations of cytokines produced by Jurkat T cells in response to the to the PCM and BCM of planktonic and biofilm cultures of clinical *C. amycolatum* strains.

We observed a statistically significant ($p=0.0328$) lower concentration of anti-inflammatory IL-10 produced by Jurkat T cells in response to the supernatant of the biofilm culture of *C. amycolatum* when compared to the planktonic culture (Fig. 1F).

A similar tendency was observed when the planktonic and biofilm types of growth of *C. amycolatum*

ATCC 700207 and *S. aureus* ATCC 25923 mono-cultures were compared. Namely, the supernatants of planktonic forms of both reference strains caused a greater stimulation of the cytokine production including the anti-inflammatory IL-10 than their biofilm counterparts. The only exception was the similar level of IL-6 observed after stimulation with the

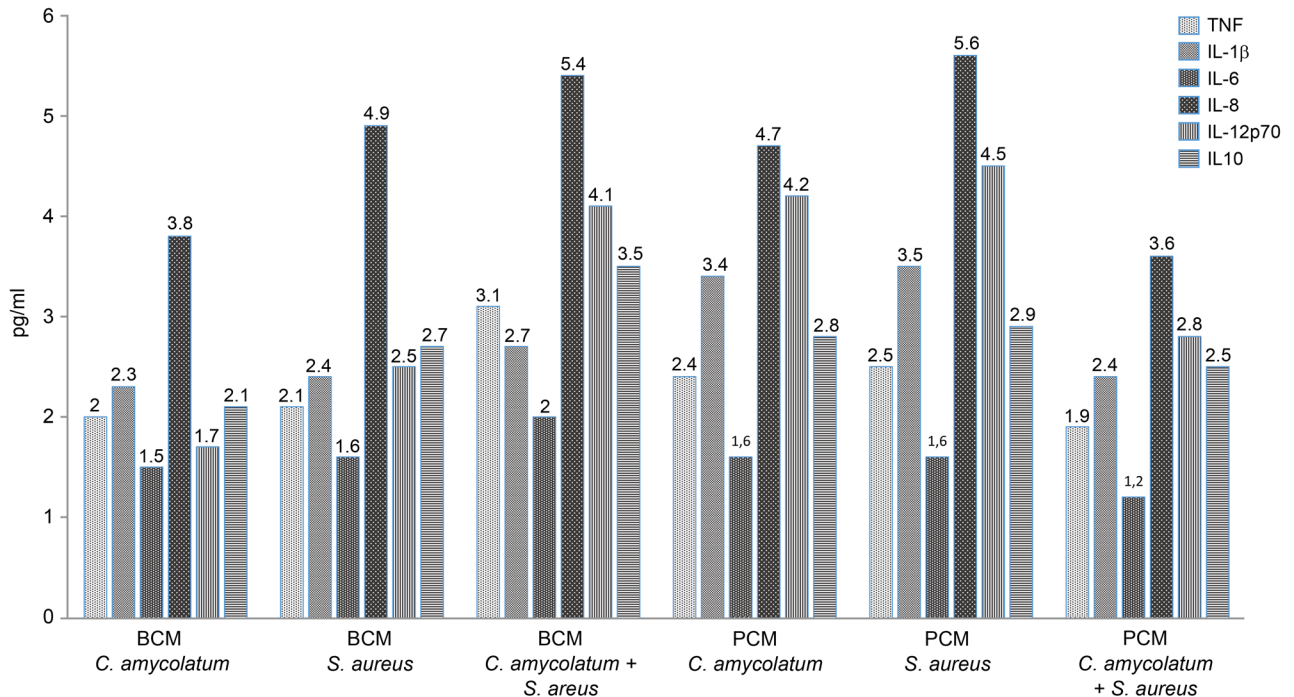


Fig. 2. Levels of cytokines (pg/ml) produced by Jurkat T cells in response to the PCM and BCM derived from mono- and mixed cultures of the reference *C. amycolatum* and *S. aureus* strains.

PCM and BCM derived from the culture of *S. aureus* ATCC 25923 (Fig. 2).

Stimulation of Jurkat T cells by the PCM and BCM from the mono- and mixed cultures of *C. amycolatum* ATCC 700207 and *S. aureus* ATCC 25923 strains revealed that the BCM derived from the mixed culture of the two species (BCMmix) stimulated the production of pro-inflammatory IL-6, TNF, and anti-inflammatory IL-10 to the highest levels (Fig. 2). When the two reference species were considered separately, it was observed that the supernatant of planktonic and biofilm *S. aureus* ATCC 25923 cultures had a stronger stimulatory effect than the monoculture of *C. amycolatum* ATCC 700207, with the greatest increase in the production of pro-inflammatory IL-8, IL-12 p70, and IL-1 β being observed for planktonic *S. aureus* (Fig. 2).

Discussion

Many potentially pathogenic bacteria grow in a planktonic state that can be attributed to acute infections and in biofilms that are associated with chronic infections. Bacteria growing within the biofilm communities secrete an extracellular matrix, form complex structures, demonstrate diverse metabolic activity and are phenotypically distinct from their planktonic counterparts. Therefore, it can be expected that the host immune response may contribute to different outcomes associated with these two disease types

(Secor et al. 2011; Brady et al. 2018). To the best of our knowledge, the immune response manifested by the cytokine release after stimulation of immune cells with the planktonic and biofilm diphtheroids has not been studied yet. In our study, the planktonic and biofilm cultures of *C. amycolatum* were conducted under conditions analogous to those used for the stimulation of Jurkat T cells. The same composition of the medium used for the planktonic and biofilm cultures and the stimulation of Jurkat T cells minimized the risk of an additional, non-specific action of the bacterial medium on the culture of eukaryotic cells.

The assessment of Jurkat T cell inflammatory responses in our study revealed a statistically significant ($p < 0.05$) increase in the levels of pro-inflammatory cytokines such as IL-1 β and IL-12 after stimulation with the PCM compared to the BCM.

These results are in line with the previously published results regarding other potentially pathogenic bacteria. Secor et al. (2011) revealed that *S. aureus* biofilm and planktonic-conditioned medium induced distinct responses in human keratinocytes *in vitro*. The authors observed that in spite of higher production of cytokines induced by the BCM after four hours of exposure, the BCM induced cytokine levels were lower when compared to the cytokine production induced by the PCM after 24 hours. After 24 hours of exposure, the supernatant of *S. aureus* biofilm induced sustained low level of cytokine production when compared to the near exponential increases of cytokines in keratinocytes

treated with the supernatant of planktonic culture. Daw et al. (2012) observed that macrophages infected with the biofilm cells of *Enterococcus faecalis* secreted lower levels of pro-inflammatory (IL-6, MCP-1, and TNF- α) cytokines. According to Mathew et al. (2010), the biofilm cells of *Enterococcus faecalis* in contact with macrophages showed higher potential for surface adherence, the intracellular survival, and produced IL-6 and TNF- α in lower concentrations when compared to planktonic cells.

An unexpected result obtained in the present study was the level of anti-inflammatory IL-10, which was significantly ($p < 0.05$) decreased after stimulation with the BCM compared to the PCM derived from *C. amycolatum* culture. As mentioned previously, there is a relative decrease in inflammation intensity in patients with the biofilm infections possibly contributing to the persistence of these infections. Hence, biofilm infections are rather associated with an increase in IL-10, which has been reported to play a role in shaping the inflammatory milieu typical of the biofilm infection (Heim et al. 2015; Gutierrez-Murgas et al. 2016).

On the other hand, according to what has been published by Saraiva and O'Garra (2010), induction of IL-10 often occurs together with pro-inflammatory cytokines, although pathways that induce IL-10 may negatively regulate these pro-inflammatory cytokines. Gutierrez-Murgas et al. (2016) reported a murine model of a catheter-associated *Staphylococcus epidermidis* biofilm infection in the central nervous system. Cytokine analysis of the tissue surrounding the catheters revealed higher levels of IL-10 in the infected group compared to the healthy mice. On the other hand, the authors observed increased levels of pro-inflammatory cytokines including IL-1 β , IL-6, CXCL2, and CXCL-1 in the homogenates of adjacent catheter-associated tissue and reported the lack of pro-inflammatory IL-12p70; thus, highlighting the role of anti-inflammatory pathways involved in response to *S. epidermidis* catheter infection. We observed that *C. amycolatum* biofilm led to the general weaker stimulation of the cytokine responses including those with pro- and anti-inflammatory activities when compared to the planktonic cells. Our results can be indicative of a weak immune stimulation by the diphtheroid species used in the study. It can result from an inherent low-virulence of this microorganism and we cannot exclude that the cytokine response can be pathogen-specific.

Another part of this study was to investigate the immunomodulatory effect of *C. amycolatum* co-cultured with *S. aureus*. According to what has been already published (Dowd et al. 2008), coaggregation of bacteria together into a functional equivalent pathogroups provides the functional equivalence of well-known pathogens, such as *Staphylococcus aureus*, giving the biofilm

community the factors necessary to maintain chronic biofilm infections.

Stimulation of the Jurkat T cell line by the PCM and BCM derived from the mono- and mixed cultures of the reference *C. amycolatum* ATCC 700207 and *S. aureus* ATCC 25923 strains revealed that the BCM derived from the mixed culture of the two species induced the highest levels of both anti-inflammatory IL-10, and pro-inflammatory IL-6 and TNF. It may support the above-mentioned hypothesis on the greater ability of co-aggregated microorganisms to maintain chronic infections what was reflected here by a stronger immunomodulatory effect. When the two reference species were considered separately, it was observed that *S. aureus* had a stronger stimulatory effect on the immune cells than *C. amycolatum* with the greatest increase in the production of pro-inflammatory IL-8, IL-12 p70, and IL-1 β observed for planktonic *S. aureus*. This may indicate that the cytokine production can be pathogen specific. On the other hand, co-existence of different bacterial species in the biofilm community can be considered an important strategy involved in the interaction with the host and facilitating the microbial persistence.

It should also be noted that the interpretation of the results obtained is burdened with some limitations. The conditions used in *in vitro* experiments and the use of selected immune cells do not reflect all pathologic processes occurring *in vivo*, and the complex interplay between other cells of the immune system and their cytokine/chemokine products secreted in response to infection. As an example, a recently discovered population of myeloid-derived suppressor cells (MDSCs) can be given. These cells have been reported to be the main source of IL-10 during *S. aureus* orthopedic implant biofilm infection. MDSCs negatively regulate inflammatory mechanisms through their suppressive action, production of IL-10, an ability to limit the monocyte/macrophage recruitment in chronic inflammation, tumors or bacterial biofilm infections (Heim et al. 2015).

Hence, the unravelling of the interplay between the immune system and the coryneform bacteria as well as other bacteria that occurs within the biofilm communities requires further studies, which would shed more light on the increasing role of these medically important microorganisms. The results presented here can be considered as a starting point in this investigation.

Conflict of interest

The authors do not report any financial or personal connections with other persons or organizations, which might negatively affect the contents of this publication and/or claim authorship rights to this publication.

Literature

- Alves DR, Perez-Esteban P, Kot W, Bean JE, Arnot T, Hansen LH, Enright MC, Jenkins AT. A novel bacteriophage cocktail reduces and disperses *Pseudomonas aeruginosa* biofilms under static and flow conditions. *Microb Biotechnol*. 2016 Jan;9(1):61–74. <https://doi.org/10.1111/1751-7915.12316>
- Bernard K. The genus *corynebacterium* and other medically relevant coryneform-like bacteria. *J Clin Microbiol*. 2012b Oct 01; 50(10):3152–3158. <https://doi.org/10.1128/JCM.00796-12>
- Bernard KA, Munro C, Wiebe D, Ongsansom E. Characteristics of rare or recently described corynebacterium species recovered from human clinical material in Canada. *J Clin Microbiol*. 2002a Nov 01;40(11):4375–4381. <https://doi.org/10.1128/JCM.40.11.4375-4381.2002>
- Brady RA, Mocca CP, Plaut RD, Takeda K, Burns DL. Comparison of the immune response during acute and chronic *Staphylococcus aureus* infection. *PLoS One*. 2018 Mar 29;13(3):e0195342. <https://doi.org/10.1371/journal.pone.0195342>
- Cacopardo B, Stefani S, Cardi F, Cardi C, Pinzone MR, Nunnari G. Surgical site infection by *Corynebacterium macginleyi* in a patient with neurofibromatosis type 1. *Case Rep Infect Dis*. 2013;2013:1–3. <https://doi.org/10.1155/2013/970678>
- Costerton JW, Stewart PS, Greenberg EP. Bacterial biofilms: a common cause of persistent infections. *Science*. 1999 May 21; 284(5418):1318–1322. <https://doi.org/10.1126/science.284.5418.1318>
- Daw K, Baghdayan AS, Awasthi S, Shankar N. Biofilm and planktonic *Enterococcus faecalis* elicit different responses from host phagocytes *in vitro*. *FEMS Immunol Med Microbiol*. 2012 Jul;65(2): 270–282. <https://doi.org/10.1111/j.1574-695X.2012.00944.x>
- Dowd SE, Wolcott RD, Sun Y, McKeenan T, Smith E, Rhoads D. Polymicrobial nature of chronic diabetic foot ulcer biofilm infections determined using bacterial tag encoded FLX amplicon pyrosequencing (bTEFAP). *PLoS One*. 2008 Oct 3;3(10):e3326. <https://doi.org/10.1371/journal.pone.0003326>
- Drancourt M, Bollet C, Carlouz A, Martelin R, Gayral JP, Raoult D. 16S ribosomal DNA sequence analysis of a large collection of environmental and clinical unidentifiable bacterial isolates. *J Clin Microbiol*. 2000 Oct;38(10):3623–3630.
- Fernández-Natal MI, Sáez-Nieto JA, Fernández-Roblas R, Asencio M, Valdezate S, Lapeña S, Rodríguez-Pollán RH, Guerra JM, Blanco J, Cachón F, et al. The isolation of *Corynebacterium coyleae* from clinical samples: clinical and microbiological data. *Eur J Clin Microbiol Infect Dis*. 2008 Mar;27(3):177–184. <https://doi.org/10.1007/s10096-007-0414-1>
- Fux CA, Costerton JW, Stewart PS, Stoodley P. Survival strategies of infectious biofilms. *Trends Microbiol*. 2005 Jan;13(1):34–40. <https://doi.org/10.1016/j.tim.2004.11.010>
- Gutierrez-Murgas YM, Skar G, Ramirez D, Beaver M, Snowden JN. IL-10 plays an important role in the control of inflammation but not in the bacterial burden in *S. epidermidis* CNS catheter infection. *J Neuroinflammation*. 2016 Dec;13(1):271. <https://doi.org/10.1186/s12974-016-0741-1>
- Heim CE, Vidlak D, Kielian T. Interleukin-10 production by myeloid-derived suppressor cells contributes to bacterial persistence during *Staphylococcus aureus* orthopedic biofilm infection. *J Leukoc Biol*. 2015 Dec;98(6):1003–1013. <https://doi.org/10.1189/jlb.4VMA0315-125RR>
- Jarzebowski T, Daca A, Witkowski JM, Bryl E, Rutkowski B, Kasprzyk J. *In vitro* estimation of the infective potential of the enterococcal strain by an analysis of monocytes' response to the formed biofilm. *Postepy Hig Med Dosw*. 2018 Apr 16;72:290–294. <https://doi.org/10.5604/01.3001.0011.7618>
- Jensen PØ, Givskov M, Bjarnsholt T, Moser C. The immune system vs. *Pseudomonas aeruginosa* biofilms. *FEMS Immunol Med Microbiol*. 2010 Aug;59(3):292–305. <https://doi.org/10.1111/j.1574-695X.2010.00706.x>
- Kang SJ, Choi SM, Choi JA, Choi JU, Oh TH, Kim SE, Kim UJ, Won EJ, Jang HC, Park KH, et al. Factors affecting the clinical relevance of *Corynebacterium striatum* isolated from blood cultures. *PLoS One*. 2018 Jun 21;13(6):e0199454. <https://doi.org/10.1371/journal.pone.0199454>
- Kimura S, Gomyo A, Hayakawa J, Akahoshi Y, Harada N, Ugai T, Komiya Y, Kameda K, Wada H, Ishihara Y, et al. Clinical characteristics and predictive factors for mortality in coryneform bacteria bloodstream infection in hematological patients. *J Infect Chemother*. 2017 Mar;23(3):148–153. <https://doi.org/10.1016/j.jiac.2016.11.007>
- Kwaszewska AK, Brewczyńska A, Szewczyk EM. Hydrophobicity and biofilm formation of lipophilic skin corynebacteria. *Pol J Microbiol*. 2006;55(3):189–193.
- Lebeaux D, Ghigo JM, Beloin C. Biofilm-related infections: bridging the gap between clinical management and fundamental aspects of recalcitrance toward antibiotics. *Microbiol Mol Biol Rev*. 2014 Sep 01;78(3):510–543. <https://doi.org/10.1128/MMBR.00013-14>
- Leid JG, Shirliff ME, Costerton JW, Stoodley P. Human leukocytes adhere to, penetrate, and respond to *Staphylococcus aureus* biofilms. *Infect Immun*. 2002 Nov 01;70(11):6339–6345. <https://doi.org/10.1128/IAI.70.11.6339-6345.2002>
- Mathew S, Yaw-Chyn L, Kishen A. Immunogenic potential of *Enterococcus faecalis* biofilm under simulated growth conditions. *J Endod*. 2010 May;36(5):832–836. <https://doi.org/10.1016/j.joen.2010.02.022>
- Miguel-Martinez I, Fernández-Fuertes F, Ramos-Macías A, Bosch-Benitez JM, Martín-Sánchez AM. Sepsis due to multiply resistant *Corynebacterium amycolatum*. *Eur J Clin Microbiol Infect Dis*. 1996 Jul;15(7):617–618. <https://doi.org/10.1007/BF01709376>
- Nhan TX, Parienti JJ, Badiou G, Leclercq R, Cattoir V. Microbiological investigation and clinical significance of *Corynebacterium* spp. in respiratory specimens. *Diagn Microbiol Infect Dis*. 2012 Nov;74(3):236–241. <https://doi.org/10.1016/j.diagmicrobio.2012.07.001>
- Qin L, Sakai Y, Bao R, Xie H, Masunaga K, Miura M, Hashimoto K, Tanamachi C, Hu B, Watanabe H. Characteristics of multi-drug-resistant *Corynebacterium* spp. isolated from blood cultures of hospitalized patients in Japan. *Jpn J Infect Dis*. 2017;70(2):152–157. <https://doi.org/10.7883/yoken.JJID.2015.530>
- Santos CS, Ramos JN, Vieira VV, Pinheiro CS, Meyer R, Alcantara-Neves NM, Ramos RT, Silva A, Hirata R Jr, Felicori L, et al. Efficient differentiation of *Corynebacterium striatum*, *Corynebacterium amycolatum* and *Corynebacterium xerosis* clinical isolates by multiplex PCR using novel species-specific primers. *J Microbiol Methods*. 2017 Nov;142:33–35. <https://doi.org/10.1016/j.mimet.2017.09.002>
- Saraiva M, O'Garra A. The regulation of IL-10 production by immune cells. *Nat Rev Immunol*. 2010 Mar;10(3):170–181. <https://doi.org/10.1038/nri2711>
- Secor PR, James GA, Fleckman P, Olerud JE, McInnerney K, Stewart PS. *Staphylococcus aureus* Biofilm and Planktonic cultures differentially impact gene expression, mapk phosphorylation, and cytokine production in human keratinocytes. *BMC Microbiol*. 2011;11(1):143. <https://doi.org/10.1186/1471-2180-11-143>

- Souza C, Faria YV, Sant'Anna LO, Viana VG, Seabra SH, Souza MC, Vieira VV, Hirata Júnior R, Moreira LO, Mattos-Guaraldi AL.** Biofilm production by multiresistant *Corynebacterium striatum* associated with nosocomial outbreak. Mem Inst Oswaldo Cruz. 2015a Apr;110(2):242–248. <https://doi.org/10.1590/0074-02760140373>
- Souza MC, dos Santos LS, Sousa LP, Faria YV, Ramos JN, Sabadini PS, da Santos CS, Nagao PE, Vieira VV, Gomes DLR, et al.** Biofilm formation and fibrinogen and fibronectin binding activities by *Corynebacterium pseudodiphtheriticum* invasive strains. *Antonie van Leeuwenhoek*. 2015b Jun;107(6):1387–1399. <https://doi.org/10.1007/s10482-015-0433-3>
- Wolcott RD, Gontcharova V, Sun Y, Zischakau A, Dowd SE.** Bacterial diversity in surgical site infections: not just aerobic cocci any more. *J Wound Care*. 2009 Aug;18(8):317–323. <https://doi.org/10.12968/jowc.2009.18.8.43630>
- Yoon S, Kim H, Lee Y, Kim S.** Bacteremia caused by *Corynebacterium amycolatum* with a novel mutation in *gyrA* gene that confers high-level quinolone resistance. *Korean J Lab Med*. 2011; 31(1):47–48. <https://doi.org/10.3343/kjlm.2011.31.1.47>

The Diversity of the Endobiotic Bacterial Communities in the Four Jellyfish Species

QING LIU¹, XINTONG CHEN^{2,3} , XIAOYA LI^{1,2}, JIANPING HONG³, GUIXIAN JIANG⁴, HONGYU LIANG^{2,5},
WENWEN LIU^{2,5}, ZHENG XU⁶, JING ZHANG⁵, WEI WANG^{7*} and LIANG XIAO^{2*}

¹ College of Animal Science and Veterinary Medicine; ShanXi Agricultural University, TaiGu, ShanXi, China

² Faculty of Naval Medicine, Second Military Medical University (Naval Medical University), Shanghai, China

³ College of Resources and Environment; ShanXi Agricultural University, ShanXi, TaiGu, China

⁴ Clinical Medicine, Grade 2015, Second Military Medical University (Naval Medical University), Shanghai, China

⁵ College of Traditional Chinese Medicine; Jilin Agricultural University, Changchun, Jilin, China

⁶ Administration Office for Scientific Research, Second Military Medical University (Naval Medical University),
Shanghai, China

⁷ Department of Otorhinolaryngology-Head and Neck Surgery, Changhai Hospital, Second Military Medical University
(Naval Medical University), Shanghai, China

Submitted 30 July 2019, revised 4 September 2019, accepted 19 September 2019

Abstract

The associated microbiota plays an essential role in the life process of jellyfish. The endobiotic bacterial communities from four common jellyfish *Phyllorhiza punctata*, *Cyanea capillata*, *Chrysaora melanaster*, and *Aurelia coerulea* were comparatively analyzed by 16S rDNA sequencing in this study. Several 1049 OTUs were harvested from a total of 130 183 reads. Tenericutes (68.4%) and Firmicutes (82.1%) are the most abundant phyla in *P. punctata* and *C. melanaster*, whereas *C. capillata* and *A. coerulea* share the same top phylum Proteobacteria (76.9% vs. 78.3%). The classified OTUs and bacterial abundance greatly decrease from the phylum to genus level. The top 20 matched genera only account for 9.03% of the total community in *P. punctata*, 48.9% in *C. capillata*, 83.05% in *C. melanaster*, and 58.1% in *A. coerulea*, respectively. The heatmap of the top 50 genera shows that the relative abundances in *A. coerulea* and *C. capillata* are far richer than that in *P. punctata* and *C. melanaster*. Moreover, a total of 41 predictive functional categories at KEGG level 2 were identified. Our study indicates the independent diversity of the bacterial communities in the four common Scyphomedusae, which might involve in the metabolism and environmental information processing of the hosts.

Key words: jellyfish, endobiotic bacteria, diversity, 16S rDNA

Introduction

Microorganisms are considered to be the most diverse and abundant organisms on Earth (Gans et al. 2005; Shanmugam et al. 2017). Microorganisms are constantly facing changing environmental conditions at the microscale, and a variety of survival strategies e.g. secondary metabolites secretion are well-developed to establish long-term relationships with their hosts. Consequently, it is important to consider that the evolution of animals and plants has occurred and will continue

to occur in the presence of microflora, forming parasitic, commensal, mutualistic, or even pathogenic relationships with their hosts (Sevellec et al. 2018). These resident microbes influence host fitness and ecological traits, ultimately forming a symbiotic organism that consists of a multicellular host and a community of associated microorganisms (Bosch 2013). The composition as well as the associations between hosts and microorganisms profoundly affects the development, maturation and almost all the biological processes of the hosted organisms (Stephens et al. 2016).

* Corresponding author: L. Xiao, Faculty of Naval Medicine, Second Military Medical University (Naval Medical University), Shanghai, China; e-mail: hormat830713@hotmail.com

W. Wang, Department of Otorhinolaryngology-Head and Neck Surgery, Changhai Hospital, Second Military Medical University (Naval Medical University), Shanghai, China; e-mail: wangw0503@163.com

© 2019 Qing Liu et al.

This work is licensed under the Creative Commons Attribution-NonCommercial-NoDerivatives 4.0 License (<https://creativecommons.org/licenses/by-nc-nd/4.0/>).

Marine animals provide a unique habitat for attachment and colonization of microorganisms, and each organism hosts a specific microbial community (Weiland-Bräuer et al. 2015; Paharik and Horswill 2016). Jellyfish are marine free-swimming with high water content (>95%) and possess a rich diversity of symbiotic microorganisms. They are generalist predators of planktonic prey, such as protists, fish eggs, and polychaeta larvae and also act as prey for a range of different animals, including other jellyfish, fish, birds, and turtles (Cleary et al. 2016). In recent decades, the frequency and duration of noteworthy jellyfish outbreaks appear to have increased at a global scale. These blooms are reported to be linked to overfishing, climate change, and eutrophication, leading to the damage to the marine ecosystems by affecting the planktonic food web (Viver et al. 2017). Meanwhile, with the considerable increase in jellyfish swarms in coastal areas, the number of victims stung by jellyfish, including swimmers, fishermen and divers, has consequently been increasing (Cleary et al. 2016; Lee et al. 2018).

Despite the great concerns raised regarding their potential harm to both the marine ecosystem and human health, little is known about the associated microbiota of jellyfish (Cortés-Lara et al. 2015). To date, cost-effective and powerful high-throughput sequencing techniques have been developed to identify microbial phylotypes and to detect rare taxa in samples. It is reasonable to speculate that the endobiotic microorganisms play a vital role in the growth and development of jellyfish with the effect of either 'harm' or 'health'. Understanding the diversity and effect of the endogenous colonies is crucial to the homeostasis and health of jellyfish, and also useful for the comprehension of the feasible microbial infection and guidance of the medication during the jellyfish envenomation. In this study, the endobiotic bacterial communities were screened by 16S rDNA sequencing in the four common species of jellyfish including *Phyllorhiza punctata*, *Cyanea capillata*, *Chrysaora melanaster* and *Aurelia coerulea*, to evaluate the diversity and richness as well as their potential functions involving the life of the four different jellyfish species.

Experimental

Materials and Methods

Jellyfish samples. Individuals of four jellyfish species (*P. punctata*, *C. capillata*, *C. melanaster*, and *A. coerulea*) were collected alive from an aquafarm in Shanghai, China. The jellyfish *P. punctata* and *A. coerulea* were fed on shrimp eggs with different temperatures 24–28°C and 18–25°C, while *C. capillata* and *C. melanaster* were both

cultured on shrimp eggs and *A. coerulea* at the same temperature 10–18°C. The jellyfish fasted for one day before sampling, and then transported to the laboratory in a 3-liter plastic bag filled with seawater to prevent damage from sloshing. All jellyfish used in this research were approved by the Faculty of Naval Medicine, Second Military Medical University (Faculty of Naval Medicine, Naval Medical University).

DNA extraction. Total bacterial genomic DNA was extracted from the jellyfish of four species using the FastDNA SPIN extraction kit (MP Biomedicals, Santa Ana, CA, USA) following the manufacturer's instructions and was stored at –20°C before further analysis. The quantity and quality of the extracted DNA were measured using a NanoDrop ND-1000 spectrophotometer (Thermo Fisher Scientific, Waltham, MA, USA) and agarose gel electrophoresis, respectively.

16S rDNA amplicon pyrosequencing. PCR amplification of the V3-V4 regions of the bacterial 16S rRNA genes was performed using the forward primer 338F (5'-ACTCCTACGGGAGGCAGCA-3') and the reverse primer 806R (5'-GGACTACHVGGGTWTCTAAT-3'). The sample-specific 7-bp barcodes were incorporated into the primers for multiplex sequencing. The PCR components included 5 µl of Q5 reaction buffer (5×), 5 µl of Q5 High-Fidelity GC buffer (5×), 0.25 µl of Q5 High-Fidelity DNA Polymerase (5 U/µl), 2 µl (2.5 mM) of dNTPs, 1 µl (10 µM) of each forward and reverse primer, 2 µl of DNA template, and 8.75 µl of ddH₂O. Thermal cycling consisted of initial denaturation at 98°C for 2 min, followed by 25 cycles consisting of denaturation at 98°C for 15 s, annealing at 55°C for 30 s, and extension at 72°C for 30 s, with a final extension of 5 min at 72°C. PCR amplicons were purified with Agencourt AMPure Beads (Beckman Coulter, Indianapolis, IN, USA) and quantified using the PicoGreen dsDNA Assay Kit (Invitrogen, Carlsbad, CA, USA). After the individual quantification step, amplicons were pooled in equal amounts, and pair-end 2 × 300 bp sequencing was performed using the Illumina MiSeq platform with the MiSeq Reagent Kit v3 at Personal Biotechnology Co. Ltd (Shanghai, China).

Sequence analysis. The QIIME (Quantitative Insights Into Microbial Ecology, v1.8.0, <http://qiime.org/>) pipeline was employed to process the sequencing data as previously described (Caporaso et al. 2010). Briefly, raw sequencing reads with exact matches to the barcodes were assigned to respective samples and identified as valid sequences. The low-quality sequences were filtered according to the following criteria: sequences that had a length of < 150 bp, had average Phred scores of < 20, contained ambiguous bases, and mononucleotide repeats of > 8 bp were removed. Paired-end reads were assembled using FLASH (v1.2.7, <http://ccb.jhu.edu/software/FLASH/>) (Magoč and

Salzberg 2011). After chimera detection, the remaining high-quality sequences were clustered into operational taxonomic units (OTUs) at 97% sequence identity with UCLUST (Edgar 2010). A representative sequence was selected from each OTU using default parameters. OTU taxonomic classification was conducted with BLAST by comparing the set of representative sequences against those in the Greengenes Database (release 13.8, <http://greengenes.secondgenome.com/>) using the best hit (DeSantis et al. 2006). An OTU table was further generated to record the abundance of each OTU in each sample and the taxonomy of these OTUs. OTUs containing less than 0.001% of the total sequences across all samples were discarded. To minimize the difference in sequencing depth across samples, an averaged, rounded, rarefied OTU table was generated by averaging 100 evenly resampled OTU subsets under 90% of the minimum sequencing depth for further analysis.

Bioinformatics and statistical analysis. Sequence data analyses were mainly performed using QIIME and R packages (v3.2.0). OTU-level alpha diversity indices, such as the Chao1 richness estimator, ACE metric (abundance-based coverage estimator), Shannon diversity index, and Simpson index, were calculated using the OTU table in QIIME. OTU-level ranked abundance curves were generated to compare the richness and evenness of OTUs among samples. Beta diversity analysis was performed to evaluate the structural variation in the microbial communities across samples using UniFrac distance metrics and visualized via principal coordinate analysis (PCoA), nonmetric multidimensional scaling (NMDS) and unweighted pair-group method with arithmetic means (UPGMA) hierarchical clustering (Ramette 2007). Differences in the UniFrac distances for pairwise comparisons among groups were determined using Student's t-test and the Monte Carlo permutation test with 1000 permutations and visualized with box-and-whisker plots. Principal component analysis (PCA) was also conducted based on the genus-level compositional profiles (Ramette 2007). The taxonomic compositions and abundances were visualized using MEGAN (Segata et al. 2011) and GraPhlAn (Lesueur et al. 2015). A Venn diagram was generated to visualize the shared and unique OTUs among samples or groups using the R package "VennDiagram" (https://en.wikipedia.org/wiki/Venn_diagram) based on the occurrence of OTUs across samples/groups regardless of their relative abundance. Taxon abundances at the phylum, class, order, family, genus, and species levels were statistically compared among samples or groups with Metastats (<http://metastats.cbcb.umd.edu/>) (White et al. 2009) and visualized with scatter plots. Co-occurrence analysis was performed by calculating Spearman's rank correlations between the dominant taxa. Correlations with $|RHO| > 0.6$ and $P < 0.01$ were visualized

as co-occurrence networks using Cytoscape (<http://www.cytoscape.org/>) (Shannon et al. 2003). Microbial functions were predicted by PICRUSt (Phylogenetic Investigation of Communities by Reconstruction of Unobserved States) based on high-quality sequences (Langille et al. 2013) (KEGG PATHWAY Database <http://www.genome.jp/kegg/pathway.html>).

Results

Diversity of the bacterial communities of the four jellyfish. According to the sequencing results, a total of 130 183 reads was obtained with the general length of 420–452 bp, of which the top three sequences occupying an overall ratio of 92.26% have the DNA lengths 425 bp (27 413 reads), 450 bp (59 837 reads) and 451 bp (32 852 reads), respectively (Fig. 1.1). For each jellyfish, *P. punctata*, *C. capillata*, *C. melanaster*, and *A. coerulea* had the PCR counts of 29 662 (22.78%), 34 232 (26.30%), 33 031 (25.37%) and 32 581 (25.03%), respectively. After removing the rare OTUs that are less than 0.001% of the total counts, a total of 1049 operational taxonomic units (OTUs) from the preliminarily divided 3813 OTUs, according to the standard of 97% sequence similarity, were finally screened, where 242 (23.07%), 561 (53.48%), 193 (18.40%), and 629 (59.96%) OTUs were distributed in the jellyfish *P. punctata*, *C. capillata*, *C. melanaster* and *A. coerulea* samples, respectively (Fig. 1.2). Consistent with the number of OTUs, the indexes including Chao1, ACE, Simpson, and Shannon were much higher in the jellyfish *C. capillata* and *A. coerulea*, indicating a higher richness and evenness of a diversity than in the jellyfish *P. punctata* and *C. melanaster* (Table I). As for the β diversity analyzed by NMDS (Nonmetric Multidimensional Scaling), the big distances on the graph indicate the obvious difference of the bacterial community structure in the four jellyfish (Fig. 1.3).

We then constructed the Venn Diagram by using the screened 1049 OTUs. The number of OTU unions of all the four jellyfish is 931 (88.75%) while the OTU intersection is 79 (7.53%) (Fig. 1.4). The number of unique OTUs in *A. coerulea*, *C. capillata*, *C. melanaster*,

Table I
Summary of α -diversity indices of the bacterial communities in the four jellyfish species.

Species	Chao1	ACE	Simpson	Shannon
<i>Phyp</i>	242	242	0.5	2.01
<i>Cyac</i>	561.93	570.29	0.96	5.96
<i>Chrm</i>	193.04	194.13	0.39	1.73
<i>Aura</i>	629.4	634.45	0.95	6.14

Notes: *Chrm* – *C. melanaster*; *Aura* – *A. coerulea*; *Phyp* – *P. punctata*; *Cyac* – *C. capillata*

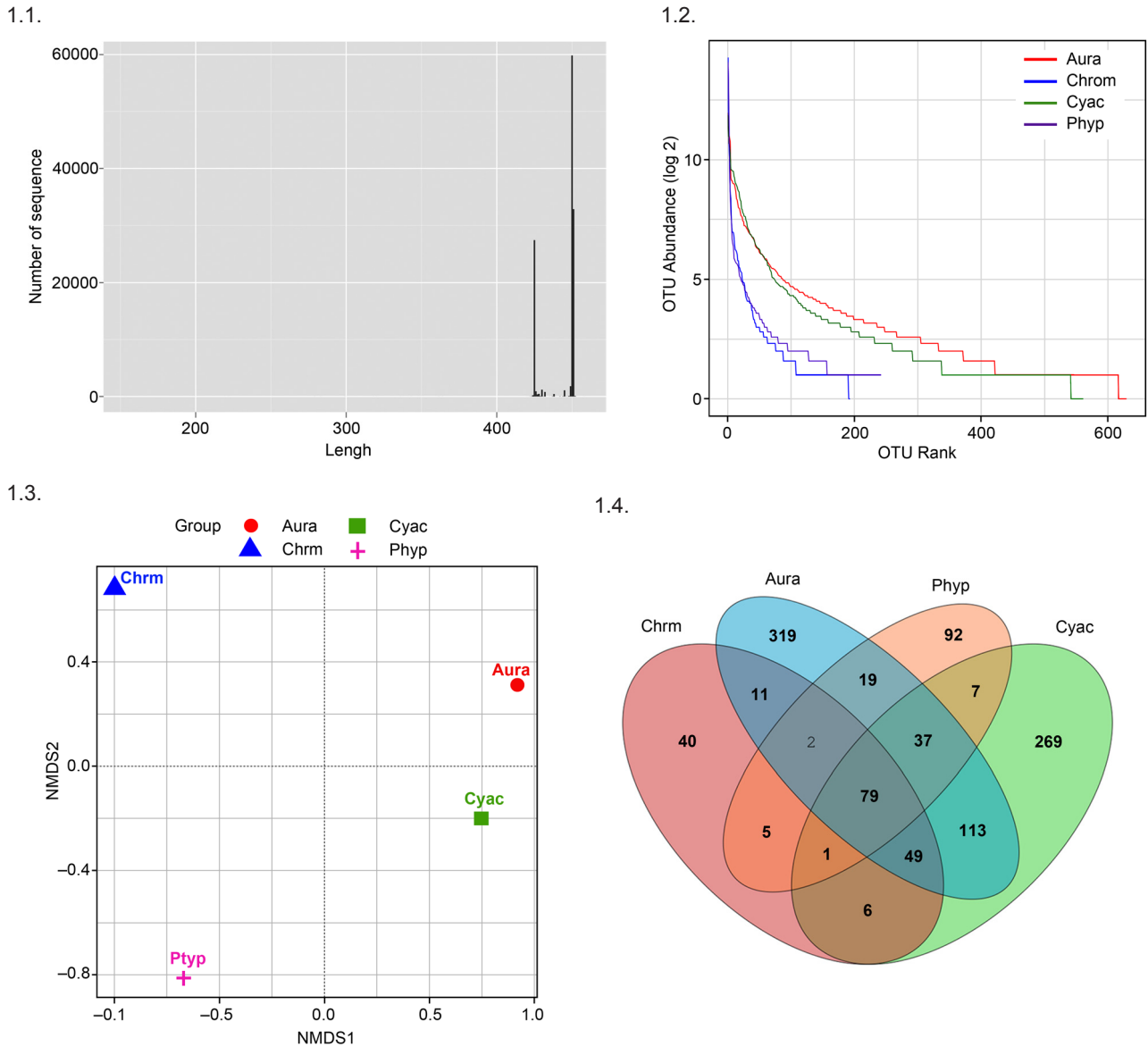


Fig. 1. Diversity of the bacterial communities of the four jellyfish species at OTU level. 1.1. Sequence length distribution of bacteria in the four jellyfish. 1.2. Rank abundance curve of the four jellyfish species. 1.3. Unweighted UniFrac NMDS plot of the bacterial communities associated with the four jellyfish species. 1.4. Venn diagram representing the shared operational taxonomic units (OTUs) among jellyfish species. *Chrm*, *C. melanaster*; *Aura*, *A. coerulea*; *Phyp*, *P. punctata*; *Cyac*, *C. capillata*.

and *P. punctata* was 319 (50.72%), 269 (47.95%), 92 (47.67%), and 40 (16.53%), respectively. The maximal and minimal numbers of overlapped OTUs between two jellyfish were 278 and 87 in the *A. coerulea* vs. *C. capillata* and *C. melanaster* vs. *P. punctata*, and the maximal and minimal numbers among three jellyfish were 128 and 80 in *A. coerulea* vs. *C. melanaster* vs. *C. capillata*, and *C. melanaster* vs. *C. capillata* vs. *P. punctata*. Also, the core microbiota (OTU intersection) mainly consisted of Firmicutes and Proteobacteria, which accounted for 11.4% (9 OTUs) and 82.3% (65 OTUs) of the total intersection (Table II). The bacterial phyla [Thermi], Actinobacteria and Planctomycetes had only one OTU, and Bacteroidetes contained two OTUs. (Table II). Among the phylum Proteobacteria,

Moraxellaceae (35 OTUs), and Pseudomonadaceae (17 OTUs) the two major families in the dominant order Pseudomonadales of the class Gammaproteobacteria were observed.

Composition of the bacterial communities from phylum to family. The assessment of different taxonomic levels is equivalent to viewing community composition structures at different resolutions, thus, the differences in the bacterial community associated with the four jellyfish species were firstly explored from the phylum to family according to the alignment of 16S rDNA sequences. A roughly equal bacterial numbers at different classification levels were obtained for *P. punctata* and *C. melanaster*, where the bacterial numbers of phylum, class, order, and family were 10 (234)

Table II
Core microbiotas (OTU intersection) of the four jellyfish species.

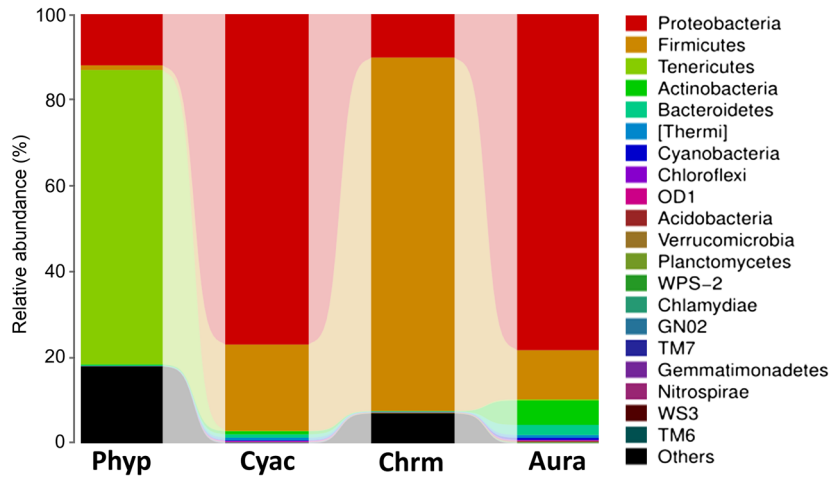
Phylum	Class	Order	Family	Genus	Matched OTUs	
Firmicutes	Bacilli	Bacillales	Staphylococcaceae	<i>Staphylococcus</i>	1528	
			Bacillaceae	<i>Bacillus</i>	1198, 1208	
				Unclassified_ Bacillaceae	238, 3199	
				<i>Geobacillus</i>	1362	
		Lactobacillales	Streptococcaceae	<i>Lactococcus</i>	1589, 2873	
			Carnobacteriaceae	<i>Carnobacterium</i>	1719	
Proteobacteria	Alphaproteobacteria	Rhizobiales	Brucellaceae	<i>Ochrobactrum</i>	1108	
			Methylobacteriaceae	<i>Methylobacterium</i>	3041	
			Methylobacteriaceae	Unclassified_ Methylobacteriaceae	2810	
			Phyllobacteriaceae	<i>Aminobacter</i>	2641	
			Sphingomonadaceae	<i>Sphingomonas</i>	2987, 3014	
		Sphingomonadales	Sphingomonadaceae	Unclassified_ Sphingomonadaceae	2284	
		Betaproteobacteria	Burkholderiales	Comamonadaceae	Unclassified_ Comamonadaceae	861
				Oxalobacteraceae	<i>Cupriavidus</i>	366
	Unclassified_ Burkholderiales			Unclassified_ Burkholderiales	476	
	Gammaproteobacteria	Pseudomonadales	Moraxellaceae	Unclassified_ Moraxellaceae	2146, 1618, 2256, 1522, 2988, 303, 2486, 303, 141, 2317, 929, 3334, 75, 1212, 2345, 1235, 3227, 1057, 2091, 3331, 3766, 2425, 2535, 389, 3630, 3372, 3440, 565, 1954, 1508, 3325, 872, 268, 1805, 2942	
			Pseudomonadaceae	<i>Pseudomonas</i>	1241, 3991, 3058, 2494, 1363, 2255, 1633, 2730, 1743, 306, 1348, 2740, 899, 3160, 909, 3051, 3320	
			Pseudomonadaceae	Unclassified_ Pseudomonadaceae	692	
			Xanthomonadales	Xanthomonadaceae	Unclassified_ Xanthomonadaceae	3013
			Vibrionales	Vibrionaceae	<i>Vibrio</i>	2553
			Actinobacteria	Actinobacteria	Actinomycetales	Pseudonocardiaceae
[Thermi]	Deinococci	Thermales	Thermaceae	<i>Thermus</i>	3649	
Bacteroidetes	[Saprosiprae]	[Saprosiprales]	Chitinophagaceae	<i>Sediminibacterium</i>	3146, 1112	
Planctomycetes	Phycisphaerae	Phycisphaerales	Unclassified_ Phycisphaerales	Unclassified_ Phycisphaerales	3775	

Square brackets indicate that the nomenclature requires updating.

vs. 12 (189), 15 (234) vs. 17 (188), 26 (228) vs. 26 (181), and 40 (218) vs. 33 (171), respectively. By comparison, the total number at different classification levels are much higher in *C. capillata* and *A. coerulea*, and the numbers of classification were 22 (558) vs. 18 (628), 39 (556) vs. 37 (622), 52 (534) vs. 56 (606), and 77 (424) vs. 95 (555), respectively (Table III).

At the phylum level, *Tenericutes* (68.4%) and *Proteobacteria* (12.1%) were the most abundant in *P. punctata*, while *Firmicutes* (82.1%) and *Proteobacteria* (10.3%) occupied the top two phyla in *C. melanaster*. A similar phylum distribution was found in *C. capillata* and *A. coerulea*, where the major phyla were *Proteobacteria* (76.9% vs. 78.3%), followed by *Firmicutes* (20.0%

2.1.



2.2.

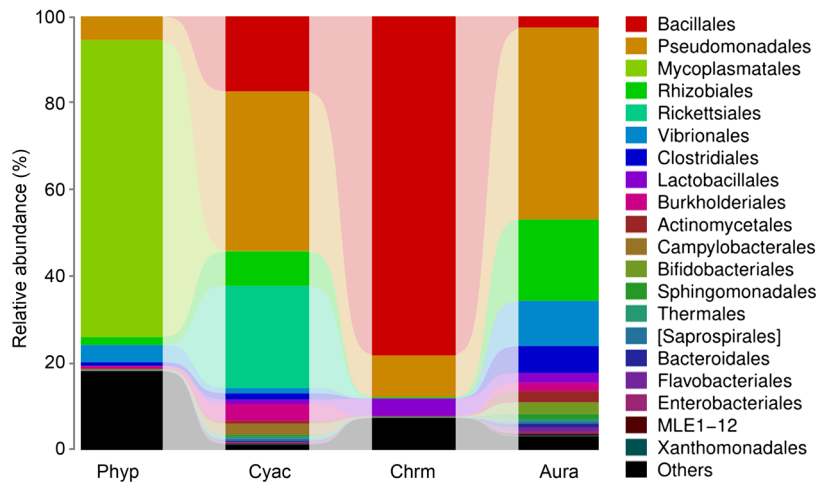


Fig. 2. Comparative analysis of the composition of the bacterial communities in the four jellyfish species across different classification levels. 2.1. Relative abundances of the representative phyla. 2.2. Relative abundances of the representative classes

vs. 11.4%) (Fig. 2.1). At the class level, Mollicutes (68.4%) from the phylum Tenericutes was the most abundant in *P. punctata*, which was followed by Gammaproteobacteria (9.5%) from Proteobacteria. In *C. melanaster*, Bacilli (82.1%) from Firmicutes and Gammaproteobacteria (9.6%) from Proteobacteria were the most abundant. By comparison, *C. capillata* and *A. coerulea* had a more dispersed distribution, where Gammaproteobacteria (38.5%) and Alphaproteobacteria (31.9%) from Proteobacteria, Bacilli (18.5%) from Firmicutes were the main classes in *C. capillata*, while Gammaproteobacteria

(55.8%) and Alphaproteobacteria (20.3%) from Proteobacteria were the top in *A. coerulea* (Fig. 2.2).

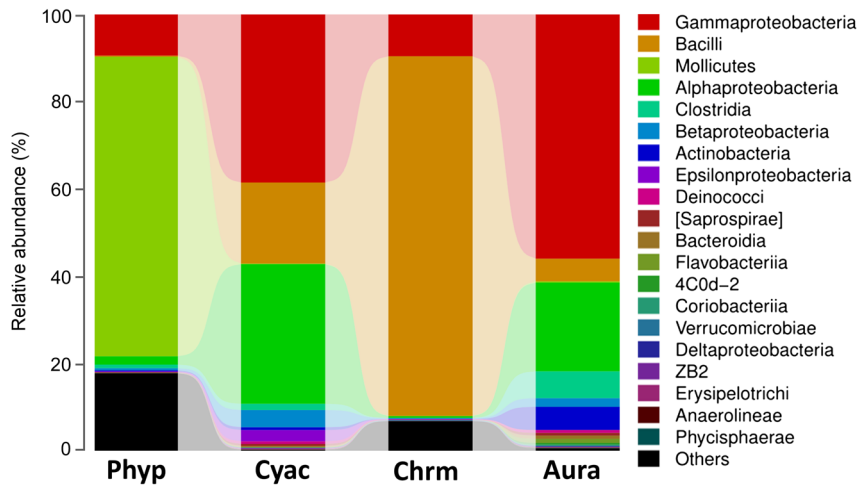
At the order level, Mycoplasmales (68.3%) from the class Mollicutes, Pseudomonadales (5.5%), and Vibrionales (4.0%) from Gammaproteobacteria were the top three orders in *P. punctata*. Bacillales (78.2%) from Bacilli and Pseudomonadales (9.6%) from Gammaproteobacteria constituted the main orders in *C. melanaster*. The order distributions of *C. capillata* and *A. coerulea* were more dispersed. Bacillales (17.5%) from Bacilli, Pseudomonadales (36.7%)

Table III
A classification table of the OTUs and bacteria of the four jellyfish at different levels.

	The jellyfish species	Phylum	Class	Order	Family	Genus
Bacteria (OTUs)	Phyp	10 (234)	16 (234)	26 (228)	40 (218)	36 (98)
	Cyac	22 (558)	39 (556)	52 (534)	77 (424)	74 (226)
	Chrm	12 (189)	17 (188)	26 (181)	33 (171)	25 (81)
	Aura	18 (628)	37 (622)	56 (606)	95 (555)	120 (308)

Notes: Chrm - *C. melanaster*; Aura - *A. coerulea*; Phyp - *P. punctata*; Cyac - *C. capillata*

2.3.



2.4.

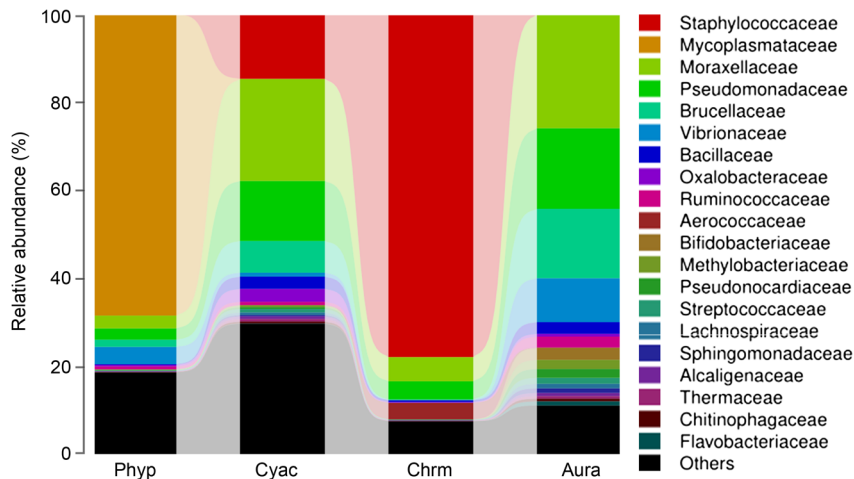


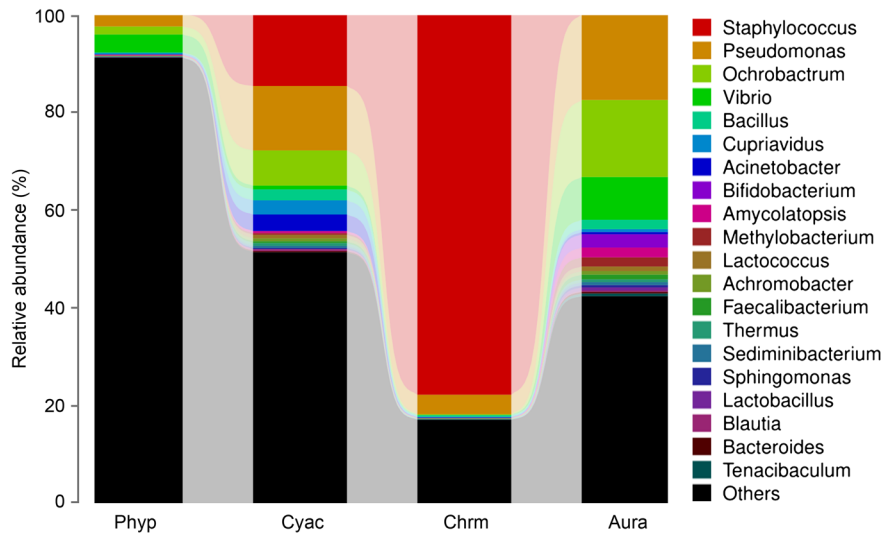
Fig. 2. Comparative analysis of the composition of the bacterial communities in the four jellyfish species across different classification levels. 2.3. Relative abundances of the representative order. 2.4. Relative abundances of the representative families.

from Gammaproteobacteria, Rhizobiales (8.0%) from Alphaproteobacteria, Rickettsiales (23.4%) from Alphaproteobacteria were the main bacterial classes in *C. capillata*, while Pseudomonadales (44.1%) from Gammaproteobacteria, Rhizobiales (18.7%) from Alphaproteobacteria, Vibrionales (10.4%) from Gammaproteobacteria, Clostridiales (6.1%) from Clostridia in *A. coerulea* (Fig. 2.3). At the family level, Mycoplasmataceae (68.3%) from the order Mycoplasmatales was the dominant in *P. punctata*, and the most abundant family in *C. melanaster* was Staphylococcaceae (77.7%) from Bacillales. Staphylococcaceae (14.7%) from Bacillales, Moraxellaceae (23.1%) from Pseudomonadales, and Brucellaceae (7.2%) from Rhizobiales were the major families in *C. capillata*. The jellyfish *A. Coerulea* has 11 families with >1% proportion, where Moraxellaceae (25.8%) from Pseudomonadales, Pseudomonadaceae (18.3%) from Pseudomonadales, and Brucellaceae (15.7%) and Vibrionaceae (9.9%) from Vibrionales were the top four components (Fig. 2.4).

Composition of the bacterial communities at the genus level. The obvious feature at the genus level is

the great increases in the unclassified OTUs and low-abundant genera among all four jellyfish species. There were 36 genera from 98 OTUs, 74 from 226, 25 from 81, and 120 from 308 that were detected in *P. punctata*, *C. capillata*, *C. melanaster*, and *A. coerulea*, respectively (Table III). The top 20 matched genera account for 9.03% of the total community in *P. punctata*, 48.9% in *C. capillata*, 83.05% in *C. melanaster*, and 58.1% in *A. coerulea* (Fig. 3.1). The top three genera in *P. punctata* were *Pseudomonas* (2.5%) from the family Pseudomonadaceae, *Vibrio* (3.7%) from Vibrionaceae, and *Ochrobactrum* (1.6%) from Brucellaceae. *Staphylococcus* from Staphylococcaceae (77.7%) was the dominant genus in *C. melanaster*, followed by *Pseudomonas* from Pseudomonadaceae with a much smaller proportion of 4.0%. The genus diversity was much richer in *C. capillata* and *A. coerulea*. There were six genera with the proportion >1% in *C. capillata*, *Staphylococcus* (14.7%), *Pseudomonas* (13.2%), and *Ochrobactrum* (7.2%) from Brucellaceae were the top three. *Pseudomonas* (17.5%), *Ochrobactrum* (15.7%), *Vibrio* (8.7%), *Bacillus* (1.9%), *Bifidobacterium* (2.7%) from Bifidobacteriaceae,

3.1.



3.2.

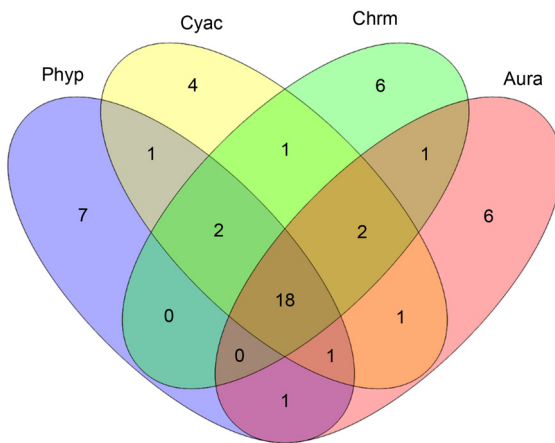


Fig. 3. Analysis of the differences in the composition of the bacterial communities associated with the four jellyfish species across the genus levels. 3.1. Relative abundances of the representative genus found in the four jellyfish species. 3.2. The Venn diagram representing the shared top 30 genera of the bacterial communities in the jellyfish species.

Amycolatopsis (2.0%) from Pseudonocardiaceae, and *Methylobacterium* (1.9%) from Methylobacteriaceae were the >1% genera (Fig. 3.1).

We then constructed the Venn diagram using the top 30 bacterial genera of the four jellyfish species, where the number of genera union is 51 and 18 genera were found in all four jellyfish species (Fig. 3.2). The numbers of unique genera were seven, four, six, and six in *P. punctata*, *C. capillata*, *C. melanaster*, and *A. coerulea*, respectively, while the number of overlapped genera between two jellyfish was 20~23, and the number of overlapped genera among three jellyfish was 18~20. The large proportions of both the overlapped and unique genera indicated the coexistence of the stabilized genera distribution and rich genera diversity of the four jellyfish species.

The direct impression of the heatmap graph with the top 50 bacterial genera was that the relative abundance in *A. coerulea* is much higher than in the other three jellyfish species. Most of the bacterial genera in *A. coerulea* were very numerous, and only nine genera were less numerous than the average in the four jellyfish species. *C. capillata* displayed as the second abun-

dant, and six bacterial genera were the most numerous, including *Salmonella*, *Geobacillus*, *Janthinobacterium*, *Cupriavidus*, *Acinetobacter*, and *Clostridium*. *P. punctata* and *C. melanaster* exhibit the lowest relative abundance, where *Alvinella* was found to be the most abundant in *P. punctata*, and *Staphylococcus* and *Rubritalea* are the most abundant in *C. melanaster* (Fig. 3.3).

Functional annotation of the microbiotas of the jellyfish species. The putative microbial functions associated with the four jellyfish species were predicted by assignment of the predicted metagenome using PICRUSt. KEGG (Kyoto Encyclopedia of Genes and Genomes) was utilized to map the pathways of the identified microbial functions. According to the Venn diagram, the number of the microbial functions is 5833 and the function intersection is 4936, thus, it accounted for a big proportion of 84.6% of the total functional groups, indicating the functional similarity of the bacteria among the four jellyfish species (Fig. 4.1). The number of unique functions in *A. coerulea*, *C. capillata*, *C. melanaster*, and *P. punctata* were only 127 (2.2%), 39 (0.7%), 25 (0.4%) and 1 (0.0%), respectively. The quantities of overlapped functions between two jelly-

3.3.

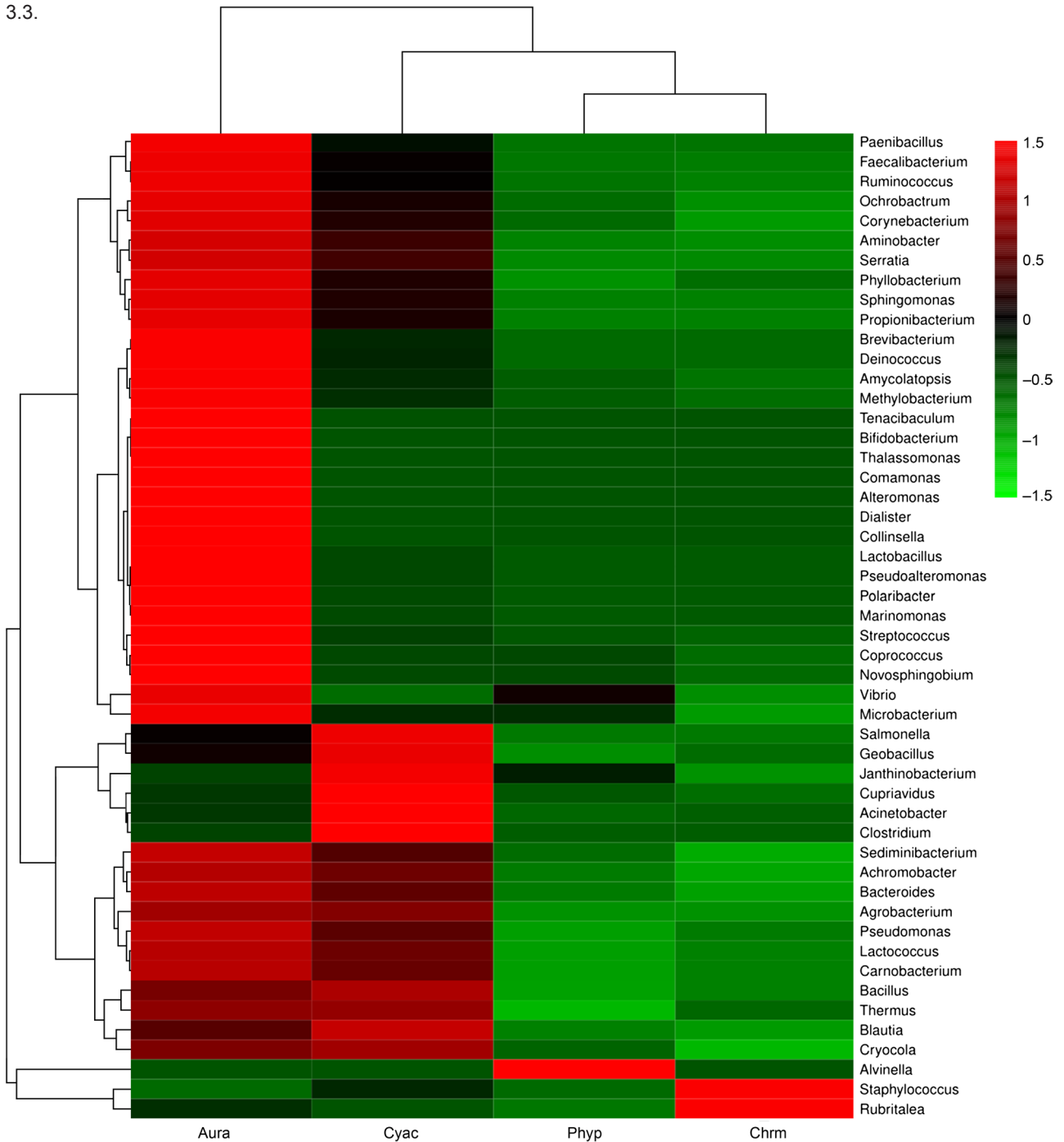


Fig. 3. Analysis of the differences in the composition of the bacterial communities associated with the four jellyfish species across the genus levels. 3.3. Heat map of the top 50 genera of the bacterial communities in the four species of jellyfish. Red represents the genera with high abundance in the corresponding jellyfish species, while green represents genera with low abundance. “Others” indicates the other bacterial genera in each jellyfish species except the top 20 genera with the highest abundance. *Chrm*, *C. melanaster*; *Aura*, *A. coerulea*; *Phyp*, *P. punctata*; *Cyac*, *C. capillata*.

fish were from 4942 in *C. melanaster* vs. *P. punctata* to 5600 in *A. coerulea* vs. *C. capillata*, and the maximal and minimal numbers among three jellyfish were 4936 in *P. punctata* vs. *C. melanaster* vs. *C. capillata* and 5111 in *C. melanaster* vs. *C. capillata* vs. *A. coerulea* (Fig. 4.1).

A total of 41 predictive categories in the KEGG level 2 functional modules were identified in the microbiota of the four jellyfish species. The relative abundances

of the functional categories among the four jellyfish were quite similar, and only tiny variations were seen in each category (Fig. 4.2). Membrane transport, amino acid metabolism, and carbohydrate metabolism were the three functional groups with the highest relative abundance. Metabolism and environmental information processing were the modules where the bacterial functions were concentrated (Fig. 4.2).

4.1.

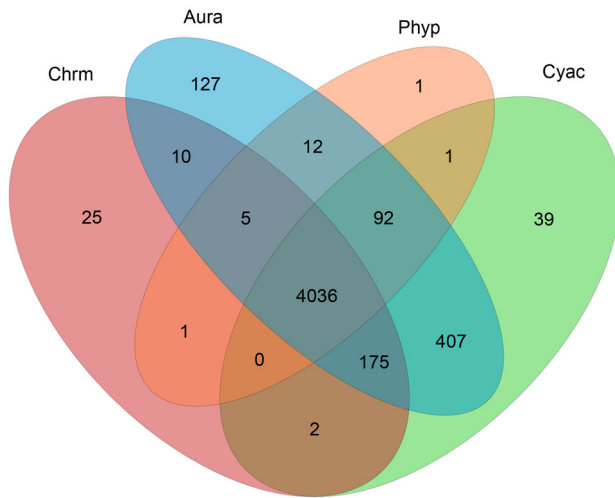
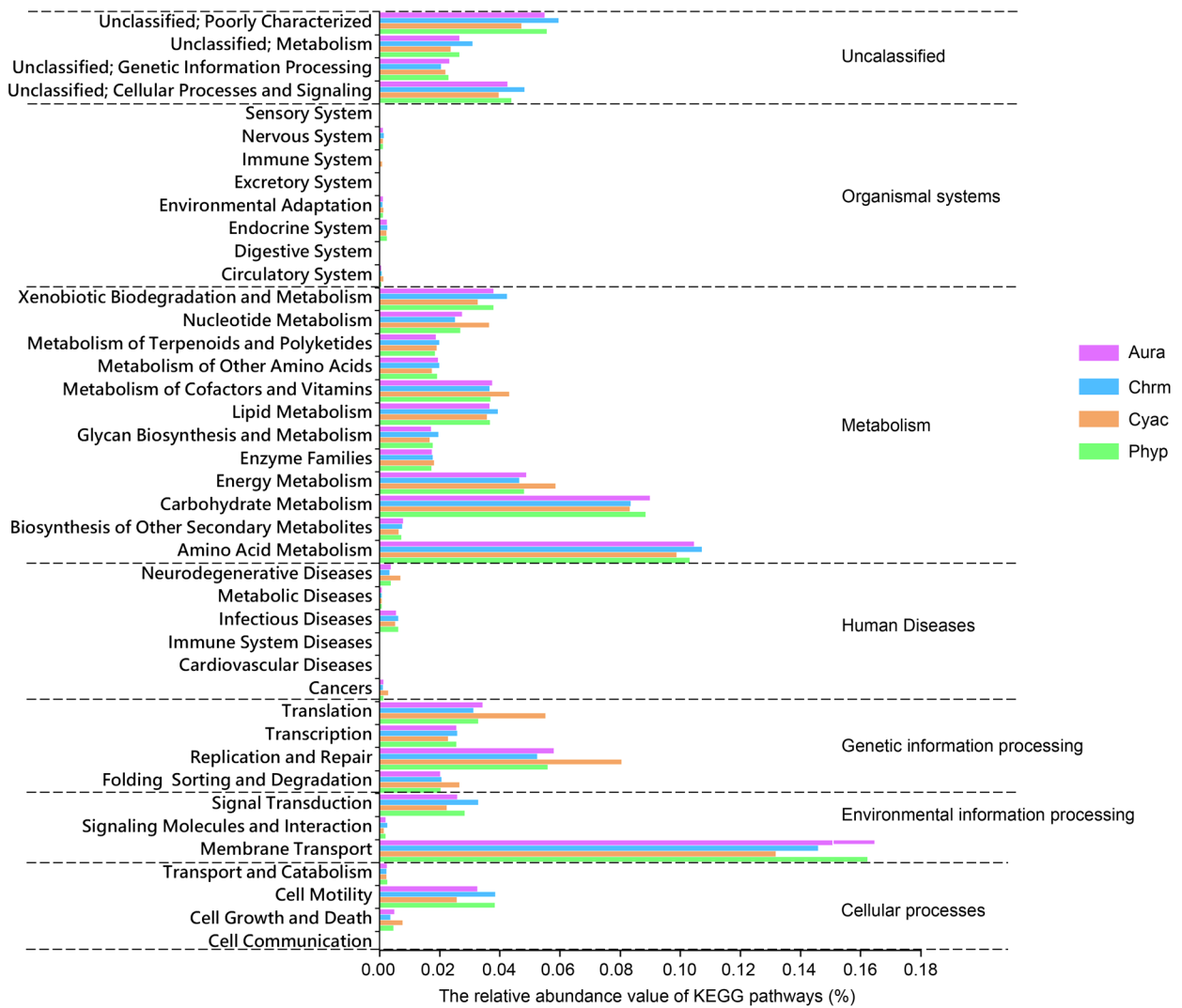


Fig. 4. The function prediction and KEGG pathway analysis of bacteria in four jellyfish species. 4.1. The Venn diagram analysis of common bacterial functional groups in the four jellyfish species. 4.2. The relative abundance of each predicted functional category given in the KEGG pathways (level 2).

4.2.



Discussion

The associated microbiota of jellyfish plays an essential role in the jellyfish life processes, and the information on the bacterial community is of great importance

to jellyfish homeostasis and its health. In this study, all the four jellyfish species belonging to Scyphozoa were raised under artificial culture conditions and the phylum Proteobacteria (76.9–78.3%, especially Moraxellaceae, *Pseudomonas*, and *Vibrio*) dominated in *C. capil-*

lata and *A. coerulea*, while Firmicutes (82.1%, mostly *Staphylococcus* and Aerococcaceae) and Tenericutes (68.4%, mainly Mycoplasmataceae) in *C. melanaster* and *P. punctata*, indicating that the bacterial diversity is host-specific. Meanwhile, the symbiotic microbes in the same or close jellyfish species are possibly diversified with their geographic distributions or breeding settings due to the variation of environmental parameters, such as temperature, salinity, and cleanness (Tinta et al. 2019). Daley et al. (2016) showed that the bacterial communities associated with *A. aurita* are mainly composed of Mycoplasmatales (Tenericutes, Mollicutes) that, in this study, is rarely found in *A. coerulea*, which is another moon jellyfish very close to *Aurelia aurita*. Similarly, the endobiotic bacteria *Pseudoalteromonas* of the tentacles of *C. capillata* (Schuett and Doepke 2010) were not detected in *C. capillata* in this study. Here, the jellyfish *P. punctata* and *A. coerulea* were fed with the same shrimp eggs under similar temperatures 18–28°C, while *C. capillata* and *C. melanaster* were both cultured on shrimp eggs and *A. coerulea* at the same temperature 10–18°C. However, the number of OTUs shared between *P. punctata* and *A. coerulea*, and between *C. capillata* and *C. melanaster* with similar breeding settings were 137 and 135 respectively. It is much less than 178 between *C. capillata* and *A. coerulea* that is the highest number, but still much higher than 87 between *C. melanaster* and *P. punctata* with different breeding conditions, which was the lowest number observed in this study. We therefore cautiously concluded that the microbiota of the four jellyfish is more dependent on the jellyfish species although we do not neglect the impact of the different breeding environments.

The host-specificity of the symbiotic bacteria is not surprising when considering that the different jellyfish species can represent distinct morphological and biological features, and, therefore, providing distinctive microniches for bacteria (Lee et al. 2018). Usually, the symbiotic bacterial communities should satisfy certain distinct host necessities, and these requirements likely help to drive corresponding differences in the structures of the associated bacterial communities. Moreover, some types of bacteria might be commonly shared because of the common phylogeny and/or ecological characteristics of their hosts. For example, three jellyfish species, including *P. punctata*, *C. capillata*, and *A. coerulea*, were found to host a small number of Cyanobacteria that have been mainly studied as the model organisms of plant-like photosynthesis or carbon and nitrogen fixation (Mulikidjanian et al. 2006; Schuergers et al. 2017), and therefore possibly photosynthesize to provide nutrients for both themselves and their hosts. Interestingly, a small number of *Vibrio* were detected in all four jellyfish species. When the inhibitory factors are removed e.g. the defensive mechanism

of jellyfish is compromised or the water temperature rises at the end of the reproductive period, the *Vibrio* will quickly increase in number to release the *Vibrio* toxic virulence factors, and their viability, resistance to antimicrobial compounds, hemolysis and cytotoxicity would significantly increase, and could finally play a dominant role in the biomass degradation of jellyfish (Shanmugam et al. 2017; Tinta et al. 2019).

Membrane transport, amino acid metabolism, and carbohydrate metabolism are the most abundant among the 41 matched KEGG pathways, supporting the conventional function of symbiotic microorganisms that involve the communication between the hosts and external environments and metabolic processes of their hosts. The host provides an ideal habitat for the microorganisms (van de Water et al. 2018). Mutually, these microorganisms play an important role in the health and adaptive response of the hosts to the environment instead of impairing their hosts (Rosenberg et al. 2007, van de Water et al. 2018). Moreover, the big proportion (84.6%) of the matched OTUs, as well as little variation of relative abundance of KEGG pathways among the four jellyfish species suggest that these microbial groups perform similar functions to meet the necessities of their hosts even when the dominant symbiotic bacteria are diversified. In conclusion, we first detected and comparatively analyzed the endobiotic bacterial community by 16S rDNA sequencing in the four common Scyphomedusae, *P. punctata*, *C. capillata*, *C. melanaster*, and *A. coerulea*. A few 1049 OTUs were harvested from a total of 130 183 reads. The number of OTU unions of all the four jellyfish species was 931 while the OTU intersection was 79. The classified OTUs and bacterial abundance greatly decrease from the phylum to genus level. The top 20 genera account for 9.03%, 48.9%, 83.1%, and 58.1% of the total community in *P. punctata*, *C. capillata*, *C. melanaster*, and *A. coerulea*, respectively. The relative abundances of top 50 genera in *A. coerulea* and *C. capillata* are far richer than that in *P. punctata* and *C. melanaster*. Moreover, 41 predictive functional categories at KEGG level 2 were identified. Our study indicates the independent diversity of the bacterial communities in the four jellyfish species that might be involved in the metabolism and environmental information processing in the hosts.

ORCID

Xintong Chen 0000-0002-4657-5833

Acknowledgments

This work was supported by the excellent youth talent program from Shanghai Municipal Health Commission (2017YQ007), Military Youth Training Program – Talent Project (18QNP016), and the general program from the National Natural Science Foundation of China (81600791, 81770329). The authors thank Li Xinshu for providing four different jellyfish samples.

Conflict of interest

The authors do not report any financial or personal connections with other persons or organizations, which might negatively affect the contents of this publication and/or claim authorship rights to this publication.

Literature

- Asnicar F, Weingart G, Tickle TL, Huttenhower C, Segata N. Compact graphical representation of phylogenetic data and meta-data with GraPhlAn. *PeerJ*. 2015 Jun 18;3:e1029. <https://doi.org/10.7717/peerj.1029>
- Bosch TCG. Cnidarian-microbe interactions and the origin of innate immunity in metazoans. *Annu Rev Microbiol*. 2013 Sep 08;67(1):499–518. <https://doi.org/10.1146/annurev-micro-092412-155626>
- Caporaso JG, Kuczynski J, Stombaugh J, Bittinger K, Bushman FD, Costello EK, Fierer N, Peña AG, Goodrich JK, Gordon JI, et al. QIIME allows analysis of high-throughput community sequencing data. *Nat Methods*. 2010 May;7(5):335–336. <https://doi.org/10.1038/nmeth.f.303>
- Cleary DFR, Becking LE, Polónia ARM, Freitas RM, Gomes NCM. Jellyfish-associated bacterial communities and bacterioplankton in Indonesian Marine lakes. *FEMS Microbiol Ecol*. 2016 May 01;92(5):fiw064. <https://doi.org/10.1093/femsec/fiw064>
- Cortés-Lara S, Urdiain M, Mora-Ruiz M, Prieto L, Rosselló-Móra R. Prokaryotic microbiota in the digestive cavity of the jellyfish *Cotylorhiza tuberculata*. *Syst Appl Microbiol*. 2015 Oct;38(7): 494–500. <https://doi.org/10.1016/j.syapm.2015.07.001>
- Daley MC, Urban-Rich J, Moisaner PH. Bacterial associations with the hydromedusa *Nemopsis bachei* and scyphomedusa *Aurelia aurita* from the North Atlantic Ocean. *Mar Biol Res*. 2016 Nov 25; 12 (10):1088–1100. <https://doi.org/10.1080/17451000.2016.1228974>
- DeSantis TZ, Hugenholtz P, Larsen N, Rojas M, Brodie EL, Keller K, Huber T, Dalevi D, Hu P, Andersen GL. Greengenes, a chimera-checked 16S rRNA gene database and workbench compatible with ARB. *Appl Environ Microbiol*. 2006 Jul 01;72(7):5069–5072. <https://doi.org/10.1128/AEM.03006-05>
- Edgar RC. Search and clustering orders of magnitude faster than BLAST. *Bioinformatics*. 2010 Oct 1;26(19):2460–2461. <https://doi.org/10.1093/bioinformatics/btq461>
- Gans J, Wolinsky M, Dunbar J. Computational improvements reveal great bacterial diversity and high metal toxicity in soil. *Science*. 2005 Aug 26;309(5739):1387–1390. <https://doi.org/10.1126/science.1112665>
- Langille MGI, Zaneveld J, Caporaso JG, McDonald D, Knights D, Reyes JA, Clemente JC, Burkpile DE, Vega Thurber RL, Knight R, et al. Predictive functional profiling of microbial communities using 16S rRNA marker gene sequences. *Nat Biotechnol*. 2013 Sep;31(9):814–821. <https://doi.org/10.1038/nbt.2676>
- Lee MD, Kling JD, Araya R, Ceh J. Jellyfish life stages shape associated microbial communities, while a core microbiome is maintained across all. *Front Microbiol*. 2018 Jul 12;9:1534. <https://doi.org/10.3389/fmicb.2018.01534>
- Magoč T, Salzberg SL. FLASH: fast length adjustment of short reads to improve genome assemblies. *Bioinformatics*. 2011 Nov 01; 27(21):2957–2963. <https://doi.org/10.1093/bioinformatics/btr507>
- Mulkidjanian AY, Koonin EV, Makarova KS, Mekhedov SL, Sorokin A, Wolf YI, Dufresne A, Partensky F, Burd H, Kaznadzey D, et al. The cyanobacterial genome core and the origin of photosynthesis. *Proc Natl Acad Sci USA*. 2006 Aug 29;103(35): 13126–13131. <https://doi.org/10.1073/pnas.0605709103>
- Paharik AE, Horswill AR. The staphylococcal biofilm: Adhesins, regulation, and host response. *Microbiol Spectr*. 2016 Apr; 4(2): 126–135. <https://doi.org/10.1128/microbiolspec.VMBF-0022-2015>
- Ramette A. Multivariate analyses in microbial ecology. *FEMS Microbiol Ecol*. 2007 Nov;62(2):142–160. <https://doi.org/10.1111/j.1574-6941.2007.00375.x>
- Rosenberg E, Koren O, Reshef L, Efrony R, Zilber-Rosenberg I. The role of microorganisms in coral health, disease and evolution. *Nat Rev Microbiol*. 2007 May;5(5):355–362. <https://doi.org/10.1038/nrmicro1635>
- Schuerger N, Mullineaux CW, Wilde A. Cyanobacteria in motion. *Curr Opin Plant Biol*. 2017 Jun;37:109–115. <https://doi.org/10.1016/j.pbi.2017.03.018>
- Schuett C, Doepke H. Endobiotic bacteria and their pathogenic potential in cnidarian tentacles. *Helgol Mar Res*. 2010 Sep;64(3): 205–212. <https://doi.org/10.1007/s10152-009-0179-2>
- Segata N, Izard J, Waldron L, Gevers D, Miropolsky L, Garrett WS, Huttenhower C. Metagenomic biomarker discovery and explanation. *Genome Biol*. 2011;12(6):R60. <https://doi.org/10.1186/gb-2011-12-6-r60>
- Sevellec M, Derome N, Bernatchez L. Holobionts and ecological speciation: the intestinal microbiota of lake whitefish species pairs. *Microbiome*. 2018 Dec;6(1):47. <https://doi.org/10.1186/s40168-018-0427-2>
- Shanmugam SG, Magbanua ZV, Williams MA, Jangid K, Whitman WB, Peterson DG, Kingery WL. Bacterial diversity patterns differ in soils developing in sub-tropical and cool-temperate ecosystems. *Microb Ecol*. 2017 Apr;73(3):556–569. <https://doi.org/10.1007/s00248-016-0884-8>
- Shannon P, Markiel A, Ozier O, Baliga NS, Wang JT, Ramage D, Amin N, Schwikowski B, Ideker T. Cytoscape: a software environment for integrated models of biomolecular interaction networks. *Genome Res*. 2003 Nov 01;13(11):2498–2504. <https://doi.org/10.1101/gr.1239303>
- Stephens WZ, Burns AR, Stagaman K, Wong S, Rawls JF, Guillemin K, Bohannan BJM. The composition of the zebrafish intestinal microbial community varies across development. *ISME J*. 2016 Mar;10(3):644–654. <https://doi.org/10.1038/ismej.2015.140>
- Tinta T, Kogovšek T, Klun K, Malej A, Herndl GJ, Turk V. Jellyfish-associated microbiome in the marine environment: exploring its biotechnological potential. *Mar Drugs*. 2019 Feb 01; 17(2):94. <https://doi.org/10.3390/md17020094>
- van de Water JAJM, Allemand D, Ferrier-Pagès C. Host-microbe interactions in octocoral holobionts – recent advances and perspectives. *Microbiome*. 2018 Dec;6(1):64. <https://doi.org/10.1186/s40168-018-0431-6>
- Viver T, Orellana LH, Hatt JK, Urdiain M, Díaz S, Richter M, Antón J, Avian M, Amann R, Konstantinidis KT, et al. The low diverse gastric microbiome of the jellyfish *Cotylorhiza tuberculata* is dominated by four novel taxa. *Environ Microbiol*. 2017 Aug; 19(8):3039–3058. <https://doi.org/10.1111/1462-2920.13763>
- Weiland-Bräuer N, Neulinger SC, Pinnow N, Künzel S, Baines JF, Schmitz RA. Composition of bacterial communities associated with *Aurelia aurita* changes with compartment, life stage, and population. *Appl Environ Microbiol*. 2015 Sep 01;81(17):6038–6052. <https://doi.org/10.1128/AEM.01601-15>
- White JR, Nagarajan N, Pop M. Statistical methods for detecting differentially abundant features in clinical metagenomic samples. *PLOS Comput Biol*. 2009 Apr 10;5(4):e1000352. <https://doi.org/10.1371/journal.pcbi.1000352>
- Yin M, Liu D, Xu F, Xiao L, Wang Q, Wang B, Chang Y, Zheng J, Tao X, Liu G, et al. A specific antimicrobial protein CAP-1 from *Pseudomonas* sp. isolated from the jellyfish *Cyanea capillata*. *Int J Biol Macromol*. 2016 Jan;82:488–496. <https://doi.org/10.1016/j.ijbiomac.2015.10.056>

Inhibition of Drug Resistance of *Staphylococcus aureus* by Efflux Pump Inhibitor and Autolysis Inducer to Strengthen the Antibacterial Activity of β -lactam Drugs

WENJING LUAN^{1*}, XIAOLEI LIU^{1*}, XUEFEI WANG¹, YANAN AN¹, YANG WANG¹, CHAO WANG¹,
KESHU SHEN², HONGYUE XU¹, SHULIN LI¹, MINGYUAN LIU^{1,3} and LU YU^{1*}

¹Key Laboratory for Zoonosis Research, Ministry of Education, Institute of Zoonosis, Department of Infectious Diseases of First Hospital of Jilin University, College of Veterinary Medicine Jilin University, Changchun, China

²Jilin Hepatobiliary Hospital, Changchun, China

³Jiangsu Co-innovation Center for Prevention and Control of Important Animal Infectious Diseases and Zoonoses, Yangzhou, China

Submitted 20 June 2019, revised 20 September 2019, accepted 21 September 2019

Abstract

This study explored a potential treatment against methicillin-resistant *Staphylococcus aureus* (MRSA) infections that combines thioridazine (TZ), an efflux pump inhibitor, and miconazole (MCZ), an autolysis inducer, with the anti-microbial drug cloxacillin (CXN). *In vitro*, the combination treatment of TZ and MCZ significantly reduced 4096-fold (Σ (FIC) = 0.1 – 1.25) the MIC value of CXN against *S. aureus*. *In vivo*, the combination therapy significantly relieved breast redness and swelling in mice infected with either clinical or standard strains of *S. aureus*. Meanwhile, the number of bacteria isolated from the MRSA135-infected mice decreased significantly ($p = 0.0427 < 0.05$) after the combination therapy when compared to monotherapy. Moreover, the number of bacteria isolated from the mice infected with a reference *S. aureus* strain also decreased significantly ($p = 0.0191 < 0.05$) after the combination therapy when compared to monotherapy. The pathological changes were more significant in the CXN-treated group when compared to mice treated with a combination of three drugs. In addition, we found that combination therapy reduced the release of the bacteria-stimulated cytokines such as IL-6, IFN- γ , and TNF- α . Cytokine assays in serum revealed that CXN alone induced IL-6, IFN- γ , and TNF- α in the mouse groups infected with ATCC 29213 or MRSA135, and the combination of these three drugs significantly reduced IL-6, IFN- γ , and TNF- α concentrations. Also, the levels of TNF- α and IFN- γ in mice treated with a combination of three drugs were significantly lower than in the CXN-treated group. Given the synergistic antibacterial activity of CXN, we concluded that the combination of CXN with TZ, and MCZ could be developed as a novel therapeutic strategy against *S. aureus*.

Key words: *Staphylococcus aureus*, mastitis, thioridazine (TZ), miconazole (MCZ), cloxacillin (CXN), combination therapy

Introduction

Staphylococcus aureus infection and drug resistance problems have caused increasing public health problems. The increase in antimicrobial resistance coupled with intracellular infection makes this bacteria the third-largest threat to human health according to the WHO (Lowy 1998; Demon et al. 2012). MRSA is of particular concern because of its ability to spread extensively and rapidly, along with its multi-drug resistance to β -lactam and aminoglycoside antibiotics (Boucher et al. 2009; Kolendi 2010). MRSA infection is always

associated with chronic or recurrent infections, including osteomyelitis, pulmonary infection, and endocardial inflammation (Que et al. 2005). In China, almost 10% of *S. aureus* clinical isolates were considered resistant to penicillin in recent years (Hu et al. 2016; Chen et al. 2017). Several new targets have been discovered and addressed in recent drugs, including ClpP protease and FtsZ of the cell division machinery. Resistance can be modified and inactivated by enzymatic drugs, enzymatic modification of drug-binding sites, drug efflux, and the others. Studies on the resistance of the current antibiotics have been reported also using drug

* These authors contributed equally to this work.

* Corresponding author: L. Yu, College of Veterinary Medicine Jilin University, Changchun, China; e-mail: yu_lu@jlu.edu.cn

© 2019 Wenjing Luan et al.

This work is licensed under the Creative Commons Attribution-NonCommercial-NoDerivatives 4.0 License (<https://creativecommons.org/licenses/by-nc-nd/4.0/>).

combinations (Foster et al. 2017). Several synergistic combinations of small molecules and antibiotics have also been provided to treat *S. aureus* infection by reversing the resistance mechanisms, attenuating *S. aureus* virulence and/or interfering with quorum sensing (Vermote et al. 2017). Thus, the urgency is required in the development of the new strategies for antimicrobial drug combinations against MRSA.

One novel strategy is to utilize helper compounds in combination with traditional antibiotics. Helper compounds are drugs approved for other therapeutic purposes that also possess antibacterial activity (Dickey et al. 2017). Thioridazine (TZ) is primarily an antipsychotic drug and also functions as an efflux pump inhibitor, which can be used as a helper compound (Klitgaard et al. 2008; Pule et al. 2016). Several *in vitro* studies have shown that TZ significantly increases the susceptibility of MRSA to β -lactam antibiotics (Poulsen et al. 2013). It has been shown that cytoderm synthesis and autolysis are linked since the inhibition of the former activates the latter. Thus, the destruction of the cytoderm is an important step in the bactericidal process of penicillin and other antibiotics (Zore et al. 2011). Miconazole (MCZ) is an antifungal drug that is considered as an autolysis inducer, which causes a release of cellular K^+ at low concentrations, and MCZ at the minimum inhibitory concentration (MIC) showed a certain antibacterial effect on clinically isolated MRSA (Falk et al. 2010). In our study, we aimed to suppress the multiple drug resistance of MRSA by combining cloxacillin (CXN) with an autolysis inducer MCZ and an efflux pump inhibitor TZ.

The previous studies have shown that the innate immune response, including pattern recognition receptors (PRR), was activated upon infection with *S. aureus* (Elazar et al. 2010). The release of cytokines is an important indicator for the evaluation of antibiotics. When inoculated with *S. aureus*, immune cells produce the inflammatory cytokines such as tumor necrosis factor- α (TNF- α), interleukin 1 β (IL-1 β), and interleukin 6 (IL-6) in high concentrations (Chen et al. 2017). *S. aureus* may also stimulate nuclear factor- κ B inhibitor (IKB), nuclear factor- κ B (NF- κ B), and mitogen-activated protein kinase phosphorylation (Gao et al. 2015). The previous studies have shown that TNF- α is the earliest and primary endogenous mediator and plays crucial role in both inflammatory and neuropathic hyperalgesia (Zhang et al. 2007). In these studies, TNF- α and IL-6 after infection were released at high concentrations for 24 h, and there was no time gradient for IFN- γ detection after infection, which was consistent with previous reports (Trigo et al. 2009; Hu et al. 2010). In the studies on the mechanism of action of antibiotics, the level of cytokines was measured at 12–24 h (Wei W et al. 2009; Fu Y et al. 2014). The

inflammatory cells including macrophages regulate inflammatory responses by the induction of significant inflammation and release of inflammatory cytokines (IL-1 β , IL-6, and TNF- α) and chemokines (Kim et al. 2015) at the high concentrations.

Our study is the first to explore the combination of TZ, MCZ, and CXN in the treatment of mastitis using a mouse model to provide a basis for subsequent combined antibacterial therapy.

Experimental

Materials and Methods

Ethics statement. The BALB/c mice were housed in micro-isolator cages and received food and water freely. The laboratory temperature was $24 \pm 1^\circ\text{C}$, and relative humidity was 40–80%. All animal studies were conducted according to the experimental practices and standards approved by the Animal Welfare and Research Ethics Committee at Jilin University (no: IZ-2009-008). The protocols were reviewed and approved by the committee. All animal studies were performed under isoflurane anesthesia, and every effort was made to minimize suffering.

Strains and growth conditions. *S. aureus* was obtained from the China Type Culture Collection (CTCC) (American Type Culture Collection [ATCC] 29213), and *S. aureus* isolates were derived from sub-clinical mastitis. The three antimicrobial agents used were CXN, MCZ (Yeyuan, Shanghai China), and TZ (MedChemexpress).

Antimicrobial susceptibility testing. To determine the MIC values for CXN, TZ, and MCZ against *S. aureus* a microdilution assay was performed according to the CLSI (formerly NCCLS) guidelines. The determination of the MIC of CXN for the mastitis isolates of *S. aureus* was performed using the Mueller-Hinton agar dilution assay according to the CLSI guidelines (CLSI 2008). Plates were incubated at $35\text{--}38^\circ\text{C}$ for 16–20 h.

Interpretation of synergy tests. The synergy test was performed in a 96-well microtiter plate containing two or three antimicrobial agents that were distributed in a two- or three-fold dilution on the day of the assay in a checkerboard pattern. Each well contained 0.1 ml of an individual antimicrobial composition or broth control. The final inoculate concentration was maintained at $3\text{--}5 \times 10^5$ CFU/ml. The plate was incubated for 20–24 h, and the MIC value was determined. *S. aureus* ATCC 29213 was used as the quality control strain.

For the first clear well in each row of the microtitre plate containing both antimicrobial agents, the fractional inhibitory concentration (FIC) of each agent was calculated as follows:

FIC of drug A (FIC_A) = MIC of drug A in combination / MIC of drug A alone

FIC of drug B (FIC_B) = MIC of drug B in combination / MIC of drug B alone

The summation of both FICs (ΣFIC) in each well ($FICI = \Sigma FIC = FIC_A + FIC_B$) was used to classify the combination of antimicrobial agents at the given concentrations as synergistic ($\Sigma FIC, \leq 0.5$), partially synergistic ($\Sigma FIC, > 0.5$ and ≤ 1.0), indifferent ($\Sigma FIC, > 1$ and ≤ 4), or antagonistic ($\Sigma FIC, > 4$) (Zore et al. 2011).

Using three-dimensional checkerboard microdilution with CXN, TZ, and MCZ the combined concentrations of each antibiotic showed synergy when their sum, FICI ($\Sigma FICs$) was lower than 1.0.

Mouse *S. aureus* mastitis model. The *S. aureus* mastitis mouse model has been used to investigate the novel prevention and treatment methods for *S. aureus* mastitis, as reported previously. Briefly, the mice weighed approximately 50 g at the beginning of the experiment. The pups were weaned 1–2 h before bacterial inoculation of the mammary glands. A mixture of oxygen and isoflurane (2–3%) was inhaled to anesthetize the lactating mice. A syringe with a 32-gauge blunt needle was used to inoculate both L4 (on the left) and R4 (on the right) glands of the fourth abdominal mammary gland pair, with approximately 10^7 CFU of *S. aureus*. A total of 18 mice were used for each mice group infected with a single strain of *S. aureus*, either ATCC 29213 or MRSA135. The 18 mice of each group were divided into the following groups, with three mice in each group: blank (I), infection control (II), MCZ monotherapy (III), TZ monotherapy (IV), CXN monotherapy (V), and CXN + TZ + MCZ treatment (VI) groups. The mice were observed for 24 h following infection before treatment was initiated, and then the results were obtained after 72 h of treatment in each drug group. In *in vivo* experiment, the concentration of cloxacillin was 20 mg/kg/d, thioridazine – 16 mg/kg/d, and miconazole – 11 mg/kg/d in the single-agent treatment group. In the combination treatment group the concentration of: cloxacillin was 0.75 mg/kg/d, thioridazine – 12 mg/kg/d, and miconazole – 1.5 mg/kg/d.

Cytokines in the mastitis mouse model. At 24 h after *S. aureus* inoculation the animal blood was centrifuged. Cytokines were detected by the double sandwich enzyme-linked immunosorbent assay technique. Different groups were compared using an independent samples *t*-test, and a paired samples *t*-test was used to analyze any significant differences in the data that originated from the same group at different time points (Moon et al. 2007).

Antimicrobial susceptibility testing. The MIC of CXN against 47 strains of *S. aureus* was determined, and the values ranged from 4 to 512 $\mu\text{g/ml}$. The MIC value of CXN against *S. aureus* ATCC 29213 was 4 $\mu\text{g/ml}$

Table II

Summary of thioridazine, miconazole and cloxacillin activity in combination (expressed as the MIC value) against *Staphylococcus aureus* strains.

Antimicrobial agents		MIC ($\mu\text{g/ml}$)		
		Range	50%	90%
Cloxacillin	Thioridazine	0.125–512	16	512
	Miconazole	0.25–512	4	512
	Thioridazine + Miconazole	0.000972–16	0.5	8

MIC – minimum inhibitory concentration

Table I

The MICs values of individual antimicrobial agents against *Staphylococcus aureus* isolates.

Antimicrobial agents	MIC ($\mu\text{g/ml}$)		
	Range	50%	90%
Cloxacillin	4–512	16	512
Thioridazine	16–64	32	64
Miconazole	1–8	4	8

MIC – minimum inhibitory concentration

and that of MRSA135 was 256 $\mu\text{g/ml}$. The drug susceptibility results showed that 23 strains of *S. aureus* were resistant to CXN, while 24 strains of *S. aureus* were sensitive to CXN. The MIC of TZ for 47 strains of *S. aureus* was determined, ranging from 16 $\mu\text{g/ml}$ to 64 $\mu\text{g/ml}$. The MIC value of TZ for *S. aureus* ATCC 29213 was 16 $\mu\text{g/ml}$ and that of MRSA135 $\mu\text{g/ml}$ was 32 $\mu\text{g/ml}$. The MIC of MCZ for 47 strains of *S. aureus* was determined, and the values ranged from 1 $\mu\text{g/ml}$ to 8 $\mu\text{g/ml}$. The MIC value of MCZ for *S. aureus* ATCC 29213 was 4 $\mu\text{g/ml}$ and that of MRSA135 was 4 $\mu\text{g/ml}$ (Table I).

Drug synergy results against *S. aureus* isolates. The FICI index, used as a predictor of synergy, was evaluated using the TZ and MCZ agents combined with CXN (Table II). The results showed that both the combination of the two drugs and the combination of the three drugs reduced the MIC value of the drugs to varying degrees. Anti-*S. aureus* activity of two drugs, CXN and TZ, was shown in Table III. Among the 47 strains tested, the combined FICI ranged from 0.14 to 1.13, of which 24 strains had synergistic effects (0.14–0.5), 13 strains had partial synergistic effects (0.56–0.75), and 10 strains had an unrelated effect (1.06–1.25). Anti-*S. aureus* activity of a combination of CXN and MCZ was reported in Table IV. Among the 47 strains tested, the combined FICI ranged from 0.14 to 2.25, of which 15 had synergistic effects (0.14–0.5), 15 had partial synergistic effects (0.51–1), and 17 had irrelevant effects (1.03–2.25). The activity of a combination of CXN, TZ, and MCZ against *S. aureus* MRSA strains was shown in Table V. The FICI ranged from 0.19 to 0.75 among

Table IV
The activity of the combination of cloxacillin and miconazole
against *Staphylococcus aureus* strains *in vitro*.

Strains	FICI
MRSA14	0.63
MRSA15	0.75
MRSA16	0.38
MRSA20	0.31
MRSA21	0.31
MRSA22	2.25
MRSA25	0.53
MRSA29	2.13
MRSA30	0.26
MRSA64	0.14
MRSA65	0.26
MRSA75	1.00
MRSA76	1.13
MRSA92	0.26
MRSA94	0.51
MRSA97	0.52
MRSA98	0.26
MRSA125	0.50
MRSA126	1.50
MRSA134	1.50
MRSA135	0.27
MRSA142	1.01
MRSA162	0.63
ATCC 29213	0.50
MSSA10	0.56
MSSA13	0.31
MSSA14	2.00
MSSA31	1.13
MSSA36	2.02
MSSA41	1.50
MSSA42	0.27
MSSA44	1.06
MSSA50	1.03
MSSA51	1.00
MSSA54	1.50
MSSA56	1.00
MSSA62	1.50
MSSA65	1.03
MSSA66	0.53
MSSA67	0.31
MSSA68	0.53
MSSA70	0.52
MSSA72	0.28
MSSA73	1.03
MSSA78	1.06
MSSA79	0.56
MSSA80	0.56

See FICI criteria for details.

Table III
The activity of the combination of cloxacillin and thioridazine
against *Staphylococcus aureus* strains *in vitro*.

Strain	FICI
MRSA14	0.38
MRSA15	0.63
MRSA16	0.75
MRSA20	0.25
MRSA21	0.50
MRSA22	0.63
MRSA25	0.31
MRSA29	0.19
MRSA30	1.06
MRSA64	0.25
MRSA65	0.25
MRSA75	1.13
MRSA76	1.13
MRSA92	0.31
MRSA94	0.19
MRSA97	0.25
MRSA98	0.19
MRSA125	0.27
MRSA126	0.50
MRSA134	0.16
MRSA135	0.16
MRSA142	0.63
MRSA162	0.38
ATCC 29213	0.28
MSSA10	0.31
MSSA13	0.56
MSSA14	0.63
MSSA31	0.63
MSSA36	0.38
MSSA41	0.63
MSSA42	0.56
MSSA44	0.38
MSSA50	0.38
MSSA51	0.14
MSSA54	0.38
MSSA56	0.63
MSSA62	0.63
MSSA65	0.63
MSSA66	1.13
MSSA67	1.13
MSSA68	1.13
MSSA70	1.13
MSSA72	1.06
MSSA73	0.63
MSSA78	1.25
MSSA79	1.25
MSSA80	0.25

See FICI criteria for details.

Table V
The activity of the combination of cloxacillin, thioridazine, and miconazole against MRSA strains *in vitro*.

Strain	CXN	TZ	MCZ	CXN	TZ	MCZ	FICI
	MICs (Single)			MICs (Synergy)			
MRSA14	512	32	2	4	4	0.25	0.26
MRSA15	512	32	2	2	4	0.25	0.25
MRSA16	512	16	4	1	4	0.25	0.31
MRSA20	256	32	2	0.25	4	0.25	0.25
MRSA21	128	16	4	0.5	4	0.25	0.32
MRSA22	64	32	4	0.25	4	0.50	0.25
MRSA25	512	16	2	0.5	4	0.50	0.50
MRSA29	256	64	4	4	4	0.50	0.20
MRSA30	512	64	4	0.5	4	0.50	0.19
MRSA64	512	32	8	8	4	0.50	0.20
MRSA65	512	32	4	0.5	4	0.50	0.25
MRSA75	512	32	2	0.5	4	0.50	0.38
MRSA76	512	32	4	8	4	0.50	0.27
MRSA92	512	16	4	0.0078	4	0.50	0.38
MRSA94	512	32	2	0.0078	4	0.50	0.38
MRSA97	256	32	2	0.0156	4	0.50	0.38
MRSA98	512	32	4	0.0078	4	0.50	0.25
MRSA125	256	16	2	0.5	4	0.50	0.50
MRSA126	256	16	1	1	4	0.50	0.75
MRSA134	512	32	1	0.0078	4	0.50	0.63
MRSA135	256	32	4	0.25	4	0.50	0.25
MRSA142	512	32	1	2	4	0.50	0.63
MRSA162	512	32	4	16	4	0.50	0.28
ATCC 29213	4	16	4	0.0156	4	0.50	0.38

See FICI criteria for details.

MCZ – miconazole; TZ – thioridazine; CXN – cloxacillin;

FIC of drug A (FIC_A) = MIC of drug A in combination / MIC of drug A alone;

FIC of drug B (FIC_B) = MIC of drug B in combination / MIC of drug B alone;

Combination FIC (AB) = $\Sigma FIC = FIC_A + FIC_B$;

Synergistic ($\Sigma FIC \leq 0.5$);

Partially synergistic ($\Sigma FIC > 0.5$ and ≤ 1.0);

Indifferent ($\Sigma FIC > 1$ and ≤ 4);

Antagonistic ($\Sigma FIC > 4$).

the 23 strains tested, of which 20 strains had synergistic effects (0.19–0.5), and three isolates have partial synergy (0.63–0.75). The activity of a combination of CXN, TZ, and MCZ against *S. aureus* MSSA strain (Table VI) showed that the FICI ranged from 0.1 to 1.25 for 23 strains tested, 19 of which had synergistic effects (0.1–0.5), one has a partial synergistic effect (0.69), and three strains have an unrelated effect (1.09–1.25). As the results of the synergistic tests, the concentration of each drug can be lowered. The *in vivo* dose of the compounds administered were referred to the ratio of the MIC value at synergistic combination (cloxacillin : thioridazine : miconazole = 0.25 $\mu\text{g/ml}$: 4 $\mu\text{g/ml}$: 0.50 $\mu\text{g/ml}$) as it was obtained by checkerboard assay *in vitro*, where the synergistic ratio of cloxacillin : thiori-

dazine : miconazole was 1 : 16 : 2. We also, referred to the dose of these compounds when they were single-administered to mouse or calculated from other animal studies already reported *in vivo* (cloxacillin ≤ 50 mg/kg/d, thioridazine ≤ 16 mg/kg/d, miconazole ≤ 20 mg/kg/d) (Hendricks et al. 2003; Choi et al. 2012). Finally, we calculated the corresponding dose of these compounds to be single-administered or in combination with animal experiments *in vivo*. The *in vivo* concentrations of three drugs in a combination treatment was as follows: cloxacillin (0.75 mg/kg/d) : thioridazine (12 mg/kg/d) : miconazole (1.5 mg/kg/d).

Statistical analysis. Comparisons of mean values from three experiments were statistically evaluated by analysis of variance, followed by the One-Way ANOVA

Table VI
The activity of the combination of cloxacillin, thioridazine, and miconazole against MSSA strains *in vitro*.

Strain	CXN	TZ	MCZ	CXN	TZ	MCZ	FICI
	MICs (Single)			MICs (Synergy)			
MSSA10	16	64	4	4	4	0.25	0.38
MSSA13	8	64	8	8	4	0.25	1.09
MSSA14	8	32	2	8	4	0.25	1.25
MSSA31	16	32	2	4	4	0.25	0.50
MSSA36	16	32	1	0.015625	4	0.25	0.38
MSSA41	8	32	1	4	4	0.25	0.88
MSSA42	16	64	8	0.125	4	0.25	0.10
MSSA44	16	32	1	0.5	4	0.25	0.41
MSSA50	16	32	1	0.125	4	0.25	0.38
MSSA51	16	32	2	0.001975	4	0.25	0.25
MSSA54	16	16	2	0.0625	4	0.25	0.38
MSSA56	16	32	2	0.03125	4	0.25	0.25
MSSA62	16	32	2	0.0009715	4	0.25	0.25
MSSA65	16	32	2	0.125	4	0.25	0.26
MSSA66	16	32	4	4	4	0.25	0.44
MSSA67	16	32	4	8	4	0.25	0.69
MSSA68	16	32	4	16	4	0.25	1.19
MSSA70	16	32	4	0.015625	4	0.25	0.19
MSSA72	16	64	8	0.5	4	0.25	0.13
MSSA73	16	32	2	0.0625	4	0.25	0.25
MSSA78	8	16	2	0.03125	4	0.25	0.38
MSSA79	8	16	4	0.03125	4	0.25	0.32
MSSA80	16	32	4	0.0078125	4	0.25	0.19
ATCC 29213	4	16	4	0.0156	4	0.50	0.38

See FICI criteria for details.

MCZ – miconazole; TZ – thioridazine; CXN – cloxacillin;

FIC of drug A (FIC_A) = MIC of drug A in combination / MIC of drug A alone;

FIC of drug B (FIC_B) = MIC of drug B in combination / MIC of drug B alone;

Combination FIC(AB) = $\Sigma FIC = FIC_A + FIC_B$;

Synergistic ($\Sigma FIC \leq 0.5$);

Partially synergistic ($\Sigma FIC > 0.5$ and ≤ 1.0);

Indifferent ($\Sigma FIC > 1$ and ≤ 4);

Antagonistic ($\Sigma FIC > 4$).

analysis. Differences with 2-sided $p < 0.05$ were considered statistically significant. All statistical analyses were performed using the GraphPad Prism 5 software (version 11.5; SPSS).

Results

Mouse mastitis treatment results. Two *S. aureus* mastitis mouse models were constructed, each injected with a single strain of *S. aureus*, either ATCC 29213 or the MRSA135 strain (Fig. 1A). Clinical observations showed that none of the mice in either the ATCC 29213 or MRSA135 groups died during the experiment, and their mental states were normal. The areolas of both

bacterial infection groups were swollen and red. The areolas in the MCZ or TZ monotherapy group were pale red and swollen, but there were no significant changes in the other groups. In the MRSA-infected groups, the mammary glands varied in color; those of the blank control group were milky white, those of the infection control group were purple, those of the MCZ or TZ treated group were red, those of a portion of the CXN treated group were red but most were milky white, and most were also milky white in the group treated with the combination of the three drugs (Fig. 1B). In the ATCC 29213-infected groups, the mammary glands varied in color; the blank control group had a normal mammary gland color, the infection control group had purple mammary glands, most of the glands in the

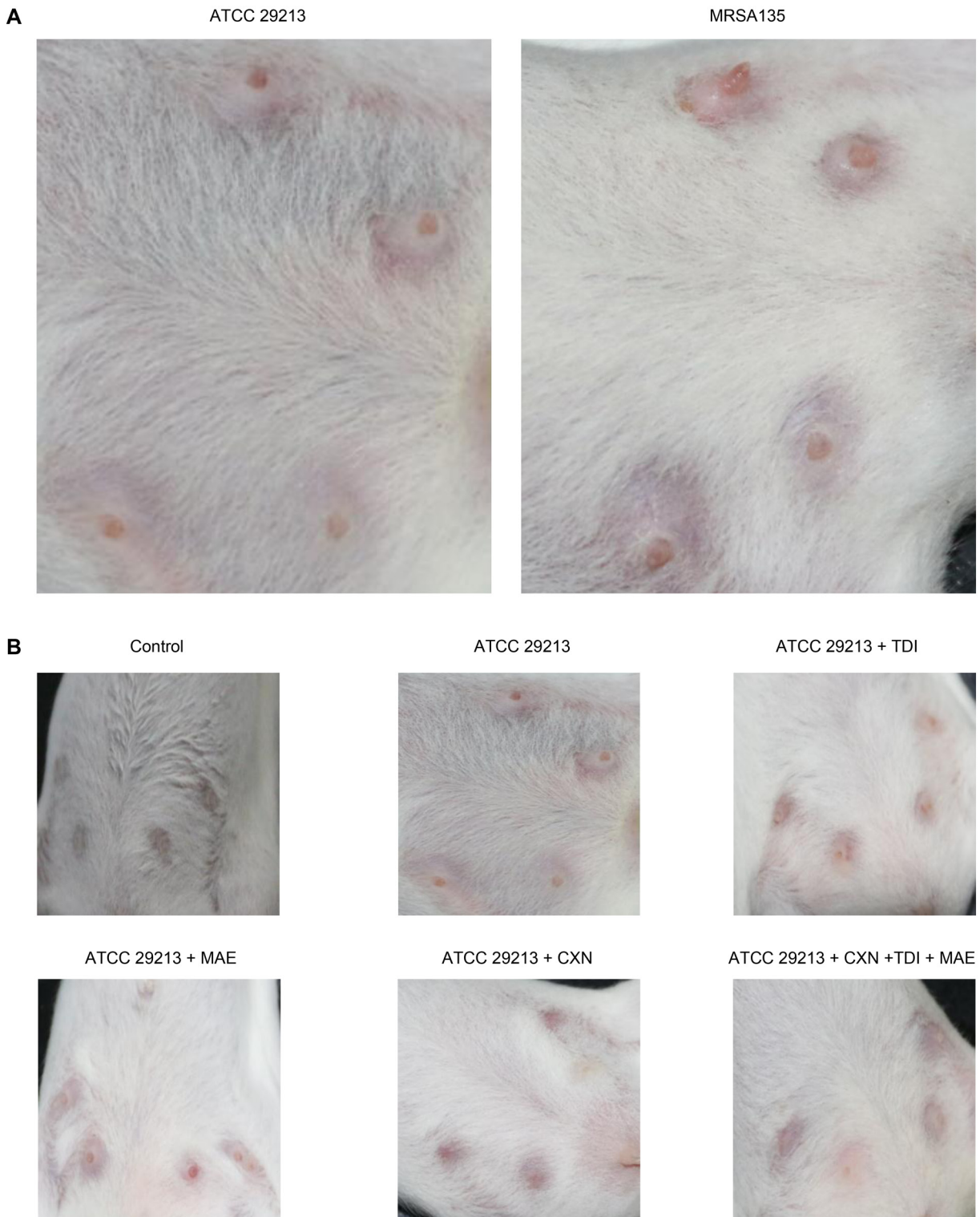


Fig. 1A i 1B. Clinical observations of mammary tissue of mouse infected with *Staphylococcus aureus* ATCC 29213 or MRSA135 before and after treatment with the drugs.

MCZ- and TZ-treated groups were red, and those of the CXN-treated and combination-treated groups were mostly milky white (Fig. 1C).

Histopathology of mammary tissue by the hematoxylin and eosin stain (H&E) was observed (Fig. 2A, and 2B). No obvious pathological changes were found in

the blank control group, which displayed normal acinar mammary glands and neat rows of acinar epithelial cells with prolactin. A large number of bacterial lumps and detached cells were seen in the infection control group, and both had red blood cell infiltrate observed in the interstitial space. The agglomerated cell mass was seen



Fig. 1C. Clinical observations of mammary tissue of mouse infected with *Staphylococcus aureus* ATCC 29213 or MRSA135 before and after treatment with the drugs.

in the acinus, and large numbers of lymphocyte infiltrate were observed in the interstitium. In the MCZ or TZ monotherapy groups, epithelial cells were swollen, obvious bacterial masses were visible, and lymphocytes had infiltrated the stroma. Few lymphocytes and certain bacterial masses were observed in the CXN group. In the combination group, few lymphocytes and very few bacteria were visible, in addition to a lack of cell shedding. The results showed that, in addition to the known effect of CXN monotherapy, the combination of CXN, TZ, and MCZ has obvious therapeutic effects against infection by both strains of *S. aureus* tested. In the group treated with the combination of the three drugs, most of the pathological changes were milder than the CXN treatment group.

S. aureus count results. Colony counts from mice of the clinical strain MRSA135-infected group showed that the bacterial concentration was 6.96×10^7 CFU/ml without therapy. Following treatment, the bacterial concentration in mice of the MCZ-treatment group was 2.23×10^7 CFU/ml; in the TZ-treatment group it was 1.73×10^7 CFU/ml; after CXN treatment it was 3.20×10^6 CFU/ml ($p=0.0447 < 0.05$), and after the combination therapy with CXN, TZ, and MCZ it was 1.10×10^6 CFU/ml ($p=0.0427 < 0.05$) (Fig. 3B). There was no significant difference between the CXN monotherapy- and the combination therapy groups (Fig. 3C). The colony counts after the mice were infected with the reference strain ATCC 29213 showed the following: the bacterial concentration without therapy was

2.34×10^5 CFU/ml; in the MCZ-treatment group it was 1.56×10^5 CFU/ml; in the TZ-treatment group it was 7.91×10^4 CFU/ml; after CXN treatment it was 1.17×10^4 CFU/ml ($p=0.0212 < 0.05$); and after the combination therapy with CXN, TZ, and MCZ was 4.43×10^3 CFU/ml ($p=0.0191 < 0.05$) (Fig. 3A). The difference between the CXN monotherapy and the three-drug treatment groups was significant ($p=0.0040 < 0.01$) (Fig. 3D).

Cytokine detection in a mouse model of mastitis.

Serum supernatants were assayed for TNF- α , IL-6 and IFN- γ levels using an ELISA kit (Fig. 4). The cytokines measured in the sera of mice infected with ATCC 29213 (the ATCC 29213 infected group) were as follows: the infected group had significantly increased levels of TNF- α , IL-6, and IFN- γ when compared to those in the control group ($p=0.0260$, $p=0.0348$, $p < 0.0001$, respectively) (Fig. 4A, 4C, and 4E). There was no significant difference in TNF- α , IL-6, and IFN- γ levels between mice treated with MCZ when compared with those of the control group. The levels of IL-6 and IFN- γ in the TZ-treated group were significantly lower than those in the ATCC 29213-infected group ($p=0.0176$, $p=0.0046$), but there was no significant difference in TNF- α levels. The levels of TNF- α , IL-6, and IFN- γ in the CXN-treated group were significantly lower than those in the infected group ($p=0.0016$, $p=0.0245$, $p < 0.0001$, respectively). The levels of TNF- α , IL-6, and IFN- γ in the group of mice treated with three drugs together were significantly lower than those in

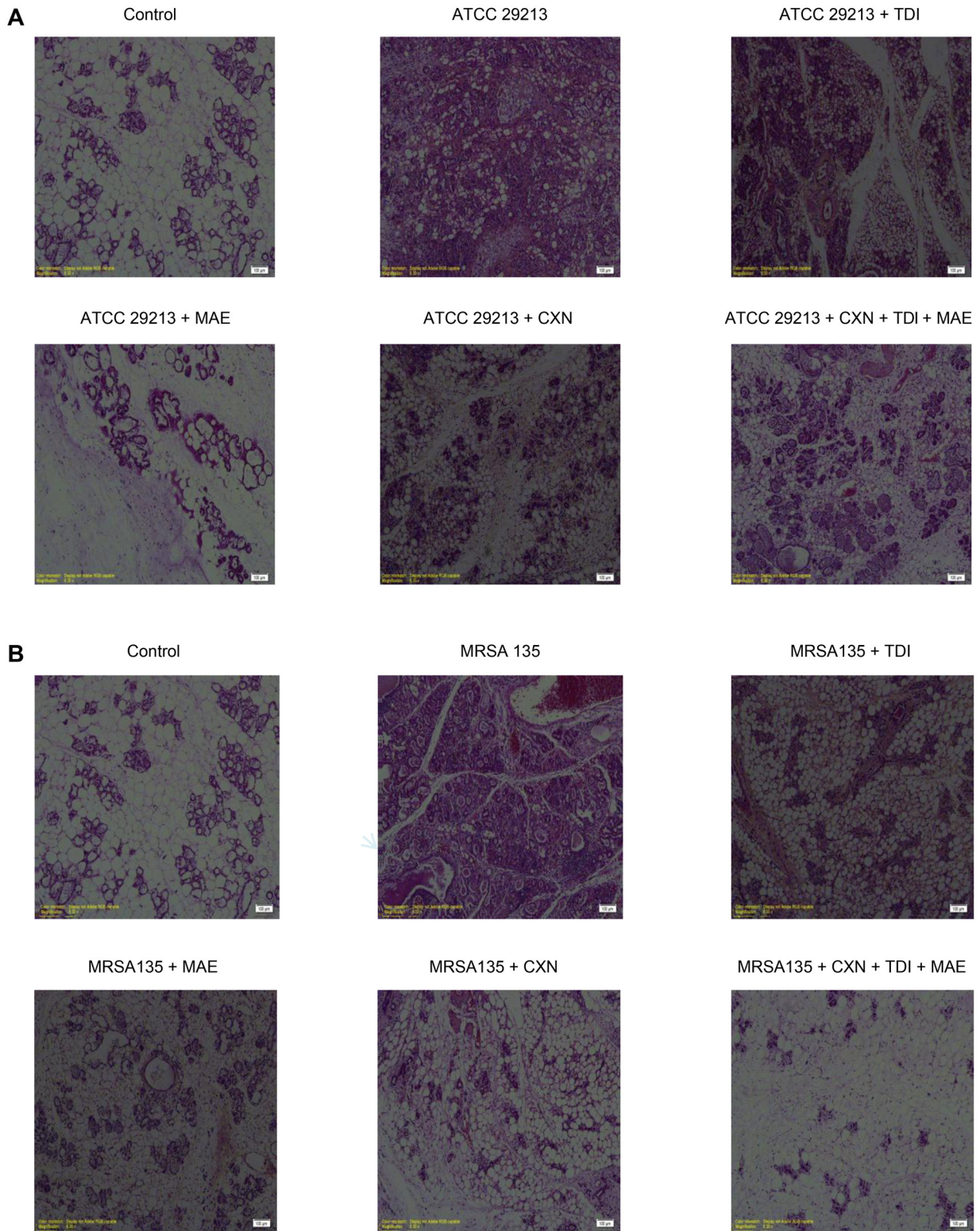


Fig. 2. Histopathological observations for each group of mice (control, infected, and treated with the drugs).

the ATCC 29213-infected group ($p=0.0004$, $p=0.0136$, $p<0.0001$). The levels of TNF- α and IFN- γ in the group of mice treated with three drugs together were significantly lower than those in the ATCC 29213-infected group ($p=0.0084$, $p=0.0280$). The cytokine results in the MRSA135-infected mice (the MRSA135-infected

group) were as follows: the MRSA135-infected group had significantly higher levels of IL-6 and IFN- γ than those in the control group ($p=0.0185$, $p=0.0148$, respectively) (Fig. 4B, 4D, and 4F). The levels of TNF- α and IL-6 in the MCZ-treated group were not significantly different from those the MRSA135-infected

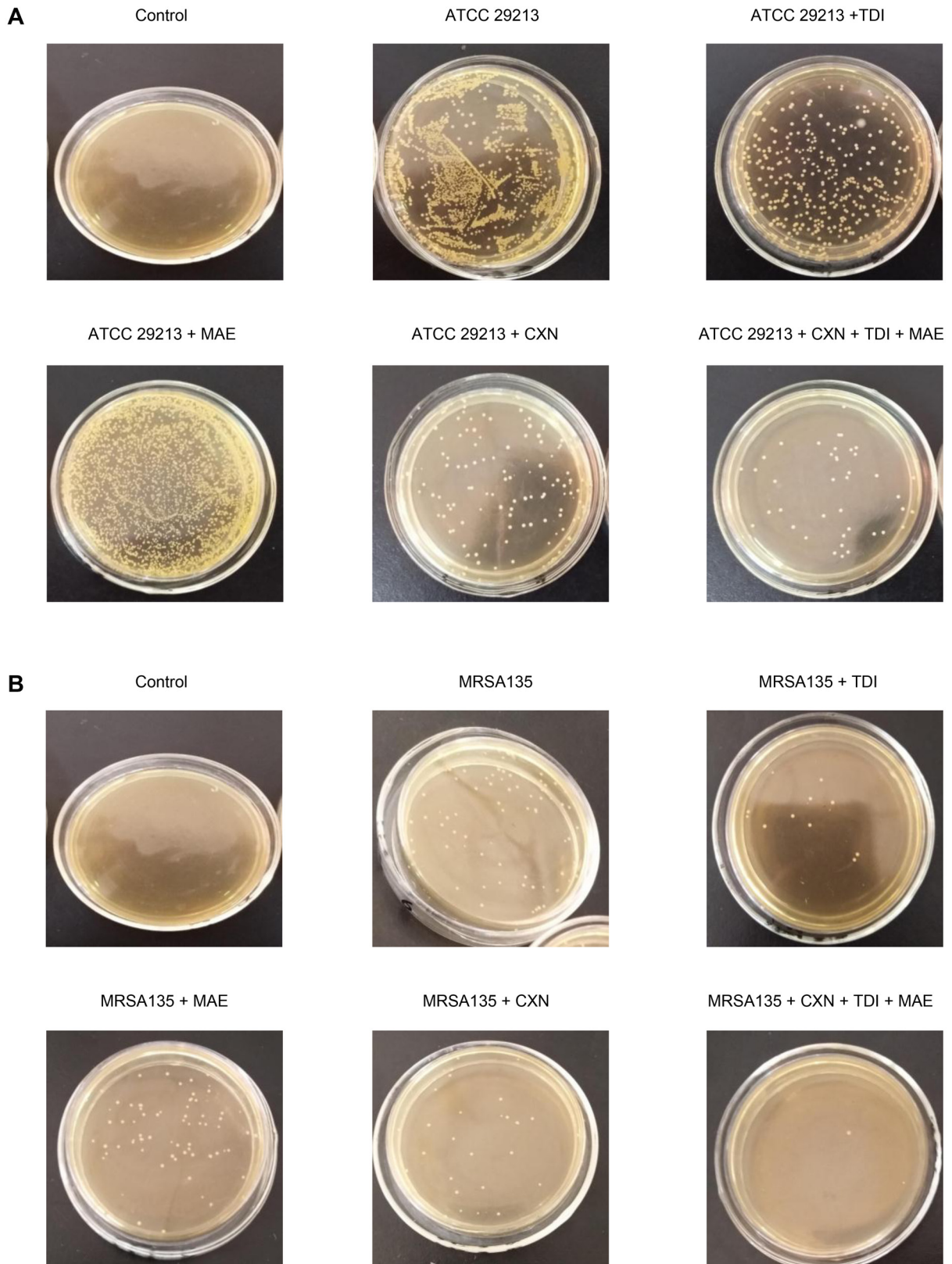


Fig. 3A i 3B

group, but the IFN- γ levels were significantly decreased ($p=0.0434$). There were no significant differences in TNF- α , IL-6, and IFN- γ levels in the TZ-treated group compared with those of the MRSA135-infected group.

The levels of IL-6 and IFN- γ in the CXN-treated group were significantly lower than those the MRSA135-infected group ($p=0.0191$, $p=0.0262$, respectively), but there was no significant difference in TNF- α levels.

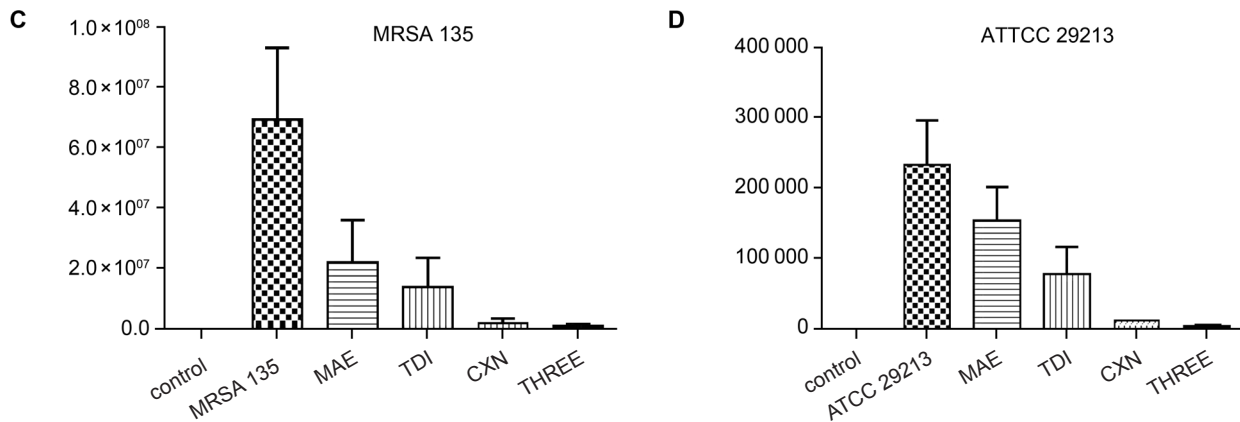


Fig. 3. The culture of *Staphylococcus aureus* isolated from each group of mice (control, infected, treated with the drugs).

MCZ – miconazole; TZ – thioridazine; CXN – cloxacillin; MCZ + TZ + CXN – the combination of miconazole, thioridazine, cloxacillin. There was no significant difference between the cloxacillin-treated and three-drugs-treated mice ($P=0.5649$). The * on the horizontal line indicates a significant difference analysis between the CXN group and the three-drug group. * $P < 0.05$, ** $p < 0.01$, *** $p < 0.0001$.

The levels of TNF- α , IL-6, and IFN- γ in mice treated with the three drugs together were significantly lower than those of the MRSA135-infected group ($p=0.0230$, $p=0.0051$, $p=0.0060$, respectively). The TNF- α levels in mice treated with the three drugs together were significantly lower than those of the MRSA135-infected group ($p=0.0010$). In summary, treatment with CXN alone or with the combination of three drugs was capable of inhibiting the expression of TNF- α and IL-6.

Discussion

A recent report indicated that developing of new natural compounds or combination therapies should be a focus on the fight against *S. aureus* (Celenza et al. 2012; Dickey et al. 2017). Combinations of antibiotics have been previously used to treat bacterial infections, including pathogens that cannot be suppressed or killed by a single antibiotic or infection with a multiplicity of microbial species (Navon-Venezia et al. 2005). A single antibiotic is hardly capable of killing bacteria that possess multiple drug resistance mechanisms against broad-spectrum β -lactams and aminoglycosides antibiotics (Wax 2008). However, bacteria can be inactivated through the joint use of a synergistically active antibacterial agent along with the antibiotic (Mascaretti 2003; Tegos and Mylonakis 2012). Combination therapy can improve the antibacterial effect and reduce the risk of drug resistance during treatment, thereby reducing drug toxicity (Tegos and Mylonakis 2012; Bresler et al. 2018). In addition, it has been found that when synthetic peptides of host defense bind to conventional antibiotics, synergistic effects can reduce the concentration of antibiotics required to eradicate certain bacterial strains of interest (Rudilla et al. 2016). Alternatively, the

two antimicrobial agents combination can also neutralize the biofilm development (Hwang et al. 2013). However, the antibiotic enhancement remains a challenge, and clinical treatment of bovine mastitis also lacks pre-clinical animal and clinical data to validate its utility (Tse et al. 2017). This study demonstrates that the drug combination provides good effects in the *in vitro* assays and in the *in vivo* treatment of mouse mastitis, and can provide a basis for clinical development. Following the CLSI recommendations, supplementary tests should be performed, even when the penicillin MIC (≤ 0.12 mg/l) is within the drug-sensitive range *in vitro* (CLSI 2015). The combination of TZ and β -lactam antibiotics may enhance efficacy against *S. aureus* as a synergistic effect. In this study, the results of *in vivo* experiments indicated that the concentration of cloxacillin alone (20 mg/kg/d) was higher than in the combination with the two other drugs (0.75 mg/kg/d), and the treatment effect was better for the combination of drugs. Thus, this study indicates the concentration of drugs that reduce drug resistance when used synergistically, providing some new ideas for drug resistance research.

Previous studies reported that TZ functions as an external pump inhibitor, and MCZ acts as an autolytic inducer against *S. aureus* (Pule et al. 2016). Therefore, we investigated these two drugs in combination with CXN to inhibit the resistance of *S. aureus* through the induction of bacterial autolysis, thus enhancing the antibacterial effect of CXN. In this study, the drug susceptibility results showed that *S. aureus* had particular resistance to CXN. Again, the two drugs showed a synergistic effect in inhibiting *S. aureus*. The synergistic effect of CXN and MCZ was better than that of CXN and TZ. The synergistic effect of the three drugs studied not only reduced the concentration of CXN required but also enhanced the antibacterial effect. Altogether, our results suggested that

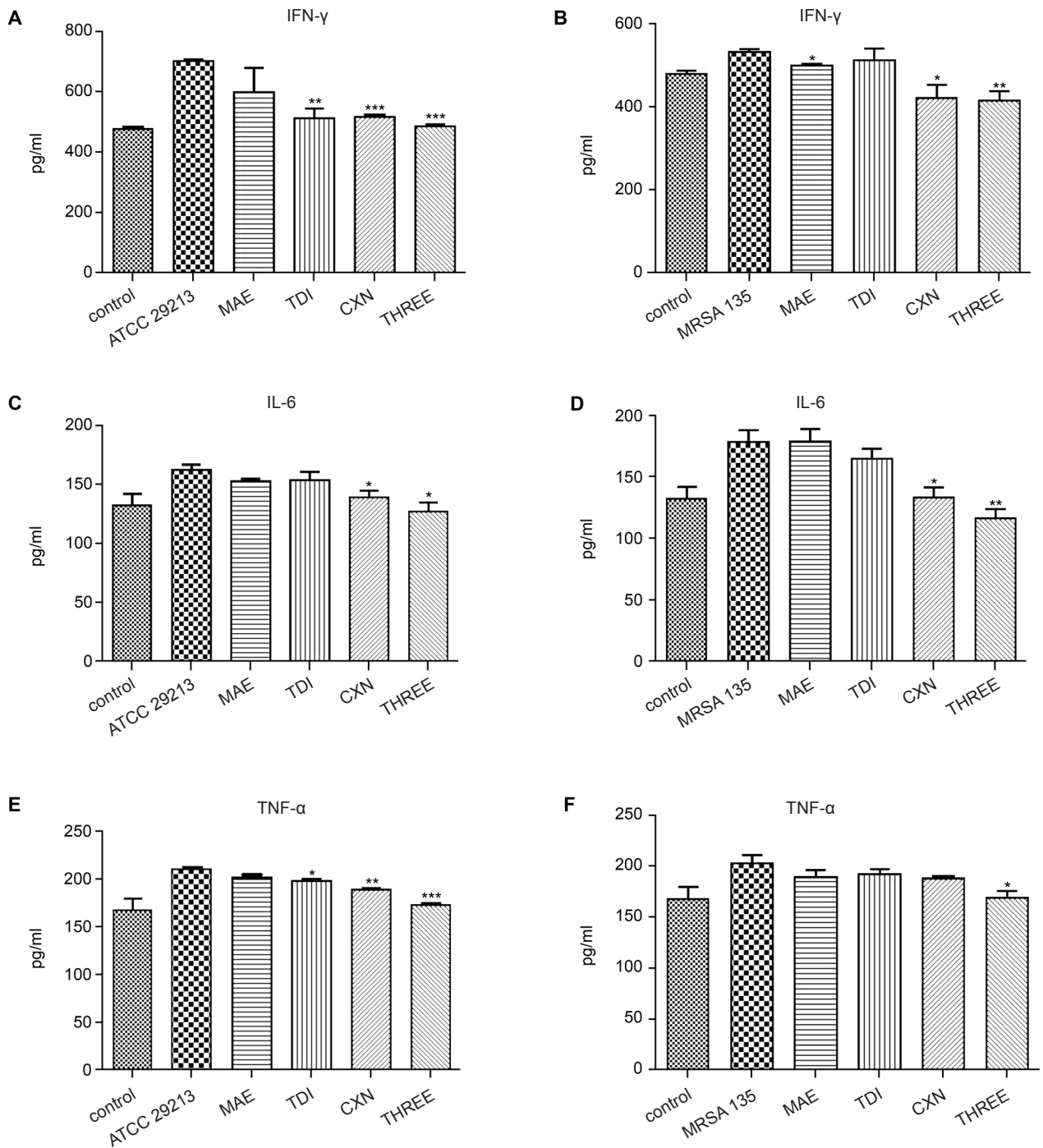


Fig. 4. Drug effects on the cytokine level in mouse mastitis models.

(A) Serum IFN- γ level in mice infected with ATCC 29213; (B) Serum IFN- γ level in mice infected with MRSA135; (C) Serum IL-6 level in mice infected with ATCC 29213; (D) Serum IL-6 level in mice infected with MRSA135; (E) Serum TNF- α level in mice infected with ATCC 29213; (F) Serum TNF- α level in mice infected with MRSA135; MCZ - miconazole; TZ - thioridazine; CXN - cloxacillin; MCZ + TZ + CXN - combination of miconazole, thioridazine, cloxacillin. The * on the horizontal line indicates a significant difference analysis between the CXN group and the three-drug group. * $P < 0.05$, ** $p < 0.01$, *** $p < 0.0001$.

treatment with a combination of TZ and CXN showed a stronger inhibitory effect against *S. aureus in vitro* when compared to the effect of CXN monotherapy. When TZ and CXN were used in combination, the MIC value was significantly reduced. In the checkerboard test, the FICI model is commonly used to determine

the synergy between anti-staphylococcal drugs. Moreover, the *in vivo* dosage of the administered combination compound was determined by the ratio of *in vitro* synergistic combination of the MIC values, the single *in vivo* doses administered in mouse studies or calculated from the other animal studies already reported.

In *S. aureus*-induced mouse mastitis, cytokines released by immune cells can aggravate the inflammatory response of mastitis (De and Mukherjee 2009). It has been suggested that TNF- α , IL-1 β , and IL-6 may play an important role in the mechanism of milk rupture (Persson et al. 2003). *In vivo* treatment of *S. aureus*-induced mouse mastitis showed that CXN monotherapy inhibited inflammation and resolved the redness of mouse mammary glands. The inflammatory response was lower in both the MCZ-treated and TZ-treated groups compared with the CXN-treated group. Redness of mammary glands was alleviated in the three-drug treatment group, and there were fewer inflammatory cells in the tissue section than in the other groups. In the pathological changes, it was shown that in both mice groups infected with the bacteria, most of the pathological changes were milder in the group treated with the combination of the three drugs than the CXN-treated group. Our results showed that the combination of three drugs could significantly inhibit the expression of TNF- α , IFN- γ , and IL-6, both *in vitro* and *in vivo*. Cytokine assays in mice sera revealed that CXN alone induced IL-6, IFN- γ , and TNF- α in the ATCC 29213-infected mouse groups, and the combination of the three drugs significantly reduced IL-6, IFN- γ , and TNF- α concentrations. The levels of TNF- α and IFN- γ in the sera of mice treated with three drugs simultaneously were significantly lower than those in the CXN-treated group. In the MRSA135-infected mouse group, CXN alone significantly reduced IL-6 and IFN- γ levels but did not significantly reduce the level of TNF- α . The combination of the three drugs significantly reduced IL-6, IFN- γ , and TNF- α concentrations. The level of TNF- α in the sera of mice treated with three drugs simultaneously was significantly lower than those in the CXN-treated group. Therefore, the results demonstrated that the combined use of the three drugs has a significant therapeutic effect on mastitis in mice infected with *S. aureus*, which may be due to the inhibition of the production of inflammatory cytokines by these three drugs applied together.

Conclusions

In our study, we investigated the effects of TZ, MCZ, and CXN on *S. aureus*, as well as the antibacterial effect of the combination of the three drugs, both *in vitro* and *in vivo*. We found that a bacterial efflux pump inhibitor and an autolysis inducer could be used in combination to inactivate the drug resistance of *S. aureus*, thus enhancing the efficacy of the antibiotic CXN. To enhance our resources against the bacterial attack, the research on gene expression effects after the combination therapy should be explored in further studies.

List of abbreviations

MRSA (methicillin-resistant *S. aureus*);
TZ (thioridazine);
MCZ (miconazole);
CXN (cloxacillin);
MIC (the minimum inhibitory concentration);
TNF- α (tumor necrosis factor- α);
IL-1 β (interleukin 1 β);
IL-6 (interleukin 6); I κ B (K-B inhibitor);
NF-KB (nuclear factor K-B);
CTCC (the China Type Culture Collection);
ATCC (American Type Culture Collection);
FIC (the fractional inhibitory concentration).

Authors' contributions

Participated in research design: L. Yu.
Conducted experiments: W. Luan, X. Wang.
Mice model construction: H. Xu, C. Wang.
Performed data analysis: Y. An, S. Li.
Figures making: Y. Wang, K. Shen.
Wrote or contributed to the writing of the manuscript: L. Yu, X. Liu.
Guide all the aspects of the study: M. Liu, L. Yu.

Ethics approval and consent to participate

Mice were housed in miniature isolation cages and were free to receive food and water. The laboratory temperature is $24 \pm 1^\circ\text{C}$ and the relative humidity is 40–80%. All animal studies were conducted in accordance with experimental practices and standards approved by the Animal Welfare and Research Ethics Committee of Jilin University (No. IZ-2009-008). *In vivo* studies in mice were performed under isoflurane anesthesia and every effort was made to meet animal welfare requirements.

Funding

This work was supported by the National Key R&D Program of China (2016YFD0501302, 2017YFD0502200); the National Nature Science Foundation of China (No. 81801972, 31172364); the Fund for Science & Technology Development of Jilin Province (20150101108JC); the Important National Science and Technology Specific Projects (2012ZX10003002); the Program for New Century Excellent Talents in University (NCET-09-0434); the Project of the Education Department of Jilin Province (No. 2016444); the Science, Technology and Innovation Commission of Shenzhen Municipality (No. JCYJ2016031100720906, JSGG20160301100442775).

Thanks to all teachers and students of the Institute of Zoonosis for their help in this experiment. Thanks to Xinrui Wang and Yi Xin for the support of this experiment.

Conflict of interest

The authors do not report any financial or personal connections with other persons or organizations, which might negatively affect the contents of this publication and/or claim authorship rights to this publication.

Literature

Anand KB, Agrawal P, Kumar S, Kapila K. Comparison of cefoxitin disc diffusion test, oxacillin screen agar, and PCR for *mecA* gene for detection of MRSA. *Indian J Med Microbiol.* 2009 Jan-Mar; 27(1):27–29.

- Boucher HW, Talbot GH, Bradley JS, Edwards JE, Gilbert D, Rice LB, Scheld M, Spellberg B, Bartlett J. Bad bugs, no drugs: no ESCAPE! An update from the Infectious Diseases Society of America. *Clin Infect Dis*. 2009 Jan;48(1):1–12. <https://doi.org/10.1086/595011>
- Bresler ML, Felipe V, Bohl LP, Orellano MS, Isaac P, Conesa A, Rivero VE, Correa SG, Bianco ID, Porporatto C. Chitosan and cloxacillin combination improve antibiotic efficacy against different lifestyle of coagulase-negative *Staphylococcus* isolates from chronic bovine mastitis. *Sci Rep*. 2018 Dec;8(1):5081. <https://doi.org/10.1038/s41598-018-23521-0>
- Celenza G, Segatore B, Setacci D, Bellio P, Brisdelli F, Piovano M, Garbarino JA, Nicoletti M, Perilli M, Amicosante G. *In vitro* antimicrobial activity of pannarin alone and in combination with antibiotics against methicillin-resistant *Staphylococcus aureus* clinical isolates. *Phytomedicine*. 2012 May;19(7):596–602. <https://doi.org/10.1016/j.phymed.2012.02.010>
- Chen K, Huang Y, Song Q, Wu C, Chen X, Zeng L. Drug-resistance dynamics of *Staphylococcus aureus* between 2008 and 2014 at a tertiary teaching hospital, Jiangxi Province, China. *BMC Infect Dis*. 2017 Dec;17(1):97. <https://doi.org/10.1186/s12879-016-2172-0>
- Choi JY, Kim CH, Jeon TJ, Kim BS, Yi CH, Woo KS, Seo YB, Han SJ, Kim KM, Yi DI, et al. Effective MicroPET imaging of brain 5-HT_{1A} receptors in rats with [¹⁸F]MeFWAY by suppression of radioligand defluorination. *Synapse*. 2012 Dec;66(12):1015–1023. <https://doi.org/10.1002/syn.21607>
- De UK, Mukherjee R. Expression of cytokines and respiratory burst activity of milk cells in response to *Azadirachta indica* during bovine mastitis. *Trop Anim Health Prod*. 2009 Feb;41(2):189–197. <https://doi.org/10.1007/s11250-008-9174-x>
- Demon D, Ludwig C, Breyné K, Guédé D, Dörner JC, Froyman R, Meyer E. The intramammary efficacy of first generation cephalosporins against *Staphylococcus aureus* mastitis in mice. *Vet Microbiol*. 2012 Nov;160(1-2):141–150. <https://doi.org/10.1016/j.vetmic.2012.05.017>
- Dickey SW, Cheung GYC, Otto M. Different drugs for bad bugs: antivirulence strategies in the age of antibiotic resistance. *Nat Rev Drug Discov*. 2017 Jul;16(7):457–471. <https://doi.org/10.1038/nrd.2017.23>
- Elazar S, Gonen E, Livneh-Kol A, Rosenshine I, Shpigel NY. Neutrophil recruitment in endotoxin-induced murine mastitis is strictly dependent on mammary alveolar macrophages. *Vet Res*. 2010 Jan;41(1):10. <https://doi.org/10.1051/vetres/2009058>
- Falk SP, Noah JW, Weisblum B. Screen for inducers of autolysis in *Bacillus subtilis*. *Antimicrob Agents Chemother*. 2010 Sep 01;54(9):3723–3729. <https://doi.org/10.1128/AAC.01597-09>
- Foster TJ. Antibiotic resistance in *Staphylococcus aureus*. Current status and future prospects. *FEMS Microbiol Rev*. 2017 May 01;41(3):430–449. <https://doi.org/10.1093/femsre/fux007>
- Fu Y, Zhou E, Wei Z, Liang D, Wang W, Wang T, Guo M, Zhang N, Yang Z. Glycyrrhizin inhibits the inflammatory response in mouse mammary epithelial cells and a mouse mastitis model. *FEBS J*. 2014 Jun;281(11):2543–2557. <https://doi.org/10.1111/febs.12801>
- Gao X, Wang T, Zhang Z, Cao Y, Zhang N, Guo M. Brazilin plays an anti-inflammatory role with regulating Toll-like receptor 2 and TLR 2 downstream pathways in *Staphylococcus aureus*-induced mastitis in mice. *Int Immunopharmacol*. 2015 Jul;27(1):130–137. <https://doi.org/10.1016/j.intimp.2015.04.043>
- Goering RV, Swartzendruber EA, Obradovich AE, Tickler IA, Tenover FC. Stealth MRSA: emergence of resistance in oxacillin-susceptible MRSA due to mecA sequence instability. *Antimicrob Agents Chemother*. 2019;68(3):e00558-19.
- Hendricks O, Butterworth TS, Kristiansen JE. The *in vitro* antimicrobial effect of non-antibiotics and putative inhibitors of efflux pumps on *Pseudomonas aeruginosa* and *Staphylococcus aureus*. *Int J Antimicrob Agents*. 2003 Sep;22(3):262–264. [https://doi.org/10.1016/S0924-8579\(03\)00205-X](https://doi.org/10.1016/S0924-8579(03)00205-X)
- Hu C, Gong R, Guo A, Chen H. Protective effect of ligand-binding domain of fibronectin-binding protein on mastitis induced by *Staphylococcus aureus* in mice. *Vaccine*. 2010 May;28(24):4038–4044. <https://doi.org/10.1016/j.vaccine.2010.04.017>
- Hu FP, Guo Y, Zhu DM, Wang F, Jiang XF, Xu YC, Zhang XJ, Zhang CX, Ji P, Xie Y, et al. Resistance trends among clinical isolates in China reported from CHINET surveillance of bacterial resistance, 2005–2014. *Clin Microbiol Infect*. 2016 Mar;22 Suppl 1:S9–S14. <https://doi.org/10.1016/j.cmi.2016.01.001>
- Hwang I, Hwang JS, Hwang JH, Choi H, Lee E, Kim Y, Lee DG. Synergistic effect and antibiofilm activity between the antimicrobial peptide coprisin and conventional antibiotics against opportunistic bacteria. *Curr Microbiol*. 2013 Jan;66(1):56–60. <https://doi.org/10.1007/s00284-012-0239-8>
- Intrakamhaeng M, Komutarin T, Pimpukdee K, Aengwanich W. Incidence of enterotoxin-producing MRSA in bovine mastitis cases, bulk milk tanks and processing plants in Thailand. *J Anim Vet Adv*. 2012;11(5):87–93.
- Iwase T, Uehara Y, Shinji H, Tajima A, Seo H, Takada K, Agata T, Mizunoe Y. *Staphylococcus epidermidis* Esp inhibits *Staphylococcus aureus* biofilm formation and nasal colonization. *Nature*. 2010 May;465(7296):346–349. <https://doi.org/10.1038/nature09074>
- Kim YN, Kim DW, Jo HS, Shin MJ, Ahn EH, Ryu EJ, Yong JI, Cha HJ, Kim SJ, Yeo HJ, et al. Tat-CBR1 inhibits inflammatory responses through the suppressions of NF- κ B and MAPK activation in macrophages and TPA-induced ear edema in mice. *Toxicol Appl Pharmacol*. 2015 Jul;286(2):124–134. <https://doi.org/10.1016/j.taap.2015.03.020>
- Klitgaard JK, Skov MN, Kallipolitis BH, Kolmos HJ. Reversal of methicillin resistance in *Staphylococcus aureus* by thioridazine. *J Antimicrob Chemother*. 2008 Sep 10;62(6):1215–1221. <https://doi.org/10.1093/jac/dkn417>
- Kolendi CL. Methicillin-resistant *Staphylococcus aureus* (MRSA): etiology, at-risk populations and treatment. New York (USA): Nova Science Publishers Inc.; 2010.
- Koszczol C, Bernardo K, Krönke M, Krut O. Subinhibitory quinupristin/dalfopristin attenuates virulence of *Staphylococcus aureus*. *J Antimicrob Chemother*. 2006 Jul 01;58(3):564–574. <https://doi.org/10.1093/jac/dkl291>
- Lowy FD. *Staphylococcus aureus* Infections. *N Engl J Med*. 1998 Aug 20;339(8):520–532. <https://doi.org/10.1056/NEJM199808203390806>
- Mascaretti OA. Bacteria versus antibacterial agents: an integrated approach. Washington, D.C. (USA): ASM Press; 2003.
- Moon JS, Kim HK, Koo HC, Joo YS, Nam H, Park YH, Kang MI. The antibacterial and immunostimulative effect of chitosan-oligosaccharides against infection by *Staphylococcus aureus* isolated from bovine mastitis. *Appl Microbiol Biotechnol*. 2007 Jun 13;75(5):989–998. <https://doi.org/10.1007/s00253-007-0898-8>
- Navon-Venezia S, Ben-Ami R, Carmeli Y. Update on *Pseudomonas aeruginosa* and *Acinetobacter baumannii* infections in the healthcare setting. *Curr Opin Infect Dis*. 2005 Aug;18(4):306–313. <https://doi.org/10.1097/01.qco.0000171920.44809.f0>
- Persson Waller K, Colditz IG, Lun S, Östensson K. Cytokines in mammary lymph and milk during endotoxin-induced bovine mastitis. *Res Vet Sci*. 2003 Feb;74(1):31–36. [https://doi.org/10.1016/S0034-5288\(02\)00147-9](https://doi.org/10.1016/S0034-5288(02)00147-9)
- Poulsen MØ, Jacobsen K, Thorsing M, Kristensen NRD, Clasen J, Lillebæk EMS, Skov MN, Kallipolitis BH, Kolmos HJ, Klitgaard JK. Thioridazine potentiates the effect of a beta-lactam antibiotic against *Staphylococcus aureus* independently of mecA expression. *Res Microbiol*. 2013 Feb;164(2):181–188. <https://doi.org/10.1016/j.resmic.2012.10.007>

- Pule CM, Sampson SL, Warren RM, Black PA, van Helden PD, Victor TC, Louw GE.** Efflux pump inhibitors: targeting mycobacterial efflux systems to enhance TB therapy. *J Antimicrob Chemother.* 2016 Jan;71(1):17–26. <https://doi.org/10.1093/jac/dkv316>
- Que YA, Haefliger JA, Piroth L, François P, Widmer E, Entenza JM, Sinha B, Herrmann M, Francioli P, Vaudaux P, et al.** Fibrinogen and fibronectin binding cooperate for valve infection and invasion in *Staphylococcus aureus* experimental endocarditis. *J Exp Med.* 2005 May 16;201(10):1627–1635. <https://doi.org/10.1084/jem.20050125>
- Rudilla H, Fusté E, Cajal Y, Rabanal F, Vinuesa T, Viñas M.** Synergistic antipseudomonal effects of synthetic peptide AMP38 and carbapenems. *Molecules.* 2016 Sep 12;21(9):1223–1234. <https://doi.org/10.3390/molecules21091223>
- Tegos G, Mylonakis E.** Antimicrobial drug discovery: emerging strategies. Wallingford (UK): CABI; 2012.
- Trigo G, Dinis M, França A, Bonifácio Andrade E, Gil da Costa RM, Ferreira P, Tavares D.** Leukocyte populations and cytokine expression in the mammary gland in a mouse model of *Streptococcus agalactiae* mastitis. *J Med Microbiol.* 2009 Jul 01;58(7):951–958. <https://doi.org/10.1099/jmm.0.007385-0>
- Tse BN, Adalja AA, Houchens C, Larsen J, Inglesby TV, Hatchett R.** Challenges and opportunities of nontraditional approaches to treating bacterial infections. *Clin Infect Dis.* 2017 Aug 01; 65(3): 495–500. <https://doi.org/10.1093/cid/cix320>
- Vermote A, Van Calenbergh S.** Small-molecule potentiators for conventional antibiotics against *Staphylococcus aureus*. *ACS Infect Dis.* 2017 Nov 10;3(11):780–796. <https://doi.org/10.1021/acsinfecdis.7b00084>
- Wax RG.** Bacterial resistance to antimicrobials. Boca Raton (USA): CRC Press; 2008.
- Wei W, Dejie L, Xiaojing S, Tiancheng W, Yongguo C, Zhengtao Y, Naisheng Z.** Magnolol inhibits the inflammatory response in mouse mammary epithelial cells and a mouse mastitis model. *Inflammation.* 2015 Feb;38(1):16–26. <https://doi.org/10.1007/s10753-014-0003-2>
- Zhang JM, An J.** Cytokines, inflammation, and pain. *Int Anesthesiol Clin.* 2007 1;45(2):27–37. <https://doi.org/10.1097/AIA.0b013e318034194e>
- Zore GB, Thakre AD, Jadhav S, Karuppayil SM.** Terpenoids inhibit *Candida albicans* growth by affecting membrane integrity and arrest of cell cycle. *Phytomedicine.* 2011 Oct;18(13):1181–1190. <https://doi.org/10.1016/j.phymed.2011.03.008>

Diversity, Virulence Factors, and Antifungal Susceptibility Patterns of Pathogenic and Opportunistic Yeast Species in Rock Pigeon (*Columba livia*) Fecal Droppings in Western Saudi Arabia

HUSSEIN H. ABULREESH^{1,2*}, SAMEER R. ORGANJI^{1,2}, KHALED ELBANNA^{1,2,3},
GAMAL E.H. OSMAN^{1,2,4}, MESHAL H.K. ALMALKI^{1,2}, AHMED Y. ABDEL-MALEK⁵,
ABDULLAH A.K. GHYATHUDDIN^{6,7} and IQBAL AHMAD⁸

¹Department of Biology, Faculty of Applied Science, Umm Al-Qura University, Makkah, Saudi Arabia

²Research Laboratories Center, Faculty of Applied Science, Umm Al-Qura University, Makkah, Saudi Arabia

³Department of Agricultural Microbiology, Faculty of Agriculture, Fayoum University, Fayoum, Egypt

⁴Microbial Genetics Department, Agricultural Genetic Engineering Research Institute (AGERI), Giza, Egypt

⁵Botany and Microbiology Department, Faculty of Science, Assiut University, Assiut, Egypt

⁶Fakieh Poultry Farms, Makkah, Saudi Arabia

⁷Department of Biological Sciences, King Abdulaziz University, Jeddah, Saudi Arabia

⁸Department of Agricultural Microbiology, Faculty of Agricultural Sciences, Aligarh Muslim University, Aligarh, India

Submitted 19 June 2019, revised 28 September 2019, accepted 29 September 2019

Abstract

Bird fecal matter is considered a potential source of pathogenic microbes such as yeast species that contaminate the environment. Therefore, it needs to be scrutinized to assess potential environmental health risks. The aim of this study was to investigate the diversity of the yeasts in pigeon fecal droppings, their antifungal susceptibility patterns, and virulence factors. We used culturing techniques to detect the yeasts in pigeon fecal droppings. The isolates were then characterized based on colony morphologies, microscopic examinations, and biochemical reactions. The molecular identification of all yeast isolates was performed by sequencing of the amplified ITS gene. Genes encoding virulence factors *CAP1*, *CAP59*, and *PLB* were also detected. Antifungal susceptibility patterns were examined by the disk diffusion method. A total of 46 yeast-like isolates were recovered, and they belonged to nine different genera, namely, *Cryptococcus*, *Saccharomyces*, *Rhodotorula*, *Candida*, *Meyerozyma*, *Cyberlindnera*, *Rhodospiridium*, *Millerozyma*, and *Lodderomyces*. The prevalence of two genera *Cryptococcus* and *Rhodotorula* was high. None of the yeast isolates exhibited any resistance to the antifungal drugs tested; however, all pathogenic *Cryptococcus* species were positive for virulence determinants like urease activity, growth at 37°C, melanin production, the *PLB* and *CAP* genes. This is the first report on the molecular diversity of yeast species, particularly, *Cryptococcus* species and their virulence attributes in pigeon fecal droppings in Saudi Arabia.

Key words: *Cryptococcus*, pigeon, fecal droppings, antifungal susceptibility, virulence genes, yeast

Introduction

Free-living wild birds are regarded as one of the indicators of a healthy environment. However, they also may be regarded as potential carriers of human-pathogenic viral, bacterial, fungal, and protozoan agents. Free-living rock pigeons (*Columba livia*), are found in large flocks within major cities around the world. They live in close proximity to humans, particularly in public parks, on rooftops, and sometimes close to catering

establishments. Numerous reports highlight that pigeon fecal droppings in public areas are a source of bacterial infectious agents, such as *Salmonella*, *Campylobacter*, and *E. coli* O157, and that they may significantly affect public health (Abulreesh et al. 2007; Abulreesh 2014).

Carriage of pathogenic yeast in pigeon feces is a matter of growing interest and has been investigated worldwide, with much focus on the *Cryptococcus* species. Wu et al. (2012) reported the presence of eight different genera of yeast, such as *Cryptococcus*, *Candida*,

* Corresponding author: H.H. Abulreesh, Department of Biology, Faculty of Applied Science, Umm Al-Qura University, Makkah, Saudi Arabia; e-mail: hhabulreesh@uqu.edu.sa

© 2019 Hussein H. Abulreesh et al.

This work is licensed under the Creative Commons Attribution-NonCommercial-NoDerivatives 4.0 License (<https://creativecommons.org/licenses/by-nc-nd/4.0/>).

and *Rhodotorula*, in pigeon fecal droppings in Beijing, China. They concluded that pigeon feces are a vector for medically important yeast species. Similarly, in Brazil, Costa et al. (2010) reported the predominance of *Cryptococcus*, *Candida*, and *Rhodotorula* species in pigeon feces. Other reports from Egypt (Mahmoud 1999), the Canary Islands (Rosario et al. 2010), India (Xavier et al. 2013), and Sweden (Mattsson et al. 1999) highlighted the diversity of *Cryptococcus* species found in pigeon fecal droppings and the role of domestic pigeons as potential source of environmental pathogenic yeast. Soltani et al. (2013) even suggested a direct link between pathogenic yeast flora in pigeon feces and human infections.

The genus *Cryptococcus* is a basidiomycete yeast belonging to the *Tremellales* class. The genus *Cryptococcus* consists of two species complexes: *C. neoformans* species complex (comprise of two species: *C. neoformans* and *C. deneofirmans*), and *C. gattii* species complex (comprises of five species: *C. gattii*; *C. tetragattii*; *C. decagattii*; *C. deutero-gattii* and *C. bacillisporus*); these species are known for their potential clinical significance. *C. neoformans* species complex is responsible for cryptococcosis in humans, an infection that affects the lungs, the brain, and spinal cord (central nervous system) that usually affect HIV patients and other immunocompromised individuals, while *C. gattii* species complex causes serious infections and immunocompetent as well immunocompromised individuals. These species are commonly found in the excreta of wild birds, particularly pigeons, as well as soil, rotting vegetables, wood, and associated with certain species of plants. Cryptococcosis is not a contagious disease, however, it is acquired from environmental exposure to *Cryptococcus* species. Recent epidemiological data suggest that there are around 220 000 annual cases of cryptococcal meningitis in HIV patients worldwide. Therefore, cryptococcal meningitis may be the leading cause of death among HIV patients (Cogliati 2013; Hagen et al. 2015; Rajasingham et al. 2017; Esher et al. 2018; Magalhães Pinto et al. 2019).

Molecular identification tools such as real-time PCR, multiplex PCR, and RFLP PCR have been successful in detecting and identifying various yeast species in clinical and environmental samples. Furthermore, the identification of yeast-based on fungal ribosomal DNA (rDNA) has become popular as an accurate molecular tool. This tool allows for the detection of 18S and 26S subunits of rDNA that are separated by the internal transcribed spacers ITS1 and ITS2 (Pincus et al. 2007).

The city of Makkah is a major attraction for people around the world visiting for religious and spiritual purposes. Hence, the study of biological contamination of the environment by pigeons may be of great significance from a public health perspective. Very little information exists regarding the diversity and charac-

terization of yeast species found in pigeon fecal droppings in Saudi Arabia, and particularly in Makkah city. The only available report describing the presence of *C. neoformans* in pigeon fecal droppings relied upon the phenotypical characterization of the isolates (Abulreesh et al. 2015). It did not involve the molecular identification of those isolates. The current study is, therefore, the first to report on the molecular diversity of yeast genera and their antifungal susceptibility patterns in pigeon feces within the city of Makkah, western Saudi Arabia. The paper also describes for the first time, the carriage of different genes encoding virulence factors among *Cryptococcus* and other yeast species found in pigeon feces in western Saudi Arabia.

Experimental

Materials and Methods

Sampling. A total of 100 samples of dried pigeon fecal droppings were collected from various locations within the city of Makkah, western Saudi Arabia, between May and November 2018. Each fecal sample was collected in a sterile universal bottle, protected from direct sunlight and transported to the laboratory on ice. All samples were processed within 6 h of collection.

Yeast isolation. Yeast species were isolated from pigeon fecal dropping following the methodology previously described by Abulreesh et al. (2015). First, 10 g of fecal droppings from each location was aseptically transferred to a flask containing 0.9 % saline solution with chloramphenicol ($200 \mu\text{g l}^{-1}$). Then the mixture was shaken for 20 min and allowed to settle for 30 min. An aliquot of 0.5 ml of each supernatant was streaked onto Sabouraud dextrose agar (SDA) (Oxoid, Basingstoke, UK). Plates were incubated at 25°C and were examined daily for ten days to observe the growth of yeast. Individual colonies with the mucous appearance and yeast-like colonial morphology were selected and subcultured on SDA to obtain pure cultures.

Yeast identification. The selected colonies were microscopically examined for typical yeast cell morphology, pseudomycelium (specific for *Candida* spp.), and capsule in Indian ink preparations (in the case of *Cryptococcus* spp.). Biochemical identification for all yeast isolates included carbohydrate and nitrate assimilation (Teodoro et al. 2013), urease reaction on, urea agar base (Christensen's medium) (Oxoid, Basingstoke, UK) (Canteros et al. 1996), production of melanin on esculin agar (Oxoid), and ability to grow at 37°C on SDA (Abulreesh et al. 2015).

Molecular identification. All yeast isolates were identified at a molecular level by the detection of the internal transcribed spacer (ITS) regions. The ITS1-

5.8S-ITS2 fragment was amplified using universal primers ITS1 (TCC GTA GGT GAA CCT GCG G) and ITS4 (TCC TCC GCT TAT TGA TAT GC) (White et al. 1990). Total DNA was extracted from colonies using the DNeasy Plant Mini kit (QIAGEN, Hilden, Germany), according to the manufacturer's procedure. Amplification was performed in 50 µl reaction volume, containing 5.0 µl 10× PCR Buffer, 4 µl dNTP, 0.5 µl *rTaq*, 1.0 µl ITS1 and ITS4, 3.0 µl genomic DNA, and 35.5 µl distilled water. The PCR protocol comprised of initial denaturation at 94°C for 5 min, followed by 35 cycles of 95°C for 1 min, annealing at 50°C for 1 min, and extension at 72°C for 1 min, followed by a final extension at 72°C for 10 min. The PCR products were purified using a QIAquick PCR Purification Kit (QIAGEN) and sequenced in both directions using the amplification primers on an ABI3730 automated sequencer (Applied Biosystems, Foster City, CA, USA). BLASTN (<http://blast.ncbi.nlm.nih.gov>) was employed to confirm the identified strains (Wu et al. 2012).

Detection of virulence-encoding genes. The molecular detection of virulence-encoding genes, such as the capsular genes (*CAP1* and *CAP59*) specific for *Cryptococcus* spp. and the phospholipase gene (*PLB1*) was performed on yeast isolates previously identified by ITS sequencing. *CAP1* is a 700 bp long gene on chromosome IV and is a part of the *MAT* locus that encodes a capsule-synthesis associated protein. Primers used for *CAP1* were, 5'-CGTTCGCGATAGAGAGAGGA-3' (forward) and 5'-CCTTACCTTCACAGTCGCCC-3' (reverse). *CAP59* is a 502 bp long gene on chromosome I and encodes for a capsule-synthesis associated protein. Primers used for *CAP59* were, 5'-CTCTACGTCGAGC-AAGTCAAG-3' (forward) and 5'-TCCGCTGCACAAG-TGATACCC-3' (reverse). *PLB1* is an 853 bp long gene, present on chromosome XII, encoding a phospholipase B probably involved in cell invasion. Primers used for *PLB1* were, 5'-CTTCAGGCGGAGAGAGGTTT-3' (forward) and 5'-GATTTGGCGTTGGTTTCAGT-3' (reverse) (Chowdhary et al. 2011). Each PCR reaction mixture comprised of 2.0 µl (~1ng) of the template DNA, 8.0 µl of GoTaq (*Taq* DNA polymerase + MgCl₂ at a final concentration of 1.5 mM, supplied by Promega USA), 0.2 µM of each primer, and 5.8 µl of sterile distilled water to make up a total volume of 16 µl. The thermal cycling protocol included an initial denaturing step at 95°C for 4 min. This was followed by 40 cycles of denaturation at 95°C for 1 min, primer-specific annealing temperature for 1 min, and extension at 72°C for 1 min. The final step was the primer extension at 72°C for 7 min. Primer-specific annealing temperatures for amplifying the nine gene fragments were: 59.2°C for *CAP1*, 55°C for *CAP59*, and 56°C for *PLB1* (Chowdhary et al. 2011).

Antifungal susceptibility testing. To determine the antifungal susceptibility patterns, the agar disk

diffusion method was employed as described by CLSI (2008). Four antifungal agents were used to examine the susceptibility patterns of the yeast species recovered from pigeon feces: Ciclopirox-Olamine (50 µg); Clotrimazole (10 µg); Nystatin (100 IU) and Fluconazole (25 µg), disks were purchased from Liofilchem Inc. (Waltham, USA). Fresh culture of each of the identified species was inoculated using swabs on the surface of Muller Hinton agar (Oxoid), plates supplemented with 2.0% glucose. Plates were incubated for 36 h at the optimum temperature for each fungal species. The sensitivity of the species against the antifungal compounds was determined by measuring the diameter of inhibition zones. A diameter of ≥ 15 mm for nystatin and ≥ 20 mm for the three antifungal agents was considered as susceptible. Susceptibility breakpoints of antifungal drugs used in our study are not species related (CLSI 2008). *C. albicans* ATCC 90028 was used as control.

Results

Yeast diversity in pigeon feces. A total of 46 presumptive yeast isolates representing nine different genera, were recovered from pigeon fecal samples collected within the city of Makkah. Table I consolidates the phenotypic characterization and molecular identification of each isolate. *Cryptococcus* spp. accounted for 41.3% of all the isolates (19 isolates). There were four different species belonging to the genus *Cryptococcus*; *C. neoformans* (11 isolates); *C. albidus* (5 isolates), *C. gattii* (2 isolates), and *C. liquefaciens* (1 isolate) (Fig. 1 and 2). Surprisingly, *Candida* spp. were almost absent, with only one isolate (2.1%) identified to be *C. glabrata*, however, other *Candida*-related genera such as *Meyerozyma guilliermondii* (8.7%) were present. *Saccharomyces cerevisiae* made up 10.9% of the isolates recovered from pigeon feces (Fig. 1), *Lodderomyces elongisporus*, *Milleromyza farinosa*, and *Cyberlindnera fabianii* were also present at an abundance of 4.34%, 6.5%, and 6.5%, respectively (Fig. 1). Two species belonging to *Rhodotorula*, *R. glutinis* (4.34%) and *R. mucilaginosa* (10.9 %) as well as *Rhodospiridium plaudigenum* (4.34 %) were identified in the pigeon fecal samples (Table I, Fig. 1).

Detection of virulence factors. The virulence factors were detected using (i) conventional methods, such as urease activity, and melanin production, and (ii) molecular methods probing for capsular (*CAP1* and *CAP59*) and phospholipase (*PLB1*) genes.

Table I exhibits the urease activity and melanin production of all isolates. Urease activity was observed in all the four isolated *Cryptococcus* species. *R. glutinis* and *R. plaudigenum* were the only non-*Cryptococcus* species that showed positive activity for urease. Melanin production was only observed in all *Cryptococcus* species.

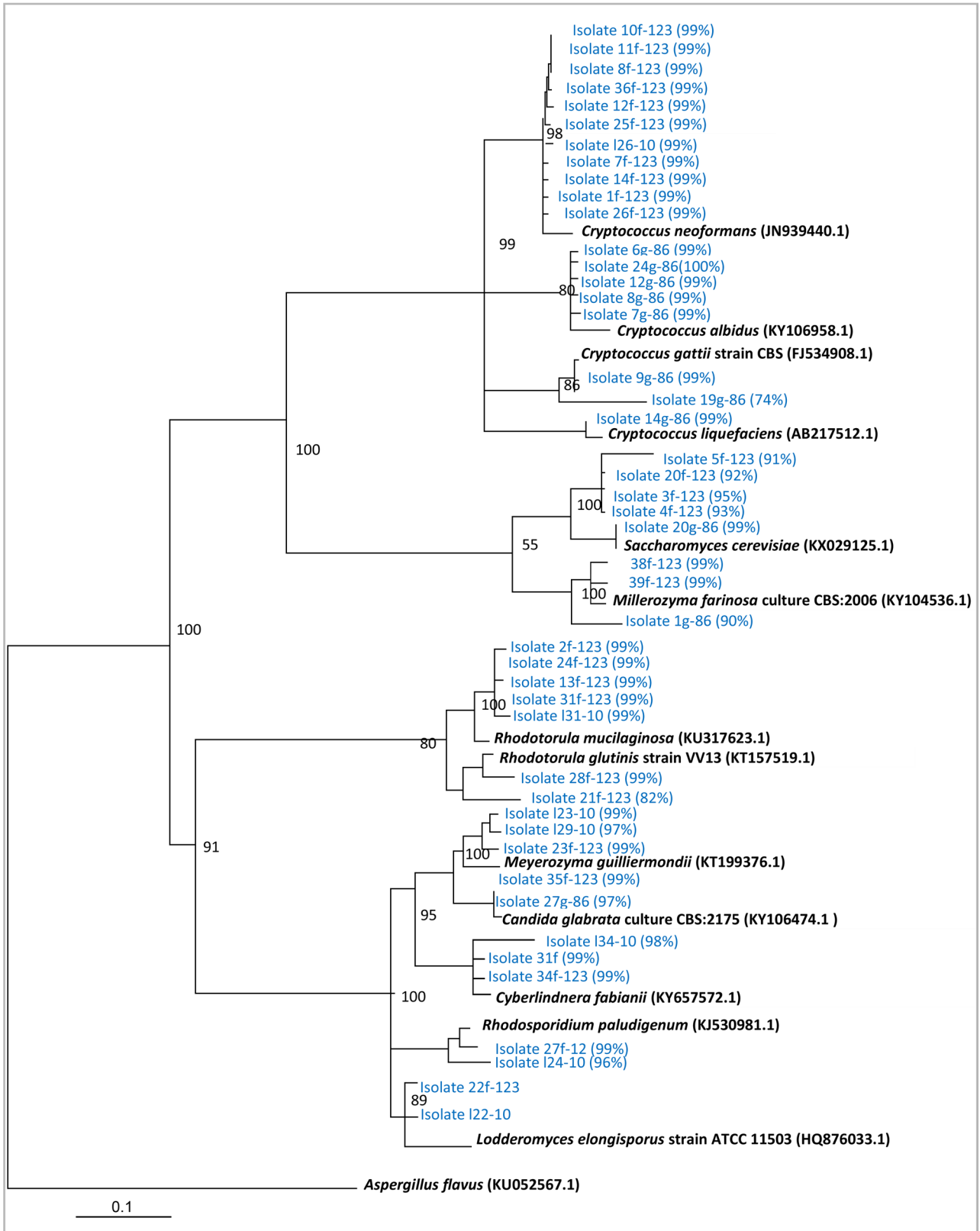


Fig. 1. Neighbor-joining tree showing the estimated phylogenetic relationship of the all fungi and yeasts strains (shown in blue) and other closely related strains. Bootstrap values out of 100 are given at the nodes based on the sequence of ITS region (amplify the ITS1-5.8S-ITS2 fragment). *Aspergillus flavus* (KU052567.1) was used as out group.

Table II shows the presence and absence of the *CAP1*, *CAP59* and *PLB1* genes for all isolates. The *CAP1* gene was detected in six of 11 *Cryptococcus neo-*

formans isolates, while the *CAP59* gene was detected in the other five isolates. Two isolates of *C. gattii* also possessed the *CAP59* gene (Fig. 3). The *PLB1* gene

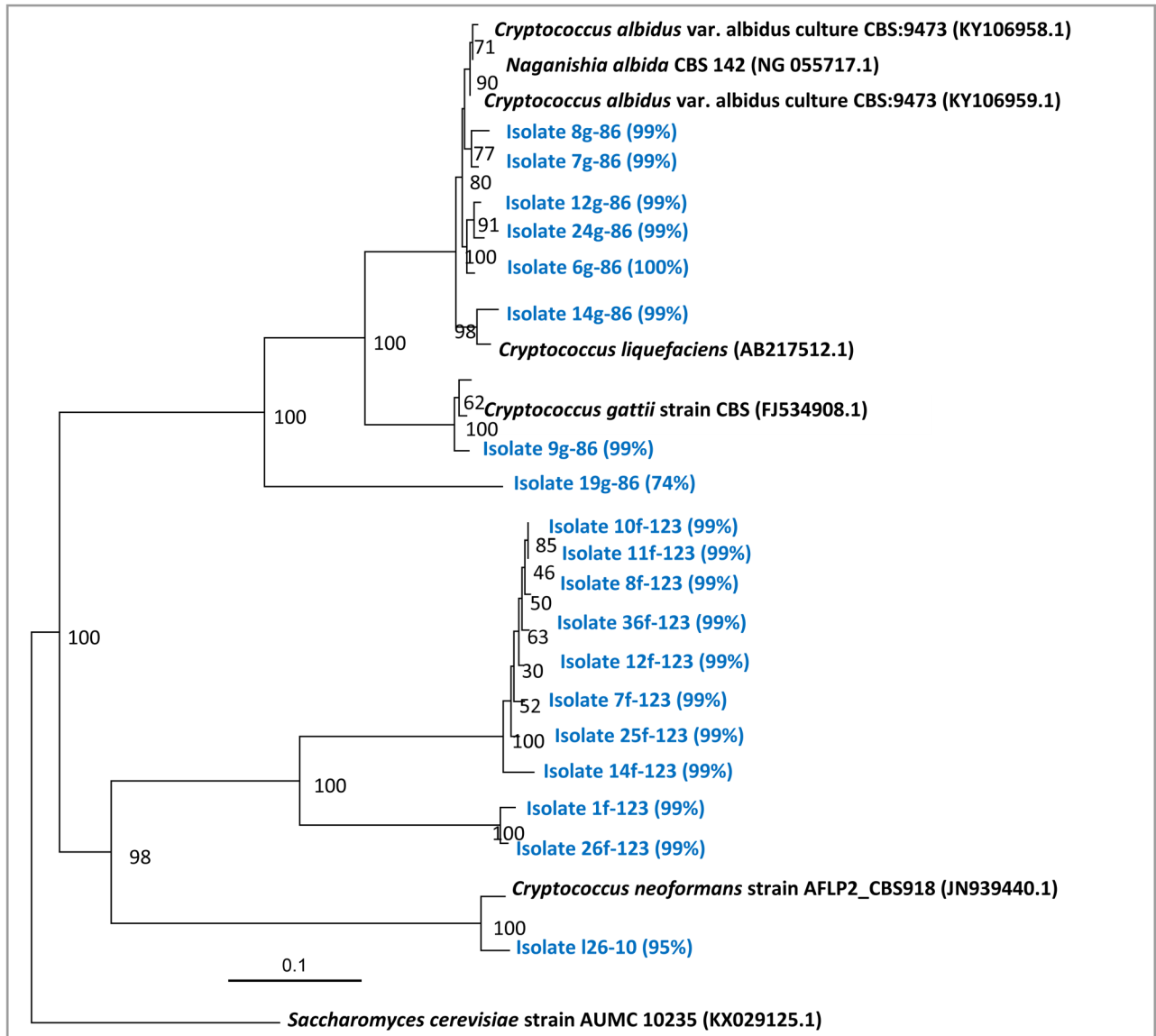


Fig. 2. Neighbor-joining tree showing the estimated phylogenetic relationship of the *Cryptococcus* strains (shown in blue) and other closely related strains. Bootstrap values out of 100 are given at the nodes, based on the sequence of ITS region (amplify the ITS1-5.8S-ITS2 fragment). *Saccharomyces cerevisiae* strain AUMC 10235 (KX029125.1) as out group

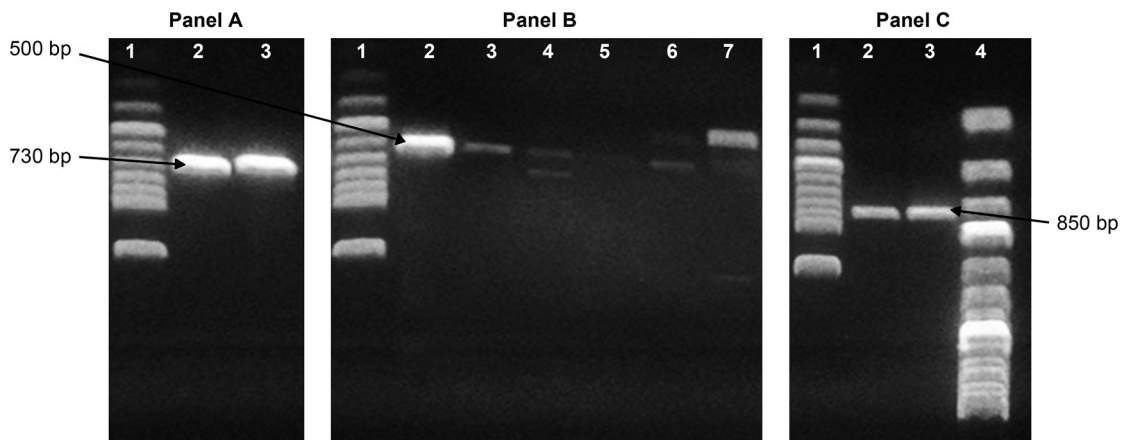


Fig. 3. Ethidium bromide stained agarose gel electrophoresis resolving the PCR Screening amplification fragments for the presence of CAP1 panel A lanes: 2 (Y33), 3 (Y38) (~730 bp), CAP59 panel B lanes 2 (Y1), 3 (Y3), 4 (Y21), 5 (Y5), 6 (Y20) and 7 (Y9) (~520 bp) and PLB1 Panel C lanes: 2 (Y44) and 3 (Y46) (~853 bp). Lane 1: 100 bp marker and lane 4 panel C: 1 Kbp ladder. Y1, Y5, Y9, Y20, Y33, Y38, Y46 = *Cryptococcus neoformans* Y44 = *Saccharomyces cerevisiae* Y3, Y21 = *Cryptococcus gattii*

Table I
Molecular identification and phenotypal traits of yeast isolates in pigeon feces.

Yeast isolates ITS ID	Number of isolates	Phenotypic traits								
		Nit*	Melanin	Urease	Pseudomy*	Capsule	Glu*†	Lact*†	Sucr*†	37°C‡
<i>Cryptococcus neoformans</i>	11	-	+	+	-	+	+	-	+	+
<i>Cryptococcus albidus</i>	5	+	+	+	-	+	+	+	+	+
<i>Cryptococcus gattii</i>	2	-	+	+	-	+	+	-	+	+
<i>Cryptococcus liquefaciens</i>	1	+	+	+	-	+	+	+	+	-
<i>Saccharomyces cerevisiae</i>	5	-	-	-	-	-	+	-	+	-
<i>Millerozyma farinosa</i>	3	-	-	-	-	-	+	+	-	+
<i>Rhodotorula mucilaginosa</i>	5	-	-	+	-	+	+	-	+	-
<i>Rhodotorula glutinis</i>	2	-	-	+	-	+	-	-	-	+
<i>Meyerozyma guilliermondii</i>	4	-	-	-	+	-	+	-	+	-
<i>Candida glabrata</i>	1	-	-	-	-	-	+	-	-	+
<i>Cyberlindnera fabianii</i>	3	+	-	-	-	-	+	-	+	+
<i>Rhodosporidium paludigenum</i>	2	+	-	+	-	-	+	-	+	-
<i>Lodderomyces elongisporus</i>	2	-	-	-	+	-	+	+	-	+

Nit* – nitrate reduction, Glu* – Glucose, Lact* – Lactose, Sucr* – Sucrose, Pseudomy* – Pseudomycelium,
Glu†, Lact†, Sucr† – assimilation
‡ – ability to grow at 37°C

Table II
Detection of virulence factors-encoding genes in yeast species isolated from pigeon feces.

Yeast isolates ITS ID	Total number of isolates	Virulence factors-encoding genes		
		<i>CAP1</i>	<i>CAP59</i>	<i>PLB</i>
<i>Cryptococcus neoformans</i>	11	6	5	11
<i>Cryptococcus albidus</i>	5	-	-	5
<i>Cryptococcus gattii</i>	2	-	2	2
<i>Cryptococcus liquefaciens</i>	1	-	-	-
<i>Saccharomyces cerevisiae</i>	5	ND	ND	5
<i>Millerozyma farinosa</i>	3	ND	ND	-
<i>Rhodotorula mucilaginosa</i>	5	ND	ND	-
<i>Rhodotorula glutinis</i>	2	ND	ND	-
<i>Meyerozyma guilliermondii</i>	4	ND	ND	-
<i>Candida glabrata</i>	1	ND	ND	1
<i>Cyberlindnera fabianii</i>	3	ND	ND	-
<i>Rhodosporidium paludigenum</i>	2	ND	ND	-
<i>Lodderomyces elongisporus</i>	2	ND	ND	-

ND – not determined

was detected in three *Cryptococcus* species, *C. neoformans*; *C. albidus*, and *C. gattii* but not in *C. liquefaciens*. *C. glabrata* and *S. cerevisiae* were also positive for the *PLB1* gene (Fig. 3).

Antifungal susceptibility patterns. None of the 46 yeast isolates showed resistance to any of the antifungal drugs, i.e., Ciclopirox-Olamine; Clotrimazole; Fluconazole and Nystatin used in this study (Table III).

Discussion

The presence of yeast species, especially the pathogenic ones, in pigeon fecal droppings and the role of pigeons in the dissemination and epidemiology of these pathogenic species have been investigated worldwide. However, in Saudi Arabia, there is a dearth of information regarding the environmental diversity of yeast,

Table III
Antifungal susceptibility patterns of yeast species isolated from pigeon feces (diameter zone, mm).

Yeast species	Number of isolates	Antifungal agents (A)‡			
		Ciclopirox-Olamine	Clotrimazole	Fluconazole	Nystatin
<i>Cryptococcus neoformans</i>	11	29 (S)	41 (S)	51 (S)	22 (S)
<i>Cryptococcus albidus</i>	5	33 (S)	46 (S)	51 (S)	22 (S)
<i>Cryptococcus gattii</i>	2	31 (S)	46 (S)	51 (S)	28 (S)
<i>Cryptococcus liquefaciens</i>	1	28 (S)	50 (S)	56 (S)	25 (S)
<i>Saccharomyces cerevisiae</i>	5	54 (S)	55 (S)	60 (S)	35 (S)
<i>Millerozyma farinosa</i>	3	41 (S)	45.3 (S)	57 (S)	25 (S)
<i>Rhodotorula mucilaginosa</i>	5	42 (S)	51 (S)	60 (S)	35 (S)
<i>Rhodotorula glutinis</i>	2	58 (S)	60 (S)	56 (S)	40 (S)
<i>Meyerozyma guilliermondii</i>	4	56 (S)	57.3 (S)	53 (S)	48 (S)
<i>Candida glabrata</i>	1	33 (S)	38 (S)	48 (S)	22 (S)
<i>Cyberlindnera fabianii</i>	3	47 (S)	45 (S)	65 (S)	51 (S)
<i>Rhodosporidium paludigenum</i>	2	53 (S)	50 (S)	60 (S)	44 (S)
<i>Lodderomyces elongisporus</i>	2	51 (S)	51 (S)	58 (S)	35 (S)
<i>Candida albicans</i> ATCC 90028	1	27 (S)	30 (S)	39 (S)	22 (S)

S – Susceptible

A‡ – Average inhibition zone reading of all isolates

including the pathogenic species. Abulreesh et al. (2015) were the first to report about *C. neoformans* in pigeon fecal droppings in Saudi Arabia. Their report was based on phenotypical identification of the presumptive isolates, and no molecular identification was performed to confirm the results. The aim of this work was to further investigate the diversity of *Cryptococcus* and other yeast species in pigeon excreta, in addition to their virulence factors and antifungal susceptibility patterns.

Diversity of yeast species in pigeon feces. In this study, nine different genera of yeast were found in pigeon fecal droppings, in comparison to other studies conducted elsewhere, the current study has identified the most diverse yeast species ever reported. For example, Wu et al. (2012) reported six different yeast species in pigeon feces from various locations in Beijing, China. In our study, we reported *C. neoformans*, *C. albidus*, and *C. gattii*, with *C. neoformans* being the most prevalent than other species. These species have frequently been associated with pigeon fecal droppings in Brazil (Costa et al. 2010), China (Wu et al. 2012), the Canary Islands (Rosario et al. 2010), Iran (Hashemi et al. 2014), Thailand (Tangwattanachuleeporn et al. 2013), India (Xavier et al. 2013), Mexico (Canónico-González et al. 2013), Korea (Chae et al. 2012), and countries in the Middle East and North Africa region (Mahmoud 1999; Mseddi et al. 2011; Abbass et al. 2017). One of our isolates is *C. liquefaciens*, which has not been reported in pigeon excreta to the best of our knowledge. We are the first to report its presence in pigeon excreta in the Middle East and Asia. In General, *Cryptococcus* spp. thrive in pigeon

fecal droppings due to the high content of urea and organic matter (Costa et al. 2010; Abulreesh et al. 2015).

Similar to the previous studies, we found that *S. cerevisiae* is less common than other saprophytic yeast species in pigeon feces (Wu et al. 2012; Rosario Medina et al. 2017). Although *S. cerevisiae* has no veterinary significance, its presence in bird excreta may be due to the physico-chemical nature of the droppings that provide a rich environment for yeasts to grow (Cafarchia et al. 2008).

Candida species, especially *C. albicans* have also been frequently found in pigeon excreta (Wu et al. 2012; Rosario Medina et al. 2017). However, *C. albicans* was not detected in our study, instead, *C. glabrata*, was the only *Candida* species encountered. Other *Candida*-related genera, *M. guilliermondii* (formerly *Candida guilliermondii*), and *Cyberlindnera fabianii* (formerly *Candida fabianii*), were also present in this study, the former has been isolated in pigeon feces in Spain (Rosario Medina et al. 2017), while the latter has been very rarely detected in pigeon excreta.

We detected two other genera in our study, *M. farinosa* (formerly *Pichia farinosa*), and *Rhodosporidium paludigenum*. Both have not been, detected in pigeon or other bird excreta worldwide. On the other hand, *R. mucilaginosa* and *R. glutinis* are very commonly found in pigeon fecal droppings (Wu et al. 2012; Marenzoni et al. 2016; Abbass et al. 2017). However, *Lodderomyces elongisporus* has seldom been reported in pigeon fecal droppings (Wu et al. 2012). It is worth noting that due to the method of sampling we adopted in the current study,

environmental contamination of fecal samples (e.g. from soil) cannot be ruled out and may play, in part, role in the diverse yeast genera reported in our study.

Virulence factors of yeast species isolated from pigeon excreta. Virulence factors play a vital role in pathogenesis. Various *Cryptococcus* species, like *C. neoformans*, *C. gattii*, and *C. albidus* possess an arsenal of such molecules. These factors enable them to successfully invade hosts, to resist defense mechanisms of their immune system and to cause infection, especially in the immunocompromised individuals. The prominent capsule of *Cryptococcus* species is an important virulence factor. All the *Cryptococcus* species isolated in this study displayed capsules in Indian ink preparations, as observed under the microscope. On a molecular level, the *CAP1* gene was detected in 54.55% of *C. neoformans* isolates, whereas, the *CAP59* gene was detected in the rest of the isolates. The *C. gattii* exhibited only the *CAP59* gene. The formation of the capsule by the *Cryptococcus* species was induced by many environmental conditions that include pH, CO₂ levels and iron deprivation (Alspaugh 2015). The polysaccharide capsule helps *Cryptococcus* species to proliferate within the phagocytic cells and to inhibit host any immune response. Once it has invaded the host cell, and colonized the vacuole, *Cryptococcus* will survive by the aid of the capsule and replicate despite the acidic nature of the vacuole (Srikanta et al. 2014). Both of the *CAP1* and *CAP59* genes are specific to *C. neoformans* and *C. gattii*, this explains the absence of these genes in other encapsulated isolates such as *C. liquefaciens*, *C. glabrata*, and *Rhodotorula* species.

Phospholipase is another virulence factor that helps the pathogenesis of *Cryptococcus* and other pathogenic yeast species. Phospholipase activity can alter the microenvironment of infection and can facilitate *Cryptococcus* species to survive better within the host cells (Alspaugh 2015). All *Cryptococcus* species detected in this study, except for *C. liquefaciens*, were positive for the *PLB1* gene, it was also detected in *C. glabrata*. The presence of the *PLB1* gene was also noted in *S. cerevisiae* isolates. The ability of phospholipase to hydrolyze phospholipids and to produce several bioactive compounds has given *S. cerevisiae* its industrial potential.

Melanin is a known protective determinant for *Cryptococcus* against environmental stressors and, hence, considered a virulence factor (Alspaugh 2015). Similarly, urease activity has been associated with pathogenesis, in pathogenic yeasts such as the *Cryptococcus* species. The ammonia produced by urease activity damages the host cell endothelium; thus, the yeast to transigrate toward the central nervous system (Feder et al. 2015). It is suggested that capsules, melanin production, and high-temperature growth (at 37°C) are key virulence determinants for pathogenic and oppor-

tunistic yeasts (Boral et al. 2018). All these characteristics were observed for the isolates of *Cryptococcus* species in this study.

In general, several environmental yeast species possess the similar virulence factors as their pathogenic clinical counterparts (Magalhães Pinto et al. 2019). Our study reports this notion and highlights the presence of pathogenic yeast in the fecal droppings of free-living pigeons, suggesting the pathogenic potential of these environmental species of yeast.

Antifungal susceptibility. None of the 46 yeast isolates representing the nine different genera reported here, was resistant to the antifungal drugs tested. These results correlate with previously reported studies, particularly for *Cryptococcus* species, that it is rare for environmental (pigeon-derived) *C. neoformans* and *C. gattii* to exhibit resistance to antifungal drugs (Costa et al. 2010; Souza et al. 2010; Tangwattanachuleeporn et al. 2013; Teodoro et al. 2013). The clinical isolates of *Cryptococcus* species exhibit similar trends of low resistance to antifungal drugs (Souza et al. 2010; Govender et al. 2011). Environmental and clinical samples of *C. glabrata* have previously exhibited susceptibility to some of the antifungal drugs used in this study (Nenoff et al. 2011; Lotfalikhani et al. 2018; Miranda-Cadena et al. 2018). The lack of antifungal resistance was also observed in clinical *R. mucilaginosa* isolates (Razzaq Abed and Mohammed Hussein 2017). Resistance to fluconazole appears to be common in clinical isolates of *R. mucilaginosa*, this perhaps due to the fact that most of the patients are administered with fluconazole when fungemia is diagnosed (Wirth and Goldani 2012). The resistance mechanism of *Rhodotorula* to fluconazole is not known, thus, the observation of repeated resistance may suggest intrinsic resistance in some isolates (Duggal et al. 2011). So far, no available reports have described antifungal susceptibility patterns of environmental *Rhodotrula* species, therefore, whether environmental isolates exhibit similar resistance patterns, particularly to fluconazole, remains to be elucidated.

There is a lack of scientific evidence on the antifungal susceptibility patterns of both environmentally and clinically derived isolates of *M. farinose*, *S. cerevisiae*, *R. glutinis*, *M. guilliermondii*, *C. fabianii*, *R. paludigenum*, and *L. elongisporus*. Hence, we are unable to compare and discuss our results for these yeast species.

The lack of resistance observed in these environmental isolates of yeasts, particularly pathogenic species, may be explained by the role of various environmental factors that are not fully understood. Possibly there might be unique ecological niches in the environment where environmental yeast species can acquire drug resistance, or there might be a pattern of spread of drug resistance among environmental yeast species through geo-climatic factors, such as wind activity or

global warming that yet to be explored. Bird migration has been playing an important role in the spread of multidrug resistance in bacteria; it is not clear whether it plays a similar role in yeast drug resistance (Kontoyianis 2017). Furthermore, it was hypothesized that environmental yeast could acquire resistance to antifungal drugs in the presence of industrial waste of pollutants that could promote altered expression of genes that may occasionally occur in pathways related to resistance (Milanezi et al. 2019). It is also possible that the disk diffusion method may have influenced the susceptibility results. It is highly likely that the use of dilution method or MIC test strips would provide more accurate susceptibility results in comparison to the disk diffusion method, i.e. some of the isolates might have exhibited resistance if tested by the dilution method or MIC strips.

Public health significance of this study. Earlier studies have implicated that free-living pigeons spread pathogens in the environment and have established a direct link between pigeon droppings and human infections (Haag-Wackernagel and Moch 2004). In this study, we observed three different species of pathogenic *Cryptococcus* in pigeon fecal droppings in western Saudi Arabia: *C. neoformans*, *C. gattii*, and *C. albidus*. Together they make up around 39% of all yeast species found in the excreta. Different *Cryptococcus* species have been reported to cause human infections, *C. neoformans* and *C. gattii* for cryptococcosis (Cogliati 2013), *C. albidus* for fungemia (Cleveland et al. 2013), and respiratory infections (Burnik et al. 2007). In Saudi Arabia, there is only one incidence of a clinical case involving *C. neoformans*. The pathogen caused abscess and osteomyelitis in an immunocompetent individual (Al-Tawfiq et al. 2007). However, this lack of reported incidents may not truly reflect low occurrence of clinical cases in the region. In contrast, we suggest that there may have been relatively few clinical investigations of medically important fungi.

Other yeast species found in pigeon feces in this study are also implicated in human infections. *C. glabrata* has been implicated in various diseases in humans including both superficial and systematic infections, such as brain abscess (Zhu et al. 2018), vertebral column (spondylodiscitis) infection (Gagliano et al. 2018), joint infection (Koutserimpas et al. 2018), and cutaneous granuloma (Fan et al. 2018).

R. mucilaginosa is an environmental yeast that has emerged as a causative agent of serious and even fatal opportunistic infections, including fungemia (Kitazawa et al. 2018) and meningitis (Miceli et al. 2011) particularly in immunocompromised patients, and immunocompetent individuals. Other species identified in our study that have been implicated in severe or fatal human infections include: *C. fabianii* (Hof et al. 2017), *L. elongisporus* (Hatanaka et al. 2016), *M. guilliermondi*

(Cebeci et al. 2017), and the emerging invasive infections of *S. cerevisiae* (Popiel et al. 2015).

The most commonly transmitted pathogens via pigeons continue to be *Chlamydomphila psittaci* and *C. neoformans* (Haag-Wackernagel and Moch 2004). Considering the relationship between environmental *C. neoformans* strains and human infection, Delgado et al. (2005) concluded that cryptococcosis could be acquired from the environmental strains in both urban and rural areas. Liaw et al. (2010) drew similar conclusions, finding strong similarities between clinical and environmental strains of *C. neoformans* and suggesting that patients might acquire yeast infection from the environment. Overall, the results of our study demonstrate that pigeon fecal droppings carried a number of pathogenic yeast species as well as emerging opportunistic yeast genera.

In Makkah city, western Saudi Arabia, massive numbers of pigeons inhabit the city. They flock in public parks, rooftops, and in close proximity to catering areas, making it almost unavoidable for humans to come in contact with their droppings. Pigeon excreta can be noted almost everywhere in the city. Additionally, dust from dried pigeon fecal droppings may contain different cryptococcal species and other opportunistic yeast. Despite the massive cleaning efforts of public spaces, dissemination of pathogenic yeast by air is inevitable, increasing the chances of acquiring infection through the respiratory system.

Risk assessment of environmental *Cryptococcus* species. *C. neoformans* and *C. gattii* are pathogenic yeasts that rarely cause infections in healthy individuals. However, immunocompromised patients, such as those who underwent organ transplant, those under medications that weaken the immune system (e.g. corticosteroid or rheumatic arthritis medications), or people with an advanced stage of HIV infection are at a high risk of getting *C. neoformans* infection. In addition, elderly individuals, over 50 years old with lung health issues may be at risk of *C. gattii* infection (Cogliati 2013). *Cryptococcus* infection is not contagious and there is low risk for healthy people to be infected when in contact with an infected individual (Delgado et al. 2005). However, *Cryptococcus* can infect healthy people when they inhale the dust containing the pathogens. This is common in the environment, in areas where pigeon fecal droppings exist in abundance. Every individual may inhale the yeast dust, yet they may not develop any symptoms immediately. *Cryptococcus* can stay hidden within the body and cause infection later, when the immune system is too weak to fight it (Esher et al. 2018). Currently, many countries around the world do not consider the detection of *Cryptococcus* in clinical routine work, particularly in meningitis cases. To mitigate the risk of *Cryptococcus* infections, it is necessary

to perform extensive surveillance of the environmental distribution of the pathogens and laboratory detection of *Cryptococcus* infections in clinical specimens. Early detection of *Cryptococcus* infection in individuals may help to treat them promptly and to reduce the mortality rate of infected people.

Conclusions

Pigeon fecal droppings in western Saudi Arabia were found to harbor a wide range of pathogenic and opportunistic yeast species. Although none of them were resistant to the common antifungal drugs, all pathogenic species and some of the opportunistic species did carry different virulence factors. Our study confirms that pigeon fecal droppings provide a rich environment for the growth of saprophytic yeasts, particularly *Cryptococcus* species. Additionally, we demonstrate that pigeons may act as reservoirs and carriers not only for pathogenic yeast (e.g. *Cryptococcus* and *Candida*), but also for opportunistic yeast species (e.g. *R. mucilaginosa*). This is the first report on the diversity and virulence factors of yeast species in pigeon fecal droppings in Saudi Arabia. Further investigations are required to understand the pathogenicity of these isolates in humans and animals using suitable experimental models.

ORCID

Hussein H. Abulreesh 0000-0002-3289-696X

Acknowledgements

We are grateful to Professor Graham Wye. Scott, Department of Biological and Marine Sciences, University of Hull, the United Kingdom for his careful reading, valuable comments and editing of the manuscript. We are also grateful to Ms. Hiyam Hasan Abureesh, King Abdulaziz Hospital, Makkah, Saudi Arabia for her assistance throughout this work.

Conflict of interest

The authors do not report any financial or personal connections with other persons or organizations, which might negatively affect the contents of this publication and/or claim authorship rights to this publication.

Literature

- Abbass MS, Yassein SN, Khalaf JM. Isolation and identification of some important mycological isolates from droppings of birds in Baghdad. *J Entomol Zool Stud.* 2017;5:671–673.
- Abulreesh H. Faecal shedding of antibiotic resistant *Escherichia coli* serogroups in pigeons with special reference to *E. coli* O157. *Annu Res Rev Biol.* 2014 Jan 10;4(13):2184–2191. <https://doi.org/10.9734/ARRB/2014/9501>
- Abulreesh HH, Goulder R, Scott GW. Wild birds and human pathogens in the context of ringing and migration. *Ring Migr.* 2007 Jan;23(4):193–200. <https://doi.org/10.1080/03078698.2007.9674363>
- Abulreesh HH, Organji SR, Elbanna K, Osman GEH, Almalki MHK, Abdel-Mallek AY. First report of environmental isolation of *Cryptococcus neoformans* and other fungi from pigeon droppings in Makkah, Saudi Arabia and *in vitro* susceptibility testing. *Asian Pac J Trop Dis.* 2015 Aug;5(8):622–626. [https://doi.org/10.1016/S2222-1808\(15\)60901-X](https://doi.org/10.1016/S2222-1808(15)60901-X)
- Alspaugh JA. Virulence mechanisms and *Cryptococcus neoformans* pathogenesis. *Fungal Genet Biol.* 2015 May;78:55–58. <https://doi.org/10.1016/j.fgb.2014.09.004>
- Al-Tawfiq JA, Ghandour J. *Cryptococcus neoformans* abscess and osteomyelitis in an immunocompetent patient with tuberculous lymphadenitis. *Infection.* 2007 Oct;35(5):377–382. <https://doi.org/10.1007/s15010-007-6109-9>
- Boral H, Metin B, Döğen A, Seyedmousavi S, Ilkit M. Overview of selected virulence attributes in *Aspergillus fumigatus*, *Candida albicans*, *Cryptococcus neoformans*, *Trichophyton rubrum*, and *Exophiala dermatitidis*. *Fungal Genet Biol.* 2018 Feb;111:92–107. <https://doi.org/10.1016/j.fgb.2017.10.008>
- Burnik C, Altıntaş ND, Özkaya G, Serter T, Selçuk ZT, Firat P, Arikan S, Cuenca-Estrella M, Topeli A. Acute respiratory distress syndrome due to *Cryptococcus albidus* pneumonia: case report and review of the literature. *Med Mycol.* 2007 Jan;45(5):469–473. <https://doi.org/10.1080/13693780701386015>
- Cafarchia C, Romito D, Caccioli C, Camarda A, Otranto D. Phospholipase activity of yeasts from wild birds and possible implications for human disease. *Med Mycol.* 2008 Jan;46(5):429–434. <https://doi.org/10.1080/13693780701885636>
- Canónico-González Y, Adame-Rodríguez JM, Mercado-Hernández R, Aréchiga-Carvajal ET. *Cryptococcus* spp. isolation from excreta of pigeons (*Columba livia*) in and around Monterrey, Mexico. *SpringerPlus.* 2013 Dec;2(1):632. <https://doi.org/10.1186/2193-1801-2-632>
- Canteros CE, Rodero L, Rivas MC, Davel G. A rapid urease test for presumptive identification of *Cryptococcus neoformans*. *Mycopathologia.* 1996 Oct;136(1):21–23. <https://doi.org/10.1007/BF00436656>
- Cebeci Güler N, Tosun İ, Aydın F. The identification of *Meyerozyma guilliermondii* from blood cultures and surveillance samples in a university hospital in Northeast Turkey: A ten-year survey. *J Mycol Med.* 2017 Dec;27(4):506–513. <https://doi.org/10.1016/j.mycmed.2017.07.007>
- Chae HS, Jang GE, Kim NH, Son HR, Lee JH, Kim SH, Park GN, Jo HJ, Kim JT, Chang KS. Classification of *Cryptococcus neoformans* and yeast-like fungus isolates from pigeon droppings by colony phenotyping and ITS genotyping and their seasonal variations in Korea. *Avian Dis.* 2012 Mar;56(1):58–64. <https://doi.org/10.1637/9703-030711-Reg.1>
- Chowdhary A, Hiremath SS, Sun S, Kowshik T, Randhawa HS, Xu J. Genetic differentiation, recombination and clonal expansion in environmental populations of *Cryptococcus gattii* in India. *Environ Microbiol.* 2011 Jul;13(7):1875–1888. <https://doi.org/10.1111/j.1462-2920.2011.02510.x>
- Cleveland KO, Gelfand MS, Rao V. Posaconazole as successful treatment for fungemia due to *Cryptococcus albidus* in a liver transplant recipient. *QJM.* 2013 Apr 01;106(4):361–362. <https://doi.org/10.1093/qjmed/hcs133>
- CLSI. Method for antifungal susceptibility testing of yeasts. Approved Standard M44-A2. Wayne (PA, USA): Clinical and Laboratory Standards Institute; 2008.
- Cogliati M. Global epidemiology of *Cryptococcus neoformans* and *Cryptococcus gattii*: An atlas of the molecular types. *Scientifica.* 2013;Article ID 675213, 23 pages.
- Costa AKF, Sidrim JJC, Cordeiro RA, Brilhante RSN, Monteiro AJ, Rocha MFG. Urban pigeons (*Columba livia*) as a potential source of pathogenic yeasts: a focus on antifungal susceptibility of

- Cryptococcus* strains in Northeast Brazil. Mycopathologia. 2010 Mar;169(3):207–213. <https://doi.org/10.1007/s11046-009-9245-1>
- Delgado ACN, Taguchi H, Mikami Y, Myiajy M, Villares MCB, Moretti ML.** Human cryptococcosis: relationship of environmental and clinical strains of *Cryptococcus neoformans* var. *neoformans* from urban and rural areas. Mycopathologia. 2005 Jan;159(1):7–11. <https://doi.org/10.1007/s11046-004-9618-4>
- Duggal S, Jain H, Tyagi A, Sharma A, Chugh TD.** *Rhodotorula fungemia*: two cases and a brief review. Med Mycol. 2011 Nov;49(8):879–882.
- Esher SK, Zaragoza O, Alspaugh JA.** Cryptococcal pathogenic mechanisms: a dangerous trip from the environment to the brain. Mem Inst Oswaldo Cruz. 2018;113(7):e180057. <https://doi.org/10.1590/0074-02760180057>
- Fan Y, Pan W, Wang G, Huang Y, Li Y, Fang W, Tao X.** Isolated cutaneous granuloma caused by *Candida glabrata*: A rare case report and literature review. Mycopathologia. 2018 Apr;183(2):417–421. <https://doi.org/10.1007/s11046-017-0228-3>
- Feder V, Kmetzsch L, Staats CC, Vidal-Figueiredo N, Ligabue-Braun R, Carlini CR, Vainstein MH.** *Cryptococcus gattii* urease as a virulence factor and the relevance of enzymatic activity in cryptococcosis pathogenesis. FEBS J. 2015 Apr;282(8):1406–1418. <https://doi.org/10.1111/febs.13229>
- Gagliano M, Marchiani C, Bandini G, Bernardi P, Palagano N, Cioni E, Finocchi M, Bellando Randone S, Moggi Pignone A.** A rare case of *Candida glabrata* spondylodiscitis: case report and literature review. Int J Infect Dis. 2018 Mar;68:31–35. <https://doi.org/10.1016/j.ijid.2018.01.003>
- Govender NP, Patel J, van Wyk M, Chiller TM, Lockhart SR.** Group for Enteric, Respiratory and Meningeal Disease Surveillance in South Africa (GERMS-SA). Trends in antifungal drug susceptibility of *Cryptococcus neoformans* isolates obtained through population-based surveillance in South Africa in 2002–2003 and 2007–2008. Antimicrob Agents Chemother. 2011 Jun;55(6):2606–2611. <https://doi.org/10.1128/AAC.00048-11>
- Haag-Wackernagel D, Moch H.** Health hazards posed by feral pigeons. J Infect. 2004 May;48(4):307–313. <https://doi.org/10.1016/j.jimf.2003.11.001>
- Hagen F, Khayhan K, Theelen B, Kolecka A, Polacheck I, Sionov E, Falk R, Parnmen S, Lumsch HT, Boekhout T.** Recognition of seven species in the *Cryptococcus gattii*/*Cryptococcus neoformans* species complex. Fungal Genet Biol. 2015 May;78:16–48. <https://doi.org/10.1016/j.fgb.2015.02.009>
- Hashemi SJ, Jabbari AG, Bayat M, Rafiei SM.** Prevalence of *Cryptococcus neoformans* in domestic birds referred to veterinary clinics in Tehran. Eur J Exp Biol. 2014;4:482–486.
- Hatanaka S, Nakamura I, Fukushima S, Ohkusu K, Matsu-moto T.** Catheter-related bloodstream infection due to *Lodderomyces elongisporus*. Jpn J Infect Dis. 2016;69(6):520–522. <https://doi.org/10.7883/yoken.JJID.2015.307>
- Hof H, Amann V, Tauber C, Paulun A.** Peritonitis in a neonate due to *Cyberlindnera fabianii*, an ascomycetous yeast. Infection. 2017 Dec;45(6):921–924. <https://doi.org/10.1007/s15010-017-1062-8>
- Kitazawa T, Ishigaki S, Seo K, Yoshino Y, Ota Y.** Catheter-related bloodstream infection due to *Rhodotorula mucilaginosa* with normal serum (1→3)-β-D-glucan level. J Mycol Med. 2018 Jun;28(2):393–395. <https://doi.org/10.1016/j.mycmed.2018.04.001>
- Kontoyiannis DP.** Antifungal resistance: an emerging reality and a global challenge. J Infect Dis. 2017 Aug 15;216 suppl_3:S431–S435. <https://doi.org/10.1093/infdis/jix179>
- Kouterimpas C, Samonis G, Velivassakis E, Iliopoulou-Kosmadaki S, Kontakis G, Kofteridis DP.** *Candida glabrata* prosthetic joint infection, successfully treated with anidulafungin: A case report and review of the literature. Mycoses. 2018 Apr;61(4):266–269. <https://doi.org/10.1111/myc.12736>
- Liaw S-J, Wu H-C, Hsueh P-R.** Microbiological characteristics of clinical isolates of *Cryptococcus neoformans* in Taiwan: serotypes, mating types, molecular types, virulence factors, and antifungal susceptibility. Clin Microbiol Infect. 2010 Jun;16(6):696–703. <https://doi.org/10.1111/j.1469-0691.2009.02930.x>
- Lotfalikhani A, Khosravi Y, Sabet NS, Na SL, Ng KP, Tay ST.** Genetic diversity, antifungal susceptibility and enzymatic characterization of Malaysian clinical isolates of *Candida glabrata*. Trop Biomed. 2018;35:1123–1130.
- Magalhães Pinto L, de Assis Bezerra Neto F, Araújo Paulo de Medeiros M, Zuza Alves DL, Maranhão Chaves G.** *Candida* species isolated from pigeon (*Columbia livia*) droppings may express virulence factors and resistance to azoles. Vet Microbiol. 2019 Aug;235:43–52. <https://doi.org/10.1016/j.vetmic.2019.05.022>
- Mahmoud YAG.** First environmental isolation of *Cryptococcus neoformans* var. *neoformans* and var. *gattii* from the Gharbia Governorate, Egypt. Mycopathologia. 1999;148(2):83–86. <https://doi.org/10.1023/A:1007166818993>
- Marenzoni ML, Morganti G, Moretta I, Crotti S, Agnetti F, Moretti A, Pitzurra L, Casagrande Proietti P, Sechi P, Cenci-Goga B, et al.** Microbiological and parasitological survey of zoonotic agents in apparently healthy feral pigeons. Pol J Vet Sci. 2016 Jun 1;19(2):309–315. <https://doi.org/10.1515/pjvs-2016-0038>
- Mattsson R, Haemig PD, Olsen B.** Feral pigeons as carriers of *Cryptococcus laurentii*, *Cryptococcus uniguttulatus* and *Debaryomyces hansenii*. Med Mycol. 1999 Oct;37(5):367–369. <https://doi.org/10.1046/j.1365-280X.1999.00241.x>
- Miceli MH, Díaz JA, Lee SA.** Emerging opportunistic yeast infections. Lancet Infect Dis. 2011 Feb;11(2):142–151. [https://doi.org/10.1016/S1473-3099\(10\)70218-8](https://doi.org/10.1016/S1473-3099(10)70218-8)
- Milanezi ACM, Witusk JPD, VAN DER Sand ST.** Antifungal susceptibility of yeasts isolated from anthropogenic watershed. An Acad Bras Cienc. 2019;91(1):e20170369.
- Miranda-Cadena K, Marcos-Arias C, Mateo E, Aguirre JM, Quindós G, Eraso E.** Prevalence and antifungal susceptibility profiles of *Candida glabrata*, *Candida parapsilosis* and their close-related species in oral candidiasis. Arch Oral Biol. 2018 Nov;95:100–107. <https://doi.org/10.1016/j.archoralbio.2018.07.017>
- Mseddi F, Sellami A, Jarbouai MA, Sellami H, Makni F, Ayadi A.** First environmental isolations of *Cryptococcus neoformans* and *Cryptococcus gattii* in Tunisia and review of published studies on environmental isolation in Africa. Mycopathologia. 2011 May;171(5):355–360. <https://doi.org/10.1007/s11046-010-9381-7>
- Nenoff P, Krüger C, Neumeister C, Schwantes U, Koch D.** *In vitro* susceptibility testing of yeasts to nystatin – low minimum inhibitory concentrations suggest no indication of *in vitro* resistance of *Candida albicans*, *Candida* species or non-*Candida* yeast species to nystatin. Clin Med Invest. 2016;1(3):71–76. <https://doi.org/10.15761/CMI.1000116>
- Pincus DH, Orena S, Chatellier S.** Yeast identification – past, present, and future methods. Med Mycol. 2007 Jan;45(2):97–121. <https://doi.org/10.1080/13693780601059936>
- Popiel KY, Wong P, Lee MJ, Langelier M, Sheppard DC, Vinh DC.** Invasive *Saccharomyces cerevisiae* in a liver transplant patient: case report and review of infection in transplant recipients. Transpl Infect Dis. 2015 Jun;17(3):435–441. <https://doi.org/10.1111/tid.12384>
- Rajasingham R, Smith RM, Park BJ, Jarvis JN, Govender NP, Chiller TM, Denning DW, Loyse A, Boulware DR.** Global burden of disease of HIV-associated cryptococcal meningitis: an updated analysis. Lancet Infect Dis. 2017 Aug;17(8):873–881. [https://doi.org/10.1016/S1473-3099\(17\)30243-8](https://doi.org/10.1016/S1473-3099(17)30243-8)
- Razzaq Abed A, Mohammed Hussein I.** A comparative study between specific and non-specific antifungal agents to treat the *Rhodotorula mucilaginosa* athletes foot. Biomed Pharmacol J. 2017 Dec 28;10(4):2153–2160. <https://doi.org/10.13005/bpj/1340>

- Rosario I, Soro G, Déniz S, Ferrer O, Acosta F, Padilla D, Acosta B.** Presence of *C. albidus*, *C. laurentii* and *C. uniguttulatus* in crop and droppings of pigeon lofts (*Columba livia*). *Mycopathologia*. 2010 Apr;169(4):315–319.
<https://doi.org/10.1007/s11046-009-9262-0>
- Rosario Medina I, Román Fuentes L, Batista Arteaga M, Real Valcárcel F, Acosta Arbelo F, Padilla del Castillo D, Déniz Suárez S, Ferrer Quintana O, Vega Gutiérrez B, Silva Sergent F, et al.** Pigeons and their droppings as reservoirs of *Candida* and other zoonotic yeasts. *Rev Iberoam Micol*. 2017 Oct;34(4):211–214.
<https://doi.org/10.1016/j.riam.2017.03.001>
- Soltani M, Bayat M, Hashemi SJ, Zia M, Pestechian N.** Isolation of *Cryptococcus neoformans* and other opportunistic fungi from pigeon droppings. *J Res Med Sci*. 2013 Jan;18(1):56–60.
- Souza LKH, Souza Junior AH, Costa CR, Faganello J, Vainstein MH, Chagas ALB, Souza ACM, Silva MRR.** Molecular typing and antifungal susceptibility of clinical and environmental *Cryptococcus neoformans* species complex isolates in Goiania, Brazil. *Mycoses*. 2010 Jan;53(1):62–67.
<https://doi.org/10.1111/j.1439-0507.2008.01662.x>
- Srikanta D, Santiago-Tirado FH, Doering TL.** *Cryptococcus neoformans*: historical curiosity to modern pathogen. *Yeast*. 2014 Feb;31(2):47–60.
<https://doi.org/10.1002/yea.2997>
- Tangwattanachuleeporn M, Somporn P, Poolpol K, Gross U, Weig M, Bader O.** Prevalence and antifungal susceptibility of *Cryptococcus neoformans* isolated from pigeon excreta in Chon Buri Province, Eastern Thailand. *Med Mycol J*. 2013;54(3):303–307.
<https://doi.org/10.3314/mmj.54.303>
- Teodoro VLI, Gullo FP, Sardi JCO, Torres EM, Fusco-Almeida AM, Mendes-Giannini MJS.** Environmental isolation, biochemical identification, and antifungal drug susceptibility of *Cryptococcus* species. *Rev Soc Bras Med Trop*. 2013 Dec;46(6):759–764.
<https://doi.org/10.1590/0037-8682-0025-2013>
- White TJ, Bruns TD, Lee SB, Taylor JW.** Amplification and direct sequencing of fungal ribosomal RNA genes for phylogenetics. In: Innis MA, Gelfand DH, Sninsky JJ, White TJ, editors. *PCR Protocols: A guide to methods and applications*. New York (USA): Academic Press; 1990. p. 315–322.
<http://doi.org/10.1016/B978-0-12-372180-8.50042-1>
- Wirth F, Goldani LZ.** Epidemiology of *Rhodotorula*: an emerging pathogen. *Interdiscip Perspect Infect Dis*. 2012;2012:1–7.
<https://doi.org/10.1155/2012/465717>
- Wu Y, Du PC, Li WG, Lu JX.** Identification and molecular analysis of pathogenic yeasts in droppings of domestic pigeons in Beijing, China. *Mycopathologia*. 2012 Sep;174(3):203–214.
<https://doi.org/10.1007/s11046-012-9536-9>
- Xavier TF, Auxilia A, Kannan M, Freeda Rose A, Senthil Kumar SR.** Isolation and identification of *Cryptococcus neoformans* from pigeon droppings in Tiruchirapalli district of Tamil Nadu, south India. *Int J Curr Microbiol Appl Sci*. 2013;2:404–409.
- Zhu Z, Huang Z, Li Z, Li X, Du C, Tian Y.** Multiple brain abscesses caused by infection with *Candida glabrata*: A case report. *Exp Ther Med*. 2018 Mar;15(3):2374–2380.

The Composition of Fungal Communities in the Rumen of Gayals (*Bos frontalis*), Yaks (*Bos grunniens*), and Yunnan and Tibetan Yellow Cattle (*Bos taurus*)

HOUFU WANG^{1#}, PENGFEI LI^{1#}, XUCHUAN LIU², CHUNYONG ZHANG^{1,2}, QIONGFEN LU^{1,2},
DONGMEI XI², RENHUI YANG¹, SHULING WANG¹, WENSHUN BAI², ZHEN YANG²,
RONGKANG ZHOU², XIAO CHENG² and JING LENG^{1,2*}

¹ Key Laboratory of Animal and Feed Science of Yunnan Provincial, Yunnan Agricultural University,
Kunming, China

² Faculty of Animal Science and Technology, Yunnan Agricultural University, Kunming, China

Submitted 30 May 2019, revised 17 October 2019, accepted 17 October 2019

Abstract

The rumen is a microbial-rich ecosystem in which rumen fungi play an important role in the feed digestion of ruminants. The composition of rumen fungi in free-range ruminants such as gayals, yaks, Tibetan yellow cattle, and the domesticated Yunnan yellow cattle was investigated by sequencing an internal transcribed spacer region 1 (ITS1) using Illumina MiSeq. A total of 285 092 optimized sequences and 904 operational taxonomic units (OTUs) were obtained from the four cattle breeds. The rumen fungi abundance and Chao and Simpson indexes were all higher in free-range ruminants than in domesticated ruminants. Three fungal phyla were identified by sequence comparison: Neocallimastigomycota, Basidiomycota, and Ascomycota. Basidiomycota and Ascomycota have very low abundance in the rumen of four breeds cattle but anaerobic fungi (AF) Neocallimastigomycota occurred in a high abundance. In Neocallimastigomycota, the dominant genera were *Piromyces*, *Anaeromyces*, *Cyllamyces*, *Neocallimastix*, and *Orpionmyces* in four cattle breeds. The composition of the major genera of Neocallimastigaceae varied greatly among the four cattle breeds. The unclassified genera were unequally distributed in gayals, yaks, Tibetan and Yunnan yellow cattle, accounting for 90.63%, 98.52%, 97.79%, and 27.01% respectively. It appears that free-range ruminants have more unknown rumen fungi than domesticated ruminants and the cattle breeds and animal diets had an impact on the diversity of rumen fungi.

Key words: gayals, yaks, Yunnan yellow cattle, Tibetan yellow cattle, rumen fungi, ITS-sequencing

Introduction

Ruminant animals lack the carbohydrate-active enzyme encoding genes, so feed (carbohydrate) metabolism is completely dependent on the microorganisms residing in their rumen (Kameshwar and Qin 2018). Current research on rumen fungi has focused on anaerobic rumen fungi. Anaerobic rumen fungi play a very important role in the digestion and metabolism of carbohydrates in the rumen (Gruninger et al. 2018; Kameshwar and Qin 2018). Anaerobic rumen fungi can secrete large amounts of cellulolytic enzymes. Their hyphae can destroy the cell wall structure of

plant feed owing to the combination of enzymes and degradable cellulose and this improves the degradation and utilization rates of plant feed (Lee et al. 2000; Gruninger et al. 2018; Kameshwar et al. 2018). Currently, the rumen AF (anaerobic fungi) are classified into phylum Neocallimastigomycota (Gruninger et al. 2014) and Neocallimasticaceae (Hibbett et al. 2007). Neocallimasticaceae was divided into eleven genera, containing a large number of monocentric rumen AF: *Neocallimastix*, *Piromyces*, *Caecomyces*, *Oontomyces* (Dagar et al. 2015a), *Pecoramyces* (Hanafy et al. 2017), *Feramyces*, *Liebetanzomyces* (Hanafy et al. 2018), and *Buwchfawromyces* (Griffith et al. 2015), as well as three

[#] These authors contributed equally to this work.

* Corresponding author: J. Leng, College of Animal Science and Technology, Yunnan Agricultural University, Kunming, China; Yunnan Provincial Key Laboratory of Animal and Feed Science, Yunnan Agricultural University, Kunming, China; e-mail: 2370140328@qq.com
© 2019 Houfu Wang et al.

This work is licensed under the Creative Commons Attribution-NonCommercial-NoDerivatives 4.0 License (<https://creativecommons.org/licenses/by-nc-nd/4.0/>).

polycentric genera: *Orpinomyces*, *Anaeromyces* (Breton et al. 1990), and *Cyllumyces* (Emin et al. 2001). The studies have shown that these AF are important in the rumen microbial system (Orpin 1975; Ho and Barr 1995). However, recent studies have shown that Basidiomycota and Ascomycota phyla play an important role in the rumen digestion of Holstein cows and cashmere goats (Zhang et al. 2017; Han et al. 2019).

Little is known about rumen AF and most of them were identified by microscopic conventional cultivation techniques, which provides important information for rumen AF (Breton et al. 1990; Ho and Barr 1995). The limitations of these methods are mainly due to the strict growing requirements and the low survival rate but molecular biology techniques can overcome these problems (Pryce et al. 2006). The fungal ribosomal RNA gene includes a gene encoding 28S ribosomal DNA, 18S ribosomal DNA, and 5.8S ribosomal DNA, which in the internal transcribed spacer Region1 evolves rapidly (Sirohi et al. 2013; Elekwachi et al. 2017). The last-mentioned gene has the interspecies specificity and intraspecies conservation, and the length of the sequence is moderate enough to get sufficient information (Pryce et al. 2006; Campa et al. 2008; Bellemain et al. 2010). ITS sequencing is used to study the diversity of the community of rumen AF and provide genetic information for the classification and identification of fungi (Liggenstoffer et al. 2010; Koljalg et al. 2013).

The free-range gayals are mainly distributed in the Nujiang River and Dulong River areas of Yunnan Province, China. Yaks live exclusively on the Qinghai-Tibetan Plateau, China (An et al. 2005) and are well adapted to harsh environmental conditions. Yunnan yellow cattle and Tibetan yellow cattle are common, wide-ranging cattle. Yunnan yellow cattle live in the same region as gayals and Tibetan yellow cattle in the same region as yaks (Deng et al. 2007; Leng et al. 2012). Rumen bacteria in gayals, Yunnan yellow cattle and yak have been already studied (Deng et al. 2007), but there is no research on their rumen fungi. Rumen anaerobic fungi are the first microorganisms attached to fibers during rumen microbial degradation (Bauchop 1979) and play an important role in the degradation process (Dagar et al. 2015b). Anaerobic fungi degrade lignocellulose using a large portfolio of Carbohydrate-Active enZymes (CAZymes) and penetrating hyphae that physically disrupt the ultrastructure of the plant cell wall; such action may help to increase the surface area for bacterial colonization and further enzymatic digestion (Lee et al. 2000; Gruninger et al. 2018; Kameshwar et al. 2018). Rumen anaerobic fungi have great application potential in industrial production. The AF cellulose degradation ability shows that it can increase biogas production in co-culture with methanogens (Cheng 2018). Studies have also shown that

rumen AF can reduce animal energy loss by reducing CH₄ (greenhouse gas) production during digestion, and it can also be used to improve the straw lignocellulosic structure in biofuels and biochemical production (Andrea et al. 2018; Oliver and Schilling 2018). These four cattle breeds are very important cattle species in China, and there are very few studies on their rumen fungi. Therefore, this paper conducted a comprehensive analysis of rumen fungi from four breeds of cattle to help us understand their rumen fungi function.

Experimental

Materials and methods

Animals and sampling. Sixteen male samples (3 ± 0.25 years old) were used in this study, including four cattle breeds and each breed comprised four cattle. Gayals and Yunnan yellow cattle were from the Nujiang Region, Yunnan Province, China ($27^{\circ} 46' 55.15''$ N, $98^{\circ} 39' 49.99''$ E above sea level 2260 m). Yaks and Tibetan yellow cattle were from the Diqing Region, Yunnan Province, China ($27^{\circ} 51' 30.61''$ N, $99^{\circ} 41' 42.82''$ E, above sea level 3280 m). Gayals, yaks, and Tibetan yellow cattle lived outside, ate mainly wild grass, without any supervision. Yunnan yellow cattle lived in cattle lairs and were fed rice bran and corn (Table II). Rumen contents were collected by gastric tube, filtered through four layers of cheesecloth and stored at -80°C before DNA extraction.

DNA extraction, PCR amplification, and sequencing. DNA was extracted from 0.5 g of rumen contents per sample after thawing and mixing well, with the E.Z.N.A DNA kits for soil, following the manufacturer's introduction. PCR was conducted using universal fungal primers for ITS1, which are as follows: forward primer ITS1 5'-GGAAGTAAAAGTCGTAACAAGG-3' and reverse primer ITS2 5'-GCTGCGTTCTTCATC-GATGC-3' (Man et al. 2018). Each tube for amplification contained 4 μl 5 \times FastPfu Buffer, 2 μl dNTPs at a concentration of 2.5 mM, 0.8 μl each primer at a concentration of 5 μM , 0.4 μl FastPu polymerase, and 10 ng DNA template with double-distilled H₂O (ddH₂O) added to 20 μl . PCR was performed at 95°C for 2 min, and 33 cycles of 95°C for 30 s, 55°C for 30 s, and 72°C for 30 s followed by incubation at 72°C for 5 min. The PCR product was purified using AxyPrep DNA gel extraction kits and eluted with Tris-HCl buffer. PCR products were quantified using the PicoGreen[®] dsDNA Assay Kit and QuantiFluor[™]-ST Blue Fluorescence System (Promega).

Phylogenetic analysis. Amplicons of ITS-1 sequences, which were moderately conserved regions of the 18S rRNA gene, were used for the sequence-specific

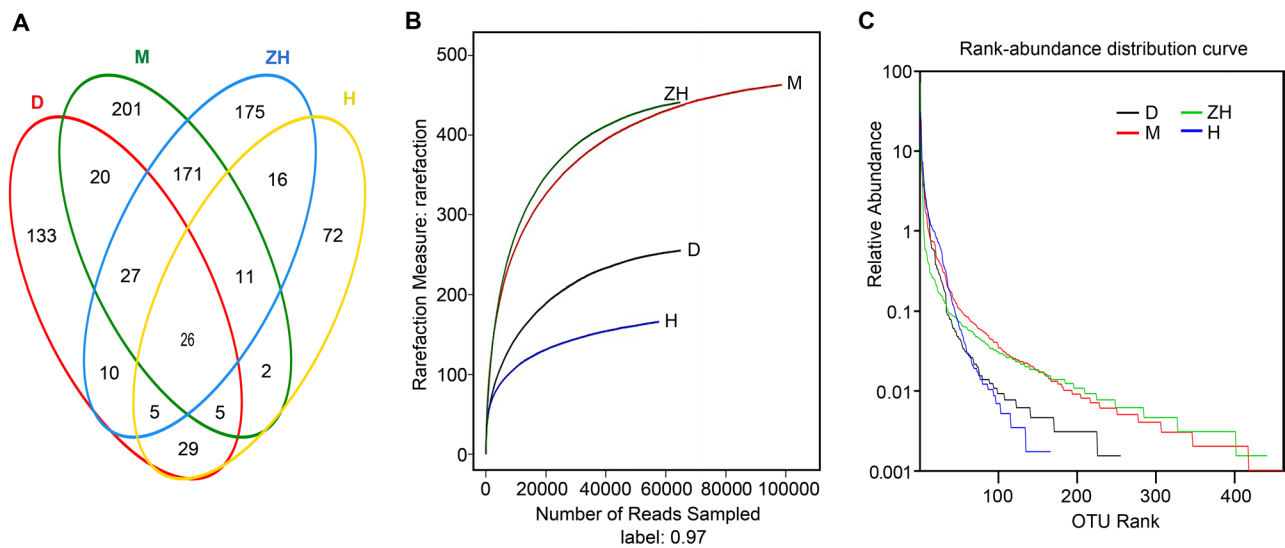


Fig. 1. Venn diagram, rarefaction index, and abundance distribution curves for D, H, M and ZH based on OTUs from cattle breeds, which had $\geq 97\%$ similarity.

D – gayals; H – Yunnan yellow cattle; M – yaks; ZH – Tibetan yellow cattle. Red line represents D. Blue line represents ZH. Green line represents M. Yellow line represents H.

separation. ITS-1 sequencing was regarded as an effective method for recognizing the diversity and structure of rumen fungi. The PE reads obtained by Miseq sequencing are first spliced according to the overlapping relationship, and the quality and quality of the sequence were quality-controlled and filtered. The operational taxonomic units (OTUs) cluster analysis and species taxonomic analysis were performed after the samples were distinguished. The various diversity index analysis could be performed based on OTUs. Cluster analysis results could be used to analyze the diversity index of OTUs and the establishment of the sequencing depth. Based on the taxonomic information, the statistical analysis of community structure could be performed at each classification level. Based on 97% similarity of OTUs the successful identification of species from *Piromyces* and *Neocallimastix* in the goat and buffalo rumen was performed (Brookman et al. 2000). The 97% similarity level to partition OTUs was used in this work. Basic diversity estimates and rarefaction curves were computed as $OTU_{0.05}$ outputs using Mothur (Schloss et al. 2011), including analyses of diversity indexes ACE, Chao, Shannon and Simpson. In addition to the diversity curves, rarefaction and rank-abundance curves were also generated to describe the sequencing depth using Mothur. The Unite database (Koljalg et al. 2013) was used to determine taxonomic information on OTUs. Based on taxonomic information such as abundance and the genera of all OTUs, phylogenetic trees were built that included abundance and structure of rumen fungi using MEGAN and NCBI databases. Venn and Heatmap diagrams were built using the R language (Jami et al. 2013).

Results

A total of 622 176 original sequences were obtained from four cattle breeds by Illumina sequencing of which 297 745 sequences remained after quality control measures, and 285 092 sequences were used for phylogenetic analyses. The average length of trim sequences used for analyses was 317.6 bp. The average number of sequences from the different cattle breeds is shown in Table I. Rarefaction curve analysis (Fig. 1B) indicated that sequences collected in this study comprised the majority of rumen fungi sequences from the four cattle breeds. The taxonomic analysis was reflected in the cluster analysis of OTUs, with 904 OTUs from the four cattle breeds: 255 OTUs from gayals, 166 from Yunnan yellow cattle, 463 from yaks, and 441 from Tibetan yellow cattle (Table I). The four cattle breeds had unique OTUs of rumen AF and shared OTUs across rumen AF (Fig. 1A).

Diversity analysis. ACE, Chao, Shannon and Simpson diversity indexes were calculated to determine the diversity of rumen fungi in the cattle breeds. In this study, the largest ACE and Chao indexes were for yaks, followed by Tibetan yellow cattle, gayals, and Yunnan yellow cattle, which indicated that yaks had a larger number of rumen fungi than the other three species. Although the abundance of rumen fungi in gayals and Yunnan yellow cattle was lower than in yaks and Tibetan yellow cattle, their diversity was close to yaks and higher than Tibetan yellow cattle as demonstrated by the Shannon and Simpson indexes (Table I).

With increasing sequencing depth, the number of OTUs was unchanged (Fig. 1B). A rank-abundance

Table I
Diversity index of anaerobic fungal communities among the cattle breeds.

Cattle breeds	Feed	Reads	0.97 (level)				
			OTU _{0.05}	Ace	Chao	Shannon	Simpson
D	weeds	64818	255	^a 272 (^b 263, ^c 288)	^a 263 (^b 258, ^c 276)	^a 2.17 (^b 2.15, ^c 2.18)	^a 0.3102 (^b 0.3063, ^c 0.3142)
H	feed	57567	166	^a 193 (^b 180, ^c 220)	^a 191 (^b 176, ^c 225)	^a 2.78 (^b 2.76, ^c 2.79)	^a 0.1352 (^b 0.1332, ^c 0.1372)
M	weeds	98550	463	^a 487 (^b 476, ^c 505)	^a 477 (^b 470, ^c 494)	^a 2.82 (^b 2.80, ^c 2.83)	^a 0.1622 (^b 0.1606, ^c 0.1639)
ZH	weeds	64694	441	^a 461 (^b 452, ^c 477)	^a 451 (^b 445, ^c 466)	^a 1.74 (^b 1.72, ^c 1.76)	^a 0.4905 (^b 0.4858, ^c 0.4953)

Weeds: bamboo or other wild grass; feed: rice bran and corn

a – average; b – minimum number; c – maximum number;

D – gayals; H – Yunnan yellow cattle; M – yaks; ZH – Tibetan yellow cattle

distribution curve was constructed to reflect the abundance and uniformity of rumen fungi. The width of the curve indicated the highest abundance of rumen fungi for yaks and the least abundance for Yunnan yellow cattle; the abundance of Tibetan yellow cattle was close to yaks (Fig. 1C). According to the sequence abundance of the top 50 OTUs, the relative abundance of rumen fungi was similar. However, abundance differed among the different cattle breeds with increasing OTU ranking (Fig. 1C). The uniformity of rumen fungi was similar when the relative abundance was under 0.01, indicating that yaks, Tibetan yellow cattle, and gayals had a similar abundance and uniformity of fungi (Fig. 1C).

Phylogenetic analysis. A phylogenetic tree based on OTUs was constructed (Fig. 3). Rumen fungi from the

ITS-1 phylogenetic tree were mainly divided into three subdivisions. Three fungal phyla were identified by sequence comparison: Neocallimastigomycota, Basidiomycota, and Ascomycota (Table III), the remaining sequences were unclassified. We detected 62 dominant genera from Ascomycota, but the abundance was very low of each genus. The most abundant genus was *Cladosporium*, accounting for 306 sequences, mainly distributed in yaks. *Udeniomyces* was the most abundant among 29 genera from Basidiomycota, accounting for 2021 sequences, and was mainly distributed in Yunnan yellow cattle (Fig. 3). Further analysis showed large differences in the composition of the primary genera of Neocallimastigaceae between different cattle breeds. The dominant genera were *Piromyces*, *Anaeromyces*,

Table II
Cattle diet and nutrient levels.

Feeds	Dietary nutrients (%)				
	DM	CP	EE	NDF	ADF
Bamboo diet	48.10 ± 9.85	13.06 ± 1.20	3.08 ± 0.69	72.13 ± 1.54	42.76 ± 3.02
Wild grass	70.24 ± 0.56	1.44 ± 0.10	0.04 ± 0.02	30.12 ± 0.17	18.83 ± 0.10
Rice bran	87.03 ± 0.22	12.82 ± 0.16	16.53 ± 0.18	22.91 ± 0.21	13.44 ± 0.52
Corn	86.15 ± 0.14	8.38 ± 0.13	3.01 ± 0.24	8.59 ± 0.62	3.27 ± 0.54

DM – Dry matter; CP – Crude protein; EE – Ether extract; NDF – Neutral detergent fiber;

ADF – Acid detergent fiber

Table III
Fungal classification and the percentage statistics.

Total sequence	Phylum	Sequences	Percents	Dominant genus
285092	Neocallimastigomycota	63 535	22.28%	<i>Piromyces</i> , <i>Anaeromyces</i> , <i>Cyllamyces</i> , <i>Neocallimastix</i> and <i>Orpionmyces</i>
	Basidiomycota	6 030	2.11%	<i>Udeniomyces</i>
	Ascomycota	2 740	0.96%	<i>Cladosporium</i>

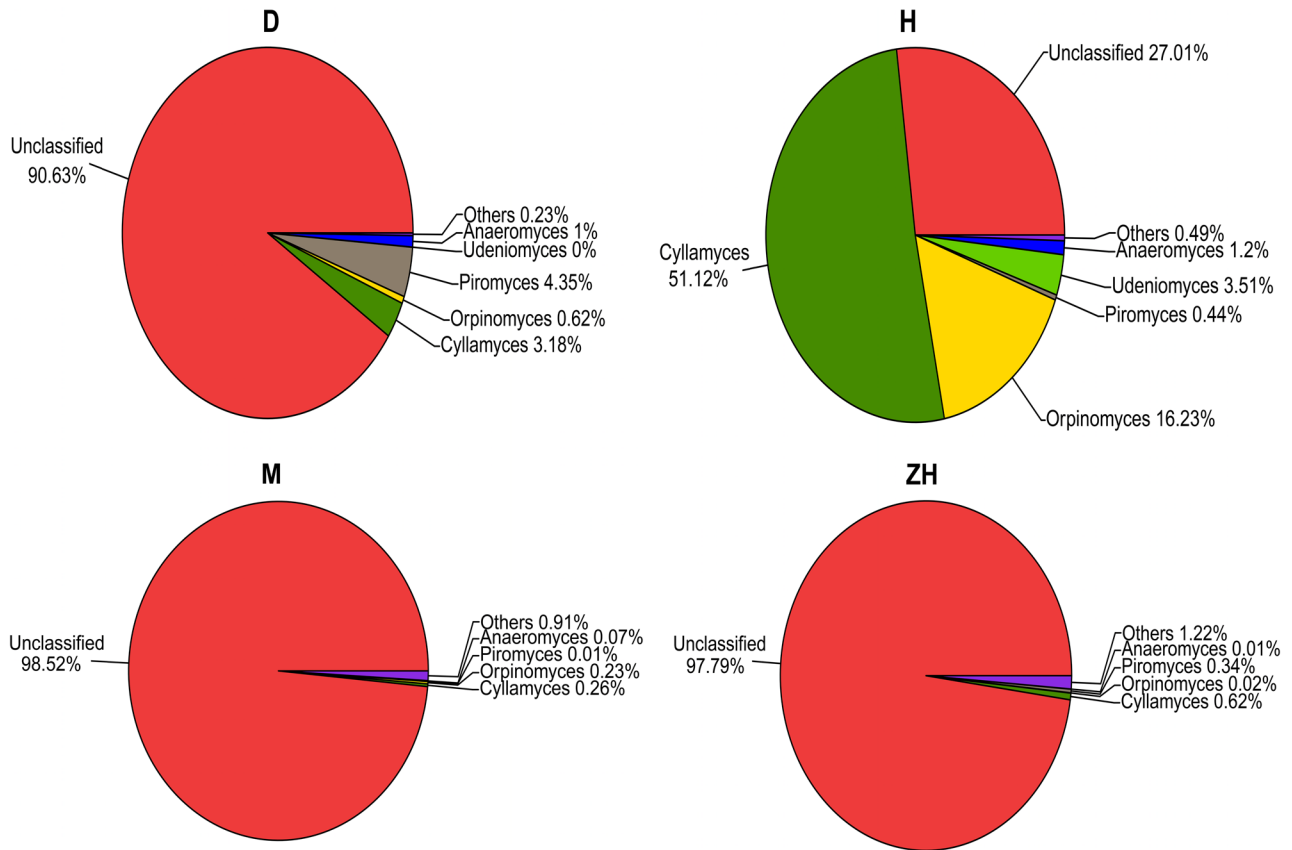


Fig. 2. Composition of rumen fungi genera. Others represent the abundance of rumen fungi lower than 1%.

D – gayals; H – Yunnan yellow cattle; M – yaks; ZH – Tibetan yellow cattle.

Cyllamyces, *Neocallimastix*, and *Orpinomyces*. In gayals, *Piromyces*, *Cyllamyces*, and *Anaeromyces* were the classified dominant rumen AF, accounting for 4.35%, 3.18%, and 1% of total sequences. *Cyllamyces* and *Orpinomyces* dominated in Yunnan yellow cattle, accounting for 51.12%, and 16.23% respectively. *Piromyces*, *Anaeromyces*, *Cyllamyces*, and *Orpinomyces* accounted for less than 1% of the total sequences in yaks and Tibetan yellow cattle. *Neocallimastix* was detected only in yaks and Tibetan yellow cattle and accounted for less than 0.01% of the total sequences. The most dominant genus was *Cyllamyces*, accounting for 32 146 sequences and 50.64% of the total *Neocallimastigaceae* sequences (Fig. 2). *Cyllamyces* accounted for 51.12% of the total sequences in Yunnan yellow cattle, was the second-most abundant (3.18%) in gayals, and the least abundant (0.26%) in yaks. *Piromyces* accounted for 4.35% of the total sequences in gayals, was the second-most abundant (0.44%) in Yunnan yellow cattle, and the least abundant (0.01%) in yaks. *Orpinomyces* accounted for 16.23% of the total sequences in Yunnan yellow cattle, was the second-most abundant (0.62%) in gayals, and the least abundant (0.02%) in Tibetan yellow cattle. *Anaeromyces* accounted for less than 1% of all species. *Udeniomyces* from Basidiomycota were detected only in Yunnan yellow cattle and comprised 3.51% of total sequences.

The hierarchical clustering heatmap analysis was performed at the class level based on the top 95 most abundant communities across the four cattle breeds (Fig. 4). Results were separated into five clusters. The abundance of *Anaeromyces*, *Orpinomyces*, *Piromyces*, and *Cyllamyces* was higher than for the other genera in the first cluster. In the second cluster, five fungal genera were more abundant in Yunnan yellow cattle compared to gayals, yaks, and Tibetan yellow cattle. In the third cluster, the unidentified class was the most abundant in gayals and yaks, with eight genera from Tibetan yellow cattle, which were more abundant than in gayals, yaks, and Yunnan yellow cattle. In yaks, 21 genera of fungi were more abundant than in gayals, Yunnan yellow cattle, and Tibetan yellow cattle in the fourth cluster. The 11 genera were the most dominant in gayals when compared to yaks, Tibetan yellow cattle, and Yunnan yellow cattle in the fifth cluster.

Discussion

The previous studies have shown that Illumina sequencing has a higher capacity to explore rumen bacteria diversity than culture-dependent methods (Peng et al. 2015). PCR amplification of universal primers for

conserved regions within the rRNA genes, followed by DNA sequencing of the internal transcribed spacer (ITS) is widely used in fungal identification studies (Pryce et al. 2006). Primers using ITS1 can avoid bias in PCR amplification and reliably study the fungal abundance and species richness (Bellemain et al. 2010). This study used the second-generation sequencing technology to investigate the structure and diversity of rumen fungi communities in four cattle breeds. The results provide new information about rumen fungi communities. The analysis showed that the dominant rumen fungi clusters, distribution, and abundance present major differences among the cattle breeds, location, and feeds.

Free-range ruminants that use grass as food may require more anaerobic fungal cellulase to aid digestion than domesticated ruminants. When compared with Yunnan yellow cattle, gayals, yak, and Tibetan yellow cattle have abundant rumen fungi sequences (Table I) and more unique OTUs (Fig. 1A). Analysis of ACE, Chao, and Simpson indexes showed that gayals, yaks and Tibetan yellow cattle had higher indexes than Yunnan yellow cattle, but the Shannon index was smaller than for Yunnan yellow cattle (Table I). These results suggest that free-range gayals and Tibetan cattle can have higher rumen fungi diversity than domesticated Yunnan cattle. Unclassified sequences were 90.63% for gayals, 98.52% for yaks, 97.79% for Tibetan yellow cattle, and 27.01% for Yunnan yellow cattle (Fig. 2), which was consistent with the heatmap analysis (Fig. 4). These results showed that the class levels could be divided into five clusters based on the top 95 genera. Many unidentified genera were distributed in the third cluster and were dominant in gayals, yaks, and Tibetan yellow cattle. These results indicated that free-range ruminants were more likely to have unknown yet fungi.

Animal species and location may be the important factors influencing the distribution and abundance of dominant rumen fungi clusters. Analysis of phylogenetic trees detected three dominant phyla rumen fungi: Ascomycota, Basidiomycota, and Neocallimastigomycota in the four cattle breeds in this study (Fig. 3), similar to the results of Zhang and Han studies (Zhang et al. 2017; Han et al. 2019). But the abundance of Neocallimastigomycota is superior to Ascomycota and Basidiomycota in this study, contrary to the results of the study on the cashmere goats (Han et al. 2019). However, Neocallimastigomycota predominates in the rumen, which is similar to the results on most ruminant rumen anaerobic fungi (Youssef et al. 2013; Wei et al. 2016; Rabee et al. 2018). A previous study showed that the genera of Ascomycota and Basidiomycota efficiently produce beta-glucanase (Mintz-Cole et al. 2013), possibly promoting the digestibility of feed, even though their abundance is low.

Different cattle breeds have different dominant rumen fungi clusters (Fig. 4) and the abundance of rumen fungi (Table I). *Anaeromyces* and *Piromyces*, *Orpinomyces*, and *Cyllamyces* were most abundant in gayals and Yunnan yellow cattle in the first cluster. Five genera of rumen fungi in Yunnan yellow cattle were more numerous than was shown for gayals, yaks, and Tibetan yellow cattle. The eight genera of rumen fungi in Tibetan yellow cattle were more numerous than in gayals, yaks, and Yunnan yellow cattle. The 21 genera of rumen AF in yaks were more numerous than in gayals, Yunnan yellow cattle, and Tibetan yellow cattle. Finally, the 11 genera of rumen fungi in gayals were more numerous than in Yunnan yellow cattle, Tibetan yellow cattle, and yaks in the clusters 2–5. *Piromyces*, *Cyllamyces*, and *Anaeromyces* were the most often classified abundant rumen AF in gayals (Fig. 2 and 3). These three representative genera were more prevalent in 19 ruminant and nonruminant animals (Liggenstoffer et al. 2010). However, in the other three cattle breeds, *Piromyces* accounted for less than 0.44% of the total sequences. *Cyllamyces* was the most abundant rumen AF genus in a previous report, accounting for 67% of total sequences in domesticated ruminants (Fliegerova et al. 2010). In our study, *Cyllamyces* was mainly found in Yunnan yellow cattle, accounting for 51.12% of the total sequences, and were more numerous than in gayals (3.18%), Tibetan yellow cattle (0.62%), and yaks (0.26%) (Fig. 2). *Cyllamyces* was also detected in American bison by Liggenstoffer et al. (2010) but the abundance was less than 0.7% of the total sequences, suggesting that *Cyllamyces* is more likely to be present in domesticated ruminants than other genera, which is consistent with Ozkose et al. (2001). We found two *Anaeromyces* species, *A. elegans* and *A. mucronatus* (Breton et al. 1990) that have high cellulolytic, xylanolytic, and glycoside hydrolase activities in different ruminant hosts. The β -xylosidase activities of *A. mucronatus* are higher in buffalo and endo-1,4- β -D-glucanohydrolase has the highest activity in alpaca (Fliegerova et al. 2002) and they are more effective at degrading the stem fragments of ryegrass than *Caecomyces* (Joblin et al. 2002). *Anaeromyces* occurred the least often in Tibetan yellow cattle, accounting for 0.01% of all sequences (Fig. 2). These findings were consistent with a previous study on the relationship of the abundance of *Piromyces* and *Anaeromyces* in crude feed and the host (Liggenstoffer et al. 2010). *Neocallimastix* accounted for less than 0.01% of the total sequences (Fig. 3) and was found only in yaks and Tibetan yellow cattle, which were selected from the Diqing Region. However, Kittelmann and coworkers have found that *Neocallimastix* is dominant in New Zealand cattle, accounting for 26.4% of all sequences (Kittelmann et al. 2012). This result indicates that the abundance of *Neocallimastix* may be related to cattle breeds or habitat.

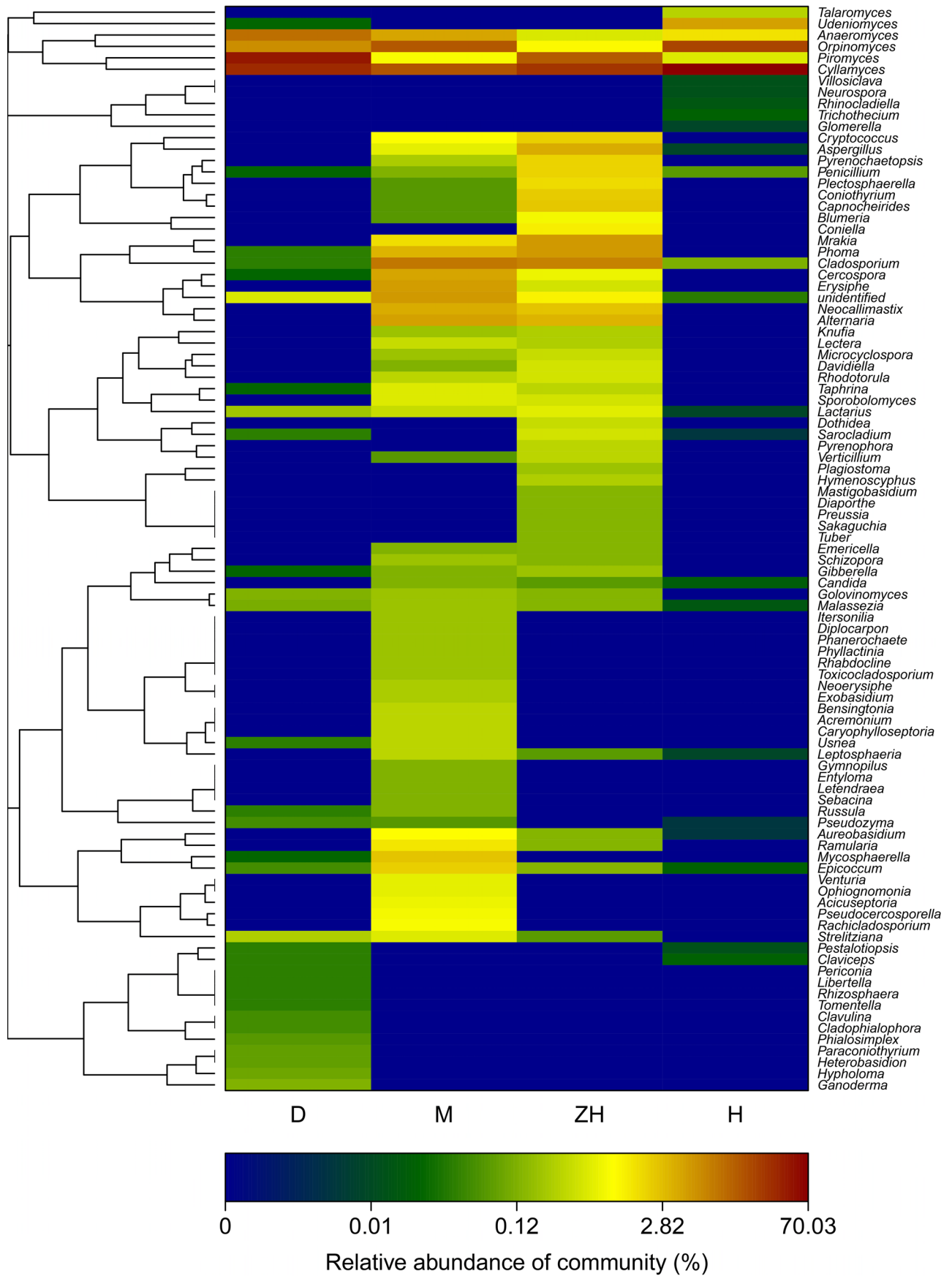


Fig. 4. Heatmap formed using the Bray-Curtis algorithm and the complete linkage method. The heatmap-plot describes the relative percentage of each fungal class within each cattle breed. Relative values for the fungal class are indicated by color intensity.

D – gayals; H – Yunnan yellow cattle; M – yaks; ZH – Tibetan yellow cattle.

Diet can also be an important factor. Han and coworkers research has shown that the concentrated feed has an important impact on the anaerobic fungal population of cashmere goats AF (Han et al. 2019). AF secrete a range of cell wall degrading enzymes such as free enzymes and cellulase multienzyme complexes (Cheng et al. 2018), which are effective degradation products of plant biomass (Haitjema et al. 2014). Screening of all rumen microbial CAZyme transcripts indicated that the AF of Neocallimastigaceae produced the largest share of cellulase transcripts (Söllinger et al. 2018). The studies have shown that *Orpinomyces* R001 and *Neocallimastix* M010 AF exhibit high digestion efficiency in the cell walls of straw silage and can cause the disappearance of *in situ* dry matter (Lee et al. 2015). The co-culture of *Neocallimastix frontalis* and *Methanobrevibacter ruminantium* showed high polysaccharide hydrolase (xylanase and FPase) and esterase activity (Wei et al. 2016). *Piromyces* sp. UH3-1 recognizes the secretion of lignin-regulating enzymes by the fungal pathway and is capable of producing a more efficient enzyme mixture (Hooker et al. 2018). Denman and coworkers have found that *Orpinomyces* had higher abundance with grain feed compared to fiber diets (Denman et al. 2008). However, another study found that the activity of cellulases and xylanases of *Orpinomyces* are related to the presence of *Neocallimastix* genus (Li et al. 1997). The biofortification of *Orpinomyces* sp. can significantly increase methane production (Akyol et al. 2019). In our study, *Orpinomyces* accounted for 16.23% of the total sequences in Yunnan yellow cattle and were more numerous than in gayals (0.62%), yaks (0.23%), and Tibetan yellow cattle (0.02%) (Fig. 2). This study suggested that *Orpinomyces* tended to be found in domesticated ruminants with easily digested diets.

This study found a large difference in rumen fungi abundance among four cattle breeds. Rumen fungi diversity and composition were mainly related to diet, and the use of its components depends on enzyme activity and quantity produced by these fungi. To better understand the relationship between fungal composition and function and the ruminant growth, as well as to extract cellulases from rumen fungi, the metagenomic and metatranscriptomic analyses should be used in future studies.

Ethical approval

All animal care procedures were approved and authorized by the animal ethics committee of Yunnan Agricultural University.

Acknowledgments

This study was financed by the National Natural Science Foundation of China (Project No: 31672452), the Key Research and Development Plan Project of Yunnan province (Project No: 2018BB001-2), and the Foundation of Yunnan Provincial Key

Laboratory of Animal and Feed Science (Project No: DYCX2015001) are acknowledged with gratitude.

Conflict of interest

The authors do not report any financial or personal connections with other persons or organizations, which might negatively affect the contents of this publication and/or claim authorship rights to this publication.

Literature

- Akyol, Ince O, Bozan M, Ozbayram EG, Ince B. Fungal bioaugmentation of anaerobic digesters fed with lignocellulosic biomass: what to expect from anaerobic fungus *Orpinomyces* sp. *Bioresour Technol.* 2019 Apr;277:1–10. <https://doi.org/10.1016/j.biortech.2019.01.024>
- An D, Dong X, Dong Z. Prokaryote diversity in the rumen of yak (*Bos grunniens*) and Jinnan cattle (*Bos taurus*) estimated by 16S rDNA homology analyses. *Anaerobe.* 2005 Aug;11(4):207–215. <https://doi.org/10.1016/j.anaerobe.2005.02.001>
- Bauchop T. The rumen anaerobic fungi: colonizers of plant fibre. *Ann Rech Vet.* 1979;10(2-3):246–248.
- Bellemain E, Carlsen T, Brochmann C, Coissac E, Taberlet P, Kauserud H. ITS as an environmental DNA barcode for fungi: an *in silico* approach reveals potential PCR biases. *BMC Microbiol.* 2010;10(1):189–197. <https://doi.org/10.1186/1471-2180-10-189>
- Breton A, Bernalier A, Dusser M, Fonty GÁ, Gaillard-Martinie B, Guillot J. *Anaeromyces mucronatus* nov. gen., nov. sp. A new strictly anaerobic rumen fungus with polycentric thallus. *FEMS Microbiol Lett.* 1990 Jul;70(2):177–182. <https://doi.org/10.1111/j.1574-6968.1990.tb13974.x>
- Brookman JL, Theodorou MK, Trinci APJ, Mennim G, Tuckwell DS. Identification and characterization of anaerobic gut fungi using molecular methodologies based on ribosomal ITS1 and 18S rRNA. *Microbiology.* 2000 Feb 01;146(2):393–403. <https://doi.org/10.1099/00221287-146-2-393>
- Campa D, Tavanti A, Gemignani F, Mogavero CS, Bellini I, Bottari F, Barale R, Landi S, Senesi S. DNA microarray based on arrayed-primer extension technique for identification of pathogenic fungi responsible for invasive and superficial mycoses. *J Clin Microbiol.* 2008 Mar 01;46(3):909–915. <https://doi.org/10.1128/JCM.01406-07>
- Cheng Y, Shi Q, Sun R, Liang D, Li Y, Li Y, Jin W, Zhu W. The biotechnological potential of anaerobic fungi on fiber degradation and methane production. *World J Microbiol Biotechnol.* 2018 Oct; 34(10):155–162. <https://doi.org/10.1007/s11274-018-2539-z>
- Dagar SS, Kumar S, Griffith GW, Edwards JE, Callaghan TM, Singh R, Nagpal AK, Puniya AK. A new anaerobic fungus (*Oontomyces anksri* gen. nov., sp. nov.) from the digestive tract of the Indian camel (*Camelus dromedarius*). *Fungal Biol.* 2015a Aug;119(8): 731–737. <https://doi.org/10.1016/j.funbio.2015.04.005>
- Dagar SS, Singh N, Goel N, Kumar S, Puniya AK. Role of anaerobic fungi in wheat straw degradation and effects of plant feed additives on rumen fermentation parameters *in vitro*. *Benef Microbes.* 2015b Jan;6(3):353–360. <https://doi.org/10.3920/BM2014.0071>
- Deng W, Wang L, Ma S, Jin B, He T, Yang Z, Mao H, Wanapat M. Comparison of Gayal (*Bos frontalis*) and Yunnan yellow cattle (*Bos taurus*): rumen function, digestibilities and nitrogen balance during feeding of pelleted lucerne (*Medicago sativum*). *Asian-Australas J Anim Sci.* 2007 Jun 1;20(6):900–907. <https://doi.org/10.5713/ajas.2007.900>
- Denman SE, Nicholson MJ, Brookman JL, Theodorou MK, McSweeney CS. Detection and monitoring of anaerobic rumen

- fungi using an ARISA method. *Lett Appl Microbiol.* 2008 Dec;47(6):492–499. <https://doi.org/10.1111/j.1472-765X.2008.02449.x>
- Elekwachi CO, Wang Z, Wu X, Rabee A, Forster RJ.** Total rRNA-Seq analysis gives insight into bacterial, fungal, protozoal and archaeal communities in the rumen using an optimized RNA isolation method. *Front Microbiol.* 2017 Sep 21;8:1814–1827. <https://doi.org/10.3389/fmicb.2017.01814>
- Fliegerov K, Mrázek J, Hoffmann K, Zábransk J, Voigt K.** Diversity of anaerobic fungi within cow manure determined by ITS1 analysis. *Folia Microbiol (Praha).* 2010 Jul;55(4):319–325. <https://doi.org/10.1007/s12223-010-0049-y>
- Fliegerov K, Pažoutov S, Mrázek J, Kopečn J.** Special properties of polycentric anaerobic fungus *Anaeromyces mucronatus*. *Acta Vet Brno.* 2002;71(4):441–444. <https://doi.org/10.2754/avb200271040441>
- Griffith GW, Callaghan TM, Podmirseg SM, Hohlweck D, Edwards JE, Puniya AK, Dagar SS.** *Buwchfawromyces eastonii* gen. nov., sp. nov.: a new anaerobic fungus (Neocallimastigomycota) isolated from buffalo faeces. *MycKeys.* 2015 Mar 04;9:11–28. <https://doi.org/10.3897/mycokeys.9.9032>
- Gruninger RJ, Nguyen TTM, Reid ID, Yanke JL, Wang P, Abbott DW, Tsang A, McAllister T.** Application of transcriptomics to compare the carbohydrate active enzymes that are expressed by diverse genera of anaerobic fungi to degrade plant cell wall carbohydrates. *Front Microbiol.* 2018 Jul 16;9:1581–1595. <https://doi.org/10.3389/fmicb.2018.01581>
- Gruninger RJ, Puniya AK, Callaghan TM, Edwards JE, Youssef N, Dagar SS, Fliegerova K, Griffith GW, Forster R, Tsang A, et al.** Anaerobic fungi (phylum *Neocallimastigomycota*): advances in understanding their taxonomy, life cycle, ecology, role and biotechnological potential. *FEMS Microbiol Ecol.* 2014 Oct;90(1):1–17. <https://doi.org/10.1111/1574-6941.12383>
- Haitjema CH, Solomon KV, Henske JK, Theodorou MK, O'Malley MA.** Anaerobic gut fungi: advances in isolation, culture, and cellulolytic enzyme discovery for biofuel production. *Biotechnol Bioeng.* 2014 Aug;111(8):1471–1482. <https://doi.org/10.1002/bit.25264>
- Han X, Li B, Wang X, Chen Y, Yang Y.** Effect of dietary concentrate to forage ratios on ruminal bacterial and anaerobic fungal populations of cashmere goats. *Anaerobe.* 2019 Oct;59(59):118–125. <https://doi.org/10.1016/j.anaerobe.2019.06.010>
- Hanafy RA, Elshahed MS, Ligginstoffer AS, Griffith GW, Youssef NH.** *Pecoromyces ruminantium*, gen. nov., sp. nov., an anaerobic gut fungus from the feces of cattle and sheep. *Mycologia.* 2017 Mar 04;109(2):231–243. <https://doi.org/10.1080/00275514.2017.1317190>
- Hanafy RA, Elshahed MS, Youssef NH.** *Feromyces austinii*, gen. nov., sp. nov., an anaerobic gut fungus from rumen and fecal samples of wild Barbary sheep and fallow deer. *Mycologia.* 2018 May 04;110(3):513–525. <https://doi.org/10.1080/00275514.2018.1466610>
- Hibbett DS, Binder M, Bischoff JF, Blackwell M, Cannon PF, Eriksson OE, Huhndorf S, James T, Kirk PM, Lücking R, et al.** A higher-level phylogenetic classification of the Fungi. *Mycol Res.* 2007 May;111(5):509–547. <https://doi.org/10.1016/j.mycres.2007.03.004>
- Ho YW, Barr DJS.** Classification of anaerobic gut fungi from herbivores with emphasis on rumen fungi from Malaysia. *Mycologia.* 1995 Sep;87(5):655–677. <https://doi.org/10.1080/00275514.1995.12026582>
- Hooker CA, Hillman ET, Overton JC, Ortiz-Velez A, Schacht M, Hunnicutt A, Mosier NS, Solomon KV.** Hydrolysis of untreated lignocellulosic feedstock is independent of S-lignin composition in newly classified anaerobic fungal isolate, *Piromyces* sp. UH3-1. *Biotechnol Biofuels.* 2018 Dec;11(1):293–306. <https://doi.org/10.1186/s13068-018-1292-8>
- Jami E, Israel A, Kotser A, Mizrahi I.** Exploring the bovine rumen bacterial community from birth to adulthood. *ISME J.* 2013 Jun;7(6):1069–1079. <https://doi.org/10.1038/ismej.2013.2>
- Joblin KN, Matsui H, Naylor GE, Ushida K.** Degradation of fresh ryegrass by methanogenic co-cultures of ruminal fungi grown in the presence or absence of *Fibrobacter succinogenes*. *Curr Microbiol.* 2002 Jul 1;45(1):46–53. <https://doi.org/10.1007/s00284-001-0078-5>
- Kameshwar AKS, Qin W.** Genome wide analysis reveals the extrinsic cellulolytic and biohydrogen generating abilities of *Neocallimastigomycota* fungi. *J Genomics.* 2018;6:74–87. <https://doi.org/10.7150/jgen.25648>
- Kittelmann S, Naylor GE, Koolaard JP, Janssen PH.** A proposed taxonomy of anaerobic fungi (class Neocallimastigomycetes) suitable for large-scale sequence-based community structure analysis. *PLoS One.* 2012 May 16;7(5):e36866. <https://doi.org/10.1371/journal.pone.0036866>
- Köljal U, Nilsson RH, Abarenkov K, Tedersoo L, Taylor AFS, Bahram M, Bates ST, Bruns TD, Bengtsson-Palme J, Callaghan TM, et al.** Towards a unified paradigm for sequence-based identification of fungi. *Mol Ecol.* 2013 Nov;22(21):5271–5277. <https://doi.org/10.1111/mec.12481>
- Lee SM, Guan LL, Eun JS, Kim CH, Lee SJ, Kim ET, Lee SS.** The effect of anaerobic fungal inoculation on the fermentation characteristics of rice straw silages. *J Appl Microbiol.* 2015 Mar;118(3):565–573. <https://doi.org/10.1111/jam.12724>
- Lee SS, Ha JK, Cheng KJ.** Relative contributions of bacteria, protozoa, and fungi to *in vitro* degradation of orchard grass cell walls and their interactions. *Appl Environ Microbiol.* 2000 Sep 01;66(9):3807–3813. <https://doi.org/10.1128/AEM.66.9.3807-3813.2000>
- Leng J, Cheng YM, Zhang CY, Zhu RJ, Yang SL, Gou X, Deng WD, Mao HM.** Molecular diversity of bacteria in Yunnan yellow cattle (*Bos taurus*) from Nujiang region, China. *Mol Biol Rep.* 2012 Feb;39(2):1181–1192. <https://doi.org/10.1007/s11033-011-0848-5>
- Li XL, Chen H, Ljungdahl LG.** Monocentric and polycentric anaerobic fungi produce structurally related cellulases and xylanases. *Appl Environ Microbiol.* 1997 Feb;63(2):628–635.
- Ligginstoffer AS, Youssef NH, Couger MB, Elshahed MS.** Phylogenetic diversity and community structure of anaerobic gut fungi (phylum Neocallimastigomycota) in ruminant and non-ruminant herbivores. *ISME J.* 2010 Oct;4(10):1225–1235. <https://doi.org/10.1038/ismej.2010.49>
- Man B, Wang H, Yun Y, Xiang X, Wang R, Duan Y, Cheng X.** Diversity of fungal communities in Heshang Cave of Central China revealed by Mycobiome-Sequencing. *Front Microbiol.* 2018 Jul 16;9:1400–1414. <https://doi.org/10.3389/fmicb.2018.01400>
- Mintz-Cole RA, Brandt EB, Bass SA, Gibson AM, Reponen T, Khurana Hershey GK.** Surface availability of beta-glucans is critical determinant of host immune response to *Cladosporium cladosporioides*. *J Allergy Clin Immunol.* 2013 Jul;132(1):159–169.e2. <https://doi.org/10.1016/j.jaci.2013.01.003>
- Oliver JP, Schilling JS.** Harnessing fungi to mitigate CH₄ in natural and engineered systems. *Appl Microbiol Biotechnol.* 2018 Sep;102(17):7365–7375. <https://doi.org/10.1007/s00253-018-9203-2>
- Orpin CG.** Studies on the rumen flagellate *Neocallimastix frontalis*. *J Gen Microbiol.* 1975 Dec 01;91(2):249–262. <https://doi.org/10.1099/00221287-91-2-249>
- Ozkose E, Thomas BJ, Davies DR, Griffith GW, Theodorou MK.** *Cyllamyces aberensis* gen.nov. sp.nov., a new anaerobic gut fungus with branched sporangiophores isolated from cattle. *Can J Bot.* 2001;79(6):666–673. <https://doi.org/10.1139/b01-047>
- Peng S, Yin J, Liu X, Jia B, Chang Z, Lu H, Jiang N, Chen Q.** First insights into the microbial diversity in the omasum and

- reticulum of bovine using Illumina sequencing. *J Appl Genet*. 2015 Aug;56(3):393–401.
<https://doi.org/10.1007/s13353-014-0258-1>
- Pryce TM, Palladino S, Price DM, Gardam DJ, Campbell PB, Christiansen KJ, Murray RJ.** Rapid identification of fungal pathogens in BacT/ALERT, BACTEC, and BBL MGIT media using polymerase chain reaction and DNA sequencing of the internal transcribed spacer regions. *Diagn Microbiol Infect Dis*. 2006 Apr; 54(4):289–297.
<https://doi.org/10.1016/j.diagmicrobio.2005.11.002>
- Rabee AE, Forster RJ, Elekwachi CO, Kewan KZ, Sabra EA, Shawket SM, Mahrous HA, Khamiss OA.** Community structure and fibrolytic activities of anaerobic rumen fungi in dromedary camels. *J Basic Microbiol*. 2019 Jan;59(1):101–110.
<https://doi.org/10.1002/jobm.201800323>
- Schloss PD, Gevers D, Westcott SL.** Reducing the effects of PCR amplification and sequencing artifacts on 16S rRNA-based studies. *PLoS One*. 2011 Dec 14;6(12):e27310.
<https://doi.org/10.1371/journal.pone.0027310>
- Sirohi SK, Choudhury PK, Puniya AK, Singh D, Dagar SS, Singh N.** Ribosomal ITS1 sequence-based diversity analysis of anaerobic rumen fungi in cattle fed on high fiber diet. *Ann Microbiol*. 2013 Dec;63(4):1571–1577.
<https://doi.org/10.1007/s13213-013-0620-2>
- Söllinger A, Tveit AT, Poulsen M, Noel SJ, Bengtsson M, Bernhardt J, Frydendahl Hellwing AL, Lund P, Riedel K, Schleper C, et al.** Holistic assessment of rumen microbiome dynamics through quantitative metatranscriptomics reveals multifunctional redundancy during key steps of anaerobic feed degradation. *mSystems*. 2018 Aug 07;3(4):e00038-18.
<https://doi.org/10.1128/mSystems.00038-18>
- Wei YQ, Long RJ, Yang H, Yang HJ, Shen XH, Shi RF, Wang ZY, Du JG, Qi XJ, Ye QH.** Fiber degradation potential of natural co-cultures of *Neocallimastix frontalis* and *Methanobrevibacter ruminantium* isolated from yaks (*Bos grunniens*) grazing on the Qinghai Tibetan Plateau. *Anaerobe*. 2016 Jun;39:158–164.
<https://doi.org/10.1016/j.anaerobe.2016.03.005>
- Youssef NH, Couger MB, Struchtemeyer CG, Liggenstoffer AS, Prade RA, Najjar FZ, Atiyeh HK, Wilkins MR, Elshahed MS.** The genome of the anaerobic fungus *Orpinomyces* sp. strain C1A reveals the unique evolutionary history of a remarkable plant biomass degrader. *Appl Environ Microbiol*. 2013 Aug 01;79(15):4620–4634.
<https://doi.org/10.1128/AEM.00821-13>
- Zhang J, Shi H, Wang Y, Li S, Cao Z, Ji S, He Y, Zhang H.** Effect of dietary forage to concentrate ratios on dynamic profile changes and interactions of ruminal microbiota and metabolites in Holstein heifers. *Front Microbiol*. 2017 Nov 09;8:2206–2223.
<https://doi.org/10.3389/fmicb.2017.02206>

New Look on Antifungal Activity of Silver Nanoparticles (AgNPs)

BARBARA ŻAROWSKA¹, TOMASZ KOŹLECKI², MICHAŁ PIEGZA^{*1},
KATARZYNA JAROS-KOŹLECKA³ and MAŁGORZATA ROBAK^{1*}

¹Department of Biotechnology and Food Microbiology, Wrocław University of Environmental and Life Sciences,
Wrocław, Poland

²Department of Chemical Engineering, Wrocław University of Technology, Wrocław, Poland

³TK Nano, Wrocław, Poland

Submitted 12 June 2019, revised 18 October 2019, accepted 19 October 2019

Abstract

The progress of research on silver nanoparticles (AgNPs) has led to their inclusion in many consumer products (chemicals, cosmetics, clothing, water filters, and medical devices) as a biocide. Despite the widespread use of AgNPs, their biocidal activity is not yet fully understood and is usually associated with various factors (size, composition, surface, red-ox potential, and concentration) and, obviously, specific features of microorganisms. There are merely a few studies concerning the interaction of molds with AgNPs. Therefore, the determination of the minimal AgNPs concentration required for effective growth suppression of five fungal species (*Paecilomyces variotii*, *Penicillium pinophilum*, *Chaetomium globosum*, *Trichoderma virens*, and *Aspergillus brasiliensis*), involved in the deterioration of construction materials, was particularly important. Inhibition of bacteria (*Pseudomonas aeruginosa*, *Staphylococcus aureus*, and *Escherichia coli*) and yeasts (*Candida albicans* and *Yarrowia lipolytica*) was also assessed as the control of AgNPs effectiveness. AgNPs at the concentrations of 9–10.7 ppm displayed high inhibitory activity against moulds, yeast, and bacteria. The TEM images revealed that 20 nm AgNPs migrated into bacterial, yeast, and fungal cells but aggregated in larger particles (50–100 nm) exclusively inside eukaryotic cells. The aggregation of 20 nm AgNPs and particularly their accumulation in the cell wall, observed for *A. brasiliensis* cells, are described here for the first time.

Key words: silver nanoparticles, antimicrobial activity, *Paecilomyces*, *Chaetomium*, *Trichoderma*, building materials, TEM images, BioscreenC

Introduction

Nowadays nanomaterials within the size of 1–100 nm in at least one dimension with the novel, size-related properties have attracted the attention of many researchers in the area of chemistry, physics, material sciences, medicine, microbiology, and biotechnology (Rai et al. 2009, 2015; Tran et al. 2013). Silver nanoparticles (AgNPs) are one of the most commonly used engineered nanoproducts known for their antimicrobial activity (Kim et al. 2007; Rai et al. 2009; Martinez-Gutierrez et al. 2010). The progress in research led to the inclusion of nanoparticles as biocides in a large number of consumer products: chemicals, cosmetics, clothing, water filters, and medical devices (Kokura et al. 2010; Metak and Ajaal 2013; Zarschler et al. 2016). The application of AgNPs as a contrast agent for mammography

and micro-computed tomography for the ear imaging is based on their electric properties (Anil Kumar et al. 2007; Zou et al. 2015; Zhang et al. 2016b; Lee and Jun 2019). Despite their widespread use, the biocidal activity of AgNPs is not fully understood and the prevalence of either positive or negative effects on humans and the environment are discussed (Bartłomiejczyk et al. 2013; Flores-López et al. 2019).

The nature and the level of AgNPs' molecular cytotoxicity are related to various factors: size, composition, surface area, charge, red-ox potential, and concentration (McShan et al. 2014; Riaz et al. 2017). In general, AgNPs at the concentrations lower than 25–30 ppm do not exhibit toxicity for mammalian cells (Milic et al. 2015; Zhang et al. 2016a). However, some cytostatic and anti-cancer activity is reported at these concentrations (AshaRani et al. 2009). Antibacterial activity of AgNPs

* Corresponding authors: M. Piegza, Department of Biotechnology and Food Microbiology, Wrocław University of Environmental and Life Sciences, Wrocław, Poland; e-mail: michal.piegza@upwr.edu.pl
M. Robak, Department of Biotechnology and Food Microbiology, Wrocław University of Environmental and Life Sciences, Wrocław, Poland; e-mail: malgorzata.robak@upwr.edu.pl

© 2019 Barbara Żarowska et al.

This work is licensed under the Creative Commons Attribution-NonCommercial-NoDerivatives 4.0 License (<https://creativecommons.org/licenses/by-nc-nd/4.0/>).

is rather well documented in the literature, mainly against the following species: *Staphylococcus aureus*, *Bacillus subtilis*, *Pseudomonas aeruginosa*, and *Escherichia coli* (Yoon et al. 2007; Li et al. 2010; Guzman et al. 2012, Kanawaria et al. 2018). Some information concerning growth inhibition of other bacteria (*Enterococcus* spp.) and yeast (*Candida albicans*) by nanosilver is also available (Kim et al. 2007; Roe et al. 2008; Lara et al. 2015). However, the studies of AgNPs interaction with cell structures of bacteria and yeasts are scarce. Only in few reports the location of AgNPs inside *C. albicans* cells was demonstrated under transmission electron microscopy (TEM) or scanning electron microscopy (SEM) (Kim et al. 2009; Radhakrishnan et al. 2018).

In opposite to bacteria and yeasts, the research on the interactions of AgNPs with filamentous fungi (molds) is still evolving (Kanawaria et al. 2018). The results on AgNPs' effects on fungal growth already reported concern mainly dermatophytes and phytopathogens (Jo et al. 2009; Pulit et al. 2013; Xu et al. 2013), not the molds found in houses or the air. Studies of AgNPs interaction with species involved in biodeterioration of buildings and construction materials are scarce. The degradation of house construction materials could be observed as the action of moulds from *Aspergillus*, *Penicillium*, *Paecilomyces*, *Trichoderma*, and *Chaetomium* genera (Łukaszuk et al. 2011; Kobiałka et al. 2019). Species of those genera are commonly used in the normalized test of resistance to microbial corrosion of construction material components (PN-EN ISO 846, 2002).

The aim of the study was to determine the minimal AgNPs concentrations required for effective growth inhibition of the selected fungal species (possibly occurring as biodeterioration agents) and two unconventional yeast species (*Yarrowia lipolytica* and *C. albicans*). The selected bacterial species: *S. aureus*, *E. coli*, and *P. aeruginosa* that may cause human infections were used to control the effectiveness of the AgNPs tested. The analysis of microbial growth was performed in the microbiological analyzer Bioscreen C (Automated Growth Curve Analysis System, Lab systems, Finland) what allowed for a precise determination (for each species) the inhibitory concentration of AgNPs. TEM was used to localize the AgNPs inside microbial cells and to visualize their aggregation in eukaryotic cells and particular accumulation in the cell wall of *A. brasiliensis*.

Experimental

Materials and Methods

Nanoparticles. AgNPs have been synthesized by the TK Nano according to the procedure described by Koźlecki et al. (2011). The final concentration of

nanoparticles was 107.2 ± 0.8 mg/l. Nanoparticles were characterized by dynamic light scattering (DLS) and TEM. The DLS measurements were performed using a Photocor Complex apparatus (Photocor Instruments), equipped with a 28 mW (657 nm) laser and 288-channel autocorrelator, operating in multi-tau mode. The measurements were carried out in 14.8 mm ID round cells, submerged in analytical grade decalin (Fisher Scientific), as an index-matching liquid; the scattering angle was set at 110° , and the temperature of measurements was fixed at $298 \pm 0.05^\circ\text{K}$. The data analysis was performed with DynaLS ver. 2.8.3 software (Alango Ltd.), using a method similar to the CONTIN algorithm, but more aggressive concerning the noise (Song et al. 2011; Echegoyen and Nerin 2013; Wen et al. 2016).

The imaging with TEM was carried out with a Zeiss EM900 microscope (Carl Zeiss AG). Samples were dipped on a 300-nickel mesh, coated with Formvar (SPI Supplies), and then dried thoroughly. Microphotographs were recorded on photographic film and then scanned using a flatbed scanner with 800×800 DPI resolution (Hewlett-Packard). The images were processed using ImageJ ver. 1.50i software (Pal et al. 2007; Bundschunh et al. 2016; Koziróg et al. 2016).

Microorganisms. Microorganisms used in the study were obtained from the Deutsche Sammlung von Microorganismen und Zellkulturen (DSMZ), and the Microorganisms Collection of the Department of Biotechnology and Food Microbiology (KBiMŻ) at Wrocław University of Environmental and Life Sciences (*Aspergillus brasiliensis* DSMZ1988, *Penicillium pinophilum* DSMZ1944, *Paecilomyces variotii* DSMZ1961, *Trichoderma virens* DSMZ1963, *Chaetomium globosum* DSMZ1962, *Candida albicans* DSMZ1386, *Yarrowia lipolytica* KBiMŻ A101, *Escherichia coli* KBiMŻ, *Pseudomonas aeruginosa* DSMZ939, and *Staphylococcus aureus* subsp. *aureus* DSMZ799).

Petri dishes assay: the plate agar tests on solid medium. Filamentous fungi were cultivated on the surface of a medium composed of 30 g glucose, 2 g NaNO_3 , 0.7 g KH_2PO_4 , 0.3 g K_2HPO_4 , 0.5 g KCl, 0.5 g $\text{MgSO}_4 \times 7\text{H}_2\text{O}$, 0.01 g $\text{MnSO}_4 \times 7\text{H}_2\text{O}$, and 2g agar per 1 l of distilled water. The pH was set to 6.0–6.5 before autoclaving. AgNPs were added directly into Petri dishes before pouring sterilized medium in the following volumes of the stock suspension ($107 \text{ mg/l} = 107 \text{ ppm}$): 0, 0.5, 1 and 5 ml, corresponding to 0 or 2.14, 4.28, and 21.4 mg of AgNPs. On the solidified media, 0.05 ml of the suspension of fungal spores at the concentration of 10^5 CFU/ml was applied to the center of Petri dishes. After incubation for 192 h at 25°C , the diameters of the developed fungal colonies were measured and compared to those observed in medium without AgNPs. The analyses were performed in triplicate for each species of filamentous fungi.

Bioscreen C: the bioassay in liquid media. Biological activity of silver nanoparticles in liquid media was tested on the three groups of microorganisms (bacteria, yeasts, and filamentous fungi). The bacterial cultures were carried out in a liquid broth consisting of 15 g of dry bullion (Biocorp) and 10 g of glucose dissolved in 1 liter of distilled water. Cultures of yeast and fungi were performed in YPG medium composed of 10 g yeast extract, 10 g bacteriological peptone, and 10 g glucose per 1 liter of distilled water. The tests were performed in the automated Bioscreen C system (Automated Growth Curve Analysis System, Lab systems, Finland). The culture volume in the wells of the Bioscreen C was 300 μ l, which comprised 250 μ l of culture medium, 20 μ l of cell suspension (final concentration 10^8 CFU/ml) and 30 μ l of the AgNP stock suspension to the final concentration of 10.7 mg/l. The temperature was maintained at 28°C, and the optical density (OD) of the cell suspensions was measured automatically at 560–600 nm at regular intervals of 30 min during 72–96 hours of cultivation under constant agitation. Each culture variant was performed in 5–10 replications.

The data obtained were analyzed using the spreadsheet software (Microsoft Excel 97) and mean values were calculated from replicates for each cultured microorganism. The overall standard deviation did not exceed 15% (Robak 2007). The mean values were used for plotting growth curves for each strain studied, as the function of the incubation time and OD of the culture. The resultant growth curves were compared to control media.

After the Bioscreen C measurements, the cultures were collected and 1 ml of each sample transferred to 2 ml Eppendorf tubes, centrifuged for 10 min at 2000 \times g, using a Spectrafuge Mini Centrifuge (Labnet International), then 0.7 ml of supernatant was placed on a Costar Spin-X 0.2 μ m filter with polyamide membrane

(Corning Inc.), and centrifuged again at 2000 \times g for 10 min to remove the residual cell debris. The permeate (0.5 ml) was diluted with 1 ml of deionized water and measured using a DLS instrument as described above.

TEM observations of microorganisms and AgNPs. Biological material obtained after removal of the residual medium by centrifugation for 10 min at 2000 \times g was fixed with 2.5% glutaraldehyde and buffered with 0.1 M cacodylate buffer overnight at 4°C. Subsequently, the material was washed three times in 0.1 M cacodylate buffer, followed by post-fixation in 2% osmium tetroxide/1.5% potassium ferricyanide in 0.1 M cacodylate buffer for 1 h at 4°C. Afterward, the material was washed three times with buffer and two times with ultrapure water by centrifugation at 600 \times g for 5 min. Subsequently, the material was incubated with 1% uranyl acetate in ultrapure water overnight at 4°C. Then, the samples were washed three times with ultrapure water and dehydrated using a graded ethanol series (from 30% to 99.9%), followed by infiltration with Epon 812 resin (by replacing the pure ethanol with 1:1 ethanol to resin ratio for 2 h, followed by pure resin). Sample blocks were polymerized for 24 h at 60°C. Ultrathin sections were prepared using an ultramicrotome and glass knife (Leica EM UC7). The preparations were observed using a field-emission scanning electron microscope (FE-SEM, Auriga60, Zeiss) employing a STEM detector, at 20 kV acceleration voltages.

Results and discussion

Characterization of nanoparticles. The AgNPs were obtained at the concentration of 107.2 mg/l as electrostatically stabilized monodispersed spherical structures (Fig. 1A). The average nanoparticle diameter,

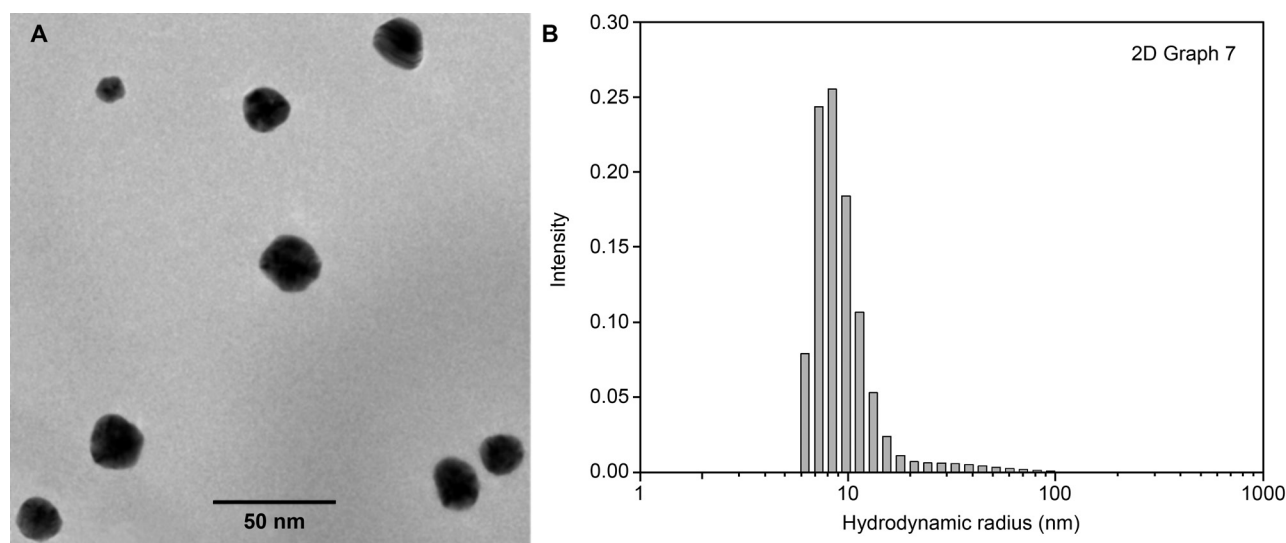


Fig. 1. Nanoparticles' shape (A) and dimensions (B).

Table I
AgNP inhibition of the filamentous fungi growth.

Fungal species	AgNPs in the medium [mg/l]			
	0	2.14	4.28	21.4
Growth [%]				
<i>Aspergillus brasiliensis</i>	100	100	83.1	3.74
<i>Trichoderma virens</i>	100	100	33.9	9.72
<i>Paecilomyces variotii</i>	100	100	0	0
<i>Penicillium pinophilum</i>	100	57.3	44.8	0
<i>Chaetomium globosum</i>	100	63.9	61.2	0

as determined with the dynamic light scattering (DLS) analysis, was 20 nm (Fig. 1B).

Microbiological analysis. The biocidal activity of AgNPs towards five species of filamentous fungi, two yeasts, and two bacterial species was evaluated. Two types of microbial growth analyses were performed: the cultivation on solid agar medium (Petri dishes) and in liquid media (Bioscreen C). The former type of growth is suitable for observation of the size of fungal colonies and the latter allows for the determination of the density of cells and hyphae during micro-batch cultures in Bioscreen C, measured every 30 minutes as an optical density (OD).

Evaluation of filamentous fungal growth on solid agar medium. Inhibition of fungal growth by AgNPs was observed for each of five tested species, however, to a different extent (Table I). The growth of *P. variotii* was completely inhibited by 4.28 mg/l of AgNPs (4.28 ppm). This concentration of nanosilver in the medium had a lower inhibitory effect on the growth of *T. virens* (66%), *P. pinophilum* (55%), *C. globosum* (39%), and *A. brasiliensis* (17%). More pronounced inhibition of growth of the last four species was noted for the highest tested concentration of AgNPs (21.4 mg/l). The growth was completely suppressed for *P. pinophilum* and *C. globosum*, and significantly impaired for *A. brasiliensis* and *T. virens* (by 96% and 90%, respectively). Pulit et al. (2013) reported a 75 – 90% inhibition of the growth of *Aspergillus niger* and *Cladosporium cladosporioides* with a higher concentration of AgNPs (50 mg/l).

This difference in the biocidal effect could be associated with the size of nanoparticles. Pulit et al. (2013) tested AgNPs particles of 60 nm in diameter, in contrast to 20 nm particles analyzed in our study. It has been well documented that smaller nanoparticles (< 10 nm) exhibit more pronounced anti-proliferative activity than larger particles. Nowicka-Krawczyk et al. (2017) demonstrated inhibition of algae by AgNPs of 3 nm in diameter. In turn, Park et al. (2011) compared the effects of AgNPs of 20, 80, and 113 nm in diameter on two mouse cell lines (RAW 264.7 and L929) to conclude more pronounced cytotoxicity for smaller nanoparti-

cles. Higher antimicrobial activity of small nanoparticles was also reported by Duran et al. (2016).

Evaluation of microbial growth in Bioscreen C. As reported by Żarowska et al. (2015), the lowest AgNP concentration to cease the growth of bacteria (*S. aureus*, *E. coli*, and *Pseudomonas fluorescens*) and yeast species (*C. albicans*, *Y. lipolytica*, and *Saccharomyces cerevisiae*) was found to be nearly 9 mg/l. Here, for Bioscreen C culture evaluation of bacterial, yeast, and fungal growth, the AgNPs in the concentration of 10.7 mg/l were applied and their antimicrobial activity was confirmed. As expected, the growth of bacteria *S. aureus*, *P. aeruginosa*, *E. coli*, and yeast *Y. lipolytica* was completely inhibited (Fig. 2A, 2B).

This followed the results reported in the literature where the AgNPs biocidal effects were observed. Sondi and Salopek-Sondi (2004) reported 70% inhibition of *E. coli* growth by AgNPs in the concentration of 10 mg/l and total inhibition at 50–60 mg/l. Dar et al. (2013) found that AgNPs of an average size of 30–70 nm displayed inhibition of bacterial growth at a concentration ten times lower (5 mg/l). Concerning filamentous fungi, AgNPs at the concentration of 10.7 mg/l seriously influenced and retarded the development of the following species: *P. variotii*, *C. globosum*, *A. brasiliensis*, *P. pinophilum*, and *T. virens* (Table II). As compared to the culture of mixed spores (of five species), the lag phase duration increased from 1.5 to nearly 10 times, and the final cell density (OD) decreased more than 36-fold showing serious growth inhibition. The intensity of *C. albicans* growth fluctuated during the time of analysis, in a period of approximately 10 hours (Fig. 2B, violet line). This fluctuation is difficult to explain but appears to be connected with the presence of AgNPs, which probably influences cell metabolism and the duplication time. According to Radhakrishnan et al. (2018) *C. albicans* cells treated with AgNPs exhibited

Table II

Lag phase duration and final OD after 96 hours of filamentous fungal and yeast growth in BioscreenC without or with AgNPs.

Filamentous fungi and yeast species	Lag phase [h]	OD		
		at 96 h	compared to	
			SM [%]	initial [× folds]
SM: spores mix (control)	10	1.592	100	36
SM: spores mix +AgNPs	20	1.308	82	5.8
<i>A. brasiliensis</i> +AgNPs	40	1.600	100	8.1
<i>P. pinophilum</i> +AgNPs	30	1.517	95	9.2
<i>P. variotii</i> +AgNPs	~68	0.633	40	3.7
<i>T. virens</i> +AgNPs	18	1.306	82	6.5
<i>C. globosum</i> +AgNPs	48	1.063	67	5.2
<i>C. albicans</i> +AgNPs	15	0.953	–	3.8
<i>Y. lipolytica</i> +AgNPs	>96	0.194	–	0

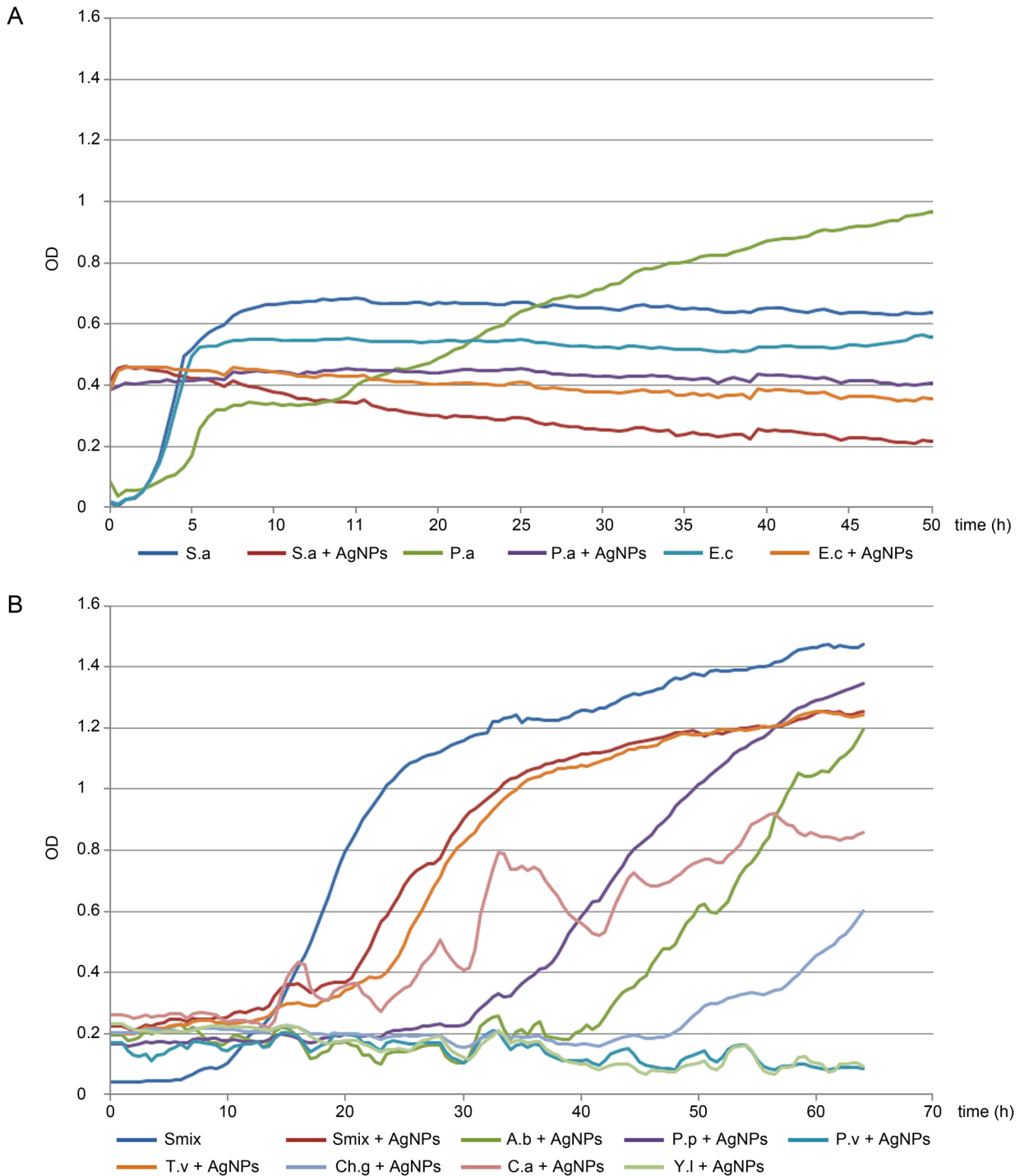


Fig. 2. Microorganism growth in BioscreenC with and without AgNPs: (A) Bacteria: S.a, *Staphylococcus aureus*; P.a, *Pseudomonas aeruginosa*; E.c, *Escherichia coli*; (B) yeasts Y.l, *Yarrowia lipolytica*, and fungi: Smix, the mixture of spores of five species of filamentous fungi; A.b, *Aspergillus brasiliensis*; P.p, *Penicillium pinophilum*; P.v, *Paecilomyces variotii*; T.v, *Trichoderma virens*, and Ch.g, *Chaetomium globosum*.

altered surface morphology and cellular ultrastructure, membrane fluidity, as well as ergosterol and fatty acids content. It was noted that the AgNP-mediated inhibition by was not only induced by ROS (reactive oxygen species) formation. The action of AgNPs on *C. albicans* was also size-dependent. According to Kim et al. (2009), AgNPs of 5 nm diameter and at the concentration of

2 mg/l effectively killed *C. albicans* yeasts. A comparable concentration (2.5 mg/l) of AgNPs was sufficient for the inhibition of *Aureobasidium pullulans*, and ten times higher concentration was needed for the *A. niger* growth inhibition (Žarowska et al. 2015). Therefore, the activity of AgNPs against yeasts and filamentous fungi requires further studies.

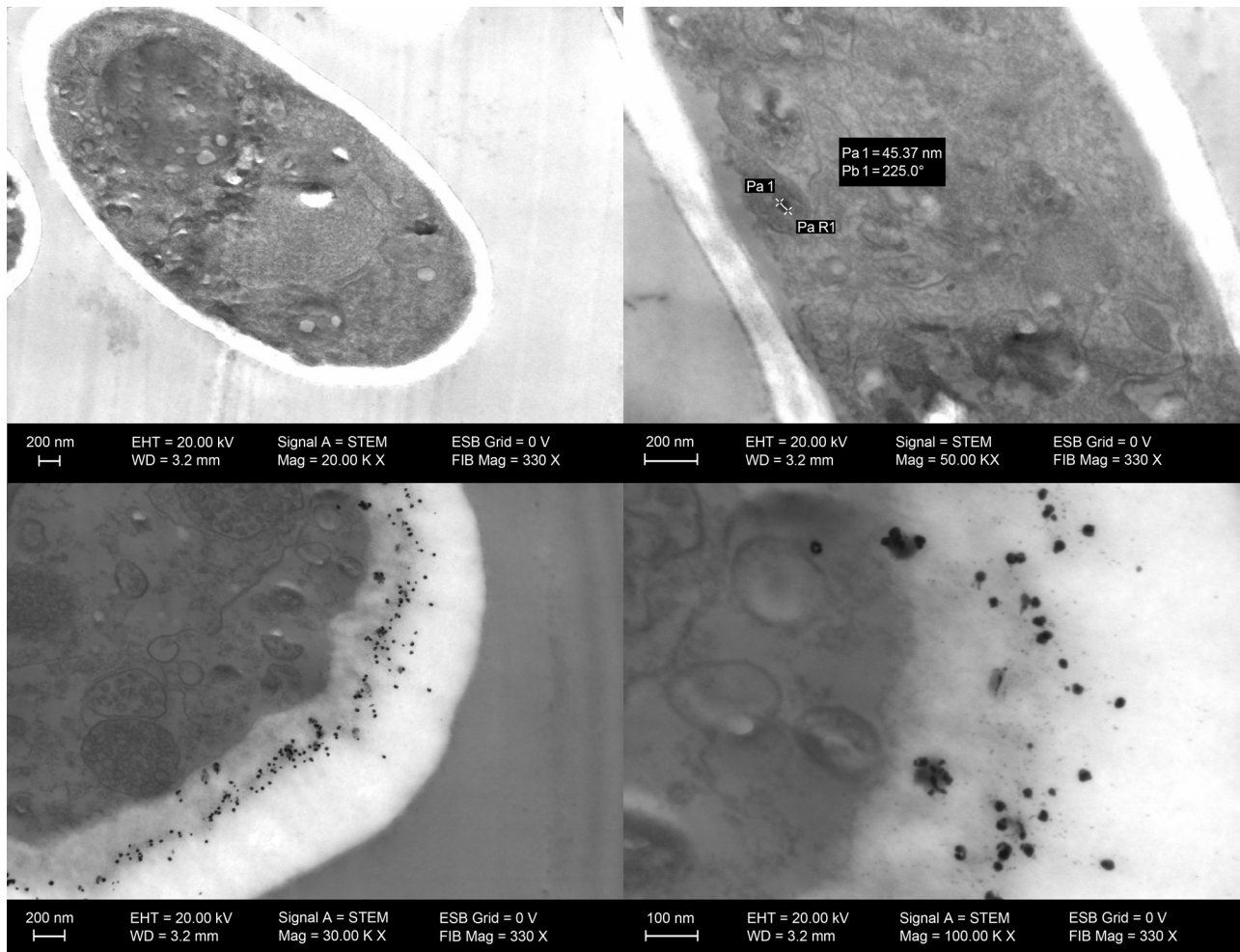


Fig. 3. TEM images of *Aspergillus brasiliensis* after the growth in the BioscreenC: (a) without AgNPs; (b) with AgNPs visible inside the cell (black points); (c, d) accumulated within the cell wall.

Also, difficult to explain is the recovery of growth after 20–48 hours of the lag phase (Table II) by four species of filamentous fungi, except *P. variotii*. The recovery of cell growth could result from at least two factors. One of them could be the microorganism's ability to synthesize and extracellularly secrete nanoparticles. This phenomenon was supported by the results of Dar et al. (2013) who proved that AgNPs could be synthesized by *Cryphonectria* spp. from silver nitrate and extracellularly secreted. Also, other mold species can synthesize and secrete AgNPs (Tran et al. 2013, Akter et al. 2018). Even autoclaved (inactivated) biomass of *Aspergillus aculeatus* was able to synthesize silver nanoparticles (Salvadori et al. 2014).

The second factor could be connected to the known fungal resistance to metals, including silver (Abou-Shanab et al. 2007). The resistance to metal as well as the nanoparticle biosynthesis could result from the activity of the same enzyme, nitrate reductase (EC 1.7.99.4). Shahverdi et al. (2007) identified nitroreductase as being responsible for the reduction of AgNO_3 to AgNPs by *Klebsiella pneumoniae*, and Anil Kumar et al.

(2007) described the green synthesis of AgNPs by this enzyme isolated from *Fusarium oxysporum*.

TEM analysis. The observations under TEM revealed the sites of AgNPs interaction with cells and filaments after nearly four days of the exposition. Nanoparticles accumulated in the cell wall without any aggregation, which was especially visible for *A. brasiliensis* (Fig. 3), and with aggregation in the cells of *P. variotii* and *P. pinophilum*. The TEM analysis was performed on microbial biomass collected after 92 h of culture with AgNPs added to the medium. Hence, at the time of microscopic observations, the fungal cells had already been adapted to the biocide (as shown in Fig. 2), and the observed accumulation of AgNPs was probably a result of its expulsion from the cells as in *A. brasiliensis*. This particular AgNPs deposition site could be due to their association with proteins present on the outer side of the cell membrane or with membrane lipids. The protein corona formation on AgNPs has been described elsewhere (Rahman et al. 2013; del Pino et al. 2014; Bargheer et al. 2015); however, the AgNPs deposition between the cell wall and cytoplasmic membrane could also involve

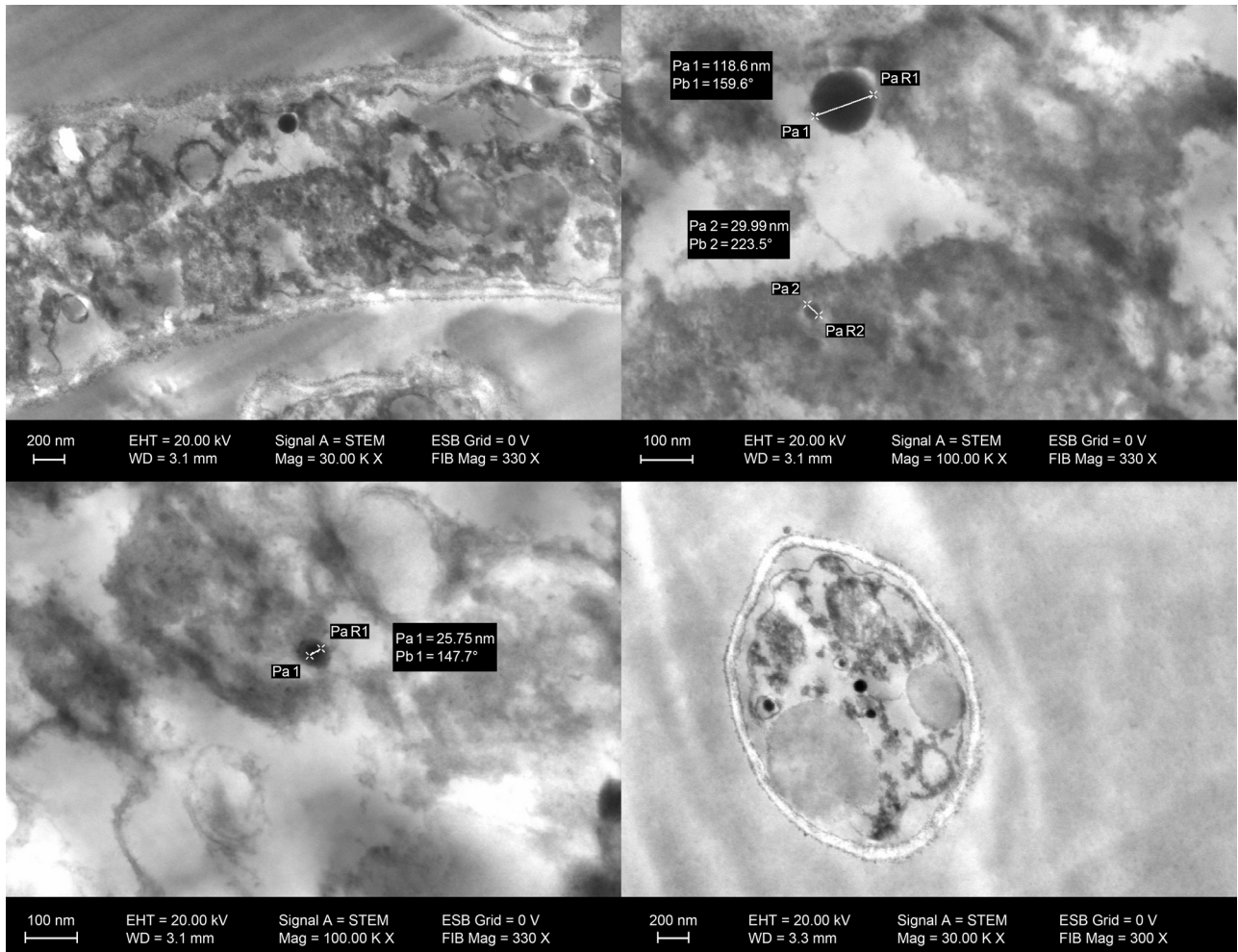


Fig. 4. TEM images of filamentous fungi after the growth with AgNPs in the Bioscreen C: (a, b) *Paecilomyces variotii*; (c, d) *Penicillium pinophilum*; AgNPs, the black structures observed inside the cell and hypha.

the binding of nanoparticles to fatty acids present as phospholipids. Recently, Radhakrishnan et al. (2018) reported an altered profile of fatty acids in the *C. albicans* cells exposed to AgNPs. However, in our study, no such abundant AgNPs deposition was denoted in any species studied, and possibly a particular cell wall compound of *A. brasiliensis* could be involved. In *A. fumigatus* the major component of the cell wall (30%) is the branched β -1,3 and β -1,6 glucans linked to chitin (Latge et al. 2005). The β -1,3 and β -1,6 glucans are not present in yeast and bacteria. So, these glucans could be involved in AgNPs localization in cell wall of *A. brasiliensis* also. It is noteworthy that for *P. variotii* and *P. pinophilum* no such type of nanoparticle accumulation was observed.

Here, besides their accumulation in cell walls, AgNPs were also found inside fungal and bacterial cells, especially in the cytoplasm, and outside of destroyed cells of *P. aeruginosa* (Fig. 4 and 5). Morones et al. (2005) have already presented similar images of AgNPs located outside *P. aeruginosa* cells.

According to many reports, the activity of AgNPs against the cell may involve generation of reactive oxy-

gen species (ROS), damage of macromolecules (DNA, proteins), and perforation of membranes due to destabilized conformation of their components, especially proteins, lipids, and glycans (Bartłomiejczyk et al. 2013; Duran et al. 2016). It appears that the observed damage was exerted by the release of Ag^+ from nanostructures (Duran et al. 2016). The mechanism of interaction of silver with the cell is best described for Gram-negative bacteria, notably *E. coli* (Kędziora et al. 2016). AgNPs uptake by the cell involves special membrane transporters, proteins of P-type ATPases (Li et al. 1997). Those P-type ATP-ases are responsible for the import of inorganic cations to the cytoplasm and the export of these ions outside the cytoplasm (Chong et al. 2012). According to Galván Márquez et al. (2018) the decreased transcription, reduced endocytosis, and dysfunctional electron transport system were observed in *S. cerevisiae* cells exposed to AgNPs.

The TEM analysis (based on the careful inspection of 300 images) allowed for the measurement of the size of the nanoparticles after interaction with the growing microorganisms. In 79% of the observed and measured

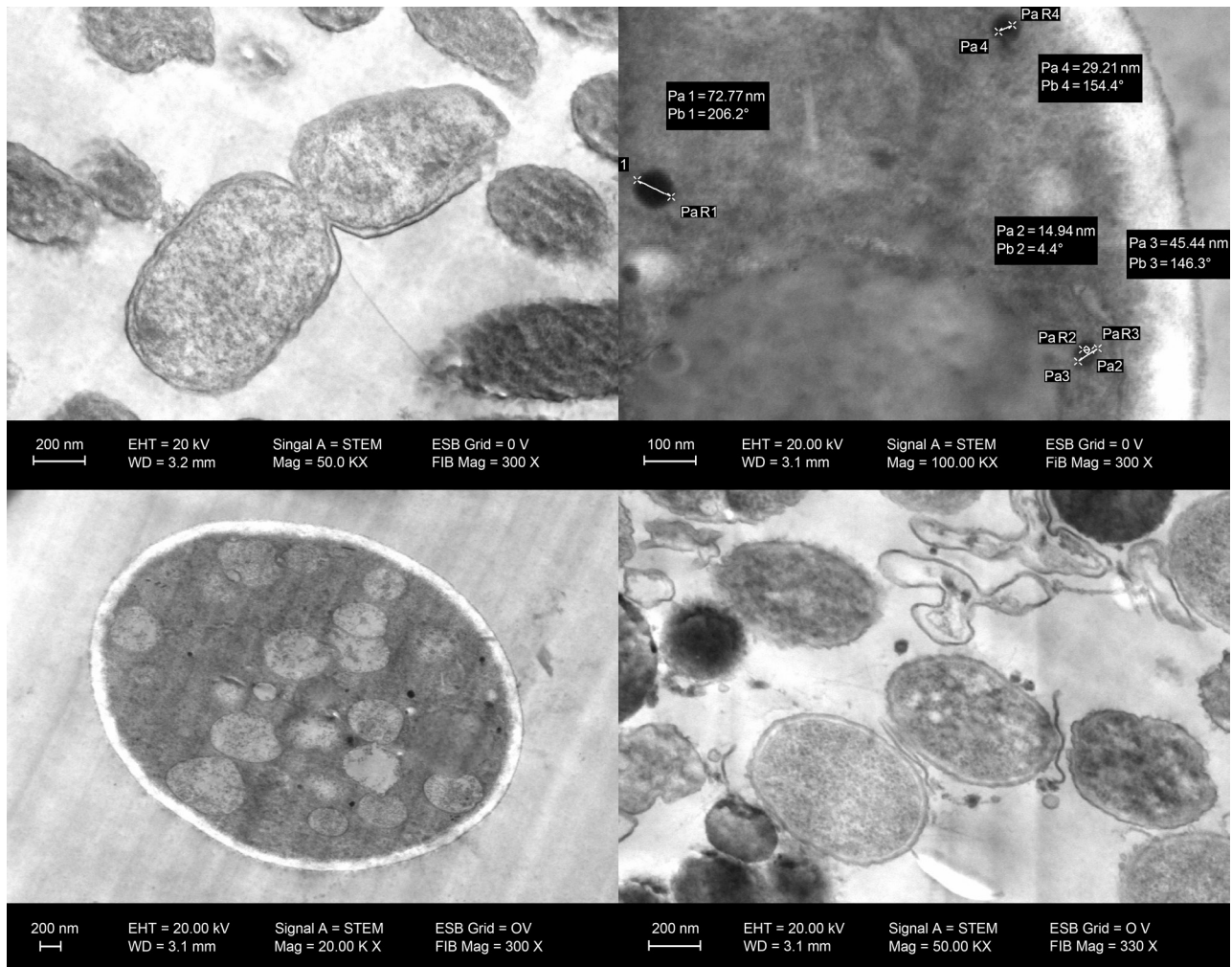


Fig. 5. TEM images of the bacterium and yeasts after the growth in the BioscreenC: (a) *Pseudomonas aeruginosa* without AgNPs; (b) *P. aeruginosa* with AgNPs; (c, d) *Candida albicans* with AgNPs, the black structures visible inside and outside of cells.

AgNPs particles, the diameter was close to 20 nm, so was the size of nanoparticles used in the study. In nearly 14%, the size was 2–2.5 times greater and in 7% diameter was 4–5 times larger. The distribution of AgNPs varied with particle diameter. Large AgNPs prevailed inside the cells while small ones dominated outside (Table III, Fig. 5).

Table III

The size and distribution (inside, outside, and within the cell wall) of AgNPs after their interaction with microorganisms.

AgNPs Size [nm]	[%]	Cell distribution according to the size [%]			
		Inside	Outside	In the cell wall	Total
21.45 ± 5.9	79.1	37.4	51.6	11	100
54.49 ± 9.1	13.9	93.8	6.25	0	100
94.62 ± 18.16	7.0	85.7	14.3	0	100
Total	100	48.7	42.6	8.7	100

The higher size of AgNPs inside the cells was probably due to cytoplasm properties to engender aggregation of AgNPs or protein corona formation. Such agglomeration was described by Rahman et al. (2013) and Bargheer et al. (2015) as the result of surface properties of proteins, as well as nanoparticles. The relatively high initial OD value for the samples with AgNPs observed in Bioscreen C microcultures (Fig. 2A and B; time 0 h) may result from the AgNP protein corona formation with the medium peptides, finally making the medium less transparent. However, the size of AgNPs found after *S. aureus* growth in Bioscreen C (with different nanoparticle doses) was not changed.

Many authors have studied the antimicrobial activity of AgNPs and found some peculiarities. Kaiser et al. (2017) described the influence of medium composition on nanosilver cytotoxicity, especially after the addition of serum and chloride. Also, food components influence the level of Ag⁺ release from the packaging material (Song et al. 2011), where Ag⁺ migration from food containers manufactured with silver and nanosil-

ver was revealed (Echegoyen and Nerin 2013). Silver ions are more toxic than AgNO₃ and nanoparticles. The minimal toxic dose of silver ions for humans is 0.014 mg/kg/day and only 1–2% accumulate in the body. Wen et al. (2016) reported that AgNPs at concentrations below 0.1 mg/l had low but observable cytotoxicity toward human buccal epithelial cells. The same concentration was the secondary maximum contaminant level of silver in drinking water (EPA 2017).

The antimicrobial activity of AgNPs also depends on the shape of nanoparticles. Pal et al. (2007) noted a stronger biocidal effect for truncated triangular silver nanoplates. These authors affirmed that for the safe use of AgNPs some questions had to be resolved (Bundschuh et al. 2016; Zarschler et al. 2016). Bundschuh et al. (2016) pointed out that long term consequences of the uptake by organisms of the engineered nanoparticles that are transferred throughout the food chain and may affect the microbial, plant, invertebrate, and fish communities, as well as the environment, is only partially understood and requires further systematic investigation. The study performed on nanoparticles used as antimicrobial agents against the molds causing deterioration of buildings and construction materials could also improve our living conditions. The environment protection becomes a very important issue for the human future and the use of AgNPs as antimicrobial agents could be in favor to overcome pollution by chemicals. Biocides used as antimicrobial agents are applied at rather high concentrations. Koziróg et al. (2016) tested seven compounds for their biocidal activity against microorganisms isolated from a wooden surface at the Auschwitz II-Birkenau Former German Nazi Concentration and Extermination Camp. Three of them were active, exhibiting biocidal activity at the concentration of 0.02–2% (200–20 000 mg/l). These active compounds were the ingredients of eight commercial biocides tested by the same researchers on wood pieces contaminated with microorganisms by triple spraying of the surface. According to the authors some of those biocides inhibited growth at the concentration of 6% (v/v), and others only at 30% (v/v). We found that the concentration of 9–10.7 mg/l of AgNPs (sized 20 nm) is sufficient to exhibit high anti-mold, anti-yeast, and anti-bacterial activity in the laboratory tests. The supplementation of materials used in the house construction with AgNPs at the low concentration (10.7 mg/l = 0.00107%) could be a better solution for the environment and human life.

Conclusions

The AgNPs tested inhibited the growth of *A. brasiliensis*, *C. globosum*, *P. pinophilum*, *P. variotii*, and *T. virens*. Therefore, AgNPs can be used to prevent

molds invasion on construction materials. The sensitivity to AgNPs depends on the molds species. Total inhibition of *P. variotii* growth was observed at a very small concentration of AgNPs (4.28 mg/l).

The TEM images revealed that AgNPs entered into the bacterial, yeast, and fungal cells and aggregated in larger particles exclusively inside cells of eukaryotic microorganisms. Such types of nanosilver aggregation have not yet been reported in literature and accumulation of AgNPs in the cell wall of *A. brasiliensis* cells was observed for the first time. Peculiarities of fungal interaction with AgNPs presented in this paper could be an interesting area of future research.

ORCID

Tomasz Koźlecki 0000-0002-7890-0936

Michał Piegza 0000-0001-9183-5692

Barbara Żarowska 0000-0002-7149-0647

Acknowledgments

We kindly thank Dr. Jakub Grzesiak from EIT, Wrocław for help in the interpretation of TEM images. The research was financed by the National Center of Research and Development (NCBR) project number No PBS 3/B1/10/2015. The publication was supported by Wrocław Centre of Biotechnology, program the Leading National Research Centre (KNOW) for years 2014–2018.

Conflict of interest

The authors do not report any financial or personal connections with other persons or organizations, which might negatively affect the contents of this publication and/or claim authorship rights to this publication.

Literature

- Abou-Shanab RAI, van Berkum P, Angle JS.** Heavy metal resistance and genotypic analysis of metal resistance genes in gram-positive and gram-negative bacteria present in Ni-rich serpentine soil and in the rhizosphere of *Alyssum murale*. *Chemosphere*. 2007 Jun;68(2):360–367. <https://doi.org/10.1016/j.chemosphere.2006.12.051>
- Akter M, Sikder MT, Rahman MM, Ullah AKMA, Hossain KFB, Banik S, Hosokawa T, Saito T, Kurasaki M.** A systematic review on silver nanoparticles-induced cytotoxicity: physicochemical properties and perspectives. *J Adv Res*. 2018 Jan;9:1–16. <https://doi.org/10.1016/j.jare.2017.10.008>
- Anil Kumar S, Abyaneh MK, Gosavi SW, Kulkarni SK, Pasricha R, Ahmad A, Khan MI.** Nitrate reductase-mediated synthesis of silver nanoparticles from AgNO₃. *Biotechnol Lett*. 2007 Feb 16;29(3):439–445. <https://doi.org/10.1007/s10529-006-9256-7>
- AshaRani PV, Hande MP, Valiyaveettil S.** Anti-proliferative activity of silver nanoparticles. *BMC Cell Biol*. 2009;10:Article 65. <https://doi.org/10.1186/1471-2121-10-65>
- Bargheer D, Nielsen J, Gébel G, Heine M, Salmen SC, Stauber R, Weller H, Heeren J, Nielsen P.** The fate of a designed protein corona on nanoparticles *in vitro* and *in vivo*. *Beilstein J Nanotechnol*. 2015 Jan 06;6:36–46. <https://doi.org/10.3762/bjnano.6.5>
- Bartomiejczyk T, Lankoff A, Kruszewski M, Szumiel I.** Silver nanoparticles – allies or adversaries? *Ann Agric Environ Med*. 2013; 20(1):48–54.

- Bundschuh M, Seitz F, Rosenfeldt RR, Schulz R.** Effects of nanoparticles in fresh waters: risks, mechanisms and interactions. *Freshw Biol.* 2016 Dec;61(12):2185–2196. <https://doi.org/10.1111/fwb.12701>
- Chong TM, Yin WF, Mondy S, Grandclément C, Dessaux Y, Chan KG.** Heavy-metal resistance of a France vineyard soil bacterium, *Pseudomonas mendocina* strain S5.2, revealed by whole-genome sequencing. *J Bacteriol.* 2012 Nov 15;194(22):6366. <https://doi.org/10.1128/JB.01702-12>
- Dar MA, Ingle A, Rai M.** Enhanced antimicrobial activity of silver nanoparticles synthesized by *Cryphonectria* sp. evaluated singly and in combination with antibiotics. *Nanomedicine.* 2013 Jan;9(1):105–110. <https://doi.org/10.1016/j.nano.2012.04.007>
- del Pino P, Pelaz B, Zhang Q, Maffre P, Nienhaus GU, Parak WJ. Protein corona formation around nanoparticles – from the past to the future. *Mater Horiz.* 2014;1(3):301–313. <https://doi.org/10.1039/C3MH00106G>
- Durán N, Durán M, de Jesus MB, Seabra AB, Fávoro WJ, Nakazato G.** Silver nanoparticles: A new view on mechanistic aspects on antimicrobial activity. *Nanomedicine.* 2016 Apr;12(3):789–799. <https://doi.org/10.1016/j.nano.2015.11.016>
- Echegoyen Y, Nerin C.** Nanoparticle release from nano-silver antimicrobial food containers. *Food Chem Toxicol.* 2013 Dec;62:16–22. <https://doi.org/10.1016/j.fct.2013.08.014>
- EPA. Secondary drinking water standards: guidance for nuisance chemicals [Internet]. Washington, DC (USA): United States Environmental Protection Agency; 2017 Mar 8 [cited 2019 May 15]. Available from <https://www.epa.gov/dwstandardsregulations/secondary-drinking-water-standards-guidance- nuisance-chemicals>
- Flores-López LZ, Espinoza-Gómez H, Somanathan R.** Silver nanoparticles: electron transfer, reactive oxygen species, oxidative stress, beneficial and toxicological effects. Mini review. *J Appl Toxicol.* 2019 Jan;39(1):16–26. <https://doi.org/10.1002/jat.3654>
- Galván Márquez I, Ghiyasvand M, Massarsky A, Babu M, Samanfar B, Omid K, Moon TW, Smith ML, Golshani A.** Zinc oxide and silver nanoparticles toxicity in the baker's yeast, *Saccharomyces cerevisiae*. *PLoS One.* 2018 Mar 19;13(3):e0193111. <https://doi.org/10.1371/journal.pone.0193111>
- Guzman M, Dille J, Godet S.** Synthesis and antibacterial activity of silver nanoparticles against gram-positive and gram-negative bacteria. *Nanomedicine.* 2012 Jan;8(1):37–45. <https://doi.org/10.1016/j.nano.2011.05.007>
- Jo YK, Kim BH, Jung G.** Antifungal activity of silver ions and nanoparticles on phytopathogenic fungi. *Plant Dis.* 2009 Oct;93(10):1037–1043. <https://doi.org/10.1094/PDIS-93-10-1037>
- Kaiser JP, Roesslein M, Diener L, Wichser A, Nowack B, Wick P.** Cytotoxic effects of nanosilver are highly dependent on the chloride concentration and the presence of organic compounds in the cell culture media. *J Nanobiotechnology.* 2017 Dec;15(1):5. <https://doi.org/10.1186/s12951-016-0244-3>
- Kanawaria SK, Sankhla A, Jatav PK, Yadav RS, Verma KS, Velraj P, Kachhwaha S, Kothari SL.** Rapid biosynthesis and characterization of silver nanoparticles: an assessment of antibacterial and antimycotic activity. *Appl Phys, A Mater Sci Process.* 2018 Apr;124(4): 320. <https://doi.org/10.1007/s00339-018-1701-7>
- Kędziora A, Krzyżewska E, Dudek B, Bugla-Płoskońska G.** [The participation of outer membranes proteins in the bacterial sensitivity to nanosilver]. *Postepy Hig Med Dosw.* 2016;70:610–617. <https://doi.org/10.5604/17322693.1250005>
- Kim JS, Kuk E, Yu KN, Kim JH, Park SJ, Lee HJ, Kim SH, Park YK, Park YH, Hwang CY, et al.** Antimicrobial effects of silver nanoparticles. *Nanomedicine.* 2007 Mar;3(1):95–101. <https://doi.org/10.1016/j.nano.2006.12.001>
- Kim KJ, Sung WS, Suh BK, Moon SK, Choi JS, Kim JG, Lee DG.** Antifungal activity and mode of action of silver nano-particles on *Candida albicans*. *Biomaterials.* 2009 Apr;22(2):235–242. <https://doi.org/10.1007/s10534-008-9159-2>
- Kobiałka N, Mularczyk M, Kosiorowska K, Pilarska K, Łaba W, Piegza M, Robak M.** New strains of filamentous fungi isolated from construction materials. *EJPAU.* 2019;22(1):#02. <https://doi.org/10.30825/5.ejpau.169.2019.22.1>
- Kokura S, Handa O, Takagi T, Ishikawa T, Naito Y, Yoshikawa T.** Silver nanoparticles as a safe preservative for use in cosmetics. *Nanomedicine.* 2010 Aug;6(4):570–574. <https://doi.org/10.1016/j.nano.2009.12.002>
- Koziróg A, Rajkowska K, Otlewska A, Piotrowska M, Kunicka-Styczyńska A, Brycki B, Nowicka-Krawczyk P, Kościelniak M, Gutarowska B.** Protection of historical wood against microbial degradation – selection and application of microbiocides. *Int J Mol Sci.* 2016 Aug 22;17(8):1364. <https://doi.org/10.3390/ijms17081364>
- Koźlecki T, Teterycz H, Sokołowski A, Polowczyk I, Sawiński W, Maliszewska I, Szydło J.** Sposób syntezy nanocząstek srebra. PL Patent deposition 2011; No P395979.
- Lara HH, Romero-Urbina DG, Pierce C, Lopez-Ribot JL, Arellano-Jiménez MJ, Jose-Yacamán M.** Effect of silver nanoparticles on *Candida albicans* biofilms: an ultrastructural study. *J Nanobiotechnology.* 2015 Dec;13(1):91–102. <https://doi.org/10.1186/s12951-015-0147-8>
- Latgé JP, Mouyna I, Tekaija F, Beauvais A, Debeaupuis JP, Nierman W.** Specific molecular features in the organization and biosynthesis of the cell wall of *Aspergillus fumigatus*. *Med Mycol.* 2005 Jan;43(s1) Suppl 1:15–22. <https://doi.org/10.1080/13693780400029155>
- Lee S, Jun BH.** Silver Nanoparticles: synthesis and application for nanomedicine. *Int J Mol Sci.* 2019 Feb 17;20(4):865. <https://doi.org/10.3390/ijms20040865>
- Li WR, Xie XB, Shi QS, Zeng HY, OU-Yang YS, Chen YB.** Antibacterial activity and mechanism of silver nanoparticles on *Escherichia coli*. *Appl Microbiol Biotechnol.* 2010 Jan;85(4):1115–1122. <https://doi.org/10.1007/s00253-009-2159-5>
- Li XZ, Nikaido H, Williams KE.** Silver-resistant mutants of *Escherichia coli* display active efflux of Ag⁺ and are deficient in porins. *J Bacteriol.* 1997 Oct;179(19):6127–6132. <https://doi.org/10.1128/jb.179.19.6127-6132.1997>
- Łukaszuk CR, Krajewska-Kułak E, Kułak W.** Effects of fungal air pollution on human health. *Prog Health Sci.* 2011;1(2):156–164.
- Martinez-Gutierrez F, Olive PL, Banuelos A, Orrantia E, Nino N, Sanchez EM, Ruiz F, Bach H, Av-Gay Y.** Synthesis, characterization, and evaluation of antimicrobial and cytotoxic effect of silver and titanium nanoparticles. *Nanomedicine.* 2010 Oct;6(5):681–688. <https://doi.org/10.1016/j.nano.2010.02.001>
- McShan D, Ray PC, Yu H.** Molecular toxicity mechanism of nano-silver. *Yao Wu Shi Pin Fen Xi.* 2014 Mar;22(1):116–127. <https://doi.org/10.1016/j.jfda.2014.01.010>
- Metak AM, Ajaal TT.** Investigation on polymer based nano-silver as packaging materials. *Int Schol Scien Res Inn.* 2013;7(12):772–778.
- Milić M, Leitinger G, Pavičić I, Zebić Avdičević M, Dobrović S, Goessler W, Vinković Vrček I.** Cellular uptake and toxicity effects of silver nanoparticles in mammalian kidney cells. *J Appl Toxicol.* 2015 Jun;35(6):581–592. <https://doi.org/10.1002/jat.3081>
- Morones JR, Elechiguerra JL, Camacho A, Holt K, Kouri JB, Ramírez JT, Yacamán MJ.** The bactericidal effect of silver nanoparticles. *Nanotechnology.* 2005 Oct 01;16(10):2346–2353. <https://doi.org/10.1088/0957-4484/16/10/059>

- Nowicka-Krawczyk P, Żelazna-Wieczorek J, Koźlecki T. Silver nano particles as a control agent against facades coated by aerial algae – A model study of *Apatococcus lobatus* (green algae). *PLoS One*. 2017 Aug 14;12(8):e0183276. <https://doi.org/10.1371/journal.pone.0183276>
- Pal S, Tak YK, Song JM. Does the antibacterial activity of silver nanoparticles depend on the shape of the nanoparticle? A study of the Gram-negative bacterium *Escherichia coli*. *Appl Environ Microbiol*. 2007 Mar 15;73(6):1712–1720. <https://doi.org/10.1128/AEM.02218-06>
- Park MVDZ, Neigh AM, Vermeulen JP, de la Fonteyne LJJ, Verharen HW, Briedé JJ, van Loveren H, de Jong WH. The effect of particle size on the cytotoxicity, inflammation, developmental toxicity and genotoxicity of silver nanoparticles. *Biomaterials*. 2011 Dec;32(36):9810–9817. <https://doi.org/10.1016/j.biomaterials.2011.08.085>
- PN-EN ISO 846. Polska norma. Tworzywa sztuczne. Ocena działania mikroorganizmów [Plastics-Evaluation of the action of the microorganisms, actualization 2019:05]. 2002 Dec.
- Pulit J, Banach M, Szczygłowska R, Bryk M. Nanosilver against fungi. Silver nanoparticles as an effective biocidal factor. *Acta Biochim Pol*. 2013;60(4):795–798.
- Radhakrishnan VS, Reddy Mudiam MK, Kumar M, Dwivedi SP, Singh SP, Prasad T. Silver nanoparticles induced alterations in multiple cellular targets, which are critical for drug susceptibilities and pathogenicity in fungal pathogen (*Candida albicans*). *Int J Nanomedicine*. 2018 May;13:2647–2663. <https://doi.org/10.2147/IJN.S150648>
- Rahman M, Laurent S, Tawil N, Yahia L, Mahmoudi M. Nanoparticle and protein corona. In: Protein-nanoparticles interactions. The Bio-Nano Interface. Springer Series in Biophysics. Berlin, Heidelberg (Germany): Springer; 2013;15. p. 21–44. https://doi.org/10.1007/978-3-642-37555-2_2
- Rai M, Ingle AP, Gaiwad S, Gupta I, Gade A, Silvério da Silva S. Nanotechnology based anti-infectives to fight microbial intrusions. *J Appl Microbiol*. 2016 Mar;120(3):527–542. <https://doi.org/10.1111/jam.13010>
- Rai M, Yadav A, Gade A. Silver nanoparticles as a new generation of antimicrobials. *Biotechnol Adv*. 2009 Jan;27(1):76–83. <https://doi.org/10.1016/j.biotechadv.2008.09.002>
- Riaz Ahmed KB, Nagy AM, Brown RP, Zhang Q, Malghan SG, Goering PL. Silver nanoparticles: significance of physicochemical properties and assay interference on the interpretation of *in vitro* cytotoxicity studies. *Toxicol In Vitro*. 2017 Feb;38:179–192. <https://doi.org/10.1016/j.tiv.2016.10.012>
- Robak M. *Yarrowia lipolytica* specific growth rate on acetate medium supplemented with glucose, glycerol or ethanol. *Acta Sci Polon Biotechnologia*. 2007;6(1):23–31.
- Roe D, Karandikar B, Bonn-Savage N, Gibbins B, Roulet JB. Antimicrobial surface functionalization of plastic catheters by silver nanoparticles. *J Antimicrob Chemother*. 2008 Feb 04;61(4):869–876. <https://doi.org/10.1093/jac/dkn034>
- Salvadori MR, Nascimento CAO, Corrêa B. Nickel oxide nanoparticles film produced by dead biomass of filamentous fungus. *Sci Rep*. 2015 May;4(1):6404. <https://doi.org/10.1038/srep06404>
- Shahverdi AR, Fakhimi A, Shahverdi HR, Minaian S. Synthesis and effect of silver nanoparticles on the antibacterial activity of different antibiotics against *Staphylococcus aureus* and *Escherichia coli*. *Nanomedicine*. 2007 Jun;3(2):168–171. <https://doi.org/10.1016/j.nano.2007.02.001>
- Sondi I, Salopek-Sondi B. Silver nanoparticles as antimicrobial agent: a case study on *E. coli* as a model for Gram-negative bacteria. *J Colloid Interface Sci*. 2004 Jul;275(1):177–182. <https://doi.org/10.1016/j.jcis.2004.02.012>
- Song H, Li B, Lin QB, Wu HJ, Chen Y. Migration of silver from nanosilver-polyethylene composite packaging into food simulants. *Food Additives & Contaminants: Part A*. 2011 Jul 08;28(12):1–5. <https://doi.org/10.1080/19440049.2011.603705>
- Tran QH, Nguyen VQ, Le A-T. Silver nanoparticles: synthesis, properties, toxicology, applications and perspectives. *Adv. Nat. Sci. Nanosci. Nanotechnol*. 2013;4:033001, 20pp. <https://doi.org/10.1088/2043-6262/4/3/033001>
- Wen R, Hu L, Qu G, Zhou Q, Jiang G. Exposure, tissue biodistribution, and biotransformation of nanosilver. *NanoImpact*. 2016 Apr;2:18–28. <https://doi.org/10.1016/j.impact.2016.06.001>
- Xu Y, Gao C, Li X, He Y, Zhou L, Pang G, Sun S. *In vitro* antifungal activity of silver nanoparticles against ocular pathogenic filamentous fungi. *J Ocul Pharmacol Ther*. 2013 Mar;29(2):270–274. <https://doi.org/10.1089/jop.2012.0155>
- Yoon KY, Hoon Byeon J, Park JH, Hwang J. Susceptibility constants of *Escherichia coli* and *Bacillus subtilis* to silver and copper nanoparticles. *Sci Total Environ*. 2007 Feb;373(2-3):572–575. <https://doi.org/10.1016/j.scitotenv.2006.11.007>
- Zarschler K, Rocks L, Licciardello N, Boselli L, Polo E, Garcia KP, De Cola L, Stephan H, Dawson KA. Ultrasmall inorganic nanoparticles: state-of-the-art and perspectives for biomedical applications. *Nanomedicine*. 2016 Aug;12(6):1663–1701. <https://doi.org/10.1016/j.nano.2016.02.019>
- Zhang X-F, Liu Z-G, Shen W, Gurunathan S. Silver nanoparticles: synthesis, characterization, properties, applications, and therapeutic approaches. *Int J Mol Sci*. 2016a;17(9):1534. <https://doi.org/10.3390/ijms17091534>
- Zhang X-F, Shen W, Gurunathan S. Silver nanoparticle-mediated cellular responses in various cell lines: an *in vitro* model. *Int J Med Sci*. 2016b;17:1603. <https://doi.org/10.3390/ijms17101603>
- Zou J, Hannula M, Misra S, Feng H, Labrador R, Aula AS, Hyttinen J, Pyykkö I. Micro CT visualization of silver nanoparticles in the middle and inner ear of rat and transportation pathway after transtympanic injection. *J Nanobiotechnology*. 2015;13(1):5. <https://doi.org/10.1186/s12951-015-0065-9>
- Żarowska B, Piegza M, Jaros-Koźlecka K, Koźlecki T, Robak M. Antimicrobial activity of silver nanoparticles. Conference material: Wrocław (Poland): BRIA; 2015;55.

Illumina MiSeq Analysis and Comparison of Freshwater Microalgal Communities on Ulleungdo and Dokdo Islands

HYUN-SIK YUN^{1,2}, YOUNG-SAENG KIM^{3*}, HO-SUNG YOON^{1,2*}

¹Department of Biology, College of Natural Sciences, Kyungpook National University, Daegu, South Korea

²School of Life Sciences, BK21 Plus KNU Creative BioResearch Group, Kyungpook National University, Daegu, South Korea

³Research Institute of Ulleung-do & Dok-do, Kyungpook National University, Daegu, South Korea

Submitted 25 July 2019, revised 23 October 2019, accepted 30 October 2019

Abstract

Ulleungdo and Dokdo are volcanic islands with an oceanic climate located off the eastern coast of South Korea. In the present study, we used barcoded Illumina MiSeq to analyze eukaryotic microalgal genera collected from Seonginbong, the highest peak on Ulleungdo, and from groundwater sites on Dongdo and Seodo Islands, which are part of Dokdo. Species richness was significantly greater in the Seonginbong samples than in the Dongdo and Seodo samples, with 834 operational taxonomic units (OTUs) identified from Seonginbong compared with 203 OTUs and 182 OTUs from Dongdo and Seodo, respectively. Taxonomic composition analysis was also used to identify the dominant microalgal phyla at each of the three sites, with Chlorophyta (green algae) the most abundant phyla on Seonginbong and Dongdo, and Bacillariophyta (diatoms) the most abundant on Seodo. These findings suggest that differences in the abundances of Chlorophyta and Bacillariophyta species in the Seonginbong, Dongdo, and Seodo samples are due to variations in species richness and freshwater resources at each sampling location. To the best of our knowledge, this is the first report to detail freshwater microalgal communities on Ulleungdo and Dokdo. As such, the number of species identified in the Seonginbong, Dongdo, and Seodo samples might be an indicator of the ecological differences among these sites and varying characteristics of their microbial communities. Information regarding the microalgal communities also provides a basis for understanding the ecological interactions between microalgae species and other eukaryotic microorganisms.

Key words: amplicon sequencing, Dokdo Island, microalgal community, MiSeq system, Ulleungdo Island

Introduction

Ulleungdo and Dokdo, located to the east of the Korean peninsula, are volcanic islands formed by the lava flows resulting from volcanic activity. Ulleungdo consists of one main island, with Seonginbong as its highest peak, and several small islets. Dokdo comprises two major islets, Dongdo and Seodo, and several exposed rocks (Sohn 1995; Kim et al. 2013). Ulleungdo and Dokdo share an oceanic climate due to the influence of warm and cold currents (Chang et al. 2002; Lee et al. 2010), although average annual precipitation is higher on Ulleungdo (1574 mm) than on Dokdo (660 mm). Annual average temperatures of both islands range from 12°C to 14°C (Chang et al. 2002; Lee et al. 2010). These islands are characterized by steep slopes

that facilitate significant surface runoff when it rains, and it is thereby difficult for rainwater to collect on the surface. Indeed, volcanic islands formed from the lava are often characterized by a water-deficient environment. However, Ulleungdo and Dokdo have springs or small streams that originate from the groundwater to create an environment wherein fresh surface water is available (Sohn 1995; Chang et al. 2002).

The uneven distribution of freshwater sources influences the overall vegetation community and its successional processes. Ulleungdo, due to its relatively high precipitation, has greater vegetation species richness, with 487 vascular plants species and 104 woody plant species, than Dokdo, with 46 vascular plant species and eight woody plant species (Shin et al. 2004; Kim et al. 2007; Park et al. 2010), indicating that Ulleungdo is at

* Corresponding authors: Y.S. Kim, Research Institute of Ulleung-do & Dok-do, Kyungpook National University, Daegu, South Korea; e-mail: kyslhh1228@hanmail.net

H.S. Yoon, Department of Biology, College of Natural Sciences, Kyungpook National University, Daegu, South Korea; e-mail: hsy@knu.ac.kr
© 2019 Hyun-Sik Yun et al.

This work is licensed under the Creative Commons Attribution-NonCommercial-NoDerivatives 4.0 License (<https://creativecommons.org/licenses/by-nc-nd/4.0/>).

a more advanced successional stage than Dokdo (Kim et al. 2007; Park et al. 2010; Jung et al. 2014). These patterns also extend to the microbial ecosystems, meaning that the different environments of Ulleungdo and Dokdo affect their microbial communities (Busse et al. 2006; Han et al. 2007; Djukic et al. 2010; Merilä et al. 2010). However, previous studies on the microbial communities on these islands have focused on the fungal and bacterial complements thereof (Kim et al. 2014; Nam et al. 2015), and little is known about the microalgal constituent. The discovery of new microalgal species is important in terms of the use of the algal biomass as a biological resource under different environmental conditions (Krustok et al. 2015).

Microalgae participate in carbon, nitrogen, and phosphorus cycles (Lehman 1980; Berner 1992; Vitousek et al. 2002) and, as photosynthetic organisms, are key producers and pioneers across a range of ecosystems (Booth 1941; Jackson 1971; Bellinzoni et al. 2003). In early successional stages, microalgae are the predominant production group, facilitating the subsequent arrival of herbaceous and woody plants, which can grow in the fertilized environment created by the microalgae (Booth 1941; Jackson 1971; Bellinzoni et al. 2003). The microalgal group promotes successional vegetation processes and allows for the emergence of predators and pathogenic microbes. The former mainly comprises zooplankton such as nematodes and arthropods (Havens and DeCosta 1987; Canovas et al. 1996; Mayer et al. 1997), while the latter causes disease in plants and animals and inhibits the biodegradation capacity of microbes (Littler and Littler 1998; Chen et al. 2014).

Interactions between microalgae and their abiotic and biotic environments drive the evolution of the microalgal community. Species dominance depends on environmental conditions, such as inorganic nutrient composition, water temperature, and light (Prowse and Talling 1958; Goldman and Shapiro 1973; Porter 1977). In particular, microalgae composition is dominated by large-cell and needle-type algae, which are difficult to prey. Because the microalgal community supports the ecosystem and serves the producer-consumer relationship, analysis of this community can improve our understanding of the local environment, elemental recycling (carbon, nitrogen, and phosphorus), and micro-ecosystem relationships between producer and consumer trophic levels (Berner 1992; Vitousek et al. 2002; Cardinale et al. 2011). However, microalgal community research based solely on the culturing faces certain limitations, particularly the difficulty in identifying and analyzing unculturable microorganisms (Handelsman 2004; Streit and Schmitz 2004). Consequently, amplicon sequencing analysis using Illumina MiSeq can be a powerful tool for the investigation of unculturable microorganisms in their natural environment

(Knight 2000; Handelsman 2004; Streit and Schmitz 2004; Schloss and Handelsman 2005).

Previous studies have yet to analyze the microalgal communities in the freshwater ecosystems on Ulleungdo (Seonginbong) and Dokdo (Dongdo and Seodo). This study investigated eukaryotic microalgal communities on these islands by taking freshwater samples from groundwater and tributary streams for the Illumina MiSeq analysis. Illumina MiSeq allows a large amount of sequencing information to be processed in a short time, and taxonomic analyses can then be conducted based on this information (Handelsman 2004; Streit and Schmitz 2004; Buée et al. 2009; Shokralla et al. 2012). In this study, microalgal species richness and diversity were characterized using taxonomic analysis, revealing that the composition of these communities varied by region, from phylum to species units.

Experimental

Materials and Methods

Collection of samples. Freshwater samples were collected from freshwater sources on Seonginbong (37° 30' 05.9" N 130° 52' 04.9" E) in Buk-myeon, Ulleung-gun, Gyeongsangbuk-do, South Korea, and on Dongdo (37° 14' 21.0" N 131° 52' 10.4" E) and Seodo Islands (37° 14' 31.5" N 131° 51' 51.6" E) in Dokdo-ri, Ulleung-gun, Gyeongsangbuk-do, South Korea (Supplemental Fig. S1). Seonginbong is the highest peak on Ulleungdo, and tributaries flow from here to freshwater sources. Freshwater sources are rare on Dokdo because of smaller volumes of groundwater, with only one groundwater source each on Dongdo and Seodo. Freshwater resources were harvested by collecting 100 ml from the water surfaces at each site on October 3, 2018. The collected samples were shipped to Macrogen Co., Ltd. on October 3, 2018, using the Same Day Express Courier Service and analyzed while maintained at room temperature.

DNA extraction and MiSeq system analysis. MiSeq system analysis (Macrogen, Seoul, South Korea) involved amplicon sequencing of whole DNA, with DNA extracted by the PowerSoil® DNA Isolation Kit (Cat. No. 12888, MO BIO) according to the manufacturer's protocol (Claassen et al. 2013). Extracted DNA was amplified with PCR to assess the 18S region for identifying eukaryotic microorganisms. Each sequenced sample was prepared according to the Illumina 18S MiSeq System Library protocols (Vo and Jedlicka 2014). DNA quantification and quality measurements were conducted using PicoGreen and Nanodrop. The 18S rRNA genes were amplified using 18S V4 primers (Stoeck et al. 2010; Luddington et al. 2012; Tragin et al. 2018). The amplicon PCR forward primer

sequence was TAREuk454FWD1 (5'-CCAGCA(G-C)C(C-T)GCGGTAATTCC-3'), and the amplicon PCR reverse primer sequence was TAREukREV3 (5'-ACT-TTCGTTCTTGAT(C-T)(A-G)A-3') (Stoeck et al. 2010). Input gDNA was amplified using targeted DNA fragments (18S V4 primers size, 420 bp), and subsequent limited-cycle amplification was conducted to add multiplexing indices and Illumina sequencing adapters (Meyer and Kircher 2010). The final products were normalized and pooled using PicoGreen, and the sizes of the libraries were verified using the TapeStation DNA D1000 ScreenTape system (Agilent). The Illumina MiSeq data was analyzed on the MiSeq™ platform (Illumina, San Diego, USA; Kozich et al. 2013).

Taxonomic identification analysis. After sequencing, the Illumina MiSeq data were demultiplexed using the index sequence, and a FASTQ file was generated for each sample. The adapter sequence was removed using SeqPurge (Sturm et al. 2016), and error correction was performed on the overlapping areas of the two readings, with low-quality barcode sequences (read length <400 bp or average quality value <25) trimmed and filtered out. All raw Illumina MiSeq reads were identified using a BLASTN search of the NCBI database based on their barcode sequences (Zhang et al. 2000). If the results could not be taxonomically classified into a sublevel, unclassified (uc) was added to the end of the name. Operational taxonomic units (OTUs) were analyzed using CD-HIT at a 97% sequence similarity threshold (Unno et al. 2010; Li et al. 2012; Chen et al. 2013). The mothur platform was used to calculate rarefaction curves and diversity indices (Shannon, Simpson, and Chao1; Heck et al. 1975; Schloss et al. 2009). Beta diversity, which refers to sample diversity information among samples in a comparison group, was obtained based on weighted UniFrac distances. A UPGMA tree was used to visualize the flexibility between samples (FigTree, <http://tree.bio.ed.ac.uk/software/figtree/>) and demonstrate relationships among the three sites.

Results and Discussion

Sequencing results analysis. Table I presents the total number of reads and OTUs obtained from the three study sites. A total of 580 853 reads were sequenced from Seonginbong, with 290 919 validated reads remaining after preprocessing. The mean read length was 408.1 bp, and the maximum read length was 418 bp. A total of 534 141 reads were sequenced from Dongdo, with 289 610 validated reads remaining after preprocessing. The mean read length was 416.7 bp, and the maximum read length was 418 bp. A total of 469 920 reads were sequenced from Seodo, and the number of validated reads after preprocessing was 275 387. The mean read

Table I
Illumina MiSeq results for the operational taxonomic units (OTUs) and statistical analysis.

	Seonginbong	Dongdo	Seodo
Total reads	580 853	534 141	469 920
Validated reads	290 919	289 610	275 387
Mean read length (bp)	408.1	416.7	412.54
Maximum read length (bp)	418	418	408
Number of OTUs ¹	834	203	182
Chao1 ²	834	203.75	182
Shannon ³	6.722	2.038	5.118
Simpson ⁴	0.9655	0.5569	0.9174
Goods Coverage ⁵	1	0.9999	1

¹OTUs: Operational taxonomic units

²Chao1: Species richness estimation

³Shannon: Shannon diversity index (>0, higher is more diverse)

⁴Simpson: Simpson diversity index (0–1, 1 = most simple)

⁵Goods Coverage: 1 – (number of singleton OTUs/number of sequences); 1 = 100% coverage

length was 412.54 bp, and the maximum read length was 418 bp. As seen in Table I, the Seonginbong sample contained the highest number of OTUs with 834 units, while the Dongdo and Seodo samples contained fewer OTUs at 203 and 182 units, respectively.

The species richness of the samples is represented by rarefaction curves in Fig. 1, while the Chao1 species richness, the Shannon diversity index, and the Simpson diversity index are summarized in Table I (Heck et al. 1975; Schloss et al. 2009). The Seonginbong sample had the greatest species richness for all indicators (Chao1: 934; Shannon: 6.7222; Simpson: 0.9655), while Dongdo and Seodo had similar results to one another for Chao1 (203.75 and 182, respectively). However, Seodo had Shannon and Simpson index scores (5.118 and 0.9174, respectively) that were similar to those at Seonginbong (6.722 and 0.9655, respectively), and much higher than those of Dongdo (2.038 and 0.5569, respectively). Based on the OTU and species richness results, the diversity of the eukaryotic microbial composition on Seonginbong appeared to be greater than on Dongdo and Seodo (Fig. 1 and Table I). These results confirmed differences in species diversity among Seonginbong, Dongdo, and Seodo.

Analysis of the eukaryotic microbial communities on Seonginbong, Dongdo, and Seodo. After a BLASTN search of the NCBI database, the validated reads in Table I were assigned to a eukaryotic microbial taxonomic group (Table II; Niu et al. 2010). When a BLASTN search generated a specific scientific name with regards to phylum, class, order, family, genus, or species, the OTU was labeled as classified (c); if not, it was labeled as unclassified (uc). Table II summarizes the number of classified and unclassified OTUs

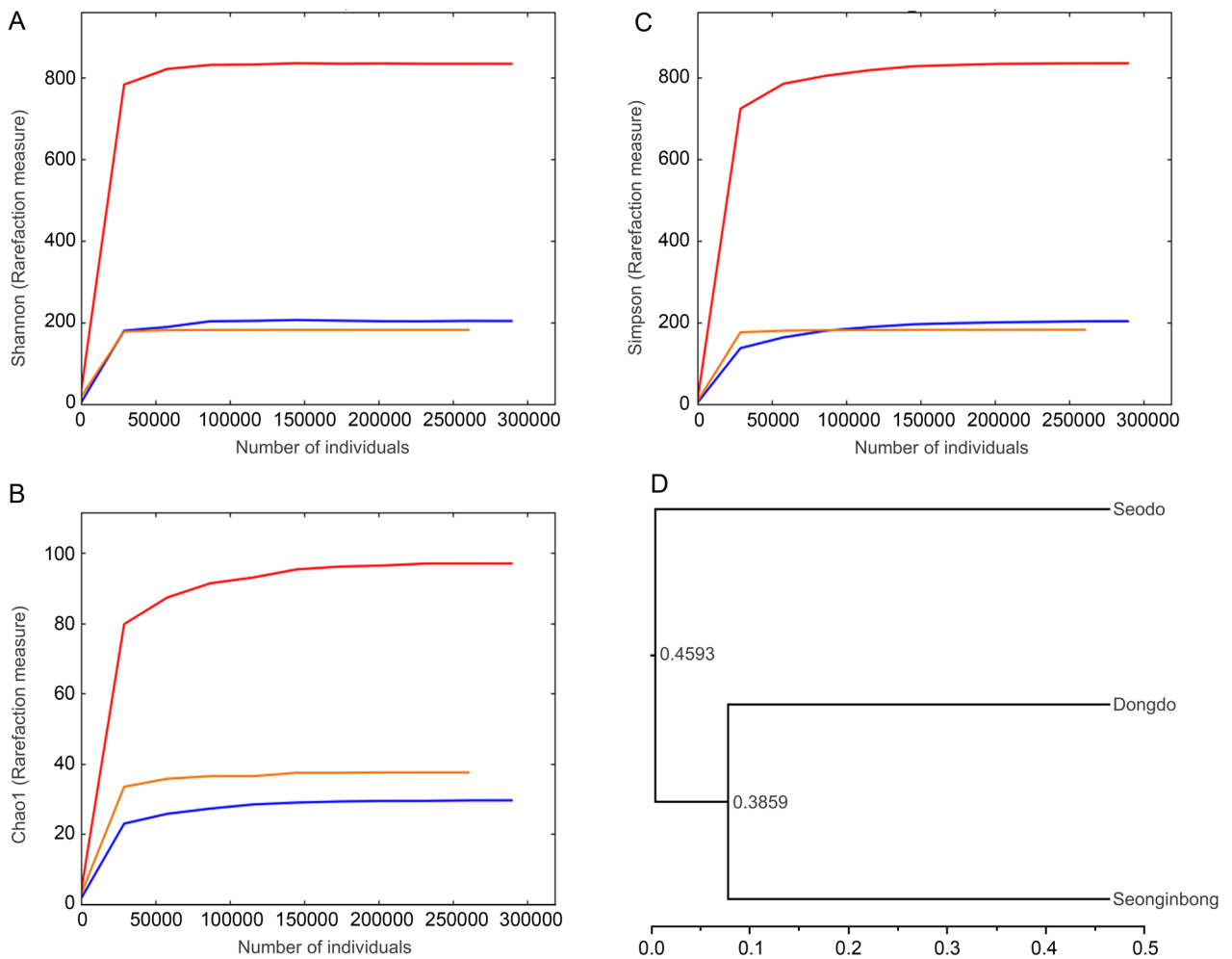


Fig. 1. Rarefaction curves for operational taxonomic units (OTUs) from the Seonginbong, Dongdo, and Seodo samples. (a) Shannon, (b) Simpson, and (c) Chao1 indexes. (d) UPGMA tree based on the community structures of Seonginbong, Dongdo, and Seodo. Seonginbong (red line), Dongdo (blue line), and Seodo (orange line).

from phylum to species for the Seonginbong, Dongdo, and Seodo samples. For the Seonginbong, Dongdo, and Seodo samples, 165 646, 30 911, and 164 678 reads were classified, and 125 273, 258 699, and 110 709 reads were unclassified at the phylum level, respectively. At

the class level, 128 160, 23 011, and 144 662 reads were classified, and 162 759, 266 599, and 130 725 reads were unclassified for the Seonginbong Dongdo and Seodo regions respectively. In addition 99 964, 22 791, and 123 329 reads, respectively, were classified at the order

Table II
Number of eukaryotic microalgal taxa observed in the Seonginbong, Dongdo, and Seodo samples.

	Seonginbong		Dongdo		Seodo	
	c ¹	uc ²	c ¹	uc ²	c ¹	uc ²
Phylum	165 646	125 273	30 911	258 699	164 678	110 709
Class	128 160	162 759	23 011	266 599	144 662	130 725
Order	99 964	190 955	22 791	266 819	123 329	152 058
Family	96 751	194 168	22 751	266 859	120 206	155 181
Genus	92 628	198 291	22 707	266 903	110 674	164 713
Species	84 154	206 765	17 930	271 680	97 541	177 846

¹Number of sequencing reads with a scientific name for the taxon (classified, *c*)

²Number of sequencing reads either unclassified into a sublevel or classified as an unknown name for the taxon (unclassified, *uc*)

level. Similarly, 96 751, 22 751, and 120 206 reads were classified at the family level, and 92 628, 22 707, and 110 674 reads were classified at the genus level. Only 84 154, 17 930, and 97 541 sequences were classified at the species level. The number of validated reads was lower than the number of total reads because of the lack of information on unculturable microorganisms in the NCBI database. Therefore, the total reads and validated reads were both utilized for microorganism classification from the phylum to species level. Total reads and validated reads at the species level could be classified using information about their taxonomic levels, such as phylum, class, order, family, and genus.

The taxonomic compositions of the eukaryotic microbial communities on Seonginbong, Dongdo, and Seodo were then analyzed. It was found that the communities contained a combination of 17 phyla: Xanthophyceae, Streptophyta, Rotifera, Porifera, Platyhelminthes, Nematoda, Eustigmatophyceae, Chytridiomycota, Chordata, Chlorophyta, Blastocladiomycota, Basidiomycota, Bacillariophyta, Ascomycota, Arthropoda, Apicomplexa, and Annelida (Fig. 2). The communities were dominated by the microalgal phyla Chlorophyta and Bacillariophyta, although their combined relative abundance was significantly higher in the Dongdo and Seodo samples (93.52% and 91.77%, respectively) than in the Seonginbong sample (31.02%). Differences in population densities were more profound in the Seonginbong sample than in the Dongdo and Seodo samples (Fig. 2). This analysis of differences in the community composition could contribute significantly to our understanding of the microbial ecosystems at each site (Wegley et al. 2007; Rodriguez-Brito et al. 2010; Fierer et al. 2012). Microbial community compositions already reported suggest a need for further research on the eukaryotic microorganisms in each

region (Knight 2000; Chiao 2004; Schloss and Handelsman 2005). In this regard, amplicon sequencing using Illumina MiSeq is a powerful tool for the identification of unculturable microalgae. More important, MiSeq system analysis can also generate useful information on new species in the natural environments of Ulleungdo and Dokdo that could be helpful in studying unculturable eukaryotic microorganisms.

Comparison of the microalgal communities on Seonginbong, Dongdo, and Seodo. We compared the structures of the microalgal communities on Seonginbong, Dongdo, and Seodo by constructing phylogenetic trees (Fig. 1) using UPGMA analysis with eukaryotic microorganisms. The taxonomic compositions of Seonginbong, Dongdo, and Seodo were analyzed from the phylum to species level. Overall, it was found that Seonginbong was more closely related to Dongdo than Seodo. At the phylum level, the microalgal communities of Seonginbong, Dongdo, and Seodo exhibited differences in their taxonomic compositions despite being dominated by two phyla: Chlorophyta (Round 1963) and Bacillariophyta (Fig. 2; Kaczmarek et al. 2007). The relative abundance of Chlorophyta was very high on Dongdo (93.52%), while Bacillariophyta was dominant on Seodo (89.13%). On Seonginbong, the relative abundance of Chlorophyta was higher than that of Bacillariophyta (Chytridiomycota 39.43%, Chlorophyta 27.1%, and Bacillariophyta 4.31%).

At the class level, five distinct microalgal classes (Bacillariophyceae, Coscinodiscophyceae, Chlorophyceae, Trebouxiophyceae, and Ulvophyceae) were detected in the overall sample (Fig. 3), with the dominant groups in each region differing: Seonginbong, Chlorophyceae; Dongdo, Trebouxiophyceae; and Seodo, Bacillariophyceae. In particular, the relative abundance of Bacillariophyceae was higher in Seodo (88.24%) than

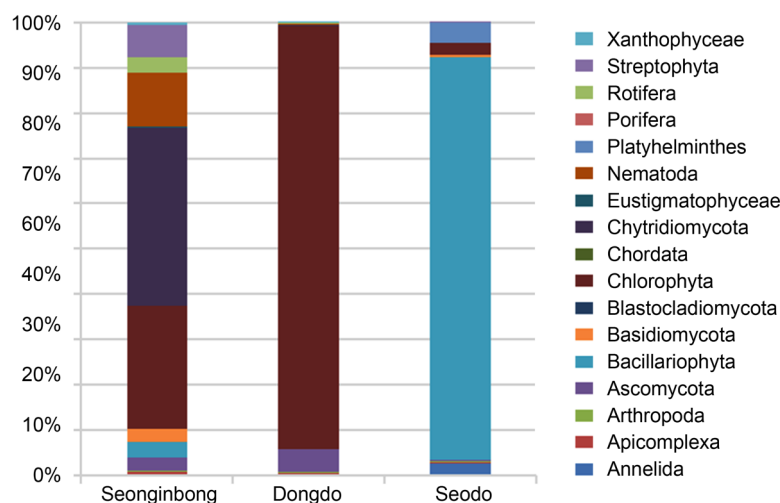


Fig. 2. Taxonomic composition of the eukaryotic microbial phyla on Seonginbong, Dongdo, and Seodo.

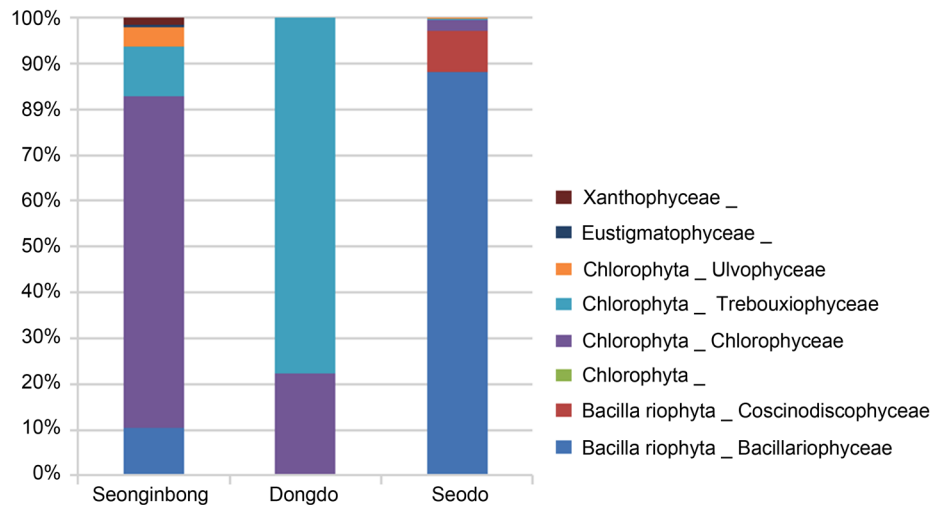


Fig. 3. Taxonomic composition of the microalgal classes on Seonginbong, Dongdo, and Seodo.

in Seonginbong (10.56%) or Dongdo (0%). The Coscinodiscophyceae was only present on Seodo (8.86%). In addition, two or three green algae classes were present at the study sites, including Chlorophyceae (73.39%), Trebouxiophyceae (11.17%), and Ulvophyceae (4.18%) on Seonginbong; Chlorophyceae (22.22%) and Trebouxiophyceae (77.67%) on Dongdo; and Chlorophyceae (2.28%), Trebouxiophyceae (0.49%), and Ulvophyceae (0.13%) on Seodo.

A total of 30 families were detected in each region. Seventeen families had identified scientific names, and nine had a relative abundance of at least 1%. These families are summarized in Table III. On Seonginbong, three diatom families (*Bacillariaceae*, *Pinnulariaceae*, and *Stauroneidaceae*) and eight green algae families (*Characiochloridaceae*, *Chlamydomonadaceae*, *Chlorococcaceae*, *Scenedesmaceae*, *Coccomyxaceae*, *Chlorellaceae*, and *Ctenocladaceae*) were identified, with the most dominant being *Chlorococcaceae* (1.53%), and two unclassified green algae families (*Chlorophyta*, *Chlorophyceae*, *Chlamydomonadales*: 3.47%; *Chlorophyta*, *Chlorophyceae*, *Sphaeropleales*: 2.53%). Conversely, only one diatom or green algae family was dominant in Dongdo and Seodo. One diatom family (*Diadesmidaceae*) and three green algae families (*Chlamydomonadaceae*, *Chlorococcaceae*, and *Chlorellaceae*) were present on Dongdo, with the most dominant being *Chlorellaceae* (64.91%), distantly followed by *Chlorococcaceae* (18.46%). Conversely, Seodo had nine diatom families (*Achnanthaceae*, *Bacillariaceae*, *Amphipleuraceae*, *Diadesmidaceae*, *Naviculaceae*, *Sellaphoraceae*, *Catenulaceae*, and *Stephanopyxidaceae*) and two green algae families (*Scenedesmaceae* and *Chlorellaceae*). The dominant family on Seodo was an unclassified diatom family (21.62%), distantly followed by three other diatom families (*Bacillariaceae*: 3.26%, *Sellaphoraceae*: 3.12%, and *Stephanopyxidaceae*: 3.14%) with relative

abundances of at least 3%. Four families were found to be unique to a specific area: *Stauroneidaceae* on Seonginbong and *Achnanthaceae*, *Sellaphoraceae*, and *Stephanopyxidaceae* on Seodo. In summary, although Dongdo and Seodo are proximally located, the species composition on Seodo differs from that on Seonginbong and Dongdo; these two regions exhibit greater similarity to one another than either does to Seodo.

A total of 50 microalgal genera were detected, with 37 identified by scientific name. Fourteen genera had a relative abundance of at least 1% (Table ???). Three diatom genera (*Nitzschia*, *Pinnularia*, and *Amphora*) known to produce toxins were identified on Seonginbong (*Pinnularia*, 0.09%) and Seodo (*Nitzschia*, 3.26%; *Amphora*, 0.12%). For the diatom genera with a relative abundance of at least 1%, genera were uniquely distributed in each region; however, microalgal genera were found at all three sites. In particular, the microalgal taxonomic compositions of Seonginbong and Dongdo were more similar to one another than either was to Seodo. There were six dominant genera (*Stauroneis*, 1.16%; *Chlorococcum*, 1.53%; *Chlorosarcinopsis*, 1.29%; *Bracteacoccus*, 1.89%), and two unclassified microalgal genera (1.48% and 1.47%) present on Seonginbong. On Dongdo, unclassified microalgal genera (63.78%), *Chlorococcum* (18.46%), and *Pseudochlorella* (1.13%) dominated. Six diatom genera were dominant on Seodo (*Achnanthidium*, 20.76%; *Achnanthes*, 1.54%; *Nitzschia*, 3.26%; *Diadesmis*, 2.15%; *Sellaphora*, 3.12%; *Stephanopyxis*, 3.14%). These findings indicate that microalgal genera are widely distributed across all three regions, whereas diatom genera are restricted to specific areas. Of note, microalgal taxonomic composition showed that the Seonginbong and Dongdo communities were closely related at the genus level.

For species-level analyses, the microalgal species identified from the Seonginbong, Dongdo, and Seodo

Table III
Relative abundance of eukaryotic microalgal families in the Seonginbong, Dongdo, and Seodo samples.

Taxonomy				Seonginbong		Dongdo		Seodo	
Phylum	Class	Order	Family	% ¹	Fr ²	% ¹	Fr ²	% ¹	Fr ²
Bacillariophyta	Bacillariophyceae	–	–	0.00	0	0.00	0	21.62	59 531
Bacillariophyta	Bacillariophyceae	–	Achnantheaceae	0.00	0	0.00	0	1.54	4 239
Bacillariophyta	Bacillariophyceae	–	Bacillariaceae	0.15	423	0.00	0	3.26	8 974
Bacillariophyta	Bacillariophyceae	Naviculales	Amphipleuraceae	0.00	0	0.00	0	0.23	645
Bacillariophyta	Bacillariophyceae	Naviculales	Diadesmidaceae	0.00	0	0.00	7	2.38	6 551
Bacillariophyta	Bacillariophyceae	Naviculales	Naviculaceae	0.00	0	0.00	0	0.29	802
Bacillariophyta	Bacillariophyceae	Naviculales	Pinnulariaceae	0.09	256	0.00	0	0.00	0
Bacillariophyta	Bacillariophyceae	Naviculales	Sellaphoraceae	0.00	0	0.00	0	3.12	8 579
Bacillariophyta	Bacillariophyceae	Naviculales	Stauroneidaceae	1.16	3 379	0.00	0	0.00	0
Bacillariophyta	Bacillariophyceae	Thalassiosiphysales	Catenulaceae	0.00	0	0.00	0	0.12	329
Bacillariophyta	Coscinodiscophyceae	Melosirales	Stephanopyxidaceae	0.00	0	0.00	0	3.14	8 660
Bacillariophyta	Coscinodiscophyceae	Paraliales	–	0.00	0	0.00	0	0.13	354
Chlorophyta	–	–	–	0.00	0	0.02	65	0.00	0
Chlorophyta	–	Chlorodendrales	–	0.00	0	0.01	21	0.00	0
Chlorophyta	Chlorophyceae	–	–	0.03	91	0.00	13	0.62	1 708
Chlorophyta	Chlorophyceae	Chlamydomonadales	–	2.53	7 368	0.09	271	0.00	0
Chlorophyta	Chlorophyceae	Chlamydomonadales	Characiochloridaceae	0.34	1 002	0.00	0	0.00	0
Chlorophyta	Chlorophyceae	Chlamydomonadales	Chlamydomonadaceae	0.38	1 096	0.02	48	0.00	0
Chlorophyta	Chlorophyceae	Chlamydomonadales	Chlorococcaceae	1.53	4 437	18.46	53 463	0.00	0
Chlorophyta	Chlorophyceae	Chlorosarcinales	–	1.29	3 761	0.00	0	0.00	0
Chlorophyta	Chlorophyceae	Sphaeropleales	–	3.47	10 096	0.00	2	0.00	0
Chlorophyta	Chlorophyceae	Sphaeropleales	Scenedesmaceae	0.08	243	0.00	0	0.22	597
Chlorophyta	Trebouxiophyceae	–	–	0.56	1 624	0.00	0	0.12	329
Chlorophyta	Trebouxiophyceae	–	Coccomyxaceae	0.01	23	0.00	0	0.00	0
Chlorophyta	Trebouxiophyceae	Chlorellales	–	0.00	0	0.00	7	0.00	0
Chlorophyta	Trebouxiophyceae	Chlorellales	Chlorellaceae	0.58	1 689	64.91	187 999	0.06	162
Chlorophyta	Trebouxiophyceae	Ctenocladales	Ctenocladaceae	0.21	604	0.00	0	0.00	0
Chlorophyta	Trebouxiophyceae	Microthamniales	–	0.11	323	0.02	48	0.00	0
Chlorophyta	Ulvophyceae	Ulotrichales	–	0.55	1 605	0.00	0	0.00	0
Chlorophyta	Ulvophyceae	Ulvales	–	0.00	0	0.00	0	0.05	136

The microalgal families detected in at least one of the three samples are shown. Unclassified taxonomic names (phylum, class, order, and family) are replaced with a dash (–)

¹Relative abundance

²Frequency of microalgae detected at each sampling site

samples were organized in a phylogenetic tree (Fig. 4). For groups without a scientific name at the genus level (Fig. 3), names were only added to those with scientific names at the species level (Fig. 4). Phylum and class boundaries were identified for the microalgal species based on species-level sequencing analysis for Seonginbong, Dongdo, and Seodo. In Fig. 4, the boundary between Bacillariophyta and Chlorophyta is marked with a yellow box, and boundaries between the classes belonging to each phylum are marked with purple boxes (Metting 1996). Among the microalgal groups, some of the Chlorophyceae belonged to Trebouxiophyceae from class via phylum (Tables III and IV). At the

species level, dominant species were identified on each island, to include six species on Seonginbong, two species on Dongdo, and six species on Seodo; these are marked by boxes in Fig. 4 (Seonginbong, red; Dongdo, blue; Seodo, green). Of the species shown on the phylogenetic tree, some have been associated with shellfish toxins (Falconer 2012) frequently found on Seodo. In particular, *Nitzschia* sp. (Bates et al. 1989; Martin et al. 1990), known to be associated with shellfish toxins, was one of the dominant species on Seodo.

We organized the three microalgal communities from the phylum to species levels to analyze the taxonomic compositions of the three study sites. The approximate

Table IV
Relative abundance of eukaryotic microalgal genera in the Seonginbong, Dongdo, and Seodo samples.

Taxonomy				Seonginbong		Dongdo		Seodo		
Phylum	Class	Order	Family	Genus	% ¹	Fr ²	% ¹	Fr ²	% ¹	Fr ²
Bacillariophyta	Bacillariophyceae	-	-	-	0.00	0	0.00	0	0.86	2 363
Bacillariophyta	Bacillariophyceae	-	-	<i>Achnanthyidium</i>	0.00	0	0.00	0	20.76	57 168
Bacillariophyta	Bacillariophyceae	-	Achnanthaceae	<i>Achnanthes</i>	0.00	0	0.00	0	1.54	4 239
Bacillariophyta	Bacillariophyceae	-	Bacillariaceae	<i>Hantzschia</i>	0.15	423	0.00	0	0.00	0
Bacillariophyta	Bacillariophyceae	-	Bacillariaceae	<i>Nitzschia</i>	0.00	0	0.00	0	3.26	8 974
Bacillariophyta	Bacillariophyceae	Naviculales	Amphipleuraceae	-	0.00	0	0.00	0	0.23	645
Bacillariophyta	Bacillariophyceae	Naviculales	Diadesmidaceae	<i>Diadesmis</i>	0.00	0	0.00	0	2.15	5 922
Bacillariophyta	Bacillariophyceae	Naviculales	Diadesmidaceae	<i>Luticola</i>	0.00	0	0.00	7	0.23	629
Bacillariophyta	Bacillariophyceae	Naviculales	Naviculaceae	<i>Navicula</i>	0.00	0	0.00	0	0.29	802
Bacillariophyta	Bacillariophyceae	Naviculales	Pinnulariaceae	<i>Pinnularia</i>	0.09	256	0.00	0	0.00	0
Bacillariophyta	Bacillariophyceae	Naviculales	Sellaphoraceae	<i>Sellaphora</i>	0.00	0	0.00	0	3.12	8 579
Bacillariophyta	Bacillariophyceae	Naviculales	Stauroneidaceae	<i>Stauroneis</i>	1.16	3 379	0.00	0	0.00	0
Bacillariophyta	Bacillariophyceae	Thalassiosiphysales	Catenulaceae	<i>Amphora</i>	0.00	0	0.00	0	0.12	329
Bacillariophyta	Coscinodiscophyceae	Melosirales	Stephanopyxidaceae	<i>Stephanopyxis</i>	0.00	0	0.00	0	3.14	8 660
Bacillariophyta	Coscinodiscophyceae	Paraliales	-	<i>Paralia</i>	0.00	0	0.00	0	0.13	354
Chlorophyta	-	-	-	-	0.00	0	0.02	65	0.00	0
Chlorophyta	-	Chlorodendrales	-	-	0.00	0	0.01	21	0.00	0
Chlorophyta	Chlorophyceae	-	-	-	0.03	91	0.00	13	0.62	1 708
Chlorophyta	Chlorophyceae	Chlamydomonadales	-	-	1.48	4 308	0.09	249	0.00	0
Chlorophyta	Chlorophyceae	Chlamydomonadales	-	<i>Actinochloris</i>	0.00	0	0.01	22	0.00	0
Chlorophyta	Chlorophyceae	Chlamydomonadales	-	<i>Ettlia</i>	0.62	1 793	0.00	0	0.00	0
Chlorophyta	Chlorophyceae	Chlamydomonadales	-	<i>Spongiochloris</i>	0.44	1 267	0.00	0	0.00	0
Chlorophyta	Chlorophyceae	Chlamydomonadales	Charactochloridaceae	<i>Charactochloris</i>	0.34	1 002	0.00	0	0.00	0
Chlorophyta	Chlorophyceae	Chlamydomonadales	Chlamydomonadaceae	-	0.02	50	0.00	0	0.00	0
Chlorophyta	Chlorophyceae	Chlamydomonadales	Chlamydomonadaceae	<i>Chlamydomonas</i>	0.35	1 026	0.00	0	0.00	0

The microalgal genera detected in at least one of the three samples are shown. Unclassified taxonomic names (phylum, class, order, family, and genus) are replaced with a dash (-)

¹Relative abundance

²Frequency of microalgae detected at each sampling site

Table IV
Continued.

Taxonomy				Seonginbong		Dongdo		Seodo		
Phylum	Class	Order	Family	Genus	% ¹	Fr ²	% ¹	Fr ²	% ¹	Fr ²
Chlorophyta	Chlorophyceae	Chlamydomonadales	Chlamydomonadaceae	<i>Chloromonas</i>	0.01	20	0.02	48	0.00	0
Chlorophyta	Chlorophyceae	Chlamydomonadales	Chlorococcaceae	<i>Chlorococcum</i>	1.53	4 437	18.46	53 463	0.00	0
Chlorophyta	Chlorophyceae	Chlorosarcinales	-	<i>Chlorosarcinopsis</i>	1.29	3 761	0.00	0	0.00	0
Chlorophyta	Chlorophyceae	Sphaeropleales	-	-	1.47	4 271	0.00	2	0.00	0
Chlorophyta	Chlorophyceae	Sphaeropleales	-	<i>Bracteacoccus</i>	1.89	5 490	0.00	0	0.00	0
Chlorophyta	Chlorophyceae	Sphaeropleales	-	<i>Dictyochloris</i>	0.12	335	0.00	0	0.00	0
Chlorophyta	Chlorophyceae	Sphaeropleales	Scenedesmaceae	<i>Coelastrella</i>	0.02	64	0.00	0	0.22	597
Chlorophyta	Chlorophyceae	Sphaeropleales	Scenedesmaceae	<i>Desmodesmus</i>	0.06	179	0.00	0	0.00	0
Chlorophyta	Trebouxiophyceae	-	-	-	0.04	102	0.00	0	0.00	0
Chlorophyta	Trebouxiophyceae	-	-	<i>Myrmecia</i>	0.51	1 487	0.00	0	0.12	329
Chlorophyta	Trebouxiophyceae	-	-	<i>Watanabea</i>	0.01	35	0.00	0	0.00	0
Chlorophyta	Trebouxiophyceae	-	Coccomyxaceae	<i>Coccomyxa</i>	0.01	23	0.00	0	0.00	0
Chlorophyta	Trebouxiophyceae	Chlorellales	-	-	0.00	0	0.00	7	0.00	0
Chlorophyta	Trebouxiophyceae	Chlorellales	Chlorellaceae	-	0.06	182	63.78	184 700	0.06	162
Chlorophyta	Trebouxiophyceae	Chlorellales	Chlorellaceae	<i>Auxenochlorella</i>	0.34	999	0.00	2	0.00	0
Chlorophyta	Trebouxiophyceae	Chlorellales	Chlorellaceae	<i>Chlorella</i>	0.04	102	0.00	0	0.00	0
Chlorophyta	Trebouxiophyceae	Chlorellales	Chlorellaceae	<i>Heveochlorella</i>	0.00	0	0.00	12	0.00	0
Chlorophyta	Trebouxiophyceae	Chlorellales	Chlorellaceae	<i>Lobosphaera</i>	0.00	14	0.00	0	0.00	0
Chlorophyta	Trebouxiophyceae	Chlorellales	Chlorellaceae	<i>Pseudochlorella</i>	0.13	392	1.13	3 285	0.00	0
Chlorophyta	Trebouxiophyceae	Ctenocladales	Ctenocladaceae	<i>Leptosira</i>	0.21	604	0.00	0	0.00	0
Chlorophyta	Trebouxiophyceae	Microthamniales	-	-	0.09	272	0.00	0	0.00	0
Chlorophyta	Trebouxiophyceae	Microthamniales	-	<i>Dictyochloropsis</i>	0.02	51	0.00	0	0.00	0
Chlorophyta	Trebouxiophyceae	Microthamniales	-	<i>Stichococcus</i>	0.00	0	0.02	48	0.00	0
Chlorophyta	Ulvophyceae	Ulotrichales	-	-	0.55	1 605	0.00	0	0.00	0
Chlorophyta	Ulvophyceae	Ulvales	-	-	0.00	0	0.00	0	0.05	136

The microalgal genera detected in at least one of the three samples are shown. Unclassified taxonomic names (phylum, class, order, family, and genus) are replaced with a dash (-)

¹Relative abundance

²Frequency of microalgae detected at each sampling site

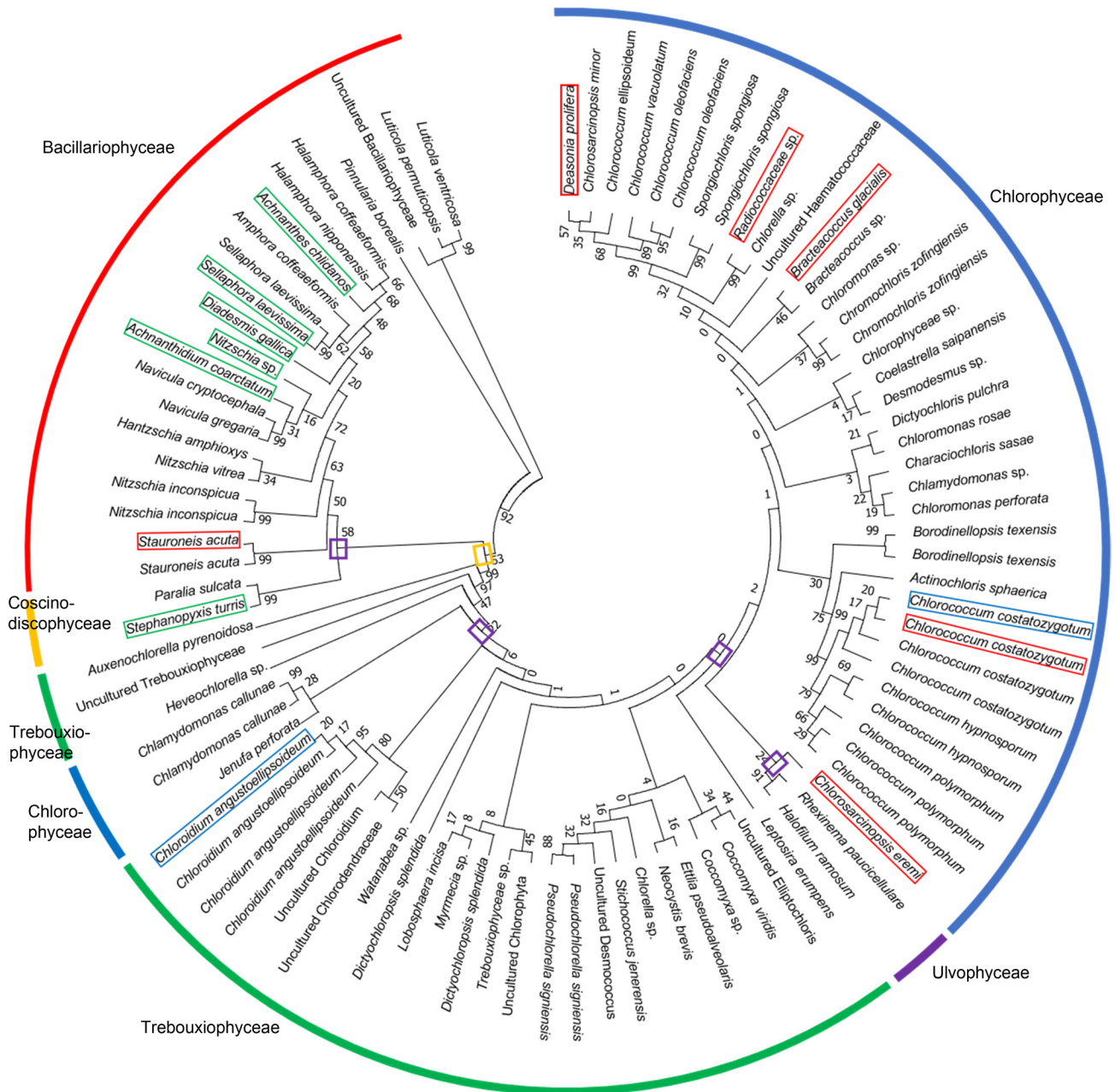


Fig. 4. Molecular phylogenetic analysis using a maximum likelihood (ML) tree. The boundary between phyla is marked with a yellow box, and the boundaries between classes are marked with purple boxes. Five classes are displayed about the species names in the phylogenetic tree. The dominant species in each sample is marked with a colored box (Seonginbong: red; Dongdo: blue; Seodo: green). The class of each group is presented at the edge (Bacillariophyceae; red, Coscinodiscophyceae; yellow, Chlorophyceae; blue, Trebouxiophyceae; green and Ulvophyceae; purple).

amount of available sunlight was highest at the Seonginbong sampling site and lowest at the Seodo site (Supplementary Fig. S1), and the relative abundance of diatoms strongly correlated with sunlight availability (Hudon and Bourget 1983; Post et al. 1984; Lange et al. 2011). Our results and those from previous studies indicate that further research on the relationship between light and microalgal community composition is required. Research also suggests that microalgal community composition is influenced by natural enemies or disease (Hudon and Bourget 1983; Post et al. 1984; Lange et al.

2011). In accordance with these findings, we observed differences in natural compositions among Seonginbong, Dongdo, and Seodo; the microalgal group was dominant on Seodo. At the phylum level, Seonginbong was characterized by zooplankton and pathogenic fungal groups (Fig. 2). At the class level, the microalgal group was dominated by Chlorophyceae on Seonginbong and Trebouxiophyceae (particularly *Chlorellaceae*) on Dongdo (Fig. 3). Trebouxiophyceae, which contains a family of small-celled organisms (*Chlorellaceae*), are relatively vulnerable to predators compared to other

classes, and results of the present study suggest that the presence of consumers (zooplankton and pathogenic fungi) affects the dominance of Chlorophyceae on Seonginbong and Dongdo to a greater extent than on Seodo (Fig. 2 and 3; Johnson and Agrawal 2003; Sarma et al. 2003; Yoshida et al. 2004; Pradeep et al. 2015).

Previous studies also indicate that microalgae can affect the external environment. A previous report found that the *Trebouxia* genus of the Trebouxiophyceae class forms a symbiotic association with lichen, fungi, and algae and is directly involved in changes to the terrestrial environment (Ahmadjian, 1988; Piercey-Normore 2006). The results of this study indicated that Trebouxiophyceae was not accurately detected at the phylum level, although a greater presence of Trebouxiophyceae at the class level was found on Seonginbong than on Dongdo and Seodo, as evidenced by the identification of microalgal communities via eukaryotic microbial communities (Table III and IV). This suggests that the microalgal group on Seonginbong engages in a symbiotic relationship with the fungi group, unlike on Dongdo and Seodo, and that this relationship directly impacts the Seonginbong natural environment. Previous studies have found that microalgae secrete a range of substances that influence their natural environment, including fungal toxins and predators (Havens and DeCosta 1987; Canovas et al. 1996; Mayer et al. 1997; Falconer 2012). The genera *Nitzschia* (Bates et al. 1989; Martin et al. 1990), *Amphora* (Daniel et al. 1980), and *Paralia* (Sar et al. 2012) are reported to be closely associated with shellfish toxins on Seodo (Falconer 2012; Sar et al. 2012) that can be harmful to human health when ingested orally. Although they only account for a small fraction of the detected microalgal community, it is nonetheless necessary to monitor their toxin-producing abilities and biological resources. Our findings indicate that microalgae are influenced both by environmental factors and the surrounding microbial community and that characteristics of the microbial community are influenced by the natural environment.

Conclusion

The present study analyzed the overall species richness and taxonomic compositions of the microalgal communities of Ulleungdo (Seonginbong) and Dokdo (Dongdo and Seodo). Amplicon sequencing analysis was performed using Illumina MiSeq, and microbiological OTUs from Seonginbong (834), Dongdo (203), and Seodo (182) were identified. Three indicators (Chao1, Shannon, and Simpson) were used to analyze species richness, and it was found that the species richness of Seonginbong was higher than those of Dongdo and Seodo. Classified reads were used for taxonomic analy-

sis, with the communities exhibiting differences in their composition from the phylum to species levels. In the Seonginbong sample, several other eukaryotic microorganisms were present in the community in addition to microalgae, while microalgae (Chlorophyta) and diatoms (Bacillariophyta) were found to be extremely dominant on Dongdo and Seodo, respectively. Analyses of the relative abundances of the different communities added details to information regarding the differences in species richness between the three regions. We obtained information on microalgae on Seonginbong, Dongdo, and Seodo via MiSeq tools; however, MiSeq analysis does have some limitations with regards to dependence on existing taxonomies in screening and identifying microalgal species. Despite these experimental limitations, MiSeq analysis provided in-depth information on the microalgal communities of Ulleungdo and Dokdo.

Acknowledgments

This work was supported by a grant from the Next-Generation BioGreen 21 Program (No. PJ01366701), Korea and the Basic Science Research Program through the National Research Foundation of Korea (NRF) and funded by the Ministry of Education (2016R1A6A1A05011910; 2017R1A2B4002016; 2018R1D1A3 B07049385), Korea.

Conflict of interest

The authors do not report any financial or personal connections with other persons or organizations, which might negatively affect the contents of this publication and/or claim authorship rights to this publication.

Literature

- Ahmadjian V.** The lichen alga *Trebouxia*: does it occur free-living? *Plant Syst Evol.* 1987;158(2-4):243–247. <https://doi.org/10.1007/BF00936348>
- Bates SS, Bird CJ, Freitas ASW, Foxall R, Gilgan M, Hanic LA, Johnson GR, McCulloch AW, Odense P, Pocklington R, et al.** Pennate diatom *Nitzschia pungens* as the primary source of domoic acid, a toxin in shellfish from eastern Prince Edward Island, Canada. *Can J Fish Aquat Sci.* 1989 Jul;46(7):1203–1215. <https://doi.org/10.1139/f89-156>
- Bellinzoni AM, Caneva G, Ricci S.** Ecological trends in travertine colonisation by pioneer algae and plant communities. *Int Biodegrad Biodegradation.* 2003 Apr;51(3):203–210. [https://doi.org/10.1016/S0964-8305\(02\)00172-5](https://doi.org/10.1016/S0964-8305(02)00172-5)
- Berner RA.** Weathering, plants, and the long-term carbon cycle. *Geochim Cosmochim Acta.* 1992 Aug;56(8):3225–3231. [https://doi.org/10.1016/0016-7037\(92\)90300-8](https://doi.org/10.1016/0016-7037(92)90300-8)
- Booth WE.** Algae as pioneers in plant succession and their importance in erosion control. *Ecology.* 1941 Jan;22(1):38–46. <https://doi.org/10.2307/1930007>
- Buée M, Reich M, Murat C, Morin E, Nilsson RH, Uroz S, Martin F.** 454 Pyrosequencing analyses of forest soils reveal an unexpectedly high fungal diversity. *New Phytol.* 2009 Oct;184(2):449–456. <https://doi.org/10.1111/j.1469-8137.2009.03003.x>
- Busse MD, Beattie SE, Powers RF, Sanchez FG, Tiarks AE.** Microbial community responses in forest mineral soil to compaction, organic matter removal, and vegetation control. *Can J For Res.* 2006 Mar;36(3):577–588. <https://doi.org/10.1139/x05-294>

- Canovas S, Picot B, Casellas C, Zulkifi H, Dubois A, Bontoux J. Seasonal development of phytoplankton and zooplankton in a high-rate algal pond. *Water Sci Technol*. 1996 Mar;33(7):199–206. <https://doi.org/10.2166/wst.1996.0139>
- Cardinale BJ, Matulich KL, Hooper DU, Byrnes JE, Duffy E, Gamfeldt L, Balvanera P, O'Connor MI, Gonzalez A. The functional role of producer diversity in ecosystems. *Am J Bot*. 2011 Mar;98(3):572–592. <https://doi.org/10.3732/ajb.1000364>
- Chang KI, Kim YB, Suk MS, Byun SK. Hydrography around Dokdo. *Ocean Polar Res*. 2002 Dec 31;24(4):369–389. <https://doi.org/10.4217/OPR.2002.24.4.369>
- Chen W, Zhang CK, Cheng Y, Zhang S, Zhao H. A comparison of methods for clustering 16S rRNA sequences into OTUs. *PLoS One*. 2013 Aug 13;8(8):e70837. <https://doi.org/10.1371/journal.pone.0070837>
- Chen Z, Lei X, Zhang B, Yang L, Zhang H, Zhang J, Li Y, Zheng W, Tian Y, Liu J, et al. First report of *Pseudobodo* sp., a new pathogen for a potential energy-producing algae: *Chlorella vulgaris* cultures. *PLoS One*. 2014 Mar 5;9(3):e89571. <https://doi.org/10.1371/journal.pone.0089571>
- Chiao JS, Sheng WG, Cheng XB. [An important mission for microbiologists in the new century-cultivation of the unculturable microorganisms]. *Sheng Wu Gong Cheng Xue Bao*. 2004 Sep;20(5):641–645.
- Claassen S, du Toit E, Kaba M, Moodley C, Zar HJ, Nicol MP. A comparison of the efficiency of five different commercial DNA extraction kits for extraction of DNA from faecal samples. *J Microbiol Methods*. 2013 Aug;94(2):103–110. <https://doi.org/10.1016/j.mimet.2013.05.008>
- Daniel GF, Chamberlain AHL, Jones EBG. Ultrastructural observations on the marine fouling diatom *Amphora*. *Helgol Meeresunters*. 1980 Jun;34(2):123–149. <https://doi.org/10.1007/BF01984035>
- Djukic I, Zehetner F, Mentler A, Gerzabek MH. Microbial community composition and activity in different Alpine vegetation zones. *Soil Biol Biochem*. 2010 Feb;42(2):155–161. <https://doi.org/10.1016/j.soilbio.2009.10.006>
- Falconer IR. *Algal Toxins in Seafood and Drinking Water*. London (UK): Academic Press; 2012.
- Fierer N, Lauber CL, Ramirez KS, Zaneveld J, Bradford MA, Knight R. Comparative metagenomic, phylogenetic and physiological analyses of soil microbial communities across nitrogen gradients. *ISME J*. 2012 May;6(5):1007–1017. <https://doi.org/10.1038/ismej.2011.159>
- Goldman JC, Shapiro J. Letter: Carbon dioxide and pH: effect on species succession of algae. *Science*. 1973 Oct 19;182(4109):306–307. <https://doi.org/10.1126/science.182.4109.306>
- Han X, Wang R, Liu J, Wang M, Zhou J, Guo W. Effects of vegetation type on soil microbial community structure and catabolic diversity assessed by polyphasic methods in North China. *J Environ Sci (China)*. 2007 Jan;19(10):1228–1234. [https://doi.org/10.1016/S1001-0742\(07\)60200-9](https://doi.org/10.1016/S1001-0742(07)60200-9)
- Handelsman J. Metagenomics: application of genomics to uncultured microorganisms. *Microbiol Mol Biol Rev*. 2004 Dec 01;68(4):669–685. <https://doi.org/10.1128/MMBR.68.4.669-685.2004>
- Havens K, DeCosta J. Freshwater plankton community succession during experimental acidification. *Arch. Hydrobiol*. 1987;111:37–65.
- Heck KL Jr, van Belle G, Simberloff D. Explicit calculation of the rarefaction diversity measurement and the determination of sufficient sample size. *Ecology*. 1975 Oct;56(6):1459–1461. <https://doi.org/10.2307/1934716>
- Hudon C, Bourget E. The effect of light on the vertical structure of epibenthic diatom communities. *Bot Mar*. 1983;26(7):317–330. <https://doi.org/10.1515/botm.1983.26.7.317>
- Jackson TA. Study of the ecology of pioneer lichens, mosses, and algae on recent Hawaiian lava flows. *Pac Sci*. 1971;25:22–32.
- Johnson MTJ, Agrawal AA. The ecological play of predator-prey dynamics in an evolutionary theatre. *Trends Ecol Evol*. 2003 Nov;18(11):549–551. <https://doi.org/10.1016/j.tree.2003.09.001>
- Jung SY, Byun JG, Park SH, Oh SH, Yang JC, Jang JW, Chang KS, Lee YM. The study of distribution characteristics of vascular and naturalized plants in Dokdo, South Korea. *J Asia-Pac Biodivers*. 2014 Jun;7(2):e197–e205. <https://doi.org/10.1016/j.japb.2014.03.011>
- Kaczmarek I, Reid C, Moniz M. Diatom taxonomy: morphology, molecules and barcodes. Paper presented at: Proceedings of the 1st Central-European Diatom meeting 2007: Botanic Garden and Botanical Museum Berlin-Dahlem FU-Berlin; 2007. p. 69–72.
- Kim CH, Park JW, Lee MH, Park CH. Detailed bathymetry and submarine terraces in the coastal area of the Dokdo volcano in the Ulleung Basin, the East Sea (Sea of Japan). *J Coast Res*. 2013 Jan 02;65:523–528. <https://doi.org/10.2112/S165-089.1>
- Kim MH, Oh YJ, Kim CS, Han MS, Lee JT, Na YE. The flora and vegetation distribution in Dokdo. *Korean J Environ Agric*. 2007 Mar 27;26(1):85–93. <https://doi.org/10.5338/KJEA.2007.26.1.085>
- Kim YE, Yoon H, Kim M, Nam YJ, Kim H, Seo Y, Lee GM, Ja Kim Y, Kong WS, Kim JG, et al. Metagenomic analysis of bacterial communities on Dokdo Island. *J Gen Appl Microbiol*. 2014;60(2):65–74. <https://doi.org/10.2323/jgam.60.65>
- Knight IT. Molecular genetic methods for detection and identification of viable but nonculturable microorganisms. In: Colwell RR, Grimes DJ, editors. *Nonculturable Microorganisms in the Environment*. Boston: (MA, USA): Springer; 2000. p. 77–85. https://doi.org/10.1007/978-1-4757-0271-2_6
- Kozich JJ, Westcott SL, Baxter NT, Highlander SK, Schloss PD. Development of a dual-index sequencing strategy and curation pipeline for analyzing amplicon sequence data on the MiSeq Illumina sequencing platform. *Appl Environ Microbiol*. 2013 Sep 01;79(17):5112–5120. <https://doi.org/10.1128/AEM.01043-13>
- Krustok I, Truu J, Odlare M, Truu M, Ligi T, Tiirik K, Nehrenheim E. Effect of lake water on algal biomass and microbial community structure in municipal wastewater-based lab-scale photobioreactors. *Appl Microbiol Biotechnol*. 2015 Aug;99(15):6537–6549. <https://doi.org/10.1007/s00253-015-6580-7>
- Lange K, Liess A, Piggott JJ, Townsend CR, Matthaei CD. Light, nutrients and grazing interact to determine stream diatom community composition and functional group structure. *Freshw Biol*. 2011 Feb;56(2):264–278. <https://doi.org/10.1111/j.1365-2427.2010.02492.x>
- Lee YG, Kim BJ, Park GU, Ahn BY. Characteristics of precipitation and temperature at Ulleung-do and Dok-do, Korea for recent four years (2005–2008). *J. Environ. Sci. Int*. 2010 Sep 30;19(9):1109–1118. <https://doi.org/10.5322/JES.2010.19.9.1109>
- Lehman JT. Release and cycling of nutrients between planktonic algae and herbivores. *Limnol Oceanogr*. 1980 Jul;25(4):620–632. <https://doi.org/10.4319/lo.1980.25.4.0620>
- Li W, Fu L, Niu B, Wu S, Wooley J. Ultrafast clustering algorithms for metagenomic sequence analysis. *Brief Bioinform*. 2012 Nov 01;13(6):656–668. <https://doi.org/10.1093/bib/bbs035>
- Littler MM, Littler DS. An undescribed fungal pathogen of reef-forming crustose coralline algae discovered in American Samoa. *Coral Reefs*. 1998 Jul 7;17(2):144. <https://doi.org/10.1007/s003380050108>
- Luddington IA, Kaczmarek I, Lovejoy C. Distance and character-based evaluation of the V4 region of the 18S rRNA gene for the identification of diatoms (Bacillariophyceae). *PLoS One*. 2012 Sep 21;7(9):e45664. <https://doi.org/10.1371/journal.pone.0045664>
- Martin JL, Haya K, Burrige LE, Wildish DJ. *Nitzschia pseudodelicatissima* – a source of domoic acid in the Bay of Fundy,

- eastern Canada. *Mar Ecol Prog Ser.* 1990;67:177–182. <https://doi.org/10.3354/meps067177>
- Mayer J, Dokulil MT, Salbrechter M, Berger M, Posch T, Pfister G, Kirschner AK, Velimirov B, Steitz A, Ulbricht T. Seasonal successions and trophic relations between phytoplankton, zooplankton, ciliate and bacteria in a hypertrophic shallow lake in Vienna, Austria. *Hydrobiologia.* 1997;342:165–174. <https://doi.org/10.1023/A:1017098131238>
- Merilä P, Malmivaara-Lämsä M, Spetz P, Stark S, Vierikko K, Derome J, Fritze H. Soil organic matter quality as a link between microbial community structure and vegetation composition along a successional gradient in a boreal forest. *Appl Soil Ecol.* 2010 Oct;46(2):259–267. <https://doi.org/10.1016/j.apsoil.2010.08.003>
- Metting F. Biodiversity and application of microalgae. *J Ind Microbiol.* 1996;17:477–489.
- Meyer M, Kircher M. Illumina sequencing library preparation for highly multiplexed target capture and sequencing. *Cold Spring Harb Protoc.* 2010 Jun 01;2010(6):pdb.prot5448. <https://doi.org/10.1101/pdb.prot5448>
- Nam YJ, Kim H, Lee JH, Yoon H, Kim JG. Metagenomic analysis of soil fungal communities on Ulleungdo and Dokdo Islands. *J Gen Appl Microbiol.* 2015;61(3):67–74. <https://doi.org/10.2323/jgam.61.67>
- Niu B, Fu L, Sun S, Li W. Artificial and natural duplicates in pyrosequencing reads of metagenomic data. *BMC Bioinformatics.* 2010;11(1):187. <https://doi.org/10.1186/1471-2105-11-187>
- Park SJ, Song IG, Park SJ, Lim DO. [The flora and vegetation of Dokdo Island in Ulleung-gun, Gyeongsanbuk-do]. *Korean J Environ Ecol.* 2010;24(3):264–278.
- Piercey-Normore MD. The lichen-forming ascomycete *Evernia mesomorpha* associates with multiple genotypes of *Trebouxia jamesii*. *New Phytol.* 2006 Jan;169(2):331–344. <https://doi.org/10.1111/j.1469-8137.2005.01576.x>
- Porter KG. The plant-animal interface in freshwater ecosystems: microscopic grazers feed differentially on planktonic algae and can influence their community structure and succession in ways that are analogous to the effects of herbivores on terrestrial plant communities. *Am Sci.* 1977;65:159–170.
- Post AF, Dubinsky Z, Wyman K, Falkowski PG. Kinetics of light-intensity adaptation in a marine planktonic diatom. *Mar Biol.* 1984;83(3):231–238. <https://doi.org/10.1007/BF00397454>
- Pradeep V, Van Ginkel S, Park S, Igou T, Yi C, Fu H, Johnston R, Snell T, Chen Y. Use of copper to selectively inhibit *Brachionus calyciflorus* (Predator) growth in *Chlorella kessleri* (Prey) mass cultures for algae biodiesel production. *Int J Mol Sci.* 2015 Aug 31;16(9):20674–20684. <https://doi.org/10.3390/ijms160920674>
- Prowse GA, Tallng JF. The seasonal growth and succession of plankton algae in the White Nile. *Limnol Oceanogr.* 1958 Apr;3(2):222–238. <https://doi.org/10.4319/lo.1958.3.2.0222>
- Rodríguez-Brito B, Li L, Wegley L, Furlan M, Angly F, Breitbart M, Buchanan J, Desnues C, Dinsdale E, Edwards R, et al. Viral and microbial community dynamics in four aquatic environments. *ISME J.* 2010 Jun;4(6):739–751. <https://doi.org/10.1038/ismej.2010.1>
- Round FE. The taxonomy of the Chlorophyta. *Brit Phycol Bull.* 1963 Dec;2(4):224–235. <https://doi.org/10.1080/00071616300650061>
- Sar EA, Sunesen I, Goya AB, Lavigne AS, Tapia E, García C, Lagos N. First report of diarrhetic shellfish toxins in mollusks from Buenos Aires province (Argentina) associated with *Dinophysis* spp.: evidence of okadaic acid, dinophysistoxin-1 and their acyl-derivatives. *Bol Soc Argent Bot.* 2012;47:5–14.
- Sarma SSS, Trujillo-Hernández HE, Nandini S. Population growth of herbivorous rotifers and their predator (*Asplanchna*) on urban wastewaters. *Aquat Ecol.* 2003;37(3):243–250. <https://doi.org/10.1023/A:1025896703470>
- Schloss PD, Handelsman J. Metagenomics for studying unculturable microorganisms: cutting the Gordian knot. *Genome Biol.* 2005;6(8):229. <https://doi.org/10.1186/gb-2005-6-8-229>
- Schloss PD, Westcott SL, Ryabin T, Hall JR, Hartmann M, Hollister EB, Lesniewski RA, Oakley BB, Parks DH, Robinson CJ, et al. Introducing mothur: open-source, platform-independent, community-supported software for describing and comparing microbial communities. *Appl Environ Microbiol.* 2009 Dec 01;75(23):7537–7541. <https://doi.org/10.1128/AEM.01541-09>
- Shin H, Park S, Kang K, Yoo J. The establishment of conservation area and conservation strategy in Ulnung Island. *Korean J Environ Ecol.* 2004;18:221–230.
- Shokralla S, Spall JL, Gibson JF, Hajibabaei M. Next-generation sequencing technologies for environmental DNA research. *Mol Ecol.* 2012 Apr;21(8):1794–1805. <https://doi.org/10.1111/j.1365-294X.2012.05538.x>
- Sohn YK. Geology of Tok Island, Korea: eruptive and depositional processes of a shoaling to emergent island volcano. *Bull Volcanol.* 1995 Feb;56(8):660–674. <https://doi.org/10.1007/BF00301469>
- Stoeck T, Bass D, Nebel M, Christen R, Jones MDM, Breiner HW, Richards TA. Multiple marker parallel tag environmental DNA sequencing reveals a highly complex eukaryotic community in marine anoxic water. *Mol Ecol.* 2010 Mar;19 Suppl 1:21–31. <https://doi.org/10.1111/j.1365-294X.2009.04480.x>
- Streit WR, Schmitz RA. Metagenomics – the key to the uncultured microbes. *Curr Opin Microbiol.* 2004 Oct;7(5):492–498. <https://doi.org/10.1016/j.mib.2004.08.002>
- Sturm M, Schroeder C, Bauer P. SeqPurge: highly-sensitive adapter trimming for paired-end NGS data. *BMC Bioinformatics.* 2016 Dec;17(1):208. <https://doi.org/10.1186/s12859-016-1069-7>
- Tragin M, Zingone A, Vaultot D. Comparison of coastal phytoplankton composition estimated from the V4 and V9 regions of the 18S rRNA gene with a focus on photosynthetic groups and especially Chlorophyta. *Environ Microbiol.* 2018 Feb;20(2):506–520. <https://doi.org/10.1111/1462-2920.13952>
- Unno T, Jang J, Han D, Kim JH, Sadowsky MJ, Kim OS, Chun J, Hur HG. Use of barcoded pyrosequencing and shared OTUs to determine sources of fecal bacteria in watersheds. *Environ Sci Technol.* 2010 Oct 15;44(20):7777–7782. <https://doi.org/10.1021/es101500z>
- Vitousek PM, Cassman K, Cleveland C, Crews T, Field CB, Grimm NB, Howarth RW, Marino R, Martinelli L, Rastetter EB. Towards an ecological understanding of biological nitrogen fixation. In: Boyer EW, Howarth RW, editors. The nitrogen cycle at regional to global scales. Dordrecht (Germany): Springer; 2002. p. 1–45. https://doi.org/10.1007/978-94-017-3405-9_1
- Vo ATE, Jedlicka JA. Protocols for metagenomic DNA extraction and Illumina amplicon library preparation for faecal and swab samples. *Mol Ecol Resour.* 2014 Nov;14(6):1183–1197. <https://doi.org/10.1111/1755-0998.12269>
- Wegley L, Edwards R, Rodríguez-Brito B, Liu H, Rohwer F. Metagenomic analysis of the microbial community associated with the coral *Porites astreoides*. *Environ Microbiol.* 2007 Nov;9(11):2707–2719. <https://doi.org/10.1111/j.1462-2920.2007.01383.x>
- Yoshida T, Hairston NG Jr, Ellner SP. Evolutionary trade-off between defence against grazing and competitive ability in a simple unicellular alga, *Chlorella vulgaris*. *Proc R Soc Lond B Biol Sci.* 2004 Sep 22;271(1551):1947–1953. <https://doi.org/10.1098/rspb.2004.2818>
- Zhang Z, Schwartz S, Wagner L, Miller W. A greedy algorithm for aligning DNA sequences. *J Comput Biol.* 2000 Feb;7(1-2):203–214. <https://doi.org/10.1089/10665270050081478>

Epidemiology, Drug Resistance, and Virulence of *Staphylococcus aureus* Isolated from Ocular Infections in Polish Patients

MARTA KŁOS¹, MONIKA POMORSKA-WESOŁOWSKA², DOROTA ROMANISZYN³,
AGNIESZKA CHMIELARCZYK³ and JADWIGA WÓJKOWSKA-MACH^{3*}

¹ Faculty of Health Sciences, Jagiellonian University Medical College, Kraków, Poland

² Department of Microbiology, Analytical and Microbiological Laboratory, KORLAB, Ruda Śląska, Poland

³ Department of Microbiology, Faculty of Medicine, Jagiellonian University Medical College, Kraków, Poland

Submitted 1 August 2019, revised 7 November 2019, accepted 7 November 2019

Abstract

Analysis of the epidemiology of *Staphylococcus aureus* (SA) ocular infections and virulence factors of the isolates with a special emphasis on their drug resistance, and the ability of biofilm formation. In a period from 2009 to 2013, 83 isolates of SA were prospectively collected and preserved in a multicenter laboratory-based study carried out in southern Poland. Epidemiological, phenotypic, and genotypic analyses were performed. The resistance and virulence genes were analyzed. Screening for the biofilm formation was provided. Among the materials derived from ocular infections from 456 patients, SA was found in 18.2% (n = 83) of cases (one SA isolate per one patient). Most infections were identified in the age group of over 65 years (OR 8.4 95%CI; 1.03–68.49). The majority of patients (73.4%) were hospitalized. Among the virulence and resistance genes, the most frequently detected were the *lukE* (72.2%, n = 60) and *ermA* (15.6%, n = 13) genes. A positive result of the CRA test (the ability of biofilm formation) was found in 66.2% (n = 55) of isolates. Among the strains under study, 6.0% (n = 5) had the methicillin-resistant *Staphylococcus aureus* phenotype, and 26.5% (n = 22) had the macrolide-lincosamide-streptogramin B phenotype. In 48 (57.8%) isolates the neomycin resistance was revealed. All isolates under study were sensitive to vancomycin. The population most susceptible to ocular SA infections consists of hospitalized patients aged 65 and more. The SA strains under study showed the increased ability to biofilm formation. In the strains tested, high susceptibility to chloramphenicol and fluoroquinolones was demonstrated. However, the high level of drug resistance to neomycin detected in this study among SA isolates and the blood-ocular barrier makes it difficult to treat ocular infections.

Key words: *Staphylococcus aureus*, ocular infections, virulence factors, epidemiology, surgical interventions, soft contact lenses

Introduction

Bacteria are considered as the main contributor to ocular infections all over the world (Teweldemedhin et al. 2017). In the study by Long et al. conducted between 1990–2009, the most frequently isolated bacteria from ocular infections were Gram-positive cocci (41.9%) (Long et al. 2014). Analysis of databases proved that *Staphylococcus aureus* (SA) is predominant regardless of the geographical area or population examined (Teweldemedhin et al. 2017). The results of the research regarding the prevalence of SA isolates from ocular infections showed their distribution in the range from 13% in India to 28.1% in Ethiopia; the average prevalence was 20.1% (Teweldemedhin et al. 2017).

The most common ocular infection is conjunctivitis, which constitutes 50–70% of infectious conjunctivitis (Bertino 2009; Galvis et al. 2014; Teweldemedhin et al. 2017). Moreover, one should also point out the frequent incidents of bacterial keratitis and endophthalmitis (West et al. 2005; Bertino 2009; Pozzi et al. 2012; Teweldemedhin et al. 2017). Untreated ocular infections may cause injuries in the ocular structure and lead to visual impairments and blindness (Bertino 2009; Teweldemedhin et al. 2017). Researchers indicate a strong relationship between ocular trauma, contact lenses, and bacterial keratitis lesions in the anatomical ocular surface that may lead to the development of staphylococcal infection (Bourcier et al. 2003; Ly et al. 2006; Teweldemedhin et al. 2017). Moreover, a patient's

* Corresponding author: J. Wójkowska-Mach, Department of Microbiology, Jagiellonian University Collegium Medicum, Kraków, Poland;
e-mail: jadwiga.wojkowska-mach@uj.edu.pl

© 2019 Marta Kłos et al.

This work is licensed under the Creative Commons Attribution-NonCommercial-NoDerivatives 4.0 License (<https://creativecommons.org/licenses/by-nc-nd/4.0/>).

immunity to ocular infections can be reduced by underlying diseases, operative procedures, the use of corticosteroids, hospitalization, and the use of medical devices (Teweldemedhin et al. 2017).

One of the main SA virulence factors that contribute to ocular infections is its ability to the formation of biofilms on the surface of biomedical implants or contact lenses (Cramton et al. 1999). Through this process, the bacteria become more resistant to various physico-chemical stresses, e.g. antibiotics (Mathur et al. 2018). Cramton and coworkers reported that SA was more frequently isolated from corneal infections related to the contact lenses wearing (Cramton et al. 1999). The extended wear of contact lenses and lack of eye hygiene increase the risk of keratitis. The morbidity of ocular infections is associated with the increasing number of cataract surgery and lens replacement (Astley et al. 2019). The ability of SA strains to aggregate and form biofilm is related to their capacity of producing slime – an extracellular mucoid substance whose main components are glycosaminoglycans. The well-established phenotypic methods, such as the Congo Red Agar (CRA) test, are still used for the identification of the virulent biofilm-forming bacteria confirming phenotypically their ability to develop a biofilm. It has been shown that the results of this method coincide with the presence of the *icaA* and *icaD* genes in staphylococci (Arciola et al. 2002).

There is little information on human SA ocular infections in databases such as PubMed, a fact that makes it impossible to work out and implement effective and plausible measures to prevent infections. Concerning Polish patients, there is no epidemiological data at all. We sought to describe the epidemiology and various types of treatment for SA ocular infections with a special emphasis on cataract postoperative complications or the consequences of soft contact lenses wearing.

Experimental

Materials and Methods

SA isolates. Isolates from this multicenter laboratory-based study were obtained by the Department of Microbiology of the Jagiellonian University Medical College and were collected in collaboration with KORLAB from 1 January to 31 December 2013. Non-repetitive samples from ocular infection were collected from hospitalized patients (62) or outpatients (21) throughout the south of Poland. In total, clinical materials from 456 patients with symptoms of infection were examined and 83 isolates of SA were found, including 47 strains from the vitreous and corneas. The remaining clinical materials were conjunctival swabs.

The relevant patient information including age, sex, and type of care (ambulatory/hospitalization) was collected. The identification of microorganisms was performed using the MALDI-TOF Biotyper (Bruker Corporation, the Netherlands) according to standard methods.

Susceptibility testing. Antimicrobial susceptibility testing of all SA isolates was performed according to the current guidelines of the European Committee on Antimicrobial Susceptibility Testing (EUCAST, http://www.eucast.org/clinical_breakpoints/; accessed December 2017) by disc diffusion or the E-test method on Müller-Hinton agar plates. The antimicrobial discs (Oxoid Ltd., UK) contained gentamicin (10 µg), amikacin (30 µg), tobramycin (10 µg), neomycin (10 µg), ciprofloxacin (5 µg), moxifloxacin (5 µg), trimethoprim/sulfamethoxazole (1.25/23.75 µg), clindamycin (2 µg), erythromycin (15 µg), chloramphenicol (30 µg), and tetracycline (30 µg). Antimicrobial susceptibility to neomycin was interpreted according to the standards of the British Society for Antimicrobial Chemotherapy Version 14.0, 05.01.2015 (BSAC, <http://bsac.org.uk/wp-content/uploads/2012/02/BSAC-Susceptibility-testing-version-14.pdf>). For vancomycin, the minimal inhibitory concentration (MIC) was determined by E-test (bioMérieux, France).

The methicillin-resistant *Staphylococcus aureus* (MRSA) phenotype was detected using a ceftoxitin disc (30 µg). The macrolide-lincosamide-streptogramin B (MLS_B) phenotype was determined according to a previously published protocol (Leclercq 2002).

The categories of antimicrobial resistance. Strains were divided into six categories based on their resistance to several antimicrobial agent categories (aminoglycosides, fluoroquinolones, folate pathway inhibitors, lincosamides, macrolides, phenicols, and tetracyclines). The susceptibility of the isolate to all antimicrobial agents from all categories examined denoted “0”; “5 or more” meant resistance to five or more categories.

DNA isolation. The bacterial strains were grown overnight at 37°C in tryptic soy broth medium and total DNA was isolated with the Genomic Mini Kit (A&A Biotechnology, Gdynia, Poland) according to the manufacturer’s instructions.

Polymerase Chain Reaction (PCR)-based detection of resistance and virulence genes. PCR amplification was used to detect the *mecA* gene using previously described primers (Pereira et al. 2010). As controls, SA ATCC 33591 (*mecA*+) and SA ATCC 25923 (*mecA*-) were employed. PCR was also used to detect the presence of a gene resistant to mupirocin (*mupA* gene) (Anthony et al. 1999). SA ATCC BAA-1708 (*mupA*+) was employed as a control. The erythromycin resistance genes (*ermA*, *ermB*, *ermC*, and *msr*) were detected by multiplex PCR (Sutcliffe et al. 1996). The bands were visualized with the UVP GelDocIT Imaging System

Table I
Staphylococcus aureus strains isolated from ocular infections in different patient age groups with consideration of gender, hospitalization, and the results of the CRA test.

Characteristics of the study group	Hospitalization (n; %)			OR (95% CI)	p-value
	Yes, n = 61 (73.4%)	No, n = 22 (26.5%)	Total, N = 83		
Age (years) by categories [n; %]					
< = 18 years	15 (24.5%)	1 (4.5%)	16 (19.2%)	2.5 (0.20–32.99)	0.027
19–64 years	12 (19.6%)	2 (9.0%)	14 (16.8%)	1.00 (ref.)	
> = 65 years	34 (55.7%)	19 (86.3%)	53 (63.8%)	8.4 (1.03–68.49)	
Gender [n; %]					
Female	26 (42.6%)	12 (54.5%)	38 (45.7%)	0.6 (0.23–1.65)	0.454
Male	35 (57.3%)	10 (45.4%)	45 (54.2%)		
The positive CRA (Congo Red Agar) biofilm test result (n; %)					
yes	45 (73.7%)	10 (45.4%)	55 (66.2%)	3.3 (1.22–9.31)	0.016
no	16 (26.2%)	12 (54.5%)	28 (33.7%)		

OR (95%CI) – 95% confidence intervals of the odds ratio

(UVP, Upland, Canada) after 1.5%-TBE-agarose electrophoresis (70 min, 90 mV) and staining with ethidium bromide (Bio-Rad, Warsaw, Poland). A DNA-ladder of 100–1000 bp (Thermo Scientific, Waltham, MA, USA) was used as a size marker.

SA isolates were verified for the presence of the following virulence genes: *lukE* (LukDE leukocidin), *pvl* (Panton-Valentine leukocidin, PVL), *tsst-1* (toxic shock syndrome toxin-1, TSST-1), *etA*, and *etB* (exfoliative toxin A or B; EtA, EtB) using PCR and the previously described primers (Johnson et al. 1991; Lina et al. 1999). The strains used as controls were kindly provided by Prof. Marek Gniadkowski, National Medicines Institute, Warsaw, Poland.

To determine the *spa* type of the polymorphic X-region of the SA protein A, the *spa* gene was amplified by PCR and sequenced. Chromatograms obtained from sequencing were analyzed using DNAGear Spa Typing Software (Al-Tam et al. 2012).

Biofilm formation. Screening for the ability of SA isolates to develop a biofilm was carried out according to the method described by Arciola et al. with the CRA test (Arciola et al. 2002). 0.8 g of Congo Red and 36 g of saccharose (Sigma, St. Louis, MO, USA) were added to 1L of brain heart infusion agar (Oxoid, Basingstoke, Hampshire, England) to prepare CRA plates. The plates were incubated at 37°C for 24 h and then overnight at room temperature. On CRA plates, black colonies were formed by slime-producing strains and red ones by non-producing strains. A six-color scale was used to accurately assess all the possible chromatic variations exhibited by the growing colonies. The scale ranged from very black (vb), thorough black (b), and almost black (ab) to burgundy (brd), red (r), and very red (vr). Very black, black, and almost black colonies were classified as the slime producer strains, while very

red, red, and burgundy-colored colonies were classified as the strains unable to produce slime.

Ethics. All SA isolates under the study were collected as part of routine clinical care. No medical records or identifying information about the patients were accessed as part of this study. The isolates and any relevant information about the cases were obtained and analyzed in a fully anonymized and de-identified form. All data analyzed during this study were blinded before analysis. The utilization of this data for analysis without patients' agreement was consistent with Polish law and approved by the Bioethics Committee of the Jagiellonian University Medical College (No. BET/227/B/2012).

Results

Among the 456 cases of ocular infections examined, 83 (18.2%) SA strains were isolated (one strain from one patient). Slightly more than half of SA strains (54.2%) came from men. The majority of patients, i.e. 73.4% (42.6% of women and 57.3% of men, respectively) constituted the hospitalized cases (Table I). The results showed a large difference in SA-ocular infection prevalence between hospitalized and ambulatory patients. The most infection cases were observed in the group of people over 65 years (63.8%); the least in the biggest group of age in the range between 19 and 64 years (16.8%). The infections in the oldest patients were treated five times more often in an outpatient setting (OR 95%CI 8.4; 1.03–68.49; $p = 0.027$, Table I).

One of the virulence characteristics, which is biofilm formation, was evaluated with the CRA test. A positive result of the CRA test was found in 66.2% of all cases (Table I). It was demonstrated that 66.2% of the strains showed biofilm formation capacity, with 22% of them

Table II
The presence of various genes encoding for the resistance and virulence factors of *Staphylococcus aureus* strains isolated from ocular infections.

Studied genes	Hospitalization (n;%)		Total n = 83
	Yes, n = 61 (73.4%)	No, n = 22 (26.5%)	
<i>mecA</i> (n = 6; 7%)	4 (6.5%)	2 (9.0%)	6 (7.2%)
<i>ermA</i> (n = 13; 16%)	8 (13.1%)	5 (22.7%)	13 (15.6%)
<i>mup</i> (n = 4; 5%)	4 (6,5%)	0	4 (4.8%)
<i>lukE</i> (n = 60; 72%)	45 (73.7%)	15 (68.1%)	60 (72.2%)
<i>tst-1</i> (n = 10; 12%)	10 (16.3%)	0	10 (12.0%)
<i>etA</i> (n = 3; 4%)	2 (3.2%)	1 (4.5%)	3 (3.6%)
<i>etB</i> (n = 2; 2%)	2 (3.2%)	N0	2 (2.4%)

etA/B – exfoliative toxin A and/or B; *lukE* – lukDE leukocidins; N/A – not applicable;
OR (95%CI) – 95% confidence intervals of odds ratio

being strong biofilm formers (very black and black colors), and 44% being weaker (almost black color). Among the biofilm-forming strains, the hospital strains dominated (73.4%), whereas among the ambulatory strains the ratio between biofilm-forming strains and non-producing ones was more even (45.4% vs. 54.5%; OR 95%CI 3.3; 1.22–9.31; $p = 0.016$, Table I).

The most frequent virulence and resistance genes were *lukE* and *ermA* (Table II). The presence of other virulence genes oscillated within the range of 1.2–12.0% of cases. The *pvl* gene was found in one strain. Strains from hospitalized patients were the main source of virulence genes. In the isolates from ambulatory patients, the *mup*, *tst-1*, *pvl* or *etB* genes were not found. Interestingly, all cases of the *pvl*, *tst* and *etB* genes detected in this study as well as two out of three the *etA* genes and 63% of the *lukE* genes were found among the strains positive in the CRA test.

Among the SA strains, most were resistant to neomycin and comprised 57.8% (n = 48). The level of erythromycin resistance amounted to 25.3%; 13.2% of isolates were resistant to ciprofloxacin, and 7.2% to moxifloxacin (Table III). Resistance to fluoroquinolones was five times more often found in ambulatory patients. Additionally, resistance to tobramycin was recorded for 14 strains (16.8%), to gentamicin for five strains (6.0%), and to chloramphenicol also for five strains (6.0%). All the isolates under study were sensitive to vancomycin, and the MIC value was equal to 1 µg/ml. Out of the isolates under study, 73.4% belonged to the category of fully susceptible to antimicrobial agents. The highest percentage of strains resistant to at least one antimicrobial was identified in hospitalized patients (40.9% for one category) and in outpatients (27.2% for two categories) (Table III). On the other hand, the strains isolated from hospitalized patients were four times more likely to show full susceptibility (they belonged to the “fully susceptible” category, Table III) than strains from non-hospitalized patients.

Among the strains under study, five isolates (6.0%) had the MRSA phenotype and 22 had the MLS_B phenotype (26.5%), including 17 strains that had the inducible (iMLS_B) and five strains that had the constitutive (cMLS_B) phenotypes (Table III). Four strains manifested both mechanisms at the same time. Each of the five MRSA strains had the *mecA* gene. Additionally, one strain had the *mecA* gene without the MRSA phenotype. Thirteen strains contained the *ermA* gene, including all those with the mechanism of cMLS_B resistance and seven with that of iMLS_B. One strain with the iMLS_B mechanism had the *mstA/B* gene, and in eight strains none of the genes of resistance under study was found.

Spa typing of five MRSA isolates showed the presence of three different *spa* types – three strains belonged to t003, one to t015, and one to t1192.

Discussion

In the studied population, the contribution of SA strains to ocular infections was slightly higher than in the American population as it has been shown by Gentile and coworkers, and where the most prevalent pathogens were coagulase-negative staphylococci (39.4%), followed by *Streptococcus viridans* (12.1%), and SA (11.1%) (Gentile et al. 2014). Similar findings came from Canada and Europe (Asencio et al. 2014; Assaad et al. 2015). A Chinese analysis of corneal samples have provided that Gram-positive cocci (69.88%) are the most commonly isolated; nevertheless, a decreasing trend was observed over the nine years of the study (Lin et al. 2019).

However, despite its non-dominant role in ocular infections, SA is an important etiologic agent of ocular infections. Callegan and coworkers have reported that ocular SA infections were more difficult to treat and the sharpness of vision was restored only in 30%

Table III
Drug resistance of *Staphylococcus aureus* strains isolated from ocular infections.

Antimicrobial category	Antimicrobial agent	Hospitalization n (%)		Total, N = 83
		Yes, n = 61 (73.4%)	No, n = 22 (26.5%)	
Aminoglycosides	Gentamicin	4 (6.5%)	1 (4.5%)	5 (6.0%)
	Amikacin	5 (8.1%)	3 (13.6%)	8 (9.6%)
	Tobramycin	9 (14.7%)	5 (22.7%)	14 (16.8%)
	Neomycin	37 (60.6%)	11 (50.0%)	48 (57.8%)
Fluoroquinolones	Ciprofloxacin	4 (6.5%)	7 (31.8%)	11 (13.2%)
	Moxifloxacin	2 (3.2%)	4 (18.1%)	6 (7.2%)
Folate pathway inhibitors	Trimethoprim/sulfamethoxazole	3 (4.9%)	2 (9.0%)	5 (6.0%)
Lincosamides	Clindamycin	13 (21.3%)	8 (36.3%)	21 (25.3%)
Macrolides	Erythromycin	13 (21.3%)	8 (36.3%)	21 (25.3%)
Phenicol	Chloramphenicol	4 (6.5%)	1 (4.5%)	5 (6.0%)
Tetracyclines	Tetracycline	11 (18.0%)	3 (13.6%)	14 (16.8%)
Non-susceptible to antimicrobial agents in (above) categories				
	fully susceptible (0 categories)	37 (60.6%)	6 (27.2%)	61 (73.4%)
	one category	25 (40.9%)	4 (18.1%)	29 (34.9%)
	2 categories	12 (19.6%)	6 (27.2%)	18 (21.6%)
	3 categories	5 (8.1%)	1 (4.5%)	6 (7.2%)
	4 categories	2 (3.2%)	1 (4.5%)	3 (3.6%)
	5 categories or more	2 (3.2%)	4 (18.1%)	5 (6.0%)
MRSA, yes		3 (4.9%)	2 (9.0%)	5 (6.0%)
MLS _B , yes		14 (22.9%)	8 (36.3%)	22 (26.5%)

MLS_B – macrolide/lincosamide/streptogramin B resistant *Staphylococcus aureus*; MRSA – methicillin-resistant *Staphylococcus aureus*;
OR (95% CI) – 95% confidence intervals of odds ratio

of the patients (Callegan et al. 2007). The research conducted by West and coworkers from 1994 to 2001 in the American population has indicated an increase in endophthalmitis incidence as a complication of cataract surgery, a fact that is challenging because this was the most common surgery in the USA (West et al. 2005; Astley et al. 2019). The reports by West and coworkers were confirmed by the results of Callegan and coworkers, which showed that postoperative endophthalmitis was a result of almost every ocular surgery, mainly cataract surgery (Callegan et al. 2007). Astley and coworkers also pointed to an increase in injection-related complications following intravitreal injections (Astley et al. 2019). One of the important elements that interfere with proper postoperative healing, and is the cause of therapeutic failures can be the virulence of pathogens. In any operation with the use of implants, such as cataract surgery, SA can present its capacity to form a biofilm. This problem was discussed by Ammendolia and coworkers who demonstrated the presence of a very high proportion of biofilm-forming strains (88.9%) higher than in the population investigated here (66.2%) (Ammendolia et al. 1999). At the same time, Ammendolia and coworkers has initially claimed that slime production was never considered as a virulence

factor, but their studies generally dealt with various types of hospital infections, not only ocular infections (Ammendolia et al. 1999). The studies considering the problem of biofilm-forming strains in ocular infections, however, have not been conducted so far. Atshan and coworkers have indicated the biofilm formation to varied extent and diverse adherence capacities of MRSA strains depending on their *spa* type (Atshan et al. 2012).

The results from the Antibiotic Resistance Monitoring in Ocular Microorganisms (ARMOR) group have shown that of MRSA amounts to 39% of ocular infections and there is also an increase in the resistance to fluoroquinolones among the ophthalmic strains in the United States (Haas et al. 2011; Vola et al. 2013). This was confirmed by a study by Morrissey and coworkers conducted in European countries, where MRSA was shown to be an etiologic agent of 22% of all ocular SA infections (Morrissey et al. 2004; Vola et al. 2013). Fortunately, according to the data analyzed and presented here, the problem of MRSA does not concern southern Poland since the prevalence of MRSA is lower. The authors' previous experience regarding other clinical forms of both hospital and outpatient infections in southern Poland indicated a high prevalence of MRSA in bloodstream infections (20.4%), and pneumonia

(32.7%) (Pomorska-Wesołowska et al. 2017). The general hospital prevalence of MRSA is 15.1%, and it is three times higher than it was established in the recent ocular infection study (Chmielarczyk et al. 2016). As reported previously, and also in this study, the *spa* typing confirmed that *spa* type t003 was the most predominant among MRSA strains (Chmielarczyk et al. 2016; Pomorska-Wesołowska et al. 2017).

Between the above-mentioned studies and ours, there was no difference in SA resistance to MLS_B, which was observed at a similar level (less than 30% in the studied patients' population with ocular infections) as well as in other populations of patients in southern Poland (Chmielarczyk et al. 2016; Pomorska-Wesołowska et al. 2017). Unfortunately, there are no known reports on MLS_B resistance in ocular infections coming from other parts of the world.

The most common antibiotics administered in ocular infections are fluoroquinolones, chloramphenicol, and aminoglycosides (Brown 2007). Unluckily, both Polish data and evidence from other centers, including those from Europe, indicate a low sensitivity of SA to aminoglycosides and some fluoroquinolones (Galvis et al. 2014; Gentile et al. 2014). Nevertheless, in the latest ARMOR surveillance studies from the USA, there was no difference in the level of resistance to older (ciprofloxacin) and newer-generation fluoroquinolones (moxifloxacin), and it was 35.8% vs 33.6%, respectively. In our study, resistance was lower to moxifloxacin (7.2%) than to ciprofloxacin (13.2%), so the newer generation of fluoroquinolones can be more effective in therapy (Thomas et al. 2019).

Given the rising resistance of 4th generation fluoroquinolones that have been observed in recent years, researches were conducted on the effectiveness of aminoglycosides (Galvis et al. 2014). Chinese research on corneal infections caused by SA confirmed the lowest resistance of the strains to neomycin (Wang et al. 2016). The possibility of treatment with the aminoglycoside group was confirmed independently by studies by Blanco and coworkers and Lin and coworkers, which showed high susceptibility of those strains to chloramphenicol (Blanco et al. 2013; Lin et al. 2019). Our results also confirm the high susceptibility of the SA isolates to fluoroquinolones and chloramphenicol. This is important information because the results of systematic review and meta-analysis suggested that fluoroquinolones might be the first choice for empirical treatment of most cases of the suspected bacterial keratitis (Hanet et al. 2012; Austin et al. 2017).

Unfortunately, the findings of this study have indicated that in Poland a serious problem, rarely described by other authors, occurs i.e. the resistance of SA to neomycin in almost 60% of strains. It appears that this is quite a rare situation because the reports of Wang and

coworkers from China have recently determined neomycin resistance in 7.8% of strains, i.e. at a considerably lower level than that established for the isolates from Polish patients (Wang et al. 2016). Therefore, this situation is surprising as neomycin is not frequently or routinely used systemically in the treatment of more common infections as opposed to ocular infections. All pharmaceutical preparations with neomycin associated with ocular treatment are available in Poland on prescription and none of them is a combined preparation. For the topical dermatological treatment, there are available over-the-counter medicines containing neomycin in combination with e.g. bacitracin, which could lead to such high neomycin resistance but the lack of Polish historical data or data from other countries makes it difficult to interpret the phenomenon observed.

Ocular antibiotics are usually administered locally, in the form of solution or suspension, to obtain a high concentration of antibacterial in the place of infection. Since the 1980s, the antibiotics can be administered in the form of injections directly into the vitreous, with the visual outcome of patients not changed considerably (Callegan et al. 2007). In ocular infections, therapeutic success depends on quick and accurate diagnosis and also on the administration of antibiotics (Callegan et al. 2007). This is due to the bacterial toxins and enzymes that may damage the integrity of the ocular tissues (Bertino 2009). Astley and coworkers reported some of those, including α -toxin (a role in the pathogenesis of SA keratitis and endophthalmitis) and PVL (cytotoxin) (Astley et al. 2019). The key anatomic barriers, such as the delicate nature of the interior of the eye and the blood-ocular barrier are factors to be considered during treatment (Callegan et al. 2007). Drug administration and contact lenses consist of a problem.

Study limitations

There are some limitations associated with this laboratory-based study. First, the demographic information on the study population is limited. For example, previous hospitalization and/or surgery and antimicrobial usage, co-morbidity, disability, and patient outcome data were not available because of the retrospective nature of the study. Additionally, these results may not be generalizable to the other parts of Poland.

Conclusions

In conclusion, the most common microorganisms in ocular infections were Gram-positive cocci, especially SA strains. The main virulence factor was the biofilm formation capacity of isolates and a high percentage of

strains with the *lukE* gene was also observed. Although high resistance to neomycin was noted, our research indicates a high efficacy of treatment with chloramphenicol and fluoroquinolones, as well as the need to implement new solutions due to the aforementioned bacteria's high resistance to neomycin and anatomic barrier difficulties.

Funding

This work was supported by the grants from Jagiellonian University Medical College ZDS/007045 and SAP N43/DBS/000014.

Acknowledgments

We would like to thank Professor Marta Wałaszek for help in statistical analysis.

Conflict of interest

The authors do not report any financial or personal connections with other persons or organizations, which might negatively affect the contents of this publication and/or claim authorship rights to this publication.

Literature

- Al-Tam F, Brunel AS, Bouzinbi N, Corne P, Bañuls AL, Shahbazkia HR. DNA Gear – a free software for spa type identification in *Staphylococcus aureus*. *BMC Res Notes* 2012;19(5):642.
- Ammendolia MG, Di Rosa R, Montanaro L, Arciola CR, Baldassarri L. Slime production and expression of the slime-associated antigen by staphylococcal clinical isolates. *J Clin Microbiol*. 1999 Oct;37(10):3235–3238.
- Anthony RM, Connor AM, Power EGM, French GL. Use of the polymerase chain reaction for rapid detection of high-level mupirocin resistance in staphylococci. *Eur J Clin Microbiol Infect Dis*. 1999 Feb 24;18(1):30–34. <https://doi.org/10.1007/s100960050222>
- Arciola CR, Campoccia D, Gamberini S, Cervellati M, Donati E, Montanaro L. Detection of slime production by means of an optimised Congo red agar plate test based on a colourimetric scale in *Staphylococcus epidermidis* clinical isolates genotyped for ica locus. *Biomaterials*. 2002 Nov;23(21):4233–4239. [https://doi.org/10.1016/S0142-9612\(02\)00171-0](https://doi.org/10.1016/S0142-9612(02)00171-0)
- Asencio MA, Huertas M, Carranza R, Tenías JM, Celis J, González-Del Valle F. [Microbiological study of infectious endophthalmitis with positive culture within a 13 year-period]. *Rev Esp Quimioter*. 2014 Mar;27(1):22–27.
- Assaad D, Wong D, Mikhail M, Tawfik S, Altomare F, Berger A, Chow D, Giavedoni L. Bacterial endophthalmitis: 10-year review of the culture and sensitivity patterns of bacterial isolates. *Can J Ophthalmol*. 2015 Dec;50(6):433–437. <https://doi.org/10.1016/j.cjco.2015.07.013>
- Astley R, Miller FC, Mursalin MH, Coburn PS, Callegan MC. An eye on *Staphylococcus aureus* toxins: roles in ocular damage and inflammation. *Toxins (Basel)* 2019;11(6):356. <https://doi.org/10.3390/toxins11060356>
- Atshan SS, Shamsudin MN, Thian Lung LT, Sekawi Z, Ghaznavi-Rad E, Pei Pei C. Comparative characterisation of genotypically different clones of MRSA in the production of biofilms. *J Biomed Biotechnol*. 2012;2012:1–7. <https://doi.org/10.1155/2012/417247>
- Austin A, Lietman T, Rose-Nussbaumer J. Update on the management of infectious keratitis. *Ophthalmology*. 2017 Nov;124(11):1678–1689. <https://doi.org/10.1016/j.ophtha.2017.05.012>
- Bertino JS Jr. Impact of antibiotic resistance in the management of ocular infections: the role of current and future antibiotics. *Clin Ophthalmol*. 2009 Sep;3:507–521. <https://doi.org/10.2147/OPTH.S5778>
- Blanco AR, Sudano Roccaro A, Spoto CG, Papa V. Susceptibility of methicillin-resistant *Staphylococci* clinical isolates to netilmicin and other antibiotics commonly used in ophthalmic therapy. *Curr Eye Res*. 2013 Aug;38(8):811–816. <https://doi.org/10.3109/02713683.2013.780624>
- Bourcier T, Thomas F, Borderie V, Chaumeil C, Laroche L. Bacterial keratitis: predisposing factors, clinical and microbiological review of 300 cases. *Br J Ophthalmol*. 2003 Jul 01;87(7):834–838. <https://doi.org/10.1136/bjo.87.7.834>
- Brown L. Resistance to ocular antibiotics: an overview. *Clin Exp Optom*. 2007 Jul;90(4):258–262. <https://doi.org/10.1111/j.1444-0938.2007.00154.x>
- Callegan M, Gilmore M, Gregory M, Ramadan R, Wiskur B, Moyer A, Hunt J, Novosad B. Bacterial endophthalmitis: therapeutic challenges and host–pathogen interactions. *Prog Retin Eye Res*. 2007 Mar;26(2):189–203. <https://doi.org/10.1016/j.preteyeres.2006.12.001>
- Chmielarczyk A, Pomorska-Wesołowska M, Szczypka A, Romaniszyn D, Pobiega M, Wójkowska-Mach J. Molecular analysis of methicillin-resistant *Staphylococcus aureus* strains isolated from different types of infections from patients hospitalized in 12 regional, non-teaching hospitals in southern Poland. *J Hosp Infect*. 2017 Mar;95(3):259–267. <https://doi.org/10.1016/j.jhin.2016.10.024>
- Cramton SE, Gerke C, Schnell NE, Nichols WW, Götz F. The intercellular adhesion (ica) locus is present in *Staphylococcus aureus* and is required for biofilm formation. *Infect Immun*. 1999 Oct;67(10):5427–5433.
- Galvis V, Tello A, Guerra A, Acuña MF, Villarreal D. [Antibiotic susceptibility patterns of bacteria isolated from keratitis and intraocular infections at Fundación Oftalmológica de Santander (FOSCAL), Floridablanca, Colombia]. *Biomedica*. 2014 Apr;34(1) Suppl 1:23–33.
- Gentile RC, Shukla S, Shah M, Ritterband DC, Engelbert M, Davis A, Hu DN. Microbiological spectrum and antibiotic sensitivity in endophthalmitis: a 25-year review. *Ophthalmology*. 2014 Aug; 121(8):1634–1642. <https://doi.org/10.1016/j.ophtha.2014.02.001>
- Haas W, Pillar CM, Torres M, Morris TW, Sahn DF. Monitoring antibiotic resistance in ocular microorganisms: results from the Antibiotic Resistance Monitoring in Ocular microOrganisms (ARMOR) 2009 surveillance study. *Am J Ophthalmol*. 2011 Oct; 152(4):567–574.e3. <https://doi.org/10.1016/j.ajo.2011.03.010>
- Hanet MS, Jamart J, Pinheiro Chaves A. Fluoroquinolones or fortified antibiotics for treating bacterial keratitis: systematic review and meta-analysis of comparative studies. *Can J Ophthalmol*. 2012 Dec;47(6):493–499. <https://doi.org/10.1016/j.cjco.2012.09.001>
- Johnson WM, Tyler SD, Ewan EP, Ashton FE, Pollard DR, Rozee KR. Detection of genes for enterotoxins, exfoliative toxins, and toxic shock syndrome toxin 1 in *Staphylococcus aureus* by the polymerase chain reaction. *J Clin Microbiol*. 1991 Mar;29(3):426–430.
- Leclercq R. Mechanisms of resistance to macrolides and lincosamides: nature of the resistance elements and their clinical implications. *Clin Infect Dis* 2002;34(4):482–492.
- Lin L, Duan F, Yang Y, Lou B, Liang L, Lin X. Nine-year analysis of isolated pathogens and antibiotic susceptibilities of microbial keratitis from a large referral eye center in southern China. *Infect Drug Resist*. 2019 May;12(12):1295–1302. <https://doi.org/10.2147/IDR.S206831>
- Lina G, Piémont Y, Godail-Gamot F, Bes M, Peter MO, Gauduchon V, Vandenesch F, Etienne J. Involvement of Panton-Valentine

- leukocidin-producing *Staphylococcus aureus* in primary skin infections and pneumonia. *Clin Infect Dis*. 1999 Nov 01;29(5): 1128–1132. <https://doi.org/10.1086/313461>
- Long C, Liu B, Xu C, Jing Y, Yuan Z, Lin X. Causative organisms of post-traumatic endophthalmitis: a 20-year retrospective study. *BMC Ophthalmol*. 2014 Dec;14(1):34. <https://doi.org/10.1186/1471-2415-14-34>
- Ly CN, Pham JN, Badenoch PR, Bell SM, Hawkins G, Rafferty DL, McClellan KA. Bacteria commonly isolated from keratitis specimens retain antibiotic susceptibility to fluoroquinolones and gentamicin plus cephalothin. *Clin Exp Ophthalmol*. 2006 Jan; 34(1): 44–50. <https://doi.org/10.1111/j.1442-9071.2006.01143.x>
- Mathur H, Field D, Rea MC, Cotter PD, Hill C, Ross RP. Fighting biofilms with lantibiotics and other groups of bacteriocins. *NPJ Biofilms Microbiomes*. 2018 Dec;4(1):9. <https://doi.org/10.1038/s41522-018-0053-6>
- Morrissey I, Burnett R, Viljoen L, Robbins M. Surveillance of the susceptibility of ocular bacterial pathogens to the fluoroquinolone gatifloxacin and other antimicrobials in Europe during 2001/2002. *J Infect*. 2004 Aug;49(2):109–114. <https://doi.org/10.1016/j.jinf.2004.03.007>
- Pereira EM, Schuenck RP, Malvar KL, Iorio NLP, Matos PDM, Olendzki AN, Oelemann WMR, dos Santos KRN. *Staphylococcus aureus*, *Staphylococcus epidermidis* and *Staphylococcus haemolyticus*: methicillin-resistant isolates are detected directly in blood cultures by multiplex PCR. *Microbiol Res*. 2010 Mar;165(3):243–249. <https://doi.org/10.1016/j.micres.2009.03.003>
- Pomorska-Wesołowska M, Chmielarczyk A, Chlebowicz M, Ziółkowski G, Szczypta A, Natkaniec J, Romaniszyn D, Pobiega M, Dzikowska M, Krawczyk L, et al. Virulence and antimicrobial resistance of *Staphylococcus aureus* isolated from bloodstream infections and pneumonia in Southern Poland. *J Glob Antimicrob Resist*. 2017 Dec;11:100–104. <https://doi.org/10.1016/j.jgar.2017.07.009>
- Pozzi C, Waters EM, Rudkin JK, Schaeffer CR, Lohan AJ, Tong P, Loftus BJ, Pier GB, Fey PD, Massey RC, et al. Methicillin resistance alters the biofilm phenotype and attenuates virulence in *Staphylococcus aureus* device-associated infections. *PLoS Pathog*. 2012 Apr 5;8(4):e1002626. <https://doi.org/10.1371/journal.ppat.1002626>
- Sutcliffe J, Grebe T, Tait-Kamradt A, Wondrack L. Detection of erythromycin-resistant determinants by PCR. *Antimicrob Agents Chemother*. 1996 Nov;40(11):2562–2566. <https://doi.org/10.1128/AAC.40.11.2562>
- Teweldemedhin M, Gebreyesus H, Atsbaha AH, Asgedom SW, Saravanan M. Bacterial profile of ocular infections: a systematic review. *BMC Ophthalmol*. 2017 Dec;17(1):212. <https://doi.org/10.1186/s12886-017-0612-2>
- Thomas RK, Melton R, Asbell PA. Antibiotic resistance among ocular pathogens: current trends from the ARMOR surveillance study (2009–2016). *Clinical Optometry*. 2019 Mar;11(11):15–26. <https://doi.org/10.2147/OPTO.S189115>
- Vola ME, Moriyama AS, Lisboa R, Vola MM, Hirai FE, Bispo PJM, Höfling-Lima AL. Prevalence and antibiotic susceptibility of methicillin-resistant *Staphylococcus aureus* in ocular infections. *Arq Bras Oftalmol*. 2013 Dec;76(6):350–353. <https://doi.org/10.1590/S0004-27492013000600006>
- Wang N, Huang Q, Tan YW, Lin LP, Wu KL. Bacterial spectrum and resistance patterns in corneal infections at a Tertiary Eye Care Center in South China. *Int J Ophthalmol*. 2016 Mar 18;9(3):384–389.
- West ES, Behrens A, McDonnell PJ, Tielsch JM, Schein OD. The incidence of endophthalmitis after cataract surgery among the U.S. Medicare population increased between 1994 and 2001. *Ophthalmology*. 2005 Aug;112(8):1388–1394. <https://doi.org/10.1016/j.ophtha.2005.02.028>

Structural Changes of *Bacillus subtilis* Biomass on Biosorption of Iron (II) from Aqueous Solutions: Isotherm and Kinetic Studies

SRI LAKSHMI RAMYA KRISHNA KANAMARLAPUDI and SUDHAMANI MUDDADA*

Department of Biotechnology, Koneru Lakshmaiah Education Foundation (KLEF), Greenfields, Vaddeswaram, Guntur, Andhra Pradesh, India

Submitted 9 June 2019, revised 9 November 2019, accepted 11 November 2019

Abstract

Various microbial biomasses have been employed as biosorbents. Bacterial biomass has added advantages because of easy in production at a low cost. The study investigated the biosorption of iron from aqueous solutions by *Bacillus subtilis*. An optimum biosorption capacity of 7.25 mg of the metal per gram of the biosorbent was obtained by the Inductive Coupled Plasma Optical Emission Spectroscopy (ICP-OES) under the experimental conditions of initial metal concentration of 100 mg/l, pH 4.5, and biomass dose of 1 g/l at 30°C for 24 hrs. The data showed the best fit with the Freundlich isotherm model while following pseudo-first-order kinetics. Scanning Electron Microscope (SEM) and Energy Dispersive X-ray (EDX) analysis confirmed iron biosorption as precipitates on the bacterial surface, and as a peak in the EDX spectrum. The functional hydroxyl, carboxyl, and amino groups that are involved in biosorption were revealed by the Fourier Transform Infrared spectroscopy (FTIR). The amorphous nature of the biosorbent for biosorption was indicated by the X-ray Diffraction (XRD) analysis. The biomass of *B. subtilis* exhibited a point zero charge (pH_{pzc}) at 2.0.

Key words: *Bacillus subtilis*, biosorption, iron, isotherms, kinetics

Introduction

Remediation of metal ions from contaminated sites is paramount. Many industries and various human activities discharge large amounts of metal ions into the water bodies where they cannot be degraded or destroyed. Ultimately, heavy metal ions reach and accumulate in the tissues of animals and humans (Iheanacho et al. 2017) posing serious health ailments.

Some metal ions act as essential micronutrients for most of the living organisms as metalloenzymes when present in sufficient quantities. However, they become toxic at high concentrations (Bhattacharya et al. 2016). Hence, metal ion concentration in wastewater and drinking water sources has to be reduced to a set levels (0.1 mg/l – Fe; 1 mg/l – Cu; 5 mg/l – Zn; 0.05 mg/l – Ar; 0.005 mg/l – Cd; 0.001 mg/l – Hg; 0.05 mg/l – Pb; 0.01 mg/l – Se) as per standards set by WHO (Puri and Kumar 2012). The traditional chemical treatments used to remediate metal ions are connected with many drawbacks like high energy requirement, the formation of

sludge or waste products, incomplete removal of ions, high cost and difficulty in implementation (Renu et al. 2017), and may become ineffective at low quantities (10–100 mg/l).

Biosorption has emerged as an alternative to traditional techniques. Biosorption is described as a naturally occurring metabolism that binds metal ions to the cellular structure of the biosorbents even from very dilute aqueous solutions (Shamim 2018). A microbial cell is a natural biosorbent of metal ions. Studies were done using microbial biomass (algae, bacteria, and fungi) as biosorbent for remediation of metal ions from polluted water resources. The biosorption process relies on nature and biosorbent type, and metal species to be biosorbed (El-Naggar et al. 2018).

The process of biosorption is associated with many advantages as a low operating cost, biosorbent reuse, the minimized disposal of chemical or biological sludge, detoxification of very dilute effluents with high efficiency, specific metal selectivity, low operation time, and no secondary toxic compounds production.

* Corresponding author: S. Muddada, Department of Biotechnology, Koneru Lakshmaiah Education Foundation (KLEF), Greenfields, Vaddeswaram, Guntur, Andhra Pradesh, India; e-mail: sudhamani1@rediffmail.com

© 2019 Sri Lakshmi Ramya Krishna Kanamarlapudi and Sudhamani Muddada

This work is licensed under the Creative Commons Attribution-NonCommercial-NoDerivatives 4.0 License (<https://creativecommons.org/licenses/by-nc-nd/4.0/>).

Hence, the process of biosorption is promising for the remediation of heavy metals from polluted water bodies (Zawierucha et al. 2016).

Among trace elements, iron is required for most of the living organisms for the formation of hemoglobin. High iron levels (200–250 mg/kg body weight) in drinking water may cause many ill effects and can be lethal (Prashanth et al. 2015). The presence of a high level of iron in the food products also affects taste, color, and appearance due to reaction with the phenolic compounds (Dueik et al. 2017). Hence, it is necessary to remove iron ions.

Bacillus is a diverse group of microorganisms. Many species of *Bacillus* are found to have metal-binding properties (Wierzba 2015; Dey et al. 2016; García et al. 2016). *Bacillus subtilis* is non-pathogenic and non-toxic with a Generally Regarded as Safe (GRAS) status. The biosorption of metal ions by *B. subtilis* has been studied (Al-Gheethi et al. 2017; Cai et al. 2018). Besides, many studies reported the biosorption of iron by various microbial biosorbents (Keshtkar et al. 2016; Migahed et al. 2017). However, there is very little information regarding the structural and functional changes occurring on the biomass of *B. subtilis* as a consequence of iron biosorption.

Hence, in the present study iron removal was done by utilizing biomass of *B. subtilis* in aqueous solutions. Optimization of experimental parameters, isotherms, and kinetic studies was done to characterize iron biosorption onto the biomass. Also, changes on the surface of the biosorbent were evaluated.

Experimental

Materials and Methods

Microorganism and growth conditions. The strain, *Bacillus subtilis* (1427) was procured from Microbial Type Culture Collection (MTCC), Chandigarh. The stock culture of *B. subtilis* was preserved on nutrient agar plates at 4°C and subcultured every month. Bacterial stocks were maintained in 50% glycerol at –80°C. Fresh biomass was obtained by inoculating the strain in nutrient broth and incubating at 37°C for 24 hrs at 150 rpm. The bacterial culture obtained after centrifugation (8000 rpm, 10 min) was washed with distilled water and used as the biosorbent for iron biosorption experiments.

Preparation of metal solution. Stock solutions of $\text{FeSO}_4 \cdot 7\text{H}_2\text{O}$ (ferrous sulfate heptahydrate) were prepared in double-distilled water. Fresh working solutions were prepared before experiments.

Biosorption experiments. Biosorption of iron ions onto biomass of *B. subtilis* was done at 30°C by

suspending different amounts of biosorbent in 100 ml metal ion solution in Erlenmeyer flasks (250 ml). The pH was adjusted by 1N NaOH or HCl before agitation at 100 rpm. The impact of various experimental parameters that influences the process of biosorption was examined. One target parameter was varied by keeping the others constant. Tests were performed with pH values varying from 3 to 9, initial metal ion concentrations differing from 4 to 40 mg/l, different inoculum sizes of 0.5 to 3 g/l, and different time intervals of 1–24 hrs. Controls (without the addition of metal) were maintained. After incubation, the biomass and supernatant obtained by centrifugation (8000 rpm, 10 min) were characterized separately.

Determination of residual Fe (II). Concentration of Fe (II) ions in the supernatant after biosorption experiments was obtained by the Inductive Coupled Plasma Optical Emission Spectroscopy (ICP-OES) at NCCCM, Hyderabad. At equilibrium conditions the percentage of biosorption and biosorption capacity of *B. subtilis* were obtained the equations:

$$q_e = \frac{(C_i - C_e) V}{m}$$

$$R\% = \frac{(C_i - C_e)}{C_i} \times 100$$

where q_e is the quantity of the metal biosorbed by the biomass (mg/g) at equilibrium; C_i is initial metal (Fe) ion concentration in the solution (mg/l); C_e is the equilibrium metal (Fe) ion concentration in solution (mg/l), V is volume of the medium (l), and m is the quantity of the biomass used in the reaction mixture (g).

Isotherm modeling. In this study, the fit of experimental data was studied by the three most widely used models, namely Freundlich, Langmuir, and Temkin isotherms.

Linearized Langmuir isotherm model is shown as:

$$\frac{C_e}{q_e} = \frac{C_e}{q_m} + \frac{1}{K_L q_m}$$

where, q_e is the mass of metal ion biosorbed per gram of the biosorbent (mg/g); C_e is the final concentration of the metal ions (mg/l) in solution; q_m is the monolayer biosorption capacity of the biosorbent (mg/g), and K_L is the Langmuir biosorption constant (l/mg). The constants K_L and q_{max} were evaluated from the slope and the intercept of the linear plot of $1/q_e$ versus $1/C_e$.

The affinity (R_L Hall isolation factor) of the biosorbent to the biosorbate can be calculated by the equation:

$$R_L = \frac{1}{1 + k_L C_i}$$

where C_i is the highest initial concentration of the biosorbate (mg/l).

Linearized Freundlich isotherm model is described as:

$$\log q_e = \log K_F + \frac{1}{n} \log C_e$$

where, K_F is a constant for relative biosorption capacity of the biosorbent and $1/n$ is an experimental parameter of biosorption intensity, which can be calculated from the linear plot of $\log q_e$ versus $\log C_e$.

Linearized Temkin isotherm model is shown as represented by the following equation:

$$q_e = \frac{RT}{b_T} \ln A_T + \frac{RT}{b_T} \ln C_e$$

where A_T is the Temkin isotherm equilibrium binding constant (L/g), b_T is the Temkin isotherm constant, R is universal gas constant (8.314 J/mol/K), and T is the temperature at 298 K. By plotting the values against q_e versus $\ln C_e$ the constants b_T and A_T can be determined.

Biosorption kinetics. In this study, pseudo-first-order and pseudo-second-order were applied.

Linear forms of the kinetic models are shown as:

$$\log (q_e - q_t) = \log q_e - \frac{k_1 t}{2.303}$$

$$\frac{t}{q_t} = \frac{1}{k_2 \cdot q_e^2} + \frac{t}{q_e}$$

where q_e and q_t are the mass of Fe (II) ions biosorbed at equilibrium and at time t (mg/l), k_1 is the pseudo-first-order equilibrium rate constant (min^{-1}), k_2 is the pseudo-second-order rate constant ($\text{g mg}^{-1} \text{min}^{-1}$), and t is the contact time (min). The parameters of the two models can be calculated from the slope and intercept of linear plots of t versus $\log (q_e - q_t)$, and t versus t/q_t , respectively.

Scanning Electron Microscopy (SEM) and Energy Dispersive X-ray spectrometry (EDX) analysis. Morphology and elemental composition of biosorbent before and after biosorption with Fe(II) ions were examined by the Field Emission Scanning Electron Microscope (FE-SEM) (CARL ZEISS SUPRA 55 GEMIN-German Technology Jena, Germany). Biomass samples were glutaraldehyde fixed, attached to 10 mm alumina-based mounts and sputtered with gold particles by using sputter coater (SC7620 'Mini' sputter coater) under vacuum. Then, the obtained specimens were observed under SEM for capturing of images. Elemental composition (EDX) was analyzed by the Energy Dispersive X-ray spectrometry (EDX) (OXFORD EDS system) at 16 KeV voltage.

Fourier Transform Infrared Spectroscopy (FTIR). The Infrared spectrum of biosorbent before and after biosorption was recorded by the FTIR spectrometer (Thermo Nicolet Avatar 370 FTIR, Madison, US) to identify the functional groups on the biosorbent surface participating in biosorption. The samples were dried and mixed with KBr (1:200) and pressed to obtain

transparent discs. The discs were analyzed immediately in the range of 400–4000 cm^{-1} , with KBr as background.

X-ray diffraction (XRD) analysis. Powdered biosorbent, before and after Fe (II) biosorption were characterized by X-ray diffraction apparatus (Bruker D8-Advance XRD model). The intensities of diffracted X-rays were noted as a function of 2θ angle by using monochromatic Cu-K α (1.5406 Å) target radiations. The patterns were recorded over the range of 3° to 80° with a scan rate of $10^\circ/\text{min}$, and a step size of 0.02° . The conditions used for operating were 40 kV and 35 mA of current.

Determination of point zero charges (pH_{pzc}). The point zero charges of biosorbent were obtained by the pH drift method. For this, different conical flasks with 50 ml of 0.01 M NaCl solution were taken and pH (initial) was adjusted within the range of 2–12 by using either 0.1 M HCl or NaOH. After adjusting the pH, 0.15 g of *B. subtilis* biomass was put into all flasks and agitated for 48 hrs at room temperature. After incubation, the flasks were withdrawn from the shaker and the final pH was taken. The pH_{pzc} can be calculated from the plot of pH_{final} vs. $\text{pH}_{\text{initial}}$. The intersection point of the curve ($\text{pH}_{\text{initial}} = \text{pH}_{\text{final}}$) was considered as the point of zero charge.

Results and Discussion

The bacterium *B. subtilis* is recognized as a GRAS organism (Sewalt et al. 2016), and hence, it is considered as a safe biosorbent for its use in metal remediation from polluted aqueous solutions.

Biosorption studies. The effect of different experimental parameters at various conditions was studied as discussed below.

Effect of initial metal ion concentration. The concentration of metal ion strongly influences the biosorbent biosorption capacity. From Fig. 1, it can be concluded that with the increase of metal ion concentration from 4 mg/l to 20 mg/l, the biosorption capacity

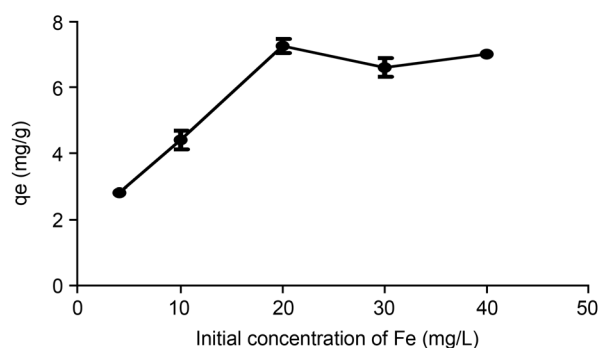


Fig. 1. Effect of initial concentration on biosorption of Fe (II) by *Bacillus subtilis* at a biomass concentration of 1 g/l, pH 4.5, and 100 rpm.

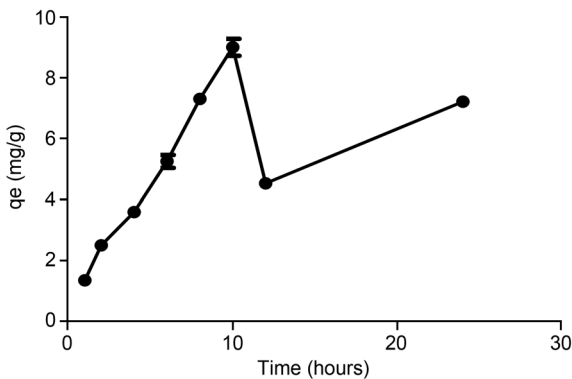


Fig. 2. Effect of contact time on biosorption Fe (II) by *Bacillus subtilis* at a biomass concentration of 1 g/l, pH 4.5, 20 mg/l of Fe (II) and 100 rpm.

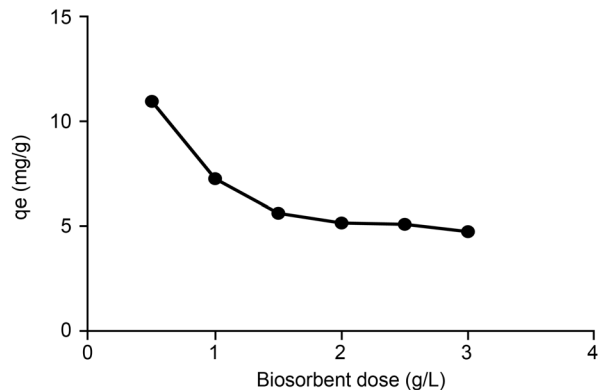


Fig. 3. Effect of biosorbent dose on biosorption Fe (II) by *Bacillus subtilis* at initial metal ion concentration of 20 mg/l, pH 4.5, and 100 rpm.

increases from 2.8 mg per gram to 7.25 mg Fe(II) per gram of biosorbent, and thereafter, it remains almost constant with further increase of metal concentration (up to 40 mg/l). This phenomenon is due to that at low metal concentration the active sites present on the biosorbent are unoccupied leading to higher biosorption capacity. Due to the attainment of saturation with increasing metal concentration, further increase leads to lower or constant biosorption capacity. Hence, 20 mg/l metal concentration was taken as the optimum with the highest biosorption capacity of 7.25 mg of Fe (II)/g of the biomass. Similarly, in other studies with As (V) concentration ranging from 500–3000 µg/l, there was an increase in biosorption capacity and it reached equilibrium at the high metal concentration (Banerjee et al. 2016).

Effect of contact time. The biosorption capacity was increased from 1.35 to 9 mg/g of biomass with the increase in contact time up to 10 hrs due to the biosorption of metal ions with the available binding sites (Fig. 2). Upon further incubation, due to lowered availability of binding sites, and as repulsive forces existed between the bound Fe (II) ions and in those in solution, another stage of biosorption was noticed. A similar pattern of two-phase biosorption was observed for Cr (VI) ions with an increase in contact time from 10 min to 10 hrs (Arbanah et al. 2012).

Effect of the biosorbent dose. Different biomass dosages were considered as represented in Fig. 3. It shows that there was a decrease in biosorption capacity with the raise of biomass dosage from 0.5 g/l to 3 g/l. At higher dosage, the biomass forms aggregates that lead to a reduction in available binding sites resulting in lower biosorption capacity. Hence, the concentration of 1 g/l of biosorbent was taken as an optimum dose for biosorption of Fe (II) ions. These results are in line with other reported studies, where, with the increase of biosorbent dose of *Bacillus cereus* from 0.5 to 3 g/l, there was the decrease in biosorption capacity

from 36.21 to 7.73 mg/g of biomass for Pb (II) ions (Todorova et al. 2019).

Effect of pH. One of the crucial parameters to be monitored during biosorption is pH because it influences the functional groups and heavy metal solution chemistry. At low pH, binding of metal ions to the biosorbent is reduced due to the existence of metal – proton competition to the same binding region (Farnane et al. 2018). However, in our experiments at a low pH of 3, the damage to the biomass occurred and resulted in the formation of flakes. At high pH values (pH > 4.5) precipitation of iron (results in yellowing of solution) and formation of hydroxides ($\text{Fe}(\text{OH})_3^-$ and $\text{Fe}(\text{OH})_4^{2-}$) occurred which hindered the biosorption. Hence, pH 4.5 was taken as an optimum in our studies to attain the highest biosorption capacity assuming that the functional groups are deprotonated and attained a negative charge for binding of positive metal ions. Also, many studies reported that biosorption is meaningless at higher pH due to the occurrence of metal hydroxides causing difficulty in concluding whether the decrease in metal concentration was due to lowered biosorption or precipitation (El-Naggar et al. 2018).

Isotherm modeling. The metal ion biosorption capacity of biosorbent was determined by the equilibrium sorption isotherms that characterize the affinity and surface properties of the biosorbent by expressing certain constant values (Kariuki et al. 2017). The present study used three biosorption isotherm models, namely Langmuir, Freundlich, and Temkin isotherms.

Langmuir isotherm can be described as a quantitative monolayer occurrence of the biosorbate on the biosorbent surface, containing the unbounded number of active sites (Saraf and Vaidya 2016). The Freundlich isotherm model explains heterogeneous surface biosorption where enthalpy of biosorption is independent of the metal ion biosorbed (Ahad et al. 2017). Temkin isotherm is showed by considering the factor of biosorbate – biosorbent interaction explicitly into

Table I
 Constants of Langmuir, Freundlich and Temkin isotherm models used
 for the biosorption of Fe (II) ions onto *B. subtilis* biomass.

Langmuir isotherm		Freundlich isotherm		Temkin isotherm	
q_{\max} (mg/g)	3.831	n	3.425	B (J/mol)	1.3583
K_L (l/mg)	1.845	K_F (mg/g)	2.766	A (l/g)	6.78 g/l
R^2	0.9353	R^2	0.9057	R^2	0.8715
R_L	0.013				

account and presume that there was a linear decrease in biosorption heat of solute molecules in the layer rather than logarithmically (Ahad et al. 2017).

From the respective linear plots, the constants of three isotherms models obtained are presented in Table I. Based on the regression coefficient value (R^2), the biosorption data expressed shows best fit with Langmuir isotherm model (0.9353) compared to Freundlich (0.9057), and Temkin isotherm models (0.8715) indicating that Fe (II) biosorption onto *B. subtilis* is monolayer with uniform binding energy. The value of $R_L = 0$ indicates favorable biosorption. The value of 'n' is greater than unity suggesting that the iron ions are favorably biosorbed onto *B. subtilis* biomass. The constants of Temkin isotherm suggest that the heat of sorption is a physical process. Various studies reported that either Freundlich (Safari and Ahmady-Asbchin 2018), Langmuir (Anuradha et al. 2018) or Temkin (Aravind et al. 2015) isotherm models are the best fit.

Biosorption kinetics. The kinetics expresses the rate of biosorption by determining the residence time of biosorbate for the completion of biosorption at the solid-solution interface. It also determines the mode of biosorption and the possible rate-controlling steps either in mass transport (pseudo-first-order) or in chemical reaction (pseudo-second-order). The kinetics of Fe (II) biosorption onto *B. subtilis* can be evaluated by subjecting the experimental data to two kinetic models – pseudo-first and second-order models.

From the respective linear plots, the parameters of two kinetic models were obtained which were summarized in Table II. With a high correlation coefficient (R^2) and the low difference between the experimental and calculated q_e values, we can interpret that the data fits well with pseudo-first-order kinetic model. The rate-controlling step is diffusion and does not depend on

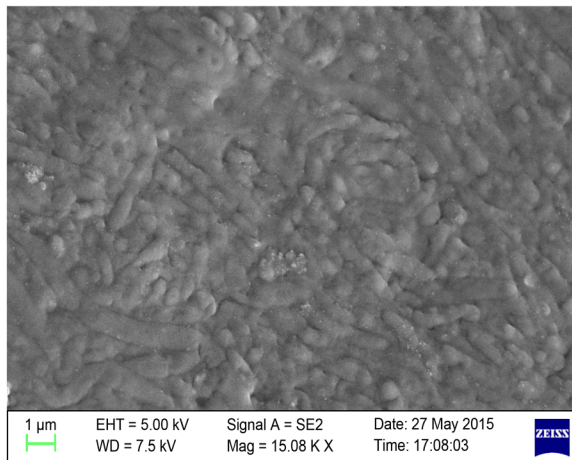
the concentration of both the reactants which implies that the biosorption is physisorption. Other studies also reported that pseudo-first-order kinetic model as a better fit for biosorption of Pb (II) and Zn (II) ions. (Hanbali et al. 2014; Singh and Chopra 2014).

SEM-EDX analysis. Morphological changes that occurred as a result of Fe (II) biosorption onto *B. subtilis* were visualized by scanning electron microscopy (SEM). SEM images revealed that before biosorption the cells were found to be plump with smooth surfaces in loosely bound form. After biosorption with Fe (II) ions, cells showed the presence of bulky particles in the form of precipitates on the surface, increase in cell size and roughness of the cell (Fig. 4 and 5). Similarly, the alteration in morphology of *Ralstonia pickettii* and lactic acid bacteria biomass was observed due to biosorption of Mn (II) and Fe (II), respectively (Ramya Krishna and Sudhamani 2017; Huang et al. 2018).

The Energy Dispersive Spectroscopy (EDX) analysis is used to indicate the presence of metal. The peak for iron in the spectrum confirmed that the Fe (II) ions were biosorbed onto the *B. subtilis* biomass (Fig. 5). The composition of elements in the biomass loaded with Fe (II) differed from that of the control biomass. The elements Magnesium, Sodium, and Calcium which were initially present in the control (Fig. 4) were not observed in the metal-loaded biomass, which indicated that iron replaced the other metal ions that already existed on the biosorbent surface. Further, the percentage composition of Oxygen, Phosphorus and Potassium in the metal loaded biomass was lowered which indicates that the mechanism of ion exchange plays a role in biosorption of Fe (II) ions. A similar mechanism of ion exchange was observed in other studies for Fe (II) biosorption by lactic acid bacteria (Ramya Krishna and Sudhamani 2017).

Table II
 Constants of pseudo-first and pseudo-second-order kinetic models obtained
 for the biosorption of Fe (II) ions onto *B. subtilis*.

Pseudo-first-order kinetic model			Pseudo-second-order kinetic model		
q_e (mg/g)	K_1 (min^{-1})	R^2	q_e (mg/g)	K_2 ($\text{gmg}^{-1} \text{min}^{-1}$)	R^2
10.6	0.2001	0.9201	17.76	0.0042	0.7154



Element	Weight %	Atomic %	Element	Weight %	Atomic %
C	66.27	73.55	P	2.33	1.00
O	29.51	24.59	S	0.37	0.15
Na	0.39	0.22	Cl	0.15	0.06
Mg	0.32	0.17	K	0.27	0.09
Si	0.17	0.08	Ca	0.22	0.07

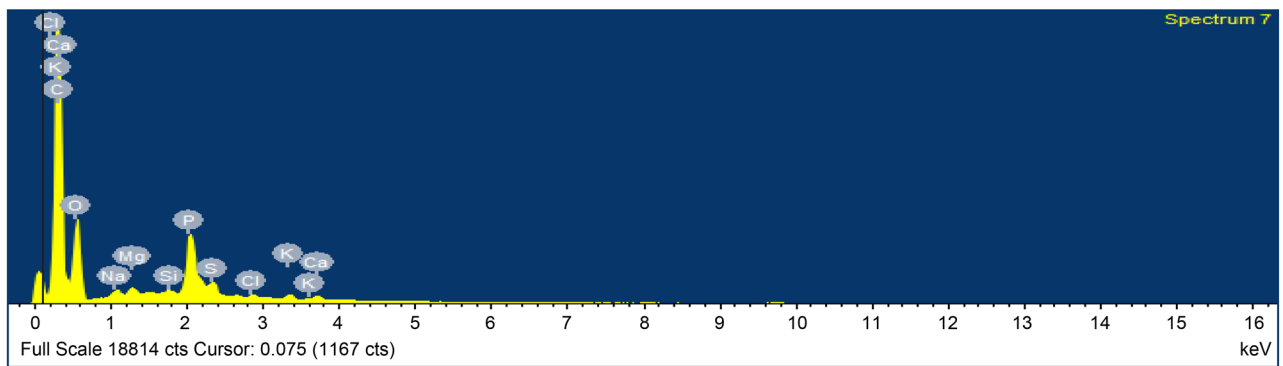
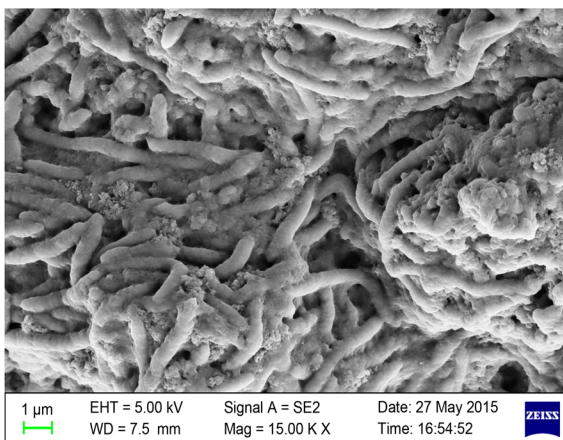


Fig. 4. SEM image, EDX spectra and elemental composition of unloaded (control) biomass of *B. subtilis*.



Element	Weight %	Atomic %	Element	Weight %	Atomic %
C	70.37	77.68	S	0.48	0.20
O	25.01	20.73	Cl	0.14	0.05
Si	0.37	0.18	K	0.08	0.03
P	1.58	0.68	Fe	1.96	0.47

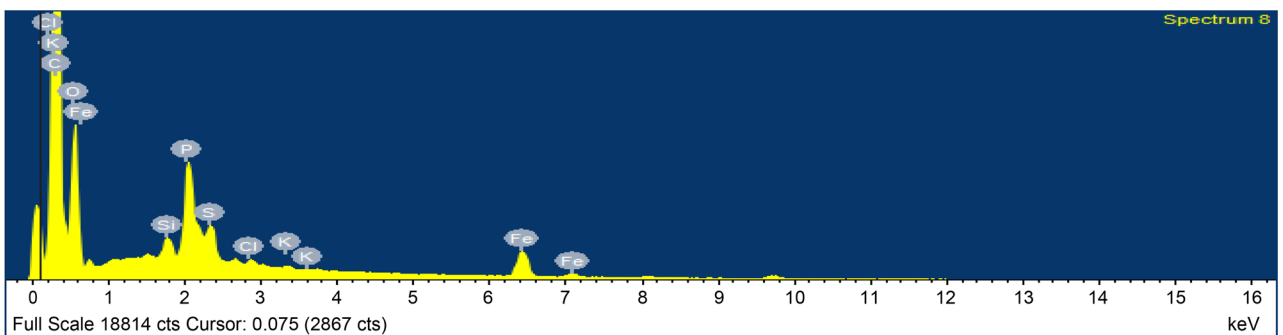


Fig. 5. SEM image, EDX spectra and elemental composition of *B. subtilis* biosorbed with Fe (II) ions.

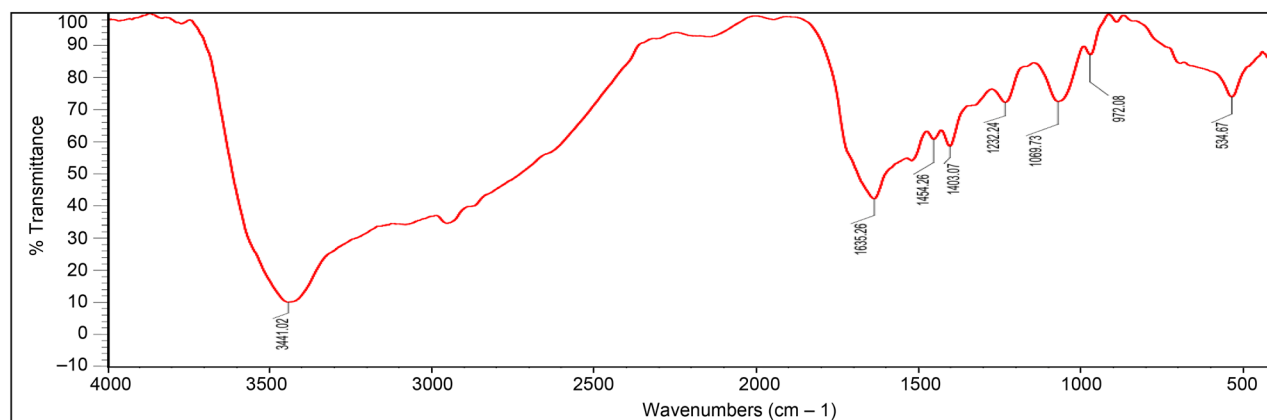


Fig. 6a. FTIR spectra of unloaded (control) biomass of *B. subtilis*.

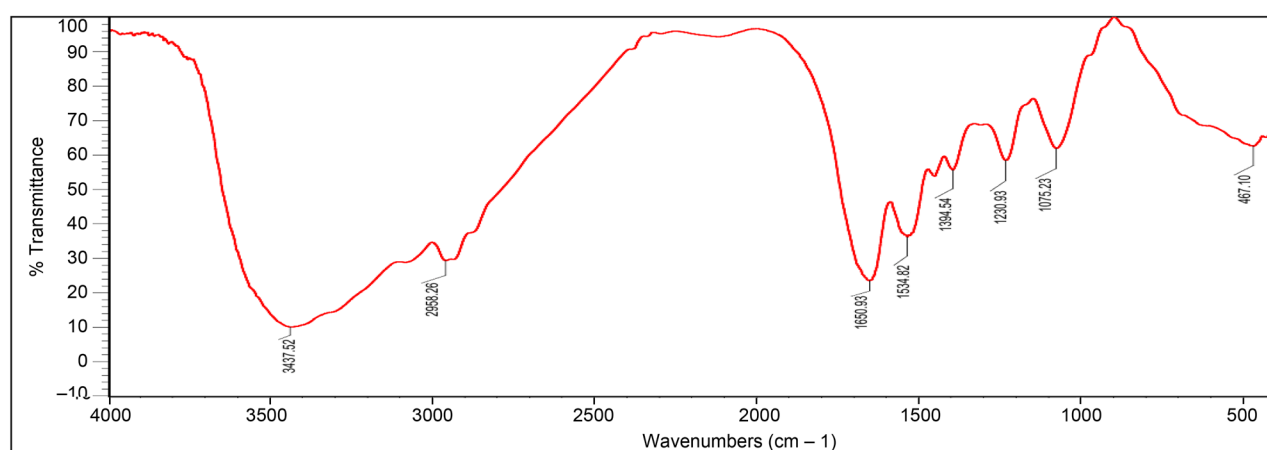


Fig. 6b. FTIR spectra of Fe (II) ion biosorbed by *B. subtilis* biomass.

FTIR analysis. FTIR spectrum discloses the functional groups that take part in Fe (II) biosorption. The spectrum of the biosorbent displayed varied biosorption peaks indicating the composite nature of the biomass. Figure 6a shows the IR spectrum of control biomass. The broad peak at 3441 cm^{-1} indicates the presence of $-\text{OH}$ and $-\text{NH}$ stretching, thus televising the occurrence of hydroxyl and amine groups. The peak at 1635 cm^{-1} represents the appearance of the amide group. Peaks at 1454 cm^{-1} and 1403 cm^{-1} shows the stretching of $-\text{C}=\text{C}$ groups and $\text{C}-\text{H}$ bending of the aromatic ring, respectively. The $-\text{C}-\text{O}$ stretching of the carboxyl group was displayed at 1232 cm^{-1} . The peaks at 1069 cm^{-1} and 972 cm^{-1} represent the $-\text{C}-\text{C}$ stretching of alcohols and $\text{C}-\text{O}-\text{C}$, $\text{C}-\text{O}$, $\text{C}-\text{O}-\text{P}$ bonds of polysaccharides.

The IR spectrum of metal loaded biomass (Fig. 6b) showed significant changes in the range of 3437 cm^{-1} , 1650 cm^{-1} , 1230 cm^{-1} , and at 1075 cm^{-1} indicating that these functional groups participate in metal ion biosorption. A new peak formed at 2958 cm^{-1} indicated the stretching of $-\text{C}-\text{H}$ bond of the aliphatic methylene group. Stretching of COO^- bond of carboxylate group

appeared at 1534 cm^{-1} . The peak at 1394 cm^{-1} indicates the $\text{C}=\text{C}$ stretching vibration of alkyl side chains. The bands below 800 cm^{-1} indicate the fingerprint zone, which can be attributed to phosphate and sulfur functional groups. Additionally, a clear shift in the protein region (3437 cm^{-1} , 1650 cm^{-1}) is exhibited indicating the protein role in Fe (II) biosorption. Conclusively, changes in the frequencies of these functional groups indicate that they participate in biosorption process. Similar changes in the FTIR spectrum due to arsenic biosorption were reported by Cristobel (Christobel and Lipton 2015). Changes at 3411 cm^{-1} , 2929 cm^{-1} , 1239 cm^{-1} , 1052 cm^{-1} , and 617 cm^{-1} peak intensities are in line with other reports (Dhanwal et al. 2018).

XRD analysis. The patterns of X-ray diffraction of *B. subtilis* prior and following iron biosorption are explained in Fig. 7a and 7b. Sharp intensity peak in the unloaded biosorbent has been observed at $2\theta = 16.610$ with d spacing value of 5.3392 , whereas the pattern in the iron-bound biosorbent showed the emergence of new peaks at 2θ values of around 8.293 and 19.659 indicating the crystalline character of the biosorbent.

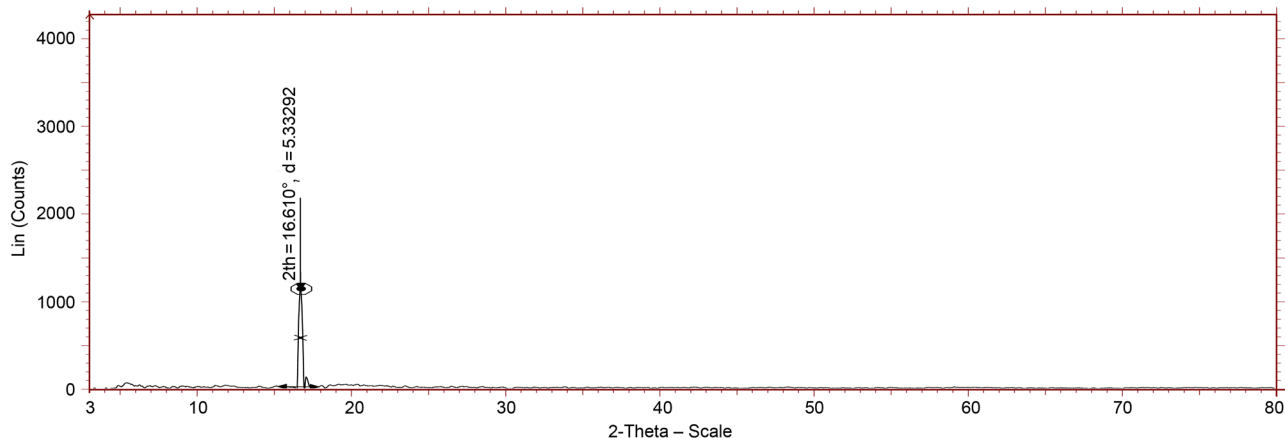


Fig. 7a. X-ray diffraction pattern of *B. subtilis* before biosorption with Fe (II) ions.

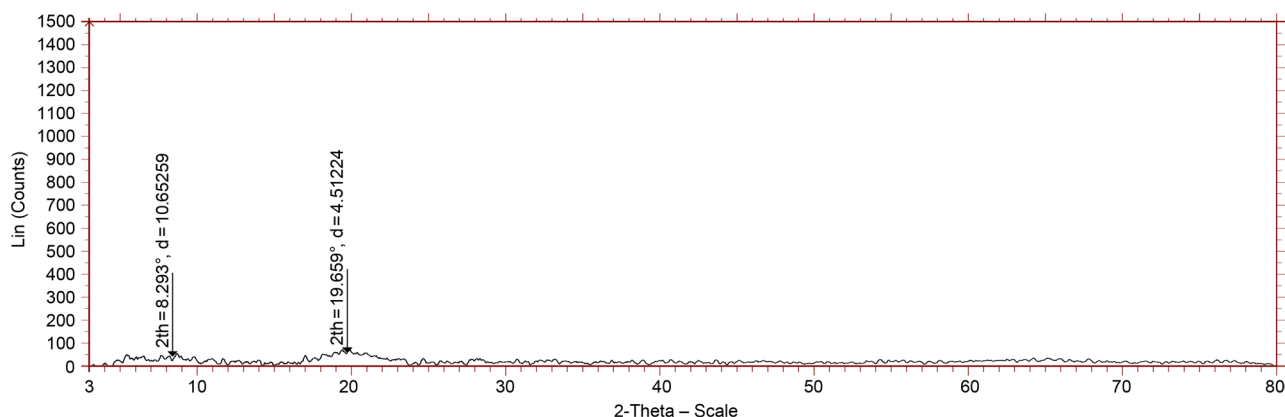


Fig. 7b. X-ray diffraction pattern of *B. subtilis* after biosorption with Fe (II) ions.

The amorphous character of biosorbent in the spectra is indicated by the poorly resolved peaks, which suggest that the metal ion can simply pierce into the surface; which is advantageous for metal biosorption from aqueous solutions. The results are in agreement with other studies (Qu et al. 2015; Santuraki and Muazu 2015).

Point zero charge of biosorbent (pH_{pzc}). Metal biosorption onto biosorbent surface is based on pH, since it influences surface available binding sites of biosorbent and metal ions in solution, respectively. Hence, the calculation of point zero charges is a critical parameter to predict metal ion biosorption. As shown in Fig. 8, the pH_{pzc} of *B. subtilis* was found to be 2 indicating the positive charge of biosorbent at pH less than 2 and a negative charge at pH greater than 2. At $\text{pH} < 2$, metal proton competition exists resulting in the decline of biosorption. On the other hand, at $\text{pH} > 2$, the biosorbent is negatively charged which facilitates the electrostatic attraction with the positively charged metal ions resulting in maximum biosorption. At higher pH ($\text{pH} < 6$), a reduction in biosorption was also observed. This is because, at high pH values, there is a probability for precipitation of metal ions as salts or

hydroxides in solution (Zaib et al. 2016). Similar results were observed using other strains of *B. subtilis*, where the pH_{pzc} of the biosorbent was 1.5 (Ng 2018).

Conclusion

Analysis by ICP-OES and SEM-EDX showed that metal ions were biosorbed onto the biosorbent. Freundlich adsorption isotherm and pseudo-first-order kinetic model proved the better fit for experimental

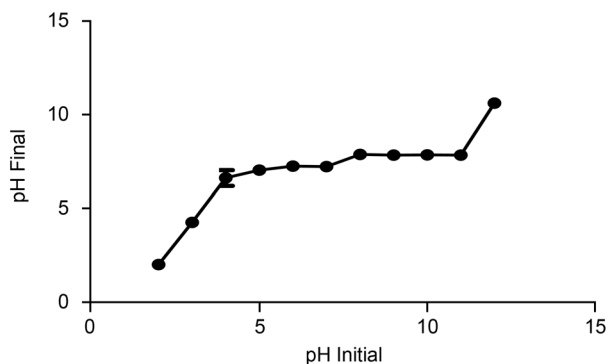


Fig. 8. Point zero charge (pH_{pzc}) of *B. subtilis*.

data. The FTIR spectrum identified the possible functional groups that interact in metal biosorption. The amorphous nature of the biosorbent which is suitable for biosorption was revealed by XRD analysis. Point zero charge of biosorbent shows that the biosorption process is facilitated at $\text{pH} > 2$. At optimized experimental conditions of 100 mg/l of the metal ion at pH 4.5, with 1 g/l of biosorbent at 30°C for 24 hrs, the biomass of *B. subtilis* showed biosorption capacity of 7.25 mg of Fe (II)/g of biomass. The biomass of *B. subtilis* can be employed as a promising biosorbent for remediation of metal ions from polluted water sources.

Acknowledgments

The authors thank Mr. Arul Maximus Rabel, Center for Nano science and Nanotechnology, Satyabhama University, Chennai for the support on SEM-EDX analysis. The authors acknowledge Sophisticated Test and Instrumentation Center (SAIF), Kochi for FTIR and XRD analysis. Additionally, the authors thank NCCCM (BARC), Hyderabad for ICP-OES analysis.

Conflict of interest

The authors do not report any financial or personal connections with other persons or organizations, which might negatively affect the contents of this publication and/or claim authorship rights to this publication.

The work was partially funded under "SEED/WS/052/2015".

Literature

- Ahad RIA, Goswami S, Syiem MB. Biosorption and equilibrium isotherms study of cadmium removal by *Nostoc muscorum* Meg 1: morphological, physiological and biochemical alterations. *3 Biotech*. 2017;7(2):104.
- Al-Gheethi A, Mohamed R, Noman E, Ismail N, Kadir OA. Removal of heavy metal ions from aqueous solutions using *Bacillus subtilis* biomass pre-treated by supercritical carbon dioxide. *CLEAN-Soil, Air, Water*. 2017;45(10):1700356.
- Anuradha R Mulik, Preeti Kulkarni, Bhadekar RK. Biosorption studies on nickel and chromium by *Kocuria sp.* *BRI 36 Biomass*. *Int J Appl Eng Res*. 2018;13(9):6886–6893.
- Aravind J, George LE, Kanmani P, Muthukumar M. Biosorption of chromium using *A. towneri* and *R. eutropha*. *Res Biotechnol*. 2015;6(3):01–09.
- Arbanah M, Najwa MM, Halim KK. Biosorption of Cr (III), Fe (II), Cu (II), Zn (II) ions from liquid laboratory chemical waste by *Pleurotus ostreatus*. *Int J Biotechnol Wellness Ind*. 2012;1(3):152–162. doi:10.6000/1927-3037/2012.01.03.01
- Banerjee A, Sarkar P, Banerjee S. Application of statistical design of experiments for optimization of As(V) biosorption by immobilized bacterial biomass. *Ecol Eng*. 2016 Jan;86:13–23. doi:10.1016/j.ecoleng.2015.10.015
- Bhattacharya PT, Misra SR, Hussain M. Nutritional aspects of essential trace elements in oral health and disease: an extensive review. *Scientifica (Cairo)*. 2016;2016:1–12. doi:10.1155/2016/5464373
- Cai Y, Li X, Liu D, Xu C, Ai Y, Sun X, Zhang M, Gao Y, Zhang Y, Yang T, et al. A Novel Pb-resistant *Bacillus subtilis* bacterium isolate for co-biosorption of hazardous Sb (III) and Pb (II): thermodynamics and application strategy. *Int J Environ Res Public Health*. 2018 Apr 09;15(4):702. doi:10.3390/ijerph15040702
- Christobel J, Lipton A. Evaluation of macroalgal biomass for removal of heavy metal arsenic (As) from aqueous solution. *Int J Appl Innov Eng Manag*. 2015;4(5):94–104.
- Dey U, Chatterjee S, Mondal NK. Isolation and characterization of arsenic-resistant bacteria and possible application in bioremediation. *Biotechnol Rep (Amst)*. 2016 Jun;10:1–7. doi:10.1016/j.btre.2016.02.002
- Dhanwal P, Kumar A, Dudgeja S, Badgujar H, Chauhan R, Kumar A, Dhull P, Chhokar V, Beniwal V. Biosorption of heavy metals from aqueous solution by bacteria isolated from contaminated soil. *Water Environ Res*. 2018 May 01;90(5):424–430. doi:10.2175/106143017X15131012152979
- Dueik V, Chen BK, Diosady LL. Iron-polyphenol interaction reduces iron bioavailability in fortified tea: competing complexation to ensure iron bioavailability. *J Food Qual*. 2017;2017:1–7. doi:10.1155/2017/1805047
- El-Naggar NEA, Hamouda RA, Mousa IE, Abdel-Hamid MS, Rabei NH. Biosorption optimization, characterization, immobilization and application of *Gelidium amansii* biomass for complete Pb^{2+} removal from aqueous solutions. *Sci Rep*. 2018 Dec;8(1):13456. doi:10.1038/s41598-018-31660-7
- Farnane M, Machrouhi A, Elhalil A, Abdennouri M, Qourzal S, Tounsadi H, Barka N. New sustainable biosorbent based on recycled deoiled carob seeds: optimization of heavy metals remediation. *J Chem*. 2018 Oct 09;2018:1–16. doi:10.1155/2018/5748493
- García R, Campos J, Cruz JA, Calderón ME, Raynal ME, Buitrón . Biosorption of Cd, Cr, Mn, and Pb from aqueous solutions by *Bacillus sp.* strains isolated from industrial waste activate sludge. *TIP*. 2016 Jan;19(1):5–14. doi:10.1016/j.recqb.2016.02.001
- Hanbali M, Holail H, Hammud H. Remediation of lead by pre-treated red algae: adsorption isotherm, kinetic, column modeling and simulation studies. *Green Chem Lett Rev*. 2014 Oct 02;7(4):342–358. doi:10.1080/17518253.2014.955062
- Huang H, Zhao Y, Xu Z, Ding Y, Zhang W, Wu L. Biosorption characteristics of a highly Mn(II)-resistant *Ralstonia pickettii* strain isolated from Mn ore. *PLoS One*. 2018 Aug 31;13(8):e0203285. doi:10.1371/journal.pone.0203285
- Iheanacho EU, Ndulaka J, Onuh C. Environmental pollution and heavy metals. *Environ Pollut*. 2017;5(5):2321–9122.
- Kariuki Z, Kiptoo J, Onyancha D. Biosorption studies of lead and copper using rogers mushroom biomass '*Lepiota hystrix*'. *South Af J Chem Eng*. 2017;23:62–70.
- Keshtkar M, Dobaradaran S, Akbarzadeh S, Bahreini M, Abadi DRV, Nasab SG, Soleimani F, Khajehmadi N, Baghmolaei M. Iron biosorption from aqueous solution by *Padina sanctae crucis* algae: isotherm, kinetic and modeling. *Int J Pharm Technol*. 2016;1:10459–10471.
- Puri A, Kumar M. A review of permissible limits of drinking water. *Indian J Occup Environ Med*. 2012;16(1):40–44. doi:10.4103/0019-5278.99696
- Migahed F, Abdelrazak A, Fawzy G. Batch and continuous removal of heavy metals from industrial effluents using microbial consortia. *Int J Environ Sci Technol*. 2017 Jun;14(6):1169–1180. doi:10.1007/s13762-016-1229-3
- Ng W. Surface charge characteristics of *Bacillus subtilis* NRS-762 cells. *Peer J Preprints*. 2018;6:e26626v1.
- Prashanth L, Kattapagari KK, Chitturi RT, Baddam VRR, Prasad LK. A review on role of essential trace elements in health and disease. *J Dr NTR Univ Health Sci*. 2015;4(2):75–85. doi:10.4103/2277-8632.158577
- Qu J, Zang T, Gu H, Li K, Hu Y, Ren G, Xu X, Jin Y. Biosorption of copper ions from aqueous solution by *Flammulina velutipes* spent substrate. *BioResources*. 2015 Oct 16;10(4):8058–8075. doi:10.15376/biores.10.4.8058-8075

- Ramyakrishna K, Sudhamani M.** The metal binding potential of a dairy isolate. *J Water Reuse Desalin.* 2017 Dec;7(4):429–441. doi:10.2166/wrd.2016.127
- Renu NA, Agarwal M, Singh K.** Methodologies for removal of heavy metal ions from wastewater: an overview. *Interdiscip Environ Rev.* 2017;18(2):124–142. doi:10.1504/IER.2017.087915
- Safari M, Ahmady-Asbchin S.** Biosorption of zinc from aqueous solution by cyanobacterium *Fischerella ambigua* ISC67: optimization, kinetic, isotherm and thermodynamic studies. *Water Sci Technol.* 2018 Oct 15;78(7):1525–1534. doi:10.2166/wst.2018.437
- Santuraki AH, Muazu AA.** Accessing the potential of *Lonchocarpus laxiflorus* roots (LLR) plant biomass to remove Cadmium (II) ions from aqueous solutions: equilibrium and kinetic studies. *Afr J Pure Appl Chem.* 2015 May 31;9(5):105–112. doi:10.5897/AJPAC2015.0620
- Saraf S, Vaidya VK.** Elucidation of sorption mechanism of *R. arrhizus* for reactive blue 222 using equilibrium and kinetic studies. *J Microb Biochem Technol.* 2016;8(3):236–246. doi:10.4172/1948-5948.1000292
- Sewalt V, Shanahan D, Gregg L, La Marta J, Carrillo R.** The Generally Recognized as Safe (GRAS) process for industrial microbial enzymes. *Ind Biotechnol (New Rochelle NY).* 2016 Oct; 12(5):295–302. doi:10.1089/ind.2016.0011
- Shamim S.** Biosorption of heavy metals. In: Derco J, Vrana B, editors. *Biosorption.* London (UK): IntechOpen Ltd.; 2018. p. 21–49.
- Singh PP, Chopra AK.** Removal of Zn²⁺ and Pb²⁺ using new isolates of *Bacillus* spp. PPS03 and *Bacillus subtilis* PPS04 from paper mill effluents using indigenously designed Bench-top Bioreactor. *J Appl Nat Sci.* 2014 Jun 01;6(1):47–56. doi:10.31018/jans.v6i1.374
- Todorova K, Velkova Z, Stoytcheva M, Kirova G, Kostadinova S, Gochev V.** Novel composite biosorbent from *Bacillus cereus* for heavy metals removal from aqueous solutions. *Biotechnol Bio-technol Equip.* 2019 Jan;33(1):730–738. doi:10.1080/13102818.2019.1610066
- Wierzbna S.** Biosorption of lead(II), zinc(II) and nickel(II) from industrial wastewater by *Stenotrophomonas maltophilia* and *Bacillus subtilis*. *Pol J Chem Technol.* 2015 Mar 1;17(1):79–87. doi:10.1515/pjct-2015-0012
- Zaib M, Athar MM, Saeed A, Farooq U, Salman M, Makhoo MN.** Equilibrium, kinetic and thermodynamic biosorption studies of Hg(II) on red algal biomass of *Porphyridium cruentum*. *Green Chem Lett Rev.* 2016 Oct;9(4):179–189. doi:10.1080/17518253.2016.1185166
- Zawierucha I, Kozłowski C, Malina G.** Immobilized materials for removal of toxic metal ions from surface/groundwaters and aqueous waste streams. *Environ Sci - Proc Imp.* 2016;18(4):429–444.

Differentially Marked IncP-1 β R751 Plasmids for Cloning via Recombineering and Conjugation

ASHVEEN BAINS and JAMES W. WILSON*

Department of Biology, Villanova University, Villanova, PA, USA

Submitted 20 August 2019, revised 8 October 2019, accepted 22 October 2019

Abstract

We demonstrate here for the first time the use of an IncP-1 β plasmid, R751, as a gene capture vehicle for recombineering/conjugation strategies to clone large segments of bacterial genomes (20–100 + Kb). We designed R751 derivatives containing alternative markers for greater flexibility when using the R751 vehicle across different bacteria. These markers are removable if desired as part of the cloning procedure (with no extra steps needed). We demonstrated utility via cloning of 38 and 22 kb genomic segments from *Salmonella enterica* serovar Typhimurium and *Escherichia coli*, respectively. The plasmids expand the options available for use in recombineering/conjugation-based cloning applications.

Key words: IncP-1, R751, FRT, FLP, Pdu, MCP

IncP-1 plasmids have facilitated numerous studies on the promiscuous nature of plasmid-based genetic elements in nature and have allowed broad range transfer of genes across a variety of cell types (Trieu-Cuot et al. 1987; Heinemann and Sprague 1989; Pansegrau et al. 1994; Thorsted et al. 1998; Waters 2001). The IncP-1 group is divided into five subgroups termed α , β , δ , ϵ , and γ based largely on phylogenetic analysis (Pansegrau et al. 1994; Thorsted et al. 1998; Norberg et al. 2011; Sen et al. 2013). In this report, we demonstrate the first-time use of an IncP-1 β plasmid (R751) as a gene capture vehicle via the FRT-Capture technique. Recombineering-based approaches such as FRT Capture and other techniques allow the convenient cloning and/or manipulation of large DNA fragments using PCR and associated insertional/recombination steps (Wilson and Nickerson 2006; Narayanan and Chen 2011; Zeng, Zang, et al. 2017; Zeng, Hao, et al. 2017; Graf et al. 2018; Zeng et al. 2018). The development of a range of plasmid vehicles for these techniques improves their application and utility (Datsenko and Wanner 2000; Quick et al. 2010; Santiago et al. 2011; Wang et al. 2016; Bubnov et al. 2018). Since R751 encodes only a single resistance marker for trimethoprim resistance and this marker may not be suitable

in certain bacteria due to background resistance, we engineered a series of R751 derivatives containing additional markers (such a series of IncP-1 β plasmids does not exist in the literature to our knowledge). The use of the FRT-Capture technique using a choice of R751 plasmid vehicles is a robust, flexible, and convenient option for the cloning and transfer of large genomic segments in bacteria.

R751 is a self-transmissible IncP-1 β plasmid encoding Tp-R that is 53.3 Kb in size and fully sequenced (Thorsted et al. 1998). To utilize this plasmid as a gene capture vehicle in a recombineering/conjugation-based approach like FRT-Capture and other techniques, we engineered R751 derivatives containing FRT sites and a range of different antibiotic resistance markers termed R751 Km, R751 Cm, and R751 Sp (Table I). We used standard Lambda Red recombination to insert the markers and FRT sites in the R751 *qacE* gene, an accessory efflux pump gene located next to the *dhfr* gene encoding Tp-R (Thorsted et al. 1998; Datsenko and Wanner 2000). Briefly, PCR primers were designed to amplify the Km-R, Cm-R, and Sp-R genes from pKD4, pKD3, and pJW102, respectively, such that the PCR products contained homology to the R751 *qacE* gene for insertion via recombineering (Datsenko and

* Corresponding author: J.W. Wilson, Department of Biology, Villanova University, Villanova, PA, USA;
e-mail: james.w.wilson@villanova.edu

© 2019 Ashveen Bains and James W. Wilson

This work is licensed under the Creative Commons Attribution-NonCommercial-NoDerivatives 4.0 License (<https://creativecommons.org/licenses/by-nc-nd/4.0/>).

Table I
Plasmids used in this study.

Plasmid	Reference
R751	(Thorsted et al. 1998)
R751 Km	this study
R751 Cm	this study
R751 Sp	this study
pCP20	(Datsenko and Wanner 2000)
pKD3	(Datsenko and Wanner 2000)
pKD4	(Datsenko and Wanner 2000)
pKD46	(Datsenko and Wanner 2000)
pJW102	(Quick et al. 2010)

Wanner 2000; Quick et al. 2010). Lambda Red recombination was used for recombineering with PCR products as described previously (Datsenko and Wanner 2000; Quick et al. 2010). The sequence of the PCR primers for this recombineering were as follows: P1*qacE*: AGCACATAATTGCTCACAGCCAAACTATCAGGTCAAGTCTGTGTAAGGCTGGAGCTGCTTC; P2*qacE*: TTTGCCCATGAAGCAACCAGGCAATGGCTGTAATTATGACCATATGAATATCCTCCTTAGTTCC. The same primers as listed could be used for each template (pKD4, pKD3, and pJW102). The PCR products were electroporated into the *E. coli* strain TOP10 containing both R751 and pKD46, the latter plasmid expressing the Lambda Red recombination products for DNA insertion. The transformants were selected on media containing the appropriate antibiotic, and pooled colonies from the transformation were used as donors in a conjugation to the *E. coli* recipient strain MG1655 (Blattner et al. 1997). Tranconjugants were selected on M9 minimal medium containing the appropriate antibiotic (since recipient strain MG1655 is prototrophic and the donor TOP10 is auxotrophic). The plasmid DNA from selected transconjugants was isolated and confirmed via PCR analysis and DNA sequencing. To confirm that conjugation was not affected by these manipulations, we compared the conjugation frequency of R751 Km, R751 Cm, and R751 Sp to the control R751 in separate conjugation experiments (Fig. 1A). The results showed no difference between the new R751 derivatives and WT R751 in conjugation ability. In addition, plasmid stability assays showed no difference between R751 Km, R751 Cm, and R751 Sp and the WT R751 for plasmid maintenance under non-selective conditions (data not shown).

The FRT-Capture technique is diagrammed in Fig. 1B. This technique allows for convenient *in vivo* cloning of large, intact genomic segments (20 – 100 Kb+) (Santiago et al. 2011; Graf et al. 2018). This allows large gene systems to be cloned and subsequently transferred to a range of other bacterial recipients for evolution-

ary studies, complementation analysis, and bacterial engineering applications (Wilson and Nickerson 2006; Blondel et al. 2010; Graf et al. 2018). To test the new R751 derivatives as cloning vehicles in the FRT-Capture technique, we targeted two separate regions for cloning in *S. Typhimurium* and *E. coli*. The *S. Typhimurium pdu* region is 38 Kb in size and contains 43 genes that code for the formation of a protein microcompartment (MCP) that houses associated Pdu enzymes to catalyze the metabolism of 1,2 PD (Chowdhury et al. 2014; Bobik et al. 2015). The *E. coli rimL* region is 22 Kb and contains *rimL* (an acetyltransferase), *ydci* (a DNA binding gene regulator), and numerous other genes of unknown function (Blattner et al. 1997; Jennings et al. 2011). For both regions, FRT sites were inserted into locations flanking the target genes (using standard recombineering) such that a Km-R gene would be removed with the genes upon excision via FLP recombinase (Fig. 1B) (Datsenko and Wanner 2000). In the presence of one of the R751 derivatives (R751 Sp is shown in Fig. 1B as an example), the excised target genes would be inserted into the plasmid via FLP, and then this molecule is isolated via conjugation to a differentially marked recipient strain. For cloning the *S. Typhimurium pdu* genes, the cloning plasmid was R751 Sp and the target DNA strain was χ 3477 containing FRT sites flanking the *pdu* genes such that a Km-R marker would be excised with the *pdu* genes (as diagrammed in Fig. 1B) (Graf et al. 2018). For cloning the *rimL* region from *E. coli*, the cloning plasmid was R751 Cm and the target DNA strain was TOP10 containing FRT sites similarly flanking the *rimL* region (inserted at the b1422 and b1444 genes) (Blattner et al. 1997). The Ap-R plasmid pCP20, which expresses the FLP

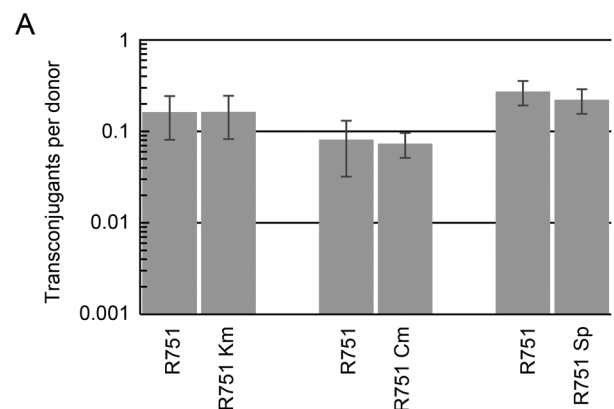


Fig. 1. Characterization of R751 plasmid derivatives.

Panel A: Conjugation frequency (transconjugant per donor) of R751 derivatives compared to WT R751. Each conjugation was performed with different recipients with appropriate counterselective markers, and each R751 derivative is compared to the associated R751 control for that corresponding recipient performed simultaneously.

recombinase, was electroporated into competent target DNA strains containing the R751 derivative, and colonies were selected on either LB Sp Km Ap or LB Cm Km Ap for the *pdu* or *rimL* clonings, respectively.

Pooled colonies from a given electroporation were used as donor to the *E. coli* recipient strain TOP10 Rif (Graf et al. 2018), and transconjugants were selected on either LB Rif Sp Km (for the *pdu* cloning) or LB Rif Cm Km

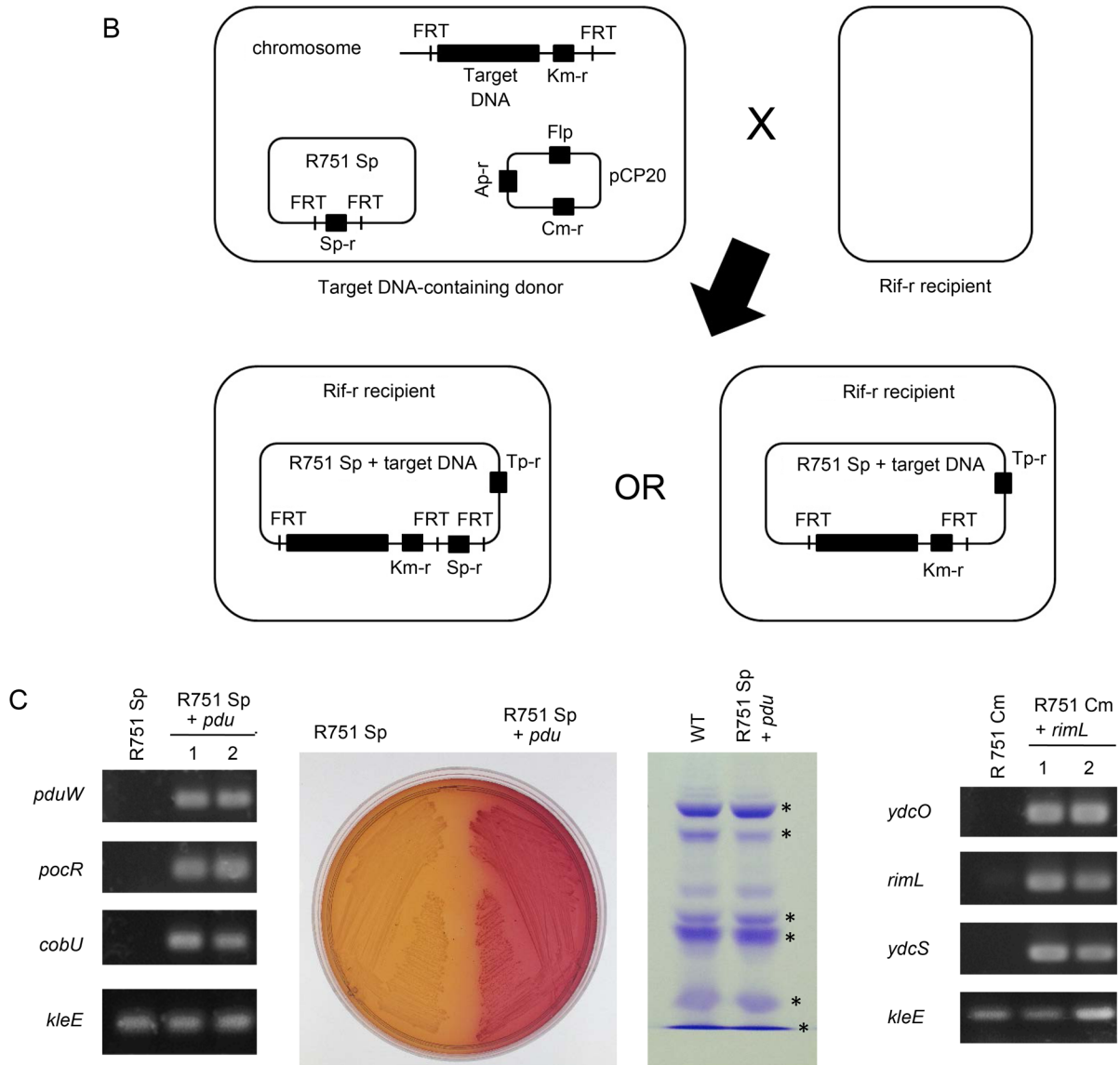


Fig. 1. Characterization of R751 plasmid derivatives.

Panel B: Diagram of the FRT-Capture technique using plasmid R751 Sp as the cloning vehicle. The Sp-r marker can either be retained (via selection for Sp-r) or removed (by using solely Tp-r as the R751 plasmid selection) via this procedure (see text for details). Please, note that when the Sp-r marker is retained, insertion of the target DNA could occur on either side of the Sp-r marker (only one such insertion is shown). The insertion location can be easily verified using PCR or DNA sequencing of the plasmid.

Panel C: Left-most picture: R751 Sp + *pdu* plasmid DNA was isolated and used as a template in PCR reactions using primers hybridizing to the *pduW*, *pocR*, and *cobU* genes. Primers hybridizing to the R751 Sp plasmid vector (*kleE* gene) were used as control. PCR products were run on 1.5% agarose and stained with SYBR Safe stain. The lanes labeled “1” and “2” are separate isolates of R751 Sp + *pdu*.

Middle two pictures: *E. coli* TOP10 Rif strains containing either R751 Sp or R751 Sp + *pdu* were streaked onto MacConkey agar containing 1,2 PD as carbon source and supplemented with coenzyme B12. Red colony color indicates the expression of the *pdu* genes and metabolism of 1,2 PD. In addition, intact MCPs were isolated from TOP10 Rif (R751 Sp + *pdu*) and approximately 15 micrograms were run on an SDS-PAGE gel and stained with Coomassie. Asterisks on the gel photo indicate bands of known Pdu MCP proteins. Corresponding negative control strains display no bands (or a very faint non-MCP background band) via this analysis (data not shown).

Right-most picture: R751 Cm + *rimL* plasmid DNA was isolated and used as a template in PCR reactions using primers hybridizing to the *ycdO*, *rimL*, and *ycdS* genes, and the samples were analyzed as above. The lanes labeled “1” and “2” are separate isolates of R751 Cm + *rimL*.

(for the *rimL* cloning). In regard to the efficiency of this process, when using approximately 5×10^7 cells of both the electroporated target DNA strain and the TATG-GCAGATGCGCAGGTGACAATTAAGAC; *pduW3*³: TGACAACAAATCACCCGTAATGCGCTGAGT; *pocR5*⁵: GCAGGTTCGTTTAAGTAATGACGTGGA-GCT; *pocR3*³: ATAGACATGTGAGTOP10 Rif recipient, we regularly obtain hundreds of transconjugant colonies (each representing independent clones).

After isolation of R751 Sp + *pdu* and R751 Cm + *rimL*, we used PCR to confirm the presence of the indicated genes (located at 5', center, and 3' locations in these regions) on these clones (Fig. 1C). Plasmid DNA from individual transconjugants was isolated and screened using PCR and relevant phenotypic assays (Fig. 1C). PCR primers used to confirm the presence of cloned *pdu* and *rimL* genes and the R751 *kleE* gene were as follows: *pduW5*⁵: TATGGCAGATGCGCAGGTGACAATTAAGAC; *pduW3*³: TGACAACAAATCACCCGTAATGCGCTGAGT; *pocR5*⁵: GCAGGTTCGTTTAAGTAATGACGTGGA-GCT; *pocR3*³: ATAGACATGTGAGGCGACATCCTCAAGACG; *cobU5*⁵: ACCTCATCCGCCGCTGCCGCCAGTCGTTGG; *cobU3*³: CTTAATTGGCGATGCGCCGACAGTACTGTA; *ycdO5*⁵: GCCGCGTCTCGCTCACGCTCATTATGCAGC; *ycdO3*³: GATCGTCATCGCGCAAGGTGACGTTGTCAC; *rimL5*⁵: AAGCGAATCACTTGAATTACATGCTGTTGC; *rimL3*³: CTCAGCCTGTTTCAGGCAACCTTCAAGGAT; *ycdS5*⁵: CAGCAGCCTGTGTGCGCTCAGCATGACAAT; *ycdS3*³: GCCTTATTTGCTCTTGCCGTCCGGCAGATT; *kleE5*⁵: CGCGTTCAGTGCCGCGAAGTACGCCAGGAA; *kleE3*³: TGGCACACCGTAACCATGCTTCCGAGTGGG.

For R751 Sp + *pdu*, we also used MacConkey agar containing 1,2 PD as a carbon source to confirm *pdu* gene expression and functional MCP formation from this plasmid (Fig. 1C) (Graf et al. 2018). In addition, we used an MCP isolation procedure to confirm recovery of intact MCP particles from an R751 Sp + *pdu* strain (analyzed via SDS-PAGE and Coomassie staining) (Fig. 1C) (Graf et al. 2018). Briefly, for MCP isolation, we harvested cells via centrifugation from 10 ml of stationary phase culture (grown in the presence of 1,2 PD), resuspended the cells in 4 ml of buffer A (50 mM Tris-HCl pH=7.5, 500 mM KCl, 12.5 mM MgCl₂, 5 mM beta-mercaptoethanol, 100 micrograms/ml lysozyme, 2 units/ml DNase I, 30% B-PER lysis reagent), and allowed lysis to occur over 1 hour at room temperature with gentle tube inversion. After the sample was centrifuged at 12 000 × g to remove the insoluble fraction, we recovered the supernatant and centrifuged this at 16 000 × g to pellet the MCPs. The pelleted MCPs were washed, resuspended in 150 μl buffer B (50 mM Tris-HCl pH=7.5, 50 mM KCl, 5 mM MgCl₂), and stored at minus 80°C until SDS-PAGE analysis. Taken together, the PCR and phenotypic assays demonstrate the successful utilization of R751 derivatives as gene capture

vehicles in a recombineering/conjugation approach to clone large genomic segments from different species.

A convenient feature of the R751 derivatives reported here is that the alternative marker on each can be removed during the FRT-Capture process and replaced with the target DNA (a deletion/replacement of the marker) (Fig. 1B). This is achieved with high efficiency when selection for the marker is removed during the steps for FRT-Capture. To perform the deletion/replacement, the same procedure as above is followed, but trimethoprim resistance (Tp-R) is used as the plasmid selection (as opposed to Sp-R or Cm-R in the above examples). When this is done, transconjugants can be screened for loss of Sp-R or Cm-R (using the examples above), which would have been removed in the donor strain via FLP from pCP20 (with 100% efficiency in our hands).

The range of different marker combinations found on the R751-derived cloning vehicles allows great flexibility for use in FRT-Capture and other similar approaches, and the deletion/replacement option allows convenient removal of a given alternative marker during this process. We emphasize the underdeveloped potential in using recombineering/conjugation-based systems to clone large genomic segments from bacterial genomes. This allows multi-gene systems that function together to be obtained on a single intact fragment that is easily isolated and transferred for subsequent applications. This will have increasing relevance in the post-genomic era as we discover novel large gene systems that can function independently in different bacteria for beneficial microbial bioengineering and evolutionary studies.

Acknowledgments

We acknowledge the Villanova University Biology Department and College for Liberal Arts and Sciences for supporting the work in this project. We thank Dr. David Figurski for plasmid R751.

Conflict of interest

The authors do not report any financial or personal connections with other persons or organizations, which might negatively affect the contents of this publication and/or claim authorship rights to this publication.

Literature

- Blattner FR, Plunkett G 3rd, Bloch CA, Perna NT, Burland V, Riley M, Collado-Vides J, Glasner JD, Rode CK, Mayhew GE, et al. The complete genome sequence of *Escherichia coli* K-12. *Science*. 1997 Sep 5;277(5331):1453–1462. <https://doi.org/10.1126/science.277.5331.1453>
- Blondel CJ, Yang HJ, Castro B, Chiang S, Toro CS, Zaldívar M, Contreras I, Andrews-Polymeris HL, Santiviago CA. Contribution of the type VI secretion system encoded in SPI-19 to chicken colonization by *Salmonella enterica* serotypes Gallinarum and Enteritidis. *PLoS One*. 2010 Jul 22;5(7):e11724. <https://doi.org/10.1371/journal.pone.0011724>

- Bobik TA, Lehman BP, Yeates TO.** Bacterial microcompartments: widespread prokaryotic organelles for isolation and optimization of metabolic pathways. *Mol Microbiol.* 2015 Oct;98(2):193–207. <https://doi.org/10.1111/mmi.13117>
- Bubnov DM, Yuzbashev TV, Vybornaya TV, Netrusov AI, Sineoky SP.** Development of new versatile plasmid-based systems for λ Red-mediated *Escherichia coli* genome engineering. *J Microbiol Methods.* 2018 Aug;151:48–56. <https://doi.org/10.1016/j.mimet.2018.06.001>
- Chowdhury C, Sinha S, Chun S, Yeates TO, Bobik TA.** Diverse bacterial microcompartment organelles. *Microbiol Mol Biol Rev.* 2014 Sep 01;78(3):438–468. <https://doi.org/10.1128/MMBR.00009-14>
- Datsenko KA, Wanner BL.** One-step inactivation of chromosomal genes in *Escherichia coli* K-12 using PCR products. *Proc Natl Acad Sci USA.* 2000 Jun 06;97(12):6640–6645. <https://doi.org/10.1073/pnas.120163297>
- Graf L, Wu K, Wilson JW.** Transfer and analysis of *Salmonella pdu* genes in a range of Gram-negative bacteria demonstrate exogenous microcompartment expression across a variety of species. *Microb Biotechnol.* 2018 Jan;11(1):199–210. <https://doi.org/10.1111/1751-7915.12863>
- Heinemann JA, Sprague GF Jr.** Bacterial conjugative plasmids mobilize DNA transfer between bacteria and yeast. *Nature.* 1989 Jul;340(6230):205–209. <https://doi.org/10.1038/340205a0>
- Jennings ME, Quick LN, Soni A, Davis RR, Crosby K, Ott CM, Nickerson CA, Wilson JW.** Characterization of the *Salmonella enterica* serovar Typhimurium *ycdI* gene, which encodes a conserved DNA binding protein required for full acid stress resistance. *J Bacteriol.* 2011 May 01;193(9):2208–2217. <https://doi.org/10.1128/JB.01335-10>
- Narayanan K, Chen Q.** Bacterial artificial chromosome mutagenesis using recombineering. *J Biomed Biotechnol.* 2011;2011:1–10. <https://doi.org/10.1155/2011/971296>
- Norberg P, Bergström M, Jethava V, Dubhashi D, Hermansson M.** The IncP-1 plasmid backbone adapts to different host bacterial species and evolves through homologous recombination. *Nat Commun.* 2011 Sep;2(1):268. <https://doi.org/10.1038/ncomms1267>
- Pansegrau W, Lanka E, Barth PT, Figurski DH, Guiney DG, Haas D, Helinski DR, Schwab H, Stanisich VA, Thomas CM.** Complete nucleotide sequence of Birmingham IncP alpha plasmids. Compilation and comparative analysis. *J Mol Biol.* 1994 Jun; 239(5):623–663. <https://doi.org/10.1006/jmbi.1994.1404>
- Quick LN, Shah A, Wilson JW.** A series of vectors with alternative antibiotic resistance markers for use in lambda Red recombination. *J Microbiol Biotechnol.* 2010 Apr;20(4):666–669. <https://doi.org/10.4014/jmb.0909.09045>
- Santiago CP, Quick LN, Wilson JW.** Self-transmissible IncP R995 plasmids with alternative markers and utility for Flp/FRT cloning strategies. *J Microbiol Biotechnol.* 2011 Nov 28;21(11):1123–1126. <https://doi.org/10.4014/jmb.1106.06032>
- Sen D, Brown CJ, Top EM, Sullivan J.** Inferring the evolutionary history of IncP-1 plasmids despite incongruence among backbone gene trees. *Mol Biol Evol.* 2013 Jan;30(1):154–166. <https://doi.org/10.1093/molbev/mss210>
- Thorsted PB, Macartney DP, Akhtar P, Haines AS, Ali N, Davidson P, Stafford T, Pocklington MJ, Pansegrau W, Wilkins BM, et al.** Complete sequence of the IncP β plasmid R751: implications for evolution and organisation of the IncP backbone. *J Mol Biol.* 1998 Oct;282(5):969–990. <https://doi.org/10.1006/jmbi.1998.2060>
- Trieu-Cuot P, Carlier C, Martin P, Courvalin P.** Plasmid transfer by conjugation from *Escherichia coli* to Gram-positive bacteria. *FEMS Microbiol Lett.* 1987 Dec;48(1-2):289–294. <https://doi.org/10.1111/j.1574-6968.1987.tb02558.x>
- Wang H, Li Z, Jia R, Hou Y, Yin J, Bian X, Li A, Müller R, Stewart AF, Fu J, et al.** RecET direct cloning and Red $\alpha\beta$ recombineering of biosynthetic gene clusters, large operons or single genes for heterologous expression. *Nat Protoc.* 2016 Jul;11(7):1175–1190. <https://doi.org/10.1038/nprot.2016.054>
- Waters VL.** Conjugation between bacterial and mammalian cells. *Nat Genet.* 2001 Dec;29(4):375–376. <https://doi.org/10.1038/ng779>
- Wilson J, Nickerson C.** A new experimental approach for studying bacterial genomic island evolution identifies island genes with bacterial host-specific expression patterns. *BMC Evol Biol.* 2006;6(1):2. <https://doi.org/10.1186/1471-2148-6-2>
- Zeng F, Hao Z, Li P, Meng Y, Dong J, Lin Y.** A restriction-free method for gene reconstitution using two single-primer PCRs in parallel to generate compatible cohesive ends. *BMC Biotechnol.* 2017 Dec;17(1):32. <https://doi.org/10.1186/s12896-017-0346-5>
- Zeng F, Zang J, Zhang S, Hao Z, Dong J, Lin Y.** AFEAP cloning: a precise and efficient method for large DNA sequence assembly. *BMC Biotechnol.* 2017 Dec;17(1):81. <https://doi.org/10.1186/s12896-017-0394-x>
- Zeng F, Zhang S, Hao Z, Duan S, Meng Y, Li P, Dong J, Lin Y.** Efficient strategy for introducing large and multiple changes in plasmid DNA. *Sci Rep.* 2018 Dec;8(1):1714. <https://doi.org/10.1038/s41598-018-20169-8>

CONTENTS

Vol. 68, 1–4, 2019

No 1

ORIGINAL PAPERS

Antibiotic susceptibility of <i>Cronobacter</i> spp. isolated from clinical samples HOLÝ O., ALSONOSI A., HOCHÉL I., RÖDEROVÁ M., ZATLOUKALOVÁ S., MLYNÁRČIK P., KOLÁŘ M., PETRŽELOVÁ J., ALAZRAQ A., CHMELAR D., FORSYTHE S.	5
Interferon gamma release assays in patients with respiratory isolates of non-tuberculous mycobacteria – a preliminary study AUGUSTYNOWICZ-KOPEĆ E., SIEMION-SZCZEŚNIAK I., ZABOST A., WYROSTKIEWICZ D., FILIPCZAK D., ONISZH K., GAWRYLUK D., RADZIKOWSKA E., KORZYBSKI D., SZTURMOWICZ M.	15
Bioactive compounds of <i>Pseudoalteromonas</i> sp. IBRL PD4.8 inhibit growth of fouling bacteria and attenuate biofilms of <i>Vibrio alginolyticus</i> FB3 SUPARDY N.A., IBRAHIM D., MAT NOR S.R., MD NOORDIN W.N.	21
Mycosynthesis of size-controlled silver nanoparticles through optimization of process variables by response surface methodology SHAHZAD A., IQTEDAR M., SAEED H., HUSSAIN S.Z., CHAUDHARY A., ABDULLAH R., KALEEM A.	35
Thermoregulation of prodigiosin biosynthesis by <i>Serratia marcescens</i> is controlled at the transcriptional level and requires HexS ROMANOWSKI E.G., LEHNER K.M., MARTIN N.C., PATEL K.R., CALLAGHAN J.D., STELLA N.A., SHANKS R.M.Q.	43
Clinical interpretation of detection of IgM anti- <i>Brucella</i> antibody in the absence of IgG and <i>vice versa</i> ; a diagnostic challenge for clinicians AL JINDAN R., SALEEM N., SHAFI A., AMJAD S.M.	51
<i>In vitro</i> and <i>in vivo</i> activity of zafloxacin and other fluoroquinolones against MRSA isolates from a University Hospital in Egypt MOHAMED N.M., ZAKARIA A.S., EDWARD E.A., ABDEL-BARY A.	59
Biodiversity of bacteria associated with eight <i>Pleurotus ostreatus</i> (Fr.) P. Kumm. strains from Poland, Japan and the USA ADAMSKI M., PIETR S.J.	71
Microbiota and chemical compounds in fermented <i>Pinelliae Rhizoma</i> (Banxiaqu) from different areas in the Sichuan Province, China SHU B., YING J., WANG T., XIA M., ZHAO W., YOU L.	83
New insight into genotypic and phenotypic relatedness of <i>Staphylococcus aureus</i> strains from human infections or animal reservoirs LISOWSKA-ŁYSIAK K., KOSECKA-STROJEK M., BIAŁECKA J., KASPROWICZ A., GARBACZ K., PIECHOWICZ L., KMET V., SAVINI V., MIĘDZOBRODZKI J.	93
The influence of temperature and nitrogen source on cellulolytic potential of microbiota isolated from natural environment WITA A., BIAŁAS W., WILK R., SZYCHOWSKA K., CZACZYK K.	105
Dengue outbreaks in Khyber Pakhtunkhwa (KPK), Pakistan in 2017: an integrated disease surveillance and response system (IDSRS)-based report ABDULLAH, ALI S., SALMAN M., DIN M., KHAN K., AHMAD M., KHAN F.H., ARIF M.	115
Dependence of volonization of the large intestine by <i>Candida</i> on the treatment of Crohn's disease KOWALSKA-DUPLAGA K., KRAWCZYK A., SROKA-OLEKSIK A., SALAMON D., WĘDRYCHOWICZ A., FYDEREK K., GOSIEWSKI T.	121
Predominance of <i>Lactobacillus plantarum</i> strains in Peruvian Amazonian fruits SÁNCHEZ J., VEGAS C., ZAVALETA A.I., ESTEVE-ZARZOSO B.	127

SHORT COMMUNICATIONS

Comparison of performance characteristics of DxN VERIS system versus Qiagen PCR for HBV genotype D and HCV genotype 1b quantification SAYAN M., ARIKAN A., SANLIDAG T.	139
--	-----

No 2

MINIREVIEW

- The state of research on antimicrobial activity of cold plasma
 NIEDŹWIEDŹ I., WAŹKO A., PAWŁAT J., POLAK-BERECKA M. 153

ORIGINAL PAPERS

- Hand, foot, and mouth disease caused by Coxsackievirus A6: a preliminary report from Istanbul
 CEYLAN A.N., TUREL O., GULTEPE B.S., INAN E., TURKMEN A.V., DOYMAZ M.Z. 165
- Evaluation of a *Salmonella* strain isolated from honeybee gut as a potential live oral vaccine against lethal infection of *Salmonella* Typhimurium
 ZAFAR H., RAHMAN S.U., ALI S., JAVED M.T. 173
- Evaluation of the pathogenic potential of insecticidal *Serratia marcescens* strains to humans
 KONECKA E., MOKRACKA J., KRZYMIŃSKA S., KAZNOWSKI A. 185
- An investigation of petrol metabolizing bacteria isolated from contaminated soil samples collected from various fuel stations
 MUCCEE F., EJAZ S. 193
- Prevalence and antimicrobial properties of lactic acid bacteria in Nigerian women during the menstrual cycle
 ADEOSHUN F.G., RUPPITSCH W., ALLERBERGER F., AYENI F.A. 203
- In situ* impact of the antagonistic fungal strain, *Trichoderma gamsii* T30 on the plant pathogenic fungus, *Rhizoctonia solani* in soil
 ANEES M., ABID M., CHOCHAN S., JAMIL M., AHMED N., ZHANG L., RHA E.S. 211
- Campylobacter fetus* is internalized by bovine endometrial epithelial cells
 CAMPOS-MÚZQUIZ L.G., MÉNDEZ-OLVERA E.T., ARELLANO-REYNOSO B., MARTÍNEZ-GÓMEZ D. 217
- Patterns of drug-resistant bacteria in a general hospital, China, 2011–2016
 MAO T., ZHAI H., DUAN G., YANG H. 225
- Analysis of the amino acid sequence variation of the 67–72p protein and the structural pili proteins of *Corynebacterium diphtheriae* for their suitability as potential vaccine antigens
 BRODZIK K., KRYSZTOPA-GRZYBOWSKA K., POLAK M., LACH J., STRAPAGIEL D., ZASADA A.A. 233
- Gastric microbiota alteration in *Klebsiella pneumoniae*-caused liver abscesses mice
 CHEN N., JIN T.-T., LIU W.-N., ZHU D.Q., CHEN Y.-Y., SHEN Y.-L., LING Z.-X., WANG H.-J., ZHANG L.-P. 247
- Influence of environmental and genetic factors on proteomic profiling of outer membrane vesicles from *Campylobacter jejuni*
 GODLEWSKA R., KLIM J., DĘBSKI J., WYSZYŃSKA A., ŁASICA A. 255
- Effects of sodium tripolyphosphate on oral commensal and pathogenic bacteria
 MOON J.-H., NOH M.H., JANG E.-Y., YANG S.B., KANG S.W., KWACK K.H., RYU J.-I., LEE J.-Y. 263
- The joint effect of pH gradient and glucose feeding on the growth kinetics of *Lactococcus lactis* CECT 539 in glucose-limited fed-batch cultures
 MALVIDO M.C., GONZÁLEZ E.A., JÁCOME R.J.B., GUERRA N.P. 269

SHORT COMMUNICATIONS

- Bacterial diversity in soybean rhizosphere soil at seedling and mature stages
 WANG L., LI Z., LIU R., LI L., WANG W. 281

No 4

CONTENTS

MINIREVIEW

Antibiotic resistance among uropathogenic <i>Escherichia coli</i> KOT B.	403
Colistin resistance in Enterobacterales strains – a current view STEFANIUK E.M., TYSKI S.	417

ORIGINAL PAPERS

Molecular identification of <i>Vibrio alginolyticus</i> causing vibriosis in shrimp and its herbal remedy HANNAN MD. A., RAHMAN MD. M., MONDAL MD. N., DEB S.C., CHOWDHURY G., ISLAM MD. T.	429
<i>Salmonella</i> -infected aortic aneurysm: investigating pathogenesis using <i>Salmonella</i> serotypes CHU C., WONG M.Y., CHIU C.-H., TSENG Y.-H., CHEN C.-L., HUANG Y.-K.	439
Molecular epidemiology of hepatitis B virus in Turkish Cypriot SUMER U., SAYAN M.	449
Cytokine levels in the <i>in vitro</i> response of T cells to planktonic and biofilm <i>Corynebacterium amycolatum</i> OLENDER A., BOGUT A., MAGRYŚ A., TABARKIEWICZ J.	457
The diversity of the endobiotic bacterial communities in the four jellyfish species LIU Q., CHEN X., LI X., HONG J., JIANG G., LIANG H., LIU W., XU Z., ZHANG J., WANG W., XIAO L.	465
Inhibition of drug resistance of <i>Staphylococcus aureus</i> by efflux pump inhibitor and autolysis inducer to strengthen the antibacterial activity of β -lactam drugs LUAN W., LIU X., WANG X., AN Y., WANG Y., WANG C., SHEN K., XU H., LI S., LIU M., YU L.	477
Diversity, virulence factors, and antifungal susceptibility patterns of pathogenic and opportunistic yeast species in rock pigeon (<i>Columba livia</i>) fecal droppings in Western Saudi Arabia ABULREESH H.H., ORGANJI S.R., ELBANNA K., OSMAN G.E.H., ALMALKI M.H.K., ABDEL-MALEK A.Y., GHYATHUDDIN A.A.K., AHMAD I.	493
The composition of fungal communities in the rumen of gayals (<i>Bos frontalis</i>), yaks (<i>Bos grunniens</i>), and Yunnan and Tibetan yellow cattle (<i>Bos taurus</i>) WANG H., LI P., LIU X., ZHANG C., LU Q., XI D., YANG R., WANG S., BAI W., YANG Z., ZHOU R., CHENG X., LENG J.	505
New look on antifungal activity of silver nanoparticles (AgNPs) ŻAROWSKA B., KOŹLECKI T., PIEGZA M., JAROS-KOŹLECKA K., ROBAK M.	515
Illumina MiSeq analysis and comparison of freshwater microalgal communities on Ulleungdo and Dokdo Islands YUN X.-S., KIM Y.-S., YOON H.-S.	527
Epidemiology, drug resistance, and virulence of <i>Staphylococcus aureus</i> isolated from ocular infections in Polish patients KŁOS M., POMORSKA-WESOŁOWSKA M., ROMANISZYN D., CHMIELARCZYK A., WÓJKOWSKA-MACH J.	541
Structural changes of <i>Bacillus subtilis</i> biomass on biosorption of Iron (II) from aqueous solutions: isotherm and kinetic studies KANAMARLAPUDI S.L.R.K., MUDDADA S.	549

SHORT COMMUNICATIONS

Differentially marked IncP-1 β R751 plasmids for cloning via recombineering and conjugation BAINS A., WILSON J.W.	559
---	-----

Polish Journal of Microbiology
Vol. 68, 1–4, 2019

Author Index

A

Abdel-Bary A. 59
Abdel-Malek A.Y. 493
Abdullah 115
Abdullah R. 35
Abid M. 211
Abulreesh H.H. 493
Adamski M. 71
Adeoshun F.G. 203
Ahmad I. 493
Ahmad M. 115
Ahmed N. 211
Akcali S. 317
Al Jindan R. 51
Alazraq A. 5
Ali S. 115, 173
Allerberger F. 203
Almalki M.H.K. 493
Alsonosi A. 5
Amjad S.M. 51
An Y. 477
Anees M. 211
Arellano-Reynoso B. 217
Arif M. 115
Arikan A. 139, 317
Augustynowicz-Kopeć E. 15, 303
Ayeni F.A. 203

B

Bai W. 505
Bains A. 559
Batura-Gabryel H. 377
Białas W. 105
Białęcka J. 93
Biedka M. 343
Bogut A. 457
Borysewicz-Lewicka M. 377
Brodzik K. 233
Brzychczy-Włoch M. 323
Bulanda M. 323

C

Callaghan J.D. 43
Campos-Múzquiz L.G. 217
Catania M.R. 309
Ceylan A.N. 165
Chaudhary A. 35
Chen C.-L. 439
Chen N. 247
Chen X. 465
Chen Y.-Y. 247
Cheng X. 505
Chiu C.-H. 439
Chmelař D. 5
Chmielarczyk A. 541

Chohan S. 211
Chowdhury G. 429
Chu C. 439
Cofta S. 377
Czaczyk K. 105

D

Deb S.C. 429
Dębski J. 255
Din M. 115
Domański D. 303
Doymaz M.Z. 165
Duan G. 225

E

Edward E.A. 59
Ejaz S. 193
Elbanna K. 493
Esteve-Zarzoso B. 127

F

Filipczak D. 15
Forsythe S. 5
Fu P. 383
Fyderek K. 121

G

Garbacz K. 93
Gawryluk D. 15
Ghyathuddin A.A.K. 493
Godlewska R. 255
Golas-Pradzynska M. 303
Gong S. 331
González E.A. 269
Gosiewski T. 121
Gospodarek-Komkowska E. 353
Grudlewska K. 353
Gryń G. 353
Grzegorzczak A. 371
Guerra N.P. 269
Gultepe B.S. 165
Guo G. 383
Guvenir M. 317

H

Hannan Md. A. 429
Hochel I. 5
Holý O. 5
Hong J. 465
Huang Y.-K. 439
Hussain S.Z. 35

I

Ibrahim D. 21
Inan E. 165

Iqtedar M. 35
Islam Md. T. 429
Iwaniak W. 295

J

Jácome R.J.B. 269
Jamil M. 211
Jang E.-Y. 263
Jaros-Koźlecka K. 515
Javed M.T. 173
Jiang G. 465
Jin T.-T. 247
Ju J. 331
Juszczak K. 353

K

Kacem Chaouche N. 309
Kaczmarek A. 353
Kaleem A. 35
Kanamarlupudi S.L.R.K. 549
Kang S.W. 263
Kasela M. 371
Kasprowicz A. 93
Kaznowski A. 185
Khan F.H. 115
Khan K. 115
Kim Y.-S. 527
Klim J. 255
Kłós M. 541
Kmet V. 93
Kolář M. 5
Konecka E. 185
Korzybski D. 15
Kosecka-Strojek M. 93
Kosek-Paszowska K. 353
Kot B. 403
Kovalenko V. 295
Kowalska-Duplaga K. 121
Koźlecki T. 515
Krawczyk A. 121
Krysztopa-Grzybowska K. 233
Krzymińska S. 185
Kuthan R. 303
Kwack K.H. 263
Kwiecińska-Piróg J. 353

L

Lach J. 233
Lee J.-Y. 263
Lehner K.M. 43
Leng J. 505
Li B.-Y. 383
Li L. 281
Li P. 505
Li S. 477

Li X. 465
 Li Y. 331
 Li Z. 281
 Liang H. 465
 Ling Z.-X. 247
 Lisowska-Łysiak K. 93
 Liu D. 331
 Liu M. 477
 Liu Q. 465
 Liu R. 281
 Liu W. 465
 Liu W.-N. 247
 Liu X. 477
 Liu X. 505
 Lu Q. 505
 Luan W. 477
 Łasica A. 255

M

Magryś A. 457
 Malm A. 371
 Malvido M.C. 269
 Mao T. 225
 Martin N.C. 43
 Martínez-Gómez D. 217
 Mat Nor S.R. 21
 Md Noordin W.N. 21
 Méndez-Olvera E.T. 217
 Międzobrodzki J. 93
 Mikołajczyk E. 323
 Młynarczyk P. 5
 Mohamed N.M. 59
 Mokracka J. 185
 Mondal Md. N. 429
 Moon J.-H. 263
 Muccee F. 193
 Muddada S. 549
 Muhammad M. 331

N

Nedosekov V. 295
 Niedźwiedź I. 153
 Noh M.H. 263
 Nowikiewicz T. 343
 Nychyk S. 295

O

Ochońska D. 323
 Olender A. 457
 Onish K. 15
 Organji S.R. 493
 Osman G.E.H. 493

P

Paluszak Z. 353
 Patel K.R. 43
 Pawlaczyk-Kamieńska T. 377
 Pawłat J. 153
 Peng J. 383
 Petrželová J. 5
 Piechowicz L. 93
 Piegza M. 515
 Pietr S.J. 71
 Piskorska-Malolepsza K. 303

Polak M. 233
 Polak-Berecka M. 153
 Pomorska-Wesołowska M. 541
 Pyskun A. 295
 Pyskun O. 295

R

Radzikowska E. 15
 Rahman Md. M. 429
 Rahman S.U. 173
 Rha E.S. 211
 Ritieni A. 309
 Robak M. 515
 Röderová M. 5
 Romaniszyn D. 541
 Romanowski E.G. 43
 Ruppitsch W. 203
 Ryu J.-I. 263

S

Saeed H. 35
 Sakhri A. 309
 Salamon D. 121, 323
 Saleem N. 51
 Salman M. 115
 Sánchez J. 127
 Sanlidag T. 139
 Sanlidag T. 317
 Santini A. 309
 Savini V. 93
 Sayan M. 139, 317, 449
 Shafi A. 51
 Shahzad A. 35
 Shanks R.M.Q. 43
 Shen K. 477
 Shen Y.-L. 247
 Shi Y. 331
 Shu B. 83
 Siemion-Szcześniak I. 15
 Sikora M. 303
 Skowron K. 353
 Sroka-Oleksiak A. 121
 Stefaniuk E.M. 417
 Stella N.A. 43
 Strapagiel D. 233
 Su P.-P. 383
 Suer K. 317
 Sumer U. 449
 Supardy N.A. 21
 Swoboda-Kopec E. 303
 Sytiuk M. 295
 Szturmowicz M. 15
 Szychowska K. 105
 Szymankiewicz M. 343
 Śniatała R. 377

T

Tabarkiewicz J. 457
 Tseng Y.-H. 439
 Turel O. 165
 Turkmen A.V. 165
 Tyski S. 417

U

Ukhovskiy V. 295

V

Vegas C. 127

W

Wałęcka-Zacharksa E. 353
 Wang C. 477
 Wang H. 505
 Wang H.-J. 247
 Wang L. 281
 Wang S. 505
 Wang T. 83
 Wang W. 281
 Wang W. 465
 Wang X. 477
 Wang Y. 477
 Waśko A. 153
 Wędrychowicz A. 121
 Wiktorczyk N. 353
 Wilk R. 105
 Wilson J.W. 559
 Wita A. 105
 Wojak I. 323
 Wong M.Y. 439
 Wójkowska-Mach J. 541
 Wyrostkiewicz D. 15
 Wyszyńska A. 255

X

Xi D. 505
 Xia M. 83
 Xiao L. 465
 Xiu J.-F. 383
 Xu H. 477
 Xu Z. 465

Y

Yang H. 225
 Yang L.-B. 383
 Yang R. 505
 Yang S.B. 263
 Yang Z. 505
 Ying J. 83
 Yoon H.-S. 527
 You L. 83
 Yu L. 477
 Yun X.-S. 527

Z

Zabost A. 15
 Zafar H. 173
 Zakaria A.S. 59
 Zasada A.A. 233
 Zatloukalová S. 5
 Zavaleta A.I. 127
 Zhai H. 225
 Zhang C. 505
 Zhang J. 465
 Zhang L. 211
 Zhang L.-P. 247
 Zhao B. 331
 Zhao W. 83
 Zhao X.-Y. 383
 Zhou R. 505
 Zhu D.Q. 247
 Żarowska B. 515

Polish Journal of Microbiology
Vol. 68, 1–4, 2019

ACKNOWLEDGEMENTS

The Editors of *Polish Journal of Microbiology* wish to express their gratitude to colleagues who have reviewed the manuscripts submitted to our Journal in the past year:

A

Abbas Aqleem (Pakistan)
Abdel-Hamid Marwa S. (Egypt)
Adamczyk-Popławska Monika (Poland)
Akar Tarik (Turkey)
Albores Silvana (Uruguay)
Allen Richard C. (Switzerland)
Alloing Genvieve (France)
Alpati Kavitha (India)
Antonelli Alberto (Italy)
Ardebili Abdollah (Iran)
Athanasίου Christos (Greece)
Aung Meiji S. (Japan)

B

Balabanova Larissa (Russian Federation)
Barati Mohammad (Iran)
Barde Pradip (India)
Barzkar Noora (Iran)
Blackard Jason (USA)
Boehm Manja (Germany)
Borewicz Klaudyna (Netherlands)
Boyanova Lyudmila (Bulgaria)
Boyd Joseph S. (USA)
Braiek Olfa B. (Tunisia)
Brook Itzhak G. (USA)
Bugla-Płoskońska Gabriela (Poland)
Bulgac Elena (USA)

C

Calix Juan (USA)
Chiciudean Iulia (Romania)
Chu Maoping (China)
Chudzicka-Strugała Izabela (Poland)
Chusri Sasitorn (Thailand)
Clark Clifford G. (Canada)
Costa Vanessa D. (Brazil)
Cycoń Mariusz (Poland)
Cyplik Paweł (Poland)

D

D'Souza Jacinta S. (India)
Daghio M. (Italy)
Dangel Alexandra (Germany)
Das Pratyush K. (India)
David Michael Z. (USA)
Dénes Béla (Hungary)
Deng Yang (China)
Ding Jie (China)
Dorrell Nick (United Kingdom)
Doyle Christine J. (Australia)
Dudek Bartłomiej (Poland)

E

Edelmann Mariola J. (USA)
Eguchi Hiroshi (Japan)
Ehlers Marthie M. (South Africa)
Etchegaray Augusto (Brazil)

F

Fan Boyi (China)
Filho Ruy O. (Brazil)
Flores Geane L. (Brazil)
Flynn Padrig B. (United Kingdom)
Fracchia Letizia (Italy)
Furlaneto Marcia C. (Brazil)

G

Gibson Brian (Finland)
Gościniak Grażyna (Poland)
Grys Thomas E. (USA)
Guler Emrah (United Kingdom)

H

Hamel Chantal (Canada)
Hille Katja (Germany)
Ho Jemima (United Kingdom)
Homan E. Jane (USA)
Huang Danlian (China)

I

Iida Tadayuki (Japan)
Iraola Gregorio (Uruguay)

J

Jackowiak Paulina (Poland)
Jaroszek-Ścisła Jolanta (Poland)
Javanmard Davod (Iran)
Joshi Naveen C. (India)
Junka Feliks (Poland)

K

Kachhwaha Sumita (India)
Kaczorek Ewa (Poland)
Kang Xiaoming (China)
Kaviyarasu Kasina (South Africa)
Khatami Mehrdad (Iran)
Kilic Ayse B. (Turkey)
Kohli Seema (India)
Kordalewska Milena (USA)
Koziel Jacek (USA)
Krzywonos Małgorzata (Poland)
Kumar Anoop (India)
Kunicka-Styczyńska Alina (Poland)

L

Lampila Lucina E. (USA)
Laudy Agnieszka E. (Poland)
Lazar Zbigniew (Poland)
Lee I Learn-Han (Malaysia)
Lee Young-Chul (Korea)
Li Fu-Li (China)
Lin Yibin (USA)
Lingala Rajendra (India)
Liu Po-Yu (Taiwan)
Luo Li (China)
Lüthje Petra (Germany)

M

Malama Sydney (Zambia)
 Malloy Katherine M. (USA)
 Mandon Karine (France)
 Mariottini Gian. L (Italy)
 Matsukawa Masanori (Japan)
 McConville Thomas (USA)
 Memar Mohammad Y. (Iran)
 Mikulski Dawid (Poland)
 Miller Darlene (USA)
 Morse Daniel (United Kingdom)
 Munir Mohammad K. (Pakistan)
 Murad Yanal (Pakistan)

N

Nadella Ranjit K. (India)
 Naruishi Koji (Japan)
 Naughton Patrick J. (United Kingdom)
 Nawrot Urszula (Poland)
 Nordmann Patrice (Switzerland)
 Norton Raymond (Australia)
 Nugen Sam R. (USA)

O

O'Callaghan Richard J. (USA)
 Ogórek Rafał (Poland)
 Olaimat Amin N. (Jordan)
 Olender Alina M. (Poland)
 Olofsson Magnus (Sweden)
 Ong Song-Quan (Malaysia)
 Ouedraogo Samiratou (Canada)

P

Paget Timothy (United Kingdom)
 Pan Hong (China)
 Peng Quan-Hui (China)
 Perez Alonso Vanessa P. (Brazil)
 Philip Koshy (Malaysia)
 Piątek Jacek (Poland)
 Pierre Joseph F. (USA)
 Poirel Laurent (Switzerland)
 Portela Ricardo W. (Brazil)
 Pradeep Bulagonda E. (India)
 Przybyla-Kelly Katarzyna (USA)

Q

Qian Haifeng (China)

R

Rabee Asmaa E. (Egypt)
 Rafiq Mohammad (United Kingdom)
 Raina Satish (Poland)
 Ramli Norolhuda M. (Netherlands)
 Rastawicki Waldemar (Poland)
 Rezende Rachel P. (Brazil)
 Reyes-Lamothe Rodrigo (Canada)
 Rizzo Carmen (Italy)
 Rodriguea Jose J. (Spain)
 Rout Simon P. (United Kingdom)
 Różalska Barbara (Poland)
 Rudolph Christian J. (United Kingdom)
 Russo Pasquale (Italy)

S

Sabu Abdulhameed (India)
Santara Sumit S. (USA)
Sato Helia H. (Brazil)
Saxena Shailendra K. (India)
Sergi Consolato (Canada)
Shukla Pratyosh (India)
Skurnik Michael (Finland)
Sopirala Madhuri M. (USA)
Spano Giuseppe (Italy)
Staniszewska Monika (Poland)
Stefaniuk Elżbieta M. (Poland)
Sturtevant Joy (USA)
Sunder Jai (India)
Supono Supono (Indonesia)

T

Taner Ferdiye (Australia)
Tang Ying Z. (China)
Tanrikulu Yusuf (Turkey)
Tarlton Nicole J. (USA)
Tellez Guillermo (USA)
Tian Chunjie (China)

V

van Calenbergh Serge (Belgium)
Varjani Sunita J. (India)
Verma Pradeep (India)

W

Wang Changxian (United Kingdom)
Wang Wenjun (China)
Wójkowska-Mach Jadwiga (Poland)
Wolf Jonas (Brazil)

Y

Yokota Shin-ichi (Japan)
Youssef Noha Y. (USA)
Yun Jin-Ho (Korea)
Yurkov Andrey (Germany)

Z

Zakeri Amin (Denmark)
Zaręba Tomasz W. (Poland)
Zasada Aleksandra A. (Poland)

Ż

Żabicka Dorota (Poland)

INFORMACJE Z POLSKIEGO TOWARZYSTWA MIKROBIOLOGÓW



XXIX OGÓLNOPOLSKI ZJAZD
POLSKIEGO TOWARZYSTWA
MIKROBIOLOGÓW
15-18 WRZEŚNIA 2020,
WARSZAWA



XXIX OGÓLNOPOLSKI ZJAZD POLSKIEGO TOWARZYSTWA MIKROBIOLOGÓW

15-18 WRZEŚNIA 2020,
WARSZAWA



Miejsce Zjazdu:

Sangate Hotel Airport
Warszawa, ul. Komitetu Obrony Robotników 32
(dawniej 17 Stycznia, róg ul. Żwirki i Wigury)

Główny Organizator Zjazdu:

Polskie Towarzystwo Mikrobiologów
ul. Stefana Banacha 1b, 02-097 Warszawa
ptm.zmf@wum.edu.pl, www.microbiology.pl



XXIX OGÓLNOPOLSKI ZJAZD
POLSKIEGO TOWARZYSTWA
MIKROBIOLOGÓW
15-18 WRZEŚNIA 2020,
WARSZAWA



GLOBAL CONGRESS

Warszawa, 12.09.2019 r.

Szanowni Państwo,

Polskie Towarzystwo Mikrobiologów organizuje w przyszłym roku **XXIX Ogólnopolski Zjazd PTM w Warszawie w terminie: 15–18 września 2020 r.** Jest to okazja do zdobycia wiedzy mikrobiologicznej, podzielenia się swoimi osiągnięciami badawczymi oraz do spotkania merytorycznego i towarzyskiego osób zainteresowanych wspólną tematyką naukową.

PTM zostało powołane 92 lata temu i Ogólnopolskie Zjazdy Towarzystwa organizowane są co 4 lata

(www.microbiology.pl).

Jest to największe wydarzenie naukowe związane z mikrobiologią i najliczniejsze spotkanie polskich mikrobiologów w tym okresie. Zwykle bierze w nim udział ponad pół tysiąca mikrobiologów: naukowców, nauczycieli akademickich, lekarzy, diagnostów laboratoryjnych, specjalistów pracujących w służbie zdrowia, weterynarii, instytucjach naukowych i uczelniach, a także w przemyśle, rolnictwie oraz wykonujących mikrobiologiczne badania kontrolne w rozmaitych obszarach. W Zjazdach PTM udział biorą firmy diagnostyczne, chemiczne, farmaceutyczne, kosmetyczne, wytwarzające żywność, środki przeciwdrobnoustrojowe, odczynniki, testy oraz aparaturę kontrolną i badawczą stosowaną w rozmaitych działach mikrobiologii.

Wiele mikrobiologicznych badań naukowych, rozwojowych i użytkowych dotyczy aktualnych problemów: narastającej lekooporności drobnoustrojów chorobotwórczych, doskonalenia diagnostyki mikrobiologicznej, badań genetycznych drobnoustrojów, badań mikrobiologicznego zanieczyszczenia środowiska, GMO, poprawy systemu jakości i metod kontroli żywności, leków, wyrobów medycznych, produktów biobójczych i kosmetycznych.

Planujemy, że obrady będą odbywały się w sesjach naukowych:

- * Mikrobiom człowieka i probiotyki; * Zakażenia układu pokarmowego; * Zakażenia układu oddechowego;
- * Zakażenia układu moczowo-płciowego; * Oporność bakterii na antybiotyki – mechanizmy lekooporności;
- * Genetyka drobnoustrojów; * Dochodzenie epidemiologiczne z zastosowaniem metod molekularnych;
- * Nowe terapie przeciwbakteryjne – kandydaci na leki; * Bakteriofagi i peptydy – jako nowe terapie alternatywne;
- * Aktualne problemy w wakcynologii; * Immunologia zakażeń;
- * Nowości w obszarze sterylizacji, dezynfekcji i antyseptyki; * Patomechanizmy zakażeń; * Mykologia;
- * Wirusologia; * Mikrobiologia środowiskowa naturalnego, bioróżnorodność i bioremediacja;
- * Mikrobiologia środowiska przemysłowego i biotechnologia; * Mikrobiologia żywności;
- * Mikrobiologia weterynaryjna; * Varia.

Planujemy również prezentacje najnowszych prac habilitacyjnych i doktorskich z obszaru mikrobiologii, a także sesje sponsorowane przez firmy.

Zachęcamy wszystkie zainteresowane osoby do zarezerwowania sobie terminu 15–18.09.2020 na uczestnictwo w tym wielkim wydarzeniu w świecie mikrobiologii polskiej. Zachęcamy również wszystkich mikrobiologów, a zwłaszcza młodych adeptów tej nauki do przygotowania interesujących wystąpień i podzielenia się wynikami swoich badań naukowych, jak również rutynowych.

Sekretarz Komitetu Organizacyjnego
XXIX Zjazdu PTM

SEKRETARZ
Polskiego Towarzystwa Mikrobiologów

A. Laudy
dr hab. n. farm. Agnieszka E. Laudy

Przewodniczący Komitetu Organizacyjnego
XXIX Zjazdu PTM

PREZES
Polskiego Towarzystwa Mikrobiologów

Stefan Tyski
prof. dr hab. Stefan Tyski



INFORMACJE Z POLSKIEGO TOWARZYSTWA MIKROBIOLOGÓW

Od ostatniej informacji o działalności Zarządu Głównego Polskiego Towarzystwa Mikrobiologów, zamieszczonej w zeszytach nr 3 z 2019 r. kwartalników Postępy Mikrobiologii i Polish Journal of Microbiology, Prezydium ZG PTM zajmowało się następującymi sprawami:

1. W dniu 01.10.2019 r., zorganizowano spotkanie redakcji PM i PJM w celu omówienia działań, które mogłyby podnieść notowania PM w rankingach, postanowiono:
 - redakcja PM będzie starała się pozyskać recenzentów i autorów manuskryptów spoza Polski. W tym celu porozumie się z redakcją PJM oraz będzie się starała rozpropagować PM poza granicami Polski;
 - podjęte zostaną działania w celu uzyskania większej liczby manuskryptów do PM oraz popularyzacji ukazujących się w PM i PJM publikacji. W tym celu informacje o pojawiających się zeszytach PM i PJM będą ukazywały się na głównej stronie PTM z możliwością dotarcia do artykułu. Ponadto na wszystkich przyszłych zjazdach organizowanych, współorganizowanych lub objętych patronatem przez PTM powinny ukazywać się informacje propagujące obydwie kwartalniki PTM i zachęcające do publikowania na ich łamach artykułów;
 - podjęte zostaną działania w celu pozyskiwania manuskryptów autorów polskich w wersji anglojęzycznej, w tym celu dla manuskryptów nadsyłanych począwszy od dnia 01.01.2020 r. wprowadzone zostaną zmiany w opłacie redakcyjnej.

Obecnie obowiązuje opłata, bez względu na przysłane wersje językowe: dla autora korespondencyjnego – członka PTM 250 zł + VAT 23% (307,50 zł), a jeżeli autor korespondencyjny nie jest aktywnym członkiem PTM (nie ma opłaconych składek w roku bieżącym), opłata wynosi 350 zł + VAT 23% (430,50 zł).

Nowa opłata od 01.01.2020 r.:

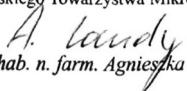
- a) dla autora korespondencyjnego – członka PTM (z opłaconą składką za rok bieżący), gdy manuskrypt jest w języku angielskim lub przysyłane są obie wersje językowe (angielska i polska): 200 zł + VAT* [dla autorów z Polski VAT wynosi 23%] (tj. 246 zł brutto), gdy manuskrypt jest przysyłany tylko w języku polskim – opłata wynosi 400 zł + VAT* [dla autorów z Polski VAT wynosi 23%] (tj. 492 zł brutto);
- b) dla pozostałych autorów korespondencyjnych, którzy nie są aktywnymi członkami PTM (nie mają opłaconych składek w roku bieżącym), gdy manuskrypt jest w języku angielskim lub przysyłane są obie wersje językowe (angielska i polska): 300 zł + VAT* [dla autorów z Polski VAT wynosi 23%] (tj. 369 zł brutto), gdy manuskrypt jest przysyłany tylko w języku polskim – opłata wynosi 600 zł + VAT* [dla autorów z Polski VAT wynosi 23%] (tj. 738 zł brutto);

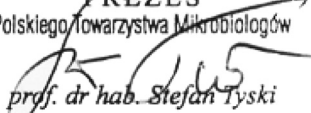
VAT* – wysokość VAT-u jest zależna od kraju, z którego autor korespondencyjny dokonuje opłaty.

- redakcje PM i PJM zwracały uwagę na złą współpracę z wydawcą – firmą EXELEY, która nie w pełni wywiązuje się ze swoich obowiązków.

2. W dniu 02.10.2019 r. odbyło się spotkanie Komitetu Organizacyjnego XXIX Ogólnopolskiego Zjazdu PTM. Pojawiła się możliwość przeprowadzenia Zjazdu PTM w nowej lokalizacji. Zdecydowano, że zostanie przeprowadzona wizja lokalna w „Sangate Hotel Airport” (dawniej Hotel Gromada) i ewentualna zmiana lokalizacji Zjazdu z Centrum Konferencyjno-Szkoleniowego przy ul. Bobrowieckiej 9 do „Sangate Hotel Airport” przy ul. Komitetu Obrony Robotników 32 (dawniej 17 Stycznia 32, róg Żwirki i Wigury) w Warszawie. Przekazano firmie Global Congress dane ponad 250 firm, do których mają być wysłane e-maile z informacją o Zjeździe i zaproszeniu do uczestnictwa w nim. Zdecydowano, że w grudniu zostanie utworzona przez firmę Global Congress strona internetowa Zjazdu, zaś rejestracja na Zjazd zostanie uruchomiona w styczniu 2020 r. Rozważano miejsca na otwarcie Zjazdu i lokalizację przeprowadzenia imprezy towarzyszącej. Ponadto dyskutowano możliwości wystąpienia o dofinansowanie Zjazdu do MNiSW, FEMS oraz do ISME.
3. W dniu 09.10.2019 r. kilku członków Komitetu Organizacyjnego Zjazdu PTM wraz z Prezesem firmy Global Congress udało się do Sangate Hotel Airport w celu przeprowadzenia wizji lokalnej odnośnie możliwości organizacji Zjazdu w tym hotelu. Po obejrzeniu pomieszczeń hotelu i odbyciu rozmów z dyrektorem hotelu oraz zastępcą kierownika ds. organizacji konferencji na terenie hotelu zdecydowano, że XXIX Zjazd PTM odbędzie się w Sangate Hotel Airport, natomiast impreza towarzysząca Zjazdowi w Koneserze. Będą prowadzone dalsze rozmowy w celu wybrania optymalnych rozwiązań do umowy.

4. W dniu 31.10.2019 r. odbyło się spotkanie kilku osób z Komitetu Naukowego Zjazdu, wymieniono informacje na temat organizacji sesji naukowych. Postanowiono w ramach popularyzacji mikrobiologii, w pierwszym dniu Zjazdu, przed jego oficjalnym otwarciem zorganizować 2 sesje popularno-naukowe, dostępne dla wszystkich zainteresowanych osób – zwłaszcza nauczycieli biologii ze szkół średnich z Warszawy i okolic. Sesje, każda obejmująca 4 wykłady uznanych polskich specjalistów, będą dotyczyły tematyki związanej z mikrobiologią środowiska (z elementami ochrony środowiska) oraz mikrobiologii lekarskiej (z zaznaczeniem problemu lekooporności drobnoustrojów oraz problemu – epidemiologia zakażeń, a szczepienia). Ponadto planujemy specjalną sesję plakatową dla uczniów szkolnych kół biologicznych, tak aby każde koło mogło zaprezentować plakat związany ze swoją działalnością. W ostatnim dniu Zjazdu zostaną przyznane nagrody za najciekawsze prezentacje plakatowe.
5. W dniu 06.11.2019 r. odbyło się zebranie kilku osób Komitetu Organizacyjnego Zjazdu PTM, W związku z trudnościami rezerwacji pomieszczeń w Koneserze, zdecydowano, że impreza towarzysząca Zjazdowi odbędzie się w Arkadach Kubickiego u podnóża Zamku Królewskiego. Omawiano sprawy finansowania Zjazdu i tworzenia strony internetowej Zjazdu.
6. Pan dr Mariusz Worek z Klinicznego Szpitala Wojewódzkiego Nr 1 im. Fryderyka Chopina w Rzeszowie, Podkarpackie Centrum Chorób Płuc, Kliniczny Zakład Diagnostyki Laboratoryjnej, Regionalne Referencyjne Laboratorium Prątka Gruźlicy w województwie podkarpackim, zwrócił się do ZG PTM z prośbą o powołanie Oddziału Terenowego PTM w Rzeszowie. Pan doktor deklaruje, że chęć przystąpienia do nowego Oddziału Terenowego PTM zgłosiło ponad 30 osób. Z dużym zadowoleniem witamy tę inicjatywę. Prośba Pana doktora zostanie rozpatrzona na posiedzeniu ZG PTM w marcu 2020 r.
7. Pan prof. dr hab. Grzegorz Woźniakowski zgłosił problemy związane z funkcjonowaniem Oddziału Terenowego PTM w Puławach. Zarząd Oddziału podjął uchwałę o likwidacji Oddziału Terenowego PTM w Puławach, która będzie rozpatrywana na dorocznym posiedzeniu ZG PTM w marcu 2020 r.
8. Złożyliśmy odpowiednie wnioski do Ministerstwa Nauki i Szkolnictwa Wyższego, FEMS, ISME, a także ORLENU, LOTOSU i KGHM z prośbą o dofinansowanie XXIX Ogólnopolskiego Zjazdu PTM. Odzew firm, do których wysłano informacje o Zjeździe z prośbą o deklaracje uczestnictwa i wsparcie finansowe Zjazdu, jest na razie niewielki.
9. Ustalono, że informacja o Zjeździe PTM rozpowszechniana będzie w dwumiesięczniku „Zakażenia XXI wieku” wydawanym przez firmę MAVIPURO Polska Sp. z o.o.
10. Dnia 2 grudnia 2019 r. odbyła się na Wydziale Biologii Uniwersytetu Warszawskiego konferencja historyczno-naukowa „MAKRO-kierunki w MIKRO-biologii” z okazji 70-lecia powołania Oddziału Terenowego PTM w Warszawie. Konferencja obejmowała dwie sesje. Sesja historyczna była poświęcona sylwetkom założycieli i animatorów Oddziału. W jej trakcie wręczono medale i dyplomy zasłużonym członkom Oddziału. W sesji naukowej, osiągnięcia współczesnej mikrobiologii prezentowali specjaliści z zakresu m.in. mikrobiologii farmaceutycznej, weterynaryjnej, środowiskowej i żywności. W konferencji wzięło udział ponad 150 osób. Prezentowano ponad 60 plakatów w 5 sesjach tematycznych. Autorom najlepszych plakatów, w każdej sesji, przyznano dyplomy i nagrody ufundowane przez sponsora. Konferencję zorganizował Oddział Warszawski PTM we współpracy z Polskim Towarzystwem Mikrobiologów, a także Urzędem Marszałkowskim Województwa Mazowieckiego, Wydziałem Biologii i Instytutem Mikrobiologii Uniwersytetu Warszawskiego oraz American Society for Microbiology. Patronat nad wydarzeniem sprawowali: Marszałek Województwa Mazowieckiego, Prezydent m.st. Warszawy, Rektor Uniwersytetu Warszawskiego, Dyrektor Narodowego Instytutu Zdrowia Publicznego – Państwowego Zakładu Higieny, Prezes Polskiego Towarzystwa Mikrobiologów.

SEKRETARZ
Polskiego Towarzystwa Mikrobiologów

dr hab. n. farm. Agnieszka E. Laudy

PREZES
Polskiego Towarzystwa Mikrobiologów

prof. dr hab. Stefan Tyski

CZŁONKOWIE WSPIERAJĄCY PTM

Członek Wspierający PTM – Złoty
od 27.03.2017 r.



HCS Europe – Hygiene & Cleaning Solutions
ul. Warszawska 9a, 32-086 Węgrzce k. Krakowa
tel. (12) 414 00 60, 506 184 673, fax (12) 414 00 66
www.hcseurope.pl

Firma projektuje profesjonalne systemy utrzymania czystości i higieny dla klientów o szczególnych wymaganiach higienicznych, m.in. kompleksowe systemy mycia, dezynfekcji, osuszania rąk dla pracowników służby zdrowia, preparaty do dezynfekcji powierzchni dla służby zdrowia, systemy sterylizacji narzędzi.

Członek Wspierający PTM – Srebrny
od 12.09.2017 r.



Firma Ecolab Sp. z o.o. zapewnia: najlepszą ochronę środowiska pracy przed patogenami powodującymi zakażenia podczas leczenia pacjentów, bezpieczeństwo i wygodę personelu, funkcjonalność posiadanego sprzętu i urządzeń. Firma jest partnerem dla przemysłów farmaceutycznego, biotechnologicznego i kosmetycznego.

Członek Wspierający PTM – Srebrny
od 12.12.2017 r.



Od ponad 100 lat siedziba Wodociągów Krakowskich mieści się przy ul. Senatorskiej. Budowę obiektu ukończono w 1913 roku. W 2016 r. do sieci wodociągowej wtłoczono ponad 56 mln m³ wody. Szacuje się, że ponad 99,5% mieszkańców Gminy Miejskiej Kraków posiada możliwość korzystania z istniejącej sieci wodociągowej.

Członek Wspierający PTM – Zwyczajny
od 12.09.2017 r.



Merck Sp. z o.o. jest częścią międzynarodowej grupy Merck KGaA z siedzibą w Darmstadt, Niemcy i dostarcza na rynek polski od roku 1992 wysokiej jakości produkty farmaceutyczne i chemiczne, w tym podłoża mikrobiologiczne

**Członek Wspierający PTM – Zwyczajny
od 06.06.2019 r.**



BART Spółka z o.o. Sp. K
ul. Norwida 4, 05-250 Słupno
NIP: 1180741884, KRS: 0000573068
<https://bart.pl/>, email: info@bart.pl

Firma BART jest producentem i dystrybutorem surowców oraz dodatków dla przemysłu spożywczego i farmaceutycznego. Specjalizujemy się w probiotykach oraz surowcach uzyskiwanych metodami biotechnologicznymi. Współpracujemy z renomowanymi producentami: Probiotical, Gnosis, Lesaffre